February 2005 Volume 208 • Number 1

THE BIOLOGICAL BULLETIN

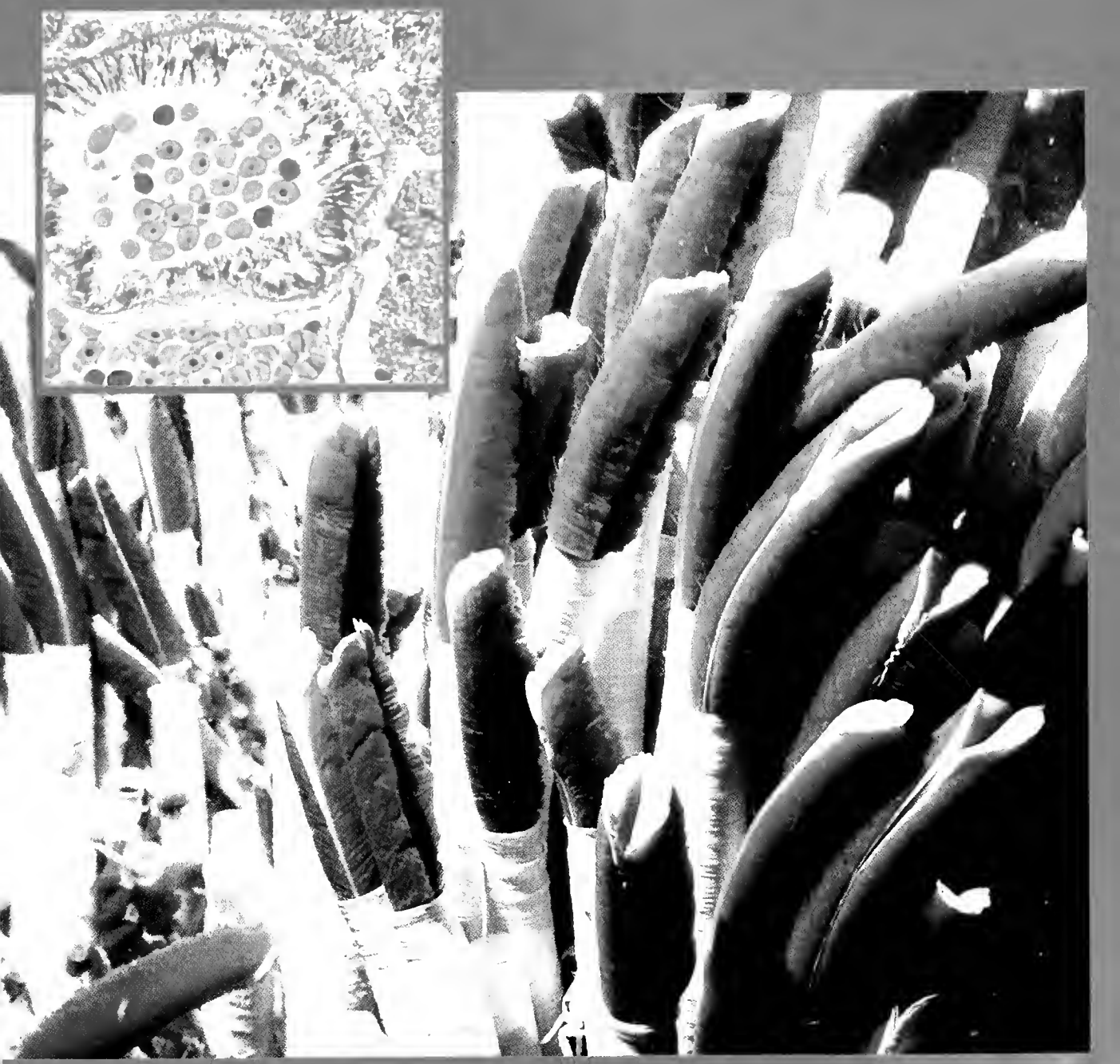

Published by the Marine Biological Laboratory

Woods Hole, Massachusetts

THE BIOLOGICAL BULLETIN

FEBRUARY 2005

Published by
MARINE BIOLOGICAL LABORATORY
WOODS HOLE, MASSACHUSETTS

http://www.biolbull.org

Cover

Riftia pachyptila, a species of vestimentiferan tubeworm, is shown here in an aggregation on Tubeworm Pillar, a large hydrothermal chimney on the East Pacific Rise. Vestimentiferans—those odd gutless worms found at hydrothermal vents and cold seeps in the deep ocean—have strange helical spermatozoa that are bound together in bundles; they also have external ciliated grooves that connect to the openings of the gonoducts. These traits suggest the possibility of sperm transfer and internal fertilization. Indeed, direct transfer of large sperm masses (spermatozeugmata) has been described in two species. It is therefore puzzling that neither mature eggs nor developing embryos have ever been discovered in the oviducts; oocytes removed by dissection always have large germinal vesicles. In estimates of the dispersal time of tubeworm larvae, it had been assumed that fertilization is external and that the dispersal period includes the entire embryonic and larval period. If this assumption is incorrect (*e.g.*, if early embryos are brooded), then dispersal time and distance could be overestimated by as much as 60%.

Using inverted plankton nets floating above clumps of *Riftia pachyptila* at hydrothermal vents in the Eastern Pacific, Hilário, Young, and Tyler (page 20, this issue) show that eggs released by females are still in the primary oocyte stage, an observation that was initially interpreted as evidence for free spawning and external fertilization. However, they also show that oocytes dissected carefully from the oviducts of seep tubeworms (*Lamellibrachia luymesi*) mature and undergo embryogenesis without the addition of spermatozoa, suggesting that oocytes are somehow inseminated internally even before egg maturation is complete.

Histological sections through the trunks of five vestimentiferan species from both seeps and vents revealed a previously unknown sperm storage structure at the far posterior end of the female reproductive tract. Here, in the portion of the tract lying between the ovary and the oviduct, sperm are stored in a spermatheca that consists of distinct outpocketings of the oviduct epithelium. The inset on the cover shows a histological section through the spermatheca of *R. pachyptila*, stained with hematoxylin and eosin. Pink oocytes near the bottom of the image are in the ovary; the central oocytes lie in the lumen of the spermatheca, surrounded by pockets containing purple-stained sperm. Oocytes are presumably inseminated when they pass from the ovary through the spermatheca to the oviduct, where they are stored in the primary oocyte stage until release. Thus, despite the earlier erroneous assumption of external fertilization, the dispersal estimates remain valid.

Credits: Photograph of *R. pachyptila* aggregation: taken by *Alvin* pilot Blee Williams, while diving with co-authors Craig Young and Paul Tyler. Inset: micrograph by author Ana Hilário. Cover design: Beth Liles (Marine Biological Laboratory).

CONTENTS

VOLUME 208, NO. 1: FEBRUARY 2005

NOTICE

The Editorial Office of *The Biological Bulletin* is seeking to acquire back issues of the journal dating from the start of publication in 1897 through 1960. These issues will be used to make their content freely available online. Anyone who has issues from this period and is willing to contribute them is asked to contact the Managing Editor, Pamela Clapp Hinkle, by telephone (at 508-289-7276) or e-mail (pclapp@mbl.edu). The journal will pay the cost of shipping.

THE BIOLOGICAL BULLETIN

THE BIOLOGICAL BULLETIN is published six times a year by the Marine Biological Laboratory, 7 MBL Street, Woods Hole, Massachusetts 02543.

Subscriptions and similar matter should be addressed to Subscription Administrator, THE BIOLOGICAL BULLETIN, Marine Biological Laboratory, 7 MBL Street, Woods Hole, Massachusetts 02543. Subscription includes both print and online journals. Subscription per year (six issues, two volumes): $360 for libraries; $120 for individuals. Subscription per volume (three issues): $180 for libraries; $70 for individuals. Back and single issues (subject to availability): $75 for libraries; $25 for individuals.

Communications relative to manuscripts should be sent to James L. Olds, Editor-in-Chief, or Pamela Clapp Hinkle, Managing Editor, at the Marine Biological Laboratory, 7 MBL Street, Woods Hole, Massachusetts 02543. Telephone: (508) 289-7149. FAX: 508-289-7922. E-mail: pclapp@mbl.edu.

http://www.biolbull.org

THE BIOLOGICAL BULLETIN is indexed in bibliographic services including *Index Medicus* and MEDLINE, *Chemical Abstracts, Current Contents, Elsevier BIOBASE/Current Awareness in Biological Sciences*, and *Geo Abstracts*.

Printed on acid free paper,
effective with Volume 180, Issue 1, 1991.

POSTMASTER: Send address changes to THE BIOLOGICAL BULLETIN, Marine Biological Laboratory, 7 MBL Street, Woods Hole, MA 02543.

Periodicals postage paid at Woods Hole, MA, and additional mailing offices.
ISSN 0006-3185

INSTRUCTIONS TO AUTHORS

The Biological Bulletin accepts outstanding original research reports of general interest to biologists throughout the world. Papers are usually of intermediate length (10–40 manuscript pages). A limited number of solicited review papers may be accepted after formal review. A paper will usually appear within four months after its acceptance.

Very short, especially topical papers (less than 9 manuscript pages including tables, figures, and bibliography) will be published in a separate section entitled "Research Notes." A Research Note in *The Biological Bulletin* follows the format of similar notes in *Nature*. It should open with a summary paragraph of 150 to 200 words comprising the introduction and the conclusions. The rest of the text should continue on without subheadings, and there should be no more than 30 references. References should be referred to in the text by number, and listed in the Literature Cited section in the order that they appear in the text. Unlike references in *Nature*, references in the Research Notes section should conform in punctuation and arrangement to the style of recent issues of *The Biological Bulletin*. Materials and Methods should be incorporated into appropriate figure legends. See the article by Lee (October 2003, Vol **205:** 99–101) for sample style. A Research Note will usually appear within two months after its acceptance.

The Editorial Board requests that regular manuscripts conform to the requirements set below; those manuscripts that do not conform will be returned to authors for correction before review.

1. ***Manuscripts.*** Manuscripts, including figures, should be submitted in quadruplicate, with the originals clearly marked. (Xerox copies of photographs are not acceptable for review purposes.) Please include an electronic copy of the text of the manuscript. Label the disk with the name of the first author and the name and version of the wordprocessing software used to create the file. If the file was not created in some version of Microsoft Word, save the text in rich text format (rtf). The submission letter accompanying the manuscript should include a telephone number, a FAX number, and (if possible) an E-mail address for the corresponding author. The original manuscript must be typed in no smaller than 12 pitch or 10 point, using double spacing (*including* figure legends, footnotes, bibliography, etc.) on one side of 16- or 20-lb. bond paper, 8 by 11 inches. Please, no right justification. Manuscripts should be proofread carefully and errors corrected legibly in black ink. Pages should be numbered consecutively. Margins on all sides should be at least 1 inch (2.5 cm). Manuscripts should conform to the *Council of Biology Editors Style Manual*, 5th Edition (Council of Biology Editors, 1983) and to American spelling. Unusual abbreviations should be kept to a minimum and should be spelled out on first reference as well as defined in a footnote on the title page. Manuscripts should be divided into the following components: Title page, Abstract (of no more than 200 words), Introduction, Materials and Methods, Results, Discussion, Acknowledgments, Literature Cited, Tables, and Figure Legends. In addition, authors should supply a list of words and phrases under which the article should be indexed.

2. ***Title page.*** The title page consists of a condensed title or running head of no more than 35 letters and spaces, the manuscript title, authors' names and appropriate addresses, and footnotes listing present addresses, acknowledgments or contribution numbers, and explanation of unusual abbreviations.

3. ***Figures.*** The dimensions of the printed page, 7 by 9 inches, should be kept in mind in preparing figures for publication. We recommend that figures be about 1 times the linear dimensions of the final printing desired, and that the ratio of the largest to the smallest letter or number and of the thickest to the thinnest line not exceed 1:1.5. Explanatory matter generally should be included in legends, although axes should always be identified on the illustration itself. Figures should be prepared for reproduction as either line cuts or halftones. Figures to be reproduced as line cuts should be unmounted glossy photographic reproductions or drawn in black ink on white paper, good-quality tracing cloth or plastic, or blue-lined coordinate paper. Those to be reproduced as halftones should be mounted on board, with both designating numbers or letters and scale bars affixed directly to the figures. All figures should be numbered in consecutive order, with no distinction between text and plate figures and cited, in order, in the text. The author's name and an arrow indicating orientation should appear on the reverse side of all figures.

Digital art: The Biological Bulletin will accept figures submitted in electronic form; however, digital art must conform to the following guidelines. Authors who create digital images are wholly responsible for the quality of their material, including color and halftone accuracy.

Format. Acceptable graphic formats are TIFF and EPS. Color submissions must be in EPS format, saved in CMKY mode.

Software. Preferred software is Adobe Illustrator or Adobe Photoshop for the Mac and Adobe Photoshop for Windows. Specific instructions for artwork created with various software programs are available on the Web at the Digital Art Information Site maintained by Cadmus Professional Communications at http://epc.cadmus.com/da/

Resolution. The minimum requirements for resolution are 1200 DPI for line art and 300 for halftones.

Size. All digital artwork must be submitted at its actual printed size so that no scaling is necessary.

Multipanel figures. Figures consisting of individual parts (*e.g.*, panels A, B, C) must be assembled into final format and submitted as one file.

Hard copy. Files must be accompanied by hard copy for use in case the electronic version is unusable.

Disk identification. Disks must be clearly labeled with the following information: author name and manuscript number; format (PC or Macintosh); name and version of software used.

Color: The Biological Bulletin will publish color figures and plates, but must bill authors for the actual additional cost of printing in color. The process is expensive, so authors with more than one color image should—consistent with editorial concerns, especially citation of figures in order—combine them into a single plate to reduce the expense. On request, when supplied with a copy of a color illustration, the editorial staff will provide a pre-publication estimate of the printing cost.

4. ***Tables, footnotes, figure legends, etc.*** Authors should follow the style in a recent issue of *The Biological Bulletin* in preparing table headings, figure legends, and the like. Because of the high cost of setting tabular material in type, authors are asked to limit such material as much as possible. Tables, with their headings and footnotes, should be typed on separate sheets, numbered with consecutive Arabic numerals, and placed after the Literature Cited. Figure legends should contain enough information to make the figure intelligible separate from the text. Legends should be typed double spaced, with consecutive Arabic numbers, on a separate sheet at the end of the paper. Footnotes should be limited to authors' current addresses, acknowledgments or contribution numbers, and explanation of unusual abbreviations. All such footnotes should appear on the title page. Footnotes are not normally permitted in the body of the text.

5. ***Literature cited.*** In the text, literature should be cited by the Harvard system, with papers by more than two authors cited as Jones *et al.*, 1980. Personal communications and material in preparation or in press should be cited in the text only, with author's initials and institutions, unless the material has been formally accepted and a volume number can be supplied. The list of references following the text should be headed Literature Cited, and must be typed double spaced on separate pages, conforming in punctuation and arrangement to the style of recent issues of *The Biological Bulletin*. Citations should include complete titles and inclusive pagination. Journal abbreviations should normally follow those of the U. S. A. Standards Institute (USASI), as adopted by BIOLOGICAL ABSTRACTS and CHEMICAL ABSTRACTS, with the minor differences set out below. The most generally useful list of biological journal titles is that published each year by BIOLOGICAL ABSTRACTS (BIOSIS List of Serials; the most recent issue). Foreign authors, and others who are accustomed to using THE WORLD LIST OF SCIENTIFIC PERIODICALS, may find a booklet published by the Biological Council of the U.K. (obtainable from the Institute of Biology, 41 Queen's Gate, London, S.W.7, England, U.K.) useful, since it sets out the WORLD LIST abbreviations for most biological journals with notes of the USASI abbreviations where these differ. CHEMICAL ABSTRACTS publishes quarterly supplements of additional abbreviations. The following points of reference style for THE BIOLOGICAL BULLETIN differ from USASI (or modified WORLD LIST) usage:

A. Journal abbreviations, and book titles, all underlined (for *italics*)

B. All components of abbreviations with initial capitals (not as European usage in WORLD LIST *e.g., J. Cell. Comp. Physiol.* NOT *J. cell. comp. Physiol.*)

C. *All* abbreviated components must be followed by a period, whole word components *must not* (*i.e., J. Cancer Res.*)

D. Space between all components (*e.g., J. Cell. Comp. Physiol.*, not *J.Cell.Comp.Physiol.*)

E. Unusual words in journal titles should be spelled out in full, rather than employing new abbreviations invented by the author. For example, use *Rit Visindafjélags Islendinga* without abbreviation.

F. All single word journal titles in full (*e.g., Veliger, Ecology, Brain*).

G. The order of abbreviated components should be the same as the word order of the complete title (*i.e., Proc.* and *Trans.* placed where they appear, not transposed as in some BIOLOGICAL ABSTRACTS listings).

H. A few well-known international journals in their preferred forms rather than WORLD LIST or USASI usage (*e.g., Nature, Science, Evolution* NOT *Nature, Lond., Science, N.Y.; Evolution, Lancaster, Pa.*)

6. ***Sequences.*** By the time a paper is sent to the press, all nucleotide or amino acid sequences and associated alignments should have been deposited in a generally accessible database (*e.g.*, GenBank, EMBL, SwissProt), and the sequence accession number should be provided.

7. ***Reprints, page proofs, and charges.*** Authors may purchase reprints in lots of 100. Forms for placing reprint orders are sent with page proofs. Reprints normally will be delivered about 2 to 3 months after the issue date. Authors will receive page proofs of articles shortly before publication. They will be charged the current cost of printers' time for corrections to these (other than corrections of printers' or editors' errors). Other than these charges for authors' alterations, *The Biological Bulletin* does not have page charges.

Reference: *Biol. Bull.* **208:** 1–2. (February 2005)

A Message From the Editor

It is a great honor to have been appointed the 10th editor-in-chief of *The Biological Bulletin*. I am humbled to have been chosen to lead this important journal for the next five years and owe a great debt of gratitude to Michael J. Greenberg, the 9th editor-in-chief of the *Bulletin*, who served the journal well for 15 years and has been so kind and generous to me personally through the recent transition.

Mike has been a visionary editor-in-chief. A fine biologist and a skilled and thoughtful editor, he understands deeply the organic relationship between editorial work, peer review, and the impact a journal can have upon the world of science. During his tenure, Mike put together an outstanding and hard-working editorial board, to whom I am also most grateful. He also set a standard for editorial excellence and journal quality that the Board and I intend to sustain and nurture at *The Biological Bulletin* going forward.

Mike's accomplishments while editor are many, but one that stands out among the rest is bringing the journal successfully into the electronic age in partnership with Stanford University's HighWire Press (www.biolbull.org). This transition was achieved while maintaining extraordinarily high editorial standards and with resources that were quite limited relative to other scholarly publications facing similar challenges. Thanks to Mike's leadership and an anonymous benefactor, issues of the journal dating back to Volume 1, Issue 1, will soon be made freely available online (in PDF format) as well.

So, thank you, Mike, on behalf of the *Bulletin*'s many readers, authors, editors, and staff, for your leadership, stewardship, helpful advice, and wonderful sense of humor. We wish you all the best in your future endeavors and look forward to working with you in your new role as a member of the editorial board.

As most readers know, the *Bulletin* was established in 1897; it is among the oldest peer-reviewed biological publications in the United States. Now in its 208th volume, the *Bulletin* is a valuable scientific resource and archive with a distinguished place in some of the most revered scientific libraries around the world.

The *Bulletin* is also among the most precious assets of its publisher, the Marine Biological Laboratory (MBL) in Woods Hole, Massachusetts. The MBL is America's oldest private marine laboratory, an international gathering place for some 1400 of the world's best and brightest biologists and advanced graduate students each summer, and home to a productive and renowned resident research program.

My own affiliation with the MBL goes back more than 25 years when, as a student, I spent a winter in the NIH's Laboratory of Biophysics program, and later returned as a visiting investigator. Although it has been a while since I last worked at a bench in Woods Hole, I remember fondly the eagerness and excitement of the place, and the remarkable quality of science that was being done in the labs and courses there day after day by scientists from institutions across the globe.

From a personal perspective, taking a leadership role with the journal is enabling me to once again immerse myself in the dynamic international scientific community that is the MBL. As an institution, the Laboratory seeks to have a disproportionate impact on the biological sciences. It follows, then, that its flagship journal, *The Biological Bulletin*, should seek to do the same: articles published in *The Biological Bulletin* should be of concrete significance to the entire field of biology.

During my tenure as editor-in-chief, I plan to build upon my predecessors' successes by exploring ways to further enhance this already significant journal. I will work to improve the journal's impact factor by encouraging the top laboratories and scientists in the world—including members of the MBL Corporation, course faculty and alumni, resident researchers, and summer investigators and students—to publish some of their best work in the *Bulletin*. I will continue to build a quality editorial board. As an aside, I believe it is extraordinarily important to involve more MBL scientists in the editorial leadership of the journal. Their collective expertise is just too valuable a resource for the journal to ignore. Hence, as we build out the editorial board, we will welcome investigators who are actively connected with the scientific enterprise at MBL as well as continuing to nurture existing relationships. To counteract the perception that some have that the *Bulletin* is too provincial, I will also work very hard to foster the international nature of science at the journal by, among other strategies, actively recruiting manuscripts from top international labs.

Finally, and perhaps most importantly, I plan to broaden the focus of the journal somewhat toward marine biomed-

ical models, especially within the context of translational research. Although we'll face significant competition from other journals, this move will increase our potential base of submissions and make the journal more attractive to prospective contributors, many of whom we believe already have some affection for or loyalty to the *Bulletin* and its publisher. I want to assure our loyal readers and authors that we will continue to accept high-quality manuscripts in our traditional areas of excellence: neurobiology, behavior, physiology, ecology, evolution, development and reproduction, cell biology, biomechanics, symbiosis, and systematics.

Ultimately, the *Bulletin* is looking for the opportunity to publish scientifically significant work. Such work tends to be, in general, transdisciplinary and, above all, presents a "full story." To use my own field of neurobiology as an example, the most powerful scientific stories deploy the tools of molecular biology to regulate brain-specific genes within specific cell populations, while using the sophisticated tools of electrophysiology and imaging to access the effects of the molecular manipulations. Often there is a computational modeling side to the hypothesis generation and an informatics side to the data itself.

I will be looking for science that is transdisciplinary because I believe such approaches can ask fundamentally more basic questions than investigations restricted to a single domain of marine biology. Five years from now, I hope *The Biological Bulletin* will be known as a journal for transdisciplinary marine biologists.

In today's competitive world of specialty journals, tenure and promotions committees, and most recently, open access initiatives (which we endorse philosophically, but question financially), general journals like the *Bulletin* face many challenges. Ultimately, my tenure as editor-in-chief will be judged by the quality of the science that is published in *The Biological Bulletin*. I am confident that with the help and commitment of our superb editorial board, our loyal readers and authors, members of the MBL community at large, and our outstanding managing staff at the MBL, *The Biological Bulletin* will thrive. I look forward to the next five years.

—James L. Olds
Editor-in-Chief

Reference: *Biol. Bull.* **208:** 3–6. (February 2005)

Increased Zooxanthellae Nitric Oxide Synthase Activity Is Associated With Coral Bleaching

HENRY TRAPIDO-ROSENTHAL[1,*], SANDRA ZIELKE[1], RICHARD OWEN[1,2], LUCY BUXTON[1,3], BRIAN BOEING[1,4], RANJEET BHAGOOLI[1,5], AND JESSICA ARCHER[1,6]

[1] *Bermuda Biological Station for Research, Inc., Ferry Reach GE-01, Bermuda;* [2] *Environment Agency, Westbury-on-Trym, Bristol BS106BF, UK;* [3] *Department of Environmental Sciences, University of Technology, Sydney, New South Wales 2065, Australia;* [4] *Department of Oceanography, University of Hawaii, Honolulu, Hawaii 96822;* [5] *Department of Chemistry, Biology and Marine Sciences, University of the Ryukyus, Nishihara, Okinawa, 903-0213 Japan; and* [6] *Department of Biology, Evergreen State University, Olympia, Washington 98505*

Coral bleaching, the breakdown of the symbiotic relationship between host corals and their photosynthetic dinoflagellate endosymbionts, is a phenomenon of major ecological significance. The cellular and molecular mechanisms underlying bleaching are poorly understood. Here we report substantial increases in nitric oxide synthase (NOS) activity in symbionts associated with bleaching corals. Nitric oxide (NO), a product of NOS activity, is a highly reactive and membrane-permeable molecule that has the potential to exert cytotoxic effects in host cells either directly or in combination with molecular oxygen or superoxide radicals. This potential allows us to suggest that coral bleaching may be a stress response initiated by the symbiont, rather than by the host.

Coral reefs are biodiverse ecosystems of enormous ecological and economic importance (1, 2). The corals that constitute the foundations of these ecosystems are symbiotic assemblages consisting of the host coral and symbiotic dinoflagellate algae of the genus *Symbiodinium*, known as zooxanthellae, which provide the host organism with photosynthetically derived nutrients and promote calcification. Environmental stressors can induce the phenomenon of bleaching, which refers to the loss of symbiotic algae or, less commonly, the degradation of algal pigments (3). Severely bleached corals can suffer depressed growth rates, increased susceptibility to disease and, at the extreme, mortality (4, 5). The cellular and molecular mechanisms that underlie the breakdown of the symbiotic partnership are still poorly understood. The study of these mechanisms is an active research area, in which a consensus is developing that a primary step in the bleaching process occurs in the zooxanthellae (3, 6).

Many investigations into the molecular mechanisms of bleaching have used experimentally bleached symbioses—that is, assemblages exposed to acute temperature stress 2–5 °C above or below ambient for 12–72 h (4). However, bleaching in the field is not usually associated with such abrupt, acute changes in temperature and usually occurs after a more gradual onset of temperature stress that may persist for several weeks (7). The extent to which the mechanisms of experimental bleaching relate to the observed declines in symbiont densities in the field is uncertain, unless these mechanisms are investigated under both experimental and field conditions. Results from our laboratory indicate that nitric oxide (NO), generated by algal nitric oxide synthase (NOS), is closely associated with coral bleaching both in artificially induced bleaching in the laboratory setting and during naturally occurring bleaching episodes in the field.

Nitric oxide synthases convert arginine to citrulline and NO (8). Zooxanthellae that have been freshly isolated from a non-stressed symbiotic relationship with a host cnidarian have a free amino acid pool that is dominated by arginine (9). In addition, these symbionts possess a low basal level of NOS activity (10). We examined the effects of elevated or depressed water temperatures that induce the breakdown of cnidarian-dinoflagellate symbioses on symbiont NOS activity, which was mea-

Received 6 November 2003; accepted 30 November 2004.

* To whom correspondence should be addressed, at School of Ocean and Earth Science and Technology, University of Hawaii, Honolulu 96822. E-mail: hank@hbsr.edu

sured by monitoring the conversion of radiolabeled arginine to citrulline (8, 10).

We examined the effect of elevated temperature on zooxanthellar NOS activity (amol citrulline/zooxanthella/min) isolated from the branching scleractinian coral *Madracis mirabilis* (*sensu* Wells, 1973). Corals, from the coastal waters of Bermuda collected by scuba diving, were kept in seawater collected at the site and returned to the laboratory within 1 h. For temperature treatments in the laboratory, corals were maintained at ambient temperature in continuously flowing seawater for at least 48 h before treatment. Corals were subjected to temperature stress by placing them in beakers of artificial seawater (ASW; 423 m*M* NaCl, 26 m*M* $MgSO_4 \cdot 7H_2O$, 23 m*M* $MgCl_2 \cdot 6H_2O$, 9 m*M* KCl, 12.6 m*M* $CaCl_2 \cdot 2H_2O$, 0.2 m*M* $NaHCO_3$, 10 m*M* HEPES; pH 7.8). The beakers were then placed into incubators set at the desired temperatures and remained there at constant temperature and irradiance for 24 h. Algal NOS activity was determined for those zooxanthellae retained within the coral host tissue (*i.e., in hospite*) over the course of the incubation and for those zooxanthellae that had left the host as a result of temperature stress. For *in hospite* zooxanthellae, corals were removed from the incubation at selected time points; zooxanthellae were then separated from the host tissue, as described by Owen *et al.* (11). For determination of algal NOS activity for zooxanthellae that had left the host, algae were quantitatively collected from beakers by centrifugation. In all cases zooxanthellar numbers were determined by counting with a hemacytometer; cells were then rinsed with homogenization buffer (HB; 50 m*M* HEPES, 1 m*M* EDTA; pH 7.4, ambient temperature) and homogenized in HB, in a total volume of 1 ml, by vortexing with sterile borosilicate glass beads (a single 5-mm bead, 0.4 g 710–1180-μm beads, and 0.2 g 15–212-μm beads). Homogenates were centrifuged at 16,000 $\times$ *g* for 10 min, after which NOS activity in the supernatant fraction was determined by measuring conversion of the NOS substrate ^{3}H-arginine (New England Nuclear, specific activity adjusted to 3.22 mCi/mmol) to ^{3}H-citrulline as previously described (8, 10, 12). Results are presented as the amount of citrulline generated per cell per unit time.

Specimens of *M. mirabilis* that are subjected to acute heat shock in the laboratory undergo visible bleaching. After 16 h of exposure to a water temperature of 32 °C (4 degrees above the ambient temperature of 28 °C), *in hospite* zooxanthellae isolated from corals subjected to such treatment had higher levels of NOS activity ($6.09 \pm 0.60 \times 10^{-18}$ mol citrulline/zooxanthella/min, $n = 3$) than did zooxanthellae isolated from non-heat-stressed control corals ($0.13 \pm 0.04 \times 10^{-18}$ moles citrulline/zooxanthella/min, $n = 3$); this difference was significant (Student's $t = 17.31$, df $= 4$, $P < 0.0001$). Time-course thermal stress experiments also showed that *in hospite* zooxanthellae within the coral, as well as those that had vacated the symbiosis, showed increases in algal NOS activity associated with thermal stress and the bleaching response (Fig. 1).

In Bermuda, *M. mirabilis* undergoes characteristic periods of colony paling and bleaching during midwinter or late summer periods of thermal stress, at which times sea surface temperature can be below 18 °C (winter) or above 29 °C (summer) for several weeks or more. It is thus possible to collect corals during and outside these periods of bleaching (Fig. 2), immediately extract *in hospite* zooxanthellae upon return to the laboratory, and determine algal NOS activities as described above. Increases in *M. mirabilis* algal NOS activity were seen to be associated with bleaching corals (*i.e.*, when zooxanthella densities are below approximately 2×10^6 cells/cm^2; Fig. 2), irrespective of whether the bleaching is associated with periods of stress caused by high or low ambient water temperature. Outside the bleaching period, basal levels of NOS activity were restored. Additionally, algal cells from bleaching corals ($0.4 \pm 0.2 \times 10^6$ zooxanthellae/cm^2) had higher NOS activities (12.6 ± 0.6 amol citrulline/zooxanthella/min) when compared to those from nonbleaching corals ($5.6 \pm 1.3 \times 10^6$ zooxanthellae/cm^2; 0.7 ± 1.0 amol citrulline/zooxanthella/min) collected during the same week (22–29 August 2002) at the same location and depth. This suggests that elevated NOS activity is related to the bleaching phenomenon.

Low levels of NO production typically result from constitutive NOS (cNOS) activity, with many associated physiological actions of this molecule resulting from the activation of guanylate cyclase and that enzyme's production of

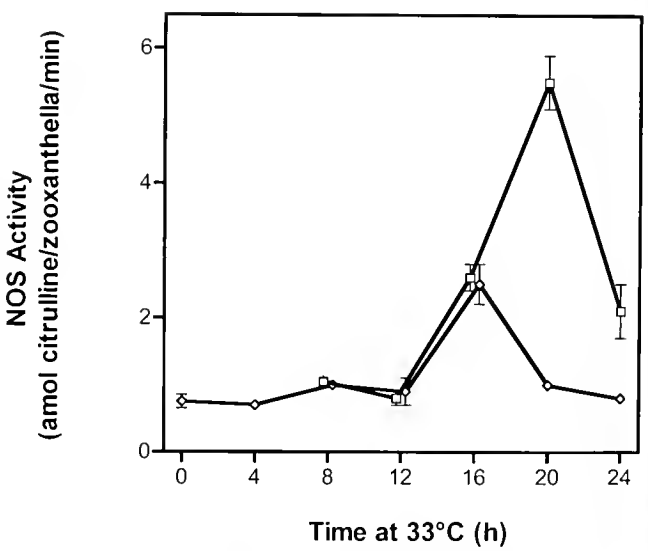

Figure 1. The effect of a 4 °C increase in temperature (from 29 to 33 °C) on NOS activity in zooxanthellae from *Madracis mirabilis*. NOS activities of *in hospite* zooxanthellae (●) and zooxanthellae released (□) from host corals were determined as described in the text. Activities are represented as means and standard deviations, in attomoles (amol; 10^{-18} moles) of citrulline generated per cell per minute of triplicate incubations; when no error bars are depicted, the bars lie within the graphical representation of the mean.

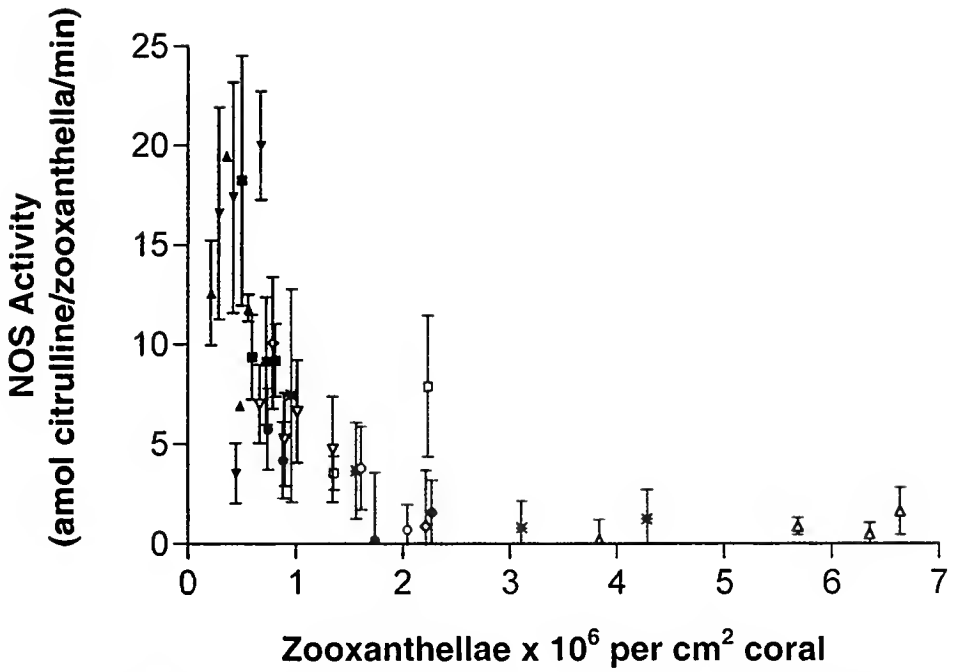

Figure 2. Relationship between *in hospite* zooxanthellar NOS activities (amol citrulline/zooxanthella/min) and algal density for specimens of *Madracis mirabilis* colonies collected from the coastal waters of Bermuda, March 2002–May 2003. NOS activities of zooxanthellae present in these corals were determined as described in the text. Each data point represents the mean activity ± 1 standard deviation of four replicates taken from a single coral colony. Zooxanthellar densities per unit coral surface area were determined by hemacytometer to calculate the total number of zooxanthellae in each airbrushed cell preparation, and the method of Stimson and Kinzie (25) was used to determine the amount of coral surface subjected to airbrushing. Symbols indicate the dates on which corals were collected, the sea surface water temperature (°C) at the time of collection, and the mean sea surface water temperature over the 2 weeks prior to collection (in brackets) as determined from daily measurements, as follows: ▽, 12-Mar-02, 17.8 (18.2); ▼, 18-Mar-02, 20.0 (18.6); △, 22-Aug-02, 28.4 (28.7); ▲, 28-Aug-02, 29.8 (28.9); □, 5-Sep-02, 28.8 (29.4); ■, 19-Sep-02, 26.9 (29.4); ○, 10-Dec-02, 20.6 (20.8); ●, 12-Dec-02, 20.8 (20.8); ◇, 12-Feb-03, 18.7 (17.8); ✻, 6-May-03, 23.2 (21.9). Green symbols indicate that the corals appeared well pigmented at time of collection, whereas black symbols indicate that the corals appeared weakly pigmented at time of collection.

cyclic GMP (13). The low levels of NOS activity in algae from nonbleaching corals collected from the field are in line with cNOS activities from a variety of other organisms (8, 13), as well as with activities previously reported for zooxanthellae isolated from non-stressed hosts (10).

Morrall and colleagues have shown that the host fractions of symbiotic cnidarians exhibit NOS activity, but that, unlike the zooxanthellae, their NOS activity decreases when they are subjected to either heat (33 °C) or cold (17 °C) shock (12). In light of our current studies, their results can be interpreted as a compensatory response of the host to the higher, possibly cytotoxic levels of symbiont-generated NO within the coral endodermal cells.

Cytotoxic reactions resulting from elevated amounts of NO can be direct and indirect. Direct reactions of NO may cause cytotoxicity by inactivating key metabolic pathways (14). The reaction of NO with photosynthetically generated molecular oxygen or superoxide also has the potential to form reactive nitrogen oxide species (RNOS), notably N_2O_3, the major NO autoxidation intermediate in aqueous media, and peroxynitrite (15). RNOS are generally thought to cause deleterious effects such as chemical damage to proteins and DNA and irreversible inhibition of mitochondrial respiration (15, 16, 17) by modifying important biomacromolecules. Notable key reactions of RNOS are nitration reactions (particularly of tyrosine), nitrosation of sulfhydryl-containing moieties (*e.g.*, glutathione and cysteine), and oxidation of various substrates (17); proteins containing reduced thiol-rich environments are particularly susceptible, forming stable and biologically active protein *S*-nitrosothiols.

Since NO and O_2 are more than 20 times more soluble in the lipid layers of cells than in aqueous media (13, 16), cell membranes are predicted to be a primary site of RNOS formation. Cell-membrane-associated proteins would be vulnerable to nitrosation and nitration reactions, forming species such as *S*-nitrosothiols (themselves NO-donors), nitrosamines, and nitrotyrosine. Histological studies have shown that, in addition to degradation of zooxanthellae *in situ* and loss of algal cells (18), loss of intact host endoder-

mal cells containing algae can be a feature of the bleaching process; the shedding of these cells is suggested to result from cell adhesion dysfunction (19). It is worth noting that the most abundant, symbiosis-enhanced protein in the symbiotic anemone *Anthopleura elegantissima* has been identified as a protein that shares significant homology with the fasciclin I (Fas 1) family of cysteine-containing cell adhesion proteins (20), which are themselves significant targets for RNOS nitrosative reactions.

Algal stress is a common initiating feature of the bleaching response, with reports of bleaching-associated destabilization of photosystem II D1 reaction centers and photosynthetic dysfunction (21, 22), and photosynthetic inhibition by *Vibrio* toxins (23). We hypothesize that upregulation of NOS activity is an important component of the zooxanthellar response to such stress. Such upregulation might be analogous to the process of induction of NOS by a number of cell types (*e.g.*, activated macrophages) as a cytotoxic defense response against microbial infection (15). This may provide the zooxanthellae with the means to vacate the now stressful conditions of the symbiosis by induction of host cell necrosis and bleaching; the algal cells can emerge from the symbiosis in photosynthetically active, and thus presumably healthy and viable, condition (24). It is interesting to speculate that bleaching may be an adaptive response of the zooxanthellae rather than the coral host, as one aspect of a multiphased dinoflagellate life cycle.

Acknowledgments

This work was supported by NSF grant OCE-0243762 and the Ocean Fund, Miami. We thank Dr. Angela Douglas for critical comments on an earlier version of this work. This is contribution # 1656 from the Bermuda Biological Station for Research, Inc.

Literature Cited

1. **Connell, J. H. 1978.** Diversity in tropical rain forests and coral reefs. *Science* **199:** 1302–1310.
2. **Moberg, F., and C. Folke. 1999.** Ecological goods and services of coral reef ecosystems. *Ecol. Econ.* **29:** 215–233.
3. **Douglas, A. E. 2003.** Coral bleaching—how and why? *Mar. Pollut. Bull.* **46:** 385–392.
4. **Brown, B. E. 1997.** Coral bleaching: causes and consequences. *Coral Reefs* **16:** S129–S138.
5. **Wilkinson, C. R. 1999.** Global and local threats to coral reef functioning and existence: review and predictions. *Mar. Freshw. Res.* **50:** 867–878.
6. **Downs, C. A., J. E. Fauth, J. C. Halas, P. Dustan, J. Bemiss, and C. M. Woodley. 2002.** Oxidative stress and coral bleaching. *Free Radical Biol. Med.* **33:** 533–543.
7. **Fitt, W. K., F. K. McFarland, M. E. Warner, and G. C. Chilcoat. 2000.** Seasonal patterns of tissue biomass and densities of symbiotic dinoflagellates in reef corals and relation to coral bleaching. *Limnol. Oceanogr.* **45:** 677–685.
8. **Bredt, D. S., and S. H. Snyder. 1989.** Nitric oxide mediates glutamate-linked enhancement of cGMP levels in the cerebellum. *Proc. Natl. Acad. Sci. USA* **86:** 9030–9033.
9. **Ferrier, M. D. 1992.** Fluxes and metabolic pools of amino acids in algal-cnidarian symbioses. Ph.D. Dissertation. University of Maryland, College Park, MD.
10. **Trapido-Rosenthal, H. G., K. H. Sharp, T. S. Galloway, and C. E. Morrall. 2001.** Nitric oxide and cnidarian-algal symbioses: pieces of a puzzle. *Am. Zool.* **41:** 111–121.
11. **Owen, R., A. H. Knap, M. Toaspern, and K. Carbery. 2002.** Inhibition of coral photosynthesis by the antifouling herbicide Irgarol 1051. *Mar. Pollut. Bull.* **44:** 623–632.
12. **Morrall, C. E., T. H. Galloway, M. H. Depledge, and H. G. Trapido-Rosenthal. 2000.** Characterisation of nitric oxide synthase activity in the tropical sea anemone *Aiptasia pallida*. *Comp. Biochem. Physiol. B* **125:** 483–491.
13. **Wink, D. A., and J. B. Mitchell. 1998.** Chemical biology of nitric oxide: insights into regulatory, cytotoxic, and cytoprotective mechanisms of nitric oxide. *Free Radical Biol. Med.* **25 (4/5):** 434–456.
14. **Brown, G. C., and B. Borutaite. 2002.** Nitric oxide inhibition of mitochondrial respiration and its role in cell death. *Free Radical Biol. Med.* **33:** 1440–1450.
15. **James, S. L. 1995.** Role of nitric oxide in parasitic infections. *Microbiol. Rev.* **59 (4):** 533–547.
16. **Wink, D. A., M. B. Grisham, J. B. Mitchell, and P. C. Ford. 1996.** Direct and indirect effects of nitric oxide in chemical reactions relevant to biology. *Methods Enzymol.* **268:** 12–31.
17. **Stamler, J. S., D. I. Simon, J. A. Osborne, M. E. Mullins, O. Jakari, T. Michel, D. J. Singel, and J. Loscalzo. 1992.** S-Nitrosylation of proteins with nitric oxide: synthesis and characterization of biologically active compounds. *Proc. Natl. Acad. Sci. USA* **89:** 444–448.
18. **Brown, B. E., M. D. A. Le Tissier, and J. C. Bythell. 1995.** Mechanisms of bleaching deduced from histological studies of reef corals sampled during a natural bleaching event. *Mar. Biol.* **122:** 655–663.
19. **Gates, R. D., G. Baghdasarian, and L. Muscatine. 1992.** Temperature stress causes host cell detachment in symbiotic cnidarians: implications for coral bleaching. *Biol. Bull.* **182:** 324–332.
20. **Reynolds, W. S., J. A. Schwarz, and V. M. Weis. 2000.** Symbiosis-enhanced gene expression in cnidarian-algal associations: cloning and characterization of a cDNA, sym32, encoding a possible cell adhesion protein. *Comp. Biochem. Physiol. A* **126:** 33–44.
21. **Warner, M. E., W. K. Fitt, and G. W. Schmidt. 1999.** Damage to photosystem II in symbiotic dinoflagellates: a determinant of coral bleaching. *Proc. Natl. Acad. Sci. USA* **96:** 8007–8012.
22. **Jones, R. J., O. Hoegh-Guldberg, A. W. D. Larkum, and U. Schreiber. 1998.** Temperature-induced bleaching of corals begins with impairment of the CO_2 fixation mechanism in zooxanthellae. *Plant Cell Environ.* **21:** 1219–1230.
23. **Banin, E., K. H. Sanjay, F. Naider, and E. Rosenberg. 2001.** A proline-rich peptide from the coral pathogen *Vibrio shiloi* that inhibits photosynthesis of zooxanthellae. *Appl. Environ. Microbiol.* **67:** 1536–1541.
24. **Ralph, P. J., R. Gademann, and A. W. D. Larkum. 2001.** Zooxanthellae expelled from bleached corals at 33 °C are photosynthetically competent. *Mar. Ecol. Prog. Ser.* **220:** 163–168.
25. **Stimson, J., and R. A. Kinzie. 1991.** The diel pattern of release of zooxanthellae by colonies of *Pocillopora damicornis* maintained under control and nitrogen-enriched conditions. *J. Exp. Mar. Biol. Ecol.* **153:** 63–74.

Reference: *Biol. Bull.* **208:** 7–11. (February 2005)

Disruptive Body Patterning of Cuttlefish (*Sepia officinalis*) Requires Visual Information Regarding Edges and Contrast of Objects in Natural Substrate Backgrounds

CHUAN-CHIN CHIAO[1,2], EMMA J. KELMAN[1,3], AND ROGER T. HANLON[1,*]

[1] *Marine Biological Laboratory, Woods Hole, Massachusetts;* [2] *Department of Life Science, National Tsing Hua University, Hsinchu, Taiwan; and* [3] *College of Life Sciences, University of Sussex, Brighton, UK*

Cuttlefish (Sepia officinalis *Linnaeus, 1758) on mixed light and dark gravel show disruptive body patterns for camouflage. This response is evoked when the size of the gravel is equivalent to the area of the "White square," a component of its dorsal mantle patterns. However, the features of natural substrates that cuttlefish cue on visually are largely unknown. Therefore, we aimed to identify those visual features of background objects that are required to evoke disruptive coloration. At first, we put young cuttlefish in a circular experimental arena, presented them with natural gravel and photographs of natural gravel, and established that the animals would show a disruptive pattern when presented either with three-dimensional natural gravel or its two-dimensional photographic representation. We then manipulated the digital photographs by applying (i) a low-pass filter to remove the edges of the fragments of gravel, and (ii) a high-pass filter to remove the contrast among them. The body patterns produced by the cuttlefish in response to these altered visual stimuli were then video-recorded and graded. The results show that, to evoke disruptive coloration in cuttlefish, visual information about the edges and contrast of objects within natural substrate backgrounds is required.*

Cephalopods have a remarkable ability to change the color and pattern of their skin, and research has demonstrated that visual input regulates these changes. Cuttlefish skin can show 20–50 chromatophore patterns that are used for both camouflage and communication (1). Cuttlefish can change their body patterns within a fraction of a second because chromatophore organs are innervated directly from the brain (2, 3). Because of its speed and diversity, body patterning in cuttlefish is the most sophisticated form of adaptive coloration in the animal kingdom (4). Although many aspects of cephalopod vision are known (5), the visual features of a given substrate that evoke adaptive coloration are relatively unstudied.

Recently we developed a quantifiable behavioral assay based upon single, static, computer-generated images that allow us to control detailed aspects of visual input. With this method, we first showed that certain visual background features were used by cuttlefish to produce disruptive coloration (6). Specifically, when the size of white squares on a checkerboard was similar to that of the "White square" component in the animal's skin, the cuttlefish produced a disruptive color pattern; this response occurred over a large contrast range and required only that a few white checks be present in the visual background. A subsequent study (7) showed that, to produce disruptive body patterns for camouflage, cuttlefish cue visually on the area—not the shape or aspect ratio—of light objects in a dark substrate. Most recently, we found that if the background was composed of a high density of small light and dark objects, the cuttlefish would produce mottled skin patterns; but if the background was uniform, uniformly stippled skin patterns would be produced (8). We also applied this behavioral assay to the study of the polarization vision of cuttlefish; although the results were mixed, they indicated that cuttlefish perceive differently polarized checks as light or dark objects and

Received 2 September 2004; accepted 10 December 2004.

* To whom correspondence should be directed. E-mail: rhanlon@mbl.edu

usually generate disruptive body patterns in response. The perceptual mechanisms underlying this polarization sensitivity are still unclear (9).

Taken together, this series of studies has demonstrated the utility of a laboratory sensorimotor assay in which sensory input can be measured quantitatively and its fine-tuned motor output (*i.e.*, chromatophore skin patterns) can be easily seen and measured quantitatively in an intact, behaving cuttlefish (see also 10). This approach was first developed to study changeable coloration in flatfish (11,12,13).

In these earlier investigations, cuttlefish were exposed to artificial—although readily quantified—substrates. We now examine the responses of cuttlefish to natural substrates and a variety of computer-manipulated digital photographs of those natural substrates. To achieve camouflage, animals must match various aspects of light and pattern. Thus, we expect that cuttlefish are attuned to certain elements of the spatial information in the background. Spatial frequency may be defined generally as the number of regular cycles in perceived light intensity per unit distance. The edge of an object, for example, might be characterized by a sharp transition in intensity, which is due to higher spatial frequencies of reflected light. In this paper, we show that for cuttlefish to detect light objects on a dark background and then produce disruptive body patterns, they require spatial frequency information about both the edges and contrast of background objects.

Four young cuttlefish, *Sepia officinalis* (5–8 cm mantle length), were reared from eggs in the MBL Marine Resources Center (Woods Hole, MA) and were maintained in the same facility throughout these experiments. Each animal was placed in a tank (30 cm × 50 cm × 15 cm) with running seawater and was restricted by a circular arena (25 cm in diameter, 12 cm in height; walls were black) in which natural gravel and digital photographs of gravel backgrounds (laminated to be waterproof) were presented as the substratum. Natural gravel, collected at the local beach, was

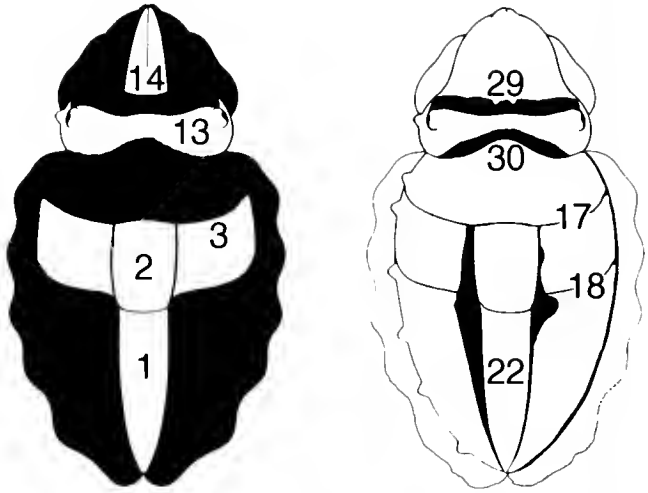

Figure 1. Ten chromatic skin components were used in grading the disruptive body patterns of the cuttlefish. The numbers of the components are the same as those used in reference 1. Five light components (left drawing) are numbered: (1) White posterior triangle; (2) White square; (3) White mantle bar, which includes White square and extends the full width of the mantle; (13) White head bar; and (14) White arm triangle. Five dark components (right drawing) are numbered: (17) Anterior transverse mantle line; (18) Posterior transverse mantle line; (22) Median mantle stripes (one on either side of the midline); (29) Anterior head bar; and (30) Posterior head bar. See text for grading method.

selected to be about the size of the White square component shown on the animal's dorsal mantle (illustrated as #2 in Fig. 1). All of the gravel was glued, with standard acid-free rubber cement, onto sheets of acrylic plastic (25 cm × 25 cm × 0.5 cm); thus the identical pattern of substrate could be presented in each trial. A digital picture of the glued gravel was taken with a Nikon Coolpix 5400 camera (5 megapixel image), and subsequent filtering and image enhancement were done in Photoshop CS (Adobe Systems, Inc.). A digital video camera (Sony VX-1000) was used to record the body patterning of *S. officinalis* over a period of 30 min. The camera was set to record for 2 s every minute,

Figure 2. A–F: Responses of cuttlefish to a natural gravel substrate and to digital photographs of that identical substrate. (A) Cuttlefish (bottom right at 4 o'clock; near white mark in margin) shows a disruptive body pattern for camouflage on a natural gravel background. (B) Cuttlefish shows similar disruptive body pattern on a digital photograph of the gravel shown in (A). Low-pass (C) and high-pass (D) filtered images of the photograph shown in (B). On both backgrounds, the cuttlefish shows uniform or stippled patterns. The background shown in (E) is an enhanced contrast image of (C), and (F) is an enhanced contrast image of (D). In both, the body patterns of cuttlefish are similar to the original low-pass and high-pass filtered images (C and D, respectively). Note, however, that the animal in (F) shows weak traces of the disruptive chromatic components White head bar, White square, and White posterior triangle. G–M: Statistical properties of processed images used in this study. The two-dimensional Fourier transform of the original digital image (G), the low-pass (H) and high-pass (I) filtering. The profiles of brightness distribution: the low-pass filtered image (J), the high-pass filtered image (K), the low-pass (L) and the high-pass (M) after Histogram Equalization. The gray scale (0–255) is shown on the abscissa, and the number of pixels of each brightness level is indicated on the ordinate. Artifacts (*i.e.*, two valleys form a sharp peak in the middle) can be seen in the Equalized high-pass filtered image (M) due to the obscured brightness distribution of the high-pass filtered image (K), yet the overall contrasts of these filtered images were enhanced substantially (*i.e.*, Fig. E and F).

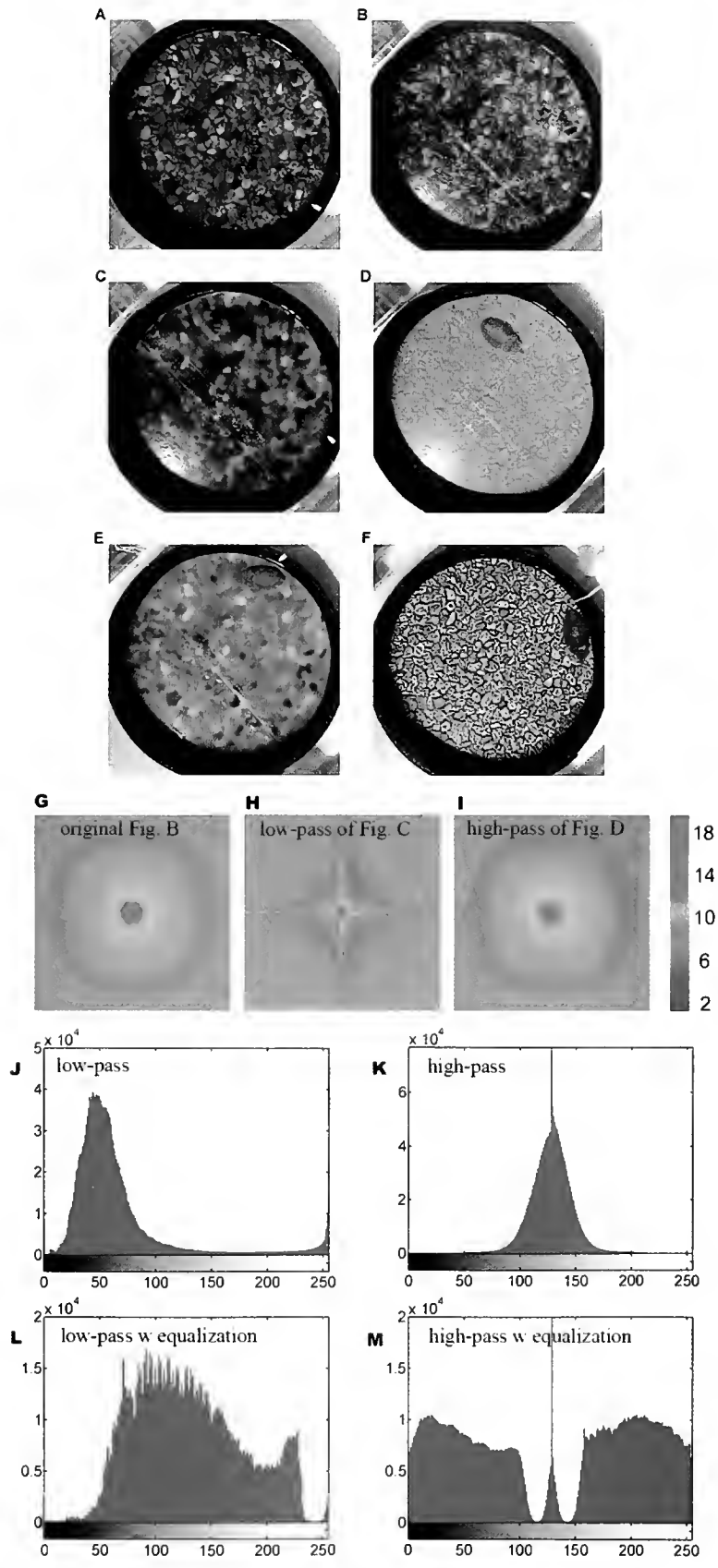
A
B
C
D
E
F
G
original Fig. B
H
low-pass of Fig. C
I
high-pass of Fig. D
18
14
10
6
2
J
low-pass
x 10^4
K
high-pass
x 10^4
L
low-pass w equalization
x 10^4
M
high-pass w equalization
x 10^4
0
50
100
150
200
250

giving a total recording time of 60 s per animal per substrate. A 500-W tungsten light was used in all experiments. In earlier experiments (6, 7, 8, 9), the cuttlefish took several minutes to settle down on the black-and-white checkerboard substratum. In the present experiments, cuttlefish easily settled, not only on natural gravel, but also on the pictures of gravel.

To determine the responses of the animals to different substrata, a more precise grading scheme was applied to patterning of the skin (6, 7). In this refined grading scheme, five light and five dark disruptive chromatic components of the skin of head and mantle were evaluated and scored (1). The components are diagrammed in Figure 1, but also note the natural disruptive body patterns in Figure 2A, B. The following grades were assigned to each component: 2, strong presence; 1, partial presence; and 0, absence. Partial or strong presence was determined by the relative degree of contrast between the light and dark components of the skin. Grading was conducted by playing the videotape and assigning a grade (whole integers 0, 1, 2) every 6 s for each component on the skin. Thus, since all tapes lasted 60 s, the components on each animal were graded 10 times on each substratum. Each disruptive chromatic component was graded separately and with equal weight, and grades for all components were summed to yield the final scores. For example, a score of 20 represents the maximal disruptive appearance: strong presence (grade 2) of all 10 disruptive components. A score of zero represents the minimal disruptive appearance: uniform or stippled patterns. Scores of 8–15 represent typical disruptive patterns, as described often (1, 2, 4, 6, 7, 9).

Figure 2 illustrates various manipulations of the substrate image. First, we removed the high spatial frequency information from the scene (*i.e.*, the edges of objects in the substrate). In brief, we used Photoshop to apply a low-pass (or Gaussian) blur filter to the original image, which was 900 pixels in diameter. The Gaussian filter had a radius of 10 pixels and a cutoff frequency at 1.3% of the Nyquist frequency of the image (14). Second, we removed low spatial frequency information from the substrate image (*i.e.*, local contrast between objects in the substrate) by applying a high-pass filter in Photoshop (14); this filter had a 10-pixel radius and a cutoff frequency at 98% of the Nyquist frequency of the image. Thus, the effects of the Gaussian filter (Fig. 2C) and the high-pass filter (Fig. 2D) are opposed. Two-dimensional Fourier transforms of the original image and the low-pass and high-pass-filtered images are compared in Figure 2G, H, and I. The rationale for using Fourier transformations to analyze spatial frequency information—and the methodology for carrying the analysis out—are provided elsewhere (15). Since images tend to lose overall contrast due to filtering effects, we applied a maximal contrast-enhancing tool to boost the contrast of the filtered images. The Equalize function in Photoshop was used; this is identical to Histogram Equalization, where a brightness distribution is normalized so that all values are equally probable. The profiles of the brightness distribution of the low-pass and the high-pass filtered images, before and after maximal contrast enhancement (Histogram Equalization), are shown in Figure 2J–M. Note that Histogram Equalization can only approximate the equally probable intensity values for these images.

Cuttlefish showed strongly disruptive patterns on natural gravel (Fig. 2A), as expected from previous results (1, 2). More important, cuttlefish also showed similarly disruptive patterns on the exact photograph of natural gravel (Fig. 2B). This indicates that cuttlefish use mainly visual cues for camouflage; *i.e.*, a tactile cue is not required (1). These results imply further that cuttlefish can sense the essential visual cues for disruptive camouflage from two-dimensional images, and that the three-dimensional cues are less vital for this particular task.

After establishing that animals responded similarly to three-dimensional natural gravel and two-dimensional gravel pictures, we sought to examine those gross aspects of spatial frequency in the scene that might contain critical visual cues informing the cuttlefish's choice of camouflage patterning. From earlier experiments (7), we knew that to produce disruptive body patterns, cuttlefish cue visually on the area—not shape or aspect ratio—of white objects on a dark background. This suggested that cuttlefish may determine the size of white objects by visually integrating the areas of whiteness. But whether cuttlefish use the edges or the local contrast between white objects and the dark background (or both) to make this determination is not known.

Cuttlefish did not show disruptive colorations on either the low-pass (Fig. 2C) or the high-pass (Fig. 2D) filtered images. Furthermore, cuttlefish did not respond to the filtered images of enhanced overall contrast (Fig. 2E, F). Although only two animals were tested, this result suggests that cuttlefish require both edges and local contrast to recognize the objects, and that global-contrast-enhanced images have little effect on their patterning. Responses from four animals are summarized in Figure 3. There was no significant difference (Student's t test) between the animals' responses on natural gravel and on the original digital photograph of gravel ($P > 0.38$). However, there were significant differences between the cuttlefishes' body patterns on the original digital photograph and on the various modified images ($P < 0.01$, low-pass; $P < 0.001$, enhanced low-pass; $P < 0.001$, high-pass; $P < 0.013$, enhanced high-pass).

The result, that animals responded differently on the original digital photograph of gravel and the blurred picture of gravel, supports the notion that the cuttlefish visual system has good spatial resolution (16), and that the details of the scene (*e.g.*, the edges of objects) are important for cuttlefish to produce appropriate camouflage patterns. Ver-

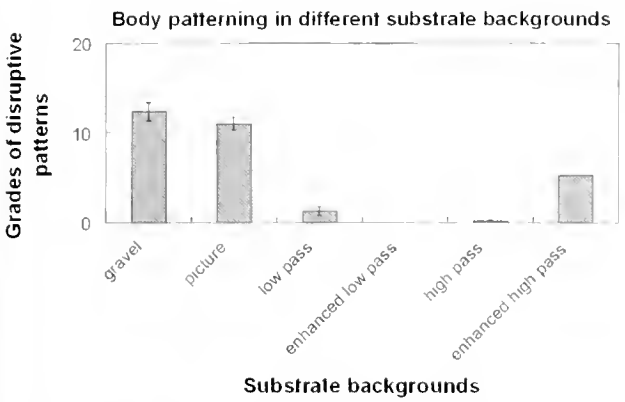

Figure 3. Grades of cuttlefish disruptive body patterning on natural gravel substrate and various digital photographs of natural gravel. Averaged grades of four cuttlefish on different substrata are shown, and bars represent the standard errors. For enhanced contrast images (enhanced low-pass and enhanced high-pass), only two animals were tested.

tebrate visual systems tend to use edge detection to recognize an object. In our experimental design, however, edge alone did not provide a sufficient cue for cuttlefish to produce disruptive coloration. Cuttlefish visually discern light objects (6), thus to show disruptive patterns for camouflage on the mixed light and dark natural gravel backgrounds (Fig. 2A), the local contrast between light and dark gravel is an essential visual cue. This finding is also consistent with our earlier results showing that reducing the contrast of black-and-white checkerboards affected the cuttlefishes' disruptive pattern (6), although in those trials only the stark black-and-white checkerboards were tested, whereas in the current trials, the gravel had many more shades of gray. Figure 2F is interesting because the edges are discernible to human vision and contrast is noticeable; yet the cuttlefish responded with only a very weak White square, White head bar, and White posterior triangle, possibly indicating a threshold of edge detection.

Sepia officinalis lives in a variety of substrata and uses a complex repertoire of changeable body patterns for camouflage (1). Our results show that the type of patterning chosen for display in a cuttlefish's skin is based upon a wide range of visual information. Our study also provides insight into how cuttlefish extract visual information from natural substrates. However, the animals' responses on various filtered images of a natural substrate were not thoroughly examined in this somewhat preliminary study; nor were the quantitative characteristics of the animals' responses to edges and contrast determined. Future studies will take advantage of this noninvasive behavioral assay to examine these matters and other visual processing mechanisms of cuttlefish.

Acknowledgments

We appreciate valuable comments from Phil McFadden, Lydia Mathger, Eric Warrant, the editor, and two anonymous reviewers. We are grateful for funding from the Sholley Foundation and Anteon contract #USAF-5408-04-SC-0002. Alexandra Barbosa and staff of the Marine Resources Center provided important animal care.

Literature Cited

1. **Hanlon, R. T., and J. B. Messenger. 1988.** Adaptive coloration in young cuttlefish (*Sepia officinalis* L.): the morphology and development of body patterns and their relation to behaviour. *Philos. Trans. R. Soc. Lond. B* **320:** 437–487.
2. **Hanlon, R. T., and J. B. Messenger. 1996.** *Cephalopod Behaviour.* Cambridge University Press, Cambridge.
3. **Messenger, J. B. 2001.** Cephalopod chromatophores: neurobiology and natural history. *Biol. Rev.* **76:** 473–528.
4. **Cott, H. B. 1940.** *Adaptive Coloration in Animals.* Methuen, London.
5. **Messenger, J. B. 1991.** Photoreception and vision in molluscs. Pp. 364–397 in *Evolution of the Eye and Visual System,* J. R. Cronly-Dillon and R. L. Gregory, eds. Macmillan Press, London.
6. **Chiao, C.-C., and R. T. Hanlon. 2001.** Cuttlefish camouflage: visual perception of size, contrast and number of white squares on artificial checkerboard substrata initiates disruptive coloration. *J. Exp. Biol.* **204:** 2119–2125.
7. **Chiao, C.-C., and R. T. Hanlon. 2001.** Cuttlefish cue visually on area—not shape or aspect ratio—of light objects in the substrate to produce disruptive body patterns for camouflage. *Biol. Bull.* **201:** 269–270.
8. **Barbosa, A., C. F. Florio, C.-C. Chiao, and R. T. Hanlon. 2004.** Visual background features that elicit mottled body patterns in cuttlefish, *Sepia officinalis*. *Biol. Bull.* **207:** 154 (Abstract).
9. **Grahle, M. M., N. Shashar, N. L. Gilles, C.-C. Chiao, and R. T. Hanlon. 2002.** Cuttlefish body patterns as a behavioral assay to determine polarization perception. *Biol. Bull.* **203:** 232–234.
10. **Marshall, N. J., and J. B. Messenger. 1996.** Colour-blind camouflage. *Nature* **382:** 408–409.
11. **Mast, S. O. 1914.** Changes in shade, color, and pattern in fishes, and their bearing on the problems of adaptation and behavior, with especial reference to the flounders *Paralichthys* and *Ancylopsetta*. *Bulletin of the Bureau of Fisheries, Wash.* **34:** 173–238.
12. **Saidel, W. M. 1988.** How to be unseen: an essay in obscurity. Pp. 487–513 in *Sensory Biology of Aquatic Animals,* R.R. Fay, A.N. Popper, and W.N. Tavolga, eds. Springer-Verlag, New York.
13. **Ramachandran, V., C. W. Tyler, R. L. Gregory, D. Rogers Ramachandran, S. Duensing, C. Pillsbury, and C. Ramachandran. 1996.** Rapid adaptive camouflage in tropical flounders. *Nature* **379:** 815–818.
14. **Russ, J. C. 1995.** *The Image Processing Handbook,* 2nd ed. CRC Press, Boca Raton, FL.
15. **Godfrey, D., J. N. Lythgoe, and D. A. Rumball. 1987.** Zebra stripes and tiger stripes: The spatial frequency distribution of the pattern compared to that of the background is significant in display and crypsis. *Biol. J. Linn. Soc.* **32:** 427–433.
16. **Watanuki, N., G. Kawamura, S. Kaneuchi, and T. Iwashita. 2000.** Role of vision in behavior, visual field, and visual acuity of cuttlefish *Sepia esculenta*. *Fish. Sci.* **66:** 417–423.

Reference: *Biol. Bull.* **208:** 12–19. (February 2005)

Behavioral and Electrophysiological Experiments Suggest That the Antennular Outer Flagellum Is the Site of Pheromone Reception in the Male Helmet Crab *Telmessus cheiragonus*

MICHIYA KAMIO[1,*], MAKOTO ARAKI[2], TOSHIKI NAGAYAMA[2], SHIGEKI MATSUNAGA[1], AND NOBUHIRO FUSETANI[1]

[1] *Laboratory of Aquatic Natural Products Chemistry, Graduate School of Agricultural and Life Sciences, The University of Tokyo, 1-1-1 Yayoi, Bunkyo-ku Tokyo 113-8657, Japan; and* [2] *Hokkaido University, Division of Biological Science, Graduate School of Science, Sapporo, Hokkaido 060, Japan*

Abstract. Sexually competent females of *Telmessus cheiragonus* (helmet crab) release two pheromones that elicit grasping and copulation behaviors in males (Kamio *et al.*, 2000, 2002, 2003). Our study aimed to use behavioral and electrophysiological techniques to identify the site of reception of these sex pheromones. In behavioral experiments, either the inner or the outer flagella of the antennules were ablated bilaterally from male crabs, and responses of male crabs to female odor were examined. When the inner flagella were surgically ablated, the sexual response (*i.e.*, grasping and copulation behavior) of male crabs was not significantly changed relative to control animals that had their second antennae ablated. In contrast, the sexual response was significantly reduced when the outer flagella of the antennules were ablated, suggesting that the outer flagellum is the receptor organ that detects the sex pheromones. In electrophysiological experiments, urine, which in females contains the pheromone that elicits grasping behavior by males but does not contain the pheromone eliciting copulation, whose release site is not known, was tested. Female and male urine as well as shrimp extract evoked phasic responses of chemosensory afferents innervating aesthetase sensilla on the outer flagellum of male crabs. The response of the afferents had significantly higher magnitude and lower threshold when female urine was applied. Thus, behavioral and electrophysiological observations suggest that in male helmet crabs, the outer flagellum of the antennule is the chemosensory organ that detects female sex pheromone.

Received 22 June 2004; accepted 16 October 2004.

* To whom correspondence should be sent at Georgia State University, Department of Biology, P.O. Box 4010, Atlanta, GA 30302-4010. E-mail: mkamio@gsu.edu

Introduction

Sex pheromones are crucial chemosensory signals that trigger and modulate reproductive behaviors in conspecifics. In many animals, pheromones are detected by specialized receptor organs. For example, many vertebrates detect pheromones through their vomeronasal systems (Halpern and Martínez-Marcós, 2003), whereas insects have sensilla on their antennae dedicated to sensing pheromones (Hecker and Butenandt, 1984). Identification of receptor organs and electrophysiological analyses of chemoreception are powerful methods for isolating and identifying pheromone compounds (Bjostad, 1998; Li *et al.*, 2002).

In decapod crustaceans, chemoreceptors occur in high densities at multiple loci on the body and appendages. The antennules (first antennae), the pereiopod dactyls, and the mouthparts are the primary chemoreceptor organs (Ache, 1982). Among these organs, the antennules so far have been reported as pheromone receptors in certain crabs, including *Portunus sanguinolentus* (Christofferson, 1972), *Callinectes sapidus* (Gleeson, 1980), *Carcinus maenus* (Bamber and Naylor, 1996), and *Chionoecetes opilio* (Bouchard *et al.*, 1996). The antennules are biramous, with an inner and an outer flagellum. (The inner and outer flagella of crabs are equivalent to the medial and lateral flagella, respectively, of some other decapod crustaceans.) One type of sensillum

located exclusively on the ventral side of the outer flagella is the aesthetasc. Ablation experiments suggested that pheromones are detected by the outer flagella (Christofferson, 1972), specifically the aesthetascs (Gleeson, 1980). In the crayfish *Procambarus clarkii*, both inner and outer flagella are involved in mating behavior (Dunham and Oh, 1992), but the animals can still mate without their antennules (Corotto *et al.*, 1999). Ablation of antennules also affects mating behavior of female American lobsters, *Homarus americanus* (Cowan, 1991). However, only a small body of neurological evidence supporting these behavioral observations has been obtained. No electrophysiological analyses were performed to demonstrate chemosensory responses of the afferents of the outer flagellum to sex pheromones.

Mating behaviors of male helmet crabs, *Telmessus cheiragonus* (Tilesius, 1815) (Decapoda: Brachyura: Cheiragonidae) are elicited by pheromones that are released from females (Kamio *et al.*, 2003). One pheromone, present in the urine, elicits precopulatory guarding (Kamio *et al.*, 2000), whereas another pheromone, from unknown sources of the postmolt female, subsequently elicits copulation behavior. These findings are based on a series of observations of the behavior of males towards artificial sponges that contain female odors. Sponges that contained aquarium water conditioned by the presence of postmolt females elicited grasping and then copulation behavior, while sponges that contained aquarium water of premolt females elicited only grasping behavior. Moreover, urine from both pre- and postmolt females elicited grasping behavior but did not elicit copulation behavior (Kamio *et al.*, 2002).

In the present paper, the location of pheromone receptors was assessed by behavioral experiments using males that underwent surgical ablation of the inner or outer flagella. Mating behavior of male crabs was eliminated after ablation of the outer flagella. Chemosensory responses of the outer flagella afferents were examined using electrophysiological recordings that integrate multiunit responses of the chemosensory afferents. These recordings showed significantly stronger responses of the afferents to female urine than to male urine. Thus, the behavioral experiments suggest that the outer flagellum possesses pheromone receptors, and the electrophysiological experiments support this idea.

Materials and Methods

Animals

Pre-copula pairs of *Telmessus cheiragonus* (helmet crabs) were collected during the mating season between May and June 2001 and 2002 from pier walls in Usujiri, Hokkaido, Japan (N 41° 57′, E 140° 58′). Males were separated from their partner females and were maintained at 10.5 ± 1 °C in an aquarium with a recirculating seawater system under natural photoperiod. Females were housed in a separate flow-through seawater system until used at ambient temperature. Behavioral experiments were conducted at the Usujiri Marine Biological Station, and electrophysiological experiments were conducted at Hokkaido University, Graduate School of Science, Sapporo. Males were fed shrimp, but females were not fed because premolt females and newly postmolt females do not eat.

Behavioral experiments

Behavioral experiments were conducted to test the effects of bilateral ablation of inner or outer flagella on the responsiveness of male crabs towards female pheromones. Three types of ablated males were prepared: (1) *inner flagellum ablated*, in which the inner flagella of the antennules (first antennae) of males were ablated at their base; (2) *outer flagellum ablated*, in which the outer flagella of the antennules of males were ablated at their base (see Fig. 1); and (3) *second antenna ablated*, in which second antennae were removed as a control for the trauma of surgery. All surgeries were carried out 3 days before the experiments, because no negative effects of the surgery alone on feeding behavior were observed at this time. Behavioral experiments were performed blind, with the observer being unaware of the type of ablation received by the crab under study.

The responses of the three types of ablated males toward female pheromone were observed using artificial sponges as female dummies (Kamio *et al.*, 2002). The sponges were washed with seawater before use. Male crabs were individually maintained at 10 °C in aquaria with a recirculating seawater system. For behavioral testing, a crab was transferred to a test aquarium with still water (31.5 × 18.5 × 24.4 cm), acclimated at 15 °C for 4 h, and then observed under artificial red light. A sponge (2.5 × 2.5 × 4 cm), which had been incubated for 20 h in a 5-liter aquarium containing 10 postmolt females that had molted 2–3 days before, was placed, using forceps, in front of a male until it contacted his chelae. Then the behavior of the male crab was observed for 1 h. Two particular behaviors were recorded as unmistakable and reliable criteria for sexual reaction: (1) *grasping*, a behavior in which the male grasps and fumbles with the sponge, without eating behavior, and places the sponge into the precopulatory guard position; and (2) *copulation*, a behavior in which the male first grasps the sponge, then opens his abdomen to expose the sexual appendages, and then moves the sponge onto the gonopods for insertion.

Electrophysiology

Electrophysiological recordings were performed to test the responses of chemoreceptor neurons in the outer flagellum of males to female odors. Multiunit spike responses of these neurons were recorded, using oil-hook extracellular electrodes, from nerve bundles innervating the antennule (Fig. 1). The excised antennule was placed in a recording

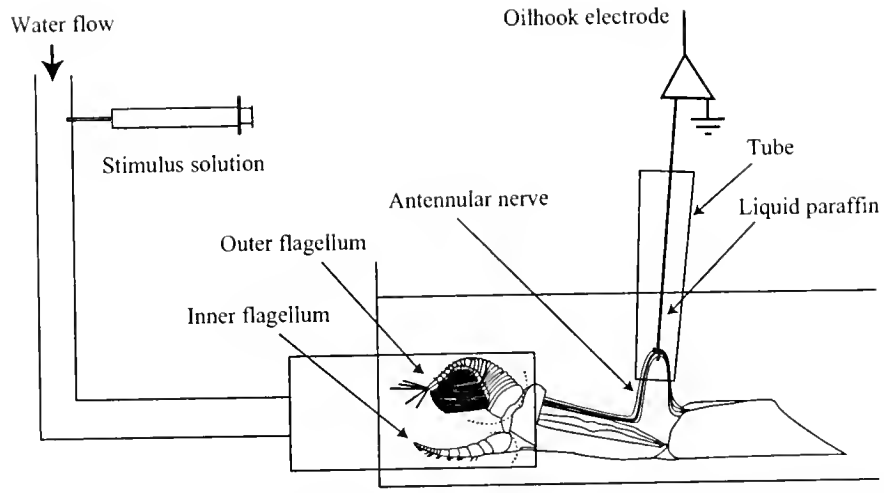

Figure 1. Diagram of the olfactometer used in recording from the antennular nerve of male specimens of *Telmessus cheiragonus*, and ablation points in behavioral experiments. Drawing of lateral view of left antennule. Ablation points of outer and inner flagella are indicated by dashed lines.

chamber. The dorsal cuticle of the distal podomere of the antennule was removed to expose the nerve bundles of the antennule. The nerve bundles were lifted up at the joint of the antennule and placed on a silver hook electrode that could be drawn into a capillary filled with liquid paraffin (Wilkens and Wolf, 1974). A carrier stream of cooled artificial seawater (ASW) (12–16 °C) continuously flowed in a tube past the tip of the antennule. After the inner flagellum had been ablated at the base, the outer flagellum was placed inside the tube.

Electrical signals were amplified with a bioelectric amplifier (NIHON KOUDEN MEG-2100), recorded digitally, and analyzed off-line using a microcomputer with hardware/software utilities (Powerlab, AD Instrumental). The multiunit response of the sensory afferents was integrated with a time constant of 2 s to obtain a measure of the magnitude of response (Caprio and Robinson, 1989; Sveinsson and Hara, 2000). Test stimulus solutions were kept cool during the experiment. Ten microliters of each stimulus solution was injected into the tube.

A food odor—shrimp extract—was prepared by homogenizing a small piece of fresh shrimp muscle (1.5 ml) in 30 ml of ASW. This mixture was centrifuged, which yielded a supernatant that was diluted 10 times and constituted the shrimp extract. Instead of aquarium water, the urine of female and male crabs was used for this experiment because it represents a more highly concentrated and less contaminated source of pheromone. Female urine, which contains pheromone that elicits grasping behavior by males (Kamio *et al.*, 2002), was collected and pooled from 426 postmolt female crabs. Urine was collected from the antennal gland opening by lifting up the operculum covering the gland opening and using a peristaltic pump to collect the urine as it streamed out of the opening (Kamio *et al.*, 2000). Male urine was collected from 20 individuals. Urine was tested at a 1/10 dilution.

Chemosensory responses of male crabs to ASW, shrimp extract, male urine, and female urine were recorded sequentially. Subsequently, the outer flagellum was removed at a point described in Figure 2 and used in a test of shrimp extract to determine whether the chemosensory response recorded before was actually derived from the outer flagellum ($n = 11$). The magnitude of the responses was normalized to the response obtained with shrimp extract. In a different experiment to compare the sensitivity of chemoreceptor neurons of the male crab to female and male urines, a recording and data analysis strategy similar to that of Sveinsson and Hara (1990) was used. Solutions were always tested in order of ascending concentration with 3-min intervals. L-Serine (Wako Chemical Co.) at 10^{-3} *M* was used as a standard reference stimulus (STD), because the response to L-serine was phasic and did not seem to affect any subsequent responses. The STD was tested at the beginning and end of each test period. If the magnitude of STD changed more than 30% during a test period, the results were excluded from the data analysis. The responses of chemosensory neurons were normalized as relative magnitudes of STD for each test period. Differences in sensitivity of male crabs to both male and female urines at each concentration and to amino acids were statistically tested by Wilcoxon matched pairs test ($n = 6$).

To compare the concentrations of common stimulants for the aesthetasc, amino acids and other nitrogenous compounds (Spencer, 1986; Derby and Atema, 1988) were analyzed. To determine the contents of free amino acid in the pooled urine of intermolt males and the pooled urine of postmolt females, 2-ml aliquots of the urines were lyophilized, dissolved in 100 μl of distilled water, and centrifuged.

To remove proteins, a 200-μl portion of a 0.5% aqueous 5-sulfosalicylic acid solution was added to the supernatant. A 20-μl aliquot of this solution was injected into a model L 8500A Hitachi amino acid analyzer. This method allowed determination of concentrations of 20 common amino acids, as well as phosphoserine (P-Ser), taurine (Tau), urea, citrulline (Cit), sarcosine (Sar), α-aminoadipic acid (α-AAA), β-alanine (β-Ala), β-aminoisobutyric acid (β-AiBA), γ-aminobutyric acid (GABA), ethanolamine ($EtONH_2$), ammonia (NH_3), δ-*allo*-hydroxylysine (δ-HyLys), ornithine (Orn), 3-methylhistidine (MeHis), anserine (Ans), and carnosine (Car). The significance of overall concentration differences of the chemicals between male and female urine was tested using Wilcoxon matched pairs test.

Results

Ablation behavioral experiments

To identify the sensory organs of male helmet crabs involved in the detection of female sex pheromones, behavioral experiments were performed on selectively ablated crabs (Fig. 2). When the second antenna were ablated, 7 of the 9 male crabs tested showed grasping behavior, while 2 of them also showed copulation behavior toward sponges treated with postmolt female pheromone. With bilateral ablation of the inner flagella of the antennules, all 10 male crabs tested showed grasping behavior, and 5 of them also showed copulation behavior. In contrast, neither grasping nor copulation behaviors were observed in any of the 10 animals that had their antennular outer flagella bilaterally ablated. Differences in grasping or copulation behavior were not significant for crabs with their second antenna ablated and crabs with antennular inner flagella ablated (Fisher's exact test, $P = 0.21$ and 0.35 respectively). The occurrence of both grasping and copulation behaviors of the crabs with outer flagella ablated was significantly different (Fisher's exact test, $P < 0.01$ and <0.05 respectively) from those of the crabs with inner flagella ablated. Between controls and crabs with outer flagella ablation, the difference in grasping behavior was significant (Fisher's exact test, $P < 0.01$), while it was not significant for copulation behavior (Fisher's exact test, $P = 0.47$).

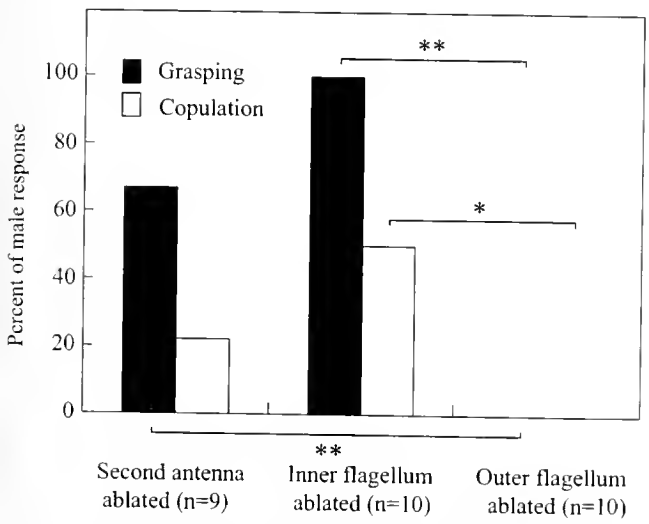

Figure 2. Behavioral responses of males with different sensory ablations to postmolt female aquarium water. $^{**}P < 0.01$; $^{*}P < 0.05$.

Electrophysiological experiments

Since behavioral experiments indicated that the outer flagella of males are involved in perception of sex pheromones released from females, responses of chemosensory neurons in the outer flagellum were analyzed by extracellular multiunit recordings. (Chemoreceptors on the inner flagellum also responded to shrimp extract and male and female urines [pers. obs.], but they were not considered further here in our experiments.) In a typical recording, substantial spontaneous activity was observed throughout the experiment, probably reflecting the activity of tonically active mechanosensory afferents. Presentation of shrimp extract produced a phasic discharge of action potentials; this response occurred about 4 s after stimulus introduction, which reflects the time for the stimulus to reach the recording chamber and sensilla (Fig. 3A). During a response to chemical stimulation, several units with different spike amplitudes were active. However, the high spike frequency prevented reliable discrimination of single units (Fig. 3B, C). Therefore, the magnitude of the responses was evaluated by integration (top trace in Fig. 3A).

The activity of these chemosensory neurons did not change significantly when ASW was injected as a control (Fig. 4A). In contrast, the afferents were strongly activated after injection of female (Fig. 4C) or male urine (Fig. 4D), as well as after injection of shrimp extract (Fig. 4B). The relative magnitude of the response to female urine compared to the response to shrimp extract varied from 53% to 324% (148 ± 24; mean ± SEM, $n = 11$). The relative magnitude of the response to male urine compared to the response to shrimp extract ranged from 41% to 264% (127 ± 21; $n = 11$). The relative magnitude of the response to female urine compared to the response to male urine ranged from 99% to 147% (119 ± 5; $n = 11$), and this difference was statistically significant (Wilcoxon matched pairs test, $z = 2.84$, $P < 0.01$). After the ablation of the outer flagellum, the baseline amplitude of integrated activity declined due to a decrease in spike number of mechanosensory afferents innervating exteroceptors on the outer flagellum. Chemosensory responses were no longer observed after injection of shrimp extract (Fig. 4E).

To characterize the difference in the sensitivity of the

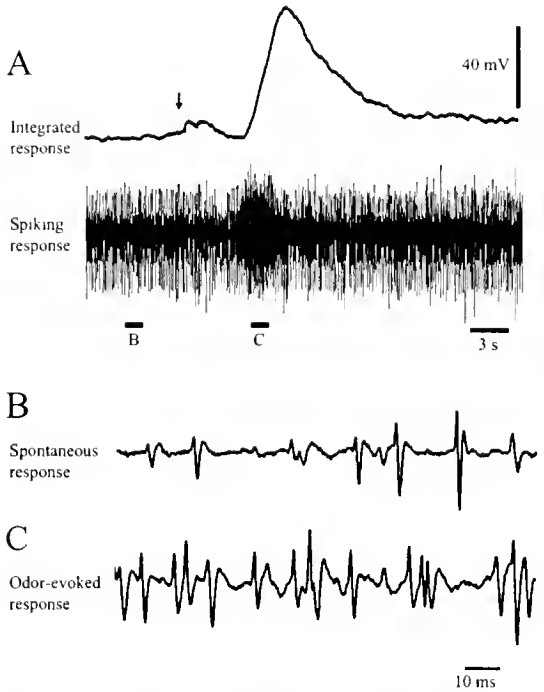

Figure 3. Responses of chemosensory neurons in the antennular outer flagellum of a male specimen of *Telmessus cheiragonus* to shrimp extract. (A) Extracellular recording from antennular nerve to the injection of shrimp extract (lower trace) and its integrated activity (upper trace). Time of injection is indicated by arrow. (B) Spike activity of the antennular nerve before injection of shrimp extract. (C) Spike activity of the antennular nerve in response to injection of shrimp extract. (B) and (C) correspond to part "B" and "C" of the lower trace of Figure 3A.

chemoreceptors on the outer flagellum to both female and male urines, the responses of outer flagellum afferents to various concentrations of female and male urine were analyzed quantitatively by normalizing them to the response to 1 m*M* L-serine (standard reference stimulus: STD) (Fig. 5). The outer flagellum showed larger responses to female urine than to male urine at all dilutions, and the differences were significant at dilutions of 10^{-3} ($z = 2.20$, $P < 0.05$; Wilcoxon matched pairs test) and 10^{-4} ($z = 1.99$, $P < 0.05$). Overall differences among ASW, female urine, and male urine were also significant (Friedman ANOVA, $P < 0.001$).

Amino acid analysis

Male and female urines contained detectable amounts of common amino acids and nitrogenous compounds; taurine, urea, and ammonia were most abundant in the urine, ranging from 49 to 248 μM, while the rest of the compounds were present at less than 20 μM. Concentrations of compounds were higher in male urine than in female urine, except for ethanolamine, γ-aminobutyric acid, and phosphoserine (Fig. 6). Overall, concentration differences of the chemicals between male and female urines were significant (Wilcoxon matched pairs test, $z = 4.52$, $P < 0.001$).

Discussion

Our ablation experiments suggest that the antennular outer flagellum of males is the site of reception of female

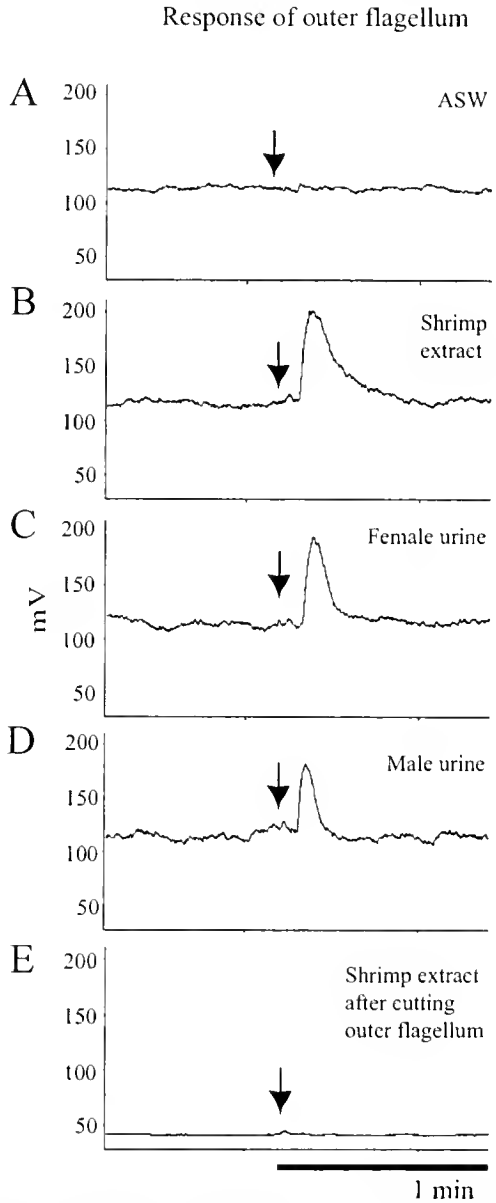

Figure 4. Responses of chemosensory neurons of the outer flagellum of a male specimen of *Telmessus cheiragonus* to various chemical stimuli. Integrated activity in response to artificial seawater (ASW) (A), shrimp extract (B), female urine (C), and male urine (D). No significant response to the injection of shrimp extract was observed after ablation of the outer flagella (E). Time of injection is indicated by arrow.

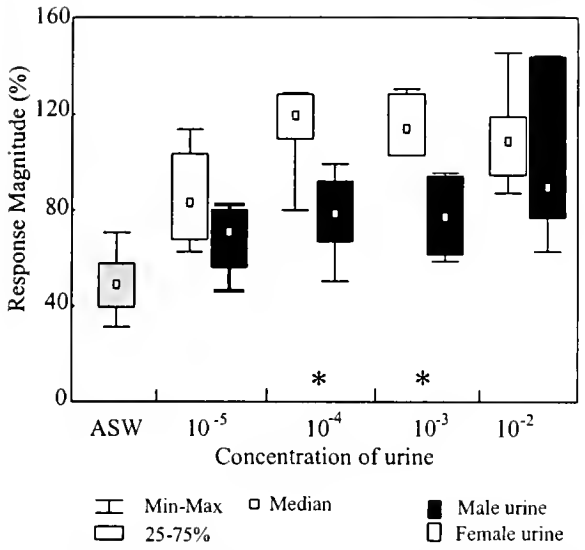

Figure 5. Concentration-response relationships of chemosensory afferents of the antennular outer flagellum of males of *Telmessus cheiragonus* to male and female urines. The response magnitudes were normalized to a percentage of the response to 10^{-3} *M* L-serine for each recording. The responses shown are the median, the 25%–75% quartiles, and the minimum-maximum values. Data are from 6 preparations. * indicates responses that are statistically different between male and female urine (Wilcoxon matched pairs test, $P < 0.05$).

pheromones in *Telmessus cheiragonus*. Furthermore, this behavioral observation is supported by our electrophysiological finding that chemosensory afferents of the outer flagellum respond more sensitively to female urine than to male urine, the former of which contained the sex pheromone that elicits grasping behavior (Kamio *et al.*, 2000). Thus, as with *Portunus sanguinolentus* (Christofferson, 1972) and *Callinectes sapidus* (Gleeson, 1982), *T. cheiragonus* detects sex pheromones by means of the antennular outer flagellum.

Urine of crustacean species contains many small nitrogenous molecules such as ammonia, urea, uric acid, and amino acids, which are nitrogenous excretory metabolites from tissues and hemolymph (Claybrook, 1983). Some of these nitrogenous compounds stimulate aesthetasc sensilla (Spencer, 1986; Derby and Atema, 1988). In the present study, many kinds of amino acids and nitrogen excretory products are found both in male urine and in female urine. The concentration of most of these compounds is higher in male urine than in female urine, and overall the amino acid concentration was higher in male urine than in female urine. Perhaps higher concentrations of these compounds in male

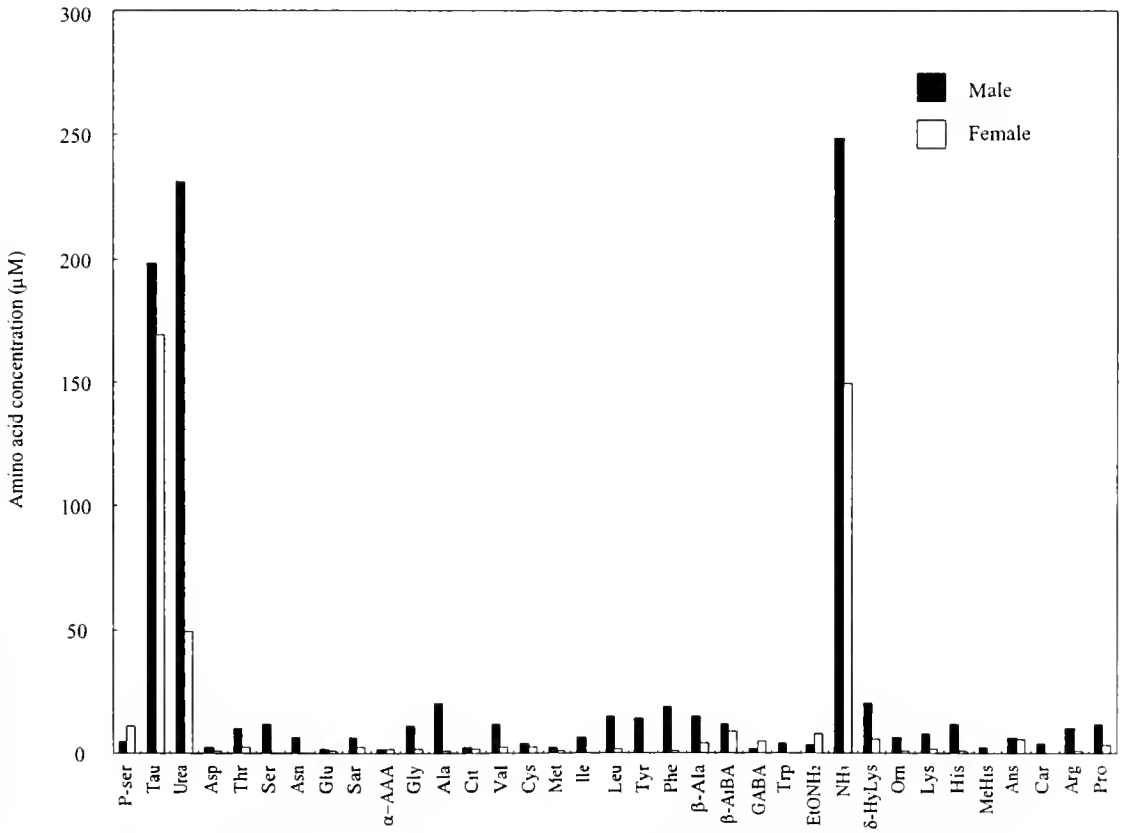

Figure 6. Concentrations of amino acids in urine of female and male specimens of *Telmessus cheiragonus*.

urine reflects the crabs' feeding history: premolt females do not eat and postmolt females were not fed during the period of urine collection, while males were fed shrimp. If the antennular chemosensory neurons respond sensitively to the nitrogenous compounds that have been detected in this amino acid analysis, the higher concentrations of nitrogenous compounds in male urine might be expected to cause a higher response of chemosensory afferents of the outer flagellum to male urine than to female urine (Fig. 4). However, the outer flagellum afferents showed significantly larger response to female urine at concentrations of less than 10^{-3} *M* (Fig. 5). The results demonstrate that compounds with higher abundance in male urine are not responsible for excitation of the afferents in the outer flagellum of male helmet crab. Compounds such as ethanolamine, GABA, and phosphoserine, which are more abundant in female urine than in male urine, may contribute to the excitation (Fig. 6). It is also possible that compounds not detected in the amino acid analysis contribute to the afferent response. Without the purified pheromone molecules, we can infer but not be certain that this differential electrophysiological responsiveness is due to sex pheromones.

At the moment, it still remains to be clarified exactly where the pheromone-specific receptors are located on the outer flagellum. Gleeson (1982) noted that the aesthetasc tuft on the outer flagellum of the antennule in *C. sapidus* is divided into mesial and lateral halves by a region of cuticle from which no sensilla arise. Ablation of mesial or lateral halves of the outer flagellum partially reduced the behavioral response of males to female sex pheromone, thus suggesting that pheromone receptors are located on both sides of the outer flagellum. Further anatomical and physiological studies will be necessary to clarify which sensilla on the outer flagellum of male helmet crab are responsible for detecting female pheromones.

Postmolt female urine contains grasping pheromone but not copulation-eliciting pheromone (Kamio *et al.*, 2002). Ablation of the outer flagellum eliminated both copulatory behavior and grasping behavior by male crabs toward postmolt-female-conditioned water. Although the present electrophysiological studies did not test the copulation pheromone, its reception site may also be on the outer flagellum. However, it is also possible that the reception site of copulation pheromone is not located on the antennular flagella. In this case, grasping pheromone may be necessary to elicit copulatory behavior. The release site of the copulation pheromone must be identified to answer this question.

Future studies will focus on identifying the sex pheromone molecules of the helmet crab. A combination of behavioral and electrophysiological techniques, such as used in this study, together with analytical chemistry, will guide the search.

Acknowledgments

We are indebted to the staff of the Usujiri Fisheries Laboratory of Hokkaido University for maintenance of crabs and allowing us the use of their facilities. Thanks are also due to Dr. Charles Derby and Dr. Manfred Schmidt, Georgia State University, for helpful discussions on this manuscript. A research fellowship from the Japan Society for Promotion of Science for Young Scientists to M. K. is acknowledged.

Literature Cited

Ache, B. W. 1982. Chemoreception and thermoreception. Pp. 369–398 in *The Biology of Crustacea. 3: Neural Integration and Behavior*, D. C. Sandeman and H. L. Atwood, eds. Academic Press, New York.

Bamber, S. D., and E. Naylor. 1996. Mating behavior of male *Carcinus maenas* in relation to a putative sex pheromone: behavioral changes in response to antennule restriction. *Mar. Biol.* **125:** 483–488.

Bjostad, L. B. 1998. Electrophysiological methods. Pp. 339–375 in *Methods in Chemical Ecology*, Vol. 2, J. G. Millar and K. F. Haynes, eds. Kluwer Academic Publishers, Norwell, MA.

Bouchard, S., B. Sainte-Marie, and J. N. McNeil. 1996. Indirect evidence indicates female semiochemicals release male precopulatory behavior in the snow crab, *Chionoecetes opilio* (Brachyura: Majidae). *Chemoecology* **7:** 39–44.

Caprio, J., and J. J. Robinson II. 1989. Electro-olfactogram and multiunit olfactory receptor responses to binary and trinary mixtures of amino acids in the channel catfish, *Ictalurus punctatus*. *J. Gen. Physiol.* **93:** 245–262.

Christofferson, J. P. 1972. The site of chemoreceptors sensitive to the sex pheromone of the female crab, *Portunus sanguinolentus* (Herbst). *Am. Zool.* **12:** 690.

Claybrook, D. L. 1983. Nitrogen metabolism. Pp. 163–213 in *The Biology of Crustacea. 5: Internal Anatomy and Physiological Regulation*, L. H. Mantel, ed. Academic Press, New York.

Corotto, F. S., D. M. Bonenberger, J. M. Bounkeo, and C. C. Dukes. 1999. Antennule ablation, sex discrimination, and mating behavior in the crayfish *Procambarus clarkii*. *J. Crustac. Biol.* **19:** 708–712.

Cowan, D. F. 1991. The role of olfaction in courtship behavior of the American lobster *Homarus americanus*. *Biol. Bull.* **181:** 402–407.

Derby, C. D., and J. Atema. 1988. Chemoreceptor cells in aquatic invertebrates: peripheral filtering mechanisms in decapod crustaceans. Pp. 365–388 in *Sensory Biology of Aquatic Animals*, J. Atema, R. R. Fay, A. N. Popper, and W. N. Tavolga, eds. Springer-Verlag, New York.

Dunham, D. W., and J. W. Oh. 1992. Chemical sex discrimination in the crayfish *Procambarus clarkii*: role of antennules. *J. Chem. Ecol.* **18:** 2363–2372.

Gleeson, R. A. 1980. Pheromone communication in the reproductive behavior of the blue crab, *Callinectes sapidus*. *Mar. Behav. Physiol.* **7:** 119–134.

Gleeson, R. A. 1982. Morphological and behavioral identification of the sensory structures mediating pheromone reception in the blue crab, *Callinectes sapidus*. *Biol. Bull.* **163:** 162–171.

Halpern, M., and A. Martínez-Marcós. 2003. Structure and function of the vomeronasal system: an update. *Prog. Neurobiol.* **70:** 245–318.

Hecker, E., and A. Butenandt. 1984. Bombykol revisited—reflections on a pioneering period and on some of its consequence. Pp. 1–44 in *Techniques in Pheromone Research*, H. E. Hummel and T. A. Miller, eds. Springer-Verlag, New York.

Kamio, M., S. Matsunaga, and N. Fusetani. 2000. Studies on sex

pheromones of the Helmet crab, *Telmessus cheiragonus*. I. An assay based on precopulatory mate-guarding. *Zool. Sci.* **17:** 731–733.

Kamio, M., S. Matsunaga, and N. Fusetani 2002. Copulation pheromone in the crab *Telmessus cheiragonus*. *Mar. Ecol. Prog. Ser.* **234:** 183–190.

Kamio, M., S. Matsunaga, and N. Fusetani. 2003. Observation on mating behavior of helmet crab, *Telmessus cheiragonus*. *J. Mar. Biol. Assoc. UK* **83:** 1007–1013.

Li, W., A. P. Scott, M. J. Siefkes, H. Yan, S. Yun, and D. A. Gage. 2002. Bile acid secreted by male sea lamprey that acts as a sex pheromone. *Nature* **296:** 138–141.

Spencer, M. 1986. The innervation and chemical sensitivity of single aesthetasc hairs. *J. Comp. Physiol. A* **158:** 59–68.

Sveinsson, T., and T. Hara. 1990. Analysis of olfactory responses to amino acids in Arctic char (*Salvelinus alpinus*) using a linear multiple-receptor model. *Comp. Biochem. Physiol. A* **97:** 279–287.

Sveinsson, T., and T. Hara. 2000. Olfactory sensitivity and specificity of Arctic char, *Salvelinus alpinus*, to putative male pheromone, prostaglandin $F_{2\alpha}$. *Physiol. Behav.* **69:** 301–307.

Wilkens, L. A., and G. E. Wolfe. 1974. A new electrode design for en passant recording, stimulation and intracellular dye injection. *Comp. Biochem. Physiol.* **48:** 217–220.

Reference: *Biol. Bull.* **208:** 20–28. (February 2005)

Sperm Storage, Internal Fertilization, and Embryonic Dispersal in Vent and Seep Tubeworms (Polychaeta: Siboglinidae: Vestimentifera)

ANA HILÁRIO[1], CRAIG M. YOUNG[2,*], AND PAUL A. TYLER[1]

[1] *School of Ocean and Earth Science, University of Southampton, SOC, European Way, Southampton SO14 3ZH UK; and* [2] *Oregon Institute of Marine Biology, University of Oregon, P.O. Box 5389, Charleston, Oregon 97420*

Abstract. Vestimentiferan tubeworms are ecologically important members of deep-sea chemosynthetic communities, including hydrothermal vents and cold seeps. Some are community dominants and others are primary colonists of new vent sites; they include some of the longest living and fastest growing marine invertebrates. Their mechanisms of propagation, dispersal, and genetic exchange have been widely discussed. Direct sperm transfer from males to females has been documented in one species, *Ridgeia piscesae*, but others are known to discharge what are apparently primary oocytes. Brooding of embryos has never been observed in any vestimentiferan. These observations have led to the supposition that fertilization might be external in most species. Here we report sperm storage at the posterior end of the oviduct in five species, including tubeworms from both vents and seeps. We show experimentally that most eggs are inseminated internally, that fertilization rate is typically lower than 100%, that meiosis is completed after eggs are released from the female, and that the dispersal phase includes the entire embryonic period.

Introduction

The discovery of hydrothermal vents in 1977 heralded the description of large vestimentiferan tubeworms that were initially placed as a class in the phylum Pogonophora (Jones, 1981) and then elevated to the phylum level (Jones, 1985). Genetic and embryological evidence now shows convincingly that these gutless, deep-sea tubeworms are polychaetes (Young *et al.*, 1996; McHugh, 1997; Rouse and Fauchald, 1997) currently classified within the polychaete family Siboglinidae (Rouse and Fauchald, 1997), which includes the frenulate, vestimentiferan, and moniliferan Pogonophora of previous authors.

Vestimentiferan tubeworms came to symbolize hydrothermal vents in the Pacific, and with their discovery at cold seeps in the Gulf of Mexico and elsewhere, became the icon of communities driven by chemosynthetic primary production. Species of vestimentiferans are known to be among the first colonizers of newly formed vents (Hessler *et al.*, 1988; Shank *et al.*, 1997), some of the fastest growing marine invertebrates (Lutz *et al.*, 1994), and the longest lived nonclonal animals known (Fisher *et al.*, 1997). Because of their ecological importance at vents and seeps, there has been considerable interest in their reproductive and dispersal biology.

In vestimentiferan tubeworms, small, yolky, and slightly buoyant eggs develop into nonfeeding trochophore larvae that are thought to disperse in the plankton for up to several weeks (Young *et al.*, 1996; Marsh *et al.*, 2001), facilitating genetic exchange and colonization of newly available seep and vent habitats. It has been estimated that larvae of the vent species *Riftia pachyptila* can disperse more than 100 km over a 5-week period (Marsh *et al.*, 2001). This estimate is based on the assumption that passive dispersal occurs during a 3-week embryonic period as well as a 2-week period when larvae are capable of independent ciliary movement (Marsh *et al.*, 2001). However, because the site of fertilization and the location of embryogenesis remain unresolved for all species of vestimentiferans, these dispersal estimates could be as much as 60% too high. Thus, the site of fertilization in vestimentiferans is of great interest

Received 5 October 2004, accepted 30 November 2004.

* To whom correspondence should be addressed. E-mail: cmyoung@uoregon.edu

and has been the subject of considerable debate. Internal fertilization and brooding of embryos appear to be the norm for frenulate siboglinids (Bakke, 1974; reviewed by Southward, 1999).

Free sperm have been observed in the oviduct of *Riftia pachyptila* (Gardiner and Jones, 1985), a species that apparently spawns its eggs (Van Dover, 1994). Moreover, transfer of large white spermatozeugmata (sperm masses) from male to female plumes has been documented in *Ridgeia piscesae* (Southward and Coates, 1989; MacDonald *et al.*, 2002) and *Tevnia jerichonana* (Southward, 1999). On the basis of these observations, Southward (1999) has proposed that eggs are fertilized either in the ovisac just before spawning or externally as the eggs are released. Internal fertilization is consistent with the unusual sperm morphology (sperm are elongate and have spiral mitochondria and nuclei) in all known species (Gardiner and Jones, 1985; Cary *et al.*, 1989), and also with the presence of external ciliary tracts (Fig. 1A, B) leading away from the male gonopores on the dorsal surface of the vestimentum (Gardiner and Jones, 1993). However, massive spermatozeugmata are known only in *Ridgeia piscesae* (Southward and Coates, 1989; MacDonald *et al.*, 2002) and *Tevnia jerichonana* (Southward, 1999); in other species, sperm appear to be released in smaller flame-shaped bundles (Fig. 1C, D) that are capable of swimming as coordinated units and that eventually break down in seawater (Gardiner and Jones, 1985; Cary *et al.*, 1989). The observations of modified sperm and direct sperm transfer are difficult to reconcile with numerous field and laboratory observations of apparent free spawning in both *Riftia pachyptila* and *Lamellibrachia luymesi* (Cary *et al.*, 1989; Van Dover, 1994; Young, unpubl. obs.). However, the clouds of presumed gametes observed in these "spawning events" could consist of zygotes, embryos, or even larvae if fertilization is internal.

Using histology, we have examined the female reproduc-

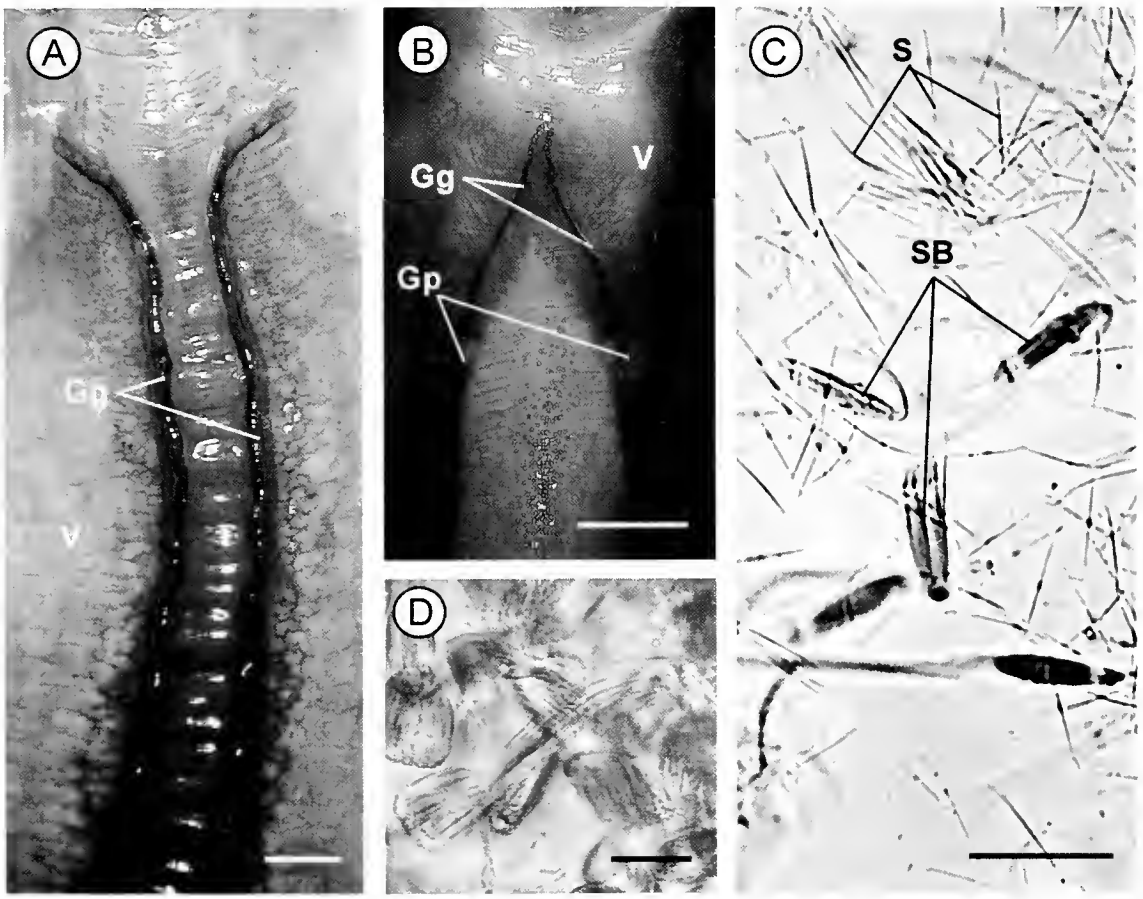

Figure 1. (A) Dorsal view of the vestimentum of a *Lamellibrachia luymesi* male, showing genital grooves leading away from paired gonopores and diverging near the anterior end (scale bar: 5 mm). (B) Dorsal view of the vestimentum in a *Riftia pachyptila* male, showing genital grooves converging (scale bar: 1 cm). (C) Actively swimming sperm bundles of *Lamellibrachia luymesi* dissected from the terminal portion of the male gonoduct. Some of the bundles have broken apart upon contact with seawater to release individual sperm (scale bar: 25 μm). (D) Sperm bundles of *Tevnia jerichonana* (scale bar: 25 μm). Gg, genital groove; Gp, gonopores; S, spermatozoa; SB, sperm bundles; V, vestimentum.

tive system of five vestimentiferan siboglinid species: *Riftia pachyptila, Ridgeia piscesae,* and *Tevnia jerichonana* from Pacific hydrothermal vents, and *Lamellibrachia luymesi* and *Seepiophila jonesi* from cold seeps in the Gulf of Mexico. In all five species we found a sperm storage region at the far posterior end of the female reproductive tract. We refer to this region as the spermatheca. We also report *in vitro* fertilization and field experiments showing that insemination is internal, that meiosis is completed after the eggs are released from the female, and that the dispersal phase of vestimentiferans includes the entire embryonic period.

Materials and Methods

Samples of *Riftia pachyptila, Ridgeia piscesae,* and *Tevnia jerichonana* were collected from a depth of 2500 m at hydrothermal vents on the East Pacific Rise (9°50′N), using the deep submergence vehicle *Alvin. Lamellibrachia luymesi* and *Seepiophila jonesi* were collected with *Johnson-Sea-Link* submersibles from various cold methane seeps between depths of 600 and 800 m on the Louisiana Slope. Major sites included GC-234 (27°44.7′N, 91°13.4′W) and Bush Hill (27°46.9′N, 91°30.5′W).

For histological studies, the worms were removed from their natural tubes, preserved in 5% seawater formalin for 48 h, and subsequently transferred to 70% ethanol. The trunk of each individual was divided into 10 equal regions, and a single section 1 mm in length was randomly chosen from each region. The segments were slowly dehydrated by transfer to 90% propan-2-ol overnight followed by a period of 9 h in 100% propan-2-ol, with change of solution every 3 h. Before being impregnated with paraffin wax at 70 °C for 12 to 24 h, the segments were cleared with 100% xylene for 6 to 12 h, depending on the size of the segment. The impregnated tissue was then embedded in wax, sectioned at 5 μm, and stained with Mayer's hematoxylin and eosin.

For electron microscopy, pieces of gonadal tissue dissected from female *Lamellibrachia luymesi* were immersed for 1.5 h at room temperature in 2.5% glutaraldehyde buffered with Millonig's 0.4 *M* phosphate buffer at pH 7.4. Due to exigencies of ship scheduling, tissue was stored in Millonig's 0.4 *M* phosphate buffer with 0.6 *M* NaCl for 2 weeks prior to post-fixation and embedding. Tissue was post-fixed for 1 h at room temperature in 1% osmium tetroxide in 0.1 *M* phosphate buffer plus 1% NaCl at pH 7.2. Tissue was then dehydrated in ascending concentrations of ethanol to 100%, immersed in acetonitrile for 10 min, left overnight in a 50% solution of acetonitrile in resin, and embedded in epoxy resin. Thin sections were stained with uranyl acetate and lead citrate and examined with a Hitachi H7000 transmission electron microscope.

Eggs of some vestimentiferans are stored in expanded distal ovisacs prior to release. We collected eggs from the ovisac or the distal region of the oviduct in all species studied and on many occasions to assess the gametogenic stage just prior to spawning. Immediately after they were removed, eggs were examined with a light microscope for the presence of visible germinal vesicles.

Oocytes were collected from the ovisacs of seven female specimens of *Lamellibrachia luymesi* and incubated without adding sperm to determine whether they had already been inseminated internally. New pipettes were used, taking special care to eliminate any possible contamination from extraneous sperm. These primary oocytes were incubated in 0.45-μm-filtered seawater for 24 h at 6 °C, after which at least 100 were examined from each individual.

To determine if tubeworms release eggs, zygotes, or embryos under natural conditions, we deployed inverted plankton nets over aggregations of *Riftia pachyptila* adults in the field (Fig. 2). Nets were 0.5 m in diameter and had 100-μm mesh. Disks of syntactic foam attached to the cod ends floated the nets upward, and polypropylene funnels at the mouths of the cod ends prevented escape of the buoyant eggs during recovery. Nets were deployed for various periods of time ranging from 3 to 10 days. They were recovered by using the submersible's manipulator and transported to the surface in closed plastic boxes to maintain temperature. Immediately after the dive, eggs and embryos were concentrated with nylon mesh filters and examined with a compound microscope to assess stages of gametogenesis or embryogenesis.

In broadcast spawners with external fertilization, fertilization rates virtually always decline as a function of distance from spawning males (*e.g.,* Pennington, 1985; Levitan, 1991; Levitan and Young, 1995; Metaxas *et al.,* 2002). We conducted a field experiment with *Lamellibrachia luymesi* eggs to determine whether distance from a dense aggregation ("bush") of tubeworms had any effect on the fertilization rate of oocytes removed from the ovisacs of females. Eggs were held 25 cm above the bottom in small plastic tubes (2-cm diameter, 2-cm length) capped on both ends with 50-μm nylon mesh. Three were deployed by submersible in a large bush of tubeworms, and the others were deployed in a straight line with three replicates each at 1.5 m, 3.0 m, 4.5 m, and 6.0 m downstream. The cultures were left to incubate for 24 h. As in the laboratory experiments mentioned above, we took special care to sterilize all containers, including the acrylic plastic box in which eggs were transported to the bottom, to eliminate spurious fertilization events.

Results

General anatomy of the female reproductive tract

The reproductive system of female vestimentiferans opens at the anterior end of the trunk, between the vestimental wings. A pair of meandering oviducts extend through the trunk, surrounded by trophosome tissue.

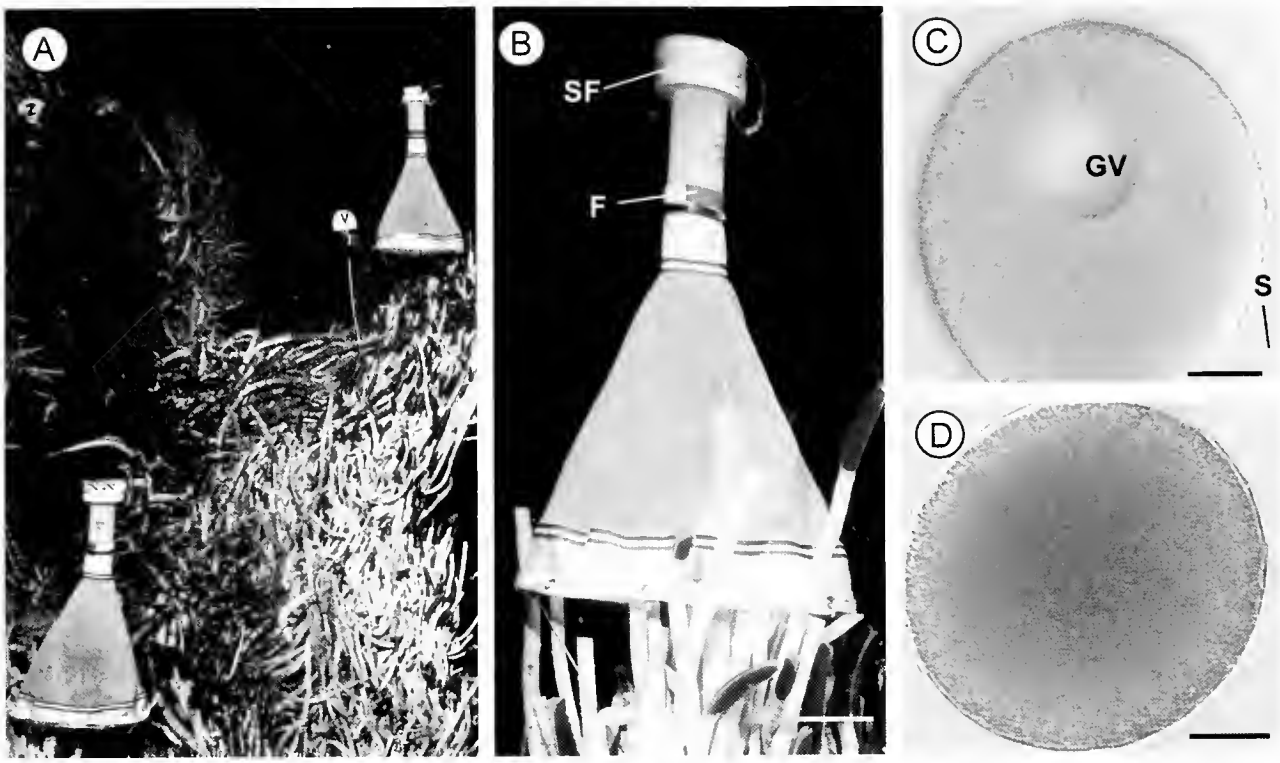

Figure 2. (A) Two egg traps deployed in a large aggregation of *Riftia pachyptila* at 9°50′N on the East Pacific Rise. Depth is 2500 m. The downward-facing net openings are 50 cm in diameter. (B) Close-up of an egg trap deployed over a clump of *R. pachyptila* (scale bar: 10 cm). SF, syntactic foam; F, position of the funnel on the inside of the cod end. (C) Light micrograph of a primary oocyte removed from the female ovisac of *R. pachyptila* and artificially inseminated with free sperm. Several filament-like sperm heads are attached to the egg surface (scale bar: 25 μm). GV, germinal vesicle; S, sperm. (D) Typical uncleaved *R. pachyptila* zygote captured in an egg trap (scale bar: 25 μm).

Whereas in *Riftia pachyptila, Ridgeia piscease,* and *Tevnia jerichonana* the gonad runs through the whole length of the trunk, in *Lamellibrachia luymesi* and *Seepiophila jonesi* it can only be found in the anterior two-thirds of the trunk. The paired gonocoels, which contain the ovaries, run parallel and dorsal to the oviducts. At the posterior end, the gonocoels bend and pass anteriorly as paired oviducts. In *Riftia pachyptila, Ridgeia piscesae,* and *Lamellibrachia luymesi,* the terminal portion of each oviduct is enlarged as an egg storage compartment known as the ovisac.

A sheet of connective tissue separates the gonocoels from each other and from the ventral blood vessel. A narrow strip of germinal epithelium grows from this connective tissue sheet into each gonocoel, filling the gonocoel cavity with rows of developing eggs. Webb (1977) described structures called "transverses," situated at irregular intervals along the length of the trunk, where the gonocoel, the oviduct, and the ventral blood vessel cross from right to left, and where the oviduct opens into the gonocoel by a nonciliated funnel. These structures were also reported by Malakhov *et al.* (1996) in *Ridgeia piscesae.* Although we have observed transverses in this same species, histological sections revealed no openings that would permit the passage of oocytes from the gonocoels to the oviducts. Thus, all eggs must pass through the posterior ends of their respective gonocoels before entering the oviducts.

The spermatheca

Through most of its length, the wall of the oviduct is composed of a ciliated cuboidal epithelium surrounded by a thin layer of circular muscle. However, in all five species examined, the oviducal epithelium is folded into a series of loops and sacs at the far posterior end of the reproductive tract, where the ovarian gonocoel joins the oviduct (Fig. 3). In every female examined, these small sacs contained clusters of spermatozoa, with the heads all aligned towards the wall of the sac (Fig. 3A–D). These sperm are no longer packaged in the discrete flame-shaped bundles released by the males (Gardiner and Jones, 1985; Cary *et al.,* 1989). We refer to this region of sperm storage as the spermatheca. In *Lamellibrachia luymesi* and *Seepiophila jonesi* the spermatheca appears as a white, hook-shaped structure easily visible with the naked eye through the body wall of the

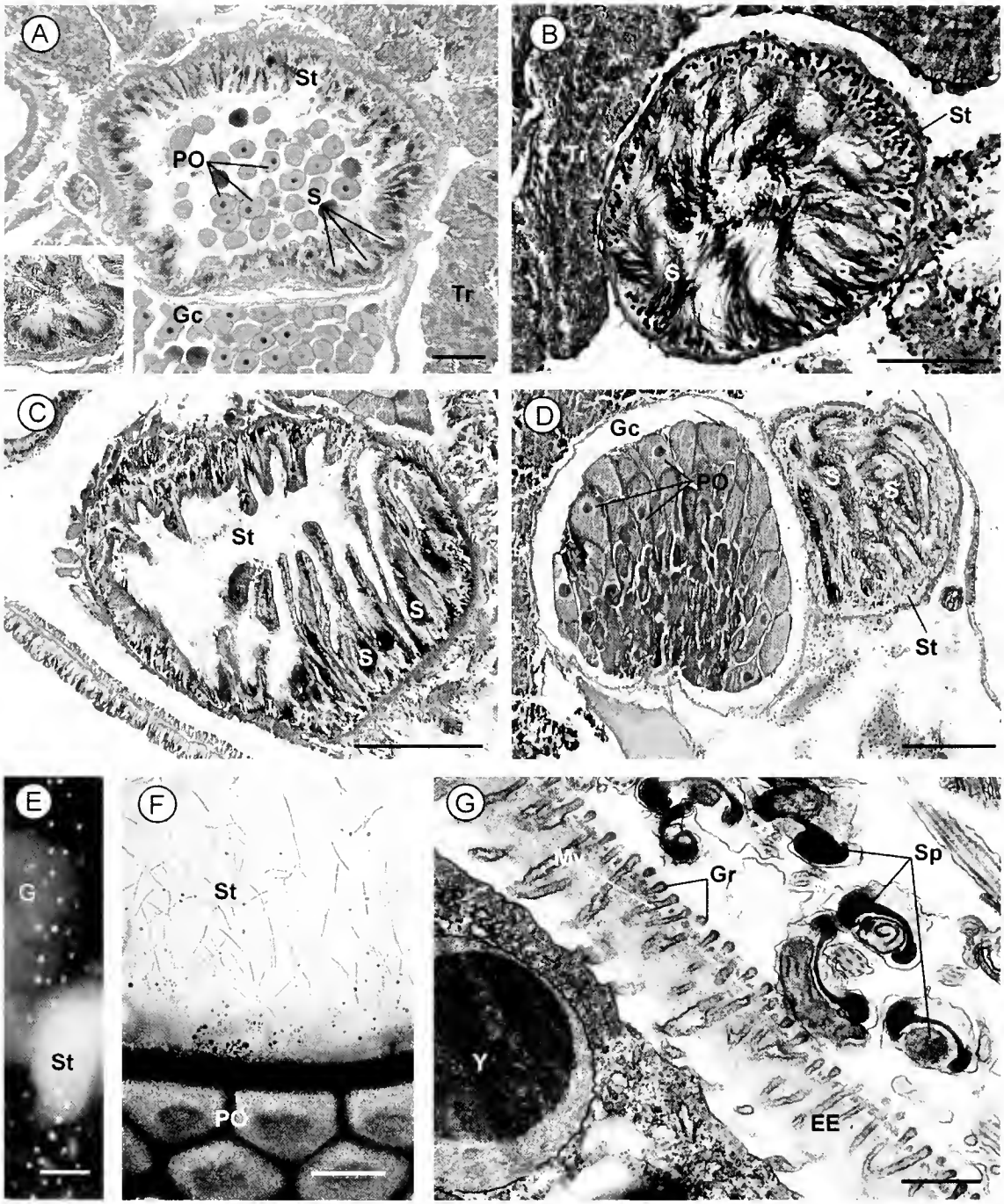

Figure 3. **(A–D)** Light micrographs of histological sections through the spermatheca regions of females of four species: *Riftia pachyptila* (A), *Tevnia jerichonana* (B), *Lamellibrachia luymesi* (C), and *Seepiophila jonesi* (D). The insert in A shows detail of the spermatheca of *Riftia pachyptila* with clusters of spermatozoa. Scale bars for A–D: 200 μm. (E) Spermatheca of *Lamellibrachia luymesi* as seen through the wall of the body (scale bar: 1 mm). (F) Squash preparation of the spermatheca from a *Lamellibrachia luymesi* female, showing isolated sperm in the lumen lying close to primary oocytes. Scale bar: 75 μm. (G) Transmission electron micrograph of the spermatheca of *Lamellibrachia luymesi*, showing an oocyte and several spermatozoa in proximity (scale bar: 0.5 μm). EE, egg envelope; G, gonad; Gc, gonocoel; Gr, granule with filamentous glycocalyx; Mv, microvilli; PO, primary oocyte; S, clusters of spermatozoa, Sp, sperm; St, spermatheca; Tr, trophosome; Y, yolk granule.

Table 1

Percentage of Riftia pachyptila *eggs, zygotes, and embryos that had not cleaved by the time they were recovered in inverted plankton nets (egg traps) deployed over adult aggregations*

Recovery Date	Site	Days Deployed	Embryos Captured	% Uncleaved
7 May 2000	Q-Vent	3	13	100.00
12 May 2000	Q-Vent	8	377	88.86
14 May 2000	Tica Vent	6	247	78.94
20 May 2000	M-Vent	6	126	61.11
21 May 2000	Biovent	7	28	71.42

worm (Fig. 3E). Free sperm are readily observed in proximity to primary oocytes in light-microscope squash preparations of the posterior oviduct (Fig. 3F). In the paraffin sections, the sperm heads do not appear to be buried in the walls of the spermatheca, but the magnifications are too low to reveal whether there are intracellular junctions that might indicate nutrient exchange between the spermatozoa and the female epithelium.

Ultrastructural examination of oocytes collected from the spermatheca shows that the egg envelope is formed of branched microvilli that terminate in a monolayer of granules situated along the outer surface of the envelope and underlying a filamentous glycocalyx (Fig. 3G). Sperm heads are often found in direct contact with the glycocalyx (Fig. 3G). However, we did not find any sperm that had penetrated the egg envelope.

Status of the oocytes at "spawning"

In all five species examined, oocytes in the spermatheca, the ovisac, and all along the length of the oviduct had large germinal vesicles (Fig. 2C), suggesting that they were primary oocytes in the first prophase of meiosis. In no instance did we encounter embryos already developing in the ovisac or in any other region of the oviduct.

Collections of eggs spawned naturally by *Riftia pachyptila* and collected in egg traps contained many uncleaved eggs (Table 1), most (but not all) of which lacked germinal vesicles (Fig. 2D) by the time they were collected. After deployments of several days, nets also contained cleaving embryos, but the high percentage of uncleaved eggs in all samples (Table 1) indicates that embryos do not begin cleavage before release from the parent. In the shortest (3-day) deployment, only uncleaved eggs were found (Table 1). As first cleavage in *R. pachyptila* occurs more than 2 days after eggs are diluted with seawater (Marsh *et al.*, 2001), these egg-trap data are completely consistent with our other observations suggesting that eggs are released as primary oocytes.

During November 2003, oocytes carefully dissected from seven female specimens of *Lamellibrachia luymesi* were incubated *in vitro* without adding additional sperm. After 24 h, a mean of 90.09% (SD: 8.45) of embryos had attained 2-cell to 16-cell embryonic stages, showing that a large percentage of oocytes had already been inseminated by the time they reached the ovisac. During a cruise in July 2004, this experiment was repeated qualitatively, using very small individuals of *L. luymesi*. Oocytes from three females yielded a high percentage of embryos without addition of sperm, but oocytes from two very small females did not develop, suggesting the possibility that these individuals, though reproductively active, had not received any sperm.

Fertilization rates

For species that fertilize internally, it is commonly assumed that all eggs are fertilized (Thorson, 1950). However, in rearing the embryos of three species of vestimentiferans in both the laboratory and the field, we found that the number of eggs developing was always less than 100%, suggesting that the internal fertilization mechanism may not function with perfect efficiency in these worms.

In laboratory pressure vessels (Marsh *et al.*, 2001), the percentage of *Riftia pachyptila* embryos cleaving ranged from 40% to 84% (Table 2), with an average of 65%. When cultures were incubated *in situ* (Table 2), about 20% more embryos cleaved; the highest value for cleaving embryos was 91%.

Fertilization rates were high (74.32% to 97.60%) in incubations of *Lamellibrachia lumesi* eggs held near the sea floor and in the laboratory (Table 3). A single field culture

Table 2

Percentage of Riftia pachyptila *embryos undergoing cleavage in laboratory pressure vessels at 250 atm (laboratory) and in mesh-covered vials outplanted to the field at a depth of 2500 m*

				Embryos Cleaving	
Location	Date	Females	Eggs	Percentage	Mean ± SD
Laboratory	12 Dec 1995	2	38	84.21	
	14 Dec 1995	1	124	60.48	
	5 Dec 1998	1	692	40.75	
	5 Dec 1998	1	300	41.66	
	15 May 1999	5	202	84.16	
	4 May 2000	6	120	77.50	
	6 May 2000	6	107	82.24	
	16 May 2000	9	100	49.00	65.00 ± 19.26
Field	25 April 1999	2	73	86.30	
	16 May 1999	2	212	90.57	
	13 Dec 1999	6	426	78.64	
	4 May 2000	6	55	76.36	
	9 May 2000	5	260	90.38	
	13 May 2000	3	232	86.21	
	17 May 2000	9	456	83.77	85.55 ± 5.71

All eggs were removed by dissection from the female ovisac and additional sperm were added *in vitro* prior to incubation.

Table 3

Percentage of Lamellibrachia lumesi *embryos undergoing cleavage at 1 atm in the laboratory and in mesh-covered vials outplanted to the field at a depth of 700 m*

			Embryos Cleaving	
Location	Date	Eggs	Percentage	Mean ± SD
Laboratory	11 Sept 1995	66	92.42	
	13 Sept 1995	222	74.32	
	17 Aug 1997	167	97.60	88.11 ± 12.23
Field	19 Aug 1997	637	96.54	NA

All eggs were removed by dissection from the female ovisac, and additional sperm were added *in vitro* prior to incubation. Eggs from numerous females were combined for each experiment.

of *Tevnia jerichonana* with combined eggs from three females yielded 87.8% development.

In a field experiment with *L. luymesi*, distance from a tubeworm bush (0 m to 6 m) had no significant effect on the fertilization rate of oocytes taken from the ovisacs of females (Fig. 4); the mean percentages of development ranged from 85% to 95%. This lack of correlation with distance strongly suggests that fertilization had already occurred before the experimental deployment. Similar experiments with freely spawning invertebrates that fertilize externally always show a strongly declining relationship between fertilization rate and distance from males (Pennington, 1985; Levitan, 1991; Levitan and Young, 1995).

Discussion

The reproductive anatomy of vestimentiferans has been studied in *Lamellibrachia luymesi* (Van der Land and Norrevang, 1977), *Lamellibrachia barhami* (Webb, 1977), and mainly in the male in *Riftia pachyptila* (Gardiner and Jones, 1985; Jones and Gardiner, 1985; Gardiner *et al.*, 1992). Early development has been described for *Riftia pachyptila* (Marsh *et al.*, 2001) and for *Lamellibrachia* sp. and *Escarpia* sp. from the Gulf of Mexico (Young *et al.*, 1996); the morphology of very young juveniles of *Ridgeia piscesae* has been described by Jones and Gardiner (1989).

Apparent spawning events have been observed in *Riftia pachyptila* (Van Dover, 1994) and *Lamellibrachia luymesi* (our unpublished observations). However, in none of these observations was it possible to ascertain whether the "spawn" consisted of unfertilized oocytes, zygotes, developing embryos, bundles of sperm, or free sperm.

Gardiner and Jones (1985) suggested that direct sperm transfer and internal fertilization might occur in *Riftia pachyptila*, because this species has modified sperm. They also reported an anecdotal observation of sperm in the female genital tract. In *Ridgeia piscesae* and *Tevnia jerichonana* sperm masses have been found attached to the female vestimentum and within the oviduct, strongly suggesting active sperm transfer when the plumes of closely juxtaposed animals brush against each other (Southward and Coates, 1989; Southward, 1999; MacDonald *et al.*, 2002), followed by internal fertilization. These observations also raise the possibility that embryos are brooded.

Except in *Ridgeia piscesae* (Southward and Coates, 1989; MacDonald *et al.*, 2002), we do not know how sperm or sperm bundles are transferred to the female, but it seems likely, on the basis of spawning observations, that sperm bundles may be released into the water column, from which they are either collected by the females or find their way into the female gonopores. The presence of spermatozoa at the posterior end of the female gonoduct demonstrates that sperm either swim or are transported deep into the reproductive system. Further work is required to determine if sperm bundles swim downward as cohesive bundles against a ciliary current that carries oocytes upward in the oviduct, or if they are transported by ciliary action or peristalsis. It is interesting that the positioning of external ciliary tracts on the male vestimentum varies from species to species and that the size and shape of sperm bundles also vary in a species-specific manner (Fig. 1). Further work is needed to determine if these characters are correlated and if they are related to the mode of sperm release or transfer.

Webb (1977), in describing the reproductive anatomy of *Lamellibrachia barhami*, noted that the gonocoel of the gonad opens into the gonoduct by nonciliated funnels situated at irregular intervals along the length of the trunk. These connections between the gonoduct and the gonocoels were not found in any of the species studied here, which suggests that all primary oocytes released from the ovary must pass through the spermatheca before they enter the

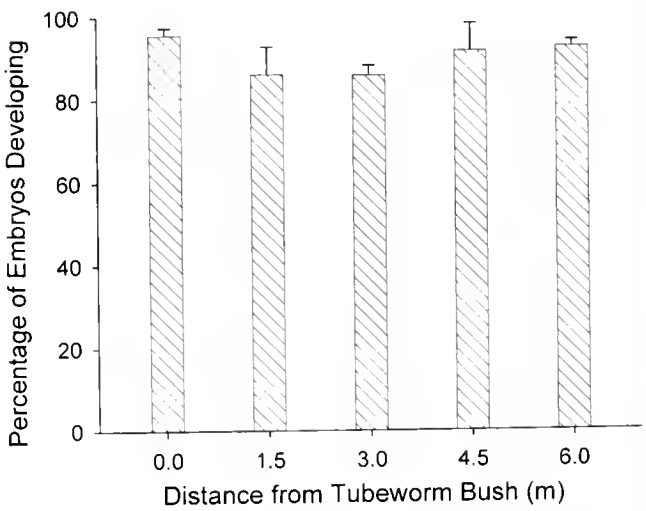

Figure 4. Percentage of fertilized eggs (mean ± 1 SD) of *Lamellibrachia luymesi* after a 24-h *in situ* deployment at various distances from a large bush of conspecifics.

gonoduct. In eggs of other polychaetes, granulated glycocalyces similar to the one found in oocytes collected from the spermatheca of *Lamellibrachia luymesi* are known to possess sperm receptors (Eckelbarger, 1992). We hypothesize that as primary oocytes pass through the spermatheca, sperm bind to the primary oocytes, which are arrested at the first meiotic prophase until they are released by the female. This hypothesis is supported by electron micrographs (Fig. 3G) showing sperm heads in direct contact with the glycocalyces of primary oocytes in the spermatheca. Westheide (1988) has categorized the sperm storage organs of polychaetes into three major types. The spermathecae of vestimentiferans, which are outpocketings of the oviduct, fall clearly into his Type 2a classification.

The breeding strategy of internal fertilization followed by zygote release rather than brooding assures a high level of fertilization without sacrificing dispersal potential. Moreover, sperm storage is an ideal strategy in an environment where periodic cues for gametogenesis and spawning synchrony are limited (Young, 1999). Indeed, hydrothermal vent polychaetes from many different families are now known to possess specialized organs for sperm storage (Zal *et al.*, 1995; Jollivet *et al.*, 2000).

Not all oocytes taken from the ovisacs of female vestimentiferans undergo development, an observation that suggests imperfect internal fertilization. However, the number of embryos undergoing development is often higher for cultures reared in the field than in the laboratory (Tables 1, 2). This raises the possibility that the percentage of eggs developing is not the same as the percentage fertilized; thus, observed rates of development lower than 100% may be caused by culture conditions rather than fertilization failure.

Previous estimates of dispersal times and distances based on lipid stores, larval metabolism, and current speeds (Marsh *et al.*, 2001) have assumed external fertilization and dispersal during the entire embryonic period. Even though the presumed location of fertilization was clearly erroneous in these studies, the dispersal estimates themselves remain valid, since embryogenesis does not begin until after inseminated oocytes are released into the water column.

Acknowledgments

This work was supported by NSF grants OCE-9619606 and OCE-0118733, NOAA/NURP UNCW grant NA96RU-0260, FCT grant SFRH/BD/7084/2001, and submersible funding from the NOAA Office of Ocean Exploration. The NSF grant that supported work on *Riftia pachyptila* was a collaborative effort that also included grants and cruises led by Donal Manahan and Lauren Mullineaux. Chuck Fisher provided samples of *Ridgeia*. We thank the Biomedical Imaging Unit, University of Southampton, for technical help in transmission electron microscopy. Sandra Brooke, Elsa Vazquez, Ana Metaxas, Tracey Griffin, Jim Welch, Cathy Allen, Shawn Arellano, Adam Marsh, Alison Green, Doug Pace and many others helped develop tubeworm culture techniques and assisted with field work on various cruises.

Literature Cited

Bakke, T. 1974. Settling of the larvae of *Siboglinum fjordicum* Webb (Pogonophora) in the laboratory. *Sarsia* **56:** 57–70.

Cary, S. C., H. Felbeck, and N. D. Holland. 1989. Observations on the reproductive biology of the hydrothermal vent tube worm *Riftia pachyptila*. *Mar. Ecol. Prog. Ser.* **52:** 89–94.

Eckelbarger, K. J. 1992. Polychaeta: Oogenesis. Pp. 109–127 in *Microscopic Anatomy of Invertebrates*, Vol. 7, F. W. Harrison and S. L. Gardiner, eds. Wiley-Liss, New York.

Fisher, C. R., I. A. Urcuyo, M. A. Simpkins, and E. Nix. 1997. Life in the slow lane: growth and longevity of cold-seep vestimentiferans. *Mar. Ecol.* **18:** 83–94.

Gardiner, S. L., and M. L. Jones. 1985. Ultrastructure of spermiogenesis in the vestimentiferan tube worm *Riftia pachyptila* (Pogonophora: Obturata). *Trans. Am. Microsc. Soc.* **104:** 19–44.

Gardiner, S. L., and M. L. Jones. 1993. Vestimentifera. Pp. 371–460 in *Microscopic Anatomy of Invertebrates*, Vol. 12, F. W. Harrison and M. E. Rice, eds. Wiley-Liss, New York.

Gardiner, S. L., S. E. Shrader, and M. L. Jones. 1992. Preliminary observations on oogenesis in the tube worm *Riftia pachyptila* Jones (Vestimentifera). *Am. Zool.* **32:** 124A.

Hessler, R. R., W. M. Smithey, M. A. Boudrias, C. H. Keller, R. A. Lutz, and J. J. Childress. 1988. Temporal change in megafauna at the Rose Garden hydrothermal vent (Galapagos Rift; eastern tropical Pacific). *Deep-Sea Res.* **35:** 1681–1709.

Jollivet, D., A. Emphis, M. C. Baker, S. Hourdez, T. Comtet, C. Jouin-Toulmond, D. Debruyères, and P. A. Tyler. 2000. Reproductive biology, sexual dimorphism, and population structure of the deep sea hydrothermal vent scale-worm, *Branchipolynoe seepensis* (Polychaete: Polynoidae). *J. Mar. Biol. Assoc. UK* **80:** 55–68.

Jones, M. L. 1981. *Riftia pachyptila* Jones: observations on the vestimentiferan worm from the Galapagos Rift. *Science* **213:** 333–336.

Jones, M. L. 1985. On the Vestimentifera, new phylum: six new species, and other taxa, from hydrothermal vents and elsewhere. *Bull. Biol. Soc. Wash.* **6:** 117–158.

Jones, M. L., and S. L. Gardiner. 1985. Light and scanning electron microscopic studies of spermatogenesis in the vestimentiferan tube worm *Riftia pachyptila* (Pogonophora: Obturata). *Trans. Am. Microsc. Soc.* **104:** 1–18.

Jones, M. L., and S. L. Gardiner. 1989. On the early development of the vestimentiferan tube worm *Ridgeia* sp. and observations on the nervous system and trophosome of *Ridgeia* sp. and *Riftia pachyptila*. *Biol. Bull.* **177:** 254–276.

Levitan, D. R. 1991. Influence of body size and population density on fertilization success and reproductive output in a free-spawning invertebrate. *Biol. Bull.* **181:** 261–268.

Levitan, D. R., and C. M. Young. 1995. Reproductive success in large populations: empirical measures and theoretical predictions of fertilization in the sea biscuit *Clypeaster rosaceus*. *J. Exp. Mar. Biol. Ecol.* **90:** 221–241.

Lutz, R. A., T. M. Shank, D. J. Fornari, R. M. Haymon, M. D. Lilley, K. L. Von Damm, and D. Desbruyères. 1994. Rapid growth at deep-sea vents. *Nature* **371:** 663–664.

MacDonald, I. R., V. Tunnicliffe, and E. C. Southward. 2002. Detection of sperm transfer and synchronous fertilization in *Ridgeia piscesae* at Endeavour Segment, Juan de Fuca Ridge. *Cah. Biol. Mar.* **43:** 395–398.

Malakhov, V. V., I. S. Popelyaev, and S. V. Galkin. 1996. Microscopic

anatomy of *Ridgeia phaeophiale* Jones, 1985 (Pogonophora, Vestimentifera) and the problem of the position of Vestimentifera in the system of the Animal Kingdom. IV. Excretory and reproductive systems and coelom. *Russ. J. Mar. Biol.* **22:** 249–260.

Marsh, A. G., L. S. Mullineaux, C. M. Young, and D. T. Manahan. 2001. Larval dispersal potential of the tubeworm *Riftia pachyptila* at deep-sea hydrothermal vents. *Nature* **411:** 77–80.

McHugh, D. 1997. Molecular evidence that echiurans and pogonophorans are derived annelids. *Proc. Natl. Acad. Sci. USA* **94:** 8006–8009.

Metaxas, A., R.E. Scheibling and C.M. Young. 2002. Estimating fertilization success in marine benthic invertebrates: a case study with the tropical sea star *Oreaster reticulatus*. *Mar. Ecol. Prog. Ser.* **226:** 87–101.

Pennington, J. T. 1985. The ecology of fertilization of echinoid eggs: the consequences of sperm dilution, adult aggregation, and synchronous spawning. *Biol. Bull.* **169:** 417–430.

Rouse, G. W., and K. Fauchald. 1997. Cladistics and polychaetes. *Zool. Scr.* **26:** 139–204.

Shank, T. M., D. J. Foranri, K. L. Von Damm, M. D. Lilley, R. M. Haymon, and R. A. Lutz. 1997. Temporal and spatial patterns of biological community development at nascent deep-sea hydrothermal vents (9° 50′N, East Pacific Rise). *Deep-Sea Res. II* **45:** 465–515.

Southward, E.C. 1999. Development of Perviata and Vestimentifera (Pogonophora). *Hydrobiologia* **402:** 185–202.

Southward, E. C., and K. A. Coates. 1989. Sperm masses and sperm transfer in a vestimentiferan, *Ridgeia piscesae* Jones, 1985 (Pogonophora: Obturata). *Can. J. Zool.* **67:** 2776–2781.

Thorson, G. 1950. Reproductive and larval ecology of marine bottom invertebrates. *Biol. Rev.* **25:** 1–45.

Van der Land, J., and A. Norrevang. 1977. Structure and relationships of *Lamellibranchia* (Annelida, Vestimentifera). *K. Dan. Vidensk. Selsk. Biol. Skr.* **21(3):** 1–102.

Van Dover, C. L. 1994. *In situ* spawning of hydrothermal vent tubeworms (*Riftia pachyptila*). *Biol. Bull.* **186:** 134–135.

Webb, M. 1977. Studies on *Lamellibrachia barhami* (Pogonophora) II—The reproductive organs. *Zool. Jahrb. Anat. Bd.* **97:** 455–481.

Westheide, W. 1988. Genital organs. Pp. 263–279 in *Ultrastructure of the Polychaeta*, W. Westheide and C.O. Hermans, eds. Gustav Fischer, Stuttgart.

Young, C. M. 1999. Synchrony and sociality: breeding strategies in constant and variable environments. Pp. 1–4 in *Aquatic Life Cycles Strategies: Survival in a Variable Environment*, M. Whitfield, J. Matthews, and C. Reynolds, eds. Mar. Biol. Assoc., Plymouth, UK.

Young, C. M., E. Vásquez, A. Metaxas, and P. A. Tyler. 1996. Embryology of vestimentiferan tube worms from deep-sea methane/sulfide seeps. *Nature* **381:** 514–516.

Zal, F., P. Chevaldonné, and D. Debruyères. 1995. Reproductive biology and population structure of the deep-sea hydrothermal vent worm *Paralvinella grasslei* (Polychaeta: Alvinellidae) at 13°N on the East Pacific Rise. *Mar. Biol.* **122:** 637–648.

Reference: *Biol. Bull.* **208:** 29–35. (February 2005)

Mechanical Properties of the Isolated Catch Apparatus of the Sea Urchin Spine Joint: Muscle Fibers Do Not Contribute to Passive Stiffness Changes

NOBUHIRO TAKEMAE* AND TATSUO MOTOKAWA

Department of Biological Sciences, Graduate School of Bioscience & Biotechnology, Tokyo Institute of Technology, W3-42, O-okayama 2-12-1, Meguro, Tokyo 152-8551, Japan

Abstract. The catch apparatus (CA) is the collagenous ligament at the spinal joint of sea urchins. It maintains spine posture by stiffening and allows spine movement by softening. A CA preparation, which was isolated from ossicles, was used to test the hypothesis that frictional forces between collagen fibers and ossicles are the source of stiffness changes. Isolated preparations of the CA changed in stiffness, thus falsifying the hypothesis. Another hypothesis proposes that muscle fibers, which represent a relatively small component of the CA, cause stiffening of the CA by contraction. Chemicals that evoked contraction in spine muscles did not always stiffen the CA: the CA of *Heterocentrotus mammillatus* softened in response to artificial seawater with potassium concentration elevated to 100 m*M*. This provided evidence against the muscle-based hypothesis. The present results suggest that the stiffness changes of the CA are based on changes in the mechanical properties of the extracellular components of the connective tissue and are therefore related to the connective tissue catch that is widespread in other echinoderms.

Introduction

Echinoderms have connective tissues that change their mechanical properties under neural control (Wilkie, 1996a). Connective tissue with such mutability is called catch connective tissue or mutable connective tissue, and the mechanical activity the tissue shows is referred to as connective tissue catch. The idea of connective tissue catch was put forward by Takahashi, based on studies on the spinal joint ligament of sea urchins (Takahashi, 1967a, b). This ligament changes its stiffness, although it is made mostly of collagenous tissue. It stiffens to hold the spine in position and softens to permit spine movement under nervous control. Takahashi named this ligament the catch apparatus (CA), because in its long-lasting holding capacity it is similar to molluscan catch muscle. Since Takahashi's pioneering work, catch connective tissue has been found in various anatomical locations in all extant echinoderm classes (Wilkie, 1996a). It has been regarded as one of the major features that characterize the phylum Echinodermata (Motokawa, 1988; Ruppert and Barnes, 1994).

It is obvious that muscles are not involved in the stiffening mechanism of catch connective tissues containing no muscle cells at all (Birenheide *et al.*, 1996, 2000). It is sometimes the case, however, that a few muscle cells are found in catch connective tissue. The role of these muscles has been studied in detail only in the CA of sea urchins. The CA is made of collagen fibrils that are parallel to the long axis of spine, and thin myocytes that contain only several thick filaments are found among the fibrils (Smith *et al.*, 1981). Hidaka and Takahashi (1983) measured the tensile stiffness of the CA and the cross-sectional area of the muscles occupying it. If the muscles directly bear all the tensile forces of stiffened CA, the muscles would produce a greater force than that produced by the strongest muscles known elsewhere in the animal kingdom. The authors concluded that the muscles are not responsible for the stiffness changes.

A different interpretation of the role of these muscles was proposed by del Castillo *et al.* (1995). In the CA, bundles of collagen fibrils insert into the calcite stereom of the spinal ossicles and wind around the pillars of the stereom. These authors suggested that the frictional forces between collagen

Received 1 June 2004; accepted 21 October 2004.

* To whom correspondence should be addressed. E-mail: ntakemae@bio.titech.ac.jp

bundles and the pillars are responsible for the resistance to the stretch of the CA. When the CA is soft, a gap appears between the collagen bundles and pillars, which permits the bundles to slide freely. Contraction of the muscles, they proposed, presses the collagen bundles tightly against the pillars, which prevents the bundles from sliding and thus makes the CA inextensible and stiff. This hypothesis invited immediate debate (Wilkie, 1996b; del Castillo and Smith, 1996; Perez-Acevedo *et al.*, 1998). Both sides of the debate invoked Occam's razor. Del Castillo's hypothesis is applicable only to ligaments that contain muscles and are attached to skeletal elements. Wilkie criticized the hypothesis because it is more parsimonious to assume that all catch connective tissues share a common mechanism. Del Castillo regarded his hypothesis as being more parsimonious because the combination of muscles and ordinary connective tissue could account for the extraordinary holding capacity and eliminate the need to suppose that the collagenous ligaments have any unusual properties.

Another challenge to the widely accepted notion that all the catch connective tissues share a common non-muscular mechanism was put forward by Elphick and Melarange (2001). Drugs that cause stiffening of catch connective tissue, such as acetylcholine and the neuropeptide NGIWY-amide, also induce contraction of muscles. This led these authors to suggest that muscle contraction is the common mechanism underlying the stiffening response of all the catch connective tissues. Wilkie (2002) again criticized this generalization by extensively reviewing the pharmacological works on catch connective tissues.

The aim of the present work was to study in detail catch connective tissue containing myocytes, using the CA as a model. The hypotheses of del Castillo and of Elphick and Melarange were examined by careful comparison of different methods and different species. These hypotheses are falsifiable. The hypothesis of del Castillo depends on the occurrence of friction between ossicles and collagen fibers. It predicts that stiffening will not be observed when the CA is isolated from the ossicles. The hypothesis of Elphick and Melarange predicts that every agent inducing muscle contraction should stiffen the CA. We used artificial seawater with elevated potassium concentration (KASW) as such an agent—elevated potassium being a universal muscle contractant that depolarizes the muscle cell membrane (Hodgkin and Horowicz, 1960). If KASW induces softening of the CA, the hypothesis is falsified.

Materials and Methods

Heterocentrotus mammillatus (Linnaeus), the slate-pencil sea urchin, was used mainly because of the large size of its catch apparatus (CA), which enabled us to isolate a block of connective tissue with precise dimensions. The sea urchins were collected near Sesoko Station, Tropical Biosphere Research Center, University of the Ryukyus, and were kept in an aquarium of artificial seawater at 24–25 °C in our laboratory. The longer diameter at ambitus was 6–8 cm. Specimens of *Diadema setosum* (Leske) were collected near Misaki Marine Biological Station, University of Tokyo. They were kept in an aquarium of natural seawater at 18 °C. The diameter at ambitus of these animals was 6–7 cm.

Isolated catch apparatus

The sea urchin spine forms a ball-and-socket-like joint with a projection on the test called the tubercle. The spine base is connected to the tubercle by three layers of conical tissues that encapsulate the joint. The most superficial layer is a thin epidermis, under which there is a layer of spine muscle, and then the CA. In *Diadema setosum*, the center of both the spine base and the tubercle is perforated and houses a central ligament connecting the two ossicles. *Heterocentrotus mammillatus* lacks the central ligament.

The isolated CA was prepared by cutting the CA free from both the junction between it and the spine base and that between it and the tubercle. The procedure was as follows. A piece of a test with a spine was cut out. All the epidermis and spine muscles covering the CA were scraped off. In *H. mammillatus*, a block of the CA was isolated and trimmed. The size of the piece for mechanical tests was 4.0 mm in the direction of the spine axis, 2.0 mm in the circumferential direction of the joint, and 1.0 mm in the direction towards the center of the joint. The isolated CA piece of *D. setosum* was trimmed to the size 4.0 mm in the circumferential direction and 1.0 mm in the direction of spine axis. The direction towards the center was about 0.3 mm, which was the non-trimmed thickness of the CA.

The CA preparation with ossicles attached was prepared as follows. All the epidermis and spine muscles covering the CA were scraped off. Most of the CA was removed, leaving a strip of CA 2 mm wide in the circumferential direction connecting the spine and the tubercle.

Creep test

Mechanical properties of the CA were measured by creep tests. The CA was subjected to a tensile load, and the elongation of the CA was measured. The tension was in the direction of the axis of the spine except in the isolated CA of *D. setosum*, in which the tension was in the circumferential direction of the spinal joint. One end of the preparation was glued to the aluminum holder at the bottom of a trough. The opposite end was attached to a clip that was connected to a lever by a thread. The trough was filled with artificial seawater (ASW), and the sample was rested for 10–15 min. A load was applied to the sample *via* the lever. The load was 1.67–16.7 g for *H. mammillatus* and 0.67–3.33 g for *D. setosum*. The preparation elongated under the load. The elongation was measured with a laser displace-

ment sensor (3Z4M-J1001-6, Omron, Japan) and recorded with a data logger (NR-2000, Keyence, Japan). The rate of elongation became rather constant in 10–20 min, and the constant rate was kept for about 1 h (see Results). Chemical stimulation was applied during this phase of constant elongation. The normal viscosity was calculated as the stress divided by the strain rate (Motokawa, 1982). It was expressed as the relative value normalized by the value at the exact time when the chemical stimulus was applied. Here we call the normal viscosity simply "viscosity."

The composition of the ASW was NaCl, 433.7 m*M*; KCl, 10.0 m*M*; $CaCl_2$, 10.1 m*M*; $MgCl_2$, 52.5 m*M*; $NaHCO_3$, 2.5 m*M* (pH 8.1). Artificial seawater with its potassium concentration elevated to 100 m*M* (KASW) was prepared by reducing the sodium concentration so as to keep the osmotic concentration constant. Acetylcholine chloride was purchased from Nacalai Tesque, Japan. It was diluted in ASW to the final concentration of 10^{-6}–10^{-3} *M*. In the control tests, ASW without chemicals was applied. All experiments were carried out at room temperature (22–28 °C). The temperature did not vary more than 2 °C in a single experiment.

Contraction of spine muscle

The isotonic contraction of the muscle bundles at the spinal joint was measured. A cut was made through the joint between the spine base and the mamelon, on which the spine base was mounted, leaving a strip of the spine muscle bundles connecting the spine base and the tubercle. A load was applied, and the shortening of the muscle bundle was measured at chemical stimulation, using the same set-up as for the creep tests. In *H. mammillatus* the width of the muscle bundle was 4 mm and the load was 0.67–1.67 g. In *D. setosum* the width was 2 mm and the load was 0.33–1.67 g.

Results

Isolated catch apparatus of Heterocentrotus mammillatus

The CA elongated rapidly on application of the load; in 10–20 min the elongation rate gradually decreased to a more-or-less constant value that was maintained for about 1 h (Fig. 1). Thereafter the rate increased rapidly until finally the CA ruptured.

Acetylcholine (ACh) at concentrations of 10^{-6}–10^{-3} *M* decreased the creep rate of the isolated CA (Fig. 2a). The decrease was apparent in about 20 s after the application of ACh, and the rate reached its lowest value in about 3.5 min. The rate kept decreasing as long as ACh was applied. When ACh was washed out with pure artificial seawater (ASW), the rate increased again to its value before the application of ACh. ACh was effective in all the samples at 10^{-3} *M*, whereas at 10^{-6}–10^{-4} *M*, 20%–30% of the samples failed to respond (Fig. 2b). The dose-response curve of the viscosity 2 min after the application of ACh is shown in Figure 2b. The viscosity in 10^{-3} *M* ACh was 2.88 ± 0.59 (average ± SEM, $n = 10$), which was significantly different ($P < 0.01$) from that of the control, as shown by the Mann-Whitney *U*-test.

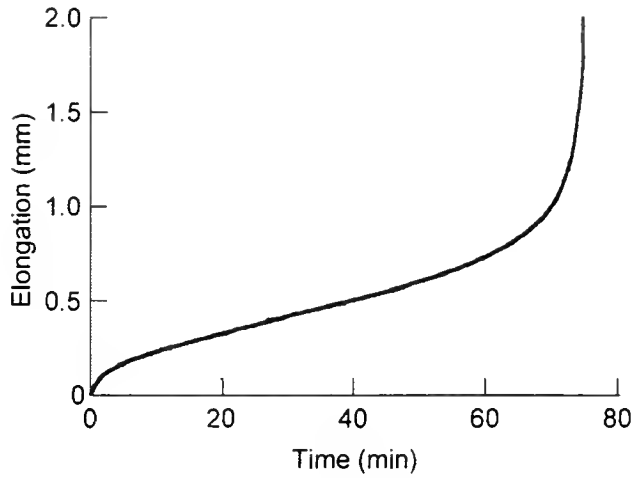

Figure 1. Typical creep curve of the isolated catch apparatus of *Heterocentrotus mammillatus*. It shows three phases: a fast elongating phase; a constant creep-rate phase; and a phase with increasing creep rate ending with tissue rupture. The sample broke at the right extremity of the curve.

Artificial seawater with elevated potassium (KASW) increased the creep rate in all samples of the isolated CA (Fig. 3a). The increase was apparent in about 20 s after the application of KASW and maximized in about 2 min. When KASW was washed out with ASW, the rate decreased again to the value before application of KASW. The viscosity 2.5 min after the application of KASW was 0.53 ± 0.09 (average ± SEM, $n = 11$), which was significantly different ($P < 0.01$) from that of the control.

Figure 3b shows the response of the CA with ossicles attached. KASW reversibly increased the creep rate as in the isolated CA. Such responses were found in 7 samples out of 9; there were no responses in 2 samples. The viscosity 2.5 min after the application of KASW was 0.77 ± 0.09 (average ± SEM, $n = 9$), which was not significantly different ($P > 0.1$) from the average of the isolated CA in KASW.

Isolated catch apparatus of Diadema setosum

Acetylcholine (ACh) at concentrations 10^{-6}–10^{-3} *M* reversibly decreased the creep rate of the isolated CA (Fig. 4a). Although these preparations were loaded circumferentially, their response was quite similar to that of the isolated CA of *H. mammillatus*, which was loaded longitudinally. The dose-response curve of the viscosity 2 min after the application of ACh is shown in Figure 4b. The viscosity in 10^{-3} *M* ACh was 2.24 ± 0.71 (average ± SEM, $n = 12$),

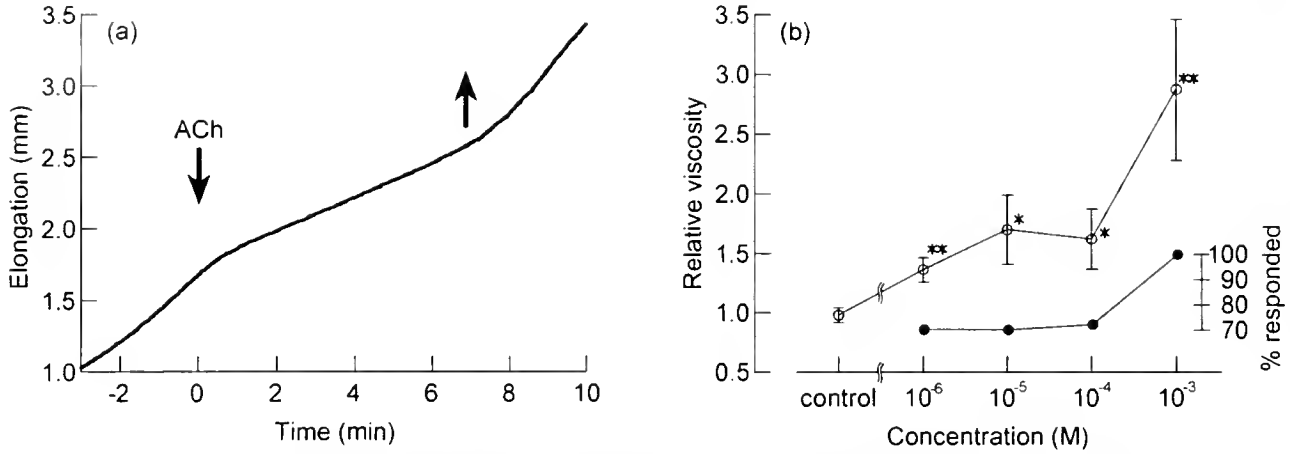

Figure 2. Response of the isolated catch apparatus of *Heterocentrotus mammillatus*. (a) Decrease in creep rate in response to 10^{-6} *M* ACh. In this and the following figures, downward arrows indicate the application of chemicals and upward ones indicate the time of washing. (b) Dose-response curves. Hollow circles give viscosity 2 min after the application of ACh. In the control test, pure ASW was applied. The average at every ACh concentration was statistically different from that of the control, as shown by the Mann-Whitney *U*-test (*, $P < 0.05$, **, $P < 0.01$). Error bar, ± SEM. Filled circles denote percentage of the samples that responded.

which was significantly different ($P < 0.01$) from that of the control. ACh 10^{-6}–10^{-3} *M* was effective in 70%–92% of samples tested (Fig. 4b).

In contrast to its effect on the CA of *H. mammillatus*, KASW decreased the creep rate of the isolated CA of *D. setosum* (Fig. 5). The decrease was apparent in about 20 s after the application of KASW, and the rate reached its lowest value in 2 min. When KASW was washed out by ASW, the rate increased again to the value before application of KASW. The viscosity 2.5 min after the application of KASW was 1.49 ± 0.11 (average ± SEM, $n = 30$), which was significantly different ($P < 0.01$) from that of the controls. The response to KASW was seen in 19 samples out of 30; there were no changes in the elongation rate in the other 11 samples.

Contraction of spine muscles

The spine muscles of *H. mammillatus* and *D. setosum* contracted in response to ACh and to KASW. The responses to ACh were similar in the two species. The contraction in low concentrations of ACh (10^{-6}–10^{-5} *M*) was phasic; the shortening reached a peak in about 1 min and was soon followed by rapid relaxation. Complete relaxation was observed in 3–4 min, even in the presence of ACh (Fig. 6a, d). In higher concentrations of ACh (10^{-4}–10^{-3} *M*), a peak was followed by oscillations that lasted as long as ACh was present (Fig. 6b, e). Similar results have been reported for the spine muscle of *Anthocidaris crassispina* (Shingyoji and Yamaguchi, 1995). KASW caused a tonic contraction in *H. mammillatus* (Fig. 6c). In *D. setosum*, KASW caused a

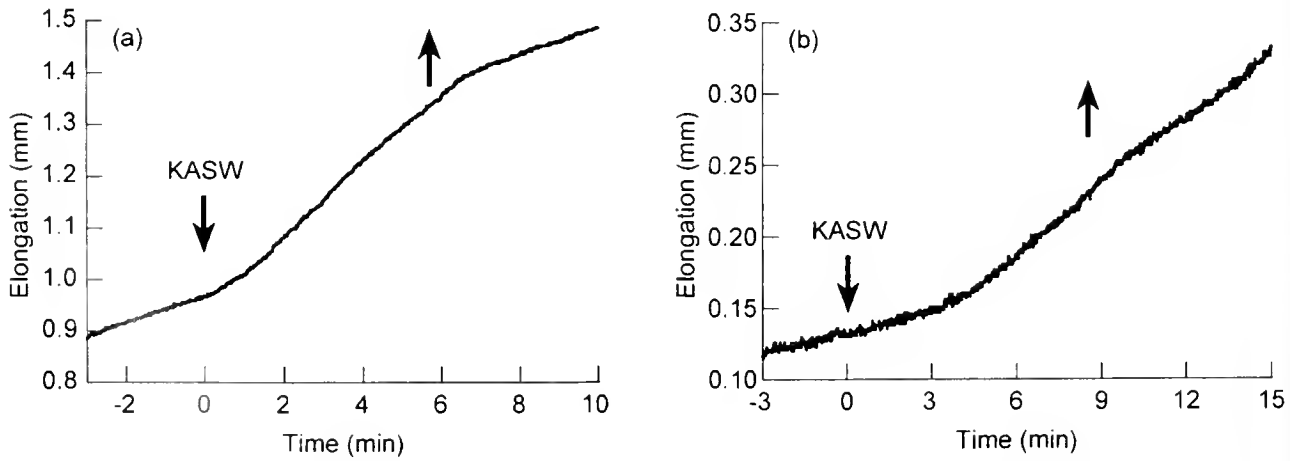

Figure 3. Increase in creep rate of catch apparatus of *Heterocentrotus mammillatus* in response to artificial seawater with elevated K concentration (KASW): (a) without ossicles; (b) with ossicles attached.

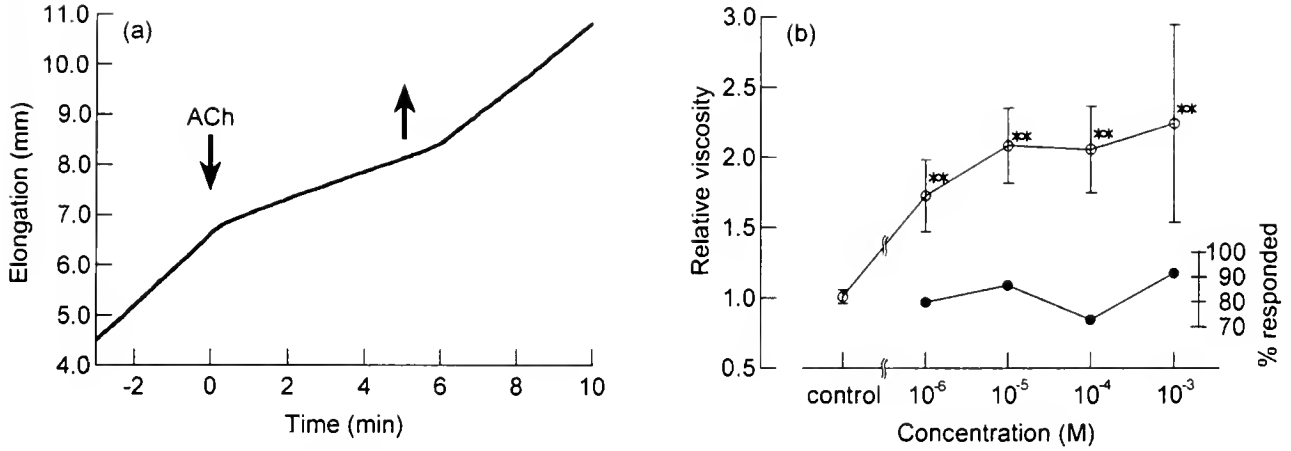

Figure 4. Response of the isolated catch apparatus of *Diadema setosum*. (a) Decrease in creep rate in response to 10^{-6} *M* ACh. (b) Dose-response curves. Hollow circles give the viscosity 2 min after the application of ACh. The average at every ACh concentration was significantly different from the control, as shown by the Mann-Whitney *U*-test (**, $P < 0.01$). Error bar, ±SEM. Filled circles denote percentage of the samples that responded.

contraction with two peaks (Fig. 6f); the contraction after the second peak decreased little or slowly.

Discussion

The mechanical properties of the isolated catch apparatus (CA) and their response to stimulation were studied for the first time. The creep curve of the isolated CA had three phases, quite similar to those of the CA with ossicles in *Anthocidaris crassispina* (Takahashi, 1967b). The responses to acetylcholine (ACh) were also similar to those of the attached CA. ACh decreases the creep rate of the attached CA of *A. crassispina* (Takahashi, 1967b) and *Heterocentrotus mammillatus* (Motokawa, 1981). We showed that the CA of both *H. mammillatus* and *D. setosum*, from which ossicles had been removed, also undergoes a decrease in creep rate in response to ACh. Artificial seawater with elevated potassium (KASW) increased the creep rate of the CA of *H. mammillatus* irrespective of whether ossicles were attached or not. The extent of the changes in the viscosity of the isolated CA was not different from that of the attached CA. All samples of the isolated CA of *H. mammillatus* responded to 10^{-3} *M* ACh and to KASW. The percentage of the samples that responded was higher than that of the attached CA. Thus the responses were qualitatively and quantitatively the same or even better in the isolated CA. These results suggest strongly that the mechanical properties and the responsiveness to stimuli of the CA are not impaired by isolation from the ossicles.

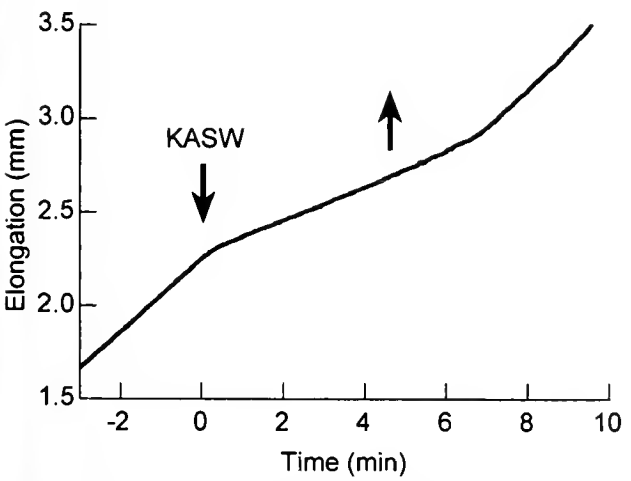

Figure 5. Increase in creep rate of catch apparatus of *Diadema setosum* in response to artificial seawater with elevated K concentration (KASW).

The isolated CA either increased or decreased its elongation rate in response to stimuli. Hereafter, we refer to a decrease in the elongation rate as stiffening and an increase as softening. The present results show clearly that the ossicles are not necessary for stiffness changes in the CA; thus they falsify the hypothesis of del Castillo *et al.* (1995), which proposed that frictional forces within the ossicles provide the mechanism of stiffness changes.

Our present study provided further evidence against the myocyte-based hypotheses. The CA of *H. mammillatus* softened in response to KASW. Media with an elevated potassium concentration generally cause contraction of muscles. The present study confirmed this in the spine muscles of *H. mammillatus* and *D. setosum*. Therefore, we would expect that the myocytes in the CA of *H. mammillatus* also contract in response to KASW. However, the CA of this species was softened by KASW. This suggests that the contraction of the myocytes in the CA has little effect on

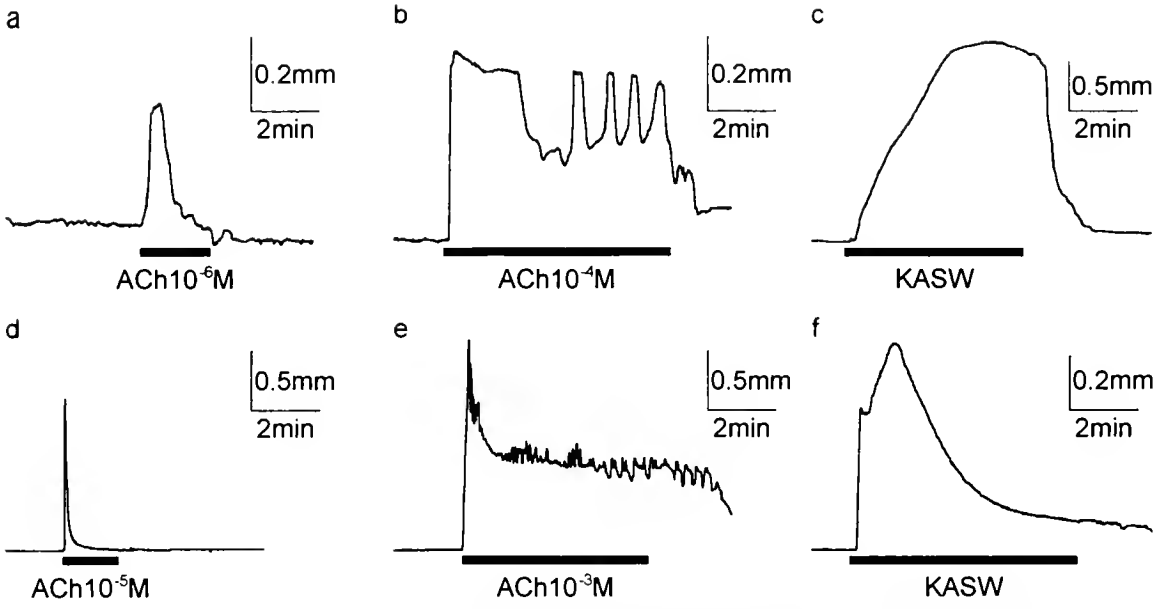

Figure 6. Contraction of spine muscles of *Heterocentrotus mammillatus* (a–c) and *Diadema setosum* (d–f). Heavy horizontal bars denote the application of chemical stimuli, either ACh or artificial seawater with elevated K concentration (KASW).

catch activities and thus provides the evidence against the myocyte-induced friction hypothesis of del Castillo *et al.* (1995) and against the hypothesis of Elphick and Melarange (2001), who claimed that the stiffening of all the catch connective tissues could be caused by muscles in the tissues.

However, the possibility remains that contraction of the myocytes in the CA may induce stiffening without the help of ossicles. The collagen bundles in the CA are parallel to the long axis of the spine. It is feasible that contraction of the myocytes could reduce the distance between adjacent bundles, thus permitting the formation of some temporary bonds between bundles. Once some bonds had been introduced, they would increase the resistance to stretch and thus stiffen the CA. Our creep experiments with the isolated CA of *D. setosum* provided evidence against this possibility. In this preparation the CA was stretched in the direction perpendicular to that of the axis of collagen bundles. Stiffening was observed even when this preparation was stretched to twice the original length. It would be highly unlikely that muscle cells oriented perpendicularly to the normal direction of the stretch could have been responsible for the stiffening of this preparation in which the distance between collagen bundles was extraordinarily large.

The time course of the muscular contraction also suggested that the sustained contraction of the myocytes is unlikely to be the basis of the catch mechanism. The CA remained stiff as long as 10^{-6} *M* ACh was applied for at least 7.5 min, while contraction of spine muscles induced by lower concentrations of ACh (10^{-6} *M*–10^{-5} *M*) were phasic, with the contraction lasting for only 2 min.

The spinal articulation of *D. setosum* is provided with a central ligament which, in addition to the CA, connects the spine base to the tubercle. The central ligament contains no myocytes and yet shows stiffening to ACh and to KASW, as does the CA of this species (Motokawa, 1983). The structure of the central ligament resembles that of the CA, except that it lacks myocytes. It is thus parsimonious to suppose that similar ligaments found side by side employ the same catch mechanism that does not depend on myocytes. The central ligament is subjected to far less strain than is the CA at the same inclination angle of the spine. As the role of the myocytes in the CA may be to reshorten it after it has been stretched by spine movements, the lack of myocytes in the central ligament may be related to the reduced strain it experiences and the consequently reduced need for a special device to restore its original length after stretching.

The present study strongly suggests that the effector cells responsible for the variable stiffness of the CA are not myocytes. Although we do not fully understand the nature of the effector cells and the force-bearing components of catch connective tissues, all available evidence supports the general conclusions that the effector cells are some type of secretory cells and that the force-bearing components are extracellular materials, not muscle cells (Wilkie, 1996a). The differences in nerves controlling the secretory cells may account for the differences in the response to KASW.

Acknowledgments

We would like to thank the staff of Sesoko Station (Tropical Biosphere Research Center, University of the

Ryukyus) for supplying *H. mammillatus* specimens, and the staff of Misaki Marine Biological Station (University of Tokyo) for supplying *D. setosum* specimens.

Literature Cited

Birenheide, R., A. Tsuchi, and T. Motokawa. 1996. To be stiff or to be soft—the dilemma of the echinoid tooth ligament. II. Mechanical properties. *Biol. Bull.* **190:** 231–236.

Birenheide, R., K. Yokoyama, and T. Motokawa. 2000. Cirri of the stalked crinoid *Metacrinus rotundus:* neural elements and the effect of cholinergic agonists on mechanical properties. *Proc. R. Soc. Lond. B* **267:** 7–16.

del Castillo, J., and D. S. Smith. 1996. We still invoke friction and Occam's razor to explain catch in the spines of *Eucidaris tribuloides. Biol. Bull.* **190:** 243–244.

del Castillo, J., D. S. Smith, A. M. Vidal, and C. Sierra. 1995. Catch in the primary spines of the sea urchin *Eucidaris tribuloides:* a brief review and a new interpretation. *Biol. Bull.* **188:** 120–127.

Elphick, M. R., and R. Melarange. 2001. Neural control of muscle relaxation in echinoderms. *J. Exp. Biol.* **204:** 875–885.

Hidaka, M., and K. Takahashi. 1983. Fine structure and mechanical properties of the catch apparatus of the sea-urchin spine, a collagenous connective tissue with muscle-like holding capacity. *J. Exp. Biol.* **103:** 1–14.

Hodgkin, A. L., and P. Horowicz. 1960. Potassium contractures in single muscle fibres. *J. Physiol.* **153:** 386–403.

Motokawa, T. 1981. The stiffness change of the holothurian dermis caused by chemical and electrical stimulation. *Comp. Biochem. Physiol. C* **70:** 41–48.

Motokawa, T. 1982. Factors regulating the mechanical properties of holothurian dermis. *J. Exp. Biol.* **99:** 29–41.

Motokawa, T. 1983. Mechanical properties and structure of the spine-joint central ligament of the sea urchin, *Diadema setosum* (Echinodermata, Echinoidea). *J. Zool. (Lond.)* **201:** 223–235.

Motokawa, T. 1988. Catch connective tissue: a key character for echinoderms' success. Pp. 39–54 in *Echinoderm Biology,* R. D. Burke, P. V. Mladenov, P. Lambert, and R. L. Parsley, eds. A. A. Balkema, Rotterdam.

Perez-Acevedo, N. L., H. Marrero, J. del Castillo, and D. S. Smith. 1998. Transient wrinkles in a variable length echinoid tendon. Pp. 783–790 in *Echinoderms: San Francisco,* R. Mooi and M. Telford, eds. A. A. Balkema, Rotterdam.

Ruppert, E. E., and R. D. Barnes. 1994. *Invertebrate Zoology,* 6th ed. Saunders, Fort Worth, TX.

Shingyoji, C., and M. Yamaguchi. 1995. Effects of acetylcholine, octopamine, ATP, dopamine, and electrical stimulation on the spine muscle of the sea urchin, *Anthocidaris crassispina. Comp. Biochem. Physiol. C* **111:** 23–32.

Smith, D. S., S. A. Wainwright, J. Baker, and M. L. Cayer. 1981. Structural features associated with movement and 'catch' of sea-urchin spine. *Tissue Cell* **13:** 299–320.

Takahashi, K. 1967a. The catch apparatus of the sea-urchin spine I. Gross histology. *J. Fac. Sci. Univ. Tokyo, Sect. IV* **11:** 109–120.

Takahashi, K. 1967b. The catch apparatus of the sea-urchin spine II. Responses to stimuli. *J. Fac. Sci. Univ. Tokyo Sect. IV* **11:** 121–130.

Wilkie, I. C. 1996a. Mutable collagenous tissues: extracellular matrix as mechano-effector. Pp. 61–102 in *Echinoderm Studies,* Vol. 5, M. Jangoux and J. M. Lawrence, eds. A. A. Balkema, Rotterdam.

Wilkie, I. C. 1996b. Mutable collagenous structure or not? A comment on the re-interpretation by del Castillo *et al.* of the catch mechanism in the sea urchin spine ligament. *Biol. Bull.* **190:** 237–242.

Wilkie, I. C. 2002. Is muscle involved in the mechanical adaptability of echinoderm mutable collagenous tissue? *J. Exp. Biol.* **205:** 159–165.

Reference: *Biol. Bull.* **208:** 36–46. (February 2005)

Dietary Preference and Digestive Enzyme Activities as Indicators of Trophic Resource Utilization by Six Species of Crab

DANIELLE JOHNSTON* AND JOEL FREEMAN#

School of Aquaculture, Tasmanian Aquaculture and Fisheries Institute, University of Tasmania, Launceston, Tasmania, Australia 7250

Abstract. The digestive physiology and stomach contents of six crab species from a variety of habitats were investigated to provide an indication of their digestive capability and dietary preferences. Stomach contents varied between species, but the key enzymes present were generally consistent with the types of dietary material being ingested. *Nectocarcinus integrifons* (red rock crab) consumed large quantities of seagrass and had high cellulase activity (0.02 ± 0.004 units mg^{-1}) to digest the constituent cellulose. *Petrolisthes elongatus* (porcelain crab) ingested brown and green phytoplankton and algae and had considerable laminarinase (0.35 ± 0.08 units mg^{-1}) and β-glucosidase (0.025 ± 0.005 units mg^{-1}) activities to digest the laminarin in its diet. *Leptograpsus variegatus* (omnivorous swift-footed shore crab) had high activities of protease (1.2 ± 0.02 units mg^{-1}), α-glucosidase, and α-amylase and appeared well equipped to utilize both dietary protein and carbohydrate. Stomach contents in *Nectocarcinus tuberculosus* (velvet crab) and *Carcinus maenas* (green crab) also suggest that these species are omnivorous. *N. tuberculosus* had high cellulase and chitinase for digesting the cellulose in plants and the chitin in invertebrate shells respectively. *C. maenas* had intermediate digestive enzyme levels and may employ more of a generalist feeding strategy than other species. *Plagusia chabrus* (speedy crab) is carnivorous, consuming encrusting bryozoans, hydroids, crustaceans, and fish. It has high protease activity, particularly trypsin (0.73 ± 0.12 units mg^{-1}), to digest the protein in its animal prey. Each species of crab studied had a complex suite of digestive enzymes, the relative activities of which reflected individual and very different species-specific dietary niches.

Received 20 May 2004; accepted 6 October 2004.

* To whom correspondence should be addressed, at WA Marine Research Laboratories, PO Box 20, North Beach, Western Australia 6920, Australia. E-mail: djohnston@fish.wa.gov.au

Current address: Photobioenergetics, Research School of Biological Sciences, The Australian National University, Australian Capital Territory 0200, Australia.

Introduction

Crabs live in a variety of habitats with varying distributions and abundance of dietary items, so stomach contents typically include a diverse range of prey (Paul, 1981; Williams, 1982; Wear and Haddon, 1987). The variation in stomach contents between species from different habitats may reflect an opportunistic or versatile feeding nature where food items are consumed in proportion to their abundance in the surrounding habitat (Choy, 1986; Wolcott and Nancy, 1992), or it may indicate that crabs actively select habitat based on the presence of suitable food. Although most studies on the feeding habits of decapod crustaceans are based on the observation of stomach contents, stomach contents do not provide any information on dietary preference or the suitability of the diet for maintaining the animal. Similarly, stomach contents cannot help discriminate between generalist and targeted feeding strategies. Digestive enzymes however, may be a complementary tool useful for determining which dietary components are most effectively metabolized (Brêthes *et al.*, 1994). By understanding the digestion and assimilation of specific dietary components, we could identify the type of prey that the animals prefer and those that they are best equipped to digest. For example, carnivorous species exhibit a wide range and high activity of proteolytic enzymes to digest their high-protein diet, whereas herbivores and omnivores that ingest large amounts of carbohydrates possess highly active carbohydrases. Previous studies on the enzymatic system of decapod crusta-

ceans have demonstrated this link between diet composition and the presence of digestive enzymes (Kristensen, 1972; Lee *et al.*, 1984; Johnston and Yellowlees, 1998; Hidalgo *et al.*, 1999; Figueiredo *et al.*, 2001).

The measurement of digestive enzyme synthesis is a tool commonly used to study trophic relationships in many invertebrate groups (McClintock *et al.*, 1991; Brêthes *et al.*, 1994). However, these studies have typically been limited to a few enzymes within one species (McClintock *et al.*, 1991; Brêthes *et al.*, 1994; Johnston and Yellowlees, 1998; Figueiredo *et al.*, 2001) or just one enzyme in a number of species (Galgani *et al.*, 1984). Our knowledge of crab digestive enzyme physiology is also limited. The few enzymes that have been documented include trypsin and carboxypeptidases A and B in *Callinectes sapidus* (blue crab) (Dendinger, 1987; Dendinger and O'Connor, 1990); α-amylase in *Carcinus maenas* (green crab) (Blandamer and Beechy, 1964); and α-glucosidase in *Cancer borealis* (jonah crab), *Cancer irroratus* (rock crab) (Brun and Wojtowicz, 1976), and *C. sapidus* (blue crab) (McClintock *et al.*, 1991). From a dietary perspective, Norman and Jones (1990) used activity of laminarinase as an indicator of the ability of *Liocarcinus puber* (velvet swimming crab) to utilize the brown algae frequently found in its stomach. Brêthes *et al.* (1994) used laminarinase and other enzymes as an index of trophic resource utilization by *Chionectes opilio* (snow crab).

The present study investigates stomach contents and digestive enzyme activities in six species of crab that inhabit a variety of habitats and specialized dietary niches. We examined the following crabs: *Nectocarcinus integrifons* (Latreille) (red rock crab), *Petrolisthes elongatus* (Milne Edwards) (porcelain crab), *Leptograpsus variegatus* (Fabricius) (swift-footed shore crab), *Carcinus maenas* (Linnaeus) (green crab), *Plagusia chabrus* (Linnaeus) (speedy crab), and *Nectocarcinus tuberculosus* (Milne Edwards) (velvet crab). The objectives of this study were (1) to determine dietary preferences for each of the six crab species, using stomach content analysis, (2) to quantify the activities of a range of digestive proteases and carbohydrases in each crab species to determine how various food sources available to the crabs are utilized, and (3) to use dietary preferences and substrate utilization to help identify the position of the crabs in the trophic network of the coastal environment.

Materials and Methods

Collection

Crabs were collected from a number of sites in Tasmania by hand or by trapping. Collection was standardized to adults of each species during their periods of active feeding. When baited traps were used, the bait was positioned such that crabs could not ingest it and thereby bias the analysis of stomach contents. *Nectocarcinus tuberculosus* was collected at night by scuba at Recherche Bay (43°0′S, 147°24′E) or in baited traps set overnight at Georges Bay (41°19′S, 148°15′E). *Petrolithes elongatus*) and *Leptograpsus variegatus*) were collected by hand from the intertidal zone at Little Beach (41°31′S, 148°16′E) and in the Derwent River (42°53′S, 147°19′E) respectively. *Carcinus maenas*) and *Nectocarcinus integrifons*) were collected in baited traps set overnight at Georges Bay (41°19′S, 148°15′E). *Plagusia chabrus*) was collected at night from the research vessel RV *Challenger*, using baited traps at Great Oyster Bay (42°15′S, 148°16′E). Following collection, each crab was placed on ice for 10–20 min, after which its carapace, digestive gland, and stomach were removed. Digestive glands were frozen in liquid nitrogen and stored at −20 °C; stomachs were fixed in 10% formalin in 35 ppt seawater.

Stomach content verification

Each stomach was visually assessed for fullness (1 = empty, 2 = 25%, 3 = 50%, 4 = 75%, 5 = 100% full), and those with a score of 3 to 5 were dissected. The contents were examined using dissecting and compound microscopes and identified to the lowest possible taxonomic grouping by using appropriate keys. The stomachs of specimens of *L. variegatus* were not collected in this study, preventing a stomach content analysis.

Enzyme analysis

Individual digestive glands were thawed and homogenized for 5 min in chilled 100 m*M* Tris, 20 m*M* NaCl buffer, pH 7.0, using an UltraTurrax homogenizer. The homogenate was centrifuged at 968 *g*, and the supernatant containing digestive gland extract was transferred into microfuge tubes and stored at −20 °C.

Detailed procedures for enzyme assays are discussed elsewhere (Johnston, 2003). Briefly, total protease activity was measured using the casein hydrolysis method (Kunitz, 1947) as modified by Walter (1984) using tyrosine as the standard. Trypsin activity was measured using *N*-α-benzoyl-arginine-ρ-nitroanalide (BAPNA) as substrate using the molar absorption coefficient, ε, of 9300 $M^{-1} \cdot cm^{-1}$ for ρ-nitroanaline (Stone *et al.*, 1991). α-Amylase activity was determined using the method of Biesiot and Capuzzo (1990), modified after Bernfeld (1955). α-Glucosidase, β-glucosidase, and chitinase activities were measured using the substrates ρ-nitrophenyl α-D-glucopyranoside, ρ-nitrophenyl β-D-glucopyranoside, and ρ-nitrophenol *N*-acetyl β-D-glucosaminide, respectively (Erlanger *et al.*, 1961). Cellulase activity was measured using the substrate sodium carboxymethyl cellulose (CM-cellulose). Laminarinase activity was measured using laminarin as the substrate.

We defined one enzyme unit (U) as the amount of en-

zyme that catalyzed the release of 1 μmol of product per minute, which we calculated using the appropriate molar extinction coefficient (ε) or a standard curve. Specific activity was defined as enzyme activity (U) per milligram of digestive gland protein (U mg protein^{-1}). Protein concentration was determined using the method of Bradford (1977), using bovine serum albumin as the standard. Enzyme assays were performed at 30 °C and the absorbances read using a TECAN Spectro Rainbow Thermo microplate reader (trypsin, α-amylase, α-glucosidase, β-glucosidase, chitinase) or a UNICAM 8625 UV/visible spectrophotometer (total protease, cellulase, laminarinase). Data points are the mean of duplicate assays accounting for the appropriate blanks, and each assay reports the mean ± standard error of five replicate crabs for each species, with the exception of *N. tuberculosus*, for which 10 individuals were used.

Statistical analysis

Based on the activities for each enzyme within a species, differences between species were analyzed using a multivariate analysis of variance (MANOVA). Unlike univariate analyses, this analysis allows for the simultaneous comparison of species means for each enzyme while maintaining the chosen magnitude of type 1 error ($P = 0.05$) as well as considering the correlation between enzymes within a species. Following MANOVA, significant differences were explored using a canonical discriminant analysis (CDA). Each species was plotted in the reduced multivariate space, in which the new axes (CDA 1, CDA 2, and CDA 3) explain a proportion of the total variability in the data. Group (species) centroids were plotted using the unstandardized canonical discriminant functions evaluated at group means, and each circle indicates the 95% confidence ellipses. Superimposed on this plot is the association between the new axes and the enzymes that were measured. This is displayed as a vector diagram in which the direction and length of the vector is a measure of the association between the enzyme and the axes. Those groups in which ellipsoids are not overlapping signify differences between species. The correlation between the position of each species relative to the vector diagram determines the enzyme or enzymes responsible for its separation.

Results

Stomach contents

Stomachs of all crabs had a large proportion of unidentifiable material that was either semi-digested or detritivorous in nature. Stomachs of *Nectocarcinus integrifons* and *Petrolisthes elongatus* contained no animal material. *N. integrifons* had large quantities of vascular plant material removed from either living or recently detached plants, whereas the stomachs of *P. elongatus* consisted largely of brown and green phytoplankton and larger algal pieces (Table 1). Stomachs of *Carcinus maenas* and *Nectocarcinus tuberculosus* had both plant and animal material (Table 1). Stomachs completely full of gastropod shells and bivalves were common in both crab species. Plant material was less common and consisted of small pieces of vascular material. Stomachs of *Plagusia chabrus* had very little identifiable

Table 1

Gut content items that were identified in the stomach of individual crabs with a stomach fullness greater than 3 (>50% full), and the corresponding diet from the literature

	Stomach content items				
Species	Animal	Plant	Literature diet	Reference	Classification
Nectocarcinus integrifons	—	Vascular plant material	Feeds predominantly on the seagrass *Posidonia australis*	Klumpp & Nichols (1983)	Herbivore
Petrolisthes elongatus	—	Brown and green phytoplankton and algal pieces	Filter feeding — phytoplankton (*e.g.*, diatoms); Deposit feeding — detritus	Achituv & Pedrotti (1999); Kropp (1981)	Herbivore
Leptograpsus variegatus	No stomachs collected		Limpets and barnacles; green and red algae	Skilleter & Anderson (1986); Griffin (1971)	Omnivore
Carcinus maenas	Molluscs	Vascular plant material	Bivalves, crustaceans, gastropods, and algae	Elner (1981)	Omnivore
Nectocarcinus tuberculosus	Molluscs, unidentifiable animal parts	Vascular plant material	—	—	Omnivore
Plagusia chabrus	Unidentifiable animal parts and small crustaceans	—	Encrusting animals — bryozoans, sponges, and hydroids	Edgar (2000)	Carnivore
			Red algae and coralline algae	Griffin (1971)	

plant matter and contained fragments of animal material, possibly small encrusting species of bryozoans and hydroids, as well as exoskeletons of small crustaceans and some fish parts (Table 1).

Digestive enzyme activity

Proteases. The highest protease activity was displayed by *Leptograpsus variegatus* (1.19 ± 0.02 units mg^{-1}) and *P. chabrus* (0.99 ± 0.05 units mg^{-1}). Lowest activity was measured in *N. integrifons* (0.34 ± 0.05 units mg^{-1}), *N. tuberculosus* (0.39 ± 0.02 units mg^{-1}), and *C. maenas* (0.46 ± 0.02 units mg^{-1}), with less than half the activity of *L. variegatus* and *P. chabrus* (Fig. 1A). The highest trypsin activity was exhibited by *P. chabrus* (0.73 ± 0.12 units mg^{-1}) and *L. variegatus* (0.46 ± 0.03 units mg^{-1}) and the lowest activity by *N. integrifons* (0.14 ± 0.03 units mg^{-1}) (Fig. 1B).

Carbohydrases. Carbohydrase activity was present in all crabs, with hydrolysis of both α- and β-linked substrates recorded in all species. α-Amylase activity was about three times higher in *Petrolisthes elongatus* (0.29 ± 0.04 units mg^{-1}) than in *N. tuberculosus* (0.09 ± 0.02 units mg^{-1}) (Fig. 2A). α-Glucosidase specific activity was highest in *L. variegatus* (0.0022 ± 0.0002 units mg^{-1}) and was about twice the level recorded for all other species. *Petrolisthes elongatus* had negligible α-glucosidase activity (Fig. 2B).

β-Glucosidase activity was highest in *P. elongatus* (0.025 ± 0.005 units mg^{-1}), about three times greater than in *L. variegatus* (0.007 ± 0.0008 units mg^{-1}) (Fig. 3A). Although variable, laminarinase activity was highest in *P. elongatus* (0.35 ± 0.08 units mg^{-1}), and *L. variegatus* also had substantial activity (0.18 ± 0.02 units mg^{-1}) (Fig. 3B). The other four species had comparatively lower activity, ranging between 0.058 ± 0.01 (*N. tuberculosus*) and 0.016 ± 0.003 (*C. maenas*) units mg^{-1}. Cellulase activity was highest for *N. integrifons* (0.019 ± 0.004 units mg^{-1}) and lowest in *C. maenas* (0.0014 ± 0.0006 units mg^{-1}) and *Plagusia chabrus* (0.0019 ± 0.0014 units mg^{-1}) (Fig. 4A). Chitinase activity was similar for most species, ranging between 0.023 ± 0.003 (*P. chabrus*) and 0.041 ± 0.005 (*L. variegatus*) units mg^{-1}. The exception was *Petrolisthes elongatus*, which had a substantially lower chitinase activity (0.006 ± 0.001 units mg^{-1}) (Fig. 4B).

Relationship between enzyme complement and crab species

Significant differences were found between crab species when the specific activities of all enzymes were compared using MANOVA (Pillai's Trace = 3.347; $F_{(40,130)} = 6.581$, $P < 0.001$). The CDA explained 72.2% of the variation on the first and second axes (CDA 1 and CDA 2) and 39.6% on the second and third axes (CDA 2 and CDA 3) (Figs. 5 and 6). The greatest difference among the species was along the first axis, CDA 1 (*x* axis), which explained 51% of the variation (Fig. 5). This difference was largely due to separation between the species on the basis of the high activity of laminarinase and β-glucosidase in *P. elongatus*, and the high activity of α-glucosidase displayed by *L. variegatus*. The second axis, CDA 2 (*y* axis) also showed differences between the species and accounted for 21.2% of variation, with *Plagusia chabrus* being separated from other species by its high activity of trypsin and total protease, while *N. integrifons* and *N. tuberculosus* were separated by their activity of cellulase and chitinase (Fig. 5). The third axis (CDA 3) explained 18.4% of the variation and, when plotted with CDA 2, shows a separation between *N. integrifons* and *N. tuberculosus* (Fig. 6). These two species are still separated along CDA 2 by their cellulase and chitinase activity, but are now separated from each other along CDA 3 by the higher activity of cellulase in *N. integrifons* and the higher

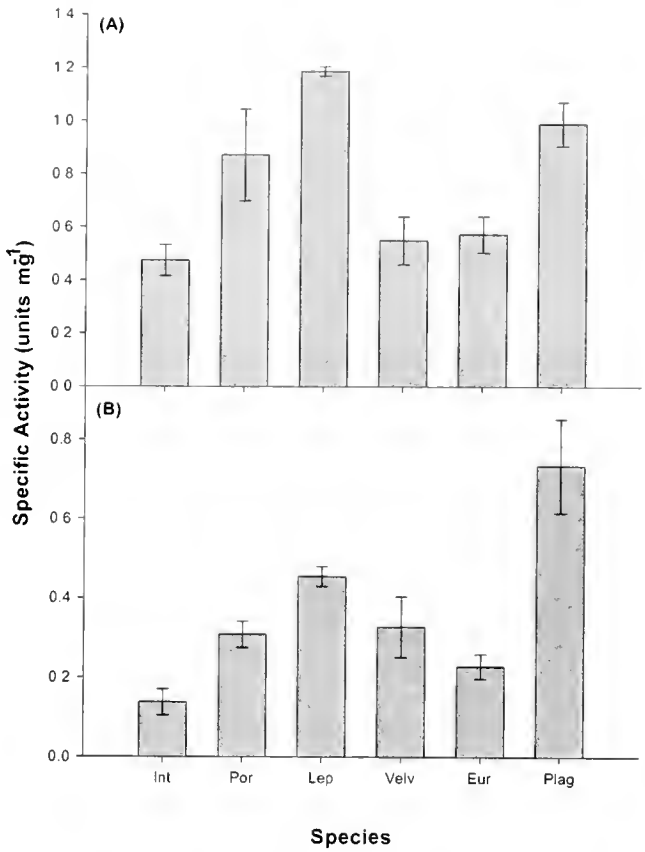

Figure 1. Specific activity of (A) total protease and (B) trypsin measured from crude digestive gland extract of six crab species with different feeding habits. Values are mean (units mg^{-1}) ± S.E. where units are in μmol ρ-nitroanalide min^{-1} for trypsin and μg tyrosine min^{-1} for total protease. Key to crab species: Int = *Nectocarcinus integrifons* (n = 5), Por = *Petrolisthes elongatus* (n = 5), Lep = *Leptograpsus variegatus* (n = 5), Velv = *Nectocarcinus tuberculosus* (n = 10), Eur = *Carcinus maenas* (n = 5), Plag = *Plagusia chabrus* (n = 5).

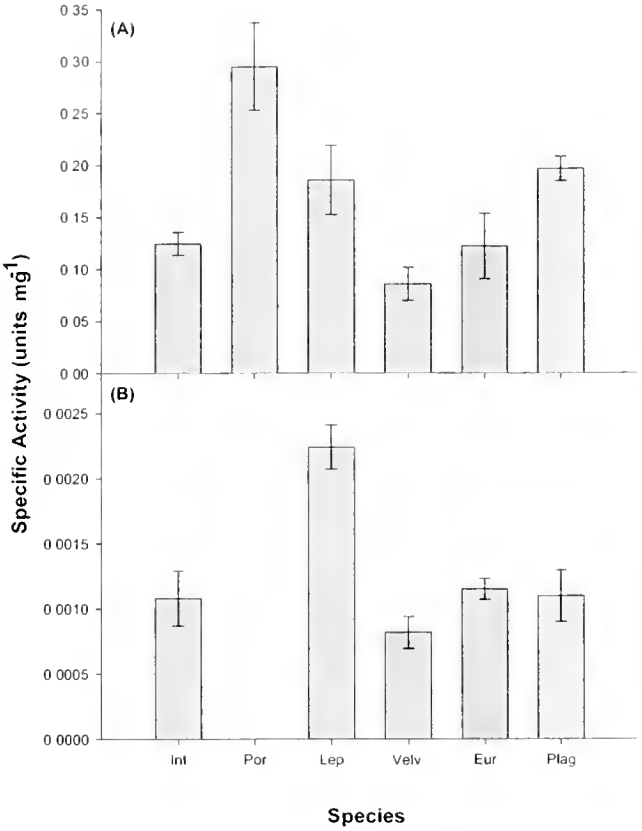

Figure 2. Specific activity of (A) α-amylase and (B) α-glucosidase measured from crude digestive gland extract of six crab species with different feeding habits. Values are mean (units mg^{-1}) ± S.E. where units are in μmol maltose min^{-1} for α-amylase and in μmol ρ-nitrophenol min^{-1} for α-glucosidase. Key to crab species: Int = *Nectocarcinus integrifons* (n = 5), Por = *Petrolisthes elongatus* (n = 5), Lep = *Leptograpsus variegatus* (n = 5), Velv = *Nectocarcinus tuberculosus* (n = 10), Eur = *Carcinus maenas* (n = 5), Plag = *Plagusia chabrus* (n = 5).

trypsin activity of *N. tuberculosus*. The *C. maenas* lies central on both plots, only being separated in Figure 6 by its relative activity of α-glueosidase.

Discussion

We investigated the dietary preference of six species of crab on the basis of their stomach contents and used analysis of digestive enzymes to determine which dietary components are most likely being assimilated. Digestive enzyme activities are an effective tool for identifying particular components of an animal's diet. High proteolytic activity reflects a diet high in protein, high carbohydrase activity reflects a diet high in starch or cellulose, and high lipase activities reflect a diet high in fat (Lee *et al.*, 1984; Johnston and Yellowlees, 1998; Johnston, 2003). Multivariate analyses (MANOVA) simultaneously compared the relative activities of proteases and carbohydrases within each species, as well as individual enzymes between species, and separated the six crab species into separate dietary preferences. For each species, one enzyme (*i.e.*, laminarinase, β-glucosidase, cellulase, trypsin, total protease, and α-glucosidase) was responsible for separating each species from the other five (Figs. 5, 6), suggesting that each species occupies a different dietary niche.

Plagusia chabrus *(speedy crab)*

Stomachs of *P. chabrus* contained fragments of animal material, possibly of small encrusting species of bryozoans and hydroids (see Edgar, 2000) (Table 1). *Plagusia chabrus* had very little identifiable plant matter within its stomach and appears to be almost totally carnivorous. However, red and coralline algae have previously been found in the stomach of this species (Griffin, 1971). This apparent discrepancy may be due to differences in the abundance and structure of potential prey communities (Paul, 1981; Haefner, 1990; Freire, 1996). Stomach contents of *P.*

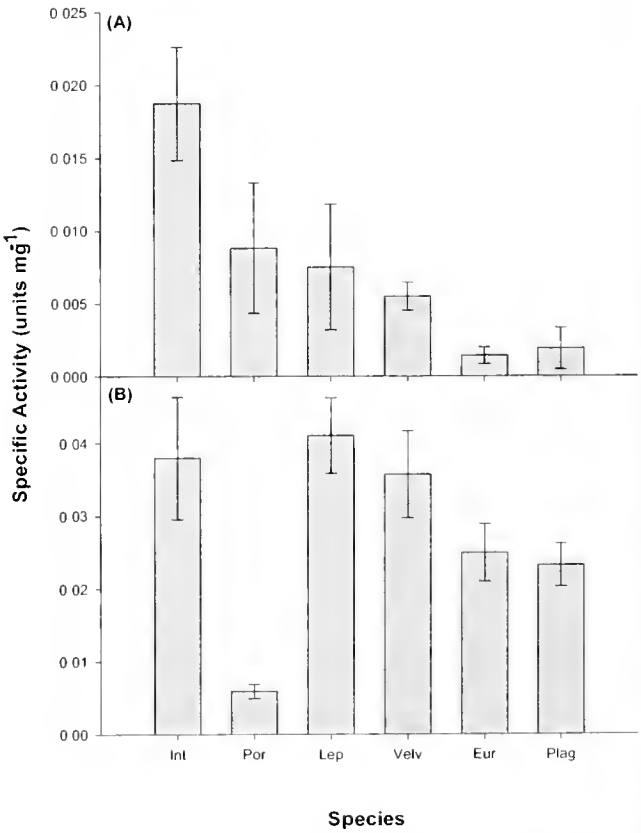

Figure 3. Specific activity of (A) cellulase and (B) chitinase measured from crude digestive gland extract of six crab species with different feeding habits. Values are mean (units mg^{-1}) ± S.E., where units are in μmol glucose min^{-1} for cellulase and in μmol ρ-nitrophenol min^{-1} for chitinase. Key to crab species: Int = *Nectocarcinus integrifons* (n = 5), Por = *Petrolisthes elongatus* (n = 5), Lep = *Leptograpsus variegatus* (n = 5), Velv = *Nectocarcinus tuberculosus* (n = 10), Eur = *Carcinus maenas* (n = 5), Plag = *Plagusia chabrus* (n = 5).

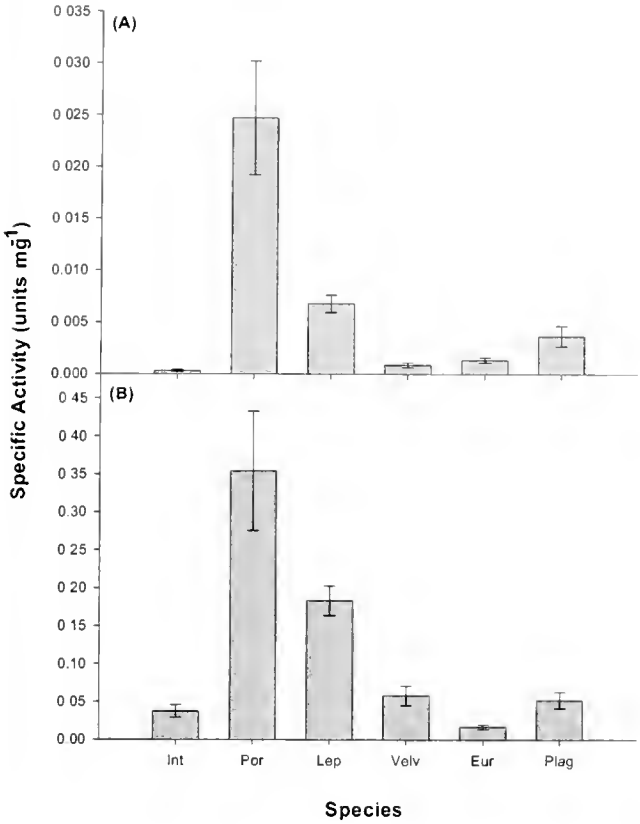

Figure 4. Specific activity of (A) β-glucosidase and (B) laminarinase measured from crude digestive gland extract of six crab species with different feeding habits. Values are mean (units mg^{-1}) ± S.E., where units are in μmol ρ-nitrophenol min^{-1} for β-glucosidase and in μmol glucose min^{-1} for laminarinase. Key to crab species: Int = *Nectocarcinus integrifons* (n = 5), Por = *Petrolisthes elongatus* (n = 5), Lep = *Leptograpsus variegatus* (n = 5), Velv = *Nectocarcinus tuberculosus* (n = 10), Eur = *Carcinus maenas* (n = 5), Plag = *Plagusia chabrus* (n = 5).

chabrus collected in this study were similar to those observed by Edgar (2000). In both studies, crabs were sampled subtidally from exposed reef in 3–5 m of water. In contrast, the majority (72%) of *P. chabrus* captured by Griffin (1971) were collected from exposed rocky platforms in the intertidal zone where red and coralline algae are more common. The greater abundance of these algae may make them a more attractive food source or more likely to be incidentally ingested.

Reflecting its carnivorous nature, *P. chabrus* displayed high protease and trypsin activity, and it was this high activity of protease and trypsin that separated *P. chabrus* from the other crab species in the MANOVA. *P. chabrus* had the highest trypsin activity encountered in any of the species studied. The trypsin activity was similar in value to that of the slipper lobster, *Thenus orientalis* (0.54 units mg^{-1}), and the karuma prawn, *Penaeus japonicus* (0.73 units mg^{-1}), two species whose diets also contain considerable amounts of protein (Maugle, 1982; Johnston and Yellowlees, 1998) (Table 2).

The low plant content in the diet of *P. chabrus* is reflected by its low activity of cellulase, an enzyme that breaks down the cellulose in plants. The high α-amylase activity is likely to reflect the high glycogen content of animal prey consumed by *P. chabrus*. Similarly high amylase activity in the carnivorous American lobster *Homarus americanus* (1.5 units mg^{-1}) also reflects digestion of glycogen in animal prey (Wojtowicz and Brockerhoff, 1972; Table 2). However, α-amylase is also involved in the digestion of starch in plant tissue (see *P. elongatus* below), so the relationship between amylase activity and carnivory is not ubiquitous.

Leptograpsus variegatus *(swift-footed shore crab)*

Two comprehensive dietary studies of *L. variegatus* revealed a mixture of plant material (the green alga *Ulva lactuca*, the coralline alga *Corallina officinalis*, and the red algae *Polysiphonia* sp. and *Ceramium* sp.) and animal material (limpets and barnacles) within its stomach (Skilleter and Anderson, 1986; Griffin, 1971). These studies suggest that *L. variegatus* is an omnivore that actively scavenges in the intertidal zone for invertebrates and algae (Table 1).

We found *L. variegatus* to have the highest protease activity of all species studied, an observation not immedi-

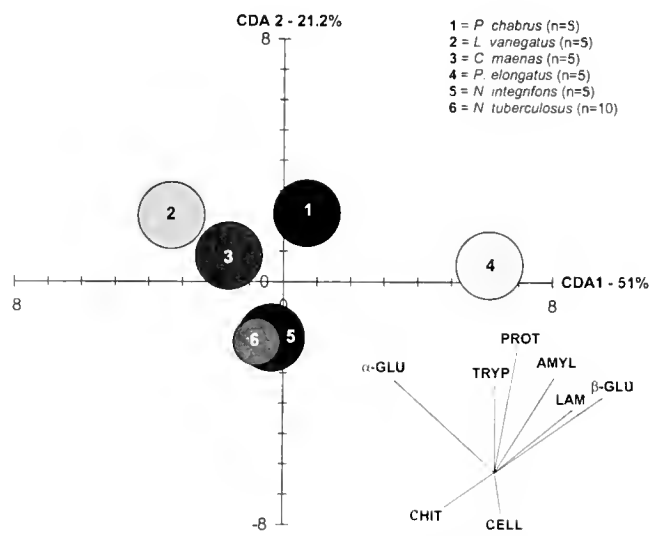

Figure 5. Results of the canonical discriminant analysis are displayed for the first (CDA 1) and second (CDA 2) canonical discriminant functions evaluated at group means. Group means are central to the 95% confidence ellipses. In the bottom right corner of each graph is a vector diagram for the enzymes measured. The direction and length for each enzyme is an indication of the association between the enzyme and the axes and can be used to interpret differences among the species. Key to vector diagram: α-GLU = α-glucosidase, AMYL = α-amylase, β-GLU = β-glucosidase, CELL = cellulase, CHIT = chitinase, LAM = laminarinase, PROT = total protease, TRYP = trypsin.

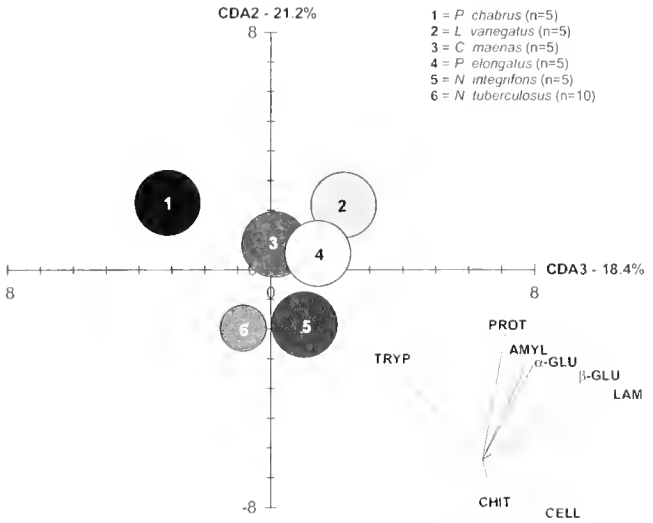

Figure 6. Results of the canonical discriminant analysis are displayed for the second (CDA 2) and third (CDA 3) canonical discriminant functions evaluated at group means. Group means are central to the 95% confidence ellipses. In the bottom right corner of each graph is a vector diagram for the enzymes measured. The direction and length for each enzyme is an indication of the association between the enzyme and the axes and can be used to interpret differences among the species. Key to vector diagram: α-GLU = α-glucosidase, AMYL = α-amylase, β-GLU = β-glucosidase, CELL = cellulase, CHIT = chitinase, LAM = laminarinase, PROT = total protease, TRYP = trypsin.

ately consistent with an omnivorous feeding strategy. Although it is generally accepted that high protease activity reflects a carnivorous diet, other studies have also found high proteolytic activity in omnivores (Jonas *et al.*, 1983; Hidalgo *et al.*, 1999). The sea lettuce (*Ulva lactuca*), which is ingested in large quantities by *L. variegatus* (Lobban and Harrison, 1997), is high in protein (15% of the organic matter) and may contribute to the high protease activity in this crab.

More in line with an omnivorous diet, the α-glucosidase activity was about twice as high in *L. variegatus* as in any other species we studied. This high α-glucosidase activity was responsible for separating *L. variegatus* from all other crab species in the MANOVA and, coupled with substantial α-amylase activity, suggests that *L. variegatus* is well equipped to utilize the carbohydrates within its diet. The strong activity of α-enzymes indicates that α-linked storage carbohydrates are important in its diet. Such storage products are present in both green algae (*i.e.*, starch, which is a mixture of amylose and amylopectin) and red algae (*i.e.*, floridean starch, a branched glucan similar to amylopectin) (Lobban and Harrison, 1997). *L. variegatus* also had substantial laminarinase activity, which suggests that this crab may also ingest brown algae, a component not described in previous dietary studies (Griffin, 1971; Skilleter and Anderson, 1986).

Carcinus maenas *(green crab) and* Nectocarcinus tuberculosus *(velvet crab)*

Carcinus maenas and *N. tuberculosus* had both plant and animal (gastropod shells and bivalves) material within their stomachs (Table 1), suggesting they are omnivores. *Carcinus maenas* is well studied and is described as a voracious predator feeding primarily on bivalve molluscs, polychaetes, and small crustaceans (Elner, 1981; MacKinnon, 1997) (Table 1). However, algae have also been frequently observed in its stomach but generally do not contribute more than about 10% to the total volume of stomach contents (Elner, 1981). The diet of *N. tuberculosus* has not been studied, but the morphology of its mouthparts, in particular the specialized mandibles, appears suited to grinding hard animals (such as molluscs) and vascular plant material (Salindeho and Johnston, 2003).

Although our stomach content analysis suggests both species to be omnivorous, their digestive enzyme complement differs from that of the omnivorous *L. variegatus*. Protease activity for both *N. tuberculosus* and *C. maenas* was less than half that of *L. variegatus*. This may be due to a reliance on plant material with lower protein content than the sea lettuce consumed by *L. variegatus*. The protease levels of *N. tuberculosus* and *C. maenas* are similar to that of the scavenging omnivorous redclaw crayfish *Cherax quadricarinatus* (0.236 units mg^{-1}) (Figueiredo *et al.*, 2001) (Table 2).

Despite the plant material in the stomach of these species, laminarinase activity was low, suggesting that brown algae are not an important dietary component of either species. In the MANOVA, *N. tuberculosus* is separated from the other crab species by its cellulase and chitinase activity, which reflects its ability to break down and digest plant cellulose as well as the chitinous shells of molluscs and other invertebrates. Interestingly, *C. maenas* lies fairly centrally on the axis of both CDA plots (Figs. 5, 6), which suggests they have intermediate levels of all digestive enzymes compared to the other crab species. *C. maenas* may be more of a generalist feeder, utilizing a broader spectrum of dietary items. Such a strategy would help to explain its incredible success in a wide range of habitats (Cohen *et al.*, 1995).

Nectocarcinus integrifons *(red rock crab)*

Herbivory is common in crabs—the consumption of vascular plants has been observed in several species (Giddins *et al.*, 1986; Kyomo, 1992; Woods and Schiel, 1997). The stomachs of *N. integrifons* contained no animal material but did contain large quantities of vascular plant material (Table 1). Klumpp and Nichols (1983) found the seagrass *Posidonia australis* to occur in the stomachs of 93% of the *N. integrifons* individuals sampled and to occupy 85% of stomach volume. Consistent with a diet low in protein (seagrass is only 7% protein), protease and trypsin activities were

Table 2

Comparison of specific activities of crustacean proteases and carbohydrases from crude digestive gland extracts

	Enzyme								
Species	Prot	Tryp	α-Am	α-Glu	β-Glu	Cell	Lam	Chit	Reference
Nectocarcinus integrifons	0.47	0.14	0.12	0.0010	0.0003	0.019	0.037	0.038	This study
Petrolisthes elongatus	0.87	0.31	0.29	Neg	0.0250	0.009	0.35	0.006	
Leptograpsus variegatus	1.2	0.46	0.19	0.0022	0.0067	0.007	0.18	0.041	
Nectocarcinus tuberculosus	0.55	0.33	0.09	0.0008	0.0009	0.005	0.058	0.036	
Carcinus maenas	0.57	0.23	0.12	0.0012	0.0013	0.001	0.017	0.025	
Plagusia chabrus	0.99	0.73	0.20	0.0011	0.0037	0.002	0.052	0.023	
Crabs									
Carcinus maenas			1.2						Blandamer & Beechy (1964)
Chionoecetes opilio			0.10						Brêthes *et al.* (1994)
Callinectes sapidus				0.0096	0.01				McClintock *et al.* (1991)
Cancer irroratus			0.24	0.001	0.008			0.23	Brun & Wojtowicz (1976)
Cancer borealis			0.12	0.001	0.009			0.09	Brun & Wojtowicz (1976)
Prawns									
Penaeus vannamei				0.07					Le Chevalier & Van Wormhoudt (1998)
P. monodon			0.13				0.45		Wigglesworth & Griffith (1994)
P. keraturus		0.060							Galgani *et al.* (1984)
P. japonicus		0.057							Galgani *et al.* (1984)
P. japonicus		0.73							Maugle (1982)
P. indicus				0.016	0.014		0.036		Omondi & Stark (1995)
Lobsters and Crayfish									
Homarus americanus			1.5						Wojtowicz & Brockerhoff (1972)
Thenus orientalis		0.54		0.022	0.004	Neg		0.42	Johnston & Yellowlees (1998)
Cherax quadricarinatus		0.236	0.821	0.11	0.041		0.12	0.15	Figueiredo *et al.* (2001)
C. quadricarinatus						0.03			Xue *et al.* (1999)

Prot = Total protease; Tryp = Trypsin; α-Am = α-Amylase; α-Glu = α-Glucosidase; β-Glu = β-Glucosidase; Cell = Cellulase; Lam = Laminarinase; Chit = Chitinase. Substrates and units are identical with those used in this study, with values in units mg^{-1} where units are $\mu mol\ min^{-1}$ except for protease, which is μg tyrosine min^{-1} Neg. = no activity detected.

lower in *N. integrifons* than in the other species. *Nectocarcinus integrifons* had the highest level of cellulase activity, and it is this enzyme that is responsible for separating this crab from other species in the MANOVA. Cellulase is required to digest cellulose, the primary structural component of vascular seagrass. Klumpp and Nichols (1983) also found high cellulase activity in both the digestive gland and stomach contents of *N. integrifons*. Using chemical analysis, they determined that with combined enzymatic and mechanical action, *N. integrifons* is able to digest up to 40% of ingested plant fiber (Klumpp and Nichols, 1983). Redclaw crayfish *C. quadricarinatus* also consumes significant amounts of plant material and has cellulase activity comparable to that of the red rock crab (0.03 units mg^{-1}) (Xue *et al.*, 1999).

Petrolisthes elongatus *(porcelain crab)*

Like *N. integrifons*, *P. elongatus* is herbivorous. Stomach contents contained no traces of animal matter and consisted largely of brown and green phytoplankton and larger algal pieces. Porcelain crabs are able to use their setose third maxillipeds to filter plankton from the water column (Caine, 1975). Although zooplankton could be captured in this fashion, they were not evident in the stomachs of crabs sampled. Alternative feeding methods, such as direct use of

the chelipeds to chop pieces of algae for ingestion or the feeding on detritus, may account for the occurrence of multicellular algae and detritus in the stomachs of *P. elongatus* (Kropp, 1981).

Surprisingly, the herbivorous *P. elongatus* had high total protease activity (Table 2). There are two explanations for this. Firstly, high protease activity may be a physiological adaptation to maximize digestion of small amounts of protein from large volumes of ingested plankton. Microphagous feeding in adult porcelain crabs is similar to planktivorous (phytoplankton) feeding by larval crustaceans. Comparative studies on the digestive enzymes of crustacean larvae indicate that protease activities may be higher in animals that consume phytoplankton than in carnivorous larvae. High protease activity may enable these species to rapidly extract the relatively small protein component from large volumes of food, so there is a net energy gain despite a relatively low overall assimilation efficiency (Kumlu and Jones, 1997; Le Vay *et al.*, 2001). Secondly, it is possible that *P. elongatus* is actually omnivorous and that zooplankton could have been ingested during filter feeding. However, zooplankton was not identified in the stomachs of animals sampled in this study. Furthermore, *P. elongatus* had substantially lower chitinase activity than the other species studied here, suggesting a poor capacity to break down chitin, a structural component of the exoskeleton of zooplankton and other invertebrates. Omnivorous species that do ingest shelled invertebrates, such as *L. variegatus* and *N. tuberculosus*, possess considerable chitinase performance.

The activities of the carbohydrases (indicative of plant digestion) were mixed, giving us an insight into the specific carbohydrates assimilated by *P. elongatus*. α-Amylase activity was very high, about three times higher than in *N. tuberculosus*. High α-amylase activity reflects the high proportion of starch in plants ingested by *P. elongatus* (Sabapathy and Teo, 1993). Interestingly, α-glucosidase activity was negligible, which suggests that although *P. elongatus* is highly efficient at digesting large structural polysaccharides such as starch using α-amylase, it is less effective at digesting smaller oligosaccharides, which are broken down using α-glucosidase.

β-Glucosidase activity was highest in the porcelain crab—about three times greater than in the next highest species, *L. variegatus*. Laminarinase, an enzyme complex that includes exo- and endo-hydrolytic β-1,3 glucanases as well as β-glucosidase, was also the highest in *P. elongatus*. It was this high laminarinase and β-glucosidase activity that separated *P. elongatus* from all other species in the MANOVA. Laminarin is a β-1,3-linked polymer of glucose stored in brown algae (Lobban and Harrison, 1997). The laminarinase and β-glucosidase enzyme combination in *P. elongatus* is ideally suited for digesting the types of algae found within the gut of this species, and these enzymes appear suitable as indicators of the dietary preference for brown algae (Figueiredo *et al.*, 2001; Wigglesworth and Griffith, 1994).

Conclusions—digestive enzyme complement as indicator of diet type

Each species of crab studied had a complex suite of digestive enzymes, the relative activities of which reflected species-specific dietary niches. As opportunistic feeders, crabs have a wide range of digestive enzymes. However, it is clear from this study that the specific enzymes dominant within each crab species are consistent with their particular diets. The porcelain crab *P. elongatus* has high activities of laminarinase and β-glucosidase for digesting dietary brown algae (laminarin). High cellulase activity is necessary to digest the vascular seagrass (cellulose) diet of the red rock crab *N. integrifons*. Significant trypsin and total protease activities break down the high-protein diet of the speedy crab *P. clabrus*. For the swift-footed shore crab *L. variegatus*, digestion of the starch in its predominantly red and green algal diet is achieved *via* high α-glucosidase and α-amylase activities. The velvet crab *N. tuberculosus* has high cellulase activity to digest the cellulose of its plant diet and high chitinase activity to digest the chitinous shells of the molluscs and other invertebrates that it also consumes. The specific nature of the enzymes in most crab species encountered here appears to favor a specific feeding behavior and dietary preference, and demonstrates different strategies of resource use. In contrast to the other species, the green crab *C. maenas* did not appear to have a dominant enzyme, which suggests that it is a generalist feeder that utilizes a broad range of dietary items, which may help to explain its incredible success in a range of diverse habitats.

Acknowledgments

We thank Sam Ibbott and Craig Mackinnon (Marine Research Laboratories, Tasmanian Aquaculture and Fisheries Institute), Rob Gurney (CSIRO), Dean Blunt and Barry Stewart (Tasmanian Clean Water Oysters) for their assistance in the collection of crab species from sites around Tasmania. We also thank Martin Lourey for critical review of final versions of this manuscript.

Literature Cited

Achituv, Y., and M. L. Pedrotti. 1999. Costs and gains of porcelain crab suspension feeding in different flow conditions. *Mar. Ecol. Prog. Ser.* **184:** 161–169.

Bernfeld, P. 1955. Amylases, α and β. *Methods Enzymol.* 1: 149–158.

Biesiot, P. M., and J. M. Capuzzo. 1990. Changes in digestive enzyme activities during early development of the American lobster *Homarus americanus* Milne Edwards. *J. Exp. Mar. Biol. Ecol.* **136:** 107–122.

Blandamer, A., and R. B. Beechy. 1964. The identification of an alpha-amylase in aqueous extracts of the hepatopancreas of *Carcinus maenas*, the common shore crab. *Comp. Biochem. Physiol.* **13:** 97–105.

Bradford, M. M. 1977. A rapid and sensitive method for the quantitation of microgram quantities of proteins utilizing the principle of protein-dye binding. *Anal. Biochem.* **72:** 248–254.

Brêthes, J., B. Parent, and J. Pellerin. 1994. Enzymatic activity as an index of trophic resource utilization by the snow crab *Chionoecetes opilio* (O. Fabricius). *J. Crustac. Biol.* **14:** 220–225.

Brun, G. L., and M. B. Wojtowicz. 1976. A comparative study of the digestive enzymes in the hepatopancreas of the jonah crab (*Cancer borealis*) and rock crab (*Cancer irroratus*). *Comp. Biochem. Physiol. B* **53:** 387–391.

Caine, E. A. 1975. Feeding and masticatory structures of selected Anomura (Crustacea). *J. Exp. Mar. Biol. Ecol.* **18:** 277–301.

Choy, S. C. 1986. Natural diet and feeding habits of the crabs *Linocarcinus puber* and *L. holsatus* (Decapoda, Brachyura, Portunidae). *Mar. Ecol. Prog. Ser.* **31:** 87–99.

Cohen, A. N., J. T. Carlton, and M. C. Fountain. 1995. Introduction, dispersal and potential impacts of the green crab *Carcinus maenas* in San Francisco Bay, California. *Mar. Biol.* **122:** 225–237.

Dendinger, J. E. 1987. Digestive proteases in the midgut gland of the Atlantic blue crab *Callinectes sapidus*. *Comp. Biochem. Physiol. B* **88:** 503–506.

Dendinger, J. E., and K. L. O'Connor. 1990. Purification and characterization of a trypsin-like enzyme from the midgut gland of the Atlantic blue crab, *Callinectes sapidus*. *Comp. Biochem. Physiol. B* **95:** 525–530.

Edgar, G. J. 2000. *Australian Marine Life: the Plants and the Animals of Temperate Waters,* 2nd ed. Reed Books, Melbourne, Australia.

Elner, R. W. 1981. Diet of the green crab *Carcinus maenas* (L.) from Port Hebert, southwestern Nova Scotia. *J. Shellfish Res.* **1:** 89–94.

Erlanger, B. F., N. Kokowsky, and W. Cohen. 1961. The preparation and properties of two chromogenic substrates of trypsin. *Arch. Biochem. Biophys.* **95:** 271–278.

Figueiredo, M. S. R. B., J. A. Kricker, and A. J. Anderson. 2001. Digestive enzyme activities in the alimentary tract of redclaw crayfish, *Cherax quadricarinatus* (Decapoda: Parastacidae). *J. Crustac. Biol.* **21:** 334–344.

Freire, J. 1996. Feeding ecology of *Liocarcinus depurator* (Decapoda: Portunidae) in the Ria de Arousa (Galicia, north-west Spain): effects of habitat, season and life history. *Mar. Biol.* **126:** 297–311.

Galgani, F. G., Y. Benyamin, and H. J. Ceccaldi. 1984. Identification of digestive proteinases of *Penaeus kerathurus* (Forskal): a comparison with *Penaeus japonicus* Bate. *Comp. Biochem. Physiol. B* **72:** 355–361.

Giddins, R. L., J. S. Lucas, M. J. Neilson, and G. N. Richards. 1986. Feeding ecology of the mangrove crab *Neosarmatium smithi* (Crustacea: Decapoda: Sesarmidae). *Mar. Ecol. Prog. Ser.* **33:** 147–155.

Griffin, D. J. G. 1971. The ecological distribution of grapsid and ocypodid shore crabs in Tasmania. *J. Anim. Ecol.* **40:** 597–562.

Haefner, P. A. 1990. Natural diet of *Callinectes ornatus* (Brachyura: Portunidae) in Bermuda. *J. Crustac. Biol.* **10:** 236–246.

Hidalgo, M. C., E. Urea, and A. Sanz. 1999. Comparative study of digestive enzymes in fish with different nutritional habits. Proteolytic and amylase activities. *Aquaculture* **170:** 267–283.

Johnston, D. J. 2003. Ontogenetic changes in digestive enzymology of the spiny lobster, *Jasus edwardsii* Hutton (Decapoda, Palinuridae). *Mar. Biol.* **143:** 1071–1082.

Johnston, D. J., and D. Yellowlees. 1998. Relationship between dietary preferences and digestive enzyme complement of the slipper lobster *Thenus orientalis* (Decapoda: Scyllaridae). *J. Crustac. Biol.* **18:** 126–135.

Jonas, E., M. Ragyanszki, J. Olah, and L. Boross. 1983. Proteolytic digestive enzymes of carnivorous (*Silurus glanis* L.), herbivorous (*Hypophthalmichthys molitrix* Val.) and omnivorous (*Cyprinus carpio* L.) fishes. *Aquaculture* **30:** 145–154.

Klumpp, D.W., and P. D. Nichols. 1983. Utilisation of the seagrass *Posidonia australis* as food by the rock crab *Nectocarcinus integrifons* (Latreille) (Crustacea: Decapoda: Portunidae). *Mar. Biol. Lett.* **4:** 331–339.

Kristensen, J. H. 1972. Carbohydrases of some marine invertebrates with notes on their food and on the natural occurrence of carbohydrates studied. *Mar. Biol.* **4:** 130–142.

Kropp, R. K. 1981. Additional porcelain crab feeding methods. *Crustaceana* **40:** 307–310.

Kumlu, M., and D. A. Jones. 1997. Digestive protease activity in planktonic crustaceans feeding at different trophic levels. *J. Mar. Biol. Assoc. UK* **77:** 159–165.

Kunitz, M. 1947. Crystalline soybean trypsin inhibitor: II. General properties. *J. Gen. Physiol.* **30:** 291–310.

Kyomo, J. 1992. Variations in the feeding habits of males and females of the crab *Sesarma internedia*. *Mar. Ecol. Prog. Ser.* **83:** 151–155.

Le Chevalier, P., and A. Van Wormhoudt. 1998. Alpha-glucosidase from the hepatopancreas of the shrimp, *Penaeus vannamei* (Crustacea-Decapoda). *J. Exp. Zool.* **280:** 384–394.

Le Vay, L., D. A. Jones, A. C. Puello-Cruz, R. S. Sangha, and C. Ngamphongsai. 2001. Digestion in relation to feeding strategies exhibited by crustacean larvae. *Comp. Biochem. Physiol. A* **128:** 623–630.

Lee, P. G., L. L. Smith, and A. L. Lawrence. 1984. Digestive proteases of *Penaeus vannamei* Boone: relationship between enzyme activity, size, and diet. *Aquaculture* **42:** 225–239.

Lobban, C. S., and P. J. Harrison. 1997. *Seaweed Ecology and Physiology.* Cambridge University Press, Cambridge.

MacKinnon, C. 1997. Preliminary evaluation of the impacts of *C. maenas* on bivalve populations in Tasmania. Pp. 48–49 in *Proceedings of the First International Workshop on the Demography, Impacts and Management of Introduced Populations of the European Crab,* Carcinus maenas, R. E. Thresher, ed. CRIMP, Hobart, Tasmania.

Maugle, P. D. 1982. Characteristics of amylase and protease of the shrimp *Penaeus japonicus*. *Bull. Jpn. Soc. Sci. Fish.* **48:** 1753–1757.

McClintock, J. B., T. S. Klinger, K. Marion, and P. Hseuh. 1991. Digestive carbohydrases of the blue crab *Callinectes sapidus* (Rathbun): implications in utilization of plant-derived detritus as a trophic resource. *J. Exp. Mar. Biol. Ecol.* **148:** 233–239.

Norman, C. P., and M. B. Jones. 1990. Utilisation of brown algae in the diet of the velvet swimming crab *Liocarcinus puber* (Brachyura: Portunidae). Pp. 491–501 in *Trophic Relationships in the Marine Environment. Proc. 24th Europ. Mar. Biol. Symp.* M. Barnes and R. N. Gibson, eds. Aberdeen University Press, Aberdeen.

Omondi, J. G., and J. R. Stark. 1995. Some digestive carbohydrases from the midgut gland of *Penaeus indicus* and *Penaeus vannamei* (Decapoda: Penaeidae). *Aquaculture* **134:** 121– 135.

Paul, R. K. G. 1981. Natural diet, feeding and predatory activity of the crabs *Callinectes arcuatus* and *C. toxotes* (Decapoda, Brachyura, Portunidaea). *Mar. Ecol. Prog. Ser.* **6:** 91– 99.

Sabapathy, U., and L. H. Teo. 1993. A quantitative study of some digestive enzymes in the rabbitfish, *Siganus canaliculatus* and the sea bass, *Lates calcarifer*. *J. Fish Biol.* **42:** 595– 602.

Salindeho, I. R., and D. J. Johnston. 2003. Functional morphology of the mouthparts and proventriculus of the rock crab *Nectocarcinus tuberculosus* (Decapoda: Portunidae). *J. Mar. Biol. Assoc. UK* **83:** 821–834.

Skilleter, G. A., and D. T. Anderson. 1986. Functional morphology of the chelipeds, mouthparts and gastric mill of *Ozius truncatus* (Milne Edwards) (Xanthidae) and *Leptograpsus variegatus* (Fabricius) (Grapsidae) (Brachyura). *Aust. J. Mar. Freshw. Res.* **37:** 67–79.

Stone, S. T., A. Betz, and J. Hofsteenge. 1991. Mechanistic studies on thrombin catalysis. *Biochemistry* **30:** 9841–9848.

Walter, H. E. 1984. Proteinases: methods with hemoglobin, casein and azocoll as substrates. Pp. 270–277 in *Methods of Enzymatic Analysis*, Vol. 5, H. U. Bergmeyer, ed. Verlag Chemie, Weinheim, Germany.

Wear, R. G., and M. Haddon. 1987. Natural diet of the crab *Ovalipes catharus* (Crustacea, Portunidae) around central and northern New Zealand. *Mar. Ecol. Prog. Ser.* **35:** 39–49.

Wigglesworth, J.M., and D. R. W. Griffith. 1994. Carbohydrate digestion in *Penaeus monodon*. *Mar. Biol.* **120:** 571–578.

Williams, M. J. 1982. Natural food and feeding in the commercial sand crab *Portunus pelagicus* Linnaeus, 1766 (Crustacea: Decapoda: Portunidae) in Moreton Bay, Queensland. *J. Exp. Mar. Biol. Ecol.* **59:** 165–176.

Wojtowicz, M. B., and H. Brockerhoff. 1972. Isolation and some properties of the digestive amylase of the American lobster (*Homarus americanus*). *Comp. Biochem. Physiol. B* **42:** 295–302.

Wolcott, D. L., and N. J. Nancy. 1992. Herbivory in crabs: adaptations and ecological considerations. *Am. Zool.* **32:** 370–381.

Woods, C. M. C., and D. R. Schiel. 1997. Use of seagrass *Zostera novazelandica* (Setchell, 1933) as habitat and food by the crab *Macrophthalmus hirtipes* (Heller 1862) (Brachyura: Ocypodidae) on rocky intertidal platforms in southern New Zealand. *J. Exp. Mar. Biol. Ecol.* **214:** 49–65.

Xue, X. M., A. J. Andersnn, N. A. Richardson, A. J. Anderson, G. P. Xue, and P. B. Mather. 1999. Characterisation of cellulase activity in the digestive system of the redclaw crayfish (*Cherax quadricarinatus*). *Aquaculture* **180:** 373–386.

Reference: *Biol. Bull.* **208:** 47–59. (February 2005)

Effects of Ambient Flow and Injury on the Morphology of a Fluid Transport System in a Bryozoan

MICHELANGELO VON DASSOW

Integrative Biology Department, 3060 VLSB #3140, Berkeley, California 94720-3140

Abstract. Many organisms use fluid transport systems that are open to the external environment for suspension feeding or gas exchange. How do factors related to the environment, such as injuries and ambient currents, affect remodeling of these systems? In the bryozoan *Membranipora membranacea,* the lophophores (crowns of ciliated tentacles) form a canopy over the colony. The lophophores pump seawater from above the colony through themselves to capture food particles. The seawater then flows under the canopy to exit the colony at chimneys (openings in the canopy) or at the canopy edge. To test whether either ambient flow speed or injury affects remodeling of this system, I measured changes in chimney size and spacing in colonies grown in flow tanks at different ambient flow speeds, and in colonies in which I killed patches of zooids. There was no effect of either ambient flow speed or injury size on chimney remodeling. Injury did not induce chimney formation. In addition, chimneys formed at the canopy edge, indicating that high pressure under the canopy did not induce chimney formation. These results suggest that ambient flow, injury, and the pressure under the canopy may have little effect on the remodeling of this fluid transport system.

Introduction

Systems in which organisms pump fluids (*e.g.,* blood, water) through themselves serve a variety of major functions including internal transport, respiration, and suspension feeding (LaBarbera, 1990). These fluid transport systems share common physical and functional principles (LaBarbera and Vogel, 1982; LaBarbera, 1990, 1995). For example, resistance to flow is greater in narrow vessels than in wide vessels; however, there is frequently a cost to building wide vessels. Therefore, vessel size tends to increase as the flow rate through the vessel increases (LaBarbera, 1990).

Many internal fluid transport systems remodel in response to changes in the flow through the system. Several studies have shown that blood vessels in the mammalian circulatory system remodel in response to changes in the flow through them (reviewed in LaBarbera, 1990, 1995; Langille, 1995). Other studies suggest that changes in flow induce remodeling in the gastrovascular canals of hydroid colonies (Dudgeon and Buss, 1996; Buss, 2001) and the veins of plasmodial slime molds (Nakagaki *et al.,* 2000, 2001). These systems all pump fluid through pipe-like conduits that are isolated from the external environment.

Organisms also use fluid transport systems for suspension feeding or respiration (LaBarbera, 1990). In contrast to internal fluid transport systems, these systems interact with the ambient flow environment through conduits that form openings onto the external fluid. These conduits are used either to take in unprocessed fluid or to expel processed fluid. They include the siphons of ascidians and clams, and the oscula of sponges. In many bryozoans that form sheet-like colonies (Banta *et al.,* 1974; Cook, 1977; Winston, 1979), and in some colonial ascidians, several individuals pump filtered seawater through the colony to exit at common excurrent openings (chimneys). Certain large, sulfur-oxidizing bacteria even form chimney-like structures that are important for maintaining proper O_2 concentrations (Fenchel and Glud, 1998). Can conduits that connect with the ambient flow environment remodel, and if so, what factors affect their remodeling?

Received 12 April 2004; accepted 29 October 2004.
E-mail: mvondass@socrates.berkeley.edu

Chimneys in the bryozoan Membranipora membranacea

The bryozoan *Membranipora membranacea* Linnaeus, 1767, is an excellent system with which to study the effects of flow on fluid transport systems involved in suspension feeding because *M. membranacea* colonies grow rapidly and form a simple fluid transport system. The colonies are composed of a sheet of physiologically connected individuals (zooids) bearing lophophores (crowns of ciliated tentacles) that form a canopy over most of the colony (Fig. 1A–D). Groups of lophophores lean away from each other to form openings called chimneys (Fig. 1; Banta *et al.*, 1974; Lidgard, 1981). Frequently, several zooids in the center of a chimney do not extend their lophophores and do not feed (Lidgard, 1981). The lophophores capture food particles from seawater that they pump from above the colony down towards the colony and between the tentacles. The seawater then flows under the canopy of closely packed lophophores to exit the colony at the canopy edge or at one of the chimneys (Fig. 1B; Banta *et al.*, 1974; Lidgard, 1981).

Previous studies have suggested that flow around and through the colony affects where new chimneys are formed in *M. membranacea* (Dick, 1987; Grünbaum, 1997; Okamura and Partridge, 1999). Okamura and Partridge (1999) found that chimney spacing decreased with increasing ambient flow speed in the field. Grünbaum (1997) found that chimney spacing was reduced in colonies with spines, an inducible defense against specific nudibranch predators, and that chimney shape depended on the shape of the substratum on which colonies were grown. Since both the presence of spines and the shape of the substratum (which determines the shape of the colony) were predicted to affect the flow through the colony, these results suggested a hydromechanical mechanism of chimney formation (Grünbaum, 1997). However, none of these studies evaluated whether chimneys could remodel after they had formed.

Remodeling of this system could result from changing the extension or orientation of lophophores, from degeneration of feeding zooids, or from regeneration of nonfeeding zooids. These processes could potentially result in new chimneys forming within the canopy as suggested by Dick (1987), or in changes in the size or position of existing chimneys. Alternatively, new chimneys could form at the canopy edge since the colony grows by addition of new zooids at the edge of the colony (Dick, 1987).

What factors might affect the remodeling of existing chimneys?

Fluid flow through and around a colony could change over time due to changes in the ambient flow speed or to injury to the colony. These two factors are likely to be important in the environment given the variable flow conditions in which these colonies grow (Okamura and Partridge, 1999) and the presence of predators that injure colonies (Yoshioka, 1982; Harvell, 1984). Ambient flow speed is known to affect the feeding performance of other sheet-like bryozoans (Okamura, 1985), as well as both the rate (Eckman and Duggins, 1993; Grünbaum, 1997) and direction (Norton, 1973) of growth in *M. membranacea*.

Ambient flow can generate passive flow through a structure. In some active suspension feeders such as sponges (Vogel, 1977) and *Styela montereyensis*, a stalked ascidian, (Young and Braithwaite, 1980), ambient flow augments active pumping. Stewart (2000) found that flow through chimneys of *M. membranacea* depended on ambient flow speed. This suggests the hypothesis that changes in the ambient flow environment might lead to remodeling of fluid transport systems that have openings onto the external environment.

Injuries to the colony would be expected to reduce flow to neighboring chimneys since injuries reduce the number of lophophores pumping fluid under the canopy to the chimneys. In addition, injuries can form new excurrent sites (Dick, 1987), which would be expected to further reduce flow to the existing chimneys. This suggests the hypothesis that injury to the colony might induce changes in the size or spacing of nearby chimneys.

What stimuli might affect remodeling of the canopy?

Two stimuli have been hypothesized to affect remodeling of the canopy: pressure under the canopy and injury (Dick, 1987). In *M. membranacea* and other bryozoans, chimneys have been observed at sites such as injuries where the canopy has been disrupted (Cook, 1977; Dick, 1987). Dick hypothesized that excurrent flow through the gap in the canopy at injured sites induces the surrounding lophophores to orient away from the site of the injury (Dick, 1987), thereby forming a chimney.

Because chimneys act to reduce the pressure under the canopy of lophophores (Grünbaum, 1995), it has been suggested that high pressure within the colony may induce chimney formation (Dick, 1987; Larsen and Riisgard, 2001). This hypothesis predicts that chimneys form within the canopy and not at the canopy edge because the canopy edge acts as an excurrent site where the pressure is low (Dick, 1987). Fluid flows under the canopy to exit the colony either at the chimneys or at the canopy edge. Since fluid flows from high-pressure sites to low-pressure sites, this indicates that both the chimneys and the canopy edge are at lower pressure than sites within the canopy (Grünbaum, 1995; Larsen and Riisgard, 2001). Therefore, the formation of chimneys at the canopy edge would disprove the hypothesis that high pressure under the canopy induces chimney formation (Dick, 1987).

Previous authors have observed structures that they interpreted to be partially formed chimneys at the canopy

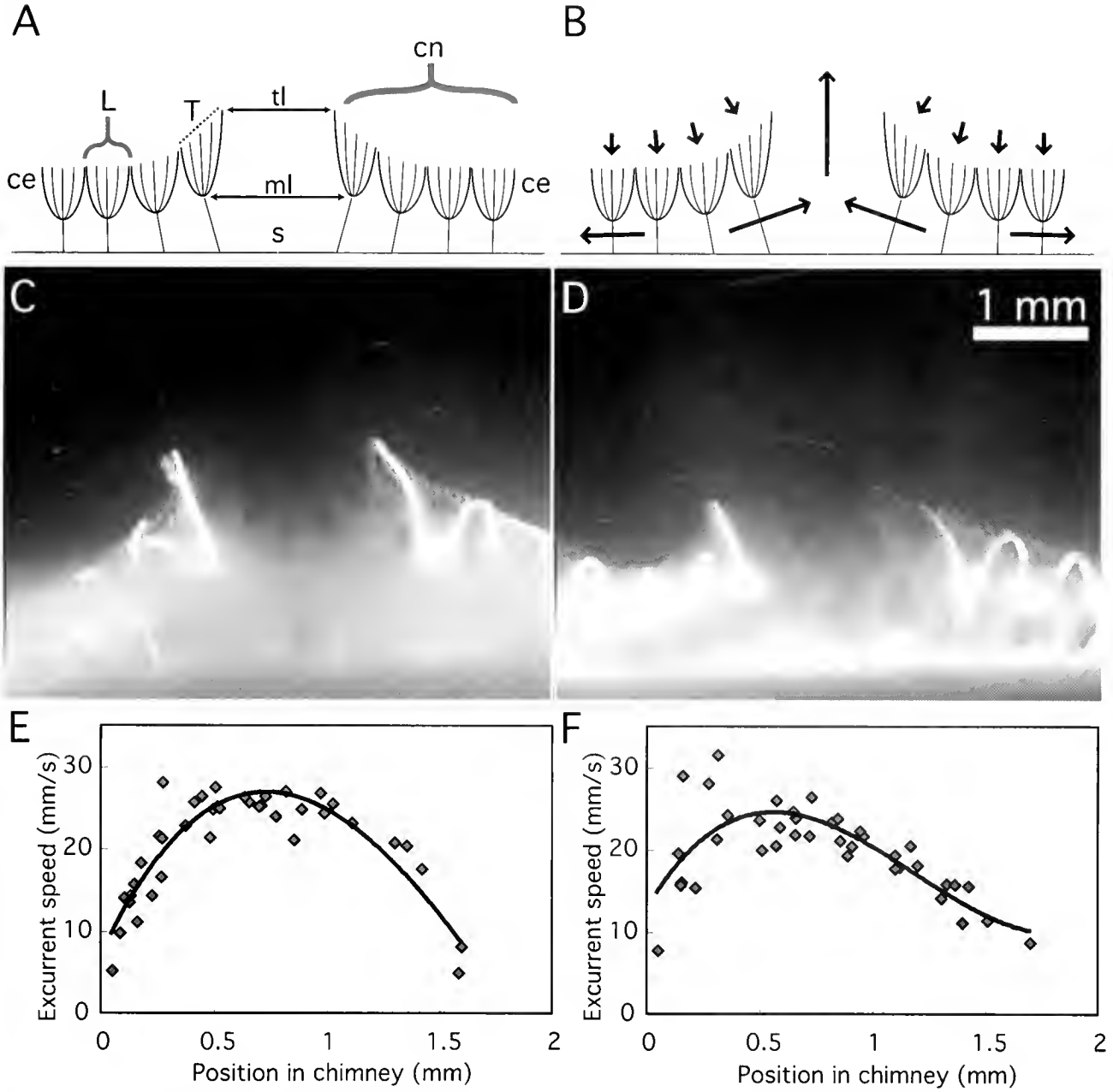

Figure 1. (A) A diagram of a *Membranipora membranacea* colony with a single chimney: canopy (cn), canopy edge (ce), lophophore (L), plane of tentacle tips (T) of a chimney lophophore, tentacle tip level (tl), and mouth level (ml) for the chimney, and colony surface (s). (B) A diagram of flow through the colony. Arrows indicate directions of flow. Small arrows indicate flow into lophophores. (C) A chimney in slow ambient flow. (D) A chimney in fast ambient flow. Colonies were illuminated with a laser sheet perpendicular to the colony surface and viewed from the side to show chimneys in cross section. Flow was to the left in both images. (E, F) Flow speeds out chimneys *versus* the distance from the downstream edge of the chimney ($x = 0$) along the line connecting the chimney edges: (E) slow ambient flow (chimney in C); (F) fast ambient flow (chimney in D).

edge (Cook and Chimonides, 1980; Dick, 1987). However, they did not observe whether these structures in fact became chimneys or just disappeared. To test whether chimneys form where the pressure under the canopy is highest, it is necessary to follow their formation through time to see where they form with respect to the canopy edge.

The goal of this study was to determine whether factors related to the environment—including ambient flow speed,

injury to the colony, or the pressure under the canopy—affect remodeling in the external fluid transport system of colonies of *M. membranacea*. I tested whether either ambient flow speed or injury to the colony influences the size or spacing of fully formed chimneys. I tested the hypothesis that new chimneys form at sites of high pressure under the canopy by observing where chimneys formed relative to excurrent sites. Finally, I tested the hypothesis that injury is sufficient to induce chimney formation by injuring groups of zooids of different sizes.

Materials and Methods

Colony collection

Colonies of *Membranipora membranacea* growing on laminarian kelp blades were collected off the Friday Harbor Laboratory dock, in Friday Harbor, Washington. Some previous studies have described the *Membranipora* species at Friday Harbor as *M. serrilamella* or *M. villosa* (Lidgard, 1981; Dick, 1987). However, recent studies indicate that these different morphotypes are the result of phenotypic plasticity for the presence of spines (Yoshioka, 1982; Harvell, 1984), and that all of the *Membranipora* colonies at Friday Harbor belong to a single interbreeding population (Schwaninger, 1999). I follow Harvell (1984) and Grünbaum (1997) in referring to colonies collected at Friday Harbor as *M. membranacea*. However, Schwaninger (1999) found significant genetic differentiation between the Friday Harbor population and the Atlantic population studied by Cook (1977), Cook and Chimonides (1980), and Okamura and Partridge (1999).

Ambient flow experiment: flow tanks

I built four flow tanks out of clear acrylic. The flow tanks were 2.3 cm wide, 5.5 cm tall, and 40 cm long. Pieces of acrylic were clipped to the tops of the tanks to close them. Dap silicon-rubber sealant was used to make a gasket around the top of the tank, and vacuum grease was spread on top of the gasket to make a tight seal. Hex-cell flow straighteners were placed towards the upstream end of the tanks. The working section was from 16.5 to 20.5 cm downstream from the flow straighteners. To maintain constant flow, the tanks were fed by a head tank and drained to a second tank. The head tank was supplied by seawater pumped from Friday Harbor.

Two flow treatments were used: the flow rate was 73.3 ± 0.5 ml/s in the fast-flow treatment, and 14.4 ± 0.2 ml/s in the slow-flow treatment. Slow flow was obtained using a single inflow tube—into which a plastic pipette tip with its end cut off was inserted—and a single outflow tube. Fast flow was obtained using two inflow and two outflow tubes (without the plastic pipette tips). This design allowed the tanks to be switched between the fast-flow and slow-flow treatments for different runs.

Colonies growing on flat pieces of kelp blades were collected. The pieces of kelp bearing the colonies were cut out and glued to pieces of plastic cut from a VWR brand weigh-boat using Duro "Quickgel" cyanoacrylate (superglue) gel. Colonies were selected that were between 3 cm^2 and 8 cm^2 in area, showed minimal damage, and were not bordered by neighboring colonies. One colony did have a very small colony (0.4 cm^2) growing next to it. Data from this colony fell within the range for the treatment and did not affect the results of any of the analyses. The colonies were placed in a sea-table with running seawater for 1 day prior to placement in the flow tanks.

A single colony, selected at random, was placed into each tank. All colonies were checked with a hand lens to remove any of the cryptic predatory nudibranch *Doridella steinbergae*. The plastic backings supporting the colonies were held onto the side of the tank by two strips of plastic cut from a weigh-boat mounted on the sides of the tanks. The colonies were held vertically to reduce fouling by debris. Seawater temperature ranged from 10 to 12 °C during the experiment.

Plan-view photographs were taken of the colonies in the flow tanks immediately before starting the flow, at about 10 min and 2 h after starting the flow, and once per day for 3 days subsequently. Photos were taken using a Nikon Coolpix 995 digital camera. A fiber optic illuminator was used for lighting in all but the first run, in which the camera flash was used.

Ambient flow experiment: flow measurements

To measure flow through the chimneys, one chimney in each colony was videotaped on the third day after the flow in the tank was started. Videos were made using a low-light, analog video camera (Watec 902A) with a macro lens. Chimneys were viewed from the side (*i.e.*, with the camera above the tank) to visualize excurrent flow (Fig. 1C, D). A red diode laser (World Star Tech) was used to make a sheet of light (<1 mm thick) that bisected the chimney. Particles naturally occurring in the seawater were used to visualize flow.

Chimneys were selected in which the lophophores were clearly visible but which were separated by no fewer than four lophophores from the canopy edge. It was difficult to get good images of chimneys in the middle of the colony because they were often obscured by chimneys closer to the colony edge. Since I could only visualize chimneys near the canopy edge and taping was done on the third day, chimneys used for these videos may not have been fully formed on the first day and therefore may not be the same ones used for measurements of chimney enlargement (see "Measurements of chimney enlargement" below). The flow rates

between these chimneys and chimneys closer to the colony center may differ, but there is no reason to expect that this would affect the shape of the flow profile within the chimneys or change the effects of ambient flow speed.

A PCI frame grabber (Scion LG3) was used to capture about 50 s of video from videotape onto a computer, where it was analyzed using NIH Image 1.62 software. Occasionally the lophophores would retract in the part of the colony in the field of view; those parts of the video were not analyzed. The video fields were separated to give 60 fields per second.

Particle streaks were selected that were bright, in focus, and intersected a line between the tentacle tips on the upstream and downstream edges of the chimney (see Fig. 1A). To ensure that the particles were visible throughout the entire 1/60 of a second covered by the field, only particles that were also visible in both the previous and subsequent fields were used. The x-y coordinates of either the beginnings or the ends of two consecutive streaks were measured to calculate particle velocities.

To calculate chimney diameter and to determine a chimney-centered coordinate system, I measured the x-y positions of the tentacle tips on the upstream and downstream edges of the chimneys. For each colony, 9 to 17 measurements were made at 3-s intervals.

The speed, the component of velocity out of the chimney (*i.e.*, normal to the colony), and the distance from the downstream edge of the chimney were calculated for each streak. I used Mathematica 3.0 to analyze data on particle streaks and tentacle-tip positions. Cubic polynomials were fitted to these data to calculate speed and velocity as a function of distance from the downstream chimney edge (Fig. 1E, F). Cubic polynomials were used because they appeared to fit the data well in both flow treatments. The maximum speed and the maximum component of velocity out of the chimney were calculated from these cubic polynomials. The relative position of maximum excurrent flow speed was measured as the distance between the downstream edge of the chimney and the site of the maximum excurrent flow speed divided by the diameter of the chimney.

To characterize the flow in the tank, imaging and streak measurements for the flow just upstream of the colony were made for one colony in the fast-flow treatment and one colony in the slow-flow treatment. The frame rate was 30 frames per second. The downstream component of velocity and the distance from the tank wall were calculated for each streak, using a computer spreadsheet. Shear rates—that is, the derivative (dU/dx) of flow velocity (U) with respect to distance (x) from a surface—were calculated from quadratic equations ($U = ax^2 + bx$) fitted to the data on particle velocities. Quadratic equations were used because laminar flow between parallel plates has a parabolic profile. Shear rates were 5 s^{-1} in the slow-flow treatment and 22 s^{-1} in the fast-flow treatment at the kelp surface, 2 mm upstream of the colony edge. These shear rates span much of the range of shear rates that colonies are likely to experience in the field (Grünbaum, 1997).

Injury experiment

To investigate whether injury to the colony affected the size or spacing of existing chimneys, and whether injury induced chimney formation, I observed the responses of colonies to injuries of different sizes. The treatments were "uninjured" controls (0 zooids killed), "4-zooid injuries" (4 zooids killed), "12-zooid injuries" (11 to 14 zooids killed), and "36-zooid injuries" (34 to 39 zooids killed). These treatments were chosen to span a range of sizes from that of typical chimneys (Lidgard, 1981) to injuries much larger than typical chimneys. I used a range of injury sizes because the local flow conditions at an injury and the flow to the neighboring chimneys are likely to depend on injury size, and because colonies in nature may receive injuries of different sizes.

I collected large colonies (>10 cm diameter) growing on flat pieces of kelp, and split the colonies into four or more pieces to form genetically identical colony fragments with intact growing edges. The pieces of algae were glued (using Duro "Quickgel" cyanoacrylate gel) to backings made from VWR-brand plastic weigh-boats. After 4 to 6 days in the sea-table, pieces from each parent colony were randomly assigned to each of the four injury treatments.

I injured patches of zooids that were located midway between three to four chimneys by breaking the zooid walls and frontal membrane with a needle. Injured zooids only rarely regenerated during the length of the experiment. Injured patches were roughly square. The colonies were then suspended vertically in the sea-tables with running seawater. Colonies were observed through a dissecting microscope and photographed in plan view before injury and at 3 and 11 days after injury.

To test whether the gaps in the canopy left by injuries were of a similar size to those produced by chimneys, I measured the area of the gaps in the canopy both at natural chimneys and at injuries. Measurements were made using images taken 3 days after injuring the colony pieces. I measured the gap area of the chimney nearest to the center of the image in each control colony piece. For both the injuries and the chimneys, I measured the area of the gaps in the canopy at the level of the tentacle tips (Fig. 1A) as the area of a polygon connecting the tentacle tips.

To test whether there was a difference in the posture of the zooids between chimneys and injuries, I calculated the "spreading ratio," the ratio of the actual area of the gap in the canopy to the expected area of the gap given the observed number of nonfeeding zooids. A spreading ratio greater than 1 indicates that the lophophores were held away

from the nonfeeding zooids, and a ratio less than 1 indicates that the lophophores were held over the nonfeeding zooids. The expected gap area was the number of nonfeeding zooids (in the injury or chimney) multiplied by the average area of non-chimney lophophores within each colony piece: it is an estimate of the total area of the lophophores removed. To determine the area of the non-chimney lophophores, I measured the area of two to three groups of 7 lophophores midway between pairs of chimneys in the same manner as I measured the gap area. In rare instances the injured zooids regenerated during the experiment, so the number of nonfeeding zooids differed slightly from the original number of injured zooids.

At 11 days, the morphology of zooids surrounding the injuries was observed using a dissecting microscope. I recorded whether the plane of the tentacle tips (Fig. 1A) of lophophores surrounding the injuries was parallel to the plane of the colony surface, tilted away from the injury, or tilted towards the injury. I also recorded whether the bases of lophophores surrounding the injuries were held higher than those of surrounding lophophores.

Measurements of chimney enlargement

I measured the enlargement in chimney area as the ratio of chimney area at time t to chimney area at time 0. I measured the enlargement in chimney spacing as the ratio of the distance between two chimneys at time t to the distance between them at time 0. Tentacle tips surrounding chimneys were sometimes difficult to see clearly in the plan-view photographs. Therefore, for measurements of chimney enlargement in both the injury and the ambient-flow experiment, I measured the area of chimneys at the level of the base of the chimney lophophores (about the level of the mouth, Fig. 1A). Chimney area and position were measured by drawing a polygon connecting the base of each of the lophophores bordering the chimney in a computer graphics program, and then measuring the area and x-y center of the polygon in NIH Image 1.62. Polygons formed by points on the colony skeleton were used as reference areas.

For the flow experiment described earlier, I measured the enlargement in chimney area and spacing from the time just prior to starting the flow to 3 days afterward. Because variation in enlargement in chimney area was high within individual colonies (see below), I calculated the median chimney enlargement of all the measurable chimneys in each colony. Colonies had between 1 and 13 (median of 5) measurable chimneys. I measured the enlargement in chimney spacing for a pair of randomly selected chimneys (using a random number generator). To ensure that chimneys were fully developed, I only measured chimneys that were separated by more than three lophophores from the canopy edge prior to starting the flow.

For the injury experiment, I measured the enlargement in chimney area and spacing from the time just prior to injury to 3 days after injury. I calculated the enlargement in area of the chimney nearest to the injury, and I calculated the enlargement in the spacing between that chimney and a second chimney close to the injury since these would be most influenced by the presence of the injury.

Measurements of chimney formation

Chimney formation was observed in colonies during the ambient flow experiment. Chimneys were selected that were completely surrounded by feeding zooids on day 3, but for which there was no sign of chimney formation on day 0. In the first image in which the chimney was visible, I measured whether the chimney was completely surrounded by lophophores and how many lophophores separated it from the canopy edge. If the lophophores were held away from the site where the chimney subsequently appeared—so that there was an indentation in the canopy edge—I scored the chimney as appearing at the canopy edge (0 lophophores from the canopy edge). If there was no sign of the chimney or of an indentation in the canopy edge, I scored the chimney as absent. I did not count chimneys in which there was an indentation in the canopy edge on day 0, since I did not want to overestimate the number of chimneys first appearing at the canopy edge relative to the number first appearing within the canopy.

Statistics and graphs

Nonparametric statistics were used because of the small sample size in all experiments. All tests were two-tailed. Most statistical tests were done using StatView 5.0. I used Mathematica 3.0 to calculate statistics for the squared ranks test, a nonparametric test for differences in variance between two independent samples (Conover, 1999). The Friedman test is a nonparametric test for comparing treatments with the data grouped into blocks (Conover, 1999), as in the injury experiment in this study in which all the pieces from the same parent colony represent a block. I implemented the method described in Conover (1999) for all comparisons of individual treatments to each other after the Friedman test. All box plots show the median, 1st and 3rd quartile, 1st and 9th decile, and minimum and maximum.

Results

Does ambient flow speed affect flow through chimneys?

Ambient flow speed affected the flow profile in the chimneys. The flow profile was nearly symmetrical in the slow-flow treatment (Fig. 1E) but not in the fast-flow treatment (Fig. 1F). Consistent with this difference in symmetry, the relative position of the maximum excurrent flow speed was significantly farther downstream of the center of the chimney in the fast-flow treatment than in the slow-flow treat-

ment (Fig. 2A; $P = 0.0002$, Mann-Whitney U test; $n = 10$ for each treatment). The maximum excurrent flow speed did not differ significantly between the two treatments (Fig. 2B; $P = 0.9$, Mann-Whitney U test), but the maximum of the component of velocity out of the chimney was significantly lower in the fast-flow treatment (Fig. 2C; $P = 0.002$, Mann-Whitney U test).

Does ambient flow speed affect chimney size and spacing?

The enlargement in chimney areas was calculated as the ratio of the chimney area at 3 days after starting the flow in the tank to the chimney area just before starting the flow. The variation in enlargement in chimney areas within individual colonies was high. The standard deviation in chimney enlargement was 23% ($n = 13$ chimneys) and 24% ($n = 11$ chimneys) for one colony in the fast-flow treatment and one colony in the slow-flow treatment.

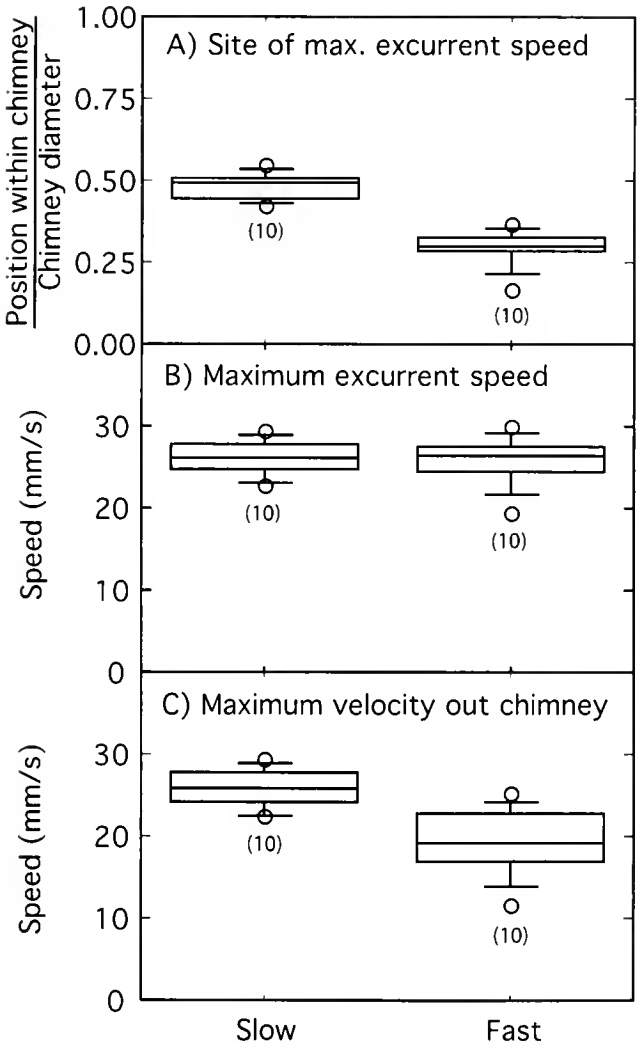

Figure 2. Effects of ambient flow speed on flow within chimneys. (A) The relative position of the site of maximum excurrent flow speed. The downstream side of the chimney is at $y = 0$, and the upstream side is at $y = 1$. The chimney center is at $y = 0.5$. (B) The maximum excurrent flow speed within the chimney in fast and slow ambient flow. (C) The maximum component of velocity out of the chimney in fast and slow ambient flow. Numbers of colonies measured are in parentheses. Box plots show the median, 1st and 3rd quartile, 1st and 9th decile, and minimum and maximum (open circles).

To test for an effect of ambient flow speed on the enlargement in chimney area, I calculated the median of the enlargement in chimney area for each colony (Fig. 3A). Chimney-area enlargement was significantly greater than 0% in the fast-flow treatment ($P = 0.005$, Wilcoxon signed-rank test; $n = 10$) but not in the slow-flow treatment ($P = 0.07$, Wilcoxon signed-rank test; $n = 9$). However, the difference in chimney-area enlargement between treatments was not statistically significant ($P = 0.09$, Mann-Whitney U test).

To test for an effect of ambient flow speed on the enlargement in chimney spacing, I measured the ratio of the distance between two randomly selected chimneys at 3 days after starting the flow in the tank to the distance between them just before starting the flow (Fig. 3B). One colony had only one measurable chimney, so that colony was excluded. The change in spacing was significantly greater than 0% in the slow-flow treatment ($P = 0.04$, Wilcoxon signed-rank test; $n = 9$), but not in the fast-flow treatment ($P = 0.1$, Wilcoxon signed-rank test; $n = 9$). However, the difference between treatments in the change in spacing was not statistically significant ($P = 0.7$, Mann-Whitney U test). The standard deviation of the change in chimney spacing was significantly greater in the fast-flow treatment (6.3%, $n = 9$) than in the slow-flow treatment (2.3%, $n = 9$; $P < 0.02$, squared-ranks test).

Where do chimneys form?

The hypothesis that high pressure under the canopy of lophophores induces chimney formation predicts that chimneys form within the canopy and not at the canopy edge (Dick, 1987). New chimneys appeared in most of the colonies in both treatments, and the process of chimney formation could be observed in photographs taken daily (Fig. 4). About half of the chimneys first appeared at the canopy edge, and no chimneys first appeared more than one lophophore from the canopy edge (Table 1).

Does injury affect nearby chimneys?

To test whether injury to the colony affected the morphology of nearby chimneys, I measured the enlargement in area and spacing for chimneys near to injuries of different sizes and in uninjured controls. None of the injury treatments differed significantly from each other or from the controls in the enlargement in either area or spacing (Fig. 5; $P = 0.6$ and $P = 1$ for area and spacing respectively, Friedman test; $n = 6$ blocks).

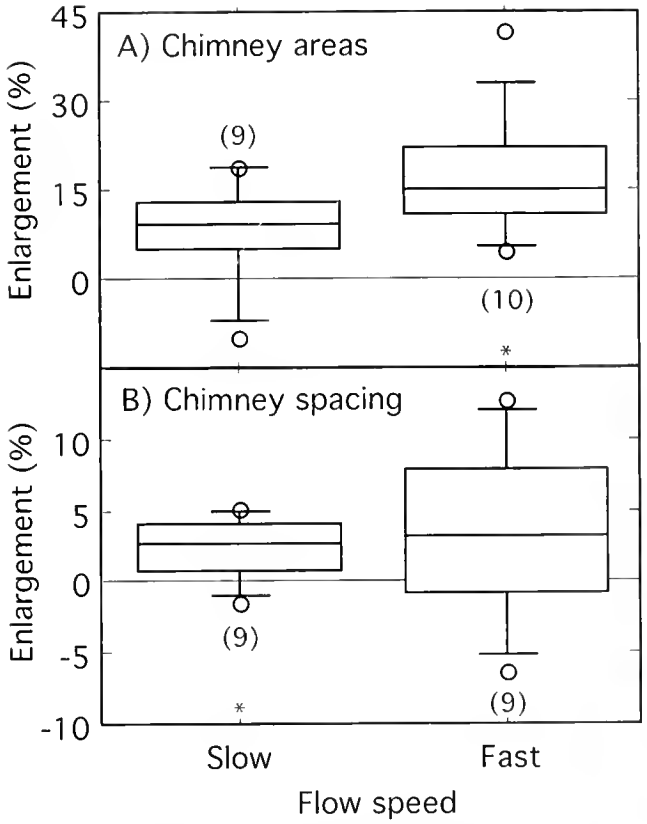

Figure 3. Changes in chimney area and spacing in fast and slow ambient flow. (A) Median enlargement in chimney area. (B) Enlargement in chimney spacing. Enlargement was significantly different from 0% for groups marked with an asterisk (*) ($P < 0.05$, Wilcoxon signed-rank test). Numbers of colonies measured are in parentheses. Box plots as in Figure 2.

Chimney areas increased significantly in all treatments (Fig. 5A; $P < 0.05$ for all treatments, Wilcoxon signed-rank tests; $n = 7$ to 8). Chimney spacing tended to increase in all treatments, but the increase was statistically significant in only one treatment, the 4-zooid injury treatment (Fig. 5B; $P = 0.03$, Wilcoxon signed-rank test; $n = 7$). The increase in spacing was not statistically significant in the other three injury treatments ($P \geq 0.3$ for all treatments, Wilcoxon signed-rank tests; $n = 7$ to 8).

Does injury induce chimney formation?

I observed the zooids bordering injured sites of different sizes to determine whether injury induces chimney formation. In normal chimneys, the stalks supporting the lophophores lean away from the chimneys so that the lophophores are held away from the chimney center, thereby forming an opening (Fig. 6A). In contrast, in every injury of all size classes, the stalks supporting the lophophores tilted towards the injured sites after 3 days, so that the lophophores surrounding the injury were held over the injury and closed or partially closed the gap in the canopy formed by the injury (Fig. 6B).

The spreading ratio (the ratio of the area of the gap in the canopy to the expected area of the gap given the number of nonfeeding zooids) provides an index of the extent to which the lophophores are held over or away from the nonfeeding zooids. There were significant differences in the spreading ratio between treatments (Fig. 6C; $P = 0.0007$, Friedman

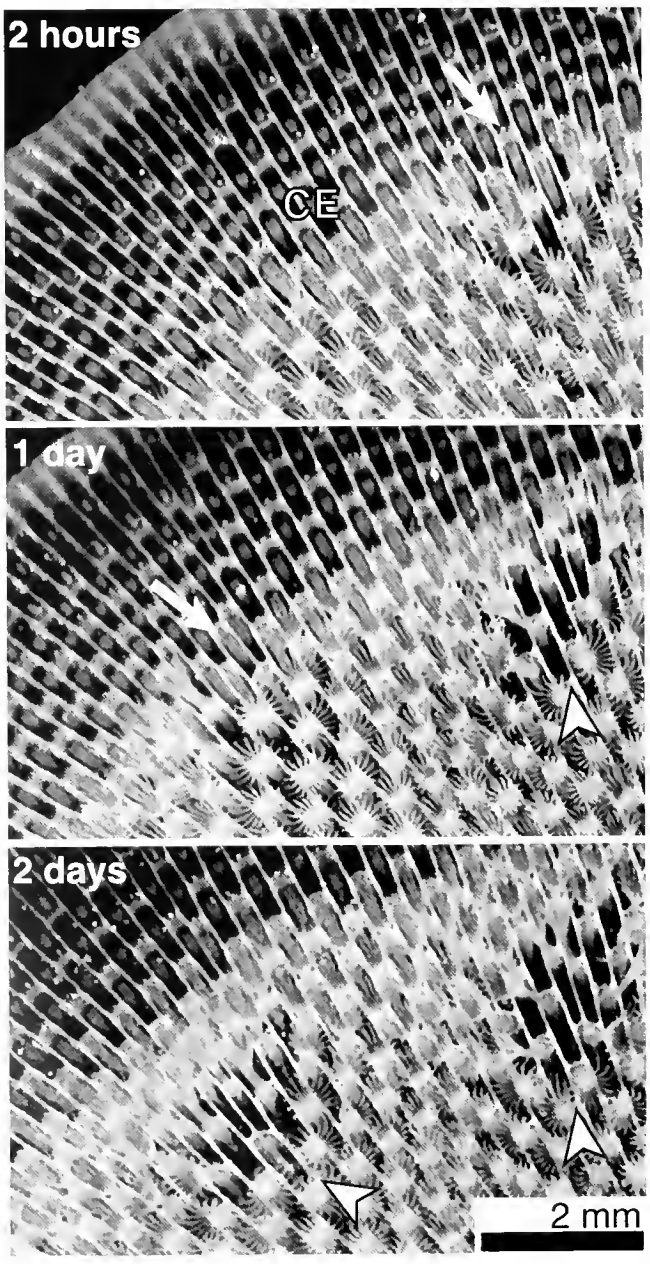

Figure 4. A time series of two chimneys forming at the canopy edge. Times shown are from when the flow was started in the tank. Canopy edge (CE), places where the lophophores spread apart to make an indentation in the canopy edge (arrows), fully formed chimneys (arrowheads). The colony edge is to the upper left.

Table 1

Numbers of chimneys formed at different distances from the canopy edge

	Separation from canopy edge (in lophophores)		
Flow treatment	0	1	≥2
Slow flow*	6	3	0
Fast flow**	11	11	0

* Slow-flow treatment: 9 chimneys formed in 5 colonies.
** Fast-flow treatment: 22 chimneys formed in 9 colonies.

test; $n = 6$ blocks). The spreading ratio for the chimneys was significantly larger than the spreading ratios for all size classes of injuries (Fig. 6C; $P < 0.05$, for all comparisons following the Friedman test; $n = 6$ blocks).

There were significant differences in the area of the gaps in the canopy between treatments (Fig. 6D; $P = 0.0005$, Friedman test; $n = 6$ blocks). The gap area at the chimneys was larger than the gap areas at injuries of all size classes (Fig. 6D). In addition, the gap area at the 36-zooid injuries was significantly larger than the gap area at both the 12-zooid and 4-zooid injuries, and the gap area at the 12-zooid injuries was significantly larger than the gap area at the 4-zooid injuries (Fig. 6D). All differences between treatments were statistically significant ($P < 0.05$, $n = 6$ blocks) in comparisons between treatments after the Friedman test. The number of nonfeeding zooids in the chimneys ranged from 1 to 14, with a median of 10 ($n = 6$).

Two other features of normal chimneys are that the planes of the tentacle tips of the chimney lophophores are tilted away from the chimney center, and the chimney lophophores are held higher than the lophophores of surrounding zooids (Fig. 1; Banta *et al.*, 1974; Lidgard, 1981). The orientation of the plane of the tentacle tips (Fig. 1A) of the lophophores surrounding the injuries was observed at 11 days in four of the sets of colony pieces. The planes of the tentacle tips of those lophophores surrounding large injuries were tilted away from the gap in the canopy left by the injury, but the planes of the tentacle tips of lophophores surrounding small injuries were held horizontally (Table 2). Injury size had a significant effect on the orientation of the plane of tentacle tips ($P = 0.04$, Friedman test; $n = 4$ blocks). There was no sign that the lophophores surrounding the injuries were held higher than the neighboring lophophores in any of the treatments.

Discussion

Does ambient flow or injury affect existing chimneys?

Flow may affect the formation of new chimneys (Grünbaum, 1997; Okamura and Partridge, 1999) but appeared to have little effect on the size and location of chimneys *after* they had formed in this study. The size of pre-existing chimneys increased significantly in several treatments in this study, suggesting that the chimneys have the capacity to enlarge after they have formed. However, neither ambient flow speed nor injury size had statistically significant effects on the magnitude of enlargement in area or in spacing of existing chimneys. Ambient flow speed did have a small but statistically significant effect on the variation in the enlargement in chimney spacing, with higher variation in faster ambient flow.

The length of time used in this study was sufficient for new chimneys to form and for old chimneys to enlarge

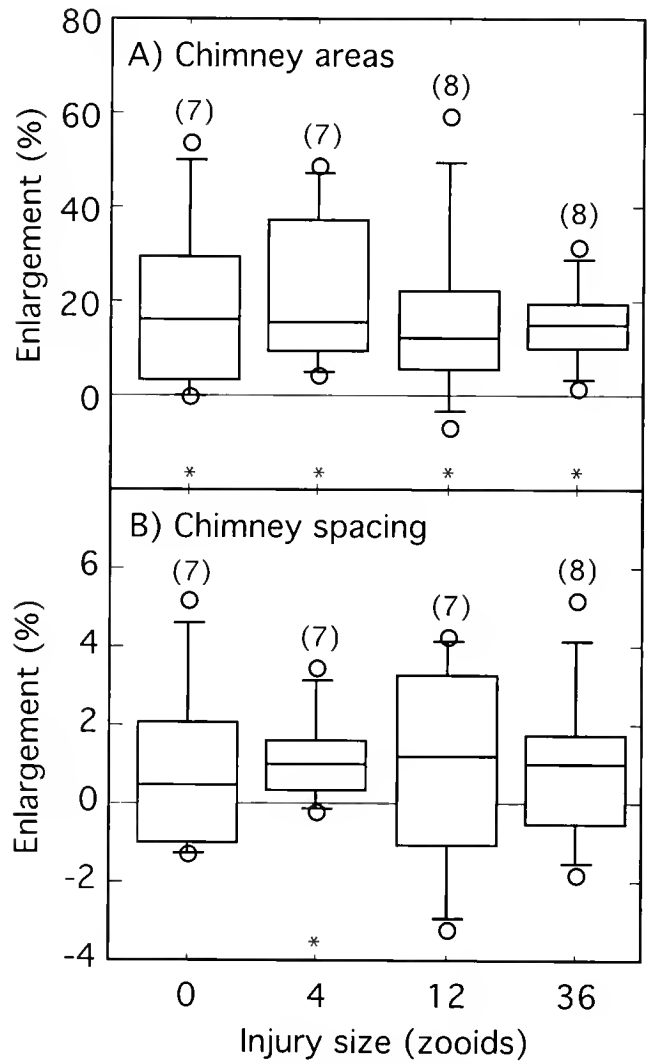

Figure 5. Changes in chimney area and spacing near injuries of different sizes. (A) Enlargement in area of individual chimneys. (B) Enlargement in chimney spacing. Enlargement was significantly different from 0% for groups marked with an asterisk (*) ($P < 0.05$, Wilcoxon signed-rank test). Numbers of colonies measured shown in parentheses. Box plots as in Figure 2.

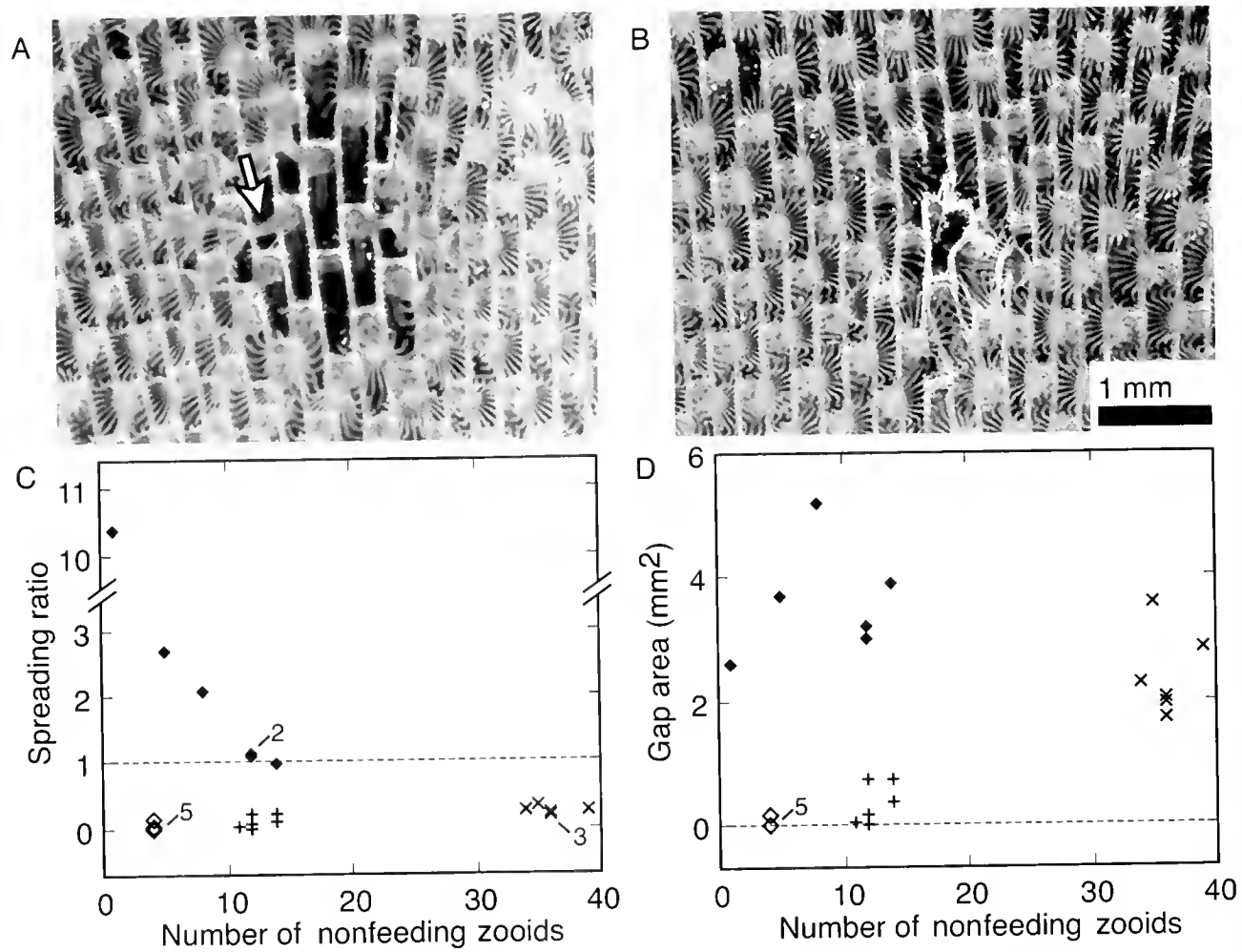

Figure 6. (A) A normal chimney with a single nonfeeding zooid viewed from above. The arrow points to a tentacle sheath (the stalk that supports the lophophore) that tilts away from the chimney center. (B) Zooids around a patch of 12 zooids that were injured 3 days before the photo was taken. (C) The spreading ratio *versus* the number of nonfeeding zooids for either chimneys or 3-day-old injuries. (D) The size of the gap in the canopy *versus* the number of nonfeeding zooids at either chimneys or 3-day-old injuries. Chimneys (filled diamonds); 4-zooid injuries (open diamonds); 12-zooid injuries (crosses); 36-zooid injuries (Xs); $n = 6$ for all treatments; numbers on plots indicate the number of overlapping values.

Table 2

Orientation of planes of tentacle tips on day 11

	Injury size (no. of zooids)		
Orientation	4	12	36
All horizontal	4	2	0
Mixed	0	1	0
All away from gap	0	1	4

Numbers shown are numbers of colonies in each category (4 colonies per treatment). Underlined treatments were not significantly different from each other ($P > 0.05$, after the Friedman test; $n = 4$ blocks).

significantly. This suggests that there was ample time for remodeling of chimneys.

Although I found little effect of ambient flow speed on the magnitude of the change in spacing of *existing* chimneys, previous studies on *Membranipora membranacea* suggest that ambient flow speed affects the spacing of the chimneys as they form (Okamura and Partridge, 1999). Okamura and Partridge (1999) found that chimney spacing depended on the ambient flow velocity at the sites in which colonies had grown in the field. In contrast, Grünbaum (1997) did not find that chimney spacing depended on the ambient flow velocity for colonies grown in flow tanks. However, he used lower flow speeds than colonies are likely to experience in the field.

The ambient flow conditions used in this study were within the range expected in the field. Grünbaum (1997) estimated that *M. membranipora* experiences shear rates from 3.5 to 45.7 s^{-1} in the field. The shear rates used in this study bracketed much of that range (from 5 to 22 s^{-1}). Grünbaum (1997) used lower shear rates (0.17 to 1.9 s^{-1}). Unfortunately, there is insufficient information to estimate the shear rates experienced by colonies in Okamura and Partridge's (1999) study.

Ambient flow speed did affect the flow profile, though not the maximum excurrent flow speed, within *M. membranacea* chimneys. Flow profiles within chimneys were clearly asymmetrical at high ambient flow speeds, but nearly symmetrical at low ambient flow speeds. In addition, the component of velocity out the chimney was lower in the treatment with high ambient flow speed than in the one with low ambient flow speed. The peak excurrent flow speeds were similar between the high and low ambient flow speeds. In contrast, previous studies done at lower ambient flow speeds than those used in this study found that excurrent flow speed increased with increasing ambient flow speed in *M. membranacea* (Stewart, 2000).

Effects of flow within the colony

Flow *within* the colony may also be important for determining where new chimneys form (Dick, 1987; Grünbaum, 1997). The odor of certain predatory nudibranchs induces the formation of defensive spines on the colony surface (Harvell, 1984; Grünbaum, 1997). These spines are expected to increase the resistance to flow under the canopy (Grünbaum, 1997). Chimney spacing is greater in colonies without spines than it is in colonies that have been induced to form spines as they grow, suggesting that new chimney spacing depends on the resistance to flow under the canopy (Grünbaum, 1997).

In contrast, I found no effect of injury on the size or spacing of the pre-existing chimneys near the injury. I expected injuries to reduce flow to neighboring chimneys both by removing lophophores that pumped fluid to those chimneys and by forming new openings in the canopy. This suggests that, in contrast to *new* chimneys (Grünbaum, 1997), the size and spacing of *existing* chimneys may not be affected by flow within the colony.

Pressure and chimney formation

Chimneys function to reduce the pressure under the canopy, so it has been hypothesized that they form where the pressure is highest (Dick, 1987; Larsen and Riisgard, 2001). Reducing the pressure under the canopy is expected to be important for *M. membranacea* colonies because high pressure is predicted to inhibit feeding by reducing the incurrent flow rate (Grünbaum, 1995; Larsen and Riisgard, 2001). Note that Pratt (2004) did not find a difference in the incurrent flow rate between isolated zooids and groups of eight zooids; however, hydrodynamic models suggest that the pressure effect would be more important for larger colonies (Grünbaum, 1995).

Two different hydrodynamic models suggest that the canopy edge should be a site of relatively low pressure because it is an excurrent site and fluid flows from high pressure to low pressure (Grünbaum, 1995; Larsen and Riisgard, 2001). Therefore, the hypothesis that high pressure under the canopy induces chimney formation predicts that chimneys should form within the canopy, and not at the canopy edge (Dick, 1987).

In this study, all newly formed chimneys started out at or very near the canopy edge, not within the canopy, indicating that chimneys do not form at sites of high pressure, but instead form at sites of low pressure. Dick (1987) and Cook and Chimonides (1980) observed indentations in the canopy edge that they interpreted as chimneys in the process of forming, but they did not observe whether these indentations subsequently became chimneys.

Injury and chimney formation

To explain his observation of chimneys at sites of damage to the colony, Dick (1987) hypothesized that excurrent flow at injured sites may induce the lophophores surrounding the injury to take on the tilted morphology of chimney lophophores.

In this study, injury did not induce chimney formation. Lophophores surrounding injuries closed over the gap in the canopy formed by the injury—the opposite of what one would find if injury induced chimney formation. However, there remained a gap in the canopy over large injuries. Lophophores surrounding these gaps tilted away from the gap, which is one of the characteristics of chimney lophophores, consistent with Dick's (1987) hypothesis. However, unlike the chimney lophophores, the lophophores around large injuries did not become noticeably taller than their neighbors. These observations suggest that injury is not sufficient to induce chimney formation.

An alternative hypothesis, that the canopy forms chimneys at sites of high excurrent flow but closes over sites of low excurrent flow, is consistent with the results of this study. This hypothesis is consistent both with the observation that chimneys form at the canopy edge (an excurrent site) and with the observation that only injuries large enough to leave a lasting opening in the canopy take on characteristics of chimneys. Many other hypotheses might also explain these observations.

Summary

I found few effects of environmental flow factors on the remodeling of the external fluid transport system of colonies

of *Membranipora membranacea*. Whereas existing chimneys tended to increase in area, neither ambient flow speed nor injury to the colony had statistically significant effects on the magnitude of the changes in the size and spacing of existing chimneys. New chimneys did not form either at sites of high pressure under the canopy or at sites of injuries. However, both the lophophores and the stalks supporting the lophophores changed orientation after injury to neighboring zooids, thereby closing or partially closing the gap in the canopy formed by the injury. This suggests that the canopy does have the capacity to remodel in response to injury. *New* chimney formation at the canopy edge appears to depend on environmental flow factors (Grünbaum, 1997; Okamura and Partridge, 1999), in contrast to my results on *existing* chimneys.

This study suggests that conduits in some fluid transport systems are capable of remodeling, but the extent of their remodeling may not be affected by changes in the flow through them. Previous studies on the effects of flow on the remodeling of conduits in biological fluid transport systems have focused on systems that are completely internal and are involved in the transport of fluids within the organism. Changing the flow through the system causes remodeling of existing conduits in the mammalian circulatory system (reviewed by LaBarbera, 1990, 1995; Langille, 1995), the gastrovascular system of hydroids (Dudgeon and Buss, 1996; Buss, 2001), and the veins of plasmodial slime molds (Nakagaki *et al.*, 2000, 2001). In contrast, I found little effect of changes in the flow on the extent of remodeling of existing conduits in *M. membranacea* colonies, though the flow does appear to affect the formation of new conduits (Grünbaum, 1997; Okamura and Partridge, 1999). The chimneys of *M. membranacea* form openings onto the ambient fluid that allow filtered water to leave the colony. It would be of interest to see whether changes in flow through conduits in other suspension-feeding systems affect the extent of remodeling of those conduits.

Acknowledgments

I thank M. Koehl for helpful discussions and Y. Rahman for assistance in conducting experiments. I also thank D. Willows, Director, for use of facilities at Friday Harbor Labs, R. Dudley for feedback on the manuscript, and J. Strother and S. Jackson for technical assistance. This work was supported by a Howard Hughes Medical Institute Predoctoral Fellowship, a summer research grant from the Department of Integrative Biology, UC Berkeley, and by grants to M. Koehl from NSF (#OCE-9907120) and ONR (#N00014-03-1-0079).

Literature Cited

Banta, W. C., F. K. McKinney, and R. L. Zimmer. 1974. Bryozoan monticules: excurrent water outlets? *Science* **185:** 783–784.

Buss, L. W. 2001. Growth by intussusception in hydractiniid hydroids. Pp. 3–26 in *Evolutionary Patterns: Growth, Form and Tempo in the Fossil Record*, J. B. C. Jackson, S. Lidgard and F. K. McKinney, eds. University of Chicago Press, Chicago, IL.

Conover, W. J. 1999. *Practical Nonparametric Statistics*, John Wiley & Sons, New York.

Cook, P. L. 1977. Colony-wide water currents in living bryozoa. *Cah. Biol. Mar.* **18:** 31–47.

Cook, P. L., and P. J. Chimonides. 1980. Further observations on water current patterns in living bryozoa. *Cah. Biol. Mar.* **21:** 393–402.

Dick, M. H. 1987. A proposed mechanism for chimney formation in encrusting bryozoan colonies. Pp. 73–80 in *Bryozoa: Present and Past*, J. R. P. Ross, ed. Western Washington University, Bellingham, WA.

Dudgeon, S. R., and L. W. Buss. 1996. Growing with the flow: on the maintenance and malleability of colony form in the hydroid *Hydractinia*. *Am. Nat.* **147:** 667–691.

Eckman, J. E., and D. O. Duggins. 1993. Effects of flow speed on growth of benthic suspension feeders. *Biol. Bull.* **185:** 28–41.

Fenchel, T., and R. N. Glud. 1998. Veil architecture in a sulphide-oxidizing bacterium enhances countercurrent flux. *Nature* **394:** 367–369.

Grünbaum, D. 1995. A model of feeding currents in encrusting bryozoans shows interference between zooids within a colony. *J. Theor. Biol.* **174:** 409–425.

Grünbaum, D. 1997. Hydromechanical mechanisms of colony organization and cost of defense in an encrusting bryozoan, *Membranipora membranacea*. *Limnol. Oceanogr.* **42:** 741–752.

Harvell, C. D. 1984. Predator-induced defense in a marine bryozoan. *Science* **224:** 1357–1359.

LaBarbera, M. 1990. Principles of design of fluid transport systems in zoology. *Science* **249:** 992–1000.

LaBarbera, M. 1995. The design of fluid transport systems: a comparative perspective. Pp. 3–27 in *Flow-Dependent Regulation of Vascular Function*, J. A. Bevan, G. Kaley, and G. M. Rubanyi, eds. Oxford University Press, New York.

LaBarbera, M., and S. Vogel. 1982. The design of fluid transport systems in organisms. *Am. Sci.* **70:** 54–60.

Langille, B. L. 1995. Blood flow-induced remodeling of the artery wall. Pp. 3–27 in *Flow-Dependent Regulation of Vascular Function*, J. A. Bevan, G. Kaley, and G. M. Rubanyi, eds. Oxford University Press, New York.

Larsen, P. S., and H. U. Riisgard. 2001. Chimney spacing in encrusting bryozoan colonies (*Membranipora membranacea*): video observations and hydrodynamic modeling. *Ophelia* **54:** 167–176.

Lidgard, S. 1981. Water flow, feeding, and colony form in an encrusting cheilostome. Pp. 135–142 in *Recent and Fossil Bryozoa*, G. P. Larwood and C. Nielson, eds. Olsen and Olsen, Fredensborg, Denmark.

Nakagaki, T., H. Yamada, and T. Ueda. 2000. Interaction between cell shape and contraction pattern in the *Physarum* plasmodium. *Biophys. Chem.* **84:** 195–204.

Nakagaki, T., H. Yamada, and Á. Tóth. 2001. Path finding by tube morphogenesis in an amoeboid organism. *Biophys. Chem.* **92:** 47–52.

Norton, T. A. 1973. Orientated growth of *Membranipora membranacea* (L.) on the thallus of *Saccorhiza polyschides* (Lightf.) Batt. *J. Exp. Mar. Biol. Ecol.* **13:** 91–95.

Okamura, B. 1985. The effects of ambient flow velocity, colony size and upstream colonies on the feeding success of bryozoa. II. *Conopeum reticulum* (Linnaeus), an encrusting species. *J. Exp. Mar. Biol.* **89:** 69–80.

Okamura, B., and J. C. Partridge. 1999. Suspension feeding adaptations to extreme flow environments in a marine bryozoan. *Biol. Bull.* **196:** 205–215.

Pratt, M. C. 2004. Effect of zooid spacing on bryozoan feeding success: Is competition or facilitation more important? *Biol. Bull.* **207:** 17–27.

Schwaninger, H. R. 1999. Population structure of the widely dispersing marine bryozoan *Membranipora membranacea* (Cheilostomata): implications for population history, biogeography, and taxonomy. *Mar. Biol.* **135:** 411–423.

Stewart, H. L. 2000. Morphological heterogeneity among zooids of encrusting colonies of *Membranipora membranacea* induces passive flow through the colony. *Am. Zool.* **40:** 1223.

Vogel, S. 1977. Current-induced flow through living sponges in nature. *Proc. Natl. Acad. Sci. USA* **74:** 2069–2071.

Winston, J. E. 1979. Current-related morphology and behavior in some Pacific coast bryozoans. Pp. 247–267 in *Advances in Bryozoology*, G. P. Larwood and M. B. Abbott, eds. Academic Press, New York.

Yoshioka, P. 1982. Predator-induced polymorphism in the bryozoan *Membranipora membranacea* (L.). *J. Exp. Mar. Biol. Ecol.* **61:** 233–242.

Young, C. M., and L. F. Braithwaite. 1980. Orientation and current-induced flow in the stalked ascidian *Styela montereyensis*. *Biol. Bull.* **159:** 428–440.

Reference: *Biol. Bull.* **208:** 60–68. (February 2005)

Diversification Before the Most Recent Glaciation in *Balanus glandula*

JOHN P. WARES* AND CLIFFORD W. CUNNINGHAM

Department of Biology, Duke University, Durham, North Carolina 27708

Abstract. A deep genetic cline between southern populations of the barnacle *Balanus glandula* (from about Monterey Bay southward) and northern populations (from northern California through Alaska) has recently been described. If this pattern is due to historical isolation and genetic drift, we expect it to have formed recently and represent a transient, nonequilibrium state. However, this cline appears to have formed well before the last glacial maximum. Our assays of sequence diversity at a region of mitochondrial cytochrome oxidase I, combined with coalescent estimators of the time of separation for these two regions, suggest that a late Pleistocene event more than 100 thousand years ago may be responsible for the initial separation. This suggests that either strong oceanographic mechanisms or natural selection have maintained the cline, because there has clearly been adequate time for this cline or polymorphism to resolve itself by genetic drift and migration. However, reliance on only a single mitochondrial marker for which the substitution rate has been estimated still limits the resolution of our analysis.

Introduction

Patterns of genetic variation in some coastal species indicate the effects of changing paleoclimate on distribution and abundance (*e.g.*, Edmands, 2001; Dawson, 2001; Hickerson and Ross, 2001; Marko, 2004). These effects may lead to significant levels of population structure, where some regions harbor significantly different frequencies of particular alleles or molecular markers (Grosberg and Cunningham, 2001). Predictions range from extreme divergence of regions, indicated by reciprocal monophyly on a gene tree of regional samples (see Avise, 2000), to gradients in overall genetic diversity. Patterns suggesting divergence between populations currently distributed to the north and south of the glacial margin at the last glacial maximum (LGM)—about 18 thousand years ago (kya)—are often explained as representing populations that survived Pleistocene glaciation in "unglaciated refugia" (Holder *et al.*, 1999; Hickerson and Ross, 2001; Wares, 2002). A finding of lower genetic diversity in populations north of the LGM glacial margin is typically interpreted as post-glacial expansion from a southern refugial distribution (see Marko, 2004). In marine organisms, the location and persistence of paleoceanographic phenomena must also be considered, such as the location of extant currents and their persistence through Pleistocene climate change (Herbert *et al.*, 2001; Wares, 2002).

Sotka *et al.* (2004) characterized the genealogical relationship among individuals of *Balanus glandula* from coastal British Columbia to southern California, using DNA sequence data from two loci (mitochondrial cytochrome oxidase I [mtCOI] and nuclear elongation factor 1α). The analysis of these data indicates a clinal pattern of allelic class frequencies, suggesting that there are surprisingly low levels of realized migration (gene flow) along the California coast from Point Arena to Monterey Bay. The divergence between the northern and southern lineages does not represent a classical "phylogeographic break" in which the two groups are genealogically distinct (class I phylogeographic status; Avise 2000). Instead, the pattern is consistent with secondary contact between historically isolated lineages, which has proceeded slowly because of selection or physical oceanographic forces. One way to distinguish among the mechanisms that may be maintaining this pattern is to estimate how long ago the cline formed. If the cline is quite

Received 26 May 2004; accepted 29 November 2004.

* To whom correspondence should be addressed, at Department of Genetics, University of Georgia, Athens, Georgia 30602. E-mail: jpwares@uga.edu

Abbreviations: kya, thousand years ago; LGM, last glacial maximum; N_e, effective population size; mtCOI, mitochondrial cytochrome oxidase I.

ancient, it becomes less likely that neutral processes could have maintained it.

The effective population size (N_e; Hudson, 1990) is a parameter that describes the idealized average number of individuals contributing genetic diversity each generation. When estimated from genealogical data using methods based on coalescent theory, this parameter represents the long-term size of the inbreeding population and thus describes the demography of a population over time scales of 10^3–10^5 years (Turner *et al.*, 2002). The time of isolation between populations can also be measured in terms of N_e. Here we apply these methods to mitochondrial data taken from *B. glandula* populations between southern Alaska and southern California (see Table 1). Although other molecular data sets are available (*e.g.*, Sotka *et al.*, 2004), estimates of the substitution rate μ have only been calculated for this portion of the mtCOI locus in balanoid barnacles (see Materials and Methods). Using these data, we estimate regional N_e and the range of divergence times between the southern and northern allelic classes of *B. glandula* to determine whether this divergence was associated with the LGM as is commonly predicted, or if it significantly predates the LGM (see Marko, 2004).

Because it is difficult to distinguish between weak selection and physical oceanographic forces in maintaining this genetic cline (Sotka *et al.*, 2004), these demographic parameters may reflect the predictions made by physical oceanographers regarding changes along the continental shelf during the Pleistocene (Gaines and Roughgarden, 1985; Roughgarden *et al.*, 1988; Wing *et al.*, 1995; Lyle *et al.*, 2001) that would create barriers to gene flow, and areas of larval retention. The formation and maintenance of this cline essentially requires such selection or oceanographic structuring, without which it should collapse quickly (Irwin, 2002; Sotka *et al.*, 2004). By narrowing the range of historical demographic scenarios associated with this cline, we can better infer the conditions that are maintaining it.

Materials and Methods

Balanus glandula (Darwin, 1854) is distributed in dense aggregates on rocky shores from northern Alaska to just south of the border between the United States and Mexico (Barnes and Barnes, 1956; Newman and Abbott, 1980) and is readily distinguished from other cirriped species by exoskeletal characters of the operculum, parieties, and basis (Newman and Abbott, 1980). Individuals (n = 370) were haphazardly collected in the field (see Table 1 for collection locations) and placed in 95% ethanol prior to DNA isolation. All molecular methods are as in Wares *et al.* (2001); a 710-bp fragment of the mitochondrial cytochrome oxidase I gene (mtCOI) was amplified using the universal primers of Folmer *et al.* (1994), with sequence data deposited in GenBank (Benson *et al.*, 2004), as AF234351-234462 and AY795085-795281, and the aligned data set available from EMBL (Kulikova *et al.*, 2004), as ALIGN-000504. This mitochondrial data set is entirely independent of the one presented in Sotka *et al.* (2004), using different individuals, mostly collected 2–3 years earlier, and a different fragment of the mtCOI gene; these data include almost three times as many individuals as in Wares *et al.* (2001) and eight newly sampled populations (Juneau, Alaska; Bamfield, British Columbia; Fogarty Creek and Strawberry Hill, Oregon; and Point St. George, Cape Mendocino, Point Arena, and Bodega Bay, California). Phylogenetic analysis of these data was performed using PAUP*4.0*b*10 (Swofford, 2002). We followed the methods of Wares *et al.* (2001) to obtain the full set of parsimony trees, and we used Arlequin 2.001 (Schneider *et al.*, 1997) to analyze sequence data for geographic associations.

We estimated effective population size (N_e) within populations and pairwise migration among populations, as well as divergence time, using four related but distinct methods. (1) To treat the continuous coalescent description of population relationships, we used the method of Wilkins and Wakeley (2002) to estimate N_e and neighborhood size (N_b; roughly the per-generation effective gene flow distance) for populations south of the cline (see Fig. 1), within the clinal region, and north of the clinal region. (2) Coalescent estimation of N_e and pairwise migration M was calculated using MIGRATE 1.7.6 (Beerli and Felsenstein, 1999). Replicate analyses were performed using the methodology of Turner *et al.* (2002). (3) Estimates of diversity in terms of θ(S) and $\theta(\pi)$ were calculated using Arlequin 2.001 (Schneider *et al.*, 1997). These estimates, combined with the estimated substitution rate at mtCOI for balanomorph barnacles (Wares, 2001; Wares and Cunningham, 2001), were used to calculate frequency-based estimates of allelic age (Slatkin and Rannala, 1997). (4) Recent improvements in Markov chain Monte Carlo (MCMC) coestimation of ancestral parameters allow the coordinated estimation of migration parameters between regions as well as the divergence time between those regions. The program IM (Hey and Nielsen, 2004) estimated these parameters, again grouping the "northern" and "southern" regions, both across Monterey Bay and across Cape Blanco, Oregon. This latter comparison is primarily used as a control estimate of divergence; because analyses of divergence time are rarely verified against populations with known divergence using an independent estimate of μ, we estimate this parameter for Cape Blanco because no phylogeographic transition is present in *B. glandula* at this location (Sotka *et al.*, 2004; see Results). Thus, only a minimal divergence is expected relative to the divergence across the observed cline.

Because of computational difficulties with searching and resolving large genealogies for ancestral population parameters, two groups of MCMC analyses were performed using IM: the full data set was separated at Monterey Bay for

analysis with 10^6 chains after discarding the first 10^5 chains. Then, as in Turner *et al.* (2002), the data partitions were randomly sampled for 20 sequences from each regional group to allow the analysis to stabilize parameter results more efficiently. A program, SEQSAMPLER.RB (written in Ruby and available from JPW), generated 40 pseudoreplicate data sets that were each analyzed twice using distinct starting seeds and the same initial parameters as for the whole data set.

Results

Sequences from the southernmost populations of *Balanus glandula* (south of Monterey Bay) are statistically distinct from those to the north. Although phylogenetic analysis shows this distinction to be robust (Wares *et al.*, 2001), the signal can be summarized by looking at only two nucleotide positions (273 and 360 in the aligned data set of 632 bp, of which 61 positions are parsimony informative and 50 are variable but parsimony uninformative; Fig. 1). The southernmost populations are fixed for an adenine residue at these nucleotide positions; the branches supporting the two clades that are limited to northern populations are themselves supported in 100% of maximum parsimony trees (consensus). This trend is significant when measured by Φ_{st} (Wares *et al.*, 2001). No populations from Cape Mendocino northward or Pacific Grove southward are significantly differentiated from each other within regions, but comparisons between regions are highly significant in analysis of molecular variance. Figure 2 shows that this pattern is driven by the secondary contact of genetically distinct populations, as the apparent isolation by distance pattern (Fig. 2a, Mantel test of pairwise F_{st} matrix against pairwise geographic distance, $P < 0.01$) breaks down when clades are analyzed separately, even though overall geographic distribution is comparable (Fig. 2b). Equilibrium isolation by distance (*sensu* Wright, 1943) represents limited dispersal and gene flow, but nonequilibrium dynamics (such as vicariance) can artificially create the same genetic patterns (Peterson and Denno 1998).

Analysis of divergence time between the lineages that dominate either northern or southern populations of *B. glandula* indicates that the initial formation of the phylogeographic discontinuity is more ancient than the last glacial maximum (LGM) by at least an order of magnitude. Here we assume that the substitution rate for cytochrome oxidase I in *B. glandula* is similar to that measured for other barnacles ($\mu \approx 1.55 \times 10^{-8}$ in *Chthamalus*, Wares, 2001; $\mu \approx 2.18 \pm 1.1 \times 10^{-8}$ in *Semibalanus*, Wares and Cunningham, 2001). The method of Wilkins and Wakeley (2002), using the mean of these two estimates, indicates that the maximum likelihood estimation of the effective population size (N_e) in populations to the north of the cline is approximately 251,200 and slightly lower in the populations to the south of the cline (199,500) and in the clinal region itself (208,900). In a purely panmictic population, the time to the most recent common ancestor is expected to be $2N_e$ (Hudson, 1990); thus the combined set of allelic classes in each region indicates that current diversity has arisen in the past 500 thousand years or so. This same method suggests that the neighborhood size is indistinguishable from infinity for the regions to the north and south of the cline, while populations within the cline have a neighborhood size of less than 1000 m, which corresponds to the results of Sotka *et al.* (2004).

Estimates of $\theta = 2N_e\mu$ for each population sampled ranged from 1.80 to 4.66 in our MIGRATE analyses. However, for some population samples we were unable to get a stable estimate from this method. Estimates of θ were somewhat correlated (0.45) with estimates of θ made using Arlequin, and log plots of this parameter show the same basic trend; because of difficulties with obtaining stable estimates using MIGRATE, however, we report only the results from Arlequin. In Table 1, N_e at each site is estimated using $\theta(\pi)$ and the above substitution rates. Frequency-based methods (Slatkin and Rannala, 1997) of estimating the age of alleles indicate that the "northern" mitochondrial haplotype groups are likely to have arisen well before the LGM, as well. The average $\theta(\pi)$ within each allelic class and the frequency of each class is used in these estimates: southern group $\theta(\pi) = 3.192$ (119–253 kya); northern groups $\theta(\pi) = 2.489$ and 1.600 (93–197 kya and 59–127 kya, respectively).

The mean time of divergence from our two full-data analyses using IM is $t = 4.66$ (4.64, 4.68 were the maximum likelihood estimates from each replicate), where $t = \mu t$ (t is time in years; Hey and Nielsen, 2004). This mean generates a divergence time of 338,000 (±113,000) years using a per-gene substitution rate of $1.4 \times 10^{-5}(\pm 6.9 \times 10^{-6}$; Wares and Cunningham, 2001). Migration across Monterey Bay was limited (estimated as $m_1 = 0.91$ from north to south, and $m_2 = 0.99$ from south to north), consistent with the finding of limited gene flow in Sotka *et al.* (2004) and the restriction indicated by analysis with the Wilkins and Wakeley (2002) method. The same values estimated from the 80 pseudoreplicate data sets were $t = 1.34 \pm 1.47$, and much lower estimates of m_1 and m_2 (0.44, 0.39). From the 82 IM analyses, the minimum divergence time between the northern and southern regions across Monterey Bay is $t = 0.595$ (43.2 ± 14.5 kya). Estimated effective population size in both regions is much higher in the IM analysis (8.7×10^6 in populations north of Monterey Bay, 7.0×10^6 in populations to the south). The pseudoreplicate analyses may be conflated by significantly higher estimates of θ because any small subsample of the complete, highly diverse data set involves long branch lengths between

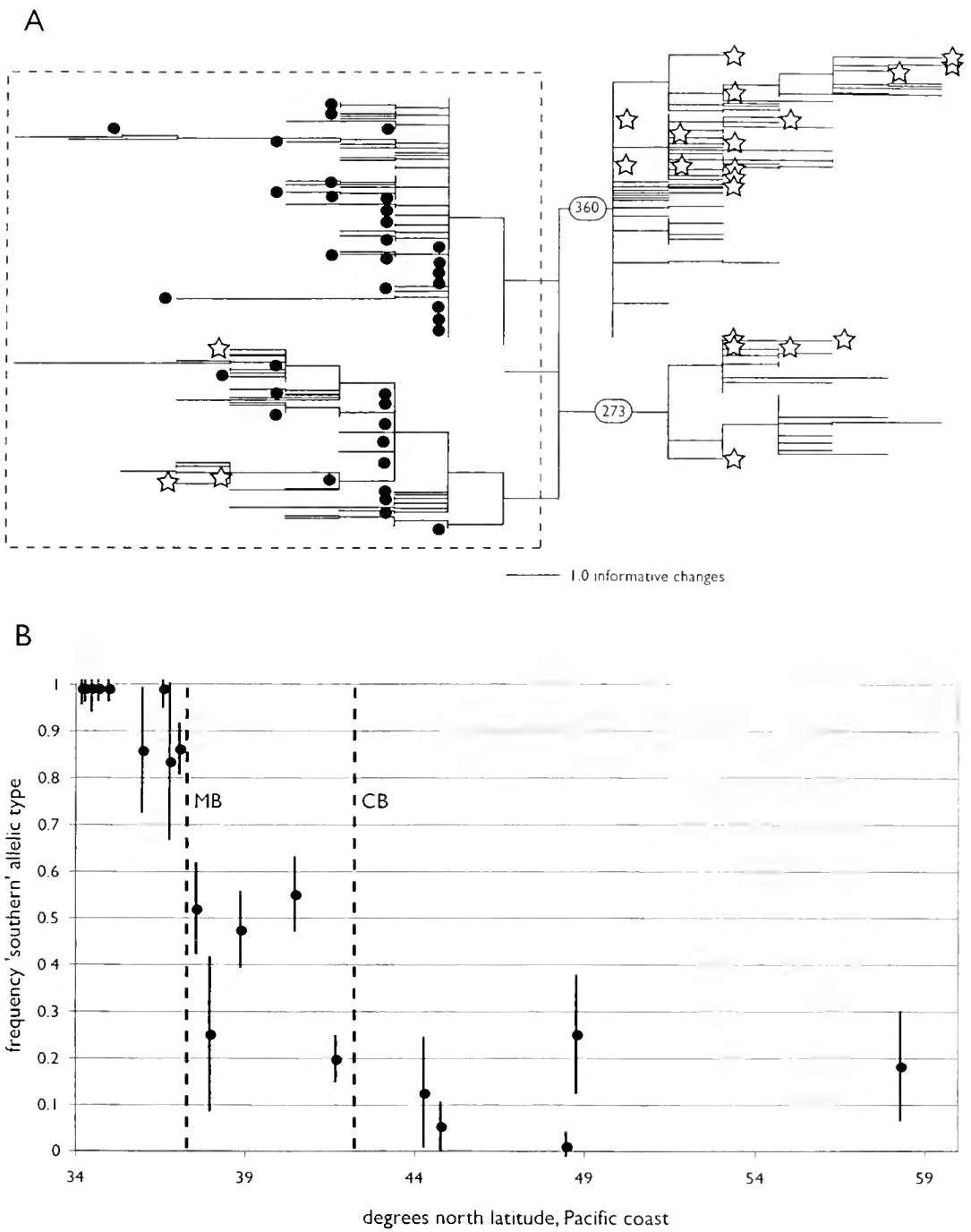

Figure 1. A. maximum-parsimony phylogram representing phylogeographic diversity of parsimony-informative sites in *Balanus glandula* ($n = 363$). For reference, dark circles represent individuals collected from south of Point Conception (34.5°N) and open stars represent individuals collected from the 3 northernmost collection sites. In general, the "northern" clades harbor only a single individual collected from south of Monterey Bay (Kirk Creek). As indicated by the plot in B, the frequency of the "southern" allelic type (see text) decreases rapidly between Monterey Bay (MB; California) and Cape Blanco (CB; Oregon). Here the southern type is defined as those individuals not found in the clades formed by substitutions at sites 273 and 360 from the reported alignment of mitochondrial cytochrome oxidase I. Binomial sampling error of the frequency of the southern type from each population is indicated.

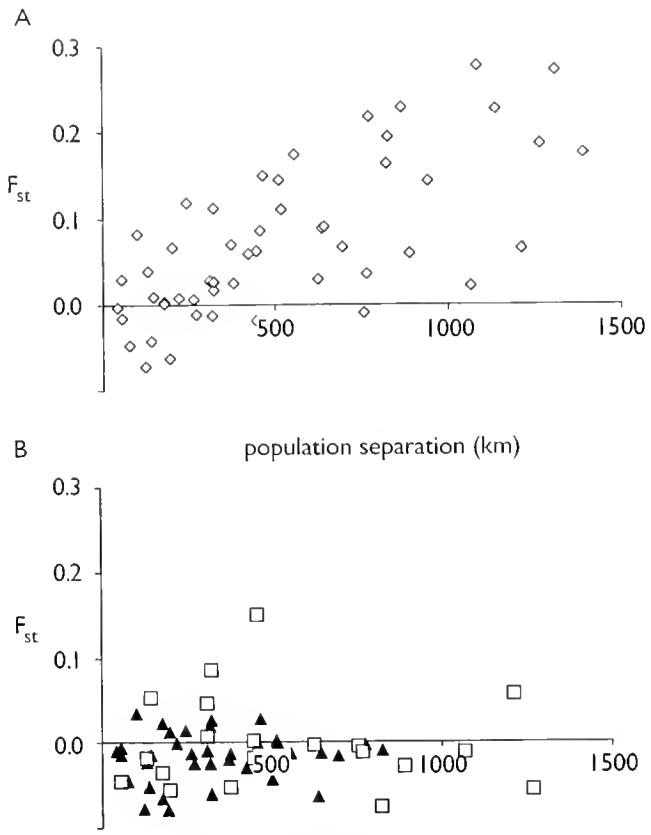

Figure 2. Isolation by distance plots for haplotype data in *Balanus glandula*. (A) All data combined; vertical axis is pairwise F_{st} between populations and horizontal is pairwise distance in kilometers between populations. A Mantel test (1000 matrix permutations) indicated that the relationship between F_{st} and distance is significant ($P < 0.01$). (B) Sequence data from the clades that predominate in northern populations (substitutions 360 and 273 on Figure 1; black) and the clade that predominates in southern populations (white) analyzed separately. Neither relationship is statistically significant.

individuals, perhaps suggesting much more unsampled diversity than exists when the entire data set is available.

Replicate comparisons of populations across Cape Blanco (excluding populations south of the clinal region), despite the lack of phylogeographic signal based on other types of analyses (Wares *et al.*, 2001; Sotka *et al.*, 2004), are not different from the Monterey Bay comparisons. The mean divergence time of pseudoreplicate data sets using IM is in fact higher ($t = 1.67 \pm 1.64$ kya), although the average estimates of migration across Cape Blanco are also much higher ($m_1 = 3.56$ and $m_2 = 4.16$). As with the pseudoreplicate analyses across Monterey Bay, estimates of θ were highly inflated by the subsampling process by nearly an order of magnitude over estimates based on $\theta(\pi)$. The average across- Cape Blanco estimate using the entire data set (excluding populations south of Monterey Bay) is $t = 4.479$ ($m_1 = 3.58$ and $m_2 = 2.72$).

Discussion

Estimating the age of an evolutionary event by using molecular data is often a circular task. Without adequate fossil or biogeographic evidence, inferences based on genetic diversity must rely on consistency among different analytical methods. Here, calculations of population age and time of separation between populations of *Balanus glandula* on either side of a significant genetic cline suggest that the separate allelic groups likely formed well before the last glacial maximum (LGM). However, these estimates have broad confidence intervals, indicating that in some cases we cannot reject a more recent event. Few molecular markers are available for which the substitution rate μ is known with confidence, and without better cases for which this parameter has been estimated independently of the biogeographic or paleontological hypothesis being tested, it will be difficult to improve such estimates. In this study, we did not obtain significantly different estimates of divergence when comparing regions on either side of the strong genetic cline than when we compared populations on either side of a separate geographic landmark for which there is no evidence of genetic differentiation. Thus, these methods and estimates must be applied with caution.

When there is complete random mating across the samples, the expected time to the most recent common ancestor is $\sim 2N_e$ generations (Hudson, 1990), but there is high variance around this prediction (Hudson and Turelli, 2003) and an inference from a single gene may be misleading. Our estimates of $N_e = \theta/2\mu$ are on the order of 10^5 for each sampled location, similar to estimates of N_e (by the method of Wilkins and Wakeley, 2004) when comparing regional groups (north and south) separated by the multilocus cline between Monterey Bay and Pt. Arena. Frequency-based methods (Slatkin and Rannala, 1997) also suggest that these groups diverged during or prior to marine isotope stage 5 (74–131 kya; Lyle *et al.*, 2001). Under panmixia, we expect similar estimates of diversity at multiple spatial scales (Hudson, 1990; Beerli, 2004). However, methods designed to estimate divergence time (t) and gene flow simultaneously (Hey and Nielsen, 2004) suggest much higher N_e in each region (on the order of 10^6–10^7) and a much older divergence. Methods that do not simultaneously account for ongoing migration following the divergence of populations frequently estimate lower separation times (Wares *et al.*, 2002). However, estimates of t are similar for populations across Cape Blanco and Monterey Bay in this study, despite strong differences in estimated migration regimes across these two geographic features. These estimates also vary widely depending on the sample size from each region. If within-region coalescence is not significantly different from among-region coalescence, it should indicate high gene flow and the homogenization of population structure.

The tendency to attribute marine phylogeographic pat-

Table 1

Summary of collection data and estimates of effective population size (N_e) *for populations of* Balanus glandulus

Population	Collection date*	Location	Sample size	N_e†	SE‡
Juneau, AK	Summer 2003	58.3°N 134.5°W	11	131,885	164,715
Bamfield, BC (Canada)	Summer 2002	48.8°N 125.1°W	10	150,360	186,675
Friday Harbor, WA	Summer 1996	48.5°N 123.0°W	12	140,215	172,035
Fogarty Creek, OR	Summer 2002	44.8°N 124.0°W	19	140,940	166,910
Strawberry Hill, OR	Summer 2002	44.3°N 124.1°W	8	134,420	174,965
Point St. George, CA	Summer 1997	41.7°N 124.2°W	76	160,870	179,335
Cape Mendocino, CA	Summer 1997	40.5°N 124.4°W	40	162,320	182,285
Pt. Arena, CA	Summer 1997	38.9°N 123.7°W	47	142,030	163,250
Bodega Bay, CA	Summer 1997	38.3°N 123.0°W	8	144,925	185,944
Pacifica, CA	Spring 1997	37.6°N 122.5°W	17	168,840	196,925
Greyhound Rock, CA	Spring 1997	37.1°N 122.3°W	39	110,505	133,965
Moss Landing, CA	Spring 1997	36.8°N 121.8°W	6	91,665	133,235
Lovers Point, CA	Spring 1997	36.6°N 121.9°W	6	65,215	101,024
Kirk Creek, CA	Spring 1997	36.0°N 121.5°W	7	93,115	131,040
Tenera Point, CA	Summer 1995	35.0°N 121.5°W	14	110,115	138,360
Vandenberg AFB, CA	Summer 1995	34.7°N 121.5°W	14	100,000	128,110
Jalama, CA	Summer 1995	34.5°N 120.5°W	4	90,580	147,145
Arroyo Hondo, CA	Summer 1995	34.3°N 121.0°W	13	138,405	169,105
Mussels Shoals, CA	Summer 1995	34.2°N 120.5°W	10	129,345	163,980

* Collections were made between 1995 and 2003.

† Effective population size estimated by $\theta(\pi)/2\mu$ at each sampled location.

‡ Standard error was calculated using Arlequin (Schneider *et al.*, 1997), incorporating error estimates for μ from Wares and Cunningham (2001).

terns to the LGM is probably associated with the overall lack of information on earlier glacial events and the impact each stage had on nearshore geography and oceanographic patterns (Valentine and Jablonski, 1993; Lyle *et al.*, 2001). Nevertheless, it is clear that divergence among populations is often far more ancient than the LGM (Edmands, 2001; Dawson *et al.*, 2001; Hickerson and Ross, 2001; Marko, 2004). The time required for significant divergence between isolated populations is generally on a much longer scale than 20–40 thousand years (Palumbi and Kessing, 1991; Wares, 2002). In *B. glandula*, the presence of similar levels of diversity [$\theta(\pi)$] throughout the studied range (Table 1) suggests long-term persistence in habitats north of glacial margins (*e.g.*, southern Alaska), indicating that unlike other coastal species (Hickerson and Ross, 2001; Hellberg *et al.*, 2001; Dawson, 2001; Jacobs *et al.*, 2004; Marko, 2004), *B. glandula* has not expanded northward from a southern refugial population.

It is important to recognize the difference between primary divergence and secondary contact in this and other systems (Endler, 1982). The statistical signal for isolation by distance in *B. glandula* is driven solely by the divergence of the northern and southern allelic types, because removal of those diagnostic nucleotide sites—or analysis within allelic "type" alone—eliminates any signal of geographic differentiation (Fig. 2). No obvious or statistically significant differences exist between settlement classes at this mitochondrial locus or at several allozyme loci across large spatial scales, different intertidal heights, or among settlement sites (Hedgecock, 1986; Wares, unpubl. data). These patterns are robust across other data types as well—although only a couple of microsatellite loci have been isolated for *B. glandula*, gene flow also appears to be quite high between populations throughout the northern range of this species, including across Cape Blanco (R. J. Toonen and J. P. Wares, unpubl. data).

The potential for the cline between northern and southern allelic types to be maintained by selection, rather than by the introgression of historically differentiated populations of this barnacle, is not yet known (Sotka *et al.*, 2004), which complicates any demographic interpretations of these data on the basis of neutral expectations. It is now recognized that although mitochondrial sequence data have their merits for phylogeographic analyses (Avise, 2000), they may also reflect non-neutral evolutionary patterns (Ballard and Kreitman, 1995; Schizas *et al.*, 2001). The current position of the cline may not reflect the original geographic disjunction, because ancient clines tend to be "attracted" to contemporary discontinuities in gene flow (Endler, 1977; Hare and Avise, 1996; Irwin, 2002). The nearshore oceanography appears to have changed dramatically during late Pleistocene glacial and interglacial periods (Hendy and Kennett, 2000), and the strength and geographic position of the cline could have been similarly affected.

Clinal genetic variation has been identified in only a few marine metapopulations (Gardner, 1996). Although some hybrid zones are known for intertidal and abyssal species (Hilbish, 1996; Won *et al.*, 2003), few represent interactions

among populations of the same species (*e.g.*, Hilbish, 1996)—a set of interactions that may represent either secondary introgression of isolated lineages or primary divergence due to environmental adaptive pressures (Endler, 1982; Nielsen *et al.*, 2003). Sotka *et al.* (2004) argue conservatively that if the northern and southern populations of *B. glandula* separated at the LGM, the rate of introgression, or "rebound," from this disruption is extremely slow considering the assumed neutral rate of gene flow for a species with broadly dispersing planktonic larvae. Here we show that this cline has been maintained for far longer, either by abiotic factors that limit the dispersal of *Balanus* across the coast of central California, or by natural selection that limits the spread of the historically differentiated lineages, or both.

Physical oceanographic patterns, including currents and gyres, probably play the greatest role in driving larval dispersal in *B. glandula* (Connolly and Roughgarden, 1999; Connolly *et al.*, 2001). If these patterns alone maintain the distinction of northern and southern genetic races of *B. glandula*, the data presented here suggest that these oceanographic mechanisms would have to be stable since well before the LGM. We still know little about coastal geology and physical oceanographic processes prior to the LGM (Lyle *et al.*, 2001; Herbert *et al.*, 2001). Thus, we must be cautious about the precision of our estimates of N_e (in Table 1, error exceeds the estimates) or the age of the separation between these populations based on estimates of μ obtained from other taxa and without the confirmation of fossil data (Marko, 2002, 2004; Clarke and Knight, 2003; Graur and Martin, 2004). Here we simply suggest that the divergence of *B. glandula* populations predates the LGM, and the maintenance of this cline—perhaps by selection, since migration and advection are expected to homogenize these populations—must be considered on this longer time scale.

Since many physical oceanographic structures are believed to be unstable during glacial maxima (Herbert *et al.*, 2001; Graham *et al.*, 2003), the transitions between glacial and interglacial periods are likely to have interrupted or moved any such "selectively neutral" barrier to gene flow. Temperature regimes along the coast also change during climatic cycling, and species are known to extend their range northward during El Niño events (Newman and McConnaughey, 1987; Engle and Richards, 2001; Connolly and Roughgarden, 1999; but see Paine 1986). However, the actual latitudinal distribution and fitness of a species may depend on a number of abiotic variables, including coastal exposure, substrate type, food availability, and other spatial components (Sanford, 2001; Helmuth *et al.*, 2002; Harley and Helmuth, 2003). It is not clear how old *B. glandula* actually is, with little fossil data available (Pleistocene, Oregon coast; Zullo, 1969, 1984), but it has persisted through many climatic changes. Except for species in the *B. amphitrite* species complex (Puspasari *et al.*, 2001), a detailed phylogeny is not available for *Balanus*. The peculiar nature of this cline, in which allele frequencies differ significantly but most alleles are still present on both sides of the region, adds to the complexity of this pattern. The long-term maintenance of diversity in both regions is important for our understanding of the interaction between abiotic environment and genetic diversity (*e.g.*, Ma *et al.*, 2000) and the extent to which historical demographics contribute to contemporary character evolution (*e.g.*, Marchinko and Palmer, 2003; Marchinko *et al.*, 2004). Further genetic and ecological analysis of *B. glandula* will be necessary to fully explain this intraspecific divergence.

Acknowledgments

The authors thank R. Toonen, N. Tsutsui, M. Hickerson, E. Sotka, T. "fujitubo" Oakley, S. Palumbi, and R. Grosberg for editorial and analytical assistance. S. Morgan, J. Abrams, C. Thornber, J. Wright, T. Shirley, A. Baldwin, T. Stokell, and D. Goldwater contributed a significant amount of taxonomic and technical effort towards this project. The editorial and technical advice of N. Knowlton and two anonymous reviewers is greatly appreciated. This research was funded by an NSF Biological Oceanography grant (DEB-96808267) to C. W. C.

Literature Cited

Avise, J. C. 2000. *Phylogeography*. Harvard University Press, Cambridge, MA.

Ballard, J. W. O., and M. Kreitman. 1995. Is mitochondrial DNA a strictly neutral marker? *Trends Ecol. Evol.* **10:** 485–488.

Barnes, H., and M. Barnes. 1956. The general biology of *Balanus glandula* Darwin. *Pac. Sci.* **10:** 415–421.

Beerli, P. 2004. Effect of unsampled populations on the estimation of population sizes and migration rates between sampled populations. *Mol. Ecol.* **13:** 827–836.

Beerli, P., and J. Felsenstein. 1999. Maximum-likelihood estimation of migration rates and effective population numbers in two populations using a coalescent approach. *Genetics* **152:** 763–773.

Benson, D. A., I. Karsch-Mizrachi, D. J. Lipman, J. Ostell, and D. L. Wheeler. 2004. GenBank: update. *Nucleic Acids Res.* **32:** D23–D30.

Clarke, T., and J. Knight. 2003. Whale genetics study leaves conservationists all at sea. *Nature* **424:** 479.

Connolly, S. R., and J. Roughgarden. 1999. Increased recruitment of northeast Pacific barnacles during the 1997 El Niño. *Limnol. Oceanogr.* **44:** 466–469.

Connolly, S. R., B. A. Menge, and J. Roughgarden. 2001. A latitudinal gradient in recruitment of intertidal invertebrates in the northeast Pacific Ocean. *Ecology* **82:** 1799–1813.

Dawson, M. N. 2001. Phylogeography in coastal marine animals: a solution from California? *J. Biogeogr.* **28:** 723–736.

Dawson, M. N., J. L. Staton, and D. K. Jacobs. 2001. Phylogeography of the tidewater goby, *Eucyclogobius newberryi* (Teleostei, Gobiidae) in coastal California. *Evolution* **55:** 1167–1179.

Edmands, S. 2001. Phylogeography of the marine copepod *Tigriopus californicus* reveals substantially reduced interpopulation divergence at northern latitudes. *Mol. Ecol.* **10:** 1743–1750.

Endler, J. A. 1977. *Geographic Variation, Speciation, and Clines*. Princeton University Press, Princeton, NJ.

Endler, J. A. 1982. Problems in distinguishing historical from ecological factors in biogeography. *Am. Zool.* **22:** 441–452.

Engle, J. M., and D. V. Richards. 2001. New and unusual marine invertebrates discovered at the California Channel Islands during the 1997–1998 El Niño. *Bull. South. Calif. Acad. Sci.* **100:** 186–198.

Folmer, O., M. Black, W. Hoeh, R. Lutz, and R. Vrijenhoek. 1994. DNA primers for amplification of mitochondrial cytochrome *c* oxidase subunit I from diverse metazoan invertebrates. *Mol. Mar. Biol. Biotechnol.* **3:** 294–299.

Gaines, S., and J. Roughgarden. 1985. Larval settlement rate: a leading determinant of structure in an ecological community of the marine intertidal zone. *Proc. Natl. Acad. Sci. USA* **82:** 3707–3711.

Gardner, J. P. A. 1996. The *Mytilus edulis* species complex in southwest England: effects of hybridization and introgression upon interlocus associations and morphometric variation. *Mar. Biol.* **125:** 385–399.

Graham, M. H., P. K. Dayton, and J. M. Erlandson. 2003. Ice ages and ecological transitions on temperate coasts. *Trends Ecol. Evol.* **18:** 33–40.

Graur, D., and W. Martin. 2004. Reading the entrails of chickens: molecular timescales of evolution and the illusion of precision. *Trends Genet.* **20:** 80–86.

Grosberg, R. K., and C. W. Cunningham. 2001. Genetic structure in the sea: from populations to communities. Pp. 61–84 in *Marine Community Ecology,* M. D. Bertness, M. E. Hay, and S. D. Gaines, eds. Sinauer, Sunderland, MA.

Hare, M. A., and J. C. Avise. 1996. Molecular genetic analysis of a stepped multilocus cline in the American oyster (*Crassostrea virginica*). *Evolution* **50:** 2305–2315.

Harley, C. D. G., and B. S. T. Helmuth. 2003. Wave exposure, thermal stress, and absolute vs. effective shore level. *Limnol. Oceanogr.* **48:** 1498–1508.

Hedgecock, D. 1986. Is gene flow from pelagic larval dispersal important in the adaptation and evolution of marine invertebrates? *Bull. Mar. Sci.* **39:** 550–564.

Hellberg, M. E., D. P. Balch, and K. Roy. 2001. Climate-driven range expansion and morphological evolution in a marine gastropod. *Science* **292:** 1707–1710.

Helmuth, B., C. D. G. Harley, P. M. Halpin, M. O'Donnell, G. E. Hofmann, and C. A. Blanchette. 2002. Climate change and latitudinal patterns of intertidal thermal stress. *Science* **298:** 1015–1017.

Hendy, I. L., and J. P. Kennett. 2000. Dansgaard-Oeschger cycles and the California Current System: planktonic foraminiferal response to rapid climate change in Santa Barbara Basin, Ocean Drilling Program hole 893A. *Paleoceanography* **15:** 30–42.

Herbert, T. D., J. D. Schuffert, D. Andreasen, L. Heusser, M. Lyle, A. Mix, A. C. Ravelo, L. D. Stott, and J. C. Herguera. 2001. Collapse of the California Current during glacial maxima linked to climate change on land. *Science* **293:** 71–76.

Hey, J., and R. Nielsen. 2004. Multilocus methods for estimating population sizes, migration rates, and divergence time, with applications to the divergence of *Drosophila pseudoobscura* and *D. persimilis*. *Genetics* **167:** 747–760.

Hickerson, M. J., and J. R. P. Ross. 2001. Post-glacial population history and genetic structure of the northern clingfish (*Gobbiesox maeandricus*), revealed from mtDNA analysis. *Mar. Biol.* **138:** 407–419.

Hilbish, T. J. 1996. Population genetics of marine species: the interaction of natural selection and historically differentiated populations. *J. Exp. Mar. Biol. Ecol.* **200:** 67–83.

Holder, K., R. Montgomerie, and V. L. Friesen. 1999. A test of the glacial refugium hypothesis using patterns of mitochondrial and nuclear DNA sequence variation in rock ptarmigan (*Lagopus mutus*). *Evolution* **53:** 1936–1950.

Hudson, R. R. 1990. Gene genealogies and the coalescent process. Pp. 1–44 in *Gene Genealogies and the Coalescent Process,* D. Futuyma and J. Antonovics, eds. Oxford University Press, Oxford.

Hudson, R. R., and M. Turelli. 2003. Stochasticity overrules the "three-times rule": genetic drift, genetic draft, and coalescence times for nuclear loci versus mitochondrial DNA. *Evolution* **57:** 182–190.

Irwin, D. E. 2002. Phylogeographic breaks without geographic barriers to gene flow. *Evolution* **56:** 2383–2394.

Jacobs, D. K., T. A. Haney, and K. D. Louie. 2004. Genes, diversity, and geologic process on the Pacific coast. *Annu. Rev. Earth Planet. Sci.* **32:** 601–652.

Kulikova, T., *et al.* 2004. The EMBL Nucleotide Sequence Database. *Nucleic Acids Res.* **32:** D27–D30.

Lyle, M., L. Heusser, T. Herbert, A. Mix, and J. Barron. 2001. Interglacial theme and variations: 500 k.y. of orbital forcing and associated responses from the terrestrial and marine biosphere, U. S. Pacific Northwest. *Geology* **29:** 1115–1118.

Ma, X. L., D. L. Cowles, and R. L. Carter. 2000. Effect of pollution on genetic diversity in the bay mussel *Mytilus galloprovincialis* and the acorn barnacle *Balanus glandula*. *Mar. Environ. Res.* **50:** 559–563.

Marchinko, K. B., and A. R. Palmer. 2003. Feeding in flow extremes: dependence of cirrus form on wave-exposure in four barnacle species. *Zoology* **106:** 127–141.

Marchinko, K. B., M. T. Nishizaki, and K. C. Burns. 2004. Community-wide character displacement in barnacles: a new perspective for past observations. *Ecol. Lett.* **7:** 114–121.

Marko, P. B. 2002. Fossil calibration of molecular clocks and the divergence times of geminate species pairs separated by the Isthmus of Panama. *Mol. Biol. Evol.* **19:** 2005–2021.

Marko, P. B. 2004. 'What's larvae got to do with it?' Disparate patterns of post-glacial population structure in two benthic marine gastropods with identical dispersal potential. *Mol. Ecol.* **13:** 597–611.

Newman, W. A., and D. P. Abbott. 1980. Cirripedia. Pp. 504–535 in *Intertidal Invertebrates of California,* R. H. Morris, D. P. Abbott, and E. C. Haderlie, eds. Stanford University Press, Stanford, CA.

Newman, W. A., and R. R. McConnaughey. 1987. A tropical eastern Pacific barnacle, *Megabalanus coccopoma* (Darwin) in Southern California, following El Niño 1982–83. *Pac. Sci.* **41:** 31–36.

Nielsen, R., and J. Wakeley. 2001. Distinguishing migration from isolation: a Markov Chain Monte Carlo approach. *Genetics* **158:** 885–896.

Paine, R. T. 1986. Benthic community-water column coupling during the 1982–1983 El Niño: Are community changes at high latitudes attributable to cause or coincidence? *Limnol. Oceanogr.* **31:** 351–360.

Palumbi, S. R., and B. D. Kessing. 1991. Population biology of the trans-Arctic exchange: mtDNA sequence similarity between Pacific and Atlantic sea urchins. *Evolution* **45:** 1790–1805.

Peterson, M. A., and R. F. Denno. 1998. The influence of dispersal and diet breadth on patterns of genetic isolation by distance in phytophagous insects. *Am. Nat.* **152:** 429–446.

Puspasari, I. A., T. Yamaguchi, and S. Kojima. 2001. Phylogeny of the *Balanus amphitrite* complex occurring in Japan (Cirripedia: Balanidae) inferred from mitochondrial COI gene nucleotide sequences and morphology. *Sessile Organisms* **18:** 7–17.

Roughgarden, J., S. Gaines, and H. Possingham. 1988. Recruitment dynamics in complex life cycles. *Science* **241:** 1460–1466.

Sanford, E. 2001. The effect of variation in water temperature on the keystone predator *Pisaster ochraceus*. *Am. Zool.* **41:** 1576.

Schizas, N. V., G. T. Chandler, B. C. Coull, S. L. Klosterhaus, and J. M. Quattro. 2001. Differential survival of three mitochondrial lineages of a marine benthic copepod exposed to a pesticide mixture. *Environ. Sci. Technol.* **35:** 535–538.

Schneider, S., J. Kueffer, D. Roessli, and L. Excoffier. 1997. Arlequin. A software for population genetic data analysis; ver. 1.1. Available: http://lgb.unige.ch/arlequin/ [Accessed November 2004.]

Slatkin, M., and B. Rannala. 1997. Estimating the age of alleles by use of intraallelic variability. *Am. J. Hum. Genet.* **60:** 447–458.

Sotka, E. E., J. P. Wares, J. A. Barth, R. K. Grosberg, and S. R. Palumbi. 2004. Strong genetic clines and geographical variation in gene flow in the rocky intertidal barnacle *Balanus glandula*. *Mol. Ecol.* **13:** 2143–2156.

Swolford, D. 2002. *Phylogenetic Analysis Using Parsimony (PAUP) v. 4.0b10.* Sinauer, Sunderland, MA.

Turner, T. F., J. P. Wares, and J. R. Gold. 2002. Genetic effective size is three orders of magnitude smaller than adult census size in an abundant, estuarine-dependent marine fish (*Sciaenops ocellatus*). *Genetics* **162:** 1329–1339.

Valentine, J. W., and D. Jablonski. 1993. Fossil communities: compositional variation at many time scales. Pp. 341–349 in *Species Diversity in Ecological Communities: Historical and Geographic Perspectives*, R. E. Ricklefs and D. Schluter, eds. University of Chicago Press, Chicago.

Wares, J. P. 2001. Patterns of speciation inferred from mitochondrial DNA in North American *Chthamalus* (Cirripedia: Balanomorpha: Chthamaloidea). *Mol. Phyogenet. Evol.* **18:** 104–116.

Wares, J. P. 2002. Community genetics in the northwestern Atlantic intertidal. *Mol. Ecol.* **11:** 1131–1144.

Wares, J. P., and C. W. Cunningham. 2001. Phylogeography and historical ecology of the North Atlantic intertidal. *Evolution* **55:** 2455–2469.

Wares, J. P., S. D. Gaines, and C. W. Cunningham. 2001. A comparative study of asymmetric migration events across a marine biogeographic boundary. *Evolution* **55:** 295–306.

Wares, J. P., D. S. Goldwater, B. Y. Kong, and C. W. Cunningham. 2002. Refuting a controversial case of a human-mediated marine species introduction. *Ecol. Lett.* **5:** 577–584

Wilkins, J. F., and J. Wakeley. 2002. The coalescent in a continuous, finite, linear population. *Genetics* **161:** 873–888.

Wing, S. R., L. W. Botsford, J. L. Largier, and L. E. Morgan. 1995. Spatial structure of relaxation events and crab settlement in the northern California upwelling system. *Mar. Ecol. Prog. Ser.* **128:** 199–211.

Won, Y., C. R. Young, R. A. Lutz, and R. C. Vrijenhoek. 2003. Dispersal barriers and isolation among deep-sea mussel populations (Mytilidae: *Bathymodiolus*) from eastern Pacific hydrothermal vents. *Mol. Ecol.* **12:** 169–184.

Wright, S. 1943. Isolation by distance. *Genetics* **28:** 139–156.

Zullo, V. A. 1969. A late Pleistocene marine invertebrate fauna from Bandon, Oregon. *Proc. Cal. Acad. Sci.* **12:** 347–361.

Zullo, V. A. 1984. New genera and species of balanoid barnacles from the Oligocene and Miocene of North Carolina. *J. Paleontol.* **58:** 1312–1338.

Reference: *Biol. Bull.* **208:** 69–76. (February 2005)

Reproductive Biology of a New Hesionid Polychaete From the Great Barrier Reef

FREDRIK PLEIJEL[1,*] AND GREG W. ROUSE[2]

[1] *Department of Marine Ecology, Tjärnö Marine Biological Laboratory, Göteborg University, SE-452 96 Strömstad, Sweden, and Muséum national d'Histoire naturelle, Département Systématique et Evolution, CNRS UMR 7138, "Systématique, Adaptation, Evolution", 43, rue Cuvier, 75231 Paris Cedex 05, France; and* [2] *South Australian Museum, Nth Terrace, Adelaide, SA 5000, Australia, and School of Environmental & Earth Sciences, University of Adelaide, SA 5005, Australia*

Abstract. We describe *Lizardia hirschi*, a new hesionid genus and species, from shallow water on the Great Barrier Reef. It is characterized by small size (maximally around 2 mm long) and by males with paired penes on the last segment or the pygidium. The sperm are elongated, with a conical acrosome; extended, cylindrical nucleus; and three mitochondria. The females have three to four pairs of eggs in segments 10–13, up to 150 μm in diameter. The female reproductive system consists of spermathecae, situated in the notopodia of segments 10–12, and oviducts opening ventrally on segment 11. Fertilization may be internal. The female (but not the male) reproductive system appears to be homologous to that in another small hesionid, *capricornia*. The phylogenetic position of *L. hirschi* within Hesionidae is currently uncertain due to the retention of many apparently larval features in the adults.

Introduction

Hesionids are generally not provided with external genital organs (Pleijel, 1998, 2001). Recently, however, two new hesionids were described (Westheide *et al.*, 1994, Pleijel and Rouse, 2000), both of which have external genital organs. In *Sinohesione genitaliphora* Westheide, Purschke and Mangerich, 1994, the males have a pair of penes situated on the ventral side of the neuropodia of segment 14, and the females have paired openings of the spermathecae in the same position but on segment 16. In *capricornia* Pleijel and Rouse, 2000 (see this description for spelling of taxon name with the initial letter in lower case), the males have a pair of large penes situated at the bases of the neuropodia of segment 9, and the females have spermathecae in the notopodia of segments 11 and 12. Based on the phylogenetic relationships (Pleijel and Rouse, 2000), the external reproductive organs in these two taxa were considered nonhomologous. Here we introduce a third taxon with external genital organs, occurring as paired penes on the posterior end on the males, collected from several localities in shallow water on the Great Barrier Reef. Similar to *capricornia*, this new hesionid is very small, reaching only 2 mm in length, and has a number of characters in common with juvenile stages of other hesionids.

Received 30 April 2004; accepted 14 October 2004.

* To whom correspondence should be addressed, at Tjärnö Marine Biological Laboratory, SE-452 96 Strömstad, Sweden. E-mail: fredrik.pleijel@tmbl.gu.se

Materials and Methods

Specimens were extracted from scuba-collected sand and gravel samples by decantation through a 250-μm sieve and relaxed in a mixture of 7% (by weight) of $MgCl_2$ $6H_2O$ (in distilled water) and filtered seawater (see Rouse and Pleijel, 2001, for details). Relaxed specimens were studied alive, then processed for long-term storage and LM (light microscopy), SEM (scanning electron microscopy), or histology and TEM (transmission electron microscopy). For long-term storage, specimens were fixed in 10% formaldehyde (*i.e.*, 25% formalin) in filtered seawater for one or a few days, rinsed in distilled water, and transferred to 70%–80% ethanol. Specimens for DNA extraction were fixed in 70% ethanol. Specimens for SEM were preserved for one hour in 1%–2% osmium tetroxide in filtered seawater, rinsed and

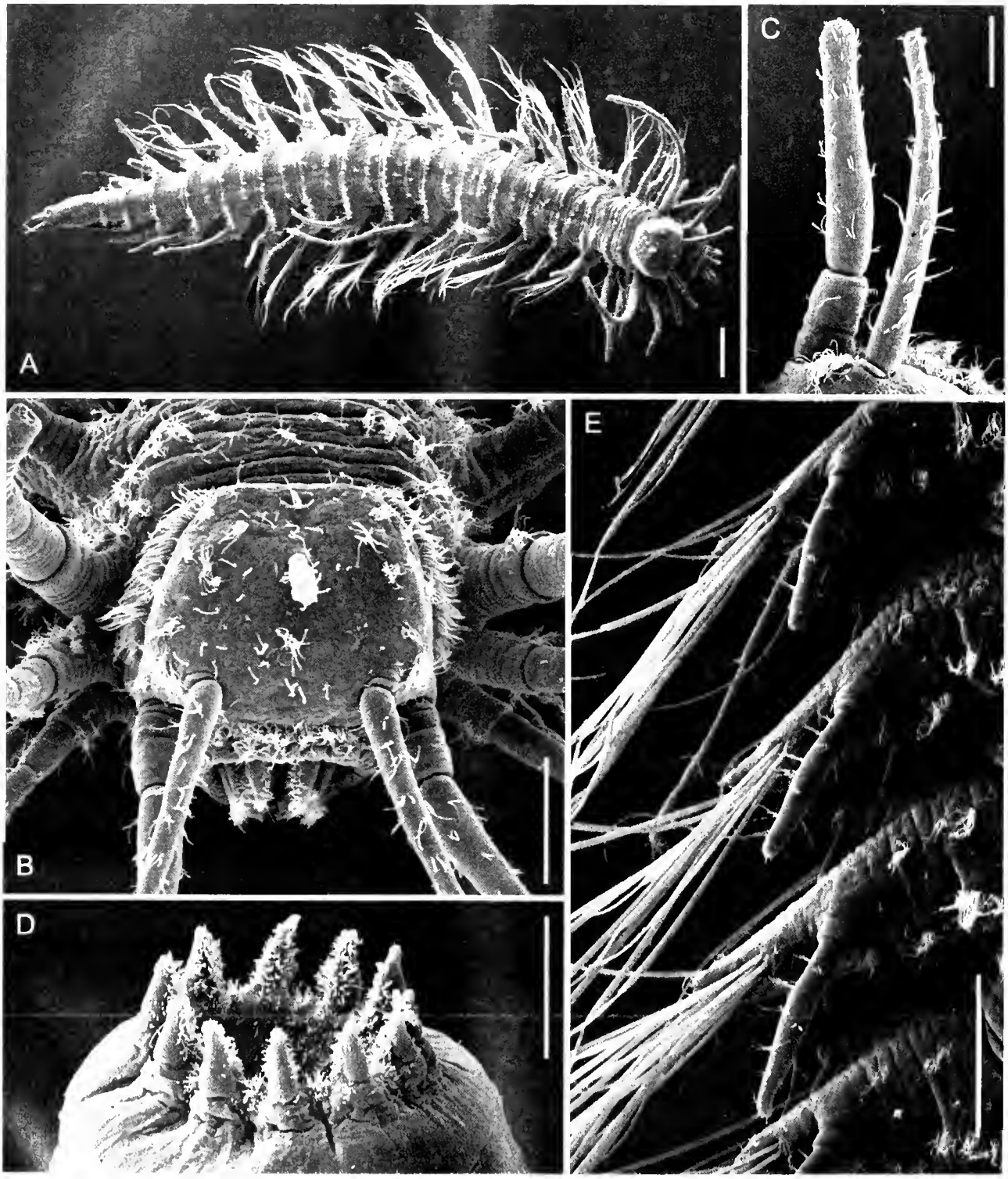

Figure 1. Scanning electron micrographs of *Lizardia hirschi*. (A) Male, dorsal view. (B) Anterior end, dorsal view. (C) Palp and palped antenna. (D) Distalmost part of everted proboscis. (E) Median parapodia, right side, ventral view. Scale lines: A, 100 μm; B, C, 25 μm; D, E, 50 μm.

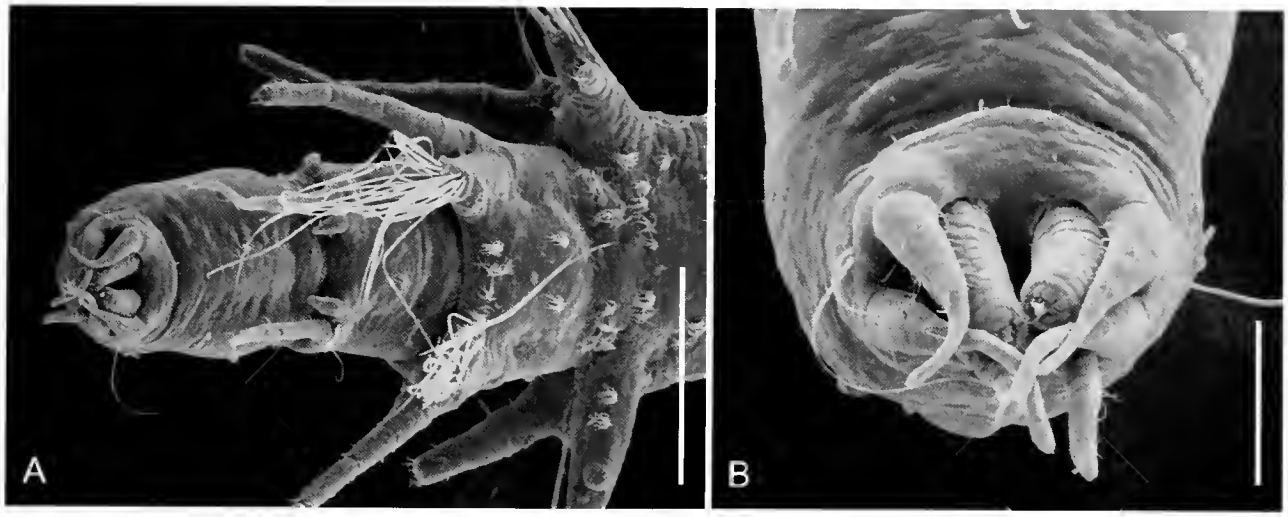

Figure 2. Scanning electron micrographs of *Lizardia hirschi*. (A) Posterior end of male, ventral view. (B) Posterior end of male, posteroventral view. The penes are the stout median projections, surrounded (from top to bottom) by ventral cirri, dorsal cirri, and pygidial cirri (partly hidden). Scale lines: A, 100 μm; B, 25 μm.

stored in distilled water, transferred to alcohol, critical-point-dried, and sputter-coated with carbon or gold (or both); microscopy was conducted at the SEM Laboratory of the National Museum of Natural History, Washington, DC. Specimens for histology and TEM were fixed in 3% glutaraldehyde (in 0.2 *M* sodium cacodylate buffer), postfixed in 1% osmium tetroxide before dehydration, and embedded in Spurr's epoxy resin. Sections of 1 μm and 70–90 nm ("ultrathin") sections were made through embedded specimens with an ultramicrotome. The 1-μm sections were stained with toluidine blue solution and photographed using a Leica DMR microscope. The ultrathin sections were stained with lead citrate and uranyl acetate and examined with a Philips CM100 transmission electron microscope. Whole mounts for LM were made from live and preserved specimens by mounting in Gurr's Aquamount, and a few additional specimens were preserved in 70% ethanol for DNA sequencing.

Formaldehyde-preserved specimens, whole specimens mounted for LM, and sections on glass slides are deposited at the South Australian Museum, Adelaide (SAM); SEM and DNA specimens are in FP's collection, and TEM sections are in GWR's collection.

Collector names are abbreviated as follows: Thomas Dahlgren (TD), Lars Jermiin (LJ), Eva Lewy (EL), Fredrik Pleijel (FP), and Greg W. Rouse (GWR).

Lizardia, new genus

Type species. Lizardia hirschi, new species.

Etymology. Named for the type locality, Lizard Island. Gender masculine.

Description. Monotypic; see *Lizardia hirschi*.

Lizardia hirschi, new species

(Figs. 1–4)

"Undescribed Hesionidae": Pleijel, 2001: fig. 18.2.

Material examined

Great Barrier Reef, Lizard Island: Holotype, immature male, fixed in formaldehyde (SAM E3366), between Palfrey and South Island, 14°42.0′S 145°26.3′E, 4 m, dead corals with algae, scuba, colls EL, FP, GWR, LJ, 27 March 2000; 1 paratype, female, fixed in formaldehyde (SAM E3363), 1 paratype mounted for LM (SAM E3364), North Point, 14°38.78′S 145°27.21′E, 8 m, coral sand, scuba, colls EL, FP, GWR, LJ, 23 March 2000; 2 spms mounted for SEM (FP), 3 spms (2 males, 1 female) preserved for LM and TEM (GWR), Bommie Bay, 14°39.13′S 145°28.031′E, 10–18 m, coral rubble, scuba, colls EL, FP, GWR, LJ, 25 March 2000; specimens for LM and TEM sectioned at 1 μm and mounted on microscope slides (SAM E3365). **Great Barrier Reef, Capricorn-Bunker Group, One Tree Island:** *ca.* 25 spms fixed in formaldehyde (SAM E3367), 2 spms mounted for LM (SAM E3368), *ca.* 15 spms mounted for SEM (FP), North Reef Flat, 23°29′S, 152°05′E, 2–3 m, scuba, colls FP, GRW, TD, among dead *Acropora*, 15 November 1996; 1 spm mounted for LM (SAM E3369), entrance Second Lagoon, 23°29′S, 152°04′E, sand and gravel, 4–6 m, scuba, colls FP, GWR, TD, 18 November 1996; 11 spms fixed in formaldehyde (SAM E3370), 2 spms fixed for DNA analyses (FP), entrance Second Lagoon,

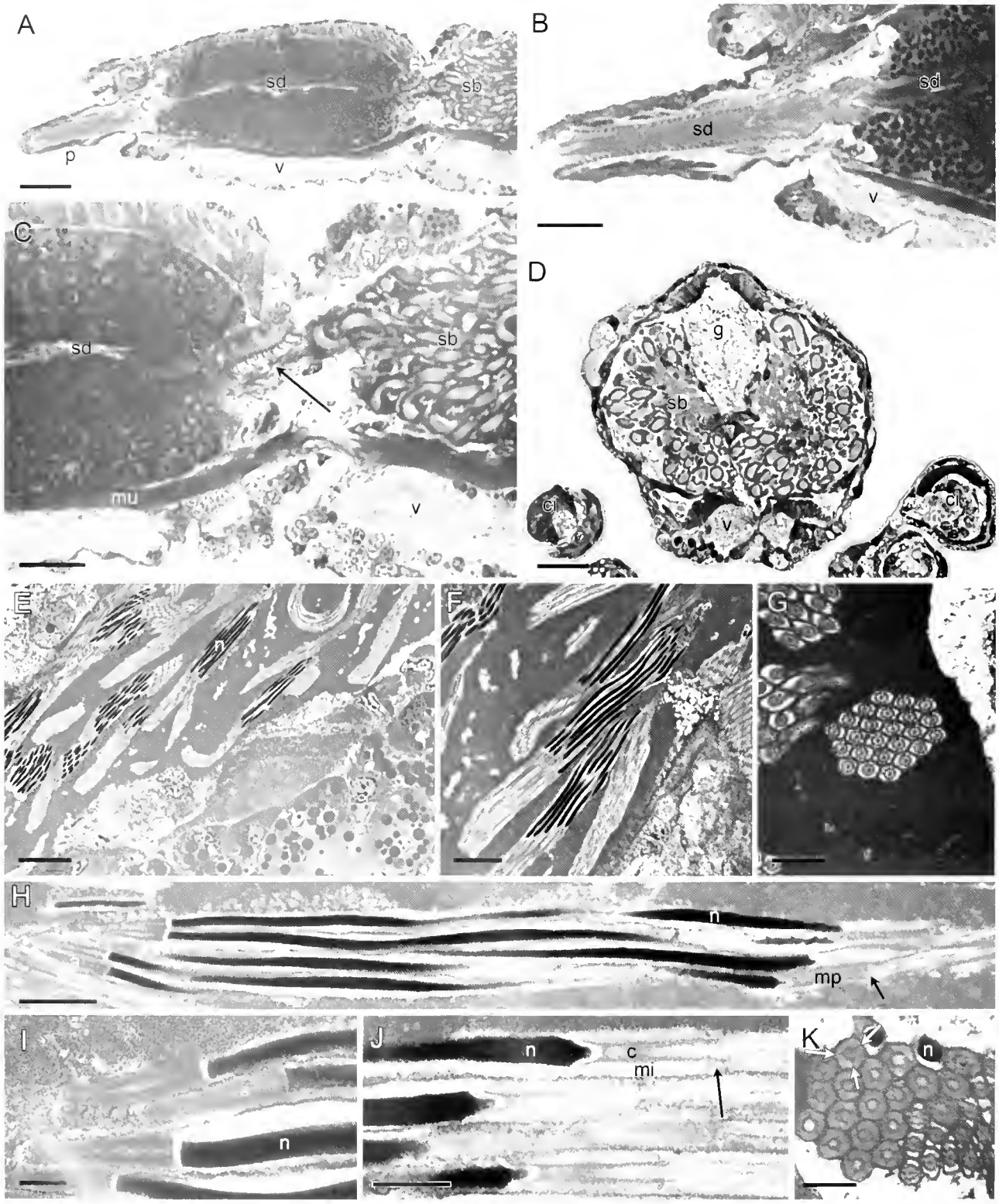
A
sd
sb
p
v
B
sd
sd
v
C
sd
sb
mu
v
D
g
sb
cl
v
cl
E
n
F
G
H
n
mp
I
n
J
n
c
mi
K
n

23°29′S, 152°04′E, sand and gravel, 4–6 m, scuba, colls FP, GWR, TD, 21 November 1996; 5 spms fixed in formaldehyde (SAM E3371), "the Bommie," 23°29′S, 152°03′E, off reef, 21 m, corals and red algae, scuba, colls FP, GWR, TD, 23 November 1996; *ca.* 70 spms fixed in formaldehyde (SAM E3372), 6 spms mounted for LM (SAM E3373) entrance Second Lagoon, 23°29′S, 152°04′E, sand and gravel, 4–6 m, scuba, colls FP, GWR, TD, 25 November 1996; 8 spms fixed in formaldehyde (SAM E3374), 1 spm (female) preserved for LM (GWR), bay in front of laboratory, 23°30′S, 152°05′E, 1 m, among dead *Tubipora*, snorkeling, coll. FP, 27 November 1996; 1 female specimen for LM sectioned at 1 μm and mounted on microscope slides (E3375).

Etymology. Named for Dr. Len Hirsch, in recognition of his contributions to polychaete systematics.

Description

Maximum length 2.1 mm, mature males always with 20 segments (including posteriormost segment surrounding penes and pygidium), mature females with 17 segments. Body elliptical in outline with truncate anterior end and tapering posterior end (Fig. 1A). Prostomium rounded rectangular, posterior margin narrower than anterior (Fig. 1A, B), posterior incision absent (Fig. 1B). Palpophores short, cylindrical; palpostyles much longer, basally slightly inflated and tapering to rounded tips (Fig. 1C). Paired antennae as long as palps, thinner than palpostyles, evenly tapered to rounded tips (Fig. 1C). Median antenna inserted mediodorsally on prostomium (Fig. 1B), between anterior pair of eyes, much shorter than paired antenna, elliptical to tapered. Anterior pair of eyes twice as large as posterior, anterior pair round to kidney-shaped, posterior pair round, both with lenses; anterior pair situated slightly farther apart than posterior pair, forming a trapezoid. Nuchal organs prominent, elongate, ciliated bands bordering posterodorsal and lateral sides of prostomium (Fig. 1B). Facial tubercle absent.

Proboscis smooth, jaws or teeth absent, terminal ring with 10 triangular, pointed and ciliated papillae (Fig. 1D). Proboscis extending posteriorly to segments 6–7 in non-everted condition.

Dorsal cirri and cirrophores segments 1–4 (possibly also 5) stouter and longer than on following segments, distinctly annulated. Ventral cirri segments 1–3 much stouter and longer than on following segments, distinctly annulated, situated on distinct cirrophores. Single noto- and neuroaciculae in segments 2 and 3, presence uncertain in segment 1. Segment 4 with neurochaetae, neuropodial lobes, and ventral cirri similar to following segments; notochaetae and notopodial lobes absent. Segment 5 similar to following ones.

Dorsal cirri median segments reaching about as far as notochaetae. Elevated dorsal cirri on segments 5, 8, 10, 12, 15, 17. Dorsal cirri segment 17 and thereafter directed posteriorly in males. Notopodial lobes small, conical, with double notoaciculae. Notochaetae of single kind, 5–8 fine, simple chaetae, internally camerate, with two longitudinal serrated rows with alternating teeth.

Neuropodial lobes conical, pointed, usually with single neuroacicula. Neurochaetae fine, all compound, *ca.* 10 each fascicle. Length of ventral and dorsalmost blades about half of median blades, with very fine and apparently unidentate tips. Shafts internally camerate. Ventral cirri inserted subdistally on small, low cirrophores, distinct annulation absent, tapering to small rounded tips (Fig. 1E), extending well beyond neuropodial lobes. No entire pair of pygidial cirri observed in females, but appear similar to dorsal cirri;

Figure 3. Reproductive system of male *Lizardia hirschi*. (A). One-micrometer longitudinal section through one of the penes, segment 20, and part of segment 19. Segment 20 contains masses of granular material and a duct for each penis. Segment 19 is filled with spermatozeugmata. (B) Detail of penis showing densely ciliated duct along its length that is continuous with the duct through segment 20. (C) One-micrometer longitudinal section through junction of segments 19 and 20. Spermatozeugmata accumulate in segment 19 and more-anterior segments and pass through to the penis *via* segment 20. Ciliated funnel into segment 20 indicated by arrow. (D) One-micrometer transverse section through segment 19 showing spermatozeugmata filling the coelom. (E) Transmission electron micrograph (TEM) showing spermatozeugmata in coleom of segment 19. Spermatozeugmata are surrounded by a uniform matrix of moderate electron density. (F) TEM of longitudinal section through spermatozeugmata. (G) TEM of transverse section through a spermatozeugma comprising 16 sperm. (H) TEM of longitudinal section through mature sperm, in a spermatozeugma, showing elongate cylindrical nuclei, conical acrosomes, short midpieces (terminates at arrow) and tails. (I). TEM of longitudinal section through acrosomes, which are simple, invaginated vesicles (J). TEM of longitudinal section through posterior end of sperm nuclei and midpieces. Note nuclear projection into midpiece, close to centriole apparatus. Midpiece termination indicated by arrow. (K). TEM of transverse section through a spermatozeugma showing midpieces comprising three mitochondria (arrows) and centriolar apparatus. Abbreviations: a, acrosome; c, centriolar apparatus; g, gut lumen; mp, sperm midpiece; mu, muscle; n, sperm nucleus; sd, sperm duct; sb, spermatozeugma; v, ventral nerve cord. Scale lines: A and D, 20 μm; B and C, 10 μm; E, 5 μm, F, 2.5 μm; G, J, and K, 0.5 μm; H, 1 μm; I, 0.25 μm.

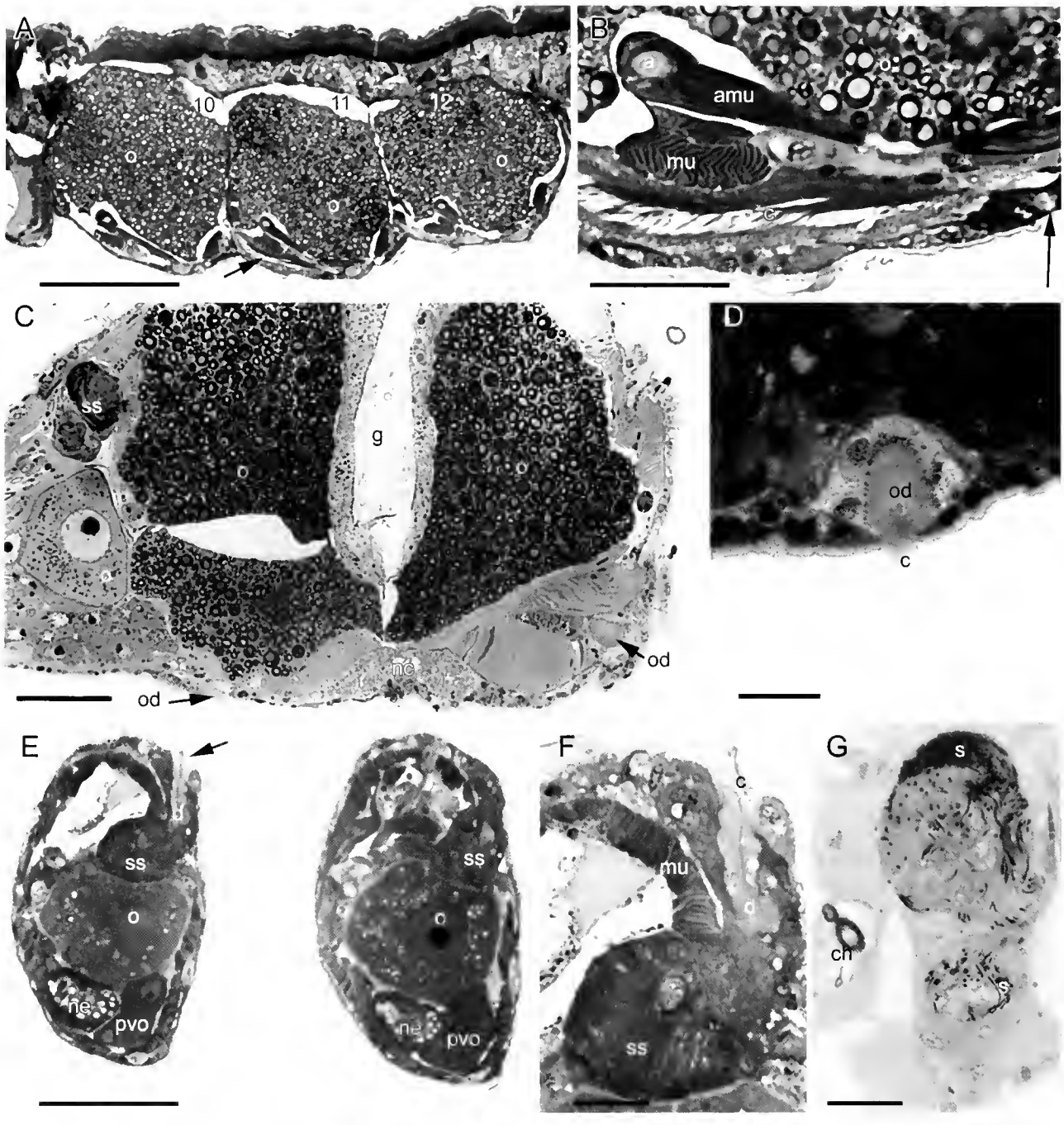

Figure 4. Reproductive system of female *Lizardia hirschi*. (A) One-micrometer longitudinal section through segments 10, 11, and 12 of a mature female from Lizard Island, showing late vitellogenic (or mature) oocytes. A pair of ciliated ducts (oviducts and/or nephridia) connect segments 10 and 11 with the funnel on the septum of segment 10 and the main duct in segment 11 (arrow). (B) Detail of sperm duct running ventrally along segment 11. Opening of the duct to the exterior (located in other sections) is indicated by arrow. (C) One-micrometer transverse section (slightly oblique) through segment 11 of female from One Tree Island, showing mature oocytes abutting gut. One spermatheca is visible, with its sperm storage area adjacent to a mature oocyte. The external opening to one of the oviducts is indicated by arrow, while the other oviduct is not emergent on this section. (D) Detail of the opening of a ciliated duct on the ventral part of segment 11. (E) One-micrometer longitudinal section through bases of parapodia in segments 11 and 12, showing a spermatheca dorsally in each. Spermathecal opening at the posterior face of the parapodium in segment 11 indicated by arrow. Oocytes or varying stages of development are visible in the coelom. (F) One-micrometer longitudinal section through spermatheca, showing duct and sperm storage area. Sperm are poorly stained in this section. (G) One-micrometer transverse section through spermatheca of female from One Tree Island, showing sperm nuclei clearly. Abbreviations: a, acicula; amu, acicula muscle; c, cilia of oviduct or spermatheca; ch, notopodial chaetae; d, spermathecal duct; g, gut; mu, muscle; nc, ventral nerve cord; ne, neuropodial chaetae; o, oocyte; od, oviduct; pvo, previtellogenic oocyte; s, sperm; ss, sperm storage area of spermatheca. Scale lines: A, 100 μm; B, 20 μm; C, 50 μm; D, 10 μm; E, 50 μm; F and G, 10 μm.

median pygidial papilla absent. Segment 20 in males with small dorsal and ventral cirri, with elongate tips and few, very fine and probably capillary chaetae in between; penes of about same size as cirri but truncate, inserted between ventral cirri (Fig. 2A, B) (penes may also be situated on pygidium). Pygidium in males with one pair of cirri of similar size and shape to dorsal and ventral cirri segment 20.

Pigmentation. Eyes orange. Live animals transparent, with conspicuous white pigmentation in large area across posterior part of prostomium and dorsally across segments 1–3, extending on cirrophores of dorsal cirri of these segments, as spots near bases of all parapodia, and on posteriormost region of gut. Light brown pigmentation also present dorsally as segmental stripes and blotches similar to, *e.g.*, *Gyptis propinqua* (Pleijel, 1993). Midgut yellowish. Eggs whitish. With exception of eye pigments, preserved specimens lose all pigmentation and become opaque.

Remarks. It may be difficult to separate immature preserved specimens and females of *L. hirschi* and *capricornia*. One useful feature is the disposal of the eyes; in *L. hirschi* the four eyes form a trapezoid approaching a quadrangle, whereas in *capricornia* the four eyes are situated on a slightly curved line.

Reproductive system and internal features. Penes on segment 20 (or, possibly, on pygidium) each with ciliated ducts running through this segment (Fig. 3A–C). Penis duct lined by cilia and many granules of varying electron density. Duct of each penis continues through segment 20 before terminating as a funnel opening in posterior region of segment 19. Coelom of segment 20 otherwise completely filled with granular material of unknown composition. Funnel in coelom of segment 19 densely ciliated and extends dorsally along septal wall (Fig. 3C). Segments 16–19 contain mature sperm, packed as spermatozeugmata (Fig. 3C–G). Spermatids found from segments 9–15. Septa between segments incomplete. Mature sperm with elongate cylindrical nucleus, 8.5 μm long, capped by conical acrosome, 3.4 μm long (Fig. 3H, I). Sperm nucleus terminates posteriorly as semi-spherical projection surrounded by three mitochondria of midpiece (Fig. 3J, K). Mitochondria extend for only 1 μm behind nucleus and also surround anchoring apparatus of flagellum. Anchoring apparatus comprised of two centrioles, both abutting base of nucleus (Fig. 3J).

Females with single pair of ciliated ducts (oviducts, nephridia, or both) opening on ventral surface of segment 11, with external opening only 10 μm in diameter (Fig. 4A–D). Oocytes of various stages of development in segment 11, as well as in segments 10 and 12 (Fig. 4A, C, E), in some specimens also in segment 13. Oocytes up to 150 μm in diameter (Fig. 4A). A pair of large, late vitellogenic or mature oocytes present in each of segments 10–12 or 10–13 in many females. Spermathecae located dorsally on posterior surfaces of each notopodia on segments 10–12 (Fig. 4C, E). Sperm embedded in spermathecal lining and tails trail along duct (Fig. 4F, G). Spermathecae appear to be blind sacs, but proximity to eggs makes internal fertilization a possibility.

Discussion

A preliminary, morphology-based phylogenetic analysis (not included here) points to a position of, first *capricornia*, and then *Lizardia hirschi*, as sister taxa to the remaining hesionids. This is in contrast to the original description of *capricornia*, where a position within Gyptini instead was obtained (Pleijel and Rouse, 2000). However, assessing the relationships of these two taxa from morphology only may be problematic due to the presence of many general hesionid characters (apart from the autapomorphies with the reproductive system). Morphologically, *capricornia* and *L. hirschi* are similar to each other, and both have a number of features that are characteristic for juvenile hesionids, including a dorsally inserted median antenna, few cephalized segments, and 10 proboscis papillae. Considering these characters, in combination with the small size of the animals, suggests the possibility that their evolution involves progenesis or neoteny and, in that case, that their indicated basal positions among hesionids may be spurious. This issue will be addressed in forthcoming studies, based also on molecular data that should be neutral *vis-à-vis* truncated ontogenies.

While the penes in *L. hirschi* and *capricornia* are clearly nonhomologous, as seen from their different positions (segment 20 or pygidium, and segment 9, respectively), the female reproductive systems of the two taxa appear to be homologous and should be treated as primary homologs in future analyses: *L. hirschi* has spermathecae dorsally on the notopodia of segments 10–12, and ventral oviduct openings on segment 11; in *capricornia* the spermathecae and oviducts are in the same position, except that spermathecae are on segments 11 and 12 only.

Among the reproductive systems of hesionids, there are other potential homologies that could be investigated. For instance, *Sirsoe methanicola* (Desbruyères and Toulmond, 1998) has a pair of sperm ducts extending through posterior chaetigers, opening into the posterior gut (Eckelbarger *et al.*, 2001). Sperm are then spawned through the anus. The possible homologous relations between the posterior sperm ducts of *Lizardia hirschi* and *Sirsoe methanicola*, notwithstanding the lack of penes in the latter group, also deserve further investigation.

Acknowledgments

This work was carried out with permit G96/539 from the Great Barrier Reef Authority. Special thanks to Thomas Dahlgren, Lars Jermiin, and Eva Lewy for collecting assistance. This work was supported by Formas, dnr 2004-0085 (FP), and the Australian Research Council and the South Australian Museum (GWR). Adelaide Microscopy provided valuable facilities.

Literature Cited

Eckelbarger, K. J., C. M. Young, E. Ramirez Llodra, S. Brooke, and P. Tyler. 2001. Gametogenesis, spawning behavior, and early development in the "iceworm" *Hesiocaeca methanicola* (Polychaeta: Hesionidae) from methane hydrates in the gulf of Mexico. *Mar. Biol.* **138:** 761–775.

Pleijel, F. 1993. Taxonomy of European species of *Amphiduros* and *Gyptis* (Polychaeta: Hesionidae). *Proc. Biol. Soc. Wash.* **106:** 158–181.

Pleijel, F. 1998. Phylogeny and classification of Hesionidae (Polychaeta). *Zool. Scr.* **27:** 89–163.

Pleijel, F. 2001. 18. Hesionidae Grube, 1850. Pp. 91–93 in *Polychaetes*, G. W. Rouse and F. Pleijel. Oxford University Press, Oxford.

Pleijel, F., and G. W. Rouse. 2000. A new taxon, *capricornia (Hesionidae, Polychaeta)*, illustrating the LITU ("Least-Inclusive Taxonomic Unit") concept. *Zool. Scr.* **29:** 157–168.

Rouse, G. W., and F. Pleijel. 2001. 1. Introduction. Pp. 1–7 in *Polychaetes*, G. W. Rouse and F. Pleijel. Oxford University Press, Oxford.

Westheide, W., G. Purschke, and W. Mangerich. 1994. *Sinohesione genitaliphora* gen. et sp. n. (Polychaeta, Hesionidae), an interstitial annelid with unique dimorphous external genital organs. *Zool. Scr.* **23:** 95–105.

THE
BIOLOGICAL BULLETIN

2005 Subscription Rates

Volumes 208-209

Paid subscriptions include both print and online versions.

	Institutional	Individual
One year subscription (6 issues - 2 volumes)	**$360.00**	**$120.00**
Single Volume (3 issues)	$180.00	$70.00
Single Issues	$75.00	$25.00

Surface delivery included in above prices.

For prompt delivery, we encourage subscribers outside the U.S. to request airmail service.

Airmail Delivery Charges:

U.S. and Canada, $45.00 Mexico, $60.00 All other locations, $100.00

The Biological Bulletin
ISSN: 0006-3185
Frequency: Bimonthly
Number of issues per year: 6
Months of Publication: February, April, June, August, October, December
Subscriptions entered for calendar year
Volume indexes contained in June and December issues
Back issues available
Claims handled upon receipt

Please address orders to:

Subscription Administrator, *The Biological Bulletin*
Marine Biological Laboratory, 7 MBL Street
Woods Hole, MA 02543 U.S.A.
Fax: 508-289-7922 • Tel: 508-289-7402 • E-mail: lreuter@mbl.edu

Orders must be prepaid in U.S. Dollars, check payable to Marine Biological Laboratory
(with reference *The Biological Bulletin*)

www.biolbull.org

Published by the Marine Biological Laboratory
Woods Hole, Massachusetts, 02543 U.S.A.

THE

BIOLOGICAL BULLETIN

2005 Subscription Form

Volumes 208-209, 6 issues

(Please print)

NAME: _____

INSTITUTION: _____

ADDRESS: _____

CITY: _____ STATE: _____ POSTAL CODE: _____

COUNTRY: _____ TELEPHONE: _____

FAX: _____ E-MAIL ADDRESS: _____

Please send me a 2005 subscription to *The Biological Bulletin* at the rate indicated below:

Price includes both print and online versions. All subscriptions run on the calendar year.

❒ Individual: $120.00 (6 ISSUES) ❒ Institutional: $360.00 (6 ISSUES)

❒ Individual: $70.00 (3 ISSUES) ❒ Institutional: $180.00 (3 ISSUES)

Check one: ❒ February, April, June or ❒ August, October, December

Please send me the following back issue(s): _____

❒ Individual: at $25.00 (PER ISSUE) ❒ Institutional: at $75.00 (PER ISSUE)

Delivery Options

❒ Surface Delivery (Surface delivery is included in the subscription price.)

❒ Air Delivery (Please add the correct amount to your payment.)

U.S. and Canada: $45.00 Mexico: $60.00 All other locations: $100.00

Payment Options

❒ Enclosed is my check or U.S. money order for $ _____

payable to Marine Biological Laboratory (with reference *The Biological Bulletin*)

❒ Please charge my ❒ VISA ❒ MasterCard ❒ Discover Card $ _____

Account No.: _____ Exp. Date: _____

Signature: _____ Date: _____

❒ Please send me an invoice. (Note: Payment must be received before subscription commences.)

Return this form with your check or credit information to:

Subscription Administrator, *The Biological Bulletin*
Marine Biological Laboratory, 7 MBL Street
Woods Hole, MA 02543 U.S.A.
Fax: 508-289-7922 • Tel: 508-289-7402 • E-mail: lreuter@mbl.edu

www.biolbull.org

Published by the Marine Biological Laboratory
Woods Hole, Massachusetts, 02543 U.S.A.

MARINE RESOURCES CENTER

MARINE BIOLOGICAL LABORATORY • WOODS HOLE, MA 02543 • (508)289-7700
WWW.MBL.EDU/SERVICES/MRC/INDEX.HTML

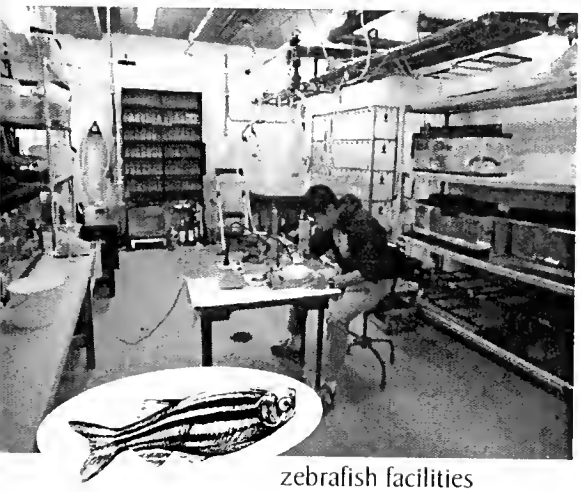

zebrafish facilities

Animal and Tissue Supply for Education & Research

- 150 aquatic species available for shipment via online catalog: <http://www.mbl.edu/animals/index.html>; phone: (508)289-7375; or e-mail: specimens@mbl.edu
- zebrafish colony containing limited mutant strains
- custom dissection and furnishing of specific organ and tissue samples

MRC Services Available

- basic water quality analysis
- veterinary services (clinical, histopathologic, microbial services, health certificates, etc.)
- aquatic systems design (mechanical, biological, engineering, etc.)
- educational tours and collecting trips aboard the R/V Gemma

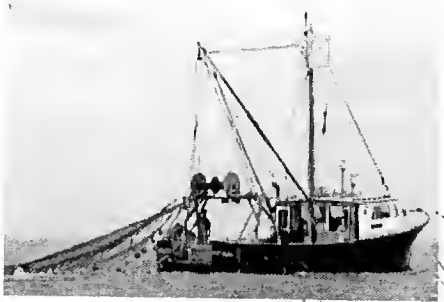

Using the MRC for Your Research

- capability for advanced animal husbandry (temperature, light control, etc.)
- availability of year-round, developmental life stages
- adaptability of tank system design for live marine animal experimentation

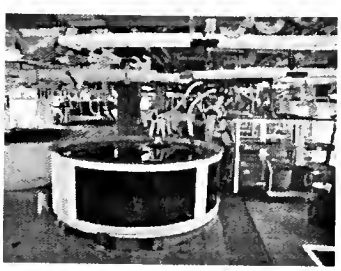

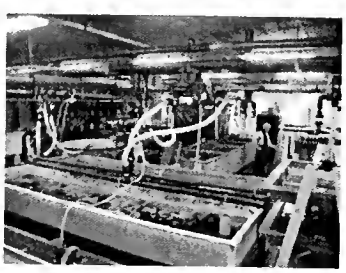

Brilliant Signals.

ew. Axio Imager.
scover New World

A new generation of microscopes is setting new standards in digital imaging. Through ultimate optimization of components, flawless integration of digital imaging and pioneering developments in optics – Axio Imager from Carl Zeiss.

Carl Zeiss MicroImaging, Inc. zeiss/axio-imager.com 800.233.2343

ZEISS

We make it visible.

April 2005

Volume 208 • Number 2

THE BIOLOGICAL BULLETIN

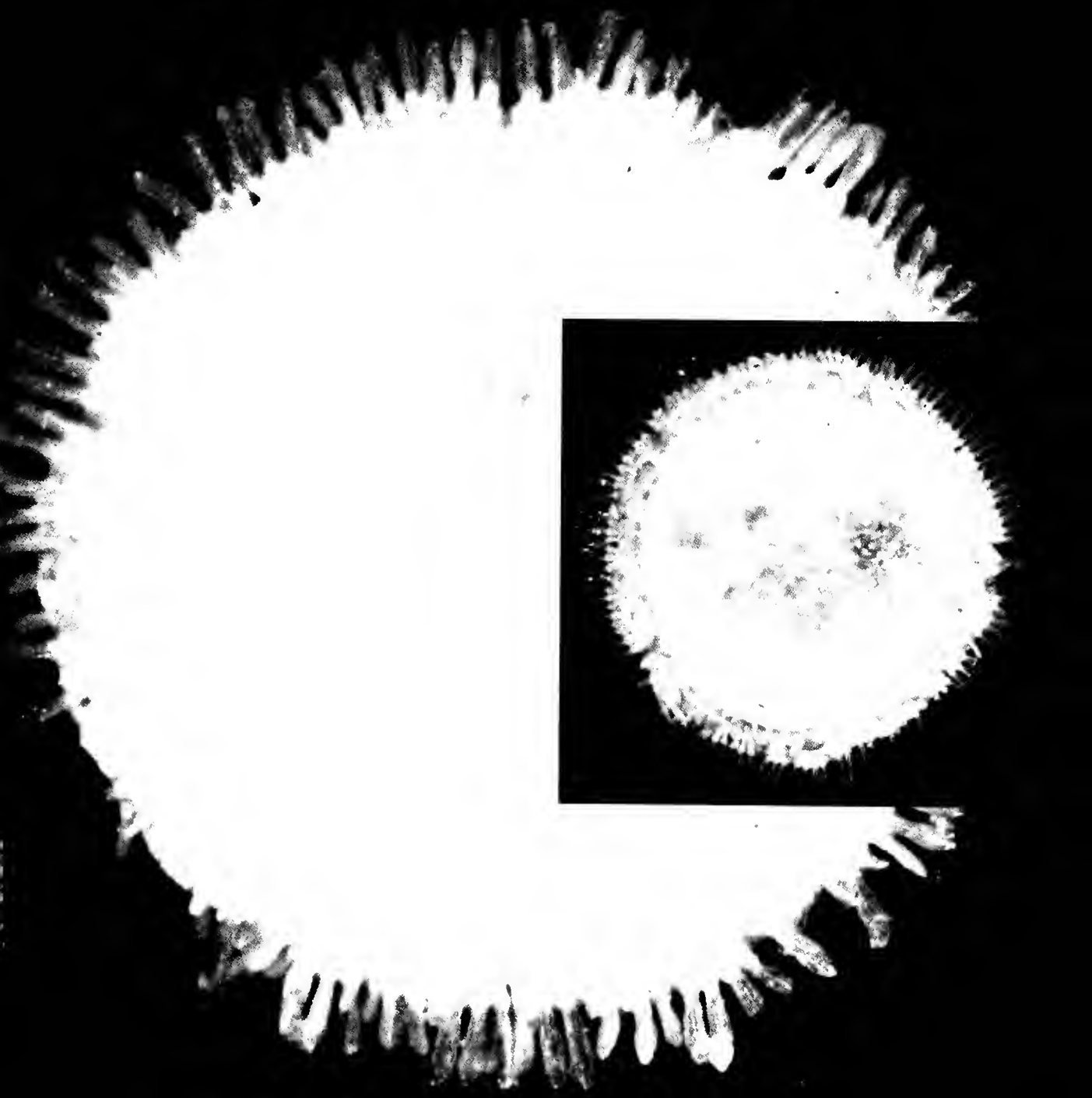

Published by the Marine Biological Laboratory

Woods Hole, Massachusetts

THE BIOLOGICAL BULLETIN

ONLINE

The Marine Biological Laboratory is pleased to announce that the full text of *The Biological Bulletin* is available online at

http://www.biolbull.org

The Biological Bulletin publishes outstanding experimental research on the full range of biological topics and organisms, from the fields of Neurobiology, Behavior, Physiology, Ecology, Evolution, Development and Reproduction, Cell Biology, Biomechanics, Symbiosis, and Systematics.

Published since 1897 by the Marine Biological Laboratory (MBL) in Woods Hole, Massachusetts, *The Biological Bulletin* is one of America's oldest peer-reviewed scientific journals.

The journal is aimed at a general readership, and especially invites articles about those novel phenomena and contexts characteristic of intersecting fields.

The Biological Bulletin Online contains the full content of each issue of the journal, including all figures and tables, beginning with the February 2001 issue (Volume 200, Number 1). The full text is searchable by keyword, and the cited references include hyperlinks to Medline. PDF files are available beginning in February 1990 (Volume 178, Number 1), some abstracts are available beginning with the October 1976 issue (Volume 151, Number 2), and some Tables of Contents are online beginning with the October 1965 issue (Volume 129, Number 2).

Each issue will be placed online approximately on the date it is mailed to subscribers; therefore the online site will be available prior to receipt of your paper copy. Online readers may want to sign up for the eTOC (electronic Table of Contents) service, which will deliver each new issue's table of contents *via* e-mail. The web site also provides access to information about the journal (such as Instructions to Authors, the Editorial Board, and subscription information), as well as access to the Marine Biological Laboratory's web site and other *Biological Bulletin* electronic publications.

Individuals and institutions who are subscribers to the journal in print or are members of the Marine Biological Laboratory Corporation must activate their online subscriptions to view articles published in the current year. All other access (*e.g.*, to articles more than a year old, Abstracts, eTOCs, searching, Instructions to Authors) is freely available. Online access is included in the print subscription price.

For more information about subscribing or activating your online subscription, visit <www.biolbull.org/subscriptions>.

THE BIOLOGICAL BULLETIN

APRIL 2005

Published by
MARINE BIOLOGICAL LABORATORY
WOODS HOLE, MASSACHUSETTS

http://www.biolbull.org

Cover

The cover photographs show dorsal and ventral (inset) views of a female of a new species of *Xyloplax*, a genus for which a new class of echinoderms, the Concentricycloidea, was erected on its discovery in 1986. Although intervening years have seen thoughtful discussion of the taxon's appropriate classification, little enlightenment on the biology of these rare animals or of their only known habitat, wood falls in the deep sea, has resulted. *Xyloplax* was previously known only from around New Zealand and off the Bahamas at depths from 1057 to 2066 m. This 9-mm-diameter female represents a population of 103 individuals collected from wood experimentally deployed at 2675 m in the North Pacific Ocean in July 2002 and recovered 25 months later by the Deep Submergence Vehicle *Alvin*. Voight (p. 77 this issue) examines aspects of the biology of this species.

The ventral view of the female shows that in this species, young are retained inside the female's body until they resemble miniature adults. This contrasts with reports of *Xyloplax turnerae*, the Atlantic species from off the Bahamas, in which young are apparently released at a much smaller size. Despite the differences in the development mode between these species, the size distribution of the populations is statistically the same.

Although this Pacific species would seem to have less opportunity for dispersal because young begin their lives at a larger size, this limitation may be overcome by an unusual growth pattern. The spines that extend beyond the edge of the body lengthen rapidly in small individuals to near their adult lengths of 0.75 mm. Their growth then nearly stops, increasing only slightly as the diameter of the body expands from 2.75 mm to over 9 mm in females, the larger sex. The spines of the Atlantic species, in contrast, lengthen uniformly as body diameter increases. In addition, the angling of the spines away from the plane of the disk-shaped body in some preserved Pacific specimens suggests that the marginal spines are under muscular control. The oversized, movable spines of the Pacific species may enhance dispersal by young individuals as they seek islands of their extremely rare and randomly distributed habitat—wood falls on the sea floor, miles away from the nearest land and 2 km beneath the ocean surface.

Credits: Photographs of *Xyloplax* n. sp. taken by Todd Haney aboard the R/V *Atlantis*. Cover design: Beth Liles (Marine Biological Laboratory).

CONTENTS

VOLUME 208, NO. 2: APRIL 2005

THE BIOLOGICAL BULLETIN

THE BIOLOGICAL BULLETIN is published six times a year by the Marine Biological Laboratory, 7 MBL Street, Woods Hole, Massachusetts 02543.

Subscriptions and similar matter should be addressed to Subscription Administrator, THE BIOLOGICAL BULLETIN, Marine Biological Laboratory, 7 MBL Street, Woods Hole, Massachusetts 02543. Subscription includes both print and online journals. Subscription per year (six issues, two volumes): $360 for libraries; $120 for individuals. Subscription per volume (three issues): $180 for libraries; $70 for individuals. Back and single issues (subject to availability): $75 for libraries; $25 for individuals.

Communications relative to manuscripts should be sent to James L. Olds, Editor-in-Chief, or Pamela Clapp Hinkle, Managing Editor, at the Marine Biological Laboratory, 7 MBL Street, Woods Hole, Massachusetts 02543. Telephone: (508) 289-7149. FAX: 508-289-7922. E-mail: pclapp@mbl.edu.

http://www.biolbull.org

THE BIOLOGICAL BULLETIN is indexed in bibliographic services including *Index Medicus* and MEDLINE, *Chemical Abstracts*, *Current Contents*, *Elsevier BIOBASE/Current Awareness in Biological Sciences*, and *Geo Abstracts*.

Printed on acid free paper,
effective with Volume 180, Issue 1, 1991.

POSTMASTER: Send address changes to THE BIOLOGICAL BULLETIN, Marine Biological Laboratory, 7 MBL Street, Woods Hole, MA 02543.

Periodicals postage paid at Woods Hole, MA, and additional mailing offices.
ISSN 0006-3185

INSTRUCTIONS TO AUTHORS

The Biological Bulletin accepts outstanding original research reports of general interest to biologists throughout the world. Papers are usually of intermediate length (10–40 manuscript pages). A limited number of solicited review papers may be accepted after formal review. A paper will usually appear within four months after its acceptance.

Very short, especially topical papers (less than 9 manuscript pages including tables, figures, and bibliography) will be published in a separate section entitled "Research Notes." A Research Note in *The Biological Bulletin* follows the format of similar notes in *Nature*. It should open with a summary paragraph of 150 to 200 words comprising the introduction and the conclusions. The rest of the text should continue on without subheadings, and there should be no more than 30 references. References should be referred to in the text by number, and listed in the Literature Cited section in the order that they appear in the text. Unlike references in *Nature*, references in the Research Notes section should conform in punctuation and arrangement to the style of recent issues of *The Biological Bulletin*. Materials and Methods should be incorporated into appropriate figure legends. See the article by Lee (October 2003, Vol. **205:** 99–101) for sample style. A Research Note will usually appear within two months after its acceptance.

The Editorial Board requests that regular manuscripts conform to the requirements set below; those manuscripts that do not conform will be returned to authors for correction before review.

1. ***Manuscripts.*** Manuscripts, including figures, should be submitted in quadruplicate, with the originals clearly marked. (Xerox copies of photographs are not acceptable for review purposes.) Please include an electronic copy of the text of the manuscript. Label the disk with the name of the first author and the name and version of the wordprocessing software used to create the file. If the file was not created in some version of Microsoft Word, save the text in rich text format (rtf). The submission letter accompanying the manuscript should include a telephone number, a FAX number, and (if possible) an E-mail address for the corresponding author. The original manuscript must be typed in no smaller than 12 pitch or 10 point, using double spacing (*including* figure legends, footnotes, bibliography, etc.) on one side of 16- or 20-lb. bond paper, 8 by 11 inches. Please, no right justification. Manuscripts should be proofread carefully and errors corrected legibly in black ink. Pages should be numbered consecutively. Margins on all sides should be at least 1 inch (2.5 cm). Manuscripts should conform to the *Council of Biology Editors Style Manual*, 5th Edition (Council of Biology Editors, 1983) and to American spelling. Unusual abbreviations should be kept to a minimum and should be spelled out on first reference as well as defined in a footnote on the title page. Manuscripts should be divided into the following components: Title page, Abstract (of no more than 200 words), Introduction, Materials and Methods, Results, Discussion, Acknowledgments, Literature Cited, Tables, and Figure Legends. In addition, authors should supply a list of words and phrases under which the article should be indexed.

2. ***Title page.*** The title page consists of a condensed title or running head of no more than 35 letters and spaces, the manuscript title, authors' names and appropriate addresses, and footnotes listing present addresses, acknowledgments or contribution numbers, and explanation of unusual abbreviations.

3. ***Figures.*** The dimensions of the printed page, 7 by 9 inches, should be kept in mind in preparing figures for publication. We recommend that figures be about 1 times the linear dimensions of the final printing desired, and that the ratio of the largest to the smallest letter or number and of the thickest to the thinnest line not exceed 1:1.5. Explanatory matter generally should be included in legends, although axes should always be identified on the illustration itself. Figures should be prepared for reproduction as either line cuts or halftones. Figures to be reproduced as line cuts should be unmounted glossy photographic reproductions or drawn in black ink on white paper, good-quality tracing cloth or plastic, or blue-lined coordinate paper. Those to be reproduced as halftones should be mounted on board, with both designating numbers or letters and scale bars affixed directly to the figures. All figures should be numbered in consecutive order, with no distinction between text and plate figures and cited, in order, in the text. The author's name and an arrow indicating orientation should appear on the reverse side of all figures.

Digital art: The Biological Bulletin will accept figures submitted in electronic form; however, digital art must conform to the following guidelines. Authors who create digital images are wholly responsible for the quality of their material, including color and halftone accuracy.

Format. Acceptable graphic formats are TIFF and EPS. Color submissions must be in EPS format, saved in CMKY mode.

Software. Preferred software is Adobe Illustrator or Adobe Photoshop for the Mac and Adobe Photoshop for Windows. Specific instructions for artwork created with various software programs are available on the Web at the Digital Art Information Site maintained by Cadmus Professional Communications at http://cpc.cadmus.com/da/

Resolution. The minimum requirements for resolution are 1200 DPI for line art and 300 for halftones.

Size. All digital artwork must be submitted at its actual printed size so that no scaling is necessary.

Multipanel figures. Figures consisting of individual parts (*e.g.*, panels A, B, C) must be assembled into final format and submitted as one file.

Hard copy. Files must be accompanied by hard copy for use in case the electronic version is unusable.

Disk identification. Disks must be clearly labeled with the following information: author name and manuscript number; format (PC or Macintosh); name and version of software used.

Color: The Biological Bulletin will publish color figures and plates, but must bill authors for the actual additional cost of printing in color. The process is expensive, so authors with more than one color image should—consistent with editorial concerns, especially citation of figures in order—combine them into a single plate to reduce the expense. On request, when supplied with a copy of a color illustration, the editorial staff will provide a pre-publication estimate of the printing cost.

4. ***Tables, footnotes, figure legends, etc.*** Authors should follow the style in a recent issue of *The Biological Bulletin* in preparing table headings, figure legends, and the like. Because of the high cost of setting tabular material in type, authors are asked to limit such material as much as possible. Tables, with their headings and footnotes, should be typed on separate sheets, numbered with consecutive Arabic numerals, and placed after the Literature Cited. Figure legends should contain enough information to make the figure intelligible separate from the text. Legends should be typed double spaced, with consecutive Arabic numbers, on a separate sheet at the end of the paper. Footnotes should be limited to authors' current addresses, acknowledgments or contribution numbers, and explanation of unusual abbreviations. All such footnotes should appear on the title page. Footnotes are not normally permitted in the body of the text.

5. ***Literature cited.*** In the text, literature should be cited by the Harvard system, with papers by more than two authors cited as Jones *et al.*, 1980. Personal communications and material in preparation or in press should be cited in the text only, with author's initials and institutions, unless the material has been formally accepted and a volume number can be supplied. The list of references following the text should be headed Literature Cited, and must be typed double spaced on separate pages, conforming in punctuation and arrangement to the style of recent issues of *The Biological Bulletin*. Citations should include complete titles and inclusive pagination. Journal abbreviations should normally follow those of the U. S. A. Standards Institute (USASI), as adopted by Biological Abstracts and Chemical Abstracts, with the minor differences set out below. The most generally useful list of biological journal titles is that published each year by Biological Abstracts (BIOSIS List of Serials; the most recent issue). Foreign authors, and others who are accustomed to using The World List of Scientific Periodicals, may find a booklet published by the Biological Council of the U.K. (obtainable from the Institute of Biology, 41 Queen's Gate, London, S.W.7, England, U.K.) useful, since it sets out the World List abbreviations for most biological journals with notes of the USASI abbreviations where these differ. Chemical Abstracts publishes quarterly supplements of additional abbreviations. The following points of reference style for The Biological Bulletin differ from USASI (or modified World List) usage:

A. Journal abbreviations, and book titles, all underlined (for *italics*)

B. All components of abbreviations with initial capitals (not as European usage in World List *e.g., J. Cell. Comp. Physiol.* NOT *J. cell. comp. Physiol.*)

C. *All* abbreviated components must be followed by a period, whole word components *must not* (*i.e., J. Cancer Res.*)

D. Space between all components (*e.g., J. Cell. Comp. Physiol.*, not *J.Cell.Comp.Physiol.*)

E. Unusual words in journal titles should be spelled out in full, rather than employing new abbreviations invented by the author. For example, use *Rit Vísindafjélags Islendinga* without abbreviation.

F. All single word journal titles in full (*e.g., Veliger, Ecology, Brain*).

G. The order of abbreviated components should be the same as the word order of the complete title (*i.e.*, *Proc.* and *Trans.* placed where they appear, not transposed as in some BIOLOGICAL ABSTRACTS listings).

H. A few well-known international journals in their preferred forms rather than WORLD LIST or USASI usage (*e.g.*, *Nature, Science, Evolution* NOT *Nature, Lond., Science, N.Y.; Evolution, Lancaster, Pa.*)

6. ***Sequences.*** By the time a paper is sent to the press, all nucleotide or amino acid sequences and associated alignments should have been deposited in a generally accessible database (*e.g.*, GenBank, EMBL, SwissProt), and the sequence accession number should be provided.

7. ***Reprints, page proofs, and charges.*** Authors may purchase reprints in lots of 100. Forms for placing reprint orders are sent with page proofs. Reprints normally will be delivered about 2 to 3 months after the issue date. Authors will receive page proofs of articles shortly before publication. They will be charged the current cost of printers' time for corrections to these (other than corrections of printers' or editors' errors). Other than these charges for authors' alterations, *The Biological Bulletin* does not have page charges.

Reference: *Biol. Bull.* **208:** 77–80. (April 2005)

First Report of the Enigmatic Echinoderm *Xyloplax* from the North Pacific

JANET R. VOIGHT

Department of Zoology, The Field Museum, 1400 S. Lake Shore Drive, Chicago, Illinois 60605

More than 100 specimens of the rare and enigmatic echinoderm Xyloplax, *a deep-sea wood-fall specialist described as the new class Concentricycloidea on the basis of nine specimens from New Zealand (1), were recently collected from a depth of 2675 m in the North Pacific. These first submersible-collected specimens of* Xyloplax *from the Pacific contrast with the submersible-collected specimens of the Atlantic's* X. turnerae *in developmental mode. Embryos of the Pacific specimens—including those from New Zealand—undergo extended development in the ovary; members of the Atlantic species apparently release small embryos or eggs. In what may be an associated difference, females appear to dominate the North Pacific population in numbers and exceed males in individual size. In addition, the marginal spines of North Pacific specimens show a nonlinear relationship to body diameter on an ln-ln plot; relatively rapid growth of marginal spines in small individuals may enhance dispersal on near-bottom currents. In the Atlantic species, the sexes are equally represented (although sexual size dimorphism exists), and marginal spines grow at a constant rate. The increased biomass of females among North Pacific specimens may reflect their increased investment in each offspring.*

Animals specialized to live on deep-sea wood falls remain little known, both taxonomically and biologically. Nine specimens from five New Zealand wood falls collected at depths from 1057 to 1208 m were assigned to the genus *Xyloplax*, which has been interpreted as composing a new class of echinoderms, the Concentricycloidea (1) and, alternatively, as a highly derived genus of the Asteroidea (2 and references therein). Detailed anatomical study of the genus (3), and a brief report of population parameters (4) were based on more than 200 specimens collected from an experimental wood deployment at 2066 m off the Bahamas. The recent collection of more than 100 specimens of the genus from an experimental wood deployment in the North Pacific provides a contrast between this viviparous species and the Atlantic species with its shorter embryonic development. Despite distinct reproductive strategies, both species exploit the rare and unpredictable habitat provided by deep-sea wood falls.

This study reports the population composition and growth patterns of specimens of the undescribed North Pacific species. The specimens probably represent the original population accurately because the deployments were recovered inside a closed box on the Deep Submergence Vehicle *Alvin*. C. Mah, University of Illinois at Urbana-Champaign, is describing the new species represented by these specimens.

The wood from which the specimens were collected had been deployed on 28 July 2002. The deployment consisted of a mesh diver's bag containing one 45.7-cm-long piece of machine-cut, bark-free, green 10.1-cm-square Douglas fir (*Pseudotsuga* sp.) and an identical piece of oak (*Quercus* sp.); cable ties secured the bag. The Remotely Operated Vehicle *Tiburon* (Monterey Bay Aquarium Research Institute) placed the bag at 2675 m near 42° 45.2′N 126° 42.5′ W. The habitat was basalt talus within a few feet of widely scattered tubeworms of *Ridgeia piscesae;* the long, thin morphology of the tubeworms is typically associated with low concentrations of sulfide (5). Down-slope and to the south was the GR-14, or SeaCliff hydrothermal vent field, an off-axis vent field located on a west-facing slope (6) that, at least during the recovery dive, was characterized by exceptionally strong bottom currents.

On 31 August 2004, the DSV *Alvin* recovered the deployment by grasping the wood through the bag with its manipulator arm and placing the bag inside a lidded box on the submersible. The box lid was then closed and secured

Received 15 November 2004; accepted 1 February 2005.
* To whom correspondence should be addressed. E-mail: jvoight@fmnh.org

with an elasticized band. No elevated temperatures associated with hydrothermal activity could be found in the area. Five hours later, the submarine was recovered and the wood was removed from the collection box and placed into cold seawater.

The bag containing the wood was opened and animals visible to the naked eye (Fig. 1) were removed from the wood by hand. Because the partially anoxic wood had been inside the closed recovery box for more than 5 h, the animals' positions on the wood could not be considered to accurately reflect normal life positions. The wood was rinsed in cold seawater and later sectioned with an electric saw. All water that had contact with the wood, including water from the recovery box on *Alvin's* basket, water into which the wood was placed after recovery, and rinse water, was sieved with a 250-μm mesh. All material retained in the sieve was preserved in 95% ethanol and later sorted under a dissecting microscope. The specimens are catalogued at The Field Museum, Chicago, Illinois, as FMNH 12458, 12459, 12460, and 12461.

The tube feet in one sector of the body were counted and multiplied by five to generate a total count, after verifying in about half of the specimens that the sectors were invariant. The diameter, including the spines, was measured for all individuals collected, except one that was badly damaged. Developing embryos visible through the adult's oral surface were used to identify gravid females; developing embryos were counted. Cygnoid spines, said to identify males of both known species (3), could not be seen in these specimens at the magnifications used. On the basis of a previous report that in *Xyloplax* the testes are kidney-shaped (3) and the observation of kidney-shaped gonads in some specimens, this character was used to identify potential males. Specimens with neither apparent developing embryos nor kidney-shaped gonads were considered to be juveniles. To test whether growth of marginal spines, which appear very large in small individuals, was non-allometric—that is, departs from the power law relationship of being linear on a plot of natural logarithms—marginal spine length and body diameter (exclusive of the spines) were measured from camera lucida drawings. To document growth, the data were transformed to natural logarithms (7). The size distribution of these specimens was compared, using a histogram, to that of *X. turnerae* reported by Rowe (4); the presence of significant differences was tested with a KS test.

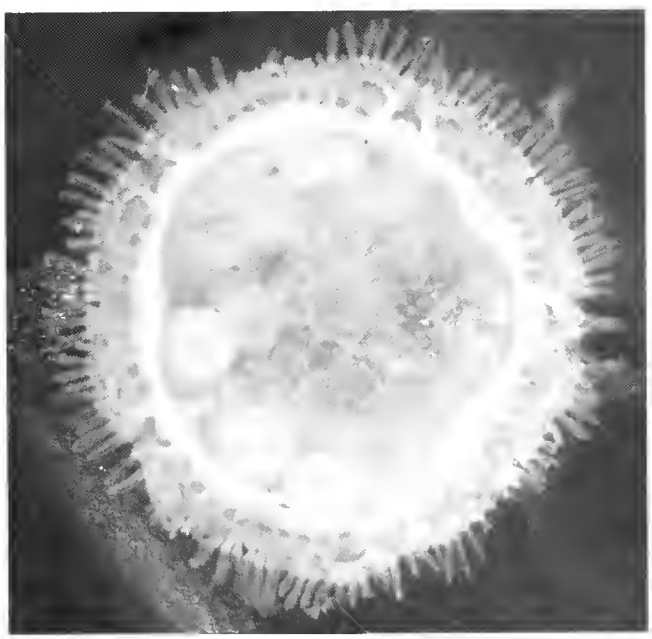

Figure 1. Digital still image of a fresh-collected female of *Xyloplax* with a diameter of about 10 mm. Developing embryos can be seen through the body, which is covered by erect spines and encircled by marginal spines. (Photo courtesy of T. Haney.)

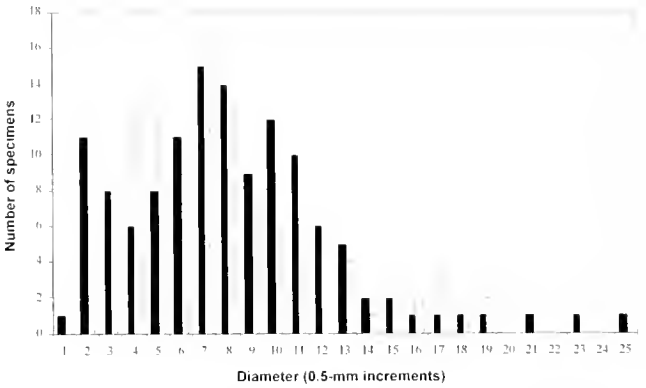

Figure 2. The diameters of the North Pacific specimens are indicated by open columns (n = 98) and those of *Xyloplax turnerae* by solid columns (n = 136); data for the latter from (3). Each increment is 0.5 mm, beginning with zero. The size distribution does not significantly differ (KS test; P = 0.414).

The size range of the specimens was from 0.75 to 9 mm (Fig. 2); largest were 14 gravid females with diameters of from 6 to 9.5 mm and a total of 55 to 65 tube feet. Only four individuals, ranging in diameter from 3.75 to 5 mm, were considered to be males on the basis of their kidney-shaped gonads. Diameters of juveniles overlapped those of males. Males had 40 to 45 tube feet; juvenile specimens had between 25 and 45 tube feet.

Individual females contained between 7 and 16 embryos in various stages of development. The most mature embryos appeared to be very similar to the smallest (0.75-mm-diameter) free-living specimen recovered. One mite was attached to each of four preserved individuals, all of which were under 2 mm in diameter and had been recovered from the sieve; that is, they had fallen off the wood, as had nearly all the smaller specimens. A free mite was also found in the sieve residue and in the vial of 74 specimens of *Xyloplax* that had been removed directly from the wood. The mites

have been sent to I. Bartsch of the Forschungsinstitut Senckenberg, Germany, for study.

Close examination of the preserved specimens revealed that in many, the marginal spines were angled relative to the plane of the body, minimizing their apparent length. Rather than risk damaging the specimens by removing the spines, specimens with detectably angled spines were eliminated from consideration, leaving only 18 individuals. Even with this reduced sample, nonlinear growth of the marginal spines was clear (Fig. 3). The spines lengthened at a consistent rate as body diameter expanded to about 2.75 mm. Beyond that point, lengthening of the roughly 0.74-mm-long spines was limited to less than 0.1 mm, even though body diameter tripled.

The wood contained very few small claims of *Xylophaga* sp. on or near its surface, but several larger clams had bored deep inside. This deployment had conspicuously fewer clams than did comparable ones from which predatory taxa such as *Xyloplax* and turbellarian flatworms were absent (unpub. data).

This report offers the first data from a Pacific population of the enigmatic genus *Xyloplax*. The other Pacific species, *X. medusiformis*, is known only from 9 specimens pulled from five pieces of wood collected at depths from 1057 to 1208 m around the islands of New Zealand. Judging from the notation that they were removed from molluscan borings (3), these animals were probably trawl-collected. More than 200 specimens of *Xyloplax turnerae* were collected on experimental wood deployments off Andros Island, Bahamas, at 2066 m. The deployments had been in place for 18 and 24 months when the recoveries were apparently performed by *Alvin* (possibly during dives 751–755, 800, 851–853, a conclusion based on the dates and position (3) and *Alvin* dive log: http://www.whoi.edu/marops/vehicles/alvin/alvin_dive_log.html). The morphology and aspects of the population biology of this species described in published reports (3, 4) contrast with those of the present species in that the Atlantic species is larger (Fig. 2; diameters of females of up 12 mm, and of males up to 7.2 mm), has more tube feet (up to 110 compared to 65), and has a stomach. The Atlantic species has a very nearly equal sex ratio, female-biased sexual size dimorphism, and linear growth of the marginal spines. Embryos contained in Atlantic females have all been smaller than 180 μm (3).

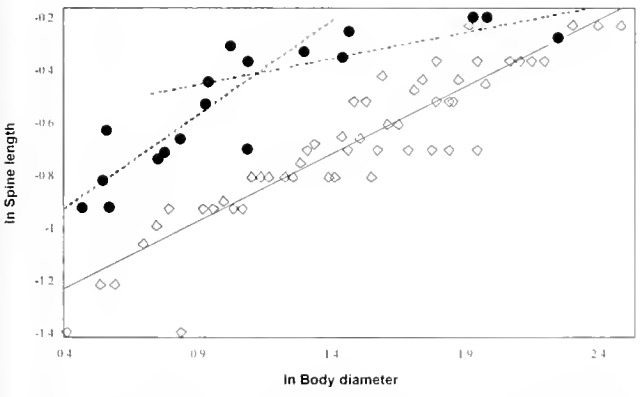

Figure 3. Natural log of marginal spine length plotted *versus* natural log of body diameter for 18 North Pacific specimens of *Xyloplax* (solid circles) and for 53 Atlantic specimens of *X. turnerae* (open diamonds). The lower end of the plot, showing only specimens of *X. turnerae*, has been truncated to emphasize the inter-specific contrast. Although scatter exists, especially among the smaller individuals, spine lengthening is nonlinear relative to increases in body diameter in the North Pacific specimens; the Atlantic specimens show a uniform increase. The spines of both species reach the same length (0.82 mm) in the largest females.

In the New Zealand *X. medusiformis*, embryos develop to a near-juvenile stage inside the ovary (3), as they appear to do in the North Pacific species. The North Pacific specimens contrast with Atlantic specimens in apparently having a strongly female-skewed sex ratio; however, the two species share a female-biased sexual size dimorphism, which is common in deep-sea animals (8). The increased female investment in each individual offspring may be associated with greater increase in female biomass in the North Pacific population.

Differences in the species' dispersal strategies may be expressed in morphological differences. *Xyloplax* has been suggested to disperse by a parachute-like mode of locomotion, apparently in reference to passively floating (1) or *via* a more active, medusoid method of locomotion driven by pulsations of the oral surface (3). The relatively large spines of young North Pacific specimens of *Xyloplax* increase the animal's surface area by nearly 50% while only minimally affecting weight. The discovery that the spines of most preserved specimens are angled supports the hypothesis that muscles control spine movements. The large, mobile marginal spines of small individuals (Fig. 1) would enhance either parachuting or medusoid locomotion. In the Atlantic *X. turnerae*, marginal spines show negatively allometric growth relative to body diameter through life, meaning that the spines are relatively longest in the smallest animals. They would therefore also enhance dispersal potential, despite being shorter than those of the Pacific species, in all but the very largest females (Fig. 1).

Acknowledgments

The pilots of the *Tiburon* and *Alvin* and the captains and crews of the R/V *Western Flyer* and R/V *Atlantis* were vital to this project. J. S. McClain and R. A. Zierenberg (NURP PO FP206164/CA-02-04), University of California Davis, and D. Clague, MBARI, aided in making the deployment. J. Martin, L. Grande, D. Blake, and C. Mah made helpful comments on the manuscript. C. Mah also provided access to the pertinent literature. NSF DEB-0103690 provided financial support.

Literature Cited

1. **Baker, A. N., F. W. E. Rowe, and H. E. S. Clark. 1986.** A new class of Echinodermata from New Zealand. *Nature* **321:** 862–864.
2. **Janies, D. 2001.** Phylogenetic relationships of extant echinoderm classes. *Can J. Zool.* **79:** 1232–1250.
3. **Rowe, F. W. E., A. N. Baker, and H. E. S. Clark. 1988.** The morphology, development and taxonomic status of *Xyloplax* Baker, Rowe and Clark (1986) (Echinodermata: Concentricycloidea), with a description of a new species. *Proc. R. Soc. Lond. B* **233:** 431–459
4. **Rowe, F. W. E. 1988.** Review of the extant class Concentricycloidea and reinterpretation of the fossil class Cyclocystoidea. Pp. 3–15 in *Echinoderm Biology*, R. D. Burke, P. V. Mladenov, P. Lambert, and R. L. Parsley, eds. A. A. Balkema, Rotterdam.
5. **Southward, E. C., V. Tunnicliffe, and M. Black. 1995.** Revision of the species of *Ridgeia* from northeast Pacific hydrothermal vents, with a redescription of *Ridgeia piscesae* Jones (Pogonophora, Obturata = Vestimentifera). *Can. J. Zool.* **73:** 282–295.
6. **Rona, P. A., R. P. Denlinger, M. R. Fisk, K. J. Howard, G. L. Taghon, K. D. Klitgord, J. S. McClain, G. R. McMurray, and J. C. Wiltshire. 1990.** Major off-axis hydrothermal activity on the northern Gorda Ridge. *Geology* **18:** 493–496.
7. **Bookstein, F., B. Chernoff, R. Elder, J. Humphries, G. Smith, and R. Strauss. 1985.** *Morphometrics in Evolutionary Biology*, Academy of Natural Sciences of Philadelphia Special Publication 15, Philadelphia, PA. 277 pp.
8. **Herring, P. 2002.** *The Biology of the Deep Ocean*. Oxford University Press, Oxford.

Reference: *Biol. Bull.* **208:** 81–91. (April 2005)

Viviparity in the Sea Star *Cryptasterina hystera* (Asterinidae)—Conserved and Modified Features in Reproduction and Development

MARIA BYRNE

Department of Anatomy and Histology, F13, University of Sydney, NSW 2006, Australia

Abstract. *Cryptasterina hystera* has a highly derived life history with intragonadal development and juveniles that emerge from the parent's reproductive tract. The gonads are ovotestes with developing eggs separated from sperm by follicle cells. *C. hystera* has typical echinosperm that must enter the gonoduct of conspecifics to achieve fertilization. During oogenesis, an initial period of yolk accumulation is followed by hypertrophic lipid deposition, the major contributor to the increase in egg size. 1-Methyladenine induces egg maturation and ovulation, but the spawning component of the hormonal cascade is suppressed. This is the major alteration in reproduction associated with evolution of viviparity in *C. hystera*. The switch to viviparity was not accompanied by major change in gonad structure, indicating there were few or no anatomical constraints for evolution of a marsupial function for the gonad. Despite their intragonadal habitat, the brachiolaria are equipped for a planktonic life, swimming in gonadal fluid. During the gastrula stage, lipid provisions are released into the blastocoel where they are stored for juvenile development. The eggs of *C. hystera* have light and dark cytoplasmic regions that mark animal-vegetal polarity. The dark pigment provided a marker to follow the fate of vegetal cells. Live birth is rare in the Echinodermata and the incidence of this form of brooding in the phylum is reviewed.

Introduction

A decoupling of selective forces on the larval and adult life stages of marine invertebrates has resulted in a remarkable diversity of life-history patterns. Markedly different larval stages within closely related species often contrast with the comparative similarity of the adults. This is exemplified by cryptic morphospecies, where new species have been discovered through observation of differences in life history, reproductive anatomy, or molecular sequence data (Reid, 1990; Knowlton, 1993; Degnan and Lavin, 1995; Ó Foighil and Smith, 1995; Byrne *et al.*, 1999a, 2003a; Huber *et al.*, 2000). Within major marine groups, some taxa (*e.g.*, syllid polychaetes, littorinid snails, lasaeid bivalves, asterinid sea stars) show greater variation in life-history patterns than closely related taxa (Pocklington and Hutcheson, 1983; Reid, 1990; Ó Foighil and Smith, 1995; Byrne *et al.*, 1999a). Why this is so is a major question for phylogeny and developmental evolution.

Within the Echinodermata, the Asterinidae, a major family of sea stars, is particularly noted for its diverse life histories (Byrne and Cerra, 1996; Hart *et al.*, 1997, 2003, 2004; Byrne *et al.*, 1999a). Species in the asterinid genera *Patiriella* and *Cryptasterina* exhibit a range of developmental modes, including a most derived method of propagation—incubation of progeny in the gonads and birth of juveniles (Byrne, 1996; Byrne and Cerra, 1996; Byrne *et al.*, 2003a). In the Asterinidae, new species have been discovered by observation of developing stages in the gonads or birth of juveniles (Dartnall, 1969; Keough and Dartnall, 1978; Hart *et al.*, 2003; Byrne *et al.*, 2003a; Dartnall *et al.*, 2003). These asterinids constitute a suite of recently diverged cryptic species in which some species exhibit as little as 1% difference in mtDNA sequence compared with congeners that have dispersive larvae (Hart *et al.*, 2003; Byrne *et al.*, 2003a).

This study documents reproduction and development in the most recently discovered viviparous species, *Cryptasterina hystera*, a member of the former pan-tropical *Patiriella pseudoexigua* group (Dartnall *et al.*, 2003). Unexpectedly, *C. hystera* has a typical lecithotrophic brachiolaria

Received 16 September 2004; accepted 21 December 2005.
E-mail: mbyrne@anatomy.usyd.edu.au

(Byrne *et al.*, 2003a). By contrast, viviparous *Patiriella* species have a vestigial brachiolaria (Byrne and Cerra, 1996). Viviparity in *C. hystera* appears to have arisen from a free-spawning ancestor with a planktonic lecithotrophic brachiolaria larva through retention and intragonadal fertilization of a large egg (Byrne *et al.*, 2003a). The gonad of *C. hystera* is an ovotestis and serves as a marsupium for the developing embryos. Reproduction and development of *C. hystera* were examined in this study to determine which life-history traits are conserved and which traits have been modified in association with the evolution of viviparity. Sperm ultrastructure was examined for modifications associated with internal fertilization. The embryos of *C. hystera* are provisioned with a conspicuous store of lipid (Byrne *et al.*, 2003a). Recent studies indicate that maternal lipid reserves are used to support juvenile development (Emlet and Hoegh-Guldberg, 1997; Byrne and Cerra, 2000; Villinski *et al.*, 2002; Byrne *et al.*, 2003b), and particular attention was paid to the fate of these reserves during development of *C. hystera*. The eggs of *C. hystera* have light and dark cytoplasmic regions that mark animal-vegetal polarity. The dark pigment was used as a marker to follow the fate of vegetal cells in development of larval territories.

Materials and Methods

Mature specimens of *Cryptasterina hystera* were collected from Statue Bay (23°15′S; 150°45′E), Queensland, during the reproductive period September–December 1997 and 1999. Ova were obtained by placing gonad lobes that appeared to be entirely female in the ovulatory hormone 1-methyladenine (10^{-5} *M* in filtered seawater [FSW]). Eggs released from the gonad were fertilized by sperm from the same or a different specimen. The larvae were reared in FSW at 21 °C until metamorphosis.

For histology, the gonads were fixed in Bouin's fluid for 24 h, rinsed in distilled water, dehydrated in graded ethanols, and embedded in paraffin. Serial sections were stained with hematoxylin and eosin. For light and transmission electron microscopy (TEM), gonads, larvae, and juveniles were fixed for 1 h at room temperature (RT) in 2.5% glutaraldehyde in 0.45 μm FSW, and then rinsed in 2.5% $NaHCO_3$ (pH 7.2). The specimens were post-fixed in 2.0% osmium tetroxide in 1.25% $NaHCO_3$ for 1 h at RT. Other specimens were fixed in 3% glutaraldehyde in 0.2 *M* cacodylate buffer (pH 7.4) with NaCl (30 mg/ml) added to the primary fixative for 2 h at 4 °C. This was followed by four rinses in 0.2 *M* cacodylate buffer with reduced amounts of NaCl added to each rinse, with the final rinse containing no NaCl. The specimens were post-fixed in 1.0% osmium tetroxide in 0.2 *M* cacodylate buffer for 2 h at 4 °C. Tissues fixed by both methods were rinsed in distilled water, dehydrated in graded ethanols, and embedded in Spurr's resin. Semithin sections were stained with 1% toluidine blue for light microscopy. Ultrathin sections were stained with 2% uranyl acetate for 30 min and 2.0% lead citrate for 10 min. The sections were viewed with a Phillips EM400 transmission electron microscope.

Results

Hermaphroditic gonad

The gonads of *Cryptasterina hystera* were a mosiac of oogenic and spermatogenic areas (Figs. 1A; 2B, D; 3A). As characteristic of asteroids (Chia and Koss, 1995), the gonad wall was formed by two tissue layers separated from each other by the genital coelom (Fig. 2D). The outer layer consisted of the outer peritoneum, a connective tissue layer, and the epithelial lining of the genital coelom (Fig. 2E). The inner layer also had three layers: the coelomic epithelium, a connective tissue layer, and the inner germinal epithelium (Fig. 2E). Both coelomic epithelia contained myoepithelial cells and occasional neurons. The inner connective tissue was the widest tissue layer in the gonad wall. It contained flocculent hemal fluid and occasional coelomocytes. The germinal layer contained somatic cells and developing gametes.

The eggs developed within a follicle formed by somatic cells (Fig. 2D–F). Follicle cells extended from the germinal epithelium to surround the egg, thereby separating them from adjacent sperm (Fig. 2E, F). Oogenesis in *C. hystera* was characterized by an initial period of yolk granule formation (Fig. 2A) in primary oocytes ($\bar{x}$ = 25 μm diam; SE = 0.71 μm; n = 15), followed by lipid accumulation. The accumulation of lipid in larger oocytes, starting at a mean diameter of 48 μm (SE = 0.9 μm; n = 21), was responsible for the major increase in egg size (Fig. 2B, C). Yolk granules were interspersed with lipid droplets, and some granules were pushed towards the egg cortex (Fig. 2B). Fully grown eggs (440 μm diameter) were dominated by lipid. A vitelline layer and jelly coat surrounded the eggs, and cortical granules were dispersed along the oolemma (Fig. 2B, E, F). Lipid droplets were not present in the cortical cytoplasm (Fig. 2B). Although looked for, egg maturation and ovulation were not observed and ova were not found in sections.

Large eggs were distinctly marked by pale olive green and dark-colored cytoplasmic regions (Fig. 1A, B). The vegetal hemisphere (confirmed by site of gastrulation) was marked by dark pigment (Fig. 1E). A small dark spot at the animal pole marked the position of the germinal vesicle (Fig. 1A, C). When the gonads were dissected, the eggs floated to the surface, animal pole up (Fig. 1B). Ultrastructural examination of the eggs did not reveal any structures at the vegetal pole that might be connected with the accumulation of dark pigment.

Spermatogenesis was usually allocated to small regions of the germinal epithelium, although entire lobes of some gonads were devoted to sperm production (Fig. 1A). Sperm

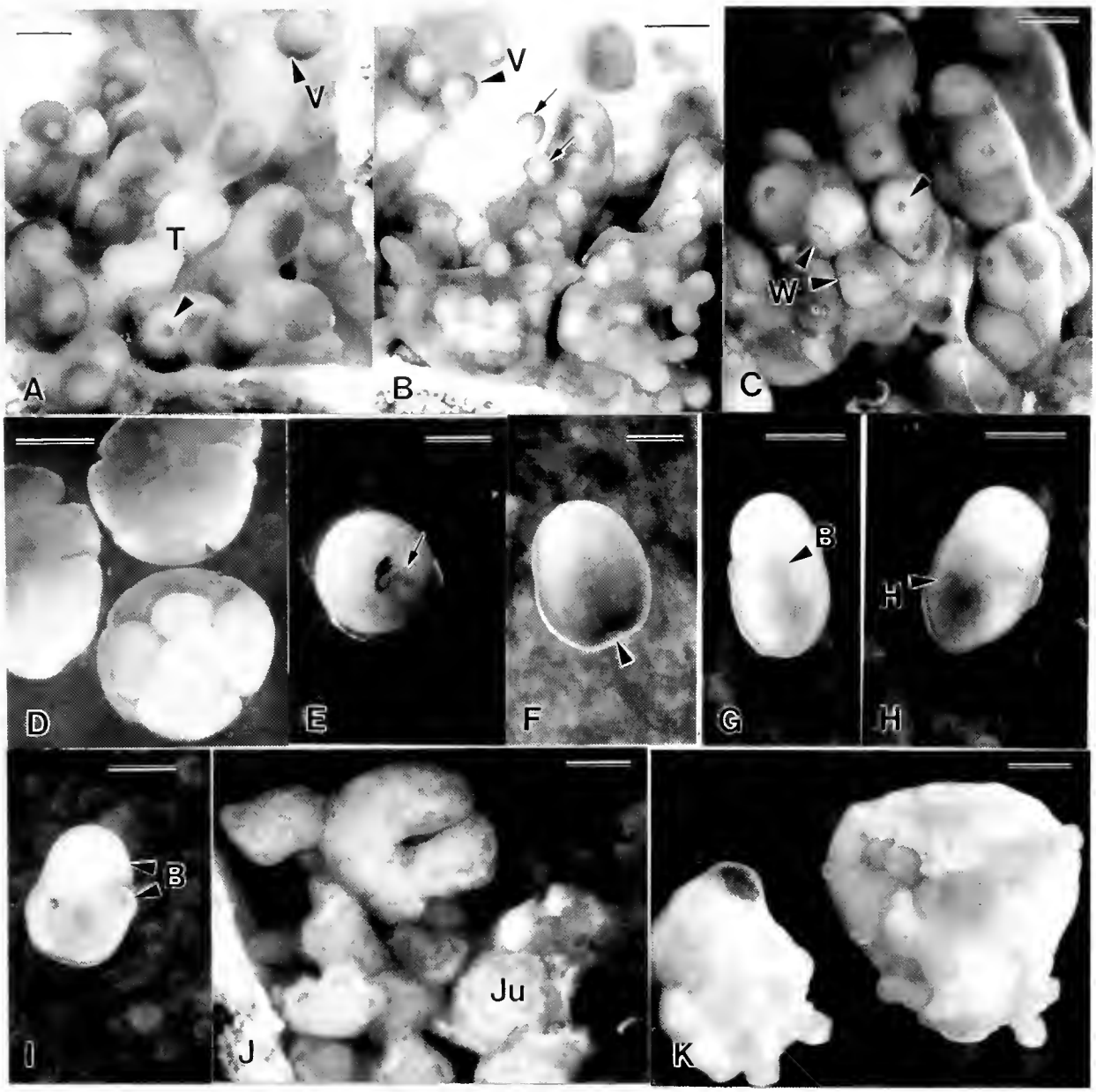

Figure 1. Light microscopy of *Cryptasterina hystera* gonads and embryos. **(A–C)** Ovotestes: The eggs have a dark vegetal region (V), and a dark spot marks the location of the germinal vesicle at the animal pole (arrowheads). The eggs float up from the dissected gonad (arrows). The gonad lobes are dominated by oocytes with occasional lobes filled with sperm (T). W, wrinkled blastulae. **(D)** Wrinkled blastulae. **(E)** Unhatched gastrula with black pigmented cells (arrow) streaming into the blastopore from one side of the embryo. The blastopore has a dark rim. **(F)** Hatched gastrula with dark pigment in vegetal hemisphere. Arrowhead, blastopore. **(G–I)** Brachiolaria larvae: The pigment remains in the posterior region. The lateral brachia (B) and hydroporic canal (H) are marked by darker cytoplasm **(J)** Gonad filled with near-term juveniles (Ju). **(K)** Moribund large juveniles dissected from gonad. Scales: A, C = 430 μm; B = 880 μm, D–F = 220 μm, G–I = 300 μm, J = 580 μm, K = 750 μm.

development in spermatocyte columns was typical of asteroid spermatogenesis. Spermatozoa were scattered in clumps intermingled with developing oocytes or in small pockets along the gonad wall (Figs. 2A, D; 3A). They remained separated from the oocytes by the follicle layer. The spermatozoa had a spherical head with the acrosome in a depression in the nucleus and surrounded by periacrosomal material, a midpiece, and a flagellum (Fig. 2F, G). These features are typical of asteroid sperm. When placed in seawater, the sperm of *C. hystera* exhibited typical motility.

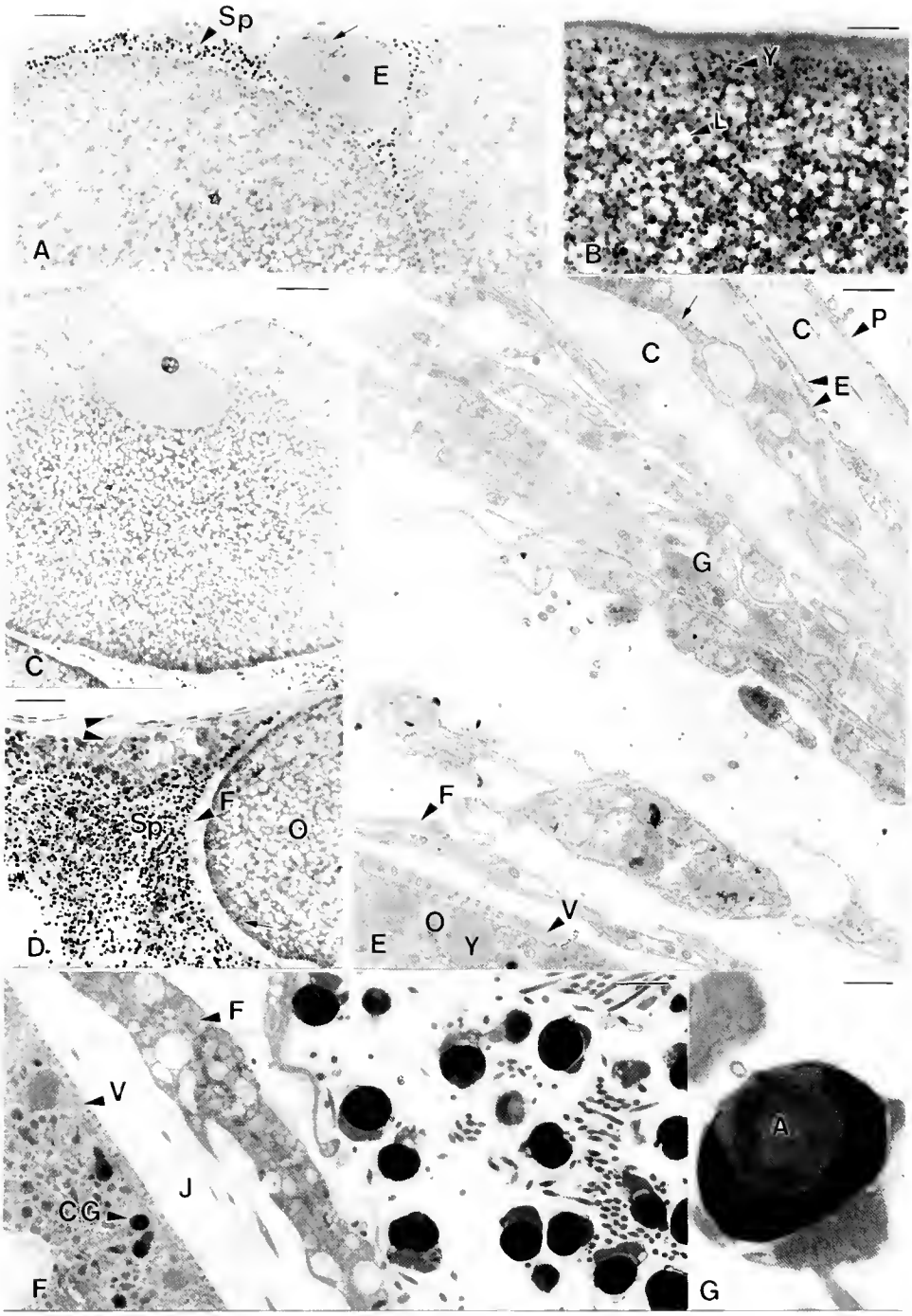

Figure 2. Light and transmission electron microscopy (TEM) of the ovotestis of *Cryptasterina hystera* **(A)** The early oocyte (E) contains a few yolk granules (arrow), and sperm (Sp) are present. **(B–C)** Advanced oocyte filled with lipid droplets (L). Yolk granules (Y) are dispersed among the lipid droplets and along the cortex. **(D)** Egg (O) and sperm (Sp) separated by the layer of follicle cells (F) around the egg. The arrowheads show the inner and outer tissue layers of the gonad wall. **(E, F)** TEM of gonad wall and oocyte (O). C, connective tissue layers; CG, cortical granule; E, epithelium of genital coelom; F, follicle cell; G, germinal epithelium; J, jelly coat; P, peritoneum; V, vitelline coat; Y, yolk granule; Arrow, phagocyte. **(G)** Sperm. A, acrosome. Scales: A, B, D = 50 μm; C = 100 μm; E = 1.5 μm; F = 2.0 μm, G = 0.4 μm.

Development

Embryos in all the gonads of individual *C. hystera* were usually at a similar stage of development, indicating that egg maturation, ovulation, and fertilization were synchronous (Figs. 1J; 3A, B, C). Among individual adults, however, the embryos were often at a different stage of development. Early in the season, cohorts of embryos developed alongside advanced gametes in the same gonad (Fig. 3A). By November and December, only a few unfertilized fully grown eggs remained in the gonad and were likely to be atretic. During these months, most gonads contained a clutch of juveniles (Fig. 1J)

Ovaries placed in 1-methyladenine (1-MA) released eggs, and many of these eggs were fertilized by sperm present in the gonad. Early cleavage was radial and holoblastic. The earliest embryos encountered in the gonad were wrinkled blastulae (Fig. 1C, D). Based on development in laboratory cultures, these embryos were about 12 h post-fertilization. Wrinkled blastulae had a highly contorted epithelium composed of cuboidal epithelial cells filled with large lipid droplets (Fig. 1C, D; 3C). The blastulae were enclosed in the fertilization envelope. The dark cytoplasm remained in the vegetal region throughout early development. In blastulae, it was confined to the lower third of the embryo. On removal from the gonad, blastulae floated at the air-water interface and continued development through the brachiolaria larval stage, metamorphosing into juveniles in 3 weeks.

The blastopore developed at the middle of the dark cytoplasm, about 24 h post-fertilization, and its rim was marked by dark pigment (Fig. 1E). During gastrulation, the dark cells around the blastopore did not move symmetrically into the embryo from around the margin of the opening (Fig. 1E). One side of the embryo appeared to contribute more dark cells to the developing archenteron than the other. As the larva elongated, dark pigmented cells moved anteriorly along the ventral surface and, to a lesser extent, the dorsal surface (Fig. 1F–H). The pigment did not extend beyond the midventral region. Although the distribution of the dark cytoplasm was variable among larvae, cells inheriting the dark pigment always remained in the posterior region of the larvae. In many larvae there was a contrast between the light anterior preoral lobe and the dark posterior region at the level of the brachiolar apparatus (Fig. 1I). The central brachium was light green, while the adjacent posterior body region was dark olive. On the dorsal side, dark cytoplasm marked the hydroporic canal (Fig. 1I).

The embryos hatched as late gastrulae at 40 h and the blastopore closed (Figs. 1F; 3A). Gastrulae and larvae swam propelled by their uniform cover of cilia. Their locomotion in gonad fluid depended on the availability of space. During the gastrula stage, lipid droplets were extruded into the blastocoel (Figs. 3D; 4A–C). Prior to extrusion, the epithelial cells changed from cuboidal to columnar, and lipid droplets were shunted to a basal location below the nucleus (Figs. 3D; 4A, B). This basal shunting was a prelude for lipid release. Lipid droplets were released into the blastocoel by an apocrine mechanism, taking part of the cell membrane with them (Figs. 3E; 4B, C). The lipid remained in the blastocoel throughout development (Figs. 3E; 4D).

Formation of the brachiolar attachment complex was first seen on external view in 5-day-old larvae as three protrusions at the anterior end (Fig. 1G). These were the developing brachia. By this stage the larvae swam at the bottom of the dish anterior end up, buoyed by the abundant lipid reserves in the blastocoel of this region of the larva. As the brachiolaria developed, the attachment complex became a prominent feature of the larva. The adhesive disc developed at the base of the brachia (Fig. 4D). Both the adhesive disc and brachiolar arms contained batteries of secretory cells that were presumably the source of adhesive material. Advanced larvae readily adhered to the substratum using their brachia and, prior to metamorphosis, attached to the surface of the culture dishes with the adhesive disc. The juvenile rudiment developed in the posterior region (Fig. 1H, I). Newly metamorphosed juveniles (600 μm in diameter, two pairs of tube feet per radius) from laboratory cultures had an amber hue due to their abundant lipid reserves. These reserves were mobilized during the perimetamorphic period. In sections of juveniles with a newly differentiated gut and well-developed skeleton, the remaining lipid droplets were seen scattered in the body wall (Fig. 3G).

Juveniles brooded by *C. hystera* appear to leave the gonad in a synchronous manner, as indicated by the appearance of hundreds of juveniles (800 μm diameter) in aquaria over a few hours. These juveniles had two pairs of podia in each radius. Some juveniles (1–2 per gonad) remained in the gonads for a longer time (Figs. 1K; 3F). These juveniles were large (1–4 mm diameter) and had four to six pairs of tube feet per radius. How they attained this size in the gonads is not known, but the presence of adjacent moribund juveniles indicated that they cannibalize their siblings. They may also utilize eggs as a source of food. The significance of this phenomenon is not clear because the presence of degenerating juveniles in the gonads indicates that at least some of them were unable to emerge from the gonad (Fig. 1K)

Discussion

Internal fertilization, intragonadal development, and live birth of juveniles is a rare form of propagation in marine invertebrates. Independent dispersive stages are completely deleted from the life history. In echinoderms, intragonadal incubation of embryos is known for one crinoid, four ophiuroids, four holothuroids, and five asteroids (Table 1). In addition, some dendrochirotid, psolid, and apodid sea

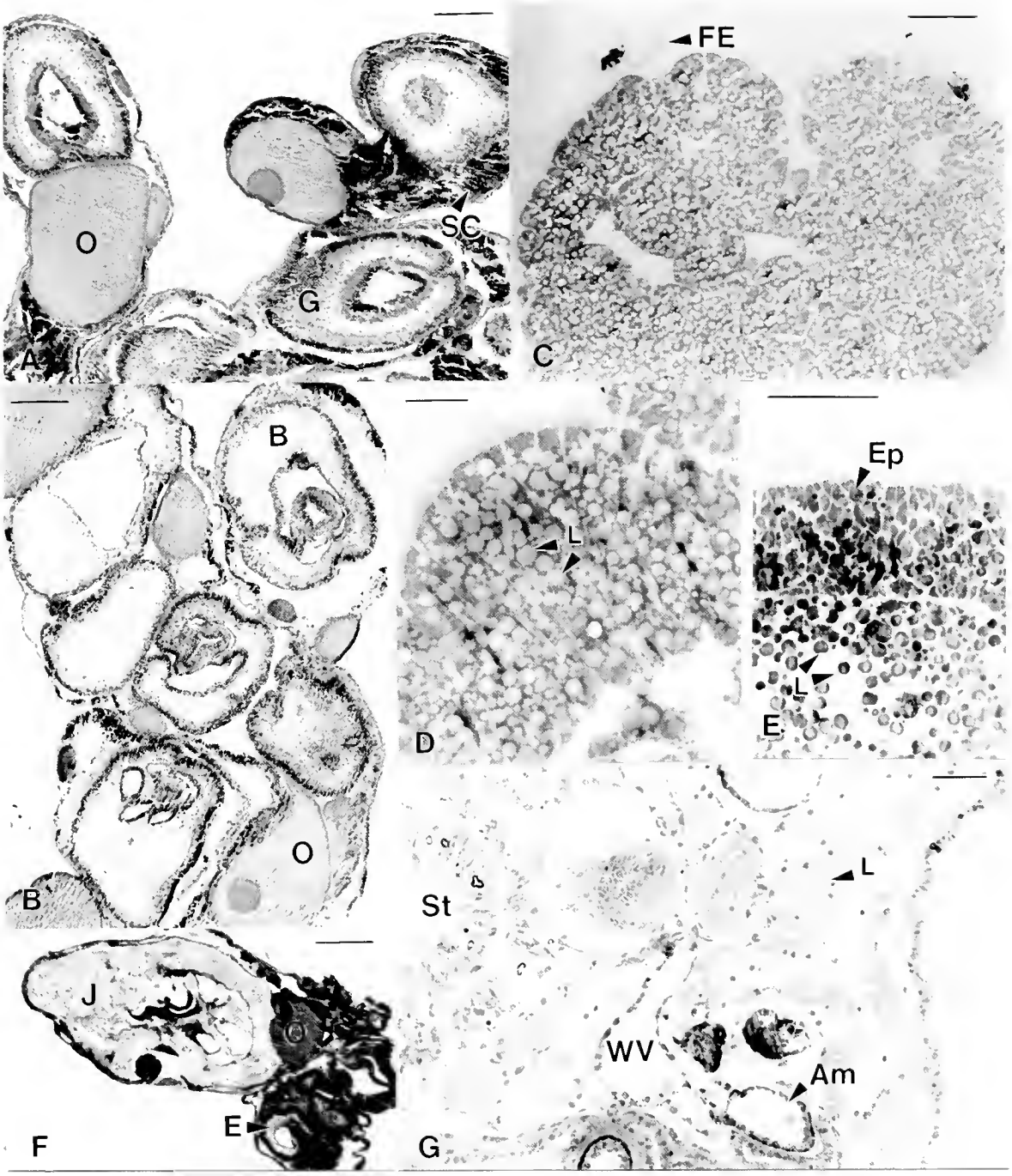

Figure 3. Light microscopy of *Cryptasterina hystera* gonads and embryos. **(A, B)** Gastrulae (G), brachiolaria larvae (B), oocytes (O), and spermatocyte columns (SC) in the gonads. **(C)** Wrinkled blastula with lipid droplets in cuboidal epithelial cells. FE, fertilization envelope. **(D)** Early gastrulae prior to extrusion of lipid (L). **(E)** Larva with lipid (L) in blastocoel. Few lipid reserves remaining in the epithelium (Ep). **(F)** Large juvenile (J), eggs (O), and embryo (E) in gonad. **(G)** Thin section of fully developed juvenile prior to the onset of feeding. The section extends from the stomach (St) to the edge of the body and shows lipid droplets (L) remaining in the body wall. WV, water vascular system; Am, ampulla of tube foot. Scales: A, B = 125 μm; C = 45 μm; D, E = 13.5 μm; F = 500 μm; G = 40 μm.

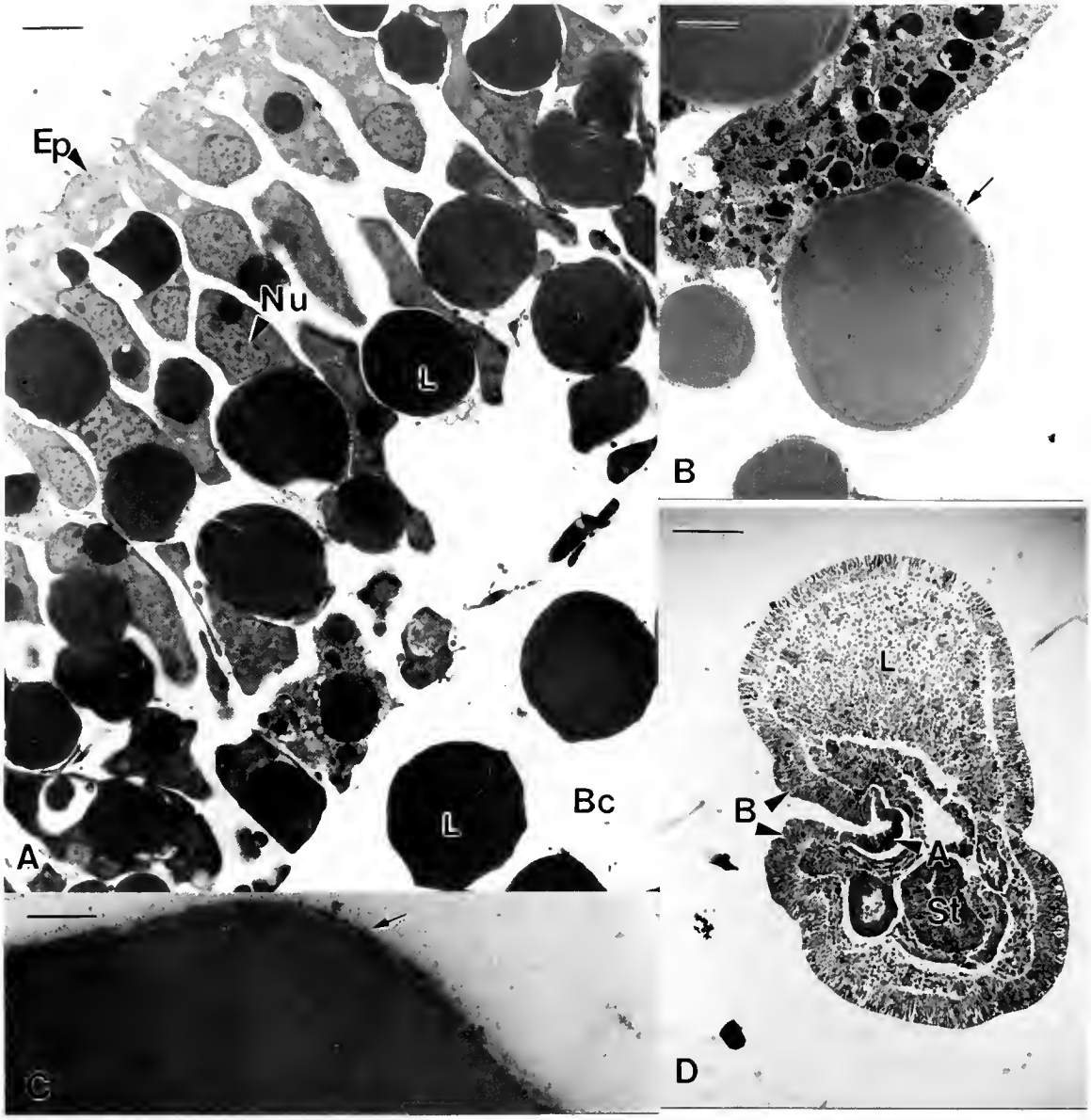

Figure 4. Light and transmission electron microscopy of *Cryptasterina hystera*. **(A–C)** Lipid reserves (L) are shunted basally below the nucleus (Nu) of the cells in the gastrula epithelium (Ep) before secretion into the blastocoel (Bc). The lipid is released by an exocrine mechanism, often taking a portion of the cell membrane (arrow). **(D)** Brachiolaria with lipid droplets (L) filling the blastocoel. A, adhesive disc; B, brachia; St, stomach. Scales: A = 3.0 μm; B = 1.5 μm; C = 0.15 μm; D = 85 μm.

cucumbers incubate their offspring in the coelom and juveniles emerge from the adult body (Reviews: Vaney, 1925; McEuen, 1986; O'Loughlin, 1994). Although live birth is rare in echinoderms, it appears that the potential for making the switch to this mode of propagation is more common in some taxa than others. The Holothuroidea contains the highest number of viviparous species (O'Loughlin, 1994). Aside from the aberrant *Xyloplax medusiformis*, all viviparous asteroids are in the Asterinidae (Table 1).

As is characteristic of viviparous asterinids, the gonads of *Cryptasterina hystera* were ovotestes (Komatsu *et al.*, 1990; Byrne, 1996). This condition is also reported in viviparous holothuroids (Miller, 1985; Frick *et al.*, 1996). Despite their intragonadal location, the sperm of *C. hystera* had a well-developed tail, were fully motile, and could fertilize eggs *in vitro*. Their ultrastructure was the asteroid "echinosperm-type" (*sensu* Jamieson, 1985) with a round head and embedded acrosome. It is likely that these sperm would be functional if released into the sea. For outcrossing to occur in *C. hystera* and other viviparous echinoderms, sperm

Table 1

Incidence of intragonadal development in the Echinodermata

Class	Reference
Crinoidea	
Comatilia iridometriformis	Messing (1984)
Holothuroidea	
Leptosynapta clarki	Sewell and Chia (1994)
Oneirophanta mutabilis	Hansen (1968)
Taeniogyrus contortus	Vaney (1925)
Trachythyone mira	Ludwig and Heding (1935) O'Loughlin (2002)
Ophiuroidea	
Amphiura microplax	Mortensen (1936)
Amphiura monorima	Mortensen (1936)
Astrochlamys sol	Madsen (1967)
Ophionotus hexactis	Mortensen (1921)
Asteroidea	
Cryptasterina pacifica	Komatsu *et al.*, (1990)
Cryptasterina hystera	Byrne *et al.* (2003a)
Patiriella vivipara	Byrne and Cerra (1996)
Patiriella parvivipara	Byrne and Cerra (1996)
Xyloplax medusiformis	Rowe *et al.* (1988)

would have to gain access to eggs by swimming through the gonopore, an activity that would require sperm chemotaxis. Sperm chemoreception and sperm-activating pheromones have been documented for several echinoderms, including asteroids (Miller, 1989; Miller and Vogt, 1996). Asterinids with benthic development gather to lay communal egg masses, with sperm deposited directly onto the eggs (Tominaga *et al.*, 1994; Byrne, 1995). Sperm exchange in *C. hystera* would be facilitated by similar mating behavior. *C. hystera* clearly has the potential for self-fertilization. Determination of paternity for *C. hystera* and other viviparous echinoderms requires genetic investigation.

Developing oocytes of *C. hystera* remained within their follicle throughout development and were thereby separated from adjacent sperm. Asteroid follicle cells release 1-methyladenine (1-MA), which induces resumption of oocyte meiosis; the follicle cells themselves respond to the hormone by separating from the oocyte, freeing it for release (Schroeder *et al.*, 1979; Chiba, 2000). Oocyte maturation and ovulation occurred in *C. hystera*, but the spawning component of the 1-MA hormone activity cascade is suppressed (Mita, 1993). This fundamental change is a major alteration in reproduction and is associated with evolution of viviparity in this sea star. Spawning in sea stars involves contraction of the myoepithelial cells in the gonad wall. It is not known if these cells have been modified or are less abundant in the gonad of *C. hystera* than in the gonads of free-spawning asteroids. Once freed from the follicle, the eggs are no longer separated from endogenous sperm. In the laboratory, eggs released after 1-MA treatment were fertilized by sperm from the same gonad. It is not known if self-fertilization occurs in the field. In free-spawning echinoderms, sperm adhere to egg jelly coats that have been hydrated by seawater, and egg jelly induces the acrosome reaction (Sousa and Azevedo, 1985). It is not known if a similar change to the egg jelly and its role in acrosome stimulation occurs in the intragonadal environment.

From an ancestral state involving planktotrophic development and small eggs dominated by yolk protein (Byrne *et al.*, 1999b, 2003b), the increase in egg size in *C. hystera* was associated with a shift to lipid-dominated eggs. An increase in lipid reserves is characteristic of echinoderms with lecithotrophic development (Emlet *et al.*, 1987; Jaeckle, 1995). The initial phase of oogenesis during which yolk protein is sequestered into yolk granules is typical of the ancestral-type oogenic pattern (Byrne *et al.*, 1999c, 2003b). This is followed by hypertrophic lipid deposition, similar to that seen in the lipid-rich eggs of the sea urchin *Heliocidaris erythrogramma* (Byrne *et al.*, 1999c). Possession of a buoyant egg in *C. hystera* and its congener *C. pacifica* was not expected in species with intragonadal development. Development in *C. hystera* and *C. pacifica* is completely supported by maternal provisioning in the egg. In contrast, *Patiriella vivipara* and *P. parvivipara* have small (120-μm diameter), secondarily reduced negatively buoyant eggs with minimal lipid stores (Byrne *et al.*, 1999b). Due to reduced egg provisioning, development in the viviparous *Patiriella* depends on sibling cannibalism (Byrne, 1996), a form of matrotrophy occasionally observed in *C. hystera* and also reported in viviparous holothuroids (Frick, 1998).

The structure of the gonad of *C. hystera*, with the inner and outer tissue layers separated by the genital coelom, is typical of asteroids (Chia and Koss, 1995). With the exception of the presence of both eggs and sperm, the structure of the gonads did not indicate any morphological specializations that might be associated with the evolution of viviparity. Similarly, the structure of the gonads of viviparous *Patiriella* and viviparous holothuroids is similar to those of broadcast spawners (Sewell and Chia, 1994; Byrne, 1996). In contrast, echinoderms that brood embryos in non-gonadal structures often have specializations for transferring nutrients to developing young (Walker and Lesser, 1989; McClary and Mladenov, 1990). *C. hystera* appears to have no anatomical impediments for acquisition of a marsupial function for the gonads. Considering this lack of morphological constraint, it is surprising that a viviparous life history is not more common in asteroids.

Most of the nutritive provisions loaded into the egg of *C. hystera* are reserved for the postlarval perimetamorphic stage. Early development is burdened by excess nutritive reserves not required for embryogenesis. Shunting of lipid into the basal cytoplasm of the epithelium, as seen in *C. hystera*, is common in lipid-rich echinoderm embryos (Patent, 1968; Henry *et al.*, 1991; Cerra and Byrne, 1995; Byrne and Cerra, 2000; Byrne *et al.*, 2003b). This is suggested to be a mechanism for partitioning excess reserves

away from the active apical region of the cell (Cerra and Byrne, 1995). In *C. hystera*, most lipid reserves are extruded into the extracellular blastocoelic space at the gastrula stage by an apocrine mechanism, similar to that documented for the sea urchin *Heliocidaris erythrogramma* (Henry *et al.*, 1991). The blastocoel thus functions as a storage space for nutrients to support juvenile development. Lipid extrusion is now reported for the embryos of two echinoderm species, both of which have highly buoyant, lipid-rich eggs. Such extrusion is the extreme outcome of the basal shunting process and may be associated with the presence of a particular class of lipid.

The presence of differently pigmented cytoplasm, as seen in the eggs of *C. hystera*, has not been reported for asteroids but is known for one echinoid, *Holopneustes purpurascens*. The animal and vegetal hemispheres of the eggs of *C. hystera* could be discerned by light and dark pigment, respectively. This is similar (but opposite) to the situation in the eggs of *H. purpurascens*, where the animal pole has dark yolk and the vegetal pole has light yolk (Morris, 1995). In that urchin, dark pigment is segregated into one blastomere at the 2-cell stage. In *C. hystera*, by contrast, the pigment remained in the vegetal region, with the major cellular segregation occurring at the third equatorial cleavage that separates cells into animal and vegetal fates. The dark cytoplasm remained in the lower third of the embryo, and the blastopore appeared where the dark pigment was most concentrated. During gastrulation, it appeared that one side of the embryo contributed more dark cells to the developing archenteron than the other. The mechanism of gastrulation in *C. hystera* may differ from the radially symmetrical pattern of involution traditionally attributed to echinoderms. Asymmetrical cell movements during gastrulation have been reported for the lecithotrophic embryos of the sea urchin *Heliocidaris erythrogramma* (Wray and Raff, 1994) and also occur in the lecithotrophic embryos of *Patiriella exigua* (Byrne and Cerra, unpubl.). More studies are required to determine whether gastrulation by asymmetrical invagination of cells from the right and left sides of the embryo is a feature of lecithotrophic development in echinoderms.

After closure of the blastopore, dark-pigmented cells that remained evident on the surface view migrated ventrally. This is consistent with migration of the blastopore region to the ventral side of planktotrophic larvae that have a functional anus. In many larvae, the dark cells formed a boundary between the preoral-postoral regions on the ventral surface, at the level of the brachiolar apparatus. The pigment may thus mark the anterior and posterior cellular domains that in feeding larvae would be bordered by the preoral and postoral ciliated bands. This is reminiscent of the oral and aboral territories marked by the ciliary band in sea urchin plutei and for which patterns of gene expression have been determined (Davidson *et al.*, 1998). On the dorsal side, dark pigment was also present in the posterior region, and the hydropore was strongly marked by dark pigment. The animal-vegetal pigment in the eggs of *C. hystera* has potential for use in cell lineage studies.

The presence of a functional brachiolaria in the gonads of *C. hystera* and *C. pacifica* indicates that these sea stars have the potential to brood and broadcast their young—an unusual form of poecilogony that has been reported for the sea star *Pteraster militaris* (McClary and Mladenov, 1988). The highly restricted distribution of *C. hystera* indicates, however, that the brachiolaria are not used for dispersal in nature and that the progeny are likely to leave the parent as juveniles (Byrne *et al.*, 2003a). In aquaria, only juveniles were released. In general, the biogeography of asterinid sea stars correlates with the presence or absence of a dispersive larva; the exception is the benthic developer *Patiriella exigua*, which occurs around the southern hemisphere (Waters and Roy, 2004; Colgan *et al.*, 2005). Viviparous asterinids have the most restricted distribution known for the Asteroidea (Byrne *et al.*, 1999a, 2003a). Three of these occur in Australia, and their distributions range from 50 km (three locations, *C. hystera*) to 100 km of coastline (seven locations, *P. vivipara*). It would be interesting to know the distribution of *C. pacifica*, the fourth viviparous asterinid, in Japan. The mangrove habitats where *C. hystera* is found are vulnerable to anthropogenic change, highlighting the need to determine the distribution of this new viviparous species.

Acknowledgments

Special thanks to Dr. S. McKillup for providing specimens. Thanks to the Electron Microscope Unit, University of Sydney, for use of facilities and to Dr. A. Cerra for assistance with microscopy. Dr. R. Emlet and an anonymous reviewer are thanked for suggestions that improved the manuscript. The research was supported by a grant from the ARC.

Literature Cited

Byrne, M. 1995. Changes in larval morphology in the evolution of benthic development by *Patiriella exigua* (Asteroidea: Asterinidae), a comparison with the larvae of *Patiriella* species with planktonic development. *Biol. Bull.* **188:** 293–305.

Byrne, M. 1996. Viviparity and intragonadal cannibalism in the diminutive asterinid sea stars *Patiriella vivipara* and *P. parvivipara*. *Mar. Biol.* **125:** 551–567.

Byrne, M., and A. Cerra. 1996. Evolution of intragonadal development in the diminutive asterinid sea stars *Patiriella vivipara* and *P. parvivipara* with an overview of development in the Asterinidae. *Biol. Bull.* **191:** 17–26.

Byrne, M., and A. Cerra. 2000. Lipid dynamics in the embryos of *Patiriella* species (Asteroidea) with divergent modes of development. *Dev. Growth Differ.* **42:** 79–86.

Byrne, M., A. Cerra, M. W. Hart, and M. J. Smith. 1999a. Life history diversity and molecular phylogeny in the Australian sea star genus *Patiriella*. Pp. 186–196 in *The Other 99%: The Conservation*

and Biodiversity of Invertebrates, W. Ponder and D. Lunney, eds. Transactions of the Royal Society of New South Wales, Sydney.

Byrne, M., A. Cerra, and J. T. Villinski. 1999b. Oogenic strategies in the evolution of development in *Patiriella* (Asteroidea). *Invertebr. Reprod. Dev.* **36:** 195–202.

Byrne M., J. T. Villinski, E. Popodi, P. Cisternas, and R. R. Raff. 1999c. Maternal factors and the evolution of developmental mode: evolution of oogenesis in *Heliocidaris erythrogramma. Dev. Genes Evol.* **209:** 275–283.

Byrne M., M. W. Hart, A. Cerra, and P. Cisternas. 2003a. Reproduction and larval morphology of broadcasting and viviparous species in the *Cryptasterina* species complex. *Biol. Bull.* **205:** 285–294.

Byrne M., P. Cisternas, P. Selvakumaraswamy, J. T. Villinski, and R. R. Raff. 2003b. Evolution of maternal provisioning in ophiuroids, asteroids and echinoids. Pp. 171–175 in *Echinoderm Research 2001,* J.P. Feral and B. David, eds. Balkema, Lisse, The Netherlands.

Cerra, A., and M. Byrne. 1995. Cellular events of wrinkled blastula formation and the influence of the fertilization envelope on wrinkling in the seastar *Patiriella exigua Acta Zool.* **76:** 155–165.

Chia, F.-S., and R. Koss. 1995. Asteroidea. Pp. 169–245 in *Microscopic Anatomy of Invertebrates,* F.W. Harrison and F.-S. Chia, eds. Wiley-Liss, New York.

Chiba, K. 2000. Meiosis reinitiation in starfish oocytes. *Zool Sci.* **17:** 413–417.

Colgan, D. J., M. Byrne, E. Rickard, and L. R. Castro. 2005. Limited nucleotide divergence over large spatial scales in the asterinid sea star *Patiriella exigua. Mar. Biol.* **146:** 263–270.

Dartnall, A. J. 1969. A viviparous species of *Patiriella* (Asteroidea, Asterinidae) from Tasmania. *Proc. Linn. Soc. N.S.W.* **93:** 294–296.

Dartnall, A. J., M. Byrne, J. Collins, and M. W. Hart. 2003. A new viviparous species of asterinid (Echinodermata, Asteroidea, Asterinidae) and a new genus to accommodate the species of pan-tropical exiguoid sea stars. *Zootaxa* **359:** 1–14.

Davidson, E. H., R. A. Cameron, and A. Ransick. 1998. Specification of cell fate in the sea urchin embryo: summary and some proposed mechanisms. *Development* **105:** 3269–3290.

Degnan, B. M., and M. F. Lavin. 1995. Highly repetitive DNA sequences provides evidence for a lack of gene flow between two morphological forms of *Herdmania momus* (Ascidiacea: Stolidobranchia). *Mar. Biol.* **124:** 293–299.

Emlet, R. B., and O. Hoegh-Guldberg. 1997. The effects of egg size on post-larval performance: experimental evidence from a sea urchin. *Evolution* **51:** 141–152.

Emlet, R. B., L. R. McEdward, and R. R. Strathmann. 1987. Echinoderm larval ecology viewed from the egg. Pp. 55–136 in *Echinoderm Studies,* M.J. Jangoux and J. M. Lawrence, eds. Balkema, Rotterdam.

Frick, J. E. 1996. Evidence of matrotrophy in the viviparous holothuroid echinoderm *Synaptula hydriformis. Invertebr. Biol.* **117:** 169–179.

Frick, J. E., E. E. Ruppert, and J. P. Wourms. 1996. Morphology of the ovotestis of *Synaptula hydriformis* (Holothuroidea, Apoda): an evolutionary model of oogenesis and the origin of egg polarity in echinoderms. *Invertebr. Biol.* **115:** 46–66.

Hansen, B. 1968. Brood-protection in a deep-sea holothuriao, *Oneirophanta mutabilis* Théel. *Nature* **217:** 1062–1063.

Hart, M. W., M. Byrne, and M. J. Smith. 1997. Molecular phylogenetic analysis of life-history evolution in asterinid starfish. *Evolution* **51:** 1846–1859.

Hart, M. W., M. Byrne, and S. L. Johnson. 2003. Cryptic species and modes of development in *Patiriella pseudoexigua. J. Mar. Biol. Assoc. UK* **83:** 1109–1116.

Hart, M. W., S. L. Johnson, J. A. Addison, and M. Byrne. 2004. Strong character incongruence and character choice in phylogeny of sea stars of the Asterinidae. *Invertebr. Biol.* **123:** 343–356.

Henry, J. J., G. A. Wray, and R. R. Raff. 1991. Mechanism of an alternate type of echinoderm blastula formation: the wrinkled blastula of the sea urchin *Heliocidaris erythrogramma. Dev. Growth Differ.* **33:** 317–328.

Huber, J. L., K. Burke da Silva, W. R. Bates, and B. J. Swalla. 2000. The evolution of anural larvae in molgulid ascidians. *Semin. Cell Dev. Biol.* **11:** 419–426.

Jaeckle, W. B. 1995. Variation in the size, energy content and biochemical composition of invertebrate eggs: correlates to mode of larval development. Pp. 79–122 in *Ecology of Marine Invertebrate Larvae,* L. McEdward, ed. CRC Press, Boca Raton, FL.

Jamieson, B. G. 1985. The spermatozoa of the Holothuroidea (Echinodermata): an ultrastructural review with data on two Australian species and phylogenetic discussion. *Zool. Scripta* **14:** 123–135.

Keough, M. J., and A. J. Dartnall. 1978. A new species of viviparous asterinid asteroid from Eyre Peninsula, South Australia. *Rec. S. Aust. Mus.* **17:** 407–416.

Knowlton, N. 1993. Sibling species in the sea. *Ann. Rev. Ecol. Syst.* **24:** 189–216.

Komatsu, M., Y. T. Kano, and C. Oguro. 1990. Development of a true ovoviviparous sea star, *Asterina pseudoexigua pacifica* Hayashi. *Biol. Bull.* **179:** 254–263.

Ludwig, H., and S. G. Heding. 1935. Die Holothurien der Deutschen Tiefsee-Expedition. 1, Fusslose und Dendrochirote Formen. *Wissenschaftliche Ergebnisse der Deutschen Expedition Tiefsee auf dem Dampher "Valdivia" 1898–9.* **24:** 121–244.

Madsen, F. J. 1967. Ophiuroidea. *B.A.N.Z. Antarctic Res. Exped. 1929–1931 Rep. Ser. B. (Zool. Bot.)* **9:** 123–145.

McClary, D. J., and P. V. Mladenov. 1988. Brood and broadcast: A novel mode of reproduction in the starfish *Pteraster militaris.* Pp. 163–168 in *Echinoderm Biology,* R.D. Burke, P.V. Mladenov, P. Lambert, and R.L. Parsley, eds. Balkema, Rotterdam.

McClary, D. J., and P. V. Mladenov. 1990. Brooding biology of the sea star *Pteraster militaris:* energetic and histological evidence for nutrient translocation to brooded juveniles. *J. Exp. Mar. Biol. Ecol.* **142:** 183–199.

McEuen, F. S. 1986. The reproductive biology and development of twelve species of holothuroids from the San Juan Islands, Washington. PhD. thesis, University of Alberta.

Messing, C. G. 1984. Brooding and paedomorphosis in the deep-water feather star *Comatilia iridometriformis* (Echinodermata: Crinoidea). *Mar. Biol.* **80:** 83–91.

Miller, J. E. 1985. Viviparity in a psolid holothurian from the tropical western Atlantic. Pp. 472 in *Proceedings of the Fifth International Echinoderm Conference.* B.F.Keegan and B.D.S. O'Connor, eds, Balkema, Rotterdam.

Miller, R. L. 1989. Evidence for the presence of sexual pheromones in free-spawning starfish. *J Exp. Mar. Biol. Ecol.* **130:** 205–222.

Miller, R. L., and R. Vogt. 1996. An o-termioal partial sequence of the 13kDa *Pycnopodia helianthoides* sperm chemoattractant "startrak" possesses sperm-attractant activity. *J. Exp. Biol.* **199:** 311–318.

Mita, M. 1993. 1-Methyladine production by ovarian follicle cells is responsible for spawning in the starfish *Asterina pectinifera. Invertebr. Reprod. Dev.* **24:** 237–242.

Morris, V. B. 1995. Apluteal development of the sea urchin *Holopneustes purpurescens* Agassiz (Echinodermata: Echinoidea: Euechinoidea). *Zool. J. Linn. Soc.* **114:** 349–364.

Mortensen, T. 1921. *Studies of the Development and Larval Forms of Echinoderms.* G.E.C. Gad, Copenhagen. 261 pp.

Mortensen, T. 1936. Echinoidea and Ophiuroidea. *Discov. Rep.* **12:** 199–348.

Ó Foighil, D., and M. J. Smith. 1995. Evolution of asexuality in the cosmopolitan marine clam *Lasaea. Evolution* **49:** 140–150.

O'Loughlin, P. M. 1994. Brood-protectiog and fissiparous cucumariids (Echinodermata, Holothuroidea). Pp. 539–547 in *Echinoderms*

Through Time, B. David, A. Guille, J.P. Féral, and M. Roux, eds. Balkema, Rotterdam.

O'Loughlin, P. M. 2002. Report on selected species of Banzare and Anare Holothuroidea, with reviews of *Meseres* Ludwig and *Heterocucumis* Panning (Echinodermata). *Mem. Mus. Vic.* **59:** 297–325.

Patent, D. H. 1968. The general and reproductive biology of the basket star *Gorgonocephalus caryi* (Echinodermata, Ophiuroidea). Ph.D. thesis, University of California, Berkeley.

Pocklington, P., and M. S. Hutcheson. 1983. New record of viviparity for the dominant benthic invertebrate *Exogone hebes* (Polychaeta: Syllidae) from the Grand Banks of Newfoundland. *Mar. Ecol. Prog. Ser.* **11:** 239–244.

Reid, D. G. 1990. A cladistic phylogeny of the genus *Littorina* (Gastropoda): implications for evolution of reproductive strategies and for classification. *Hydrobiologia* **193:** 1–19.

Rowe, F. W. E., A. N. Baker, and H. E. S. Clark. 1988. The morphology, development and taxonomic status of *Xyloplax* Baker, Rowe and Clark (1986) (Echinodermata: Concentricycloidea), with the description of a new species. *Proc. R. Soc. Lond. B* **233:** 431–459.

Schroeder, P. C., J. H. Larsen, and A. E. Waldo. 1979. Oocyte-follicle relationships in a starfish. *Cell Tissue Res.* **203:** 249–256.

Sewell, M. A., and F.-S. Chia. 1994. Reproduction of the intraovarian brooding apodid *Leptosynapta clarki* (Echinodermata: Holothuroidea) in British Columbia. *Mar. Biol.* **121:** 285–300.

Sousa, M., and C. Azevedo. 1985. Acrosomal reaction and early events at fertilization in *Marthasterias glacialis* (Echinodermata: Asteroidea). *Gamete Res.* **11:** 157–167.

Tominaga, H., M. Komatsu, and C. Oguro. 1994. Aggregation for spawning in the breeding season of the sea-star, *Asterina minor* Hayashi. Pp. 369–373 in *Echinoderms Through Time,* B. David, A. Guille, J.P. Féral, and M. Roux, eds. Balkema, Rotterdam.

Vaney, C. 1925. L'incubation chez holothuries. *Travaux de la Station Zoologique Wimereux* **8:** 254–274.

Villinski, J. T., J. L. Villinski, M. Byrne, and R. R. Raff. 2002. Convergent maternal provisioning and life history evolution in echinoderms. *Evolution* **56:** 1764–1775.

Walker, C. W., and M. P. Lesser. 1989. Nutrient and development of brooded embryos in the brittlestar *Amphipholis squamata:* do endosymbiotic bacteria play a role? *Mar. Biol.* **103:** 519–530.

Waters, J. M., and M. S. Roy. 2004. Out of Africa: the slow train to Australasia. *Syst. Biol.* **53:** 18–24.

Wray, G. A., and R. R. Raff. 1991. Rapid evolution of gastrulation mechanism in a sea urchin with lecithotrophic larvae. *Evolution* **45:** 1741–1750.

Reference: *Biol. Bull.* **208:** 92–99. (April 2005)

Larval Morphometrics and Influence of Adults on Settlement in the Gregarious Ophiuroid *Ophiothrix fragilis* (Echinodermata)

RAPHAEL MORGAN[1,*] AND MICHEL JANGOUX[1,2]

[1] *Université Libre de Bruxelles, Laboratoire de Biologie Marine (CP 160/15), 50 Av Franklin Roosevelt, B1050 Brussels, Belgium; and* [2] *Université de Mons-Hainaut, Laboratoire de Biologie Marine, 20 Place du Parc, B7000 Mons, Belgium*

Abstract. The development of *Ophiothrix fragilis* was documented using light microscopy, and the allometry of larval growth was quantified. Larval development to the suspended juvenile stage took 21 days under conditions that were probably optimal compared to those in the plankton. Larval shape changed through development as the larval body and arms grew. Growth of the posterolateral larval arms was continuous throughout development, even during metamorphosis when the larva became endotrophic. During this period, these larval arms function as locomotory organs, and their continuous growth is probably essential to support the juvenile as it increases in density through development of its calcareous plates. In induction assays using adult conspecifics, initiation of metamorphosis was spontaneous. Release of the posterolateral arms was induced by the presence of adults. This response is likely to enhance a juvenile's chance of recruiting to a suitable habitat in the *Ophiothrix fragilis* beds of the North Sea.

Introduction

Planktotrophic larvae of marine benthic invertebrates face two sets of challenges during development (McEdward and Herrera, 1999). Firstly, they must function as feeding planktonic organisms which must acquire food, swim, control their position in the water column, and select a microhabitat. Secondly, they must undergo ontogenetic transformations that result in continuous changes in body form. This is especially true in the later stages of development when the rudiment of the juvenile is constructed in preparation for settlement. As a consequence, functional requirements and ontogenic changes can impose demands on larval design (McEdward, 1984, 1986; McEdward and Herrera, 1999). Therefore, the analysis of the development of feeding larvae requires an understanding of the requirements and capabilities of particular stages as well as an understanding of the patterns of larval growth that define the developmental trajectory (McEdward and Herrera, 1999).

Planktotrophic plutei of ophiuroids can develop *via* two pathways depending on their metamorphosis, which occurs in the plankton and precedes settlement (Mladenov, 1985a). In type I developers, metamorphosis is characterized by the regression of all larval arms except for the posterolateral pair and the differentiation of a juvenile between these. In type II developers, all larval arms regress and a vitellaria that differentiates into a juvenile is formed. The larval development of type I developers has been described in detail for four species (MacBride, 1907; Narasimhamurti, 1933; Olsen, 1942; Tominaga *et al.*, 2004).

The brittle star *Ophiothrix fragilis* (Abildgaard, 1789) occurs in high densities throughout the English Channel-North Sea region where the major populations are known and have been studied throughout the late 19th and 20th centuries (Allen, 1899; Warner, 1970; Holme, 1984; Davoult *et al.*, 1990). These populations are considered stable through time and space. *O. fragilis* is a type I planktotrophic developer whose development was described by MacBride (1907). The fact that in the English Channel-North Sea region juveniles are preferentially found on adult conspecifics has led many to believe that settlement occurs preferentially on adults (Warner, 1971; Davoult *et al.*, 1990; Morgan and Jangoux, 2004). Morgan and Jangoux (2004)

Received 26 May 2004; accepted 4 February 2005.

* To whom correspondence should be addressed. E-mail: rmorgan@ulb.ac.be

have also shown the close relationship between juveniles and adults in this species; this relationship is particularly evident in the way juveniles respond to adults at a distance.

In this study, the development and growth of the larval body and skeleton of *O. fragilis* was followed to document the larval morphometric changes. Considering the well-known aggregative behavior of *O. fragilis*, the role that conspecific adults may play in induction of settlement was investigated.

Materials and Methods

In 1999, specimens of *Ophiothrix fragilis* were collected by scuba diving (20–25 m) from Wemeldinge (Zeeland, Netherlands). Individuals were taken during the period of sexual maturity between the months of May and August and brought back to the Marine Biology Laboratory in Brussels. They were kept in a closed-circuit aquarium under the same abiotic conditions of temperature and salinity as those found in the field (16–18 °C, 32‰).

Fertilizations assays were made using ripe individuals. Individuals were considered ripe when their gonads (white testes; orange ovaries) could be seen through the extended wall of the bursae. Water used for fertilizations and subsequent larval cultures came from the sampling site. Water was allowed to settle for 48 h, then filtered (15 μm) before use.

In each fertilization assay, one male and one female were placed in a small aquarium with 500 ml of filtered and aerated seawater (16 °C, 32‰). The male was agitated for 5 s every minute until it started to liberate its gametes. Release of sperm induced the female to spawn, and the male was removed (Morgan and Jangoux, 2002). Embryos at the gastrula stage were transferred to 30-l larval rearing tanks at a density of 500 embryos/liter.

Larvae from a single spawning event were reared under a 12:12 dark/light photoperiod at 16 °C and 32‰ salinity. Seawater was constantly aerated, and half the volume of water from each tank was siphoned off every 5 days and replaced with filtered seawater. At the onset of larval exotrophy (3rd day after fertilization) the larvae were fed the diatom *Chaetoceros calcitrans* at a concentration of 30,000 cells · larva^{-1} · day^{-1}.

The larvae from this culture were followed from fertilization to completion of development (settled juveniles). Every 1–2 days, a subsample of 30 to 50 larvae was photographed, using a digital camera mounted on a dissecting microscope. Measurements were then made using an image analysis program (UTHSCSA image tool developed at the University of Texas Health Science Center at San Antonio, Texas, and available from the Internet through http://ddsdx.uthscsa.edu/dig/itdesc.html). Two measurements were taken on each individual: the height of the body (body length) and the length of the longest posterolateral rod (Fig. 1).

To establish the chronology of development and morphological change, the larvae were observed every 1–2 days under a microscope with or without polarized light (observation of the skeleton). The timing of development or regression of various features (*e.g.*, larval arms, juvenile mouth) was determined and used as a quantifiable character when at least 50% of the observed larvae had acquired the new feature.

Late larvae from a culture (n = 1) were used to test for induction of metamorphosis and settlement. They were placed in a small aquaria filled with 500 ml of filtered autoclaved seawater with (experimental) or without (control) an adult conspecific. In total, 90 larvae divided into three trials were used for each experimental and control assay. The larvae were separated from the adult by a 90-μm mesh. In the case of metamorphosis induction assays, the larvae were observed for 48 h to check whether adult conspecifics could initiate or accelerate metamorphosis. In the case of settlement induction assays, the number of settled individuals was counted after 12 h in experimental and control batches.

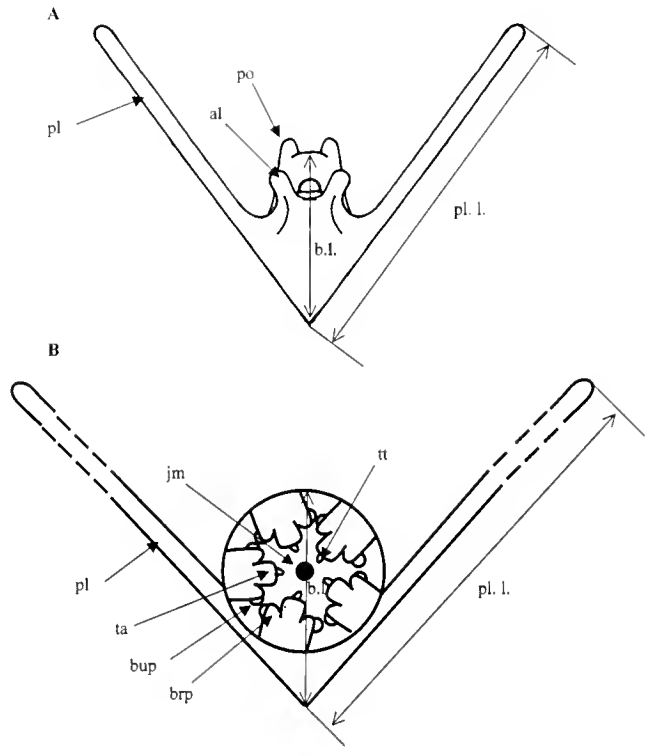

Figure 1. *Ophiothrix fragilis*. Drawing of a 5-day-old larva (A) and a 21-day-old suspended juvenile (B), showing the measurements taken (not to scale). b.l.: body length; pl. l.: posterolateral rod length; al: anterolateral arms; brp: brachial podia; bup: buccal podia; jm: juvenile mouth; pl: posterolateral arm; po: postoral arms; ta: terminal article; tt: terminal tentacle.

Results

Larval development

Table 1 gives the chronology of development of *Ophiothrix fragilis* from fertilization through appearance of settled juveniles. Under our rearing conditions, development was completed in about 21 days. A well-formed oval larva with a vacuolated crest appeared 12 h after fertilization (Fig. 2A). The first pair of arms, the posterolateral ones, appeared after 24 h (Fig. 2B), and on the 3rd day the openings of the mouth and anus marked the start of the exotrophic larval period. The following days were essentially characterized by the acquisition of additional arms : the anterolateral, postoral and postdorsal pair (Fig. 2D–G). From the 13th day, the left hydrocoele, visible by transparency, started to differentiate five lobes whose development was completed 2 days later, marking the onset of metamorphosis (Fig. 2H). Metamorphosis was initiated when the complete five-lobed hydrocoele began to encircle the esophagus and the so-called ophiurid rudiment began to appear. The larval arms, except the posterolaterals and their respective skeletal rods, started to regress (Fig. 2I, J). Rod regression occurred parallel to the development of juvenile skeletal plates (Fig. 2J). The larval esophagus and intestine regressed in turn, and the larva then entered an endotrophic period, being deprived of both mouth and anus. While endotrophic, the larva progressively became pentameric with the appearance at the rudiment level of radial and interradial areas and the differentiation of five (radial) terminal articles and tentacles. The opening of the juvenile mouth soon followed, and the rudiment continued to develop; in each radius a first pair of ambulacral podia and a pair of buccal podia formed (Fig. 2K, and Fig. 1B for schematic representation). Twenty-one days after fertilization, the resulting suspended juveniles had five podia in each radius and tended to sink to the bottom of the rearing tanks. This event was soon followed by the loss of the remaining pair of larval arms and settlement of the juveniles on the bottom of the tanks. Settled juveniles have a pair of hooked spines on the penultimate arm segment of each radius (see Morgan and Jangoux, 2004).

Table 1

Ophiothrix fragilis: *Chronology of major developmental stages and events*

Developmental stages and events	Time after fertilization (days)	
	Present study	McBride (1907)
Gastrula	0.5	0.5
2-arm endotrophic pluteus	1	1
4-arm exotrophic pluteus	3	3
6-arm exotrophic pluteus	3	4
8-arm exotrophic pluteus	7	7–10
Fully developed 8-arm pluteus	12	ND
Development of 5 lobes of hydrocoele	13	ND
5-lobed hydrocoele complete	16	16–20
Initiation of metamorphosis	16	20–23
Regression of larval mouth and anus	18	ND
Development of terminal tentacles	18	ND
Development of brachial and buccal podia	19	ND
Apparition of juvenile mouth	19	ND
Suspended juvenile (settlement stage)	21	ND
Benthic juvenile (with hooked spines)	22	26

ND, not determined.

Larval growth

The length of the longest posterolateral rod, the body length, and their ratio were followed during development. Growth of the posterolateral rod was accelerated during the first couple of days following the embryonic period (Fig. 3A). Growth then slowed down, with a gain of about 300 μm (mean: 279.04 μm; SD: 71.59 μm) between the 3rd and 11th day; it then picked up again, with a gain of 900 μm (mean: 887.91 μm; SD: 111.06 μm) between the 11th and 19th day (Fig. 3A). The posterolateral rod did not stop growing during metamorphosis, from the 16th day onward, but slowed down once it had ended.

Growth of the body was slow during the first couple of days following the embryonic period (Fig. 3B). A slow but constant increase in body length then took place, with a gain of 100 μm (mean: 103.07 μm; SD: 17.51 μm) between the 3rd and 13th day (Fig. 3B). During the differentiation of the five lobes of the left hydrocoele, growth of the body increased. The larval body grew by 70 μm (mean: 72.1 μm; SD: 25.79 μm) in 2 days. Formation of the rudiment provoked a reorganization of the body, with a decrease of 50 μm (mean: 49.47 μm; SD: 23.5 μm).

During the embryonic period, preferential growth of the posterolateral rods took place and the arm-to-body ratio increased sharply (from 1.2 to 2.8), showing allometric growth (Fig. 3C). Growth then became isometric, with the arm-to-body ratio stabilizing around 3 until the 11th day (Fig. 3C). At that point the ratio increased once again showing preferential growth of the arms; by the 15th day, at the onset of metamorphosis, the ratio exceeded 4. During metamorphosis, the decrease in the length of the body and

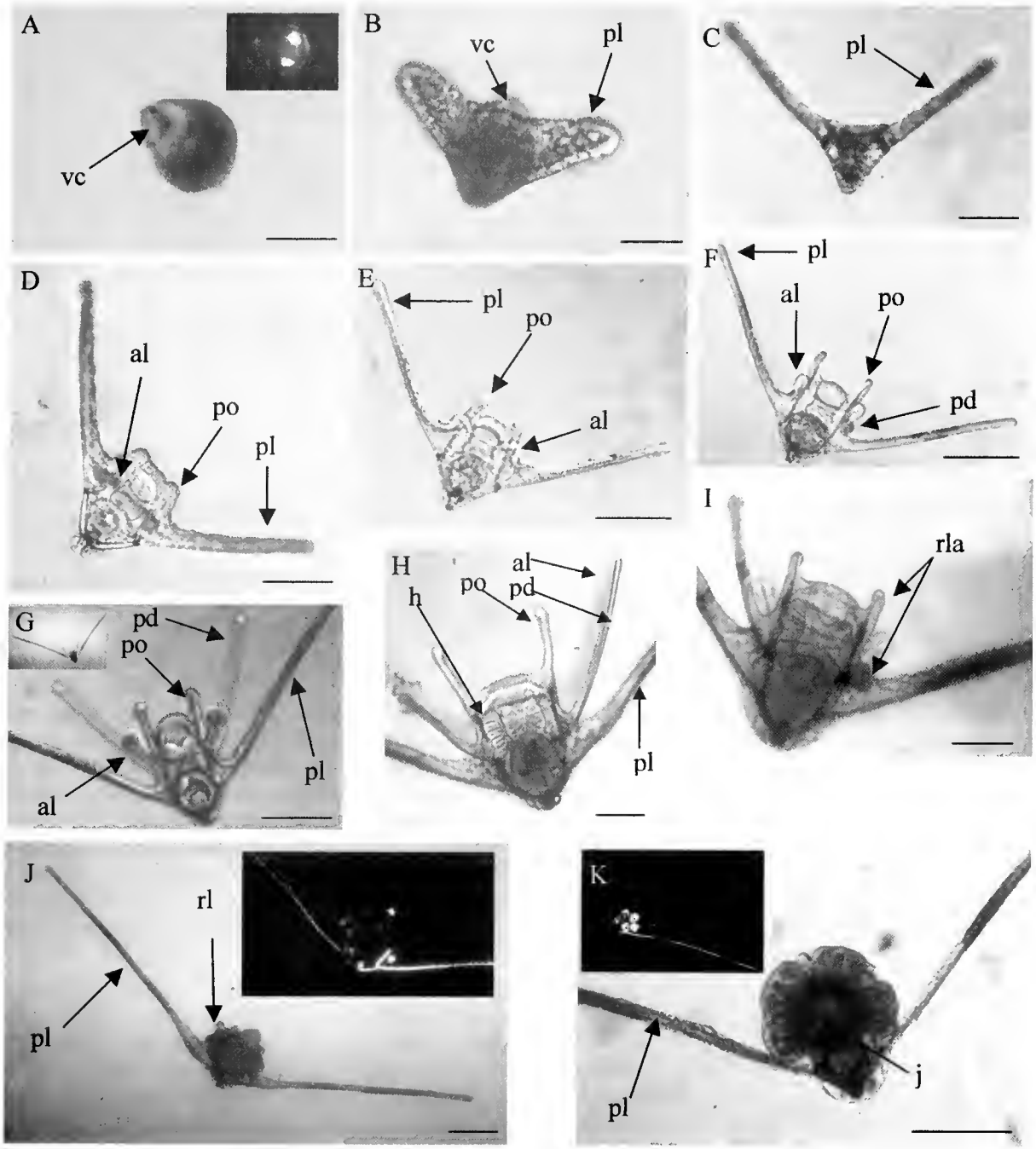

Figure 2. *Ophiothrix fragilis.* Larval development. (A) 12-hour-old larva (inset shows developing larval skeleton); (B) 24-hour-old larva (2-arm endotrophic pluteus); (C) 2-day-old larva (2-arm endotrophic pluteus); (D) 3-day-old larva (6-arm exotrophic pluteus); (E) 5-day-old larva (6-arm exotrophic pluteus); (F) 7-day-old larva (8-arm exotrophic pluteus); (G) 11-day-old larva (inset shows a general view of the 8-arm exotrophic pluteus); (H) 15-day-old larva; (I) 16-day-old larva (metamorphic larva); (J) 19-day-old individual (suspended prejuvenile) (inset shows the regression of the larval skeleton [except for the posterolateral rods] and the developing juvenile skeletal plates); (K) 21-day-old individual at the settlement stage (inset shows the complete juvenile skeleton and the remaining posterolateral rods). al: anterolateral arms; h: hydrocoele; j: juvenile; pd: postdorsal arms; pl: posterolateral arms; po: postoral arms; rla: regressing larval arms (also rl in part J); vc: vacuolated crest. Scale bars: 50 μm (A); 100 μm (B, C, F, G, H, I); 200 μm (D, J, K).

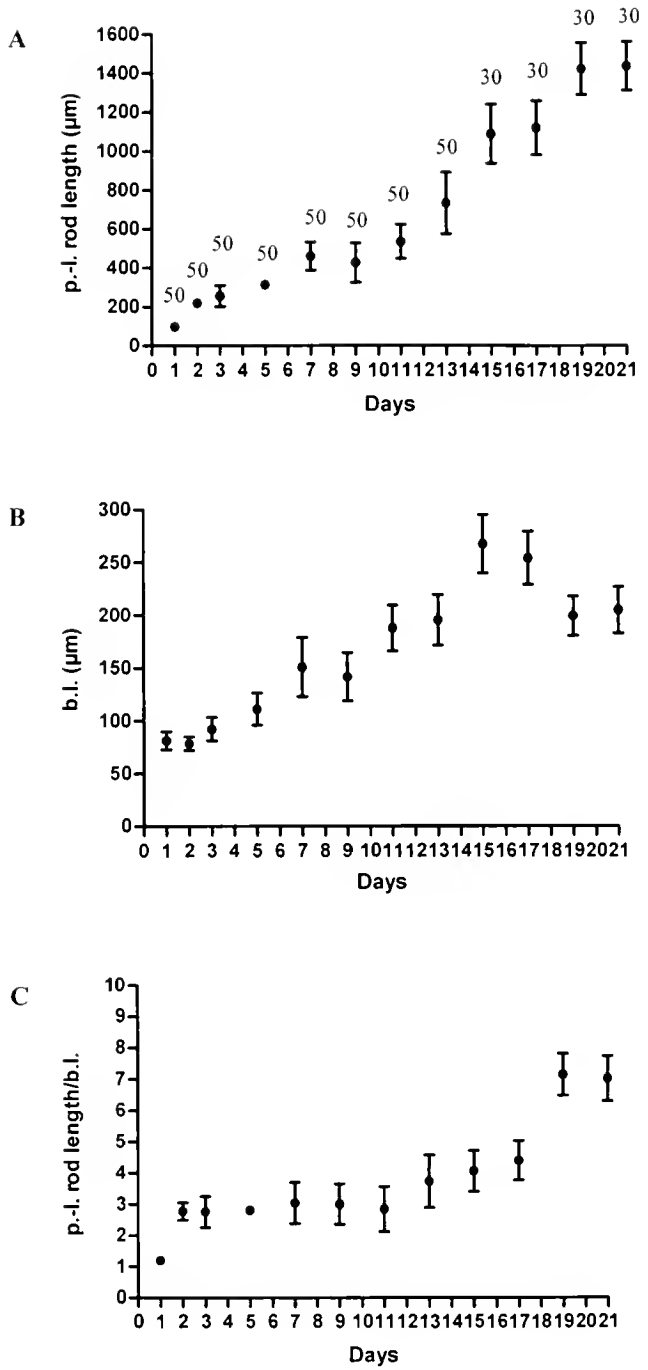

Figure 3. *Ophiothrix fragilis.* (A) Posterolateral rod growth, (B) body length growth, and (C) ratio of posterolateral rod length to body length during development. b.l.: body length; p.-l. rod length: posterolateral rod length. Values of n (number of individuals measured) for A to C are indicated in A. Bars are standard deviations.

increase in the length of the posterolateral rod further accentuated the arm-to-body ratio, which increased from 4 to 7. The arm-to-body ratio stabilized once metamorphosis was complete (Fig. 3C).

Induction of metamorphosis and settlement

The influence of the presence of adults on induction of metamorphosis and settlement was examined at the onset of metamorphosis (larva with a 5-lobed hydrocoele) and the onset of settlement (suspended juveniles), respectively. The presence (experimental) or absence (control) of adult conspecifics did not influence the initiation of metamorphosis: all individuals (n = 180) spontaneously began metamorphosis in the water column. The presence of adult conspecifics did not accelerate metamorphosis: all individuals in the presence of adults (three replicates of 30 larvae) were at the same stage of development as the controls (three replicates of 30 larvae). In the settlement induction assays, about 10% (mean: 11.1% in three replicates of 30 larvae) of suspended juveniles settled spontaneously in the controls; in the presence of adults, 90% (mean: 90% in three replicates of 30 larvae) of suspended juveniles settled.

Discussion

In our rearing conditions, *Ophiothrix fragilis* completed development in 21 days. In MacBride's (1907) study, development took 26 days (Table 1). The difference is probably due to larval nutrition. As a food supply, MacBride (1907) used seawater from the field, which is usually a poorer food source than a laboratory ration enhanced with cultured food. (Paulay *et al.*, 1985; Strathmann *et al.*, 1992).

Growth of the larva of *O. fragilis* is continuous throughout its development and can be divided into three periods. During the first period, when the larva is endotrophic, we observed a faster growth of the posterolateral rods compared to body length. This could be due to development of the feeding organs (ciliated band) before the larva becomes exotrophic. The brief endotrophic period during the first days following fertilization and the faster development of the feeding organs during this time also occurs in other echinoderms (McEdward, 1984; Chia and Walker, 1991; Pearse and Cameron, 1991). The second period is essentially characterized by the acquisition and growth of the three other pairs of larval arms, along with growth of the posterolateral rod and growth in body length so that their ratio remains stable (isometric growth). During the third period, the body and posterolateral rod continue to lengthen, with conspicuous development of the arms. Unfortunately, morphometric comparisons can be done with plutei from echinoids only. McEdward (1984, 1986) has shown in different species of sea urchins an initial rapid increase of the whole larval length (which can be equated to our posterolateral rod length). This is followed by a decrease in the rate of elongation during differentiation of further larval arms and, finally, by an increase in the rate of elongation during rudiment development. McEdward suggested that the addition of new arms and their growth during the later stage helps maintain feeding capability relative to larval body size

and metabolism, which also increase during development, especially during rudiment formation. While this could be what happens in echinoplutei, which do not lose their ability to feed during rudiment differentiation, in ophioplutei the future juvenile (or rudiment) is formed from the larval body and the larva passes through a second endotrophic period during which the juvenile digestive tract differentiates. Therefore, the posterolateral arms would essentially be used as locomotory organs and not as feeding-locomotory organs as in echinoids (McEdward, 1984, 1986). As the juvenile differentiates so do its skeletal plates, which would probably increase its weight and make it sink. Although active movement downward probably also occurs, the increase in growth rate of the posterolateral rods could help compensate for the reduction of the other larval arms during metamorphosis, thus allowing the developing juvenile to remain in the plankton.

Metamorphosis in type I developers has been studied in the past by MacBride (1907) on *Ophiothrix fragilis*, Narasimhamurti (1933) on *Ophiocoma nigra*, Olsen (1942) on *Ophiopholis aculeate*, and Tominaga *et al.* (2004) on *Ophiodaphne formata*. As numerous authors have already established (Burke, 1989; Hendler, 1991; Byrne and Selvakuramaswamy, 2002), metamorphosis begins spontaneously in the water column when the five-lobed hydrocoele starts to encircle the esophagus and the larval arms begin to regress, and ends with the loss of the two remaining posterolateral arms. Therefore, ending of metamorphosis in ophiuroids coincides with the settlement of the fully functional juvenile. Accordingly, a perimetamorphic period, as defined by Gosselin and Jangoux (1998) for echinoids, can be determined. In echinoids the perimetamorphic period starts at larval competence, includes metamorphosis and the endotrophic postlarval development, and stops at the acquisition of juvenile exotrophy. In ophiuroids the perimetamorphic period starts with the initiation of metamorphosis and ends with the settlement of an exotrophic juvenile. So metamorphosis in echinoids is rapid, but the benthic postlarva still needs to develop to become exotrophic; metamorphosis in ophiuroids is gradual, but it ends with a benthic exotrophic juvenile (juvenile mouth open; see Morgan and Jangoux, 2004). We see that, although the pathways to the exotrophic juvenile are different, both rely on a rapid establishment in the benthos.

Although delay of metamorphosis or settlement is known to occur in a number of marine invertebrates (Highsmith and Emlet, 1986; Pechenik, 1990; Vaitilingon *et al.*, 2001), it is not known if it takes place in ophiuroids and, if it does, upon which developmental stage it operates. Although McBride (1907) described a five-lobed hydrocoele appearing after 16–20 days of development in *O. fragilis*, encirclement of the esophagus, and therefore metamorphosis, did not occur until a few days later. This does not fit our observations, in which the encirclement immediately followed the appearance of the five-lobed hydrocoele. Delay could therefore have occurred, not due to the absence of an inducer as in echinoids—since in ophiuroids metamorphosis begins spontaneously—but due to some other factor, such as a shortage of food resources. In type II developers, delayed metamorphosis is also known to occur at this stage (Mladenov, 1985b). Furthermore, Turon *et al.* (2000, p. 204, fig. 1) illustrated a suspended juvenile of *O. fragilis* bearing two extra articles on each arm. Our results have shown that suspended juveniles can settle at a much earlier stage, indicating a probable delay of settlement in Turon's specimen. Delayed settlement has been observed in other species, and some authors consider the suspended juvenile to be an exploratory stage, as the vittelaria is considered to be in type II developers (Stancyk, 1973; Strathmann, 1978; Mladenov, 1979, 1985b). This interpretation would indicate a probable selection of settlement site.

The larvae of many species settle and metamorphose selectively on substrata with specific physical or biological characteristics (Scheltema, 1974; Crisp, 1976; Burke, 1986). Juveniles of *O. fragilis* in the North Sea-English Channel region have been exclusively found on conspecific adults (Warner, 1971; Davoult *et al.*, 1990; Morgan and Jangoux, 2004), whereas juveniles of their Mediterranean counterparts are found gregariously on sponges before moving to the adult habitat where, once growth has taken place, they live solitarily (Turon *et al.*, 2000). This has led many authors to think that the feeding capabilities of juveniles in the first stages of benthic life would need to be enhanced by the suspension-feeding activities of other organisms (Warner, 1971; Turon *et al.*, 2000, Morgan and Jangoux, 2004). Survival of the juveniles therefore depends on finding a suitable settlement site.

In ophiuroids, metamorphosis begins spontaneously in the plankton. However, loss of the two posterolateral rods and settlement, although it can also happen spontaneously, is clearly enhanced in *O. fragilis* by the presence of adult conspecifics. This is the first case in which an actual induction of settlement has been revealed in ophiuroids. Contact between the settlement stage and the adult is not necessary to induce the breakage of the posterolateral rods. Loss of their posterolateral rods in proximity to an *Ophiothrix fragilis* bed would ensure that the juveniles settle on a suitable site. Furthermore, the hooked spines on juveniles that have lost their posterolateral rods would help them cling to the adults (Morgan and Jangoux, 2004). While our experimental setup has shown that the proximity of an adult conspecific can induce settlement, we still do not know whether juveniles at the settlement stage need to be close to a conspecific adult or can detect them from farther away. MacBride (1907) noted that when larvae in the plankton were reaching the end of their metamorphosis, they sank lower in the water. We also observed this in our cultures.

Juveniles that lose their posterolateral rods spontaneously

will rain down on the available substrata. If it is unsuitable, heavy mortalities would supposedly occur. However, resuspension, drifting, and recolonization following settlement has been demonstrated in some ophiuroids (Hendler *et al.*, 1999). Turon *et al.* (2000) have postulated that recolonization through resuspension could contribute to the mass recruitment of *O. fragilis* juveniles on sponges in the Mediterranean. It could also be that suspended juveniles are induced to settle by some cue released by the sponges, and further studies need to be made along that line.

Induction of loss of the two posterolateral rods and settlement implies the recognition of an inducer. In echinoids, the primary podia are used to test the substrata before metamorphosis (Burke, 1980; Gosselin and Jangoux, 1998). Nothing is known of the sensory structures involved during settlement in ophiuroids, but Morgan and Jangoux (2004) have demonstrated the role that the terminal tentacles of settled juveniles of *O. fragilis* play in the recognition of adult conspecifics at a distance. These organs are already present in suspended juveniles and could therefore be implicated in their recognition of adult conspecifics and in the induction of settlement.

Acknowledgments

We are grateful to two anonymous referees for constructive comments. Our thanks go to B. Blockmans, Ph. Pernet, and D. Gillan for help during scuba diving missions. R. Morgan is a recipient of an F.R.I.A. grant and a grant from the David and Alice Van Buuren foundation. This is a contribution to the CIBIM (Centre Interuniversitaire de Biologie Marine).

Literature Cited

Allen, E. J. 1899. On the fauna and bottom-deposits near the thirty fathom line from the Eddystone grounds to Start Point. *J. Mar. Biol. Assoc. UK* **5:** 365–542.

Burke, R. D. 1980. Podial sensory receptors and the induction of metamorphosis in echinoids. *J. Exp. Mar. Biol. Ecol.* **47:** 223–234.

Burke, R. D. 1986. Pheromones and the gregarious settlement of marine invertebrate larvae. *Bull. Mar. Sci.* **39:** 323–331.

Burke, R. D. 1989. Echinoderm metamorphosis: comparative aspects of the change in form. Pp. 81–108 in *Echinoderm Biology*, Vol. 3, J. M. Lawrence and M. Jangoux, eds. A. A. Balkema, Rotterdam.

Byrne, M., and P. Selvakumaraswamy. 2002. Phylum Echinodermata: Ophiuroidea. Pp. 483–498 in *Atlas of Marine Invertebrate Larvae*, C. M. Young, ed. Academic Press, London.

Chia, F. S., and C. W. Walker. 1991. Echinodermata: Asteroidea. Pp. 301–353 in *Reproduction of Marine Invertebrates, Vol. VI, Echinoderms and Lophophorates*, A. C. Giese, J. J. Pearse, and V.B. Pearse, eds. Boxwood Press, Pacific Grove, CA.

Crisp, D. J. 1976. Settlement responses of marine organisms. Pp. 83–124 in *Adaptations to Environment*, R. C. Newell, ed. Butterworths, London.

Davoult, D., F. Gounin, and A. Richard. 1990. Dynamique et reproduction de la population d'*Ophiothrix fragilis* (Abildgaard) du détroit du Pas de Calais (Manche Orientale). *J. Exp. Mar. Biol. Ecol.* **138:** 201–216.

Gosselin, P., and M. Jangoux. 1998. From competent larva to exotrophic juvenile: a morphofunctional study of the perimetamorphic period of *Paracentrotus lividus* (Echinodermata, Echinoida). *Zoomorphology* **118:** 31–43.

Hendler, G. 1991. Echinodermata: Ophiuroidea. Pp. 355–511 in *Reproduction of Marine Invertebrates, Vol. VI, Echinoderms and Lophophorates*, A. C. Giese, J. J. Pearse, and V. B. Pearse, eds. Boxwood Press, Pacific Grove, CA.

Hendler, G., C. C. Baldwin, D. G. Smith, and C. E. Thacker. 1999. Planktonic dispersal of juvenile brittle stars (Echinodermata: Ophiuroidea) on a Caribbean reef. *Bull. Mar. Sci.* **65:** 283–288.

Highsmith, R. C., and R. B. Emlet. 1986. Delayed metamorphosis: effect on growth and survival of juveniles sand dollars (Echinoidea: Clypeasteroida). *Bull. Mar. Sci.* **39:** 347–361.

Holme, N. A. 1984. Fluctuations of *Ophiothrix fragilis* in the western English Channel. *J. Mar. Biol. Assoc. UK* **64:** 351–378.

MacBride, E. W. 1907. The development of *Ophiothrix fragilis*. *Q. J. Microsc. Sci.* **51:** 557–606.

McEdward, L. R. 1984. Morphometric and metabolic analysis of the growth and form of an echinopluteus. *J. Exp. Mar. Biol. Ecol.* **82:** 259–287.

McEdward, L. R. 1986. Comparative morphometrics of echinoderm larvae. II. Larval size, shape, growth, and the scaling of feeding and metabolism in echinoplutei. *J. Exp. Mar. Biol. Ecol.* **96:** 267–286.

McEdward, L. R., and J. C. Herrera. 1999. Body form and skeletal morphometrics during larval development of the sea urchin *Lytechinus variegatus* Lamarck. *J. Exp. Mar. Biol. Ecol.* **232:** 151–176.

Mladenov, P. V. 1979. Unusual lecithotrophic development of the Caribbean brittle star *Ophiothrix oerstedi*. *Mar. Biol.* **55:** 55–62.

Mladenov, P. V. 1985a. Observations on reproduction and development of the Caribbean brittle star *Ophiothrix suensoni* (Echinodermata: Ophiuroidea). *Bull. Mar. Sci.* **36:** 384–388.

Mladenov, P. V. 1985b. Development and metamorphosis of the brittle star *Ophiocoma pumila*: evolutionary and ecological implications. *Biol. Bull.* **168:** 285–295.

Morgan, R., and M. Jangoux. 2002. Reproductive cycle and spawning induction in the gregarious brittle-star *Ophiothrix fragilis* (Echinodermata) in the Oosterschelde (Netherlands). *Invertebr. Reprod. Dev.* **42:** 145–155.

Morgan, R., and M. Jangoux. 2004. Juvenile-adult relationship in the gregarious ophiuroid *Ophiothrix fragilis* (Echinodermata): a behavioural and morphological study. *Mar. Biol.* **145:** 265–276.

Narasimhamurti, N. 1933. The development of *Ophiocoma nigra*. *Q. J. Microsc. Sci.* **76:** 63–88.

Olsen, H. 1942. The development of the brittle-star *Ophiopholis aculeata* (O. Fr. Muller). *Bergens Mus. Arbok. Naturvid.* **6:** 1–107.

Paulay, G., L. Boring, and R. R. Strathmann. 1985. Food limited growth and development of larvae: experiments with natural sea water. *J. Exp. Mar. Biol. Ecol.* **93:** 1–10.

Pearse, J. S., and R. A. Cameron. 1991. Echinodermata: Echinoidea. Pp. 513–662 in *Reproduction of Marine Invertebrates, Vol. VI, Echinoderms and Lophophorates*, A. C. Giese, J. J. Pearse, and V. B. Pearse, eds. Boxwood Press, Pacific Grove, CA.

Pechenik, J. A. 1990. Delayed metamorphosis by larvae of benthic marine invertebrates: does it occur? Is there a price to pay? *Ophelia* **32:** 63–94.

Scheltema, R. S. 1974. Biological interactions determining larval settlement of marine invertebrates. *Thalassia Jugosl.* **10:** 263–296.

Stancyk, S. E. 1973. Development of *Ophiolepsis elegans* (Echinodermata: Ophiuroidea) and its implications in the estuarine environment. *Mar. Biol.* **21:** 7–12.

Strathmann, R. S. 1978. Length of pelagic period in echinoderms with feeding larvae from the Northeast Pacific. *J. Exp. Mar. Biol. Ecol.* **34:** 23–27.

Strathmann, R. R., L. Fenaux, and M. F. Strathmann. 1992. Heterochronic developmental plasticity in larval sea urchins and its implications for evolution of nonfeeding larvae. *Evolution* **46:** 972–986.

Tominaga, H., S. Nakamura, and M. Komatsu. 2004. Reproduction and development of the conspicuously dimorphic brittle star *Ophiodaphne formata* (Ophiuroidea). *Biol. Bull* **206:** 25–34.

Turon, X., M. Codina, I. Tarjuelo, M. J. Uriz, and M. A. Becerro. 2000. Mass recruitment of *Ophiothrix fragilis* on sponges: settlement patterns and post-settlement dynamics. *Mar. Ecol. Prog. Ser.* **200:** 201–212.

Vaitilingon, D., R. Morgan, Ph. Grosjean, P. Gosselin, and M. Jangoux. 2001. Effect of delayed metamorphosis and food rations on the perimetamorphic events in the echinoid *Paracentrotus lividus* (Lamarck, 1816) (Echinodermata). *J. Exp. Mar. Biol. Ecol.* **262:** 41–60.

Warner, G. F. 1970. Brittle-star beds in Torbay, Devon. *Underwater Association Report* **1969:** 81–85.

Warner, G. F. 1971. On the ecology of a dense bed of the brittle-star *Ophiothrix fragilis*. *J. Mar. Biol. Assoc. UK* **51:** 267–282.

Reference: *Biol. Bull.* **208:** 100–113. (April 2005)

Changes in Tissue Biochemical Composition and Energy Reserves Associated With Sexual Maturation in the Ommastrephid Squids *Illex coindetii* and *Todaropsis eblanae*

R. ROSA[1,*], P. R. COSTA[2], N. BANDARRA[1], AND M. L. NUNES[1]

[1] *Departamento de Inovação Tecnológica e Valorização dos Produtos da Pesca, IPIMAR, Avenida de Brasília, 1449-006 Lisboa, Portugal; and* [2] *Departamento de Ambiente Aquático, IPIMAR, Avenida de Brasília, 1449-006 Lisboa, Portugal*

Abstract. The aim of this study was to investigate the biochemical changes that occur during sexual maturation of the squids *Illex coindetii* and *Todaropsis eblanae*. In both species, amino acids and protein content increased in the gonad throughout maturation, but the allocation of these nitrogen compounds from the digestive gland and muscle was not evident. A significant ($P < 0.05$) increase in the content of lipids and fatty acids was observed in the gonad and digestive gland. It seems that both species take energy for egg production directly from food, rather than from stored products. Analyses for cholesterol revealed a significant ($P < 0.05$) increase in the gonad, and the lipid content differences between species are potentially related to different feeding ecologies. The glycogen reserves in the gonad increased significantly ($P < 0.05$), suggesting that glycogen has an important role in the maturation process. It was evident that sexual maturation had a significant effect upon the gonad energy content, but because the energy variation in the digestive gland and muscle was nonsignificant ($P > 0.05$), there was no evidence that storage reserves are transferred from tissue to tissue.

Introduction

Illex coindetii (Vérany, 1839) and *Todaropsis eblanae* (Ball, 1841) are neritic ommastrephid squids that are caught near the bottom on the continental shelf and slope of the Atlantic Ocean, where they are voracious opportunistic predators and important members of food webs (Clarke, 1966). Though these cephalopod species are commercially important by-catches of commercial demersal trawls in the east Atlantic (Lordan *et al.*, 1998; Robin *et al.*, 2002), several aspects of the biology and ecology remain poorly studied, including the reproductive biology (Laptikhovsky and Nigmatullin, 1999; Hernández-García, 2002). However, according to Rocha *et al.* (2001), both these squids seem to have an intermittent terminal spawning; *i.e.*, the spawning is monocyclic and eggs are laid in separate batches during the relatively long spawning period. According to Calow (1973), terminal spawning species (semelparous strategy) invest more in their single spawning event than do multiple spawning species. In fact, the complete dedication of energy to reproduction results in a terminal spawning event; in contrast, a partial cost both before and during reproduction allows individuals to spawn repeatedly throughout their adult life. Moreover, the reproductive strategy exhibited by a species is inextricably linked to its source of reproductive energy (feeding or storage) (Jackson *et al.*, 2004).

Sexual maturation and reproduction influence the status of a number of physiological processes and consequently the animal's ecology and behavior. Clarification of the energy storage and consumption patterns of these squids will shed light on the interaction between organism and environment. Cephalopods have a protein-based metabolism (Lee, 1994), and the direct use of protein as an energy reserve may account for the lack of major reserves of glycogen and lipid in cephalopod tissues (O'Dor *et al.*, 1984; Storey and Storey, 1983). The lipids in the digestive gland have also been hypothesized to be possible substrates

Received 20 July 2004; accepted 30 November 2004.

* To whom correspondence should be addressed. E-mail: rrosa@ipimar.pt

and a site for energy storage in cephalopods (O'Dor and Webber, 1986; O'Dor and Wells, 1978; Moltschaniwskyj and Semmens, 2000).

Here, we focus on the changes in biochemical composition that take place in the gonad, digestive gland, and muscle of *Illex coindetii* and *Todaropsis eblanae* during sexual maturation. Specifically, we examine the content of lipid, glycogen, cholesterol, and energy in these tissues, as well as the profiles of total amino acid and fatty acid.

Materials and Methods

Samples

Specimens of *Illex coindetii* and *Todaropsis eblanae* were collected off the Portuguese west coast (Peniche) by commercial trawlers and off the south coast (Algarve) on several cruises aboard the R/V *Noruega* and R/V *Capricórnio* of Instituto de Investigação das Pescas e do Mar (IPIMAR) in February, March, April, and June of 2002. For each animal, the following parameters were recorded: mantle length, total weight, gonad weight, digestive gland (also called "liver" in some biochemical literature) weight, and depth range of catch (Table 1). For both species, maturity stages were determined following Lipinski (1979), and the specimens were classified as immature (stages 1 and 2) or mature (stage 5). Gonadosomatic index (GSI—gonad wet weight/body wet weight, ×100) and digestive gland index (DgI—digestive gland weight/ body wet weight, ×100) were also determined. Each of the tissue types collected (gonad, digestive gland, and muscle) were pooled, after freeze-drying in a Savant VP100®. The biochemical analyses were performed in triplicate in these tissues.

Protein and amino acid analyses

Protein concentration was determined (with 100 mg of wet tissue) on the washed TCA precipitate solubilized in 1*M* sodium hydroxide (NaOH) for 24 h as described by Lowry *et al.* (1951), using the Bio-Rad protein assay (BIO-RAD). Bovine gamma globulin (BIO-RAD) was used as a standard.

To determinate the total amino acid profile, proteins were hydrolyzed with 6 N hydrochloric acid (containing 0.1% phenol) in a MLS-1200 Mega Microwave System (Milestone), at 800 W, 160 °C for 10 min. The hydrolysis was performed under inert and anaerobic conditions to prevent oxidative degradation of amino acids. The hydrolysates were filtered and dissolved in sodium citrate buffer, pH 2.2. Amino acids were separated by ion exchange liquid chromatography in an automatic analyzer Biochrom 20 (Amersham Biosciences), equipped with a column filled with a polysulfonated resin (250 × 4.6 mm), using three sodium citrate buffers—pH 3.20, 4.25, and 6.45 (Amersham Biosciences)—and three temperatures (50 °C, 58 °C, and 95 °C). The detection of amino acids was done at 440 nm and 570 nm after reaction with ninhydrin (Amersham Biosciences). Amino acids were identified by comparison of their retention time with those of specific standards (Sigma) and quantified with the software EZChrom Chromatography Data System, vers. 6.7 (Scientific Software Inc.) using norleucine (Sigma) as internal standard.

Total lipids and fatty acid analyses

Total lipids were extracted by the method of Bligh and Dyer (1959). The fatty acid profile was determined using the experimental procedure of Lepage and Roy (1986) as modified by Cohen *et al.* (1988). The fatty acid methyl esters were analyzed in a Varian 3400 gas chromatograph equipped with an auto-sampler and fitted with a flame ionization detector. The separation was carried out with helium as carrier gas in a fused silica capillary column Chrompack CPSil/88 (50 m × 0.32 mm id), programmed from 180 °C to 200 °C at 4 °C min^{-1}, held for 10 min at 200 °C, and heated to 210 °C for 14.5 min, with a detector at 250 °C. A split injector (100:1) at 250 °C was used. Fatty acid

Table 1

Summary of biological data for Illex coindetti *and* Todaropsis eblanae

Species	Sex	Maturation stage	*n*	ML (mm)	TW (g)	GW (g)	DgW (g)	GSI	HSI	Collection depth range (m)
Illex coindetii	Males	Immature	17	104.12 ± 9.08	31.30 ± 8.19	0.64 ± 0.40	1.42 ± 0.49	2.04 ± 1.25	4.56 ± 0.99	30–520
		Mature	14	132.00 ± 6.78	89.50 ± 23.60	4.25 ± 0.72	4.18 ± 1.16	4.86 ± 0.59	4.75 ± 0.91	30–520
	Females	Immature	18	117.76 ± 18.43	40.51 ± 18.79	0.31 ± 0.12	2.04 ± 1.30	2.41 ± 0.33	4.85 ± 1.20	50–500
		Mature	12	184.50 ± 26.73	199.71 ± 60.53	30.56 ± 3.43	12.70 ± 1.98	11.42 ± 0.60	4.72 ± 0.17	50–500
Todaropsis eblanae	Males	Immature	14	98.04 ± 13.87	82.20 ± 39.73	3.70 ± 2.60	4.81 ± 2.82	3.94 ± 1.24	5.90 ± 2.88	80–520
		Mature	11	127.30 ± 16.44	124.57 ± 17.06	6.81 ± 1.43	5.61 ± 2.89	5.53 ± 1.20	4.44 ± 2.16	80–520
	Females	Immature	10	96.12 ± 18.49	73.39 ± 39.89	0.33 ± 0.41	3.81 ± 1.93	0.34 ± 0.22	5.91 ± 2.60	80–520
		Mature	8	166.63 ± 18.21	290.32 ± 89.30	18.67 ± 8.89	20.45 ± 6.81	5.74 ± 2.13	6.43 ± 0.72	80–520

Abbreviations: *n*, number of individuals; ML, mantle length; TW, total weight; GW, gonad weight; DgW, digestive gland weight; GSI, gonadosomatic index; HIS, hepatosomatic index.

methyl esters were identified by comparing their retention times with those of chromatographic Sigma standards. Peak areas were determined using the Varian software.

Cholesterol analyses

The quantification of cholesterol content was based on the experimental procedure of Naemmi *et al.* (1995) as modified by Oehlenschläger (2000). The cholesterol was analyzed in a Hewlett Packard 5890 gas chromatograph. The separation was carried out with helium as carrier gas in an HP5 column (30 m × 0.5 mm id). The temperatures of the oven, injector, and detector were 280 °C, 285 °C, and 300 °C, respectively. Cholesterol was identified and quantified by comparison with standards (Sigma) from which a standard curve was prepared.

Glycogen analysis and bioenergetic calculation

Glycogen concentrations were determined according to the method described by Viles and Silverman (1949). Tissue samples were boiled with 1 ml of 33% potassium hydroxide for 15 min. After cooling, 50 μl of a saturate sodium sulfate solution and 2 ml of 96% ethanol were added. Samples were placed in an ice bath for precipitation (~30 min). Following centrifugation, the precipitate was dissolved in 0.5 ml of distilled water, again precipitated with 1 ml of ethanol, and redissolved in 0.4 ml of distilled water. Glycogen was then measured by the anthrone-reagent method (72 ml of concentrated sulfuric acid was added to 28 ml of distilled water, 0.05 g of anthrone, and 0.05 g of thiourea; the mixture was heated at 90 °C for 20 min) and the absorbance read at 620 nm. A calibration curve was prepared with a glycogen (Sigma) standard.

The energy content was estimated according to Winberg (1971), using factors of 12.6, 12.1, and 39.3 J mg^{-1} for protein, carbohydrate, and lipid, respectively. It is worth noting that the carbohydrate fraction was underestimated since it included only the glycogen content.

Statistical analysis

Data were analyzed using an ANOVA. Previously, normality and homogeneity of variances were verified by Kolmogorov-Smirnov and Bartlett tests, respectively. Having demonstrated a significant difference somewhere among the groups with ANOVA, we applied the Tukey test to find out where those differences were (Zar, 1996).

Results

Biological data

The mean mantle length, total weight, gonadosomatic index, and digestive gland index of *Illex coindetii* and *Todaropsis eblanae* are shown in Table 1. The gonadosomatic index increased through the oogenesis and spermatogenesis of both the species, but the digestive gland index showed an unclear variation trend.

Protein and amino acid content

The protein content in the gonad, digestive gland, and muscle of *Illex coindetii* and *Todaropsis eblanae* is presented in Figure 1. Both species showed an increase of these nitrogen compounds in the gonad throughout sexual maturation, the highest values being obtained during oogenesis

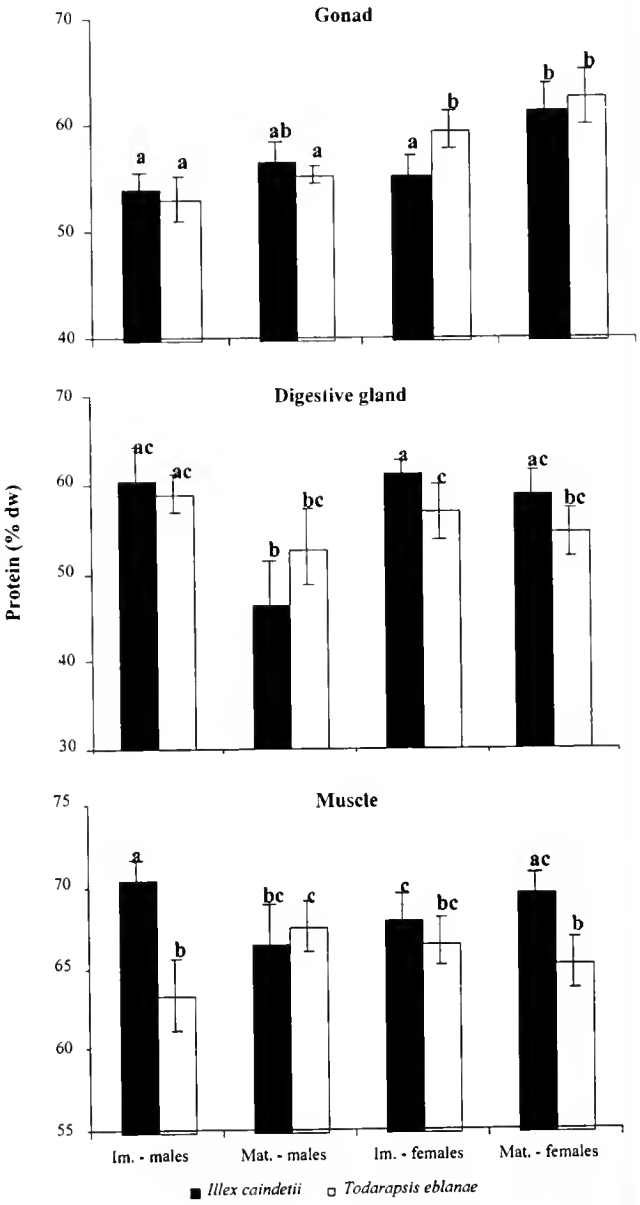

Figure 1. Protein content (% dry weight) in the gonad, digestive gland, and muscle of *Illex coindetii* and *Todaropsis eblanae* males and females at different stages of gonad development. Means ± SD with different letters represent significant differences ($P < 0.05$). Im. immature; Mat. mature.

(from 55.26% to 61.54% dry weight in *I. coindetii* and from 59.64% to 62.69% dryweight in *T. eblanae*) ($F_{7,16}$ = 11.23, Tukey test $P < 0.05$). The amino acid analyses corroborated these findings. The total (protein bound + free) amino acid composition in the gonad is shown in Appendix Table 1. The major essential amino acids were arginine, leucine, and lysine. The major nonessential amino acids were glutamic acid, aspartic acid, and alanine. In the digestive gland, the protein content decreased significantly only during spermatogenesis of *I. coindetii* ($F_{7,16}$ = 24.39, Tukey test $P <$ 0.05). The major essential amino acids were also arginine, leucine, and lysine; the major nonessential amino acids were glutamic acid, aspartic acid, and alanine (Appendix Table 2). In the muscle, both protein and amino acid analyses revealed an unclear variation throughout the maturation process of both species. The major essential and nonessential amino acids in the muscle were the same found in gonad and digestive gland (Appendix Table 3).

Lipid and fatty acid content

The lipid contents in the gonad, digestive gland, and muscle of *Illex coindetii* and *Todaropsis eblanae* are shown in Figure 2. A significant increasing trend was observed in the gonad during the maturation of both species (mainly during oogenesis), and between species, higher values were always attained in males and females of *T. eblanae* ($F_{7,16}$ = 32.22, Tukey test $P < 0.05$). Similar results were obtained with the fatty acid analyses (Appendix Table 4). Most of the saturated fatty acid content was represented by 16:0 and 18:0, monounsaturated fatty acid content by 18:1 and 20:1, and polyunsaturated fatty acid content as arachidonic acid (20:4n-6), eicosapentaenoic acid (20:5n-3), and docosahexaenoic acid (22:6n-3). Between the different tissues analyzed, the highest lipid and fatty acid levels were obtained in the digestive gland and the lowest in the muscle. In the digestive gland, a significant increase in the lipid (Fig. 2) and fatty acid (Appendix Table 5) content was observed during maturation, primarily during oogenesis (lipids and fatty acids: $F_{7,16}$ = 21.79 and 29.67, Tukey test $P <$ 0.05). In the muscle, the lipid content showed an unclear trend during maturation (Fig. 2) and, as in the other tissues, the major fatty acids in the muscle were 16:0, 18:0, 18:1, 20:1, 20:4n-6, 20:5n-3, and 22:6n-3 (Appendix Table 6).

Cholesterol, glycogen, and energy content

The cholesterol content in the gonad, digestive gland, and muscle of *Illex coindetii* and *Todaropsis eblanae* is shown in Figure 3. In the gonad, the differences during sexual maturation were not significant, with the highest values being attained by females. Between species, *T. eblanae* always had the highest values in both sexes ($F_{7,16}$ = 42.36,

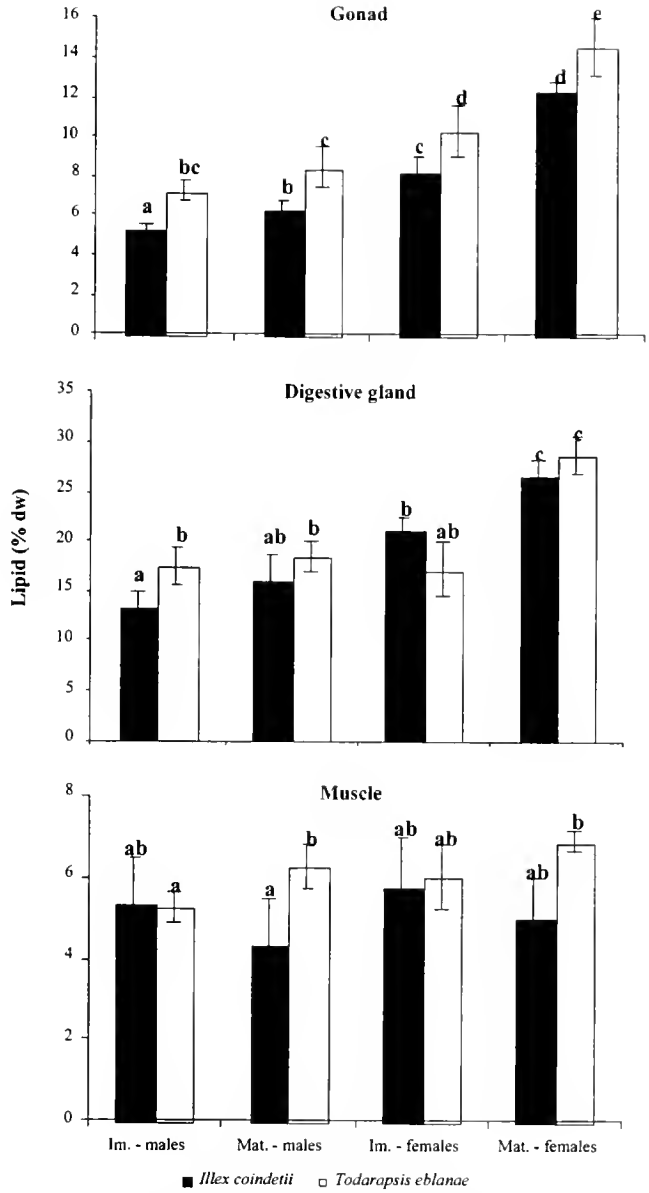

Figure 2. Lipid content (% dry weight) in the gonad, digestive gland, and muscle of *Illex coindetii* and *Todaropsis eblanae* males and females at different stages of gonad development. Means ± SD with different letters represent significant differences ($P < 0.05$). Im, immature; Mat, mature.

Tukey test $P < 0.05$). In the digestive gland, although there were significant differences between immature and mature males of both species, the differences throughout oogenesis were not significant. The muscle presented lower cholesterol values in relation to other tissues and revealed no clear pattern of variation throughout spermatogenesis and oogenesis. The glycogen content in the different tissues of *I. coindetii* and *T. eblanae* is shown in Figure 4. In the gonad, the glycogen content increased during maturation of both species. Trends of variation in the digestive gland and muscle were unclear. The energy content in the gonad,

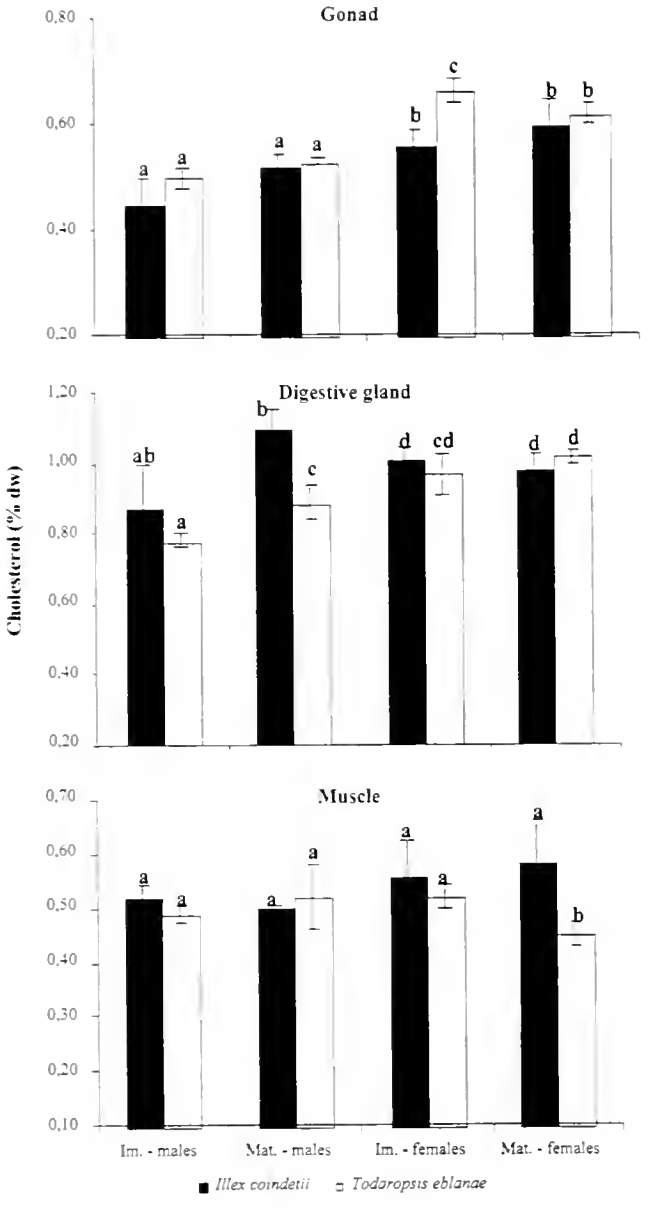

Figure 3. Cholesterol content (% dry weight) in the gonad, digestive gland, and muscle of *Illex coindetii* and *Todaropsis eblanae* males and females at different stages of gonad development. Means ± SD with different letters represent significant differences ($P < 0.05$). Im, immature; Mat, mature.

digestive gland, and muscle of *I. coindetii* and *T. eblanae* is shown in Figure 5. There was a significant increase in the gonad energy content during sexual maturation of both species ($F_{7,16} = 32.36$, Tukey test $P < 0.05$). In the digestive gland, the energy content differences did not seem to be related to sexual maturation ($F_{7,16} = 26.18$, Tukey test $P < 0.05$). In the muscle there was no significant variation between species, sexes, and maturation stages ($F_{7,16} = 2.52$, $P > 0.05$).

Discussion

In the present study, we observed a clear increase in the gonadosomatic index, but there was not a concomitant decrease in the digital gland index, which suggests that the digestive gland resources are not depleted and if resources are mobilized from this organ, then these resources seem to be compensated by those gained from feeding. The digestive gland may continue to accumulate substantial reserves of energy throughout sexual maturation, with no evidence

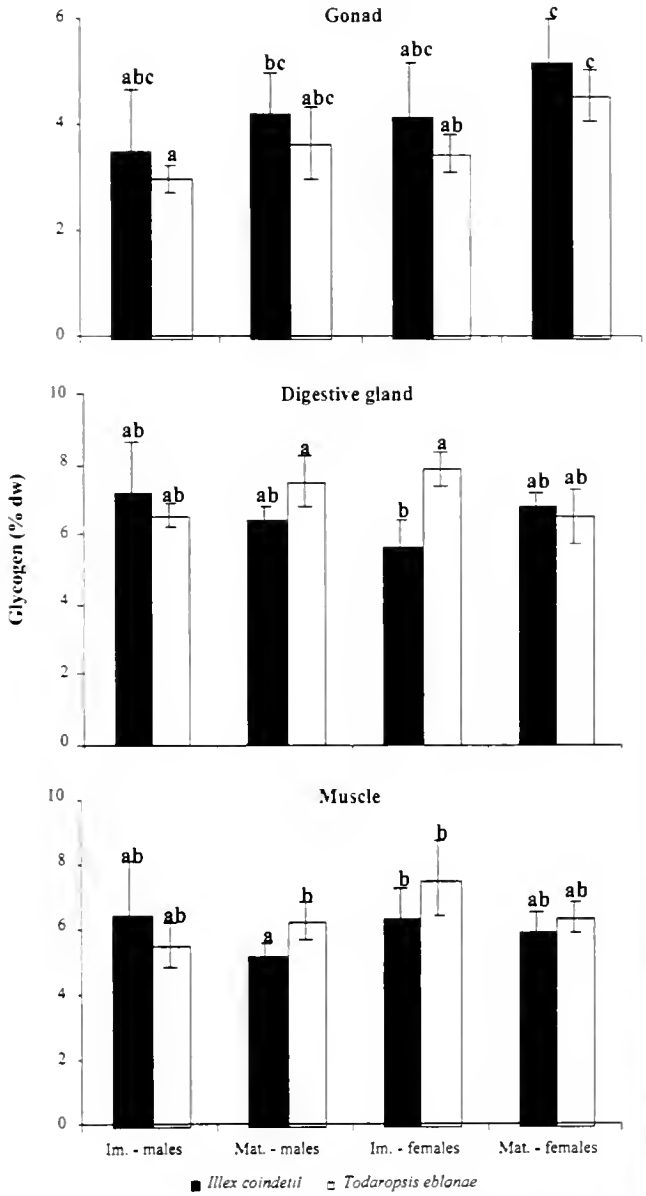

Figure 4. Glycogen content (% dry weight) in the gonad, digestive gland, and muscle of *Illex coindetii* and *Todaropsis eblanae* males and females at different stages of gonad development. Means ± SD with different letters represent significant differences ($P < 0.05$). Im, immature; Mat, mature.

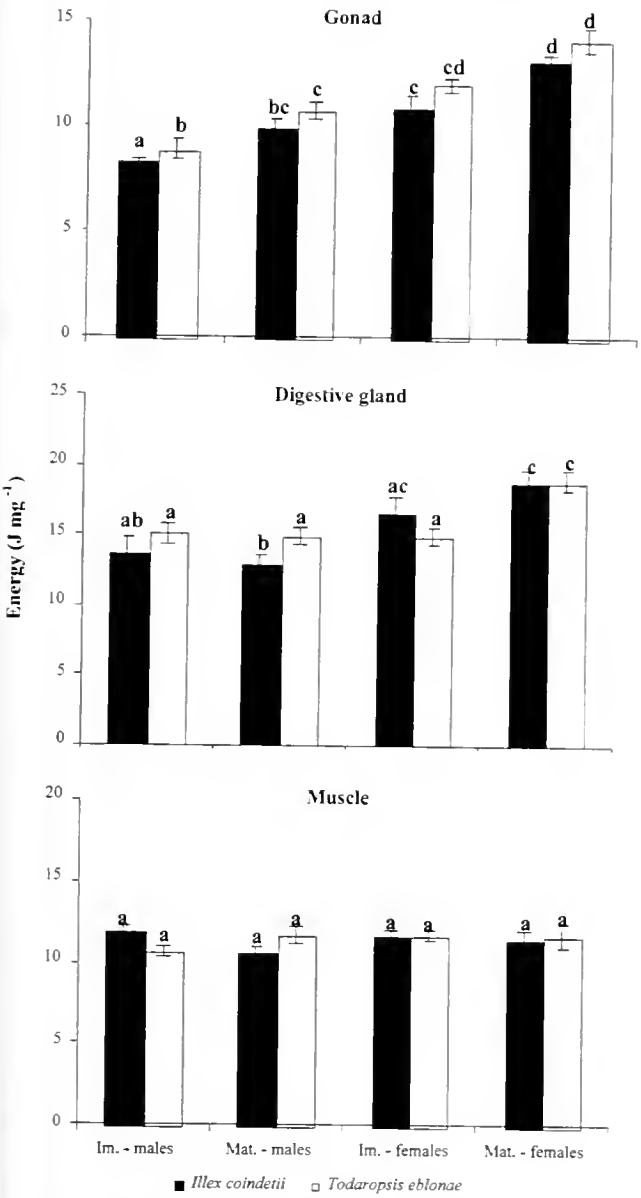

Figure 5. Energy content (J mg^{-1}) in the gonad, digestive gland, and muscle of *Illex coindetii* and *Todaropsis eblanae* males and females at different stages of gonad development. Means ± SD with different letters represent significant differences ($P < 0.05$). Im, immature; Mat, mature.

for the utilization of either digestive gland or mantle tissues to supply energy for gonads. In fact, other studies have shown that ommastrephids and other species maintain their condition, continue to growth, and fuel their reproduction from feeding rather than energy stores (Harman *et al.*, 1989; Rodhouse and Hatfield, 1990; Clarke *et al.*, 1994; Gabr *et al.*, 1999; McGrath and Jackson, 2002).

Being fast-swimming organisms, squids may not be able to utilize muscle tissue to fuel the production of gametes. However, according to Moltschaniwskyj and Semmens (2000), some species may utilize mantle tissue immediately before spawning. More recently, in a study of the deepwater squid *Moroteuthis ingens*, Jackson *et al.* (2004) found that water tended to increase in the mantle, while protein, lipid, and carbohydrate all decreased with maturity, suggesting a transfer of energy from the muscle tissue during reproductive maturation. Additionally, it is noteworthy that in some gonatid squids, the proportions of the body and the integrity of the mantle do not change in males during maturation, but do change in females. As an adaptation for a deepwater bathypelagic "brooding" of the negatively buoyant egg, some of the female's muscle tissue degenerates (gelatinizes) (Arkhipkin and Bjorke, 1999). According to Seibel *et al.* (2000), the high lipid content of the digestive gland in females provides fuel to support the extended "brooding" period of these gonatids.

Because we used only specimens in stages 1, 2 (immature) and 5 (mature) in the present study, we could not apply a size-independent method such as geometric mean regression (see McGrath and Jackson, 2002; Jackson *et al.*, 2004), to determine how somatic condition changed with maturity. Studies on captive ommastrephids will also be needed to resolve the important life-history question of whether somatic reserves are converted into gametes.

Both squid species showed an increase of amino acids and protein content in the gonad throughout sexual maturation (mainly in oogenesis), but the allocation of these nitrogen compounds from the muscle (protein catabolism) was not evident. In addition, there was little evidence that accumulated lipid storage products were being used for egg production.

A significant increasing trend in the lipid and fatty acid contents in the gonad and digestive gland was observed, mainly in oogenesis, which suggests that, for successful reproduction, females require higher energetic resources directed towards gonad development. Moreover, it is worth noting that sex-related biochemical differences can be due to distinct feeding ecologies. Female ommastrephids are typically larger than males and are perhaps able to feed on different prey; that is, they may take more fast-swimming, oily fish, while males may take slower crustaceans with lower lipid content.

Both *Illex coindetii* and *Todaropsis eblanae* seem to use energy for egg production directly from food, rather than from stored products. This direct acquisition has also been proposed by other authors for temperate (Guerra and Castro, 1994; Collins *et al.*, 1995) and tropical (Moltschaniwskyj and Semmens, 2000) squids. Some lipid classes, namely phospholipids, have an important role in the composition of the gametes (Pollero and Iribarne, 1988), because they are probably involved in the synthesis of the vitellus, which is a yolk phospholipoprotein (Fujii, 1960). Squid gonad fatty acids were dominated by polyunsaturated fatty acids and highly unsaturated fatty acids from the n-3 series (Sargent *et al.*, 1999). Eicosapentaenoic acid and arachidonic acid are

important as structural components of cell membranes and as precursors of prostaglandins (Lilly and Bottino, 1981). Docosahexaenoic acid may be important for the correct development and survival of fast-growing phospholipid-rich cephalopod paralarvae (Navarro and Villanueva, 2000, 2003). Lipid functions in the squid life cycle must include supply of essential fatty acids and membrane components like phospholipids and cholesterol to cells.

Levels of lipid, fatty acid, and cholesterol were significantly higher in digestive gland than in gonad and muscle. The digestive gland is a site of digestive absorption and intracellular digestion (Boucher-Rodoni *et al.*, 1987; Semmens, 2002), and the differences between the two squid species may be related to different feeding ecologies. In fact, comparison between stomach content and lipid analysis confirms that lipid from digestive gland is very likely to derive from the diet with little or no modification prior to deposition (Hayashi *et al.*, 1990, Phillips *et al.*, 2001). Moreover, recent findings for the southern pygmy squid *Idiosepius notoides* have shown the presence, in the digestive gland and cecum, of intracellular lipidic droplets that derive from that squid's field diet (Eyster and van Camp, 2003).

Voogt (1973) reported that cephalopods are able to synthesize sterols, although molluscs in general apparently can only carry out this biosynthesis slowly (Goad, 1978). According to Kanazawa (2001), cephalopods seem to incorporate acetate and mevalonate into sterols poorly and then require additional dietary sources of sterol for growth and survival. Squid are active carnivores, and if their component sterols are of a dietary origin, considerable variation in the cholesterol content of the digestive gland of *Illex coindetii* and *Todaropsis eblanae* might be expected on the basis of the sterol composition of their prey. Apsimon and Burnell (1980) and Ballantine *et al.* (1981) found an exogenous rather than endogenous origin for the component sterols of *Spirula spirula* and *Illex illecebrosus*.

The cholesterol content in the gonad of the two squid species exhibited variations that seem to be correlated with the maturation process. Cholesterol is known to be an important precursor of steroid hormones, molting hormones, bile salts, and vitamin D (Kanazawa, 2001). It has been also demonstrated, in other invertebrates, that exogenous cholesterol is converted to sex hormones such as pregesterone, 17 α-hydroxyprogesterone, androstenedione, and testosterone, and to molting hormones such as 20-hydroxyecdydone (Kanazawa, 2000). Our present knowledge about carbohydrate metabolism is mainly confined to studies involving muscle work (see Storey and Storey, 1983). Cephalopods can utilize carbohydrate, lipid, and protein as metabolic substrates: lipid and protein fuel routine aerobic metabolism, and carbohydrate provides the substrate for burst (anaerobic) muscle activity (Wells and Clarke, 1996). During maturation, the glycogen reserves in the gonad increased significantly. As it is in other marine organisms, glycogen may be important for maturation and embryogenesis. Carbohydrates are precursors of metabolic intermediates in the production of energy and nonessential amino acids and are a component of decapod ovarian pigments (Harrison, 1990).

Summing up the findings of this study, it is evident that sexual maturation had a significant effect upon the energy content of the gonads of *Illex coindetii* and *Todaropsis eblanae*, because it is associated with an increase in the products of biosynthesis that will support the lecithotrophic strategy of paralarvae. The energy variation in the digestive gland and muscle was nonsignificant, and because the digestive gland, gonad, and muscle constituents varied independently of one another, revealed no evidence that storage reserves were transferred from organ to organ. The biochemical composition of digestive gland and muscle may be influenced not by sexual maturation but instead by other biotic factors, such as feeding activity, food availability, and spawning.

Acknowledgments

The Portuguese Foundation for Science and Technology (FCT) supported this study through a doctoral grant to the first author. Gratitude is due to Pedro da Conceição for his technical assistance and to Dr. João Pereira for his help obtaining the specimens.

Literature Cited

Apsimon, J. W., and D. J. Burnell. 1980. Sterols from the squid, *Illex illecebrosus* (Mollusca, Cephalopoda). *Comp. Biochem. Physiol. B* **65:** 567–570.

Arkhipkin, A. I., and H. Bjorke. 1999. Ontogenetic changes in morphometric and reproductive indices of the squid *Gonatus fabricii* (Oegopsida, Gonatidae) in the Norwegian Sea. *Polar Biol.* **22:** 357–365.

Ballantine, J. A., J. C. Roberts, and R. J. Morris. 1981. Sterols of the cephalopod *Spirula spirula*. *J. Mar. Biol. Assoc. UK* **61:** 843–850.

Bligh, E. G., and W. J. Dyer. 1959. A rapid method of total lipid extraction and purification. *Can. J. Biochem. Physiol.* **37:** 911–917.

Boucher-Rodoni, R., E. Boucaud-Camou, and K. Mangold. 1987. Feeding and digestion. Pp. 85–108 in *Cephalopod Life Cycles. Vol. 2: Comparative Reviews*, P.R. Boyle, ed. Academic Press, London.

Calow, P. 1973. The relationship between fecundity, phenology, and longevity: a systems approach. *Am. Nat.* **107:** 559–574.

Clarke, A., P. G. Rodhouse, and D. J. Gore. 1994. Biochemical composition in relation to the energetics of growth and sexual maturation in the ommastrephid squid *Illex argentinus*. *Philos. Trans. R. Soc. Lond. B* **344:** 201–212.

Clarke, M. R. 1966. A review of the systematics and ecology of the oceanic squids. *Adv. Mar. Biol.* **4:** 91–300.

Cohen, Z., A. Von Shak, and A. Richmond. 1988. Effect of environmental conditions on fatty acid composition of the red algae *Porphyridium cruentum*: correlation to growth rate. *J. Phycol.* **24:** 328–332.

Collins, M. A., G. Burnell, and P. G. Rodhouse. 1995. Recruitment, maturation, and spawning of *Loligo forbesi* Steenstrup (Cephalopoda: Loliginidae) in Irish waters. *ICES J. Mar. Sci.* **52:** 127–137.

Eyster, L. S., and L. M. van Camp. 2003. Extracellular lipid droplets in *Idiosepius notoides*, the southern pygmy squid. *Biol. Bull.* **205:** 47–53.

Fujii, T. 1960. Comparative biochemical studies on the egg-yolk proteins of various animal species. *Acta Embryol. Morphol. Exp.* **3:** 260–285.

Gabr, H. R., R. T. Hanlon, S. G. El-Etreby, and M. H. Hanafy. 1999. Reproductive versus somatic tissue growth during the life cycle of the cuttlefish *Sepia pharaonis* Ehrenberg, 1831. *Fish. Bull.* **97:** 802–811.

Goad, L. J. 1978. The sterols of marine invertebrates. Pp. 75–172 in *Marine Natural Products: Chemical and Biological Perspectives,* Vol. 2, P. J. Scherer, ed. Academic Press, New York.

Guerra, A., and B. G. Castro. 1994. Reproductive-somatic relationships in *Loligo gahi* (Cephalopoda: Loliginidae) from the Falkland Islands. *Antarct. Sci.* **6:** 175–178.

Harman, R. F., R. E. Young, S. B. Reid, K. M. Mangold, T. Suzuki, and R. F. Nixon. 1989. Evidence for multiple spawning in the tropical oceanic squid *Stenoteuthis oualaniensis* (Teuthoidea: Ommastrephidae). *Mar. Biol.* **101:** 513–519.

Harrison, K. E. 1990. The role of nutrition in maturation, reproduction and embryonic development of decapod crustaceans: a review. *J. Shellfish Res.* **9:** 1–28.

Hayashi, K., H. Kishimura, and Y. Sakurai. 1990. Level and composition of diacyl glyceryl ethers in different tissues and stomach contents of giant squid *Moroteuthis robusta. Nippon Suisan Gakkaishi* **56:** 1635–1639.

Hernández-García, V. 2002. Reproductive biology of *Illex coindetii* and *Todaropsis eblanae* (Cephalopoda: Ommastrephidae) off northwest Africa (4°N, 35°N). *Bull. Mar. Sci.* **71:** 347–366.

Jackson, G. D., J. M. Semmens, K. L. Phillips, and C. H. Jackson. 2004. Reproduction in the deepwater squid *Moroteuthis ingens*: What does it cost? *Mar. Biol.* **145:** 905–616.

Kanazawa, A. 2000. Nutrition and food. Pp. 611–624 in *Spiny Lobsters: Fisheries and Culture,* S. F. Phillips and J. Kittaka, eds. Fishing News Books, London.

Kanazawa, A. 2001. Sterols in marine invertebrates. *Fish. Sci.* **67:** 997–1007.

Laptikhovsky, V. V., and C. M. Nigmatullin. 1999. Egg size and fecundity in females of the subfamilies Todaropsinae and Todarodinae (Cephalopoda: Ommastrephidae). *J. Mar. Biol. Assoc. UK* **79:** 569–570.

Lee, P. G. 1994. Nutrition of cephalopods: fueling the system. *Mar. Freshw. Behav. Physiol.* **25:** 35–51.

Lepage, G., and C. C. Roy. 1986. Direct transesterification of all classes of lipids in one-step reaction. *J. Lipid Res.* **27:** 114–119.

Lilly, M. L., and N. R. Bottino. 1981. Identification of arachidonic acid in Gulf of Mexico shrimp and degree of biosynthesis in *Penaeus setiferus. Lipids* **16:** 871–875.

Lipinski, M. 1979. Universal maturity scale for the commercially important squids. The results of maturity classification of the *Illex illecebrosus* population for the years 1973–77. International Commission for the Northwest Atlantic Fisheries (ICNAF), Research Document 79/II/38, Serial no. 5364. 40 pp.

Lordan, C., D. J. Burnell, and T. F. Cross. 1998. The diet and ecological importance of *Illex coindetii* and *Todaropsis eblanae* (Cephalopoda: Ommastrephidae) in Irish waters. *S. Afr. J. Mar. Sci.* **20:** 153–163.

Lowry, O. H., N. J. Rosenburgh, A. L. Farr, and R. J. Randall. 1951. Protein measurement with Folin phenol reagent. *J. Biol. Chem.* **193:** 265–275.

McGrath, B. L., and G. D. Jackson. 2002. Egg production in the arrow squid *Nototodarus gouldii* (Cephalopoda: Ommastrephidae), fast and furious or slow and steady? *Mar. Biol.* **141:** 699–706.

Moltschaniwskyj, N. A., and J. M. Semmens. 2000. Limited use of stored energy reserves for reproduction by the tropical loliginid squid *Photololigo* sp. *J. Zool.* **251:** 307–313.

Naemmi, E. D., N. Ahmad, T. K. Al-sharrah, and M. Behbahani. 1995. Rapid and simple method for determination of cholesterol in processed food. *J. AOAC Int.* **78:** 1522–1525.

Navarro, J. C., and R. Villanueva. 2000. Lipid and fatty acid composition of early stages of cephalopods: an approach to their lipid requirements. *Aquaculture* **183:** 161–177.

Navarro, J. C., and R. Villanueva. 2003. The fatty acid composition of *Octopus vulgaris* paralarvae reared with live and inert food: deviation from their natural fatty acid profile. *Aquaculture* **219:** 613–631.

O'Dor, R. K., and D. M. Webber. 1986. The constraints on cephalopods: Why squid aren't fish. *Can. J. Zool.* **64:** 1591–1605.

O'Dor, R. K., and M. J. Wells. 1978. Reproduction versus somatic growth: hormonal control in *Octopus vulgaris. J. Exp. Biol.* **77:** 15–31.

O'Dor, R. K., K. Mangold, M. Wells, J. Wells, and R. Boucher-Rodoni. 1984. Nutrient absorption, storage and remobilization in *Octopus vulgaris. Mar. Behav. Physiol.* **11:** 239–258.

Oehlenschläger, J. 2000. Cholesterol content in edible part of marine fatty pelagic fish species and other seafood. Pp. 107–115 in *Proceedings of 29th WEFTA Meeting,* S. A. Georgakis, ed. Pieria, Greece.

Phillips, K. L., G. D. Jacksun, and P. D. Nichols. 2001. Predation on myctophids by the squid *Moroteuthis ingens* around Macquarie and Heard Islands: stomach contents and fatty acid analyses. *Mar. Ecol. Prog. Ser.* **215:** 179–189.

Pollero, R. J., and O. O. Iribarne. 1988. Biochemical changes during the reproductive cycle of the small patagonian octopus, *Octopus tehuelchus,* D'Orb. *Comp. Biochem. Physiol. B* **90:** 317–320.

Robin, J. P., V. Denis, J. Royer, and L. Challier. 2002. Recruitment, growth and reproduction in *Todaropsis eblanae* (Ball, 1841), in the area fished by French Atlantic trawlers. *Bull. Mar. Sci.* **71:** 711–724.

Rocha, F., A. Guerra, and A. F. González, 2001. A review of reproductive strategies in cephalopods. *Biol. Rev.* **76:** 291–304.

Rodhouse, P. G., and E. M. C. Hatfield. 1990. Dynamics of growth and maturation in the cephalopod *Illex argentinus* de Castelanos, 1960 (Teuthoidea: Ommastrephidae). *Philos. Trans. R. Soc. Lond. B* **329:** 229–241.

Sargent, J. R., L. A. McEvoy, A. Estevez, G. Bell, M. Bell, J. Henderson, and D. Tocher. 1999. Lipid nutrition of marine fish during early development: current status and future directions. *Aquaculture* **179:** 217–229.

Seibel, B. A., F. G. Hochberg, and D. B. Carlini. 2000. Life history of *Gonatus onyx* (Cephalopoda: Teuthoidea): deep-sea spawning and post-spawning egg care. *Mar. Biol.* **137:** 519–526.

Semmens, J. M. 2002. Changes in the digestive gland of the loliginid squid *Sepioteuthis lessoniana* (Lesson 1830) associated with feeding. *J. Exp. Mar. Biol. Ecol.* **274:** 19–39.

Storey, K. B., and J. M. Storey. 1983. Carbohydrate metabolism in cephalopod molluscs. Pp. 91–136 in *The Mollusca, Vol. 1, Metabolic Biochemistry and Molecular Biomechanics,* P. W. Hochachka, ed. Academic Press, New York.

Viles, P., and J. Silverman. 1949. Determination of starch and cellulose with anthrone. *J. Anal. Chem.* **21:** 950–953.

Voogt, P. A. 1973. Investigations of the capacity of synthesizing 3 β-sterols in Mollusca. X. Biosynthesis of 3 β-sterols in Cephalopoda. *Arch. Int. Physiol. Biochim.* **81:** 401–407.

Wells, M. J., and A. Clarke. 1996. Energetics: the costs of living and reproducing for an individual cephalopod. *Philos. Trans. R. Soc. Lond. B* **351:** 1083–1104.

Winberg, G. C. 1971. *Methods for the Estimation of Production of Aquatic Animals.* Academic Press, London.

Zar, J. H. 1996. *Biostatistical Analysis.* Prentice Hall, Upper Saddle River, NJ.

Appendix

Supplementary data on composition of *Illex coindetii* and *Todaropsis eblanae* males and females at different stages of gonad development

Appendix Table 1. *Total (protein bound + free) amino acid composition (% dry weight) in the gonad*

Amino acids (% dw)	*Illex coindetii*				*Todaropsis eblanae*			
	Males		Females		Males		Females	
	Immature	Mature	Immature	Mature	Immature	Mature	Immature	Mature
Essential (EAA)								
Threonine	2.17 ± 0.12^{a}	2.64 ± 0.09^{b}	2.82 ± 0.01^{c}	2.91 ± 0.04^{d}	2.50 ± 0.11^{bc}	2.46 ± 0.09^{c}	2.71 ± 0.04^{b}	2.92 ± 0.06^{d}
Methionine	1.43 ± 0.00^{a}	1.48 ± 0.02^{b}	1.86 ± 0.04^{c}	1.69 ± 0.14^{cd}	1.46 ± 0.07^{ab}	1.52 ± 0.04^{b}	1.59 ± 0.03^{d}	1.71 ± 0.04^{ed}
Isoleucine	2.18 ± 0.10^{a}	2.47 ± 0.06^{b}	3.44 ± 0.03^{c}	3.16 ± 0.13^{d}	2.35 ± 0.06^{b}	2.40 ± 0.04^{b}	2.55 ± 0.05^{e}	2.75 ± 0.11^{f}
Leucine	3.65 ± 0.18^{a}	3.71 ± 0.10^{a}	5.26 ± 0.04^{b}	4.94 ± 0.14^{c}	3.61 ± 0.11^{a}	3.99 ± 0.07^{de}	3.93 ± 0.08^{d}	4.23 ± 0.17^{e}
Valine	2.17 ± 0.08^{a}	2.24 ± 0.06^{a}	2.80 ± 0.02^{b}	2.91 ± 0.01^{c}	2.23 ± 0.07^{a}	2.39 ± 0.08^{d}	2.43 ± 0.03^{d}	2.61 ± 0.08^{e}
Phenylalanine	2.91 ± 0.04^{a}	2.69 ± 0.06^{b}	3.59 ± 0.00^{c}	3.38 ± 0.17^{d}	2.63 ± 0.08^{b}	3.02 ± 0.09^{e}	2.86 ± 0.03^{a}	3.08 ± 0.09^{c}
Tyrosine	2.06 ± 0.10^{a}	2.20 ± 0.02^{b}	2.42 ± 0.06^{c}	2.52 ± 0.02^{d}	2.08 ± 0.05^{a}	2.32 ± 0.08^{c}	2.27 ± 0.04^{b}	2.44 ± 0.09^{c}
Lysine	4.86 ± 0.32^{a}	5.43 ± 0.18^{bd}	5.36 ± 0.05^{b}	5.38 ± 0.13^{bd}	4.71 ± 0.12^{a}	5.45 ± 0.07^{b}	5.13 ± 0.08^{c}	5.53 ± 0.20^{d}
Histidine	1.31 ± 0.06^{a}	1.37 ± 0.03^{a}	1.53 ± 0.05^{b}	1.65 ± 0.04^{c}	1.35 ± 0.02^{a}	1.36 ± 0.05^{a}	1.47 ± 0.03^{b}	1.58 ± 0.07^{c}
Arginine	5.77 ± 0.30^{a}	6.08 ± 0.19^{a}	3.93 ± 0.08^{b}	4.03 ± 0.10^{b}	4.92 ± 0.24^{c}	4.47 ± 0.15^{d}	5.35 ± 0.14^{c}	5.77 ± 0.16^{a}
Σ EAA	28.52 ± 0.33^{a}	30.31 ± 0.58^{b}	33.00 ± 0.27^{c}	32.55 ± 0.88^{c}	27.83 ± 0.84^{a}	29.37 ± 0.74^{b}	30.28 ± 0.21^{b}	32.62 ± 0.93^{c}
Non-essential (NEAA)								
Aspartic acid	4.36 ± 0.23^{a}	5.10 ± 0.18^{b}	5.48 ± 0.06^{c}	5.90 ± 0.16^{d}	5.41 ± 0.56^{c}	4.96 ± 0.13^{b}	5.88 ± 0.40^{d}	6.33 ± 0.32^{c}
Serine	2.35 ± 0.13^{a}	2.79 ± 0.09^{b}	3.15 ± 0.08^{c}	3.15 ± 0.02^{c}	2.71 ± 0.12^{b}	2.62 ± 0.10^{b}	2.95 ± 0.03^{d}	3.18 ± 0.06^{c}
Glutamic acid	6.13 ± 0.10^{a}	7.02 ± 0.22^{b}	5.81 ± 0.18^{c}	7.88 ± 0.29^{d}	6.16 ± 0.36^{a}	7.14 ± 0.31^{b}	6.70 ± 0.15^{c}	7.21 ± 0.09^{b}
Glycine	2.70 ± 0.11^{a}	2.99 ± 0.09^{b}	1.97 ± 0.04^{c}	2.54 ± 0.11^{d}	2.92 ± 0.15^{b}	3.15 ± 0.09^{e}	3.18 ± 0.06^{e}	3.42 ± 0.08^{f}
Alanine	3.16 ± 0.09^{a}	3.37 ± 0.13^{b}	2.78 ± 0.06^{c}	3.42 ± 0.10^{b}	3.10 ± 0.09^{a}	3.31 ± 0.11^{b}	3.38 ± 0.05^{b}	3.64 ± 0.13^{d}
Cystine	tr	0.73 ± 0.04^{a}	0.70 ± 0.02^{a}	0.53 ± 0.03^{b}	0.70 ± 0.06^{a}	0.10 ± 0.16^{c}	0.77 ± 0.09^{a}	0.83 ± 0.11^{a}
Proline	3.27 ± 0.24^{a}	2.58 ± 0.05^{b}	2.27 ± 0.06^{c}	3.04 ± 0.13^{a}	3.01 ± 0.14^{a}	3.83 ± 0.26^{d}	3.27 ± 0.11^{a}	3.53 ± 0.16^{d}
Σ NEAA	21.96 ± 1.01^{a}	24.58 ± 0.71^{b}	22.16 ± 0.48^{a}	26.46 ± 0.31^{c}	24.02 ± 1.33^{bd}	25.10 ± 0.78^{d}	26.12 ± 0.59^{d}	28.13 ± 0.58^{e}
Σ TAA	50.49 ± 2.31^{a}	54.89 ± 1.30^{b}	55.16 ± 0.70^{b}	59.01 ± 0.78^{c}	51.86 ± 2.15^{a}	54.47 ± 1.51^{b}	56.41 ± 0.48^{b}	60.75 ± 1.29^{c}

Values are mean of triplicates ± SD. Different superscript letters within rows represent significant differences ($P < 0.05$); tr—trace.

Appendix Table 2. *Total (protein bound + free) amino acid composition (% dry weight) in the digestive gland*

Amino acids (% dw)	*Illex coindetii*				*Todaropsis eblanae*			
	Males		Females		Males		Females	
	Immature	Mature	Immature	Mature	Immature	Mature	Immature	Mature
Essential (EAA)								
Chreonine	2.82 ± 0.02^{a}	2.20 ± 0.06^{b}	2.92 ± 0.10^{a}	2.74 ± 0.08^{a}	2.78 ± 0.29^{ac}	2.19 ± 0.06^{b}	2.52 ± 0.08^{c}	2.34 ± 0.07^{d}
Methionine	1.84 ± 0.07^{a}	1.40 ± 0.03^{b}	1.91 ± 0.07^{a}	1.79 ± 0.07^{a}	1.83 ± 0.18^{ac}	1.42 ± 0.01^{b}	1.64 ± 0.01^{c}	1.52 ± 0.01^{d}
Isoleucine	3.03 ± 0.04^{a}	2.58 ± 0.06^{b}	3.23 ± 0.12^{c}	3.03 ± 0.15^{ac}	3.07 ± 0.34^{acd}	2.45 ± 0.05^{d}	2.82 ± 0.07^{e}	2.62 ± 0.07^{f}
Leucine	4.41 ± 0.09^{a}	3.19 ± 0.08^{b}	4.87 ± 0.17^{c}	4.57 ± 0.19^{ac}	4.63 ± 0.51^{abc}	3.59 ± 0.03^{d}	4.13 ± 0.02^{e}	3.84 ± 0.01^{f}
Valine	3.38 ± 0.08^{a}	2.44 ± 0.05^{b}	3.50 ± 0.13^{a}	3.29 ± 0.13^{a}	3.33 ± 0.37^{a}	2.50 ± 0.04^{b}	2.88 ± 0.05^{c}	2.68 ± 0.05^{d}
Phenylalanine	3.44 ± 0.07^{a}	2.40 ± 0.06^{b}	4.19 ± 0.15^{c}	3.93 ± 0.16^{c}	4.00 ± 0.41^{c}	2.92 ± 0.33^{b}	3.36 ± 0.39^{a}	3.13 ± 0.37^{a}
Tyrosine	2.83 ± 0.16^{a}	1.77 ± 0.04^{b}	3.00 ± 0.11^{a}	2.82 ± 0.08^{a}	2.81 ± 0.38^{a}	1.88 ± 0.02^{c}	2.17 ± 0.02^{d}	2.02 ± 0.02^{e}
Lysine	5.39 ± 0.14^{a}	3.86 ± 0.09^{b}	6.09 ± 0.22^{c}	5.72 ± 0.14^{d}	5.75 ± 0.71^{d}	4.61 ± 0.07^{e}	5.30 ± 0.07^{a}	4.93 ± 0.06^{f}
Histidine	1.78 ± 0.03^{a}	1.24 ± 0.04^{bd}	0.15 ± 0.01^{c}	0.14 ± 0.01^{c}	0.77 ± 0.87^{bd}	1.17 ± 0.05^{b}	1.34 ± 0.06^{d}	1.25 ± 0.05^{bd}
Arginine	3.69 ± 0.10^{a}	2.37 ± 0.07^{b}	4.07 ± 0.15^{c}	3.82 ± 0.16^{ac}	3.89 ± 0.40^{ac}	2.80 ± 0.04^{d}	3.22 ± 0.05^{e}	2.99 ± 0.05^{f}
Σ EAA	32.59 ± 0.79^{a}	23.47 ± 0.56^{b}	33.93 ± 1.21^{ad}	31.87 ± 1.30^{ad}	32.86 ± 2.73^{ad}	25.53 ± 0.45^{c}	29.39 ± 0.58^{d}	27.33 ± 0.58^{c}
Non-essential (NEAA)								
Aspartic acid	6.15 ± 0.12^{a}	4.19 ± 0.14^{b}	6.43 ± 0.23^{a}	6.04 ± 0.25^{a}	5.64 ± 0.07^{b}	4.73 ± 0.02^{c}	5.47 ± 0.03^{d}	5.07 ± 0.03^{e}
Serine	2.65 ± 0.03^{a}	2.08 ± 0.05^{b}	2.80 ± 0.10^{a}	2.63 ± 0.11^{a}	2.70 ± 0.25^{a}	2.07 ± 0.01^{b}	2.39 ± 0.02^{c}	2.22 ± 0.02^{d}
Glutamic acid	7.30 ± 0.15^{a}	5.33 ± 0.12^{b}	8.10 ± 0.29^{c}	7.61 ± 0.31^{a}	6.30 ± 0.01^{d}	7.03 ± 0.02^{e}	8.09 ± 0.04^{c}	7.52 ± 0.05^{a}
Glycine	3.10 ± 0.12^{a}	1.97 ± 0.06^{b}	3.72 ± 0.13^{c}	3.49 ± 0.14^{d}	3.57 ± 0.34^{cd}	2.57 ± 0.03^{e}	2.96 ± 0.03^{f}	2.75 ± 0.04^{g}
Alanine	3.34 ± 0.07^{a}	2.36 ± 0.09^{b}	3.62 ± 0.13^{c}	3.40 ± 0.17^{ac}	3.49 ± 0.32^{ac}	2.89 ± 0.04^{d}	3.33 ± 0.06^{a}	3.09 ± 0.06^{a}
Cystine	tr	1.05 ± 0.03	tr	tr	tr	tr	tr	tr
Proline	2.92 ± 0.19^{a}	1.85 ± 0.10^{b}	3.78 ± 0.14^{ce}	3.55 ± 0.11^{c}	2.96 ± 0.11^{a}	3.61 ± 0.07^{c}	4.16 ± 0.08^{d}	3.87 ± 0.07^{e}
Σ NEAA	25.46 ± 0.67^{a}	18.83 ± 0.51^{b}	28.46 ± 1.02^{a}	26.73 ± 0.98^{a}	24.66 ± 0.73^{ac}	22.91 ± 0.06^{d}	26.37 ± 0.12^{c}	24.52 ± 0.15^{ac}
Σ TAA	58.05 ± 1.46^{a}	42.30 ± 1.02^{b}	59.74 ± 2.14^{a}	56.11 ± 2.21^{ad}	57.52 ± 3.46^{ad}	48.44 ± 0.51^{c}	55.76 ± 0.70^{d}	51.85 ± 0.83^{e}

Values are mean of triplicates ± SD. Different superscript letters within rows represent significant differences ($P < 0.05$); tr—trace.

Appendix Table 3. *Total (protein bound + free) amino acid composition (% dry weight) in the muscle*

Amino acids (% dw)	*Illex coindetii*				*Todaropsis eblanae*			
	Males		Females		Males		Females	
	Immature	Mature	Immature	Mature	Immature	Mature	Immature	Mature
Essential (EAA)								
Threonine	3.07 ± 0.10^{a}	2.92 ± 0.04^{a}	2.99 ± 0.13^{a}	3.04 ± 0.14^{a}	2.96 ± 0.03^{a}	2.75 ± 0.08^{b}	2.69 ± 0.39^{ab}	2.88 ± 0.06^{a}
Methionine	2.30 ± 0.09^{a}	2.19 ± 0.05^{b}	2.24 ± 0.08^{ab}	2.28 ± 0.09^{ab}	1.17 ± 1.50^{cb}	0.99 ± 1.28^{ab}	1.97 ± 0.25^{c}	2.10 ± 0.13^{b}
Isoleucine	3.22 ± 0.06^{a}	3.07 ± 0.01^{b}	3.14 ± 0.18^{ab}	3.20 ± 0.19^{ab}	2.90 ± 0.05^{c}	2.83 ± 0.12^{c}	2.82 ± 0.48^{c}	3.01 ± 0.10^{bc}
Leucine	5.65 ± 0.18^{a}	5.38 ± 0.08^{b}	5.51 ± 0.24^{a}	5.61 ± 0.27^{a}	5.26 ± 0.06^{b}	4.86 ± 0.10^{c}	4.83 ± 0.15^{c}	5.15 ± 0.25^{b}
Valine	2.97 ± 0.07^{a}	2.82 ± 0.02^{b}	2.89 ± 0.15^{ab}	2.94 ± 0.16^{ab}	2.88 ± 0.04^{ab}	2.80 ± 0.01^{b}	2.62 ± 0.12^{b}	2.80 ± 0.03^{b}
Phenylalanine	3.26 ± 0.07^{a}	3.11 ± 0.01^{b}	3.18 ± 0.17^{ab}	3.24 ± 0.19^{ab}	3.11 ± 0.03^{b}	3.25 ± 0.34^{ab}	2.81 ± 0.54^{ab}	3.02 ± 0.19^{ab}
Tyrosine	2.52 ± 0.05^{a}	2.40 ± 0.01^{b}	2.46 ± 0.14^{ab}	2.51 ± 0.15^{ab}	2.44 ± 0.04^{b}	2.55 ± 0.16^{ab}	2.28 ± 0.29^{ab}	2.45 ± 0.05^{b}
Lysine	5.88 ± 0.14^{a}	5.60 ± 0.03^{b}	5.73 ± 0.30^{ab}	5.84 ± 0.33^{ab}	5.57 ± 0.06^{b}	5.34 ± 0.22^{b}	5.17 ± 0.90^{ab}	5.52 ± 0.26^{ab}
Histidine	1.71 ± 0.04^{a}	1.63 ± 0.01^{b}	1.67 ± 0.09^{ab}	1.70 ± 0.10^{ab}	2.60 ± 0.02^{c}	1.14 ± 0.20^{d}	1.52 ± 0.28^{e}	1.62 ± 0.09^{e}
Arginine	5.65 ± 0.13^{a}	5.38 ± 0.03^{b}	5.51 ± 0.29^{ab}	5.61 ± 0.31^{ab}	4.73 ± 0.07^{c}	5.36 ± 0.41^{ab}	4.72 ± 0.74^{bc}	5.04 ± 0.15^{bc}
Σ EAA	36.23 ± 0.92^{a}	34.50 ± 1.29^{ab}	35.31 ± 1.77^{ab}	35.96 ± 1.93^{ab}	33.60 ± 1.09^{bc}	31.87 ± 1.35^{c}	31.43 ± 2.20^{c}	33.57 ± 1.30^{bc}
Non-essential (NEAA)								
Aspartic acid	7.11 ± 0.24^{a}	6.77 ± 0.11^{b}	6.93 ± 0.29^{ab}	7.05 ± 0.32^{ab}	6.53 ± 0.09^{c}	6.39 ± 0.21^{cd}	6.01 ± 0.20^{d}	6.41 ± 0.28^{cd}
Serine	3.11 ± 0.15^{a}	2.96 ± 0.09^{ab}	3.02 ± 0.09^{ab}	3.08 ± 0.10^{ab}	2.87 ± 0.02^{b}	2.83 ± 0.10^{ab}	2.68 ± 0.41^{ab}	2.87 ± 0.07^{b}
Glutamic acid	10.43 ± 0.38^{a}	9.94 ± 0.19^{a}	10.17 ± 0.40^{a}	10.35 ± 0.44^{a}	10.03 ± 0.04^{a}	9.01 ± 0.43^{b}	8.96 ± 0.53^{b}	9.57 ± 0.39^{ab}
Glycine	3.51 ± 0.12^{a}	3.34 ± 0.05^{b}	3.42 ± 0.14^{ab}	3.48 ± 0.16^{ab}	3.96 ± 0.06^{c}	4.56 ± 0.21^{d}	3.12 ± 0.25^{b}	3.32 ± 0.17^{ab}
Alanine	4.26 ± 0.15^{a}	4.06 ± 0.07^{a}	4.15 ± 0.17^{a}	4.23 ± 0.19^{a}	4.49 ± 0.01^{b}	4.05 ± 0.05^{a}	4.30 ± 0.03^{b}	4.64 ± 0.62^{ab}
Cystine	0.51 ± 0.02^{a}	0.49 ± 0.01^{a}	0.50 ± 0.02^{a}	0.51 ± 0.02^{a}	0.12 ± 0.17^{b}	0.12 ± 0.17^{b}	0.64 ± 0.15^{a}	0.69 ± 0.08^{c}
Proline	2.93 ± 0.13^{a}	2.79 ± 0.08^{a}	2.86 ± 0.09^{a}	2.91 ± 0.10^{a}	4.84 ± 0.39^{b}	3.47 ± 0.21^{c}	3.31 ± 0.39^{a}	3.59 ± 0.87^{ac}
Σ NEAA	31.86 ± 0.19^{a}	30.34 ± 0.61^{b}	31.04 ± 1.19^{ab}	31.61 ± 1.33^{ab}	32.85 ± 0.76^{b}	30.35 ± 1.28^{ab}	29.02 ± 2.12^{ab}	31.10 ± 0.51^{ab}
Σ TAA	68.09 ± 2.11^{a}	64.85 ± 0.90^{bc}	66.36 ± 2.96^{ab}	67.57 ± 3.26^{ab}	66.45 ± 0.33^{a}	62.22 ± 1.07^{b}	60.45 ± 2.41^{bc}	64.68 ± 0.78^{c}

Values are mean of triplicates ± SD. Different superscript letters within rows represent significant differences ($P < 0.05$).

Appendix Table 4. *Fatty acid composition (μg/mg dry weight) in the gonad*

Fatty acids (μg/mg DW)	*Illex coindetii*				*Todaropsis eblanae*			
	Males		Females		Males		Females	
	Immature	Mature	Immature	Mature	Immature	Mature	Immature	Mature
12:0	0.03 ± 0.01^{a}	0.01 ± 0.00^{b}	0.04 ± 0.00^{a}	0.07 ± 0.00^{c}	0.01 ± 0.01^{b}	0.02 ± 0.00^{b}	0.03 ± 0.01^{a}	0.04 ± 0.00^{a}
14:0	0.97 ± 0.14^{a}	1.30 ± 0.12^{b}	1.90 ± 0.05^{c}	4.26 ± 0.31^{d}	0.80 ± 0.13^{a}	1.26 ± 0.25^{b}	2.17 ± 0.22^{c}	4.86 ± 0.58^{d}
15:0	0.14 ± 0.02^{a}	0.27 ± 0.01^{b}	0.33 ± 0.02^{c}	0.38 ± 0.02^{d}	0.10 ± 0.01^{e}	0.22 ± 0.03^{b}	0.12 ± 0.01^{a}	0.52 ± 0.07^{f}
16:0	10.72 ± 1.31^{a}	13.35 ± 0.64^{b}	24.50 ± 0.74^{c}	40.67 ± 2.60^{d}	10.42 ± 0.74^{a}	14.10 ± 1.59^{b}	18.58 ± 0.38^{c}	50.60 ± 6.78^{f}
17:0	0.53 ± 0.05^{a}	0.64 ± 0.01^{b}	1.12 ± 0.03^{c}	1.02 ± 0.06^{d}	0.56 ± 0.03^{a}	0.90 ± 0.11^{c}	0.47 ± 0.00^{f}	1.19 ± 0.16^{cd}
18:0	2.39 ± 0.20^{a}	3.08 ± 0.15^{b}	5.34 ± 0.14^{c}	7.77 ± 0.48^{d}	5.07 ± 0.15^{c}	5.88 ± 0.41^{c}	6.03 ± 0.31^{e}	12.82 ± 1.63^{f}
19:0	0.03 ± 0.00^{a}	0.02 ± 0.00^{b}	0.04 ± 0.03^{ab}	0.13 ± 0.00^{c}	0.04 ± 0.01^{a}	0.04 ± 0.02^{abd}	0.06 ± 0.01^{d}	0.15 ± 0.02^{e}
20:0	0.07 ± 0.01^{a}	0.07 ± 0.01^{a}	0.14 ± 0.01^{b}	0.17 ± 0.01^{c}	0.08 ± 0.00^{a}	0.14 ± 0.01^{b}	0.14 ± 0.04^{b}	0.17 ± 0.02^{c}
22:0	0.03 ± 0.01^{a}	0.02 ± 0.00^{a}	0.07 ± 0.01^{b}	0.05 ± 0.01^{c}	0.04 ± 0.01^{ac}	0.03 ± 0.01^{a}	0.10 ± 0.03^{b}	0.14 ± 0.05^{d}
Σ Saturated	14.90 ± 1.70^{a}	18.72 ± 0.93^{b}	33.47 ± 0.95^{c}	54.53 ± 3.46^{d}	17.12 ± 1.07^{b}	22.58 ± 2.36^{e}	27.70 ± 0.94^{f}	70.48 ± 9.26^{g}
Iso 14:0	0.09 ± 0.10^{ab}	0.02 ± 0.00^{a}	0.01 ± 0.01^{a}	0.06 ± 0.08^{b}	0.02 ± 0.00^{a}	0.02 ± 0.01^{a}	0.01 ± 0.01^{a}	0.03 ± 0.01^{a}
Anteiso 14:0	0.03 ± 0.01^{a}	0.01 ± 0.00^{b}	0.01 ± 0.00^{b}	0.01 ± 0.00^{b}	0.00 ± 0.00^{c}	0.00 ± 0.00^{c}	0.00 ± 0.00^{c}	0.00 ± 0.00^{c}
Iso 16:0	0.04 ± 0.02^{a}	0.10 ± 0.01^{b}	0.14 ± 0.00^{c}	0.21 ± 0.02^{d}	0.10 ± 0.01^{b}	0.10 ± 0.01^{b}	0.07 ± 0.01^{e}	0.30 ± 0.04^{f}
Anteiso 16:0	0.07 ± 0.01^{a}	0.11 ± 0.01^{bc}	0.12 ± 0.01^{b}	0.10 ± 0.01^{c}	0.07 ± 0.01^{a}	0.11 ± 0.01^{bc}	0.04 ± 0.00^{d}	0.06 ± 0.02^{a}
Σ Branched	0.23 ± 0.01^{a}	0.24 ± 0.01^{a}	0.28 ± 0.01^{b}	0.39 ± 0.12^{c}	0.18 ± 0.01^{d}	0.23 ± 0.04^{a}	0.12 ± 0.02^{c}	0.39 ± 0.03^{c}
16:1n-7	0.21 ± 0.02^{a}	0.24 ± 0.02^{ad}	0.31 ± 0.02^{b}	1.12 ± 0.11^{c}	0.26 ± 0.02^{d}	0.25 ± 0.02^{ad}	0.41 ± 0.01^{e}	1.37 ± 0.19^{f}
17:1n-8	0.03 ± 0.03^{a}	0.08 ± 0.00^{b}	0.18 ± 0.01^{c}	0.18 ± 0.11^{c}	0.52 ± 0.02^{d}	0.09 ± 0.00^{b}	0.18 ± 0.02^{c}	0.46 ± 0.06^{d}
18:1n-9	1.53 ± 0.10^{a}	1.89 ± 0.10^{b}	7.62 ± 0.31^{c}	11.27 ± 0.71^{d}	2.45 ± 0.07^{e}	2.03 ± 0.21^{b}	9.58 ± 0.89^{f}	20.17 ± 2.56^{g}
18:1n-7	0.69 ± 0.05^{a}	0.85 ± 0.05^{b}	1.13 ± 0.03^{c}	2.50 ± 0.18^{d}	1.35 ± 0.03^{e}	1.44 ± 0.11^{e}	1.91 ± 0.01^{f}	5.60 ± 0.55^{g}
20:1n-9	0.24 ± 0.04^{a}	0.36 ± 0.09^{b}	0.01 ± 0.00^{c}	0.01 ± 0.00^{c}	0.01 ± 0.00^{c}	0.00 ± 0.00^{d}	0.00 ± 0.00^{d}	0.01 ± 0.00^{c}
20:1n-7	4.21 ± 0.21^{a}	4.30 ± 0.15^{a}	7.46 ± 0.22^{b}	11.51 ± 0.48^{c}	7.82 ± 0.10^{b}	10.43 ± 0.97^{c}	10.68 ± 2.70^{c}	20.78 ± 2.71^{d}
22:1n-11	0.05 ± 0.02^{a}	0.01 ± 0.00^{b}	0.07 ± 0.01^{a}	0.37 ± 0.06^{c}	0.25 ± 0.00^{d}	0.05 ± 0.01^{a}	0.14 ± 0.01^{c}	0.24 ± 0.03^{d}
22:1n-9	0.49 ± 0.03^{a}	0.43 ± 0.01^{b}	0.35 ± 0.03^{c}	0.34 ± 0.02^{c}	0.76 ± 0.01^{d}	1.02 ± 0.09^{e}	0.51 ± 0.07^{a}	0.52 ± 0.05^{a}
Σ Monounsaturated	7.45 ± 0.41^{a}	8.15 ± 0.26^{b}	17.14 ± 0.53^{c}	27.29 ± 1.60^{d}	13.42 ± 0.25^{e}	15.31 ± 1.36^{e}	23.42 ± 3.69^{d}	49.15 ± 6.01^{f}
16:4n-3	0.45 ± 0.01^{a}	0.48 ± 0.03^{a}	0.54 ± 0.02^{b}	0.52 ± 0.11^{ab}	0.51 ± 0.01^{b}	0.85 ± 0.11^{c}	0.34 ± 0.02^{d}	0.48 ± 0.05^{a}
18:2n-6	0.04 ± 0.01^{a}	0.08 ± 0.00^{b}	0.20 ± 0.02^{c}	0.35 ± 0.01^{d}	0.09 ± 0.01^{b}	0.11 ± 0.10^{abc}	0.16 ± 0.02^{c}	0.49 ± 0.06^{c}
18:3n-6	0.03 ± 0.01^{a}	0.05 ± 0.00^{b}	0.09 ± 0.02^{c}	0.13 ± 0.01^{d}	0.04 ± 0.03^{abc}	0.03 ± 0.01^{a}	0.07 ± 0.00^{e}	0.39 ± 0.04^{d}
18:3n-3	0.05 ± 0.03^{ab}	0.03 ± 0.00^{a}	0.08 ± 0.01^{b}	0.20 ± 0.00^{c}	0.12 ± 0.00^{d}	0.36 ± 0.14^{e}	0.11 ± 0.02^{d}	0.06 ± 0.01^{b}
18:4n-3	1.06 ± 0.06^{a}	1.27 ± 0.31^{ab}	0.73 ± 0.10^{c}	1.05 ± 0.40^{a}	1.27 ± 0.02^{b}	1.92 ± 0.63^{c}	0.85 ± 0.14^{d}	0.88 ± 0.14^{d}
20:2n-6	0.11 ± 0.04^{bc}	0.21 ± 0.02^{b}	0.27 ± 0.02^{c}	0.49 ± 0.08^{d}	0.16 ± 0.01^{e}	0.13 ± 0.00^{a}	0.40 ± 0.01^{f}	1.00 ± 0.07^{g}
20:4n-6	0.54 ± 0.02^{a}	1.18 ± 0.10^{b}	1.36 ± 0.05^{c}	2.66 ± 0.13^{d}	1.38 ± 0.00^{c}	1.45 ± 0.13^{c}	2.85 ± 0.01^{d}	4.81 ± 0.66^{e}
20:3n-3	0.11 ± 0.02^{a}	0.10 ± 0.02^{a}	0.15 ± 0.01^{b}	0.28 ± 0.02^{c}	0.09 ± 0.00^{a}	0.14 ± 0.00^{b}	0.23 ± 0.10^{abc}	0.50 ± 0.05^{d}
20:4n-3	0.07 ± 0.03^{ab}	0.04 ± 0.00^{a}	0.12 ± 0.02^{b}	0.38 ± 0.01^{c}	0.08 ± 0.00^{b}	0.05 ± 0.00^{a}	0.22 ± 0.00^{d}	0.72 ± 0.07^{e}
20:5n-3	10.07 ± 0.63^{a}	10.67 ± 0.48^{a}	13.06 ± 0.65^{b}	19.31 ± 0.94^{c}	15.36 ± 0.10^{d}	23.35 ± 2.13^{e}	13.85 ± 0.90^{b}	28.83 ± 1.85^{c}
22:4n-6	0.09 ± 0.01^{a}	0.04 ± 0.01^{b}	0.09 ± 0.01^{a}	0.38 ± 0.03^{c}	0.06 ± 0.01^{d}	0.06 ± 0.00^{d}	0.15 ± 0.01^{e}	0.41 ± 0.06^{c}
22:5n-6	0.07 ± 0.01^{a}	0.17 ± 0.03^{b}	0.40 ± 0.05^{c}	0.82 ± 0.11^{d}	0.23 ± 0.05^{b}	0.19 ± 0.01^{b}	0.43 ± 0.02^{c}	1.34 ± 0.27^{e}
22:5n-3	0.13 ± 0.01^{a}	0.17 ± 0.06^{a}	0.01 ± 0.00^{b}	1.54 ± 0.07^{c}	0.31 ± 0.04^{d}	0.38 ± 0.03^{d}	1.12 ± 0.21^{c}	2.16 ± 0.55^{c}
22:6n-3	9.58 ± 0.64^{a}	11.85 ± 0.54^{b}	26.45 ± 1.64^{c}	40.06 ± 2.33^{d}	14.65 ± 0.38^{e}	18.83 ± 1.82^{f}	23.03 ± 2.14^{c}	60.27 ± 8.39^{g}
Σ Polyunsaturated	22.39 ± 1.55^{a}	26.34 ± 1.52^{b}	43.54 ± 2.15^{c}	68.15 ± 3.91^{d}	34.36 ± 0.29^{e}	47.84 ± 4.83^{c}	43.82 ± 3.17^{c}	102.37 ± 12.67^{f}
Σ Total FA	44.97 ± 3.71^{a}	53.42 ± 2.66^{b}	94.43 ± 3.62^{c}	150.36 ± 9.07^{d}	65.08 ± 1.05^{e}	85.97 ± 8.49^{c}	95.06 ± 7.75^{c}	222.38 ± 28.99^{f}

Different superscript letters within rows represent significant differences ($P < 0.05$).

Appendix Table 5. *Fatty acid composition (μg/mg dry weight) in the digestive gland*

Fatty acids (μg/mg DW)	*Illex coindetii*				*Todaropsis eblanae*			
	Males		Females		Males		Females	
	Immature	Mature	Immature	Mature	Immature	Mature	Immature	Mature
12:0	0.01 ± 0.00^{a}	0.12 ± 0.02^{b}	0.03 ± 0.02^{a}	0.51 ± 0.03^{c}	0.15 ± 0.00^{b}	0.14 ± 0.01^{b}	0.10 ± 0.02^{b}	0.12 ± 0.02^{b}
14:0	6.22 ± 0.06^{a}	5.89 ± 0.05^{b}	9.79 ± 0.29^{c}	5.59 ± 0.05^{d}	4.22 ± 0.06^{e}	7.80 ± 0.29^{f}	4.18 ± 0.57^{e}	7.93 ± 0.55^{f}
15:0	1.37 ± 0.04^{a}	0.86 ± 0.13^{b}	2.13 ± 0.19^{c}	2.88 ± 0.00^{d}	0.63 ± 0.04^{e}	1.03 ± 0.05^{f}	0.47 ± 0.06^{g}	1.24 ± 0.17^{af}
16:0	34.64 ± 0.35^{a}	33.00 ± 3.93^{ac}	46.26 ± 3.08^{b}	31.66 ± 0.45^{c}	24.73 ± 0.35^{d}	45.67 ± 2.31^{b}	25.13 ± 2.59^{d}	34.99 ± 4.98^{ac}
17:0	2.10 ± 0.02^{a}	1.53 ± 0.14^{bg}	3.38 ± 0.15^{c}	4.23 ± 0.11^{d}	1.11 ± 0.02^{e}	1.78 ± 0.18^{b}	0.95 ± 0.06^{f}	1.30 ± 0.29^{g}
18:0	10.71 ± 0.02^{a}	10.68 ± 0.81^{a}	11.54 ± 0.36^{a}	19.50 ± 1.08^{b}	16.26 ± 0.02^{c}	18.00 ± 1.52^{b}	13.95 ± 0.90^{d}	16.21 ± 2.45^{bc}
19:0	0.33 ± 0.02^{a}	0.19 ± 0.01^{b}	0.18 ± 0.01^{b}	1.05 ± 0.08^{c}	0.38 ± 0.01^{d}	0.04 ± 0.01^{e}	0.29 ± 0.04^{a}	0.09 ± 0.01^{f}
20:0	0.61 ± 0.03^{a}	0.42 ± 0.01^{b}	0.62 ± 0.04^{a}	1.49 ± 0.07^{c}	0.43 ± 0.03^{b}	0.74 ± 0.07^{d}	0.47 ± 0.05^{b}	0.80 ± 0..12^{d}
22:0	0.34 ± 0.02^{a}	0.20 ± 0.02^{bc}	0.48 ± 0.09^{c}	0.73 ± 0.01^{d}	0.17 ± 0.01^{b}	0.53 ± 0.26^{cd}	0.25 ± 0.04^{e}	0.37 ± 0.00^{f}
Σ Saturated	56.33 ± 0.44^{a}	52.93 ± 1.10^{b}	74.41 ± 1.22^{c}	67.65 ± 1.82^{d}	48.08 ± 0.44^{e}	75.74 ± 1.14^{c}	45.80 ± 2.95^{c}	63.05 ± 1.58^{d}
Iso 14:0	0.37 ± 0.02^{a}	0.23 ± 0.04^{b}	0.67 ± 0.06^{c}	2.10 ± 0.04^{d}	0.47 ± 0.02^{e}	0.31 ± 0.01^{f}	0.14 ± 0.04^{g}	0.46 ± 0.09^{e}
Anteiso 14:0	0.15 ± 0.01^{a}	0.10 ± 0.02^{b}	0.35 ± 0.04^{c}	1.17 ± 0.05^{d}	0.25 ± 0.01^{e}	0.05 ± 0.01^{f}	0.06 ± 0.02^{bf}	0.08 ± 0.02^{bf}
Iso 16:0	0.95 ± 0.01^{a}	0.99 ± 0.14^{a}	1.39 ± 0.09^{b}	3.47 ± 0.08^{c}	0.62 ± 0.01^{d}	1.44 ± 0.07^{b}	0.53 ± 0.10^{d}	0.98 ± 0.15^{a}
Anteiso 16:0	0.38 ± 0.02^{a}	0.25 ± 0.02^{b}	0.52 ± 0.02^{c}	1.87 ± 0.06^{d}	0.32 ± 0.02^{e}	0.35 ± 0.02^{a}	0.16 ± 0.06^{b}	0.40 ± 0.10^{a}
Σ Branched	1.86 ± 0.03^{a}	1.57 ± 0.22^{b}	2.93 ± 0.23^{c}	8.60 ± 0.05^{d}	1.65 ± 0.03^{b}	2.14 ± 0.09^{c}	0.90 ± 0.18^{f}	1.92 ± 0.28^{a}
16:1n-7	5.51 ± 0.02^{a}	4.54 ± 0.20^{b}	4.01 ± 0.21^{c}	14.59 ± 0.79^{d}	7.26 ± 0.02^{e}	7.68 ± 0.57^{e}	4.51 ± 0.34^{b}	9.57 ± 1.52^{f}
17:1n-8	1.28 ± 0.02^{a}	0.77 ± 0.05^{b}	1.60 ± 0.17^{c}	2.88 ± 0.14^{d}	1.32 ± 0.02^{a}	1.21 ± 0.09^{a}	0.61 ± 0.06^{e}	1.70 ± 0.26^{c}
18:1n-9	30.92 ± 0.35^{a}	27.21 ± 2.01^{b}	32.11 ± 1.56^{a}	26.46 ± 1.25^{b}	43.33 ± 0.35^{c}	44.65 ± 3.56^{c}	22.20 ± 1.31^{d}	60.93 ± 9.92^{e}
18:1n-7	6.38 ± 0.52^{a}	5.16 ± 0.28^{b}	6.35 ± 0.36^{a}	18.84 ± 0.17^{c}	7.40 ± 0.52^{d}	8.07 ± 0.98^{d}	4.64 ± 0.17^{e}	11.48 ± 1.62^{f}
20:1n-9	0.69 ± 0.02^{a}	1.10 ± 0.00^{b}	0.73 ± 0.18^{a}	6.27 ± 0.18^{c}	0.01 ± 0.00^{d}	0.01 ± 0.00^{d}	2.65 ± 0.65^{e}	0.01 ± 0.00^{d}
20:1n-7	4.70 ± 0.06^{a}	12.59 ± 1.48^{b}	4.67 ± 0.12^{a}	6.72 ± 0.06^{c}	17.77 ± 0.06^{d}	22.84 ± 2.52^{e}	13.40 ± 0.95^{b}	21.86 ± 3.34^{c}
22:1n-11	1.37 ± 0.01^{a}	6.43 ± 0.70^{b}	1.50 ± 0.10^{a}	0.97 ± 0.11^{c}	4.65 ± 0.01^{d}	14.03 ± 1.26^{e}	6.28 ± 0.14^{b}	5.95 ± 0.80^{b}
22:1n-9	0.71 ± 0.02^{a}	1.11 ± 0.12^{b}	0.59 ± 0.02^{c}	1.41 ± 0.03^{d}	1.22 ± 0.02^{b}	1.91 ± 0.17^{c}	1.27 ± 0.12^{b}	2.11 ± 0.31^{e}
Σ Monounsaturated	51.56 ± 0.97^{a}	58.92 ± 2.15^{b}	51.55 ± 2.72^{a}	78.15 ± 0.41^{c}	82.95 ± 0.97^{d}	100.39 ± 8.88^{e}	55.66 ± 2.21^{b}	113.61 ± 17.76^{c}
16:4n-3	0.54 ± 0.01^{a}	0.59 ± 0.00^{b}	0.65 ± 0.01^{c}	2.96 ± 0.23^{d}	1.13 ± 0.01^{e}	0.77 ± 0.12^{bc}	1.14 ± 0.10^{e}	0.65 ± 0.13^{c}
18:2n-6	2.79 ± 0.07^{a}	1.39 ± 0.05^{b}	4.49 ± 0.18^{c}	3.00 ± 0.06^{d}	3.03 ± 0.07^{d}	2.46 ± 0.28^{a}	1.31 ± 0.05^{b}	4.15 ± 0.91^{c}
18:3n-6	0.68 ± 0.02^{a}	0.40 ± 0.02^{b}	0.87 ± 0.04^{c}	1.09 ± 0.24^{c}	0.56 ± 0.02^{d}	0.67 ± 0.07^{a}	0.24 ± 0.02^{e}	0.79 ± 0.10^{a}
18:3n-3	1.80 ± 0.07^{a}	0.82 ± 0.03^{b}	2.15 ± 0.01^{c}	0.56 ± 0.01^{d}	1.21 ± 0.07^{c}	1.20 ± 0.07^{c}	0.48 ± 0.07^{d}	1.86 ± 0.27^{a}
18:4n-3	1.21 ± 0.06^{a}	0.63 ± 0.02^{b}	1.48 ± 0.09^{c}	1.07 ± 0.13^{d}	1.55 ± 0.06^{e}	2.85 ± 0.50^{e}	4.19 ± 0.31^{f}	3.03 ± 0.65^{g}
20:2n-6	1.08 ± 0.05^{a}	0.89 ± 0.09^{b}	1.57 ± 0.04^{c}	4.84 ± 0.06^{d}	1.77 ± 0.05^{e}	1.51 ± 0.14^{c}	1.04 ± 0.08^{a}	2.37 ± 0.34^{f}
20:4n-6	3.23 ± 0.08^{a}	3.69 ± 0.15^{b}	3.56 ± 0.05^{b}	14.24 ± 0.01^{c}	4.53 ± 0.08^{d}	4.80 ± 0.52^{d}	6.20 ± 0.47^{e}	5.57 ± 0.26^{f}
20:3n-3	0.50 ± 0.02^{a}	0.51 ± 0.02^{a}	0.45 ± 0.01^{c}	0.68 ± 0.03^{c}	0.45 ± 0.02^{b}	0.49 ± 0.20^{ab}	0.29 ± 0.00^{d}	0.89 ± 0.21^{e}
20:4n-3	1.31 ± 0.05^{a}	0.84 ± 0.04^{b}	0.94 ± 0.01^{c}	1.19 ± 0.01^{d}	0.98 ± 0.05^{c}	1.19 ± 0.13^{d}	0.73 ± 0.08^{b}	1.84 ± 0.25^{e}
20:5n-3	14.48 ± 0.47^{a}	12.21 ± 0.86^{b}	22.10 ± 0.08^{c}	35.46 ± 0.37^{d}	13.41 ± 0.47^{b}	15.24 ± 1.54^{a}	20.31 ± 1.89^{c}	20.23 ± 2.42^{c}
22:4n-6	0.38 ± 0.11^{a}	0.01 ± 0.00^{b}	0.35 ± 0.01^{a}	1.66 ± 1.08^{c}	0.36 ± 0.11^{a}	0.21 ± 0.10^{d}	0.37 ± 0.07^{a}	0.49 ± 0.03^{a}
22:5n-6	0.77 ± 0.05^{a}	0.97 ± 0.09^{b}	0.94 ± 0.00^{b}	1.64 ± 0.04^{c}	0.95 ± 0.05^{b}	0.99 ± 0.11^{b}	1.10 ± 0.15^{b}	1.71 ± 0.18^{c}
22:5n-3	1.22 ± 0.00^{a}	2.14 ± 0.23^{b}	1.14 ± 0.00^{a}	4.38 ± 0.13^{d}	0.75 ± 0.00^{e}	2.70 ± 0.28^{f}	2.80 ± 0.27^{f}	3.81 ± 0.11^{g}
22:6n-3	26.40 ± 0.34^{a}	34.13 ± 1.18^{b}	39.32 ± 0.30^{c}	29.13 ± 0.76^{d}	32.79 ± 0.34^{b}	34.28 ± 3.56^{b}	45.94 ± 2.73^{c}	53.66 ± 4.66^{f}
Σ Polyunsaturated	56.38 ± 1.38^{a}	59.22 ± 1.53^{b}	80.00 ± 0.11^{c}	101.90 ± 2.09^{d}	63.46 ± 1.38^{e}	69.38 ± 6.68^{c}	86.17 ± 5.32^{c}	101.05 ± 13.01^{d}
Σ Total FA	166.13 ± 2.82^{a}	172.64 ± 15.99^{b}	208.89 ± 8.05^{c}	256.30 ± 1.63^{d}	196.15 ± 2.82^{e}	247.64 ± 18.00^{d}	188.53 ± 11.29^{c}	279.64 ± 10.64^{f}

Different superscript letters within rows represent significant differences ($P < 0.05$).

Appendix Table 6. *Fatty acid composition (μg/mg dry weight) in the muscle*

Fatty acids (μg/mg DW)	*Illex coindetii*				*Todaropsis eblanae*			
	Males		Females		Males		Females	
	Immature	Mature	Immature	Mature	Immature	Mature	Immature	Mature
12:0	0.01 ± 0.00^{a}	0.01 ± 0.00^{a}	0.01 ± 0.00^{c}	0.01 ± 0.00^{a}	0.00 ± 0.00^{a}	0.01 ± 0.00^{a}	0.01 ± 0.00^{a}	0.01 ± 0.00^{a}
14:0	0.45 ± 0.02^{a}	0.25 ± 0.01^{b}	0.73 ± 0.20^{cd}	0.59 ± 0.06^{c}	0.66 ± 0.05^{c}	0.96 ± 0.04^{d}	0.98 ± 0.07^{d}	1.22 ± 0.04^{e}
15:0	0.17 ± 0.01^{a}	0.17 ± 0.00^{a}	0.21 ± 0.06^{ab}	0.17 ± 0.02^{a}	0.21 ± 0.02^{b}	0.23 ± 0.01^{b}	0.29 ± 0.02^{c}	0.25 ± 0.01^{d}
16:0	11.64 ± 0.64^{a}	8.67 ± 0.10^{b}	11.57 ± 0.99^{a}	10.63 ± 0.89^{a}	11.07 ± 0.59^{a}	11.84 ± 0.12^{a}	12.78 ± 0.71^{a}	12.07 ± 0.38^{a}
17:0	0.42 ± 0.04^{a}	0.82 ± 0.04^{b}	0.47 ± 0.03^{ab}	0.44 ± 0.04^{a}	0.49 ± 0.02^{b}	0.43 ± 0.01^{a}	0.50 ± 0.03^{b}	0.45 ± 0.02^{a}
18:0	2.72 ± 0.07^{a}	3.01 ± 0.10^{b}	2.66 ± 0.18^{ab}	2.90 ± 0.17^{ab}	2.66 ± 0.02^{a}	3.22 ± 0.04^{c}	2.03 ± 0.08^{d}	3.53 ± 0.13^{e}
19:0	0.02 ± 0.00^{a}	0.02 ± 0.01^{a}	0.02 ± 0.01^{a}	0.01 ± 0.01^{a}	0.02 ± 0.01^{a}	0.04 ± 0.02^{b}	0.03 ± 0.00^{ab}	0.06 ± 0.01^{b}
20:0	0.06 ± 0.02^{ab}	0.04 ± 0.01^{b}	0.06 ± 0.01^{a}	0.07 ± 0.00^{ac}	0.08 ± 0.00^{c}	0.07 ± 0.01^{a}	0.05 ± 0.00^{ab}	0.08 ± 0.01^{c}
22:0	0.02 ± 0.01^{a}	0.03 ± 0.00^{a}	0.07 ± 0.01^{b}	0.06 ± 0.02^{b}	0.03 ± 0.00^{a}	0.03 ± 0.00^{a}	0.06 ± 0.01^{b}	0.05 ± 0.04^{ab}
Σ Saturated	15.51 ± 0.99^{a}	13.02 ± 0.26^{b}	15.80 ± 0.82^{a}	14.88 ± 1.19^{ab}	15.21 ± 0.70^{a}	16.83 ± 0.16^{ac}	16.73 ± 0.90^{ac}	17.72 ± 0.60^{c}
Iso 14:0	0.01 ± 0.00^{a}	0.02 ± 0.00^{a}	0.01 ± 0.00^{a}	0.01 ± 0.00^{a}	0.02 ± 0.01^{a}	0.02 ± 0.00^{a}	0.01 ± 0.00^{a}	0.02 ± 0.00^{a}
Anteiso 14:0	0.01 ± 0.00^{a}	0.02 ± 0.00^{a}	0.01 ± 0.00^{a}	0.01 ± 0.00^{a}	0.01 ± 0.00^{a}	0.01 ± 0.00^{a}	0.01 ± 0.00^{a}	0.01 ± 0.00^{a}
Iso 16:0	0.08 ± 0.01^{a}	0.08 ± 0.01^{a}	0.08 ± 0.01^{a}	0.08 ± 0.01^{a}	0.10 ± 0.00^{b}	0.08 ± 0.00^{a}	0.07 ± 0.00^{a}	0.10 ± 0.01^{b}
Anteiso 16:0	0.07 ± 0.01^{a}	0.16 ± 0.10^{b}	0.08 ± 0.02^{a}	0.07 ± 0.00^{a}	0.08 ± 0.03^{b}	0.08 ± 0.01^{a}	0.10 ± 0.00^{c}	0.08 ± 0.01^{a}
Σ Branched	0.17 ± 0.01^{a}	0.28 ± 0.11^{b}	0.17 ± 0.01^{a}	0.16 ± 0.01^{a}	0.21 ± 0.01^{a}	0.19 ± 0.02^{ab}	0.18 ± 0.01^{ab}	0.22 ± 0.02^{b}
16:1n-7	0.20 ± 0.01^{a}	0.20 ± 0.00^{a}	0.24 ± 0.02^{a}	0.22 ± 0.01^{a}	0.28 ± 0.02^{b}	0.26 ± 0.01^{b}	0.28 ± 0.02^{b}	0.44 ± 0.05^{c}
17:1n-8	0.05 ± 0.00^{a}	0.05 ± 0.02^{a}	0.06 ± 0.01^{a}	0.05 ± 0.01^{a}	0.07 ± 0.01^{a}	0.07 ± 0.01^{a}	0.07 ± 0.01^{a}	0.12 ± 0.01^{b}
18:1n-9	1.25 ± 0.10^{a}	0.80 ± 0.05^{b}	1.33 ± 0.12^{a}	1.22 ± 0.10^{a}	1.58 ± 0.08^{c}	1.80 ± 0.03^{d}	1.47 ± 0.08^{c}	2.70 ± 0.16^{e}
18:1n-7	1.03 ± 0.01^{a}	0.77 ± 0.01^{b}	0.65 ± 0.19^{b}	0.73 ± 0.08^{b}	0.86 ± 0.10^{b}	0.95 ± 0.06^{ab}	0.46 ± 0.02^{c}	1.24 ± 0.11^{d}
20:1n-9	0.01 ± 0.00^{a}	0.05 ± 0.07^{b}	0.02 ± 0.00^{a}	0.00 ± 0.00^{a}	0.01 ± 0.00^{a}	0.01 ± 0.00^{a}	0.01 ± 0.00^{a}	0.00 ± 0.00^{a}
20:1n-7	2.98 ± 0.27^{a}	1.24 ± 0.13^{b}	2.59 ± 0.20^{a}	2.85 ± 0.16^{a}	2.98 ± 0.07^{a}	3.38 ± 0.01^{c}	1.91 ± 0.05^{d}	4.17 ± 0.20^{e}
22:1n-11	0.05 ± 0.03^{a}	0.04 ± 0.00^{a}	0.04 ± 0.03^{a}	0.05 ± 0.02^{a}	0.09 ± 0.04^{ab}	0.08 ± 0.01^{b}	0.02 ± 0.00^{a}	0.04 ± 0.02^{a}
22:1n-9	0.38 ± 0.04^{a}	0.57 ± 0.05^{b}	0.45 ± 0.06^{c}	0.48 ± 0.02^{c}	0.47 ± 0.03^{c}	0.50 ± 0.02^{bc}	0.39 ± 0.05^{a}	0.42 ± 0.11^{bc}
Σ Monounsaturated	5.93 ± 0.25^{a}	3.71 ± 0.17^{b}	5.35 ± 0.75^{c}	5.61 ± 0.37^{ac}	6.32 ± 0.26^{d}	7.03 ± 0.06^{e}	4.60 ± 0.23^{f}	9.13 ± 0.49^{g}
16:4n-3	0.44 ± 0.03^{ac}	1.83 ± 0.07^{b}	0.48 ± 0.15^{ac}	0.39 ± 0.02^{a}	0.39 ± 0.01^{a}	0.48 ± 0.04^{c}	0.66 ± 0.02^{d}	0.43 ± 0.02^{ac}
18:2n-6	0.06 ± 0.01^{a}	0.30 ± 0.06^{b}	0.10 ± 0.04^{a}	0.08 ± 0.04^{a}	0.08 ± 0.02^{a}	0.16 ± 0.02^{c}	0.13 ± 0.01^{c}	0.22 ± 0.02^{d}
18:3n-6	0.05 ± 0.01^{a}	0.07 ± 0.00^{b}	0.05 ± 0.01^{a}	0.05 ± 0.01^{a}	0.06 ± 0.01^{ab}	0.06 ± 0.00^{ab}	0.03 ± 0.00^{c}	0.08 ± 0.01^{b}
18:3n-3	0.07 ± 0.05^{ab}	0.05 ± 0.00^{a}	0.04 ± 0.01^{a}	0.04 ± 0.00^{a}	0.08 ± 0.03^{ab}	0.08 ± 0.01^{b}	0.04 ± 0.00^{a}	0.08 ± 0.01^{b}
18:4n-3	0.16 ± 0.11^{a}	0.22 ± 0.00^{b}	0.08 ± 0.02^{a}	0.10 ± 0.01^{a}	0.20 ± 0.06^{ab}	0.23 ± 0.04^{b}	0.08 ± 0.03^{a}	0.14 ± 0.05^{c}
20:2n-6	0.07 ± 0.00^{a}	0.18 ± 0.05^{b}	0.11 ± 0.04^{a}	0.08 ± 0.00^{a}	0.08 ± 0.00^{a}	0.20 ± 0.01^{b}	0.17 ± 0.01^{b}	0.27 ± 0.01^{c}
20:4n-6	0.98 ± 0.01^{a}	1.17 ± 0.10^{b}	0.58 ± 0.16^{a}	0.65 ± 0.03^{c}	0.89 ± 0.12^{b}	1.19 ± 0.02^{b}	0.46 ± 0.07^{c}	1.08 ± 0.05^{d}
20:3n-3	0.07 ± 0.00^{a}	0.17 ± 0.02^{b}	0.12 ± 0.07^{ab}	0.08 ± 0.02^{a}	0.13 ± 0.04^{b}	0.18 ± 0.02^{b}	0.23 ± 0.03^{c}	0.33 ± 0.06^{d}
20:4n-3	0.04 ± 0.01^{a}	0.03 ± 0.02^{a}	0.05 ± 0.02^{ab}	0.05 ± 0.01^{a}	0.04 ± 0.01^{a}	0.07 ± 0.00^{b}	0.03 ± 0.00^{a}	0.14 ± 0.00^{c}
20:5n-3	5.12 ± 0.22^{a}	5.84 ± 0.08^{b}	5.68 ± 0.51^{ab}	5.35 ± 0.57^{ab}	5.53 ± 0.68^{ab}	5.55 ± 0.27^{ab}	6.16 ± 0.25^{c}	7.26 ± 0.28^{d}
22:4n-6	0.02 ± 0.00^{a}	0.12 ± 0.04^{bc}	0.02 ± 0.02^{a}	0.01 ± 0.00^{a}	0.08 ± 0.02^{b}	0.03 ± 0.01^{a}	0.05 ± 0.02^{a}	0.16 ± 0.09^{c}
22:5n-6	0.19 ± 0.05^{ab}	0.17 ± 0.01^{a}	0.10 ± 0.04^{b}	0.11 ± 0.04^{b}	0.19 ± 0.02^{a}	0.22 ± 0.11^{c}	0.11 ± 0.01^{b}	0.31 ± 0.04^{d}
22:5n-3	0.22 ± 0.02^{a}	0.44 ± 0.01^{b}	0.25 ± 0.08^{ac}	0.29 ± 0.02^{c}	0.32 ± 0.01^{c}	0.26 ± 0.02^{a}	0.12 ± 0.05^{d}	0.39 ± 0.06^{b}
22:6n-3	16.09 ± 0.42^{a}	10.77 ± 0.22^{b}	15.57 ± 1.10^{ac}	14.88 ± 1.38^{c}	15.74 ± 1.73^{ac}	14.75 ± 0.35^{c}	16.68 ± 1.15^{a}	17.10 ± 0.98^{a}
Σ Polyunsaturated	23.58 ± 0.50^{a}	21.34 ± 0.60^{b}	23.23 ± 1.62^{a}	22.16 ± 2.01^{ab}	23.83 ± 2.49^{a}	23.47 ± 0.33^{a}	24.94 ± 1.53^{a}	28.00 ± 1.60^{c}
Σ Total FA	45.18 ± 0.74^{ac}	38.35 ± 1.14^{b}	44.54 ± 2.43^{a}	42.80 ± 3.54^{a}	45.56 ± 3.40^{ac}	47.52 ± 0.56^{c}	46.45 ± 2.63^{ac}	55.08 ± 2.68^{d}

Different superscript letters within rows represent significant differences ($P < 0.05$).

Reference: *Biol. Bull.* **208:** 114–119. (April 2005)

Red Algae Respond to Waves: Morphological and Mechanical Variation in *Mastocarpus papillatus* Along a Gradient of Force

JUSTIN A. KITZES AND MARK W. DENNY*

Stanford University, Hopkins Marine Station, Pacific Grove, California, 93950

Abstract. Intertidal algae are exposed to the potentially severe drag forces generated by crashing waves, and several species of brown algae respond, in part, by varying the strength of their stipe material. In contrast, previous measurements have suggested that the material strength of red algae is constant across wave exposures. Here, we reexamine the responses to drag of the intertidal red alga *Mastocarpus papillatus* Kützing. By measuring individuals at multiple sites along a known force gradient, we discern responses overlooked by previous methods, which compared groups of individuals between "exposed" and "protected" sites. This improved resolution reveals that material strength and stipe cross-sectional area are both positively correlated with drag, suggesting that individual blades or populations can adjust either or both of these parameters in response to their mechanical environment. The combined effect of this variation is a stipe breaking force that is positively correlated with locally imposed drag. Owing to this response to drag, the estimated wave-imposed limit to thallus size in *M. papillatus* is larger than previously predicted and larger than sizes observed in the field, indicating that factors other than wave force alone constrain the size of this alga on wave-swept shores.

Introduction

Of all the organisms that inhabit the intertidal zone of rocky shores, sessile macroalgae face particularly great challenges in dealing with the effects of wave-induced water motion. Because algae lack the ability to "run and hide" during storms and their material strength is low relative to other biological materials (Denny *et al.*, 1989), algal distribution and abundance may be constrained by wave force (*e.g.*, Shaughnessy *et al.*, 1996). The question of whether algal populations respond to variation in wave intensity with morphological or mechanical adjustments to their shape or strength remains both open and intriguing.

Previous laboratory and field studies have demonstrated that some species of brown algae (Ochrophyta, class Phaeophyceae) exhibit considerable variability in breaking force, cross-sectional area, and material strength in response to differing exposure conditions (Charters *et al.*, 1969; Armstrong, 1987; McEacheron and Thomas, 1987; Gerard, 1987; Koehl and Alberte, 1988; Kraemer and Chapman, 1991a; Johnson and Koehl, 1994; Milligan and DeWreede, 2000). In contrast, no species of red algae (Rhodophyta) has revealed a correlation between mechanical properties and wave exposure, although differences in both biomass and planform area have been observed between exposed and protected sites (Carrington, 1990; Pratt and Johnson, 2002).

In this study, we assess the response of the common intertidal red alga *Mastocarpus papillatus* to varying levels of hydrodynamic force. In an attempt to uncover weak trends undetected in previous studies, we take a new approach to the measure of wave exposure. Whereas prior work has compared algal properties between groups of individuals from stretches of "exposed" and "protected" shore, we examine these same properties as they vary continuously along a measured gradient of imposed hydrodynamic force.

Drag is likely to be the most important hydrodynamic force applied to intertidal algae (Denny, 1988; Gaylord *et al.*, 1994), and as a result, it is the primary means by which algae interact mechanically with their flow environment. The force of drag, D, pulls an intertidal alga in the direction

Received 13 May 2004, accepted 27 December 2004.

* To whom correspondence should be addressed. E-mail: mwdenny@stanford.edu

of water flow, and is a function of both water velocity and the shape and surface area of the alga:

$$D = \tfrac{1}{2}\rho U^2 S C_d \quad (1)$$

Here ρ is the density of seawater (nominally 1025 kg m^{-3}), U is water velocity (m s^{-1}), S is maximal planform area (m^2, essentially half the wetted surface area of the frond), and C_d is the dimensionless coefficient of drag. In a comparison of groups of algae taken from "exposed" and "protected" sites, Carrington (1990) found no significant difference in stipe strength (breaking force divided by cross-sectional area at the breaking point) for *M. papillatus*, suggesting that the material properties of this species are not adjusted in response to its flow environment. However, this approach may be confounded by the fact that the planform area of this alga varies with wave exposure (Carrington, 1990). A small alga from a high-velocity, wave-exposed site might experience the same drag as a large alga from a lower-velocity, wave-protected site, in which case one might expect the strength of the two algae to be adjusted to similar values despite the difference in exposure. Here we explore how the morphological and mechanical properties of *M. papillatus* vary directly with imposed drag.

Materials and Methods

Species and location

Mastocarpus papillatus is perhaps the most common intertidal red alga along the central California coast (Abbott and Hollenberg, 1976); it grows in semi-erect clumps with multiple thalli emerging from a single crustose holdfast. ("Thallus" is the term for the combination of a stipe and the attached blade.) The alga's reproductive structures are contained in the papillae on the surface of each thallus, and, as a consequence, the potential reproductive output for a thallus is roughly proportional to its surface area (Bell, 1992). In this study, we take a single thallus as the sampling unit, without considering thallus location within a clump as a factor in the analysis. Although clumping reduces drag in the related alga *Chondrus crispus* (Johnson, 2001), Carrington (1990) found only mild drag-reducing interactions between groups of up to six closely packed thalli of *M. papillatus*. In this study, we did not encounter clumps larger than about a dozen densely packed individuals.

We collected samples from six sites along the rocky intertidal shore at Hopkins Marine Station (HMS), Pacific Grove, California (36°37′ N, 121°54′ W). All sites were within 0.5 m of locations where dynamometers had previously been used to measure wave-induced forces as a function of offshore wave height (Helmuth and Denny, 2003). These measurements allowed us to choose, *a priori*, sites with a range of wave exposures. Although these sites were not spaced equally along the shore, they were roughly equally spaced along a gradient of wave force. Sites were separated by a minimum of 10 m, and all were located at about 1.5 m above mean lower low water.

Data collection

We collected thalli during springtime low tides from April through June, 2003. Samples were fully hydrated before all experimental procedures to control for the possible effects of desiccation. We selected thalli that lacked obvious holes, tears, rotten areas, and other imperfections that could affect the breaking force. Thalli were selected with fewer than four major branches, as extensive branching patterns made accurate measurements of projected area difficult.

Blades were isolated from their neighbors and grasped with either a small alligator clip lined with rubber tubing or a small string tied with a slipknot. The clamp or string was attached to either a 500-g or a 1000-g recording spring scale (Pesola, resolution of ~0.05 N) and pulled with a steady force intended to separate the blade from the substratum within about 1 second. A small slider on the scale recorded the force at which the thallus broke.

Only samples that broke just above the holdfast at the lower part of the stipe were included in subsequent analyses. We measured the diameter of the stipe at the breaking point for each sample with a dissecting microscope and ocular micrometer (resolution of ~25 μm), and estimated cross-sectional area at the breaking point as the area of a circle having this diameter. Stipe cross sections were very nearly circular, and we do not believe this approximation introduced substantial errors into our calculations. Each sample blade was then flattened under a sheet of clear acrylic and digitally photographed. The planform area of each sample was estimated using ImageJ, an image analysis program distributed by the Research Services Branch of the National Institutes of Health. We calculated the material strength of each blade by dividing the breaking force for that sample by the cross-sectional area over which the break occurred.

Drag calculations

We modeled the drag for each sample with the standard relationship given by Equation 1. The C_d used for this study was taken from Carrington (1990) and Bell (1999), who calculated the drag coefficient of *M. papillatus* as

$$C_d = 0.156\ U^{-0.367},\ U \leq 3.5\ \text{m s}^{-1} \quad (2)$$

$$C_d = 0.099,\ U > 3.5\ \text{m s}^{-1} \quad (3)$$

Thus,

$$D = 79.9\ U^{1.633} S,\ U \leq 3.5\ \text{m s}^{-1} \quad (4)$$

$$D = 50.7\ U^2 S,\ U > 3.5\ \text{m s}^{-1} \quad (5)$$

The appropriate units are subsumed into the leading numerical coefficient. Carrington (1990) noted that for velocities less than 3.5 m s^{-1} (the flow conditions at which drag measurements were conducted), this model of drag accounted for 75.8% of variation in drag for the 60 samples she examined. The addition of nine other morphological parameters, including patterns of branching and papillar density, explained only an additional 9% of the variation, and we did not include them in the model of drag for this study. Equations 2 and 3 take into account the reconfiguration (a decrease in projected area as a blade bends over) of *M. papillatus* in flow.

A bottom-mounted wave gauge (SeaBird SBE26) deployed offshore at HMS measured significant wave height (the height of the highest one-third of waves) four times per day for 40 days just before the beginning of this study. We used the average significant wave height during this period (1.3 m) to calculate the relevant maximal water velocity for each site from the relationships reported by Helmuth and Denny (2003). These velocity calculations provide an estimate of the typical daily maximum velocity experienced by *M. papillatus* thalli at each sampling site over the 40 days immediately prior to the beginning of this study. Using this velocity and Eq. 1, we calculated the typical maximum drag imposed on each individual and used this as an index of the maximum force to which the individual thallus is subjected.

Statistical analyses were conducted using Systat 8.0 (SPSS Inc., Chicago, Illinois).

Results

We sampled a total of 121 fronds. All data (cross-sectional area, breaking force, material strength, drag) were $\log_{10}$-transformed prior to regression to correct departures from normality.

The results of our three ordinary-least-squares regressions are reported in Table 1. There are positive relationships between breaking force and drag (Fig. 1A, $r^2 = 0.212$, $P < 0.001$), cross-sectional area and drag (Fig. 1B, $r^2 = 0.048$, $P = 0.009$), and material strength and drag (Fig. 1C, $r^2 = 0.053$, $P = 0.007$); all are significant at the $\alpha = 0.017$ level ($\alpha = 0.05$ with a Dunn-Šidák correction for multiple comparisons).

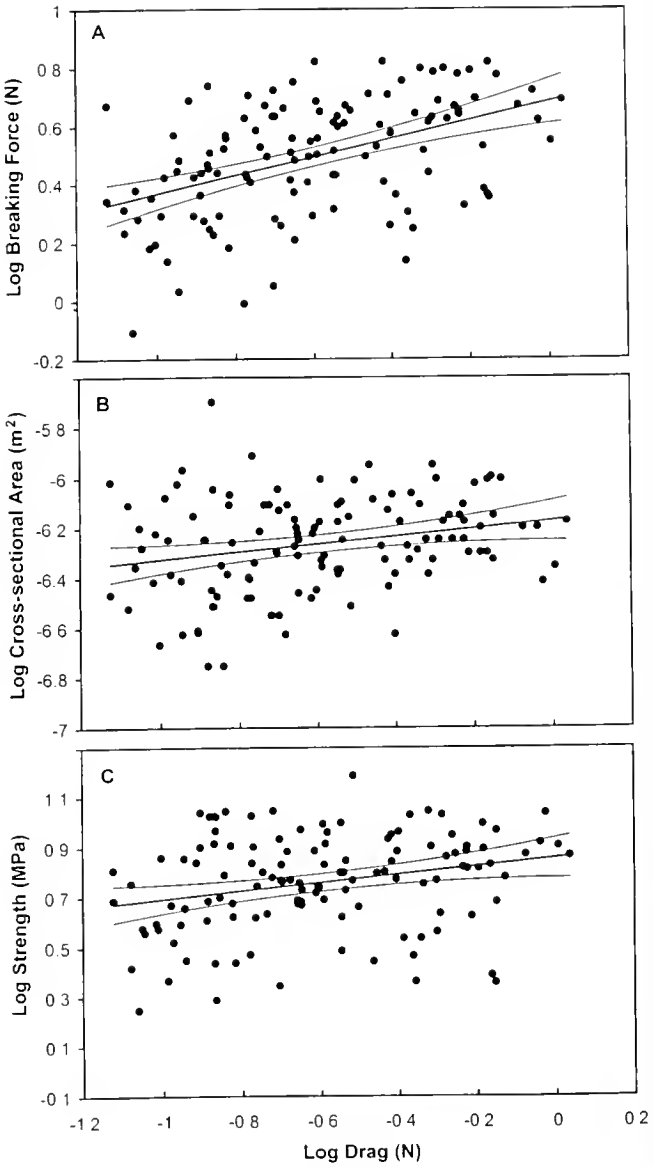

Figure 1. The $\log_{10}$ of (A) measured breaking force, (B) stipe cross-sectional area, and (C) material strength as a function of the $\log_{10}$ of calculated average maximal drag. Outer lines represent 95% confidence intervals on the regression. ($n = 121$; A: $r^2 = 0.212$, $P < 0.001$; B: $r^2 = 0.048$, $P = 0.009$; C: $r^2 = 0.053$, $P = 0.007$)

Table 1

Breaking force, stipe cross-sectional area, and stipe strength all increase with an increase in drag: results from regressions on $\log_{10}$ − $\log_{10}$ transformed data

Regression	Intercept	Slope	P	r^2
Breaking force on Drag	0.683	0.316	< 0.001	0.212
Cross-sectional area on Drag	−6.171	0.154	0.009	0.048
Strength on Drag	0.854	0.162	0.007	0.053

Probability values reported are the outcome of two-tailed Student's t tests against the null hypothesis that the slope estimates equal zero; $n = 121$ in all cases.

Discussion

Relationships along a drag gradient

Breaking force for *Mastocarpus papillatus* increases with increasing drag (Fig. 1A), implying that these algae respond

to their wave environment. This increase in breaking force can be due to an increase in stipe cross-sectional area, an increase in the breaking strength of the stipe material, or both. The trends shown in Figure 1B and 1C suggest that both adjustments are present in *M. papillatus*. The correlations between drag and strength, cross-sectional area, and breaking force may be the result either of selective forces acting on the population as a whole (by removing weak individuals) or of plastic responses to increased drag forces within individual thalli. Further investigation is needed to determine which of these two effects occurs in *M. papillatus*.

Our observed increases in stipe breaking force, cross-sectional area, and material strength with increasing drag stand in contrast to previously published results. Pratt and Johnson (2002) found no significant relationships between any of these three variables and wave exposure for the related algae *Mastocarpus stellatus* and *Chondrus crispus* when they compared groups of algae between exposed and protected sites. Carrington *et al.* (2001) also found no variation in tissue strength in *C. crispus* when using an exposed-*versus*-protected experimental design. Examining both *M. stellatus* and *C. crispus*, Dudgeon and Johnson (1992) report evidence that high wave exposure and freezing actually lower the strength of the stipes in these algae. Working with *M. papillatus*, Carrington (1990) found no significant differences in stipe strength among samples collected from sites characterized as exposed, protected, and intermediate-exposure.

The relationships between cross-sectional area and drag, although statistically significant, explains only 4.8% of the overall measured variability in cross-sectional area. Similarly, the relationship between strength and drag accounts for only 5.3% of the overall variation in strength. Thus, the natural variation within this *M. papillatus* population is large compared to the magnitude of the predictable adjustment of either cross-sectional area or strength with increasing drag. Given this variability, it is not surprising that studies based on a categorical comparison (exposed *versus* protected) failed to discern a relationship. Sampling techniques that directly quantify the drag on each individual, and therefore allow for calculation of the correlation between drag and morphological and mechanical parameters, are needed to detect such relatively weak signals. A technique similar to that used here has been used to measure the plastic variation in length of barnacle feeding legs as a function of flow speed (Arsenault *et al.*, 2001; Li and Denny, 2004).

Despite these high levels of natural variation, the observed increases in cross-sectional area and strength across the force gradient at Hopkins Marine Station may be biologically significant, an effect that may be obscured by the logarithmic plots shown in Figure 1. On average, cross-sectional area varies by 20%–25% and strength by 25%–30% over the range of drag sampled in this study, and together these trends contribute to a twofold variation in breaking force. Thus, despite the high degree of variability in these graphs and the lack of predictive power they imply, differences in strength and cross-sectional area across a drag gradient may still be of biological importance for individuals of this species.

The biological mechanisms by which tissue strength varies in red algae are unknown, although previous studies on brown algae suggest that the types and amounts of structural materials, the proportions of these materials, and the orientation of fibers in thalli may play a role (Wainwright *et al.*, 1976; Koehl and Wainwright, 1977; Babb, 1985). Modification of cell wall composition, including an augmentation of structural compounds, in response to wave forces has also been previously documented for brown algae (Kraemer and Chapman, 1991a). Kraemer and Chapman (1991b) also noted an increase in the incorporation of radioactively tagged carbon into cell wall tissue of *Egregia menziesii* under the application of a continuous force, which may play a role in strength variation.

Comparison with data from Carrington (1990)

Many of the results of this study corroborate the previous work of Carrington (1990), also at Hopkins Marine Station; a brief comparison is given in Table 2. The difference in the percentage of holdfast failures might be explained by seasonal differences: our study was conducted in spring and Carrington's in winter. Variation in the properties of *M. papillatus* between seasons has yet to be examined. Carrington reports a slightly larger mean cross-sectional area than we measured (Student's t test with unequal variances, $P = 0.005$). Since we find that cross-sectional area varies

Table 2

Comparison with data from Carrington (1990): although stipe strength is similar between these studies, our thalli had slightly smaller stipe cross sections and a higher incidence of holdfast failures

Calculations	Carrington (1990)	This study
Holdfast failures (%)	12% (n = 83)	36% (n = 240)
Mean stipe strength	6.73 MN/m^2 (n = 73, SD = 2.83)	6.27 MN/m^2 (n = 121, SD = 0.233)
Mean stipe cross-sectional area	0.71 mm^2 (n = 125, SD = 0.34)	0.60 mm^2 (n = 121, SD = 0.27)

with wave environment, this difference may be due to a higher average drag for Carrington's samples. Carrington's study did not include drag values, however, so this hypothesis cannot be tested. There is no significant difference between the two means of stipe strength (Student's t test with unequal variances, $P > 0.10$). Carrington found no differences among the mean stipe strength for her exposed, intermediate, and protected sites. However, our results suggest that within each of her sites she may have sampled across a variety of microhabitats, obscuring the relationships we found. Additional variation between our results and Carrington's could also be explained by the greater resolution of our measurements: we measured breaking force to the nearest 0.05 N and cross-sectional diameter to the nearest 25 μm; Carrington measured these two quantities to the nearest 1 N and 50 μm, respectively.

Predictions of maximum attainable size

Carrington found no significant relationship between cross-sectional area of the stipe and thallus planform area ($P \gg 0.05$), and neither did we ($r^2 = 0.023$, $P = 0.054$). Operating under the assumption that equal stipe cross-sectional area implied equal breaking force across blade sizes, Denny and Wethey (2001) proposed that Carrington's data could be used to predict the maximum size a blade could attain at a given water velocity. Setting Equation 4 (the expression for measured drag at low velocities) equal to the mean breaking force of Carrington's sample (4.8 N) and solving for planform area, they obtained the relationship:

$$S_{max} = 0.060\ U^{-1.633} \tag{6}$$

Maximum blade area (and, therefore, maximum potential reproductive output) are predicted to decrease rapidly with increasing water velocity (Fig. 2).

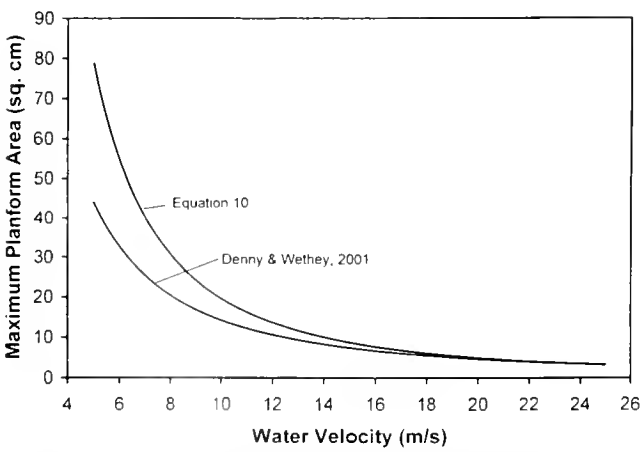

Figure 2. Prediction of maximum attainable frond size according to equation 10 ($S_{max} = 0.095\ U^{-2}$) and Denny and Wethey (2001, $S_{max} = 0.060\ U^{-1.633}$).

This prediction should be modified in two respects, however. First, Denny and Wethey (2001) assumed that the drag coefficient decreases steadily as velocity increases (Equation 2), but Bell (1999) suggests that the drag coefficient at the high velocities is constant (Equation 3). As a result, Equation 5 rather than Equation 4 should be used to describe the drag force imposed on a thallus. Second, in contrast to the supposition of Denny and Wethey (2001), our results (Table 1, Fig. 1A) show that breaking force, F, is not constant. On average:

$$\log(F) = 0.683 + 0.316 \log(D) \tag{7}$$

$$F = 4.820\ D^{0.316} \tag{8}$$

Inserting Equation 5 (the appropriate expression for drag) into Equation 8 (the expression for breaking force), we obtain an equation for breaking force as a function of water velocity and thallus area:

$$F = 16.67\ U^{0.632} S^{0.316} \tag{9}$$

Equating this expression for breaking force with Equation 5 (the expression for drag at high velocities) and solving for planform area, we find that

$$S_{max} = 0.198\ U^{-2} \tag{10}$$

This relationship is also shown in Figure 2. At low velocities, the maximum sizes it predicts are substantially larger than those predicted by Denny and Wethey (2001), and the two curves cross at a velocity of approximately 20 m s^{-1}.

The predictions of both Equations 6 and 10 appear to be larger than the sizes observed in nature. For example, *M. papillatus* is virtually absent at sites along the shore at Hopkins Marine Station that are exposed to average maximum water velocities in excess of 10 m s^{-1}, despite the prediction of Denny and Wethey (2001) that a relatively large blade of 14 cm^2 (or our prediction that an even larger blade of 20 cm^2) could survive that velocity. This disparity could have at least two causes. First, sites with an average maximum water velocity of 10 m s^{-1} may occasionally be exposed to much higher velocities (Helmuth and Denny, 2003), and it may be these rare high velocities (rather than the average maximum velocity) that limit the size and distribution of *M. papillatus*. For example, by either prediction, the single imposition of a water velocity of 20 m s^{-1} would remove all blades larger than 5 cm^2. Second, wave forces may not be the only constraint on the size of *M. papillatus* on wave-swept shores. Samples that exhibited weakening of the stipe tissue due to storm damage, repeated stress, grazing, or other factors were not included in our collection for this study. It seems likely that biotic and nonhydrodynamic abiotic stressors such as these reduce the maximum size (and reproductive output) attainable by a

frond in the field to below the size we have estimated here for intact fronds.

Conclusions

When examined along a continuous gradient of wave force, *Mastocarpus papillatus* exhibits statistically significant increases in breaking force, cross-sectional area, and material strength with an increase in estimated drag, although there is substantial variation about this trend. The finer resolution of this microhabitat-based approach allows us for the first time to discern these trends in an alga of the order Rhodophyta.

Attention should be paid to the possible biological explanations behind these relationships, especially to the relationship between strength and drag. Possible chemical or physical variation within *M. papillatus* tissue itself, particularly in the cell wall composition, might help explain this relationship.

Predictions of the wave-limited size of this alga indicate that factors other than simply wave force contribute to limiting the size of fronds in the field.

Acknowledgments

We thank Chris Harley, Patrick Martone, Luke Hunt, Luke Miller, Emily Freed, and Kallin Tea. Special thanks also go to Jim Watanabe for his help with statistical analyses. This work was supported by NSF grant OCE 9985946 to MWD.

Literature Cited

Abbott, I. A., and G. J. Hollenberg. 1976. *Marine Algae of California.* Stanford University Press, Stanford, CA. 827 pp.

Armstrong, S. L. 1987. Mechanical properties of the tissues of the brown alga *Hedophyllum sessile* (C. Ag.) Setchell: variability with habitat. *J. Exp. Mar. Biol. Ecol.* **114:** 143–151.

Arsenault, D. K., K. B. Marchinko, and A. R. Palmer. 2001. Precise tuning of barnacle leg length to coastal wave action. *Proc. R. Soc. Lond. B* **268:** 2149–2154.

Bahb, I. 1985. The biomechanics of Maine coast kelps: their distribution, morphology, and mechanical properties. M.Sc. thesis, University of Maine, Orono. 126 pp.

Bell, E. C. 1992. Consequences of morphological variation in an intertidal macroalga: physical constraints on growth and survival of *Mastocarpus papillatus* Kützing. PhD. thesis, Stanford University.

Bell, E. C. 1999. Applying flow tank measurements to the surf zone: predicting dislodgment in the Gigartinaceae. *Phycol. Res.* **47:** 159–166.

Carrington, E. 1990. Drag and dislodgment of an intertidal macroalga: consequences of morphological variation in *Mastocarpus papillatus* Kützing. *J. Exp. Mar. Biol. Ecol.* **139:** 185–200.

Carrington, E., S. P. Grace, and T. Chopin. 2001. Life history phases and the biomechanical properties of the red alga *Chondrus crispus* (Rhodophyta). *J. Phycol.* **37:** 699–704.

Charters, A. C., M. Neushul, and C. Barilotti. 1969. The functional morphology of *Eisenia arborea. Proc. Int. Seaweed Symp.* **6:** 89–105.

Denny, M. W. 1988. *Biology and the Mechanics of the Wave-Swept Environment.* Princeton University Press, Princeton, NJ.

Denny, M., and D. Wethey. 2001. Physical processes that generate patterns in marine communities. Pp. 3–37 in *Marine Community Ecology,* M. Bertness, S. Gaines, and M. Hay, eds. Sinauer Associates, Sunderland, MA.

Denny, M. W., V. Brown, E. Carrington, G. Kraemer, and A. Miller. 1989. Fracture mechanics and the survival of wave-swept macroalgae. *J. Exp. Mar. Biol. Ecol.* **127:** 211–228.

Dudgeon, S. R., and A. S. Johnson. 1992. Thick *vs.* thin: thallus morphology and tissue mechanics influence differential drag and dislodgement of two co-dominant seaweeds. *J. Exp. Mar. Biol. Ecol.* **165:** 23–43.

Gaylord, B., C. A. Blanchette, and M. W. Denny. 1994. Mechanical consequences of size in wave-swept algae. *Ecol. Monogr.* **64:** 287–313.

Gerard, V. A. 1987. Hydrodynamic streamlining of *Laminaria saccharina* Lamour in response to mechanical stress. *J. Exp. Mar. Biol. Ecol.* **107:** 237–244.

Helmuth, B., and M. W. Denny. 2003. Predicting wave exposure in the rocky intertidal zone: do bigger waves always lead to larger forces?. *Limnol. Oceanogr.* **48:** 1338–1345.

Johnson, A. S. 2001. Drag, drafting, and mechanical interactions in canopies of the red alga *Chondrus crispus. Biol. Bull.* **201:** 126–135.

Johnson, A. S., and M. A. R. Koehl. 1994. Maintenance of dynamic strain similarity and environmental stress factor in different flow habitats: thallus allometry and material properties of a giant kelp. *J. Exp. Mar. Biol. Ecol.* **195:** 381–410.

Koehl, M. A. R., and R. S. Alberte. 1988. Flow, flapping, and photosynthesis of *Nereocystis leutkeana:* a functional comparison of undulate and flat blade morphologies. *Mar. Biol.* **99:** 435–444.

Koehl, M. A. R., and S. A. Wainwright. 1977. Mechanical adaptations of a giant kelp. *Limnol. Oceanogr.* **22:** 1067–1071.

Kraemer, G. P., and D. J. Chapman. 1991a. Biomechanics and alginic acid composition during hydrodynamic adaptation by *Egregia menziesii* (Phaeophyta) juveniles. *J. Phycol.* **27:** 47–53.

Kraemer, G. P., and D. J. Chapman. 1991b. Effects of tensile force and nutrient availability on carbon uptake and cell wall synthesis in blades of juvenile *Egregia menziesii* (Turn.) Aresch. (Phaeophyta). *J. Exp. Mar. Biol. Ecol.* **149:** 267–277.

Li, N. K., and M. W. Denny. 2004. Limits to phenotypic plasticity: flow effects on barnacle feeding appendages. *Biol. Bull.* **206:** 121–124.

McEacheron, J. C. T., and M. L. H. Thomas. 1987. Attachment strength of *Ascophyllum nodosum* (L.) LeJolis and exposure to wave action. *Bot. Mar.* **30:** 217–222.

Milligan, K. L. D., and R. E. DeWreede. 2000. Variations in holdfast attachment mechanics with development stage, substratum-type, season, and wave exposure for the intertidal kelp species *Hedophyllum sessile* (C. Agardh) Setchell. *J. Exp. Mar. Biol. Ecol.* **254:** 189–209.

Pratt, M. P., and A. S. Johnson. 2002. Strength, drag, and dislodgment of two competing intertidal algae from two wave exposures and four seasons. *J. Exp. Mar. Biol. Ecol.* **272:** 71–101.

Shaughnessy, F. J., R. E. DeWreede, and E. C. Bell. 1996. Consequences of morphology and tissue strength to blade survivorship of two closely related Rhodophyta species. *Mar. Ecol. Prog. Ser.* **136:** 257–266.

Wainwright, S. A., W. D. Biggs, J. D. Currey, and J. M. Gosline. 1976. *Mechanical Design in Organisms.* Edward Arnold, London. 423 pp.

Reference: *Biol. Bull.* **208:** 120–126. (April 2005)

Sex Reversal in Pairs of *Lythrypnus dalli:* Behavioral and Morphological Changes

EDMUND W. RODGERS, SHELIA DRANE, AND MATTHEW S. GROBER*

Department of Biology, Georgia State University, P.O. Box 4010, Atlanta, Georgia 30302-4010

Abstract. In *Lythrypnus dalli*, the bluebanded goby, reproductive success is primarily determined by functional sex, and functional sex is determined largely by rank in the dominance hierarchy. In most natural social groups of *L. dalli*, one male is at the apex of the hierarchy, and 1 to 7 females are lower in rank. When a male exits the group, a female ascends to the top of the hierarchy and becomes a male. We have examined this process in a simplified environment—a pair of females—that allows us to identify behavior associated with the formation of a dominance relationship and any other phenotypic changes associated with dominance, sex change or both. We found that pairs of *L. dalli* females quickly and readily form stable dominance relationships, with the dominant fish changing sex into a male. This dominant animal also rapidly increases in body size and length of its dorsal fin. In summary, dominant *L. dalli* females change sex in this simplified environment, providing excellent opportunities to examine the early behavioral and morphological changes associated with dominance and sex change.

Introduction

Social context often determines how a given individual responds to behavioral stimuli, with individuals modifying their behavior on the basis of the behavior of the individuals around them. This is especially true in several species of protogynous (female to male) sex-changing fish, where sex reversal is socially controlled. In these species, a unique pattern of behavior stimulates one individual to change sex while inhibiting others (Robertson, 1972; Ross *et al.*, 1983). Two social factors are thought to be the primary regulators of sex change: inhibition by males and stimulation from other females (Robertson, 1972; Shapiro, 1979). Without sufficient social stimulation (*i.e.*, in isolation), fish capable of sex reversal might not initiate sex change (Cole and Shapiro, 1995; Carlisle *et al.*, 2000). Size advantage (Warner *et al.*, 1975) contributes to the determination of which animal changes sex, but behavioral interactions are also critical determinants (Lutnesky, 1996; Munday, 2002). Larger size often equates with increased success in aggressive encounters and therefore social dominance, providing a proximate mechanism for the size advantage hypothesis. In protogynous sex changers, the most reproductively significant resource that dominance affords is "maleness"; thus the reproductive payoff for dominance is extremely large, and females would be highly motivated to increase their aggressive behavior in times of social instability (*i.e.*, in the absence of a dominant male).

The study of *Lythrypnus dalli* (Gilbert, 1890) had previously dealt exclusively with larger social groups (>3), and it was not known whether sex change could be induced in pairs of females. This study used pairs of fish to closely examine changes associated with the acquisition of dominance and, potentially, sex change. In a group environment, dominance relationships are more difficult to tease apart owing to multiple interactions between individuals in the group, whereas in pairs there are fewer social variables contributing to an animal's behavior. We found that one of the pair quickly changes to male, as evidenced by male-typical behavior and male reproductive morphology.

Materials and Methods

We use four measures of "maleness" to determine if any of the fish changed sex: (1) display of male-typical courting behavior; (2) male-typical papilla ratio, defined as a length-

Received 1 July 2004; accepted 12 December 2004.
* To whom correspondence should be addressed. E-mail: mgrober@gsu.edu

to-width ratio greater than 1.6 (female ~1.0 l/w); (3) the presence of an accessory gonadal structure (AGS); and (4) the presence of fertilized eggs, an unequivocal indication of functional sex change.

Subjects

We selected 32 female specimens of *Lythrypnus dalli* with lengths between 23 and 30 mm for the study. Sex was determined by examination of the external genital papilla (Behrents, 1983). The papilla ratio in females of this species is about 1.0, compared with about 2.0 in the males (St. Mary, 1994); the largest ratio at the start of this experiment was 1.3. Fish with female-typical papilla have gonads consisting of more than 95% ovarian tissue (St. Mary, 1994). During the experiments, animals were housed in 33-l aquaria, each with an individual filter system (Marineland), at 20–21.1°C; fed twice daily using a commercially prepared diet (OSI Marine Labs); and kept on a 12-h light/dark cycle. One group of fish was collected (California Fish & Game permit # 803034-01) on Santa Catalina Island, California, in May 2002 (pre-breeding season), using an anesthetic solution of quinaldine sulfate (Sigma Chemical) and hand-nets. A second group of fish was collected, using the same methods, during the breeding season in late June 2002. Prior to the experiments, the animals were kept in 180-l holding tanks.

Experimental design

The study is divided into two experiments. In experiment 1, morphological traits and behavioral interactions were quantified between eight pairs of individuals identified as females. External morphological data were collected prior to pairing (standard length, mass, and papilla ratio, described below). The pairs were observed until eyed eggs (a marker of fertilization), indicating functional sex change, were seen, or until 14 days, an adequate amount of time for sex change in this species (Reavis and Grober, 1999), had elapsed. Experiment 2 was similar to experiment 1 and was designed to confirm a novel observation in experiment 1, that dominant fish exhibited disproportional growth of the longest rays of the dorsal fin. The behavior of the eight pair of fish in experiment 2 was not observed closely. In both experiments, the pairing and morphological measurements (with the exception of initial dorsal fin length) were identical (see below).

At the completion of each experiment, animals were given an overdose of tricaine methanesulfate (MS 222), and their morphological characters were measured again. This included measurement of the longest dorsal ray (see Results). The animals were placed in Bouin's fixative, the gonads were dissected out to examine internal morphology, and digital photographs of all the gonads were taken to aid in analysis.

During sex reversal, *L. dalli* undergoes gonadal reorganization (St. Mary, 1994), which in a number of sex-changing gobies involves degeneration of ovarian tissue (Sadovy and Shapiro, 1987) and generation of AGS and testicular tissue (Cole and Shapiro, 1990). In *L. dalli*, the presence or absence of the AGS is the primary indicator of functional sex; males have a highly developed AGS and females have none. Visual inspection was used to assess the composition of reproductive tissue, *i.e.*, presence of eggs and presence of AGS. Gonad sex was verified using standard paraffin histology followed by staining with hematoxylin and eosin.

Pairing

At the start of each experiment, animals were removed from the holding tank and anesthetized using MS 222. Mass and standard length were recorded. Papilla ratios were measured, and digital images were also taken. Animals were paired by standard length (within 2 mm of each other) and body mass (within 0.1 g). The fish were individually identified by their banding pattern, which did not appear to change nor have an effect on their behavior. Two animals were placed together into a 33-l tank with a single PVC tube to serve as the nest (St. Mary, 1994).

Observations and behavior

The behavior of each pair was observed twice daily, once in the morning and once in the afternoon, for 10 min each session. Data were recorded on paper and then transferred to a computer spreadsheet. The fish were given one day to acclimate before observations began. The observer recorded the number of approaches, displacements, jerks, bites, nips, solicitations, and tail-waggles. In addition, the observer noted which animal resided in the nest tube, if either animal was gravid, and whether eggs were present in the tube.

An approach is defined as a fish moving within 5 cm of the other fish. Movement away from the approaching fish is recorded as a displacement. Jerks are a male-typical behavior used during courtship (Behrents, 1983), and involve a saltatory swim motion with movement laterally as well. Because jerks can be directed either at the female or around the nest without being directed at a fish, a jerk towards a female is scored as both an approach and a jerk. Bites are aggressive interactions in which one fish bites the other after an approach. In contrast, nips follow a jerk to a female, with a male nipping the tail of the female. This behavior is also part of the courting process. Solicitations are produced by females when they move within 12 cm of the male in his line of view. Tail waggles are displayed by both sexes: the fish remains stationary while moving its tail back and forth.

Statistics

Morphological data were analyzed using parametric statistics. For traits that had "before" and "after" measures, we used paired student's *t*-tests (standard length and fin length in experiment 2). For fin length in experiment 1, we used an unpaired *t*-test to look at differences between males and females. We also used a *t*-test to examine whether papillar morphology was significantly different between new males and females. The distributions of the frequencies of the various behaviors for newly sex-changed males and females did not meet the criteria for parametric statistics (*e.g.*, normality, homogeneity of variance); thus we used nonparametric methods to examine group differences. All behavioral analyses were conducted with the Wilcoxon signed rank test. Values for mean and median were similar, indicating a symmetrical distribution. Simple linear regressions were employed to examine the relationship between known interdependent behaviors (*e.g.*, approaches regressed on displacements). Though the fish were size-matched, we used logistic analysis (SAS) to examine whether small differences in size predicted which individual would change sex. Significance level in all cases was set at $P < 0.05$. Mean values ± standard error of the mean (SEM) are given. All analyses were carried out using the Statview 5.01 (SAS Institute Inc.) unless otherwise noted.

Results

In all cases, the pairs readily established a stable dominance relationship, defined as one individual (the dominant) instigating the majority of encounters (Fig. 1a) and exhibiting male courtship behavior (Fig. 1b), while the other individual (the subordinate) is displaced as a result of the encounter (Fig. 1c). In all cases the dominant individual initiated spawning behavior with the subordinate individual that resulted in a clutch of eggs. Of the 8 clutches, 4 were verified as fertile; in the other 4 cases, the male consumed the clutch before verification. At the completion of the experiment, all dominants had a male papilla ratio as well as an AGS (Figs. 2, 3). Using our criteria, we demonstrated

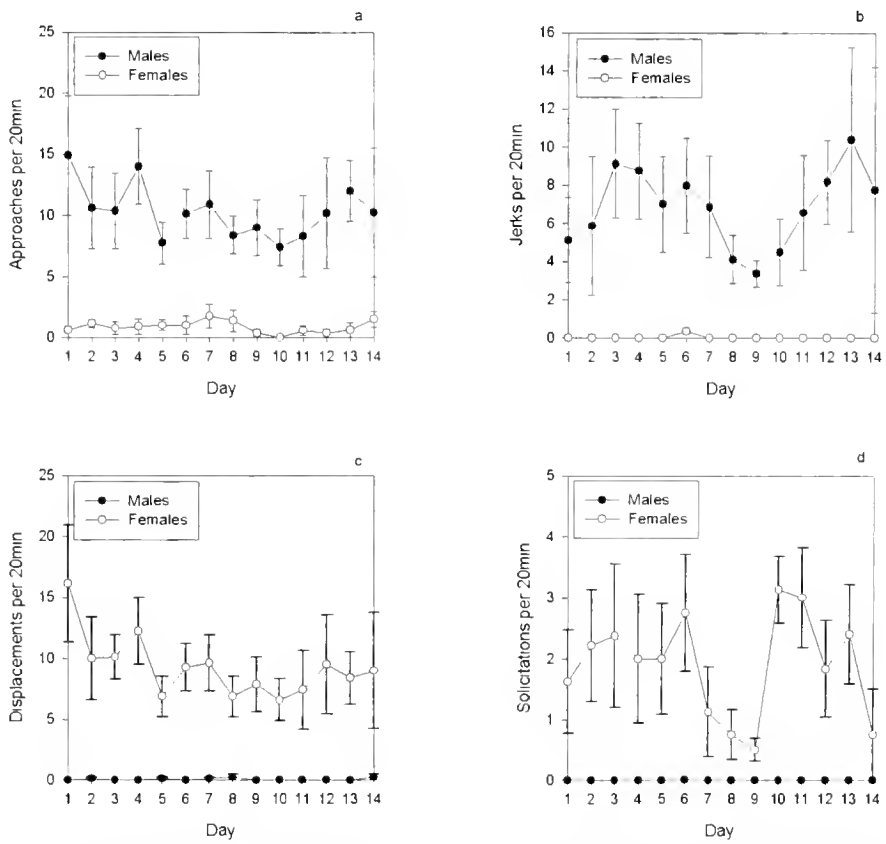

Figure 1. Changes in sex-typical behavior over the course of experiment. Animals that are labeled male are individuals that changed sex— *i.e.*, those that would become male. (a) Males approach and females rarely do, demonstrating dominance. (b) Jerking behavior, a major component of male courting behavior, is exclusively produced by males. (c) Females were displaced at high rates compared to males. (d) Solicitations, a type of female courting behavior, are exhibited exclusively by females. Note the similar pattern of behavior in b and d.

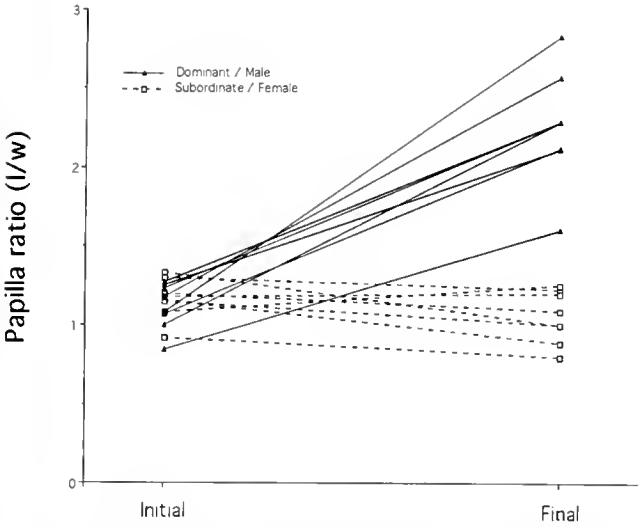

Figure 2. Papilla length/ width ratios at the start and conclusion for all animals in experiment 1. Dominants (males) had a significantly higher ratio than subordinates (females) at the end of the experiment ($t = 8.64$, df = 14, $P < 0.0001$).

that the dominant individual in a pair of females changed sex from female to male.

Morphological changes

All fish initially had a female-typical papilla ratio (mean ± SEM: 1.15 ± 0.061). There was no difference in papilla ratio at the start of the experiment ($t = 0.732$, df = 14, $P > 0.05$) between fish that became male (mean ± SEM: 1.15 ± 0.102) and those that remained female (mean ± SEM: 1.17 ± 0.086). After sex change there was a significant change to a male-typical papilla in the fish that demonstrated male-typical behavior ($t = 8.64$, df = 14, $P < 0.0001$). Female papilla ratio remained the same, 1.09 ± 0.052, whereas the ratio in sex changers more than doubled to 2.26 ± 0.127 (Fig. 2).

All dominant animals exhibited unambiguous male-typical gonad morphology that included the presence of sperm and an AGS. All subordinate individuals were gravid, and eggs were clearly visible within the ovary upon inspection. These results were verified histologically (Fig. 3).

The standard length of dominant individuals changed significantly over the course of the experiment ($P < 0.05$); that of subordinates did not ($P > 0.05$). When we examined the magnitude and direction of the change, we found that dominants grew significantly more relative to subordinates (paired *t*-test, $t = 4.528$, df = 15, $P = 0.0003$).

In experiment 1, we noted that the dorsal fin of the dominant fish was elongated. Although we had not measured initial fin length, at the conclusion of the experiment we measured the longest dorsal ray. Dominants had a mean fin length of 10.47 ± 0.539 mm, while subordinates had a mean of 5.5 ± 0.269 mm ($t = 8.475$, df = 14, $P < 0.0001$). To control for dominant fish simply growing more, we used a ratio of fin length to body length. This ratio was significantly different: subordinates had a smaller fin with an average of 4.648 ± 0.137 fin lengths per body length, and dominants had a ratio of 2.64 ± 0.143 ($t = 10.129$, df = 14, $P < 0.0001$).

Experiment 2 verified the marked change in fin length observed in the first experiment. Future dominants and subordinates did not have different fin lengths at the beginning of the experiment ($t = 1.669$, df = 8; $P > 0.05$), but the dominant fish had a significantly longer fin at the end of the experiment ($t = 4.091$, df = 8; $P = 0.0035$). Dominant individuals exhibited a pronounced lengthening of their longest dorsal ray, while many of the subordinates showed a fin shortening.

We attempted to minimize size as a major contributing factor; however, small differences in size did exist between the paired animals. To assess whether these small differences in standard length were predictive of which animal changed sex, we ran a logistical regression. Our results suggest that the size differences present in this experiment were not a good predictor of which animal would become dominant (Wald $\chi^2 = 0.034$, $P = 0.8532$, df = 1, $\beta = -0.05006$).

Behavior

Verification of egg fertility in experiment 1 was difficult because of consumption of clutches by males (see below). Four of eight pairs completed sex change in less than 14 days, as determined by the presence of fertilized eggs. In the four remaining pairs, males exhibited all other sex-typical characteristics, but consumed at least one complete clutch of eggs. Because fish that parented and fish that consumed their eggs displayed similar rates of behavior in all measures, we grouped them in the behavioral analysis.

A clear dominance relationship was evident from the first observational session and persisted unchanged throughout the experiment (Fig. 1). The dominant fish produced male-typical behavior and began courting the subordinate. The dominant fish instigated the vast majority of behavioral interactions, evidenced by high rates of approach behavior. Dominants displayed significantly higher rates of aggressive and courtship behavior (approaches and jerks, $P < 0.05$, Fig. 1a, b). Subordinates displayed significantly more submissive and female-typical behavior (displacements and solicitations, $P < 0.05$, Fig. 1c, d). All dominants jerked and subordinates generally did not jerk, although there were rare individual displays over the course of the experiment. Subordinate fish were displaced at high rates (9.138 per 20 min, Fig. 1c) compared to dominants (0.062 per 20 min). There

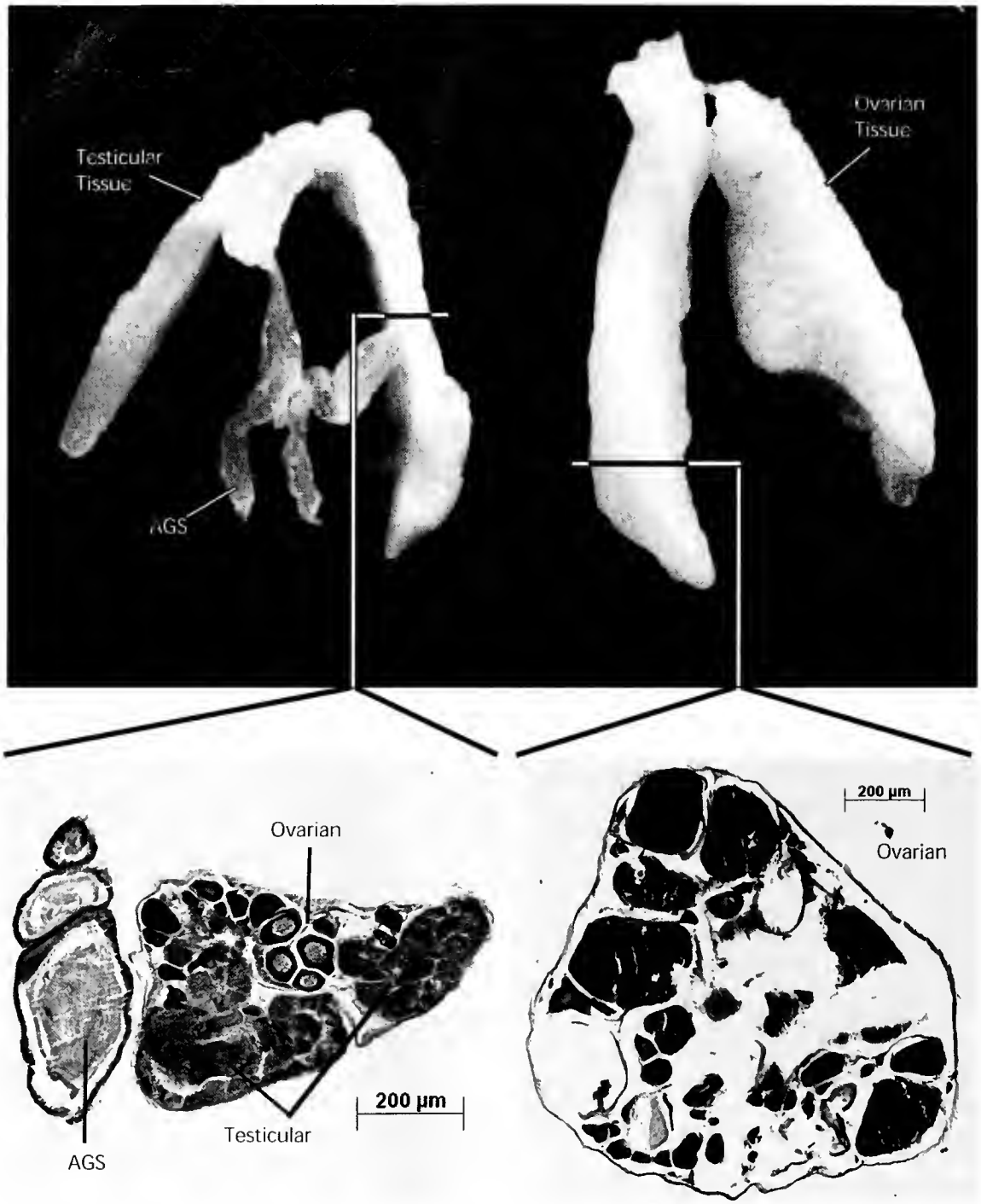

Figure 3. Gonad morphology of a typical male (left) and female (right). The cross-section of each type is shown underneath. Note that the male gonad contains mostly testicular tissue, some ovarian tissue, and an accessory gonadal structure (AGS). The female gonad contains only ovarian tissue and is visibly full of eggs.

was a significant association between approaches and displacements, such that when a dominant approached, the subordinate was usually displaced ($R^2 = 0.917$; $P < 0.001$). The dominant guarded or resided in the tube for most of the time.

Other behavior occurred at a far lower frequency, including bites, nips, and tail waggles. Dominant individuals produced bites and nips. Tail-waggle was the one behavior that did not show an overall sex/dominance bias, but was exhibited by both dominants and subordinates.

Discussion

When two female bluebanded gobies were paired, in our experimental conditions, in all cases, one fish established dominance over the other, with that fish instigating most of the encounters and winning nearly all of them. The dominant fish became male, exhibiting all behavioral and morphological characters associated with that sex. The subordinate fish remained female and exhibited all associated sex-typical behavior and morphology.

In *Lythrypnus dalli*, body size is sexually dimorphic, with males being larger (Wiley, 1976). In our work, dominant individuals grew more than subordinates and changed sex. The observed sexual dimorphism in growth rate is consistent with previous data from St. Mary (1994); however, we cannot address whether the increase in growth is a result of sex change or of dominance. Dominance rank has been shown to affect the growth rate of individuals within a hierarchy of sex-changing clown fish (Buston, 2003). We also found that the dorsal fin was elongated in the dominant, sex-changed fish. The dorsal fin is known to be sexually dimorphic (Wiley, 1976), but we did not expect the rapidity and magnitude of the changes we observed in the first experiment. Experiment 2 confirmed that the fin lengthened dramatically in the dominant individual over the course of the experiment. The dorsal fin shrank in many of the subordinate fish, but whether this is a natural process or the result of aggressive encounters with the dominant is unknown. As with the change in growth rate, we cannot say whether the fin elongation is caused by the sex-change process or is modulated by dominance status. If the latter is the case, then this trait can potentially be used as an index of rank within a hierarchy.

Simplification of the social group to a pair of animals, as in our study, revealed an interdependence of behavior between males and females that was not seen in previous studies using larger groups of fish. This is best illustrated in Figure 1b and d, where courtship behavior (solicitations and jerks) clearly shows the same pattern over time. Although the precise nature of the interaction is unclear, female behavior apparently had an impact on the rate of male behavior, an effect that would be difficult to examine in a group with multiple females.

Like Reavis and Grober (1999), we used fertilized eggs as a marker for complete sex change and allowed the experiment to run for a maximum of 14 days. All tanks had eggs in the nest within the 14 days, but only half of those nests had eggs that remained until they could be verified as fertile. In the four other groups, the males did not display paternal care. These males ate the eggs after day 10 of the experiment, making it impossible to use the presence of eyed eggs to verify fertility and thus terminate the experiment. The bulk of the data indicates that these eggs were viable. Clutch-consuming males exhibited all male-typical behavior (approaches, jerks, bites, and nips). Morphological examination revealed no differences between males that demonstrated appropriate care and those that did not. The gonads of the two groups were indistinguishable from one another, and both groups developed an AGS, the hallmark of the male sex. There were no differences in the papilla between the two groups, and all males displayed sexually dimorphic elongation of the longest dorsal rays. In addition, parenting males had fertile clutches at the same time as egg consumption was occurring, suggesting that all of the males were capable of fertilizing eggs.

In experiments with groups of fish greater than two (Reavis and Grober, 1999), the amount of time required for full sex change depended on the size of the individuals in the group upon male removal. In groups where the size asymmetry between the top two females was greater than 10%, sex change occurred more rapidly than in groups where the size asymmetry was less than 10%. The observed delay was determined to be the result of an increase in time spent resolving the dominance relationship between the top two individuals. Individuals of similar size take longer to settle a conflict than individuals of different sizes (Enquist *et al.* 1990; Koops and Grant, 1993). In this experiment, we used pairs of size-matched individuals; thus we were surprised to find that the contestants quickly resolved the dominance relationship. One possible explanation is that in a group, individuals may receive contradictory signals. This could result from being dominated by one individual but also receiving positive stimulus by dominating other individuals in the group, thus prolonging conflict resolution. In dyadic contests, the signals are straightforward; one animal wins the encounters while the other loses them, thereby shortening the time and probably the number of interactions required to form a stable dominance relationship.

In summary, two females is a sufficient group size to induce sex change in *L. dalli*, as evidenced by one individual exhibiting male typical gonads, external genitalia, behavior patterns, and often fertilized eggs. When an *L. dalli* female becomes dominant, the first noticeable morphological change is the elongation of the dorsal fin. Dominant individuals also grow more rapidly.

Acknowledgments

The authors thank Cathleen Drilling for her work in collecting the experimental animals, help with behavioral observations, and gonad histology; Michael Black for animal collection and behavioral observations; and William Lonergan and Beth Stokes for their help with behavioral observations. We also thank Ryan Earley for his help with statistical analysis, and Dr. Charles Derby and an anonymous reviewer for their comments on an earlier version of this paper. This work was supported by NSF IBN 9723817 to Matthew S. Grober, the Georgia Research Alliance and

the Center for Behavioral Neuroscience, an STC program of the NSF agreement #IBN- 9876754.

Literature Cited

Behrents, K. C. 1983. The comparative ecology and interactions between two sympatric gobies (*Lythrypnus dalli* and *Lythrypnus zebra*). Ph.D. dissertation, University of Southern California.

Buston, P. 2003. Size and growth modification in clownfish. *Nature* **424:** 145–146.

Carlisle, S. L., S. K. Marxer-Miller, A. V. M. Canario, R. F. Oliveira, L. Carneiro, and M. S. Grober. 2000. Effects of 11-ketotestosterone on genital papilla morphology in the sex changing fish *Lythrypnus dalli*. *J. Fish Biol.* **57:** 445–456.

Cole, K., and D. Y. Shapiro. 1990. Gonad structure and hermaphroditism in the gobiid genus *Coryphopterus* (Teleostei: Gobiidae). *Copeia* **4:** 996–1003.

Cole, K., and D. Y. Shapiro. 1995. Social facilitation and sensory mediation of adult sex change in a cryptic, benthic marine goby. *J. Exp. Mar. Biol. Ecol.* **186:** 65–75.

Enquist, M., O. Leimar, T. Ljundberg, Y. Mallner, and N. Segerdahl. 1990. A test of sequential assessment game: fighting in the cichlid fish *Nannacara anomala*. *Anim. Behav.* **40:** 1–14.

Koops, M. A., and J. W. A. Grant. 1993. Weight asymmetry and sequential assessment in convict cichlid contests. *Can. J. Zool.* **71:** 475–479.

Lutnesky, M. 1996. Size-dependent rate of protogynous sex change in pomacanthid angelfish. *Centropyge potteri*. *Copeia* **1:** 209–212.

Munday, P. L. 2002. Bi-directional sex change: testing the growth rate advantage model. *Behav. Ecol. Sociobiol.* **52:** 247–254.

Reavis, R., and M. S. Grober. 1999. An integrative approach to sex change: social, behavioral and neurochemical changes in *Lythrypnus dalli* (Pisces). *Acta Ethol.* **2:** 51–60.

Robertson, D. R. 1972. Social control of sex reversal in a coral-reef fish. *Science* **177:** 1007–1009.

Ross, R. M., G. S. Losey, and M. Diamond. 1983. Sex change in a coral-reef fish: dependence of stimulation and inhibition on relative size. *Science* **221:** 574–575.

Sadovy, Y., and D. Y. Shapiro. 1987. Criteria for the diagnosis of hermaphroditism in fish. *Copeia* **1:** 136–156.

Shapiro, D. Y. 1979. Social behavior, group structure and the control of sex reversal in hermaphrodite fish. *Adv. Study Behav.* **10:** 43–102.

St. Mary, C. M. 1994. Sex allocation in a simultaneous hermaphrodite, the blue banded goby (*Lythrypnus dalli*)—the effect of body size and behavioral gender and the consequences for reproduction. *Behav. Ecol.* **5:** 304–313.

Warner, R. R., D. R. Robertson, and E. G. Leigh. 1975. Sex change and sexual selection. *Science* **190:** 633–638.

Wiley, J. W. 1976. Life histories and systematics of the Western North American gobies *Lythrypnus dalli* (Gilbert) and *Lythrypnus zebra* (Gilbert). *Trans. S. Diego Soc. Nat. Hist.* **18:** 169–184.

Reference: *Biol. Bull.* **208:** 127–137. (April 2005)

Eyestalk Ablation Has Little Effect on Actin and Myosin Heavy Chain Gene Expression in Adult Lobster Skeletal Muscles

SCOTT MEDLER[1,*], KITTY J. BROWN[1], ERNEST S. CHANG[2], AND DONALD L. MYKLES[1]

[1] *Department of Biology, Colorado State University, Fort Collins, Colorado 80523; and* [2] *Bodega Marine Laboratory, University of California, P.O. Box 247, Bodega Bay, California 94923*

Abstract. The organization of skeletal muscles in decapod crustaceans is significantly altered during molting and development. Prior to molting, the claw muscles atrophy dramatically, facilitating their removal from the base of the claw. During development, lobster claw muscles exhibit fiber switching over several molt cycles. Such processes may be influenced by the secretion of steroid molting hormones, known collectively as ecdysteroids. To assay the effects of these hormones, we used eyestalk ablation to trigger an elevation of circulating ecdysteroids and then quantified myofibrillar mRNA levels with real-time PCR and myofibrillar protein levels by SDS-PAGE. Levels of myosin heavy chain (MHC) and actin proteins and the mRNA encoding them were largely unaffected by eyestalk ablation, but in muscles from intact animals, myofibrillar gene expression was modestly elevated in premolt and postmolt animals. In contrast, polyubiquitin mRNA was significantly elevated (about 2-fold) in claw muscles from eyestalk-ablated animals with elevated circulating ecdysteroids. Moreover, patterns of MHC and actin gene expression are significantly different among slow and fast claw muscles. Consistent with these patterns, the three muscle types differed in the relative amounts of myosin heavy chain and actin proteins. All three muscles also co-expressed fast and slow myosin isoforms, even in fibers that are generally regarded as exclusively fast or slow. These results are consistent with other recent data demonstrating co-expression of myosin isoforms in lobster muscles.

Received 16 April 2004; accepted 14 February 2005.

* To whom correspondence should be addressed. Current address: Department of Biological Sciences, University at Buffalo, Buffalo, NY 14260. E-mail: smedler@buffalo.edu

Introduction

Lobster muscles are complex in organization, with different muscles being composed of a distinct assortment of different fiber types. The factors responsible for establishing and maintaining these fiber types are unknown, but one possible influence is the group of molting hormones known as ecdysteroids. These steroid hormones control complex processes associated with molting and may affect muscle gene expression. Experimental removal of eyestalks causes an increase in circulating ecdysteroids and thus provides a means of manipulating hormone concentration. In this study, we examined the effects of eyestalk ablation and elevated ecdysteroids on skeletal muscle gene expression.

The muscles of the large claws of decapod crustaceans undergo a significant atrophy of up to 60%–75% of their mass prior to molting, so that the bulky muscle can be withdrawn from the narrow basi-ischial opening (Mykles and Skinner, 1990; Ismail and Mykles, 1992; Mykles, 1997; West, 1997). After the molt, muscle mass is quickly regained (Skinner, 1966; Mykles, 1997). Consistent with these findings, myofibrillar protein synthesis is elevated by about 3-fold to 10-fold immediately before and after molting (Skinner, 1965; El Haj *et al.*, 1996; El Haj, 1999). Intracellular proteinases, including calcium-activated proteinases and the ubiquitin-proteasome system, are also active at the time of molting and appear to be involved in controlling the molt-induced muscle atrophy (Mykles and Skinner, 1990; Mykles 1997, 1998). Levels of polyubiquitin protein and mRNA increase in crustacean claw muscles during premolt, when ecdysteroids are elevated (Shean and Mykles, 1995; Koenders *et al.*, 2002; Spees *et al.*, 2003). Although molting is a complex process influenced by multiple factors, one of the major factors known to regulate the

process is the synthesis and secretion of these ecdysteroids (Chang and Bruce, 1980; Landau *et al.*, 1997).

In crustaceans, ecdysteroids are synthesized in the Y-organ, which secretes the hormones as they are produced (Skinner, 1985). Ecdysteroid levels are controlled by molt-inhibiting hormone (MIH), a peptide produced by the X-organ/sinus gland complexes, one of which is located in the optic ganglion of each eyestalk (Van Herp and Kallen, 1991; Landau *et al.*, 1997). Circulating concentrations of the molting hormone, predominantly 20-hydroxyecdysone (20E), generally remain below 50 pg/μl until the animal enters the premolt period (Chang and Bruce, 1980; Snyder and Chang, 1991). At this time, hemolymph concentrations of 20E begin to rise, and remain elevated until after molting, when they return to basal levels (Chang and Bruce, 1980; Snyder and Chang, 1991). Ablation of the eyestalks removes the principal source of MIH and effectively disinhibits the production and secretion of ecdysteroids from the Y-organ (Chang and Bruce, 1980; Wheatly and Hart, 1995).

Among other operations constituting the complex molting process, ecdysteroids are thought to control muscle growth and differentiation, although the specific effects of 20E concentration on the skeletal muscles of crustaceans are ambiguous. Premolt conditions or direct treatment with 20E increase rates of muscle protein synthesis (Skinner, 1965, 1966; El Haj *et al.*, 1996; El Haj, 1999), and some studies have suggested that actin expression increases in response to 20E treatment (Whiteley *et al.*, 1992; Whiteley and El Haj, 1997). In fiddler crabs, the ecdysteroid receptor has been cloned, and receptor expression is up-regulated in the large claw muscle during premolt, a stage when muscle in the major claw atrophies dramatically (Ismail and Mykles, 1992; Chung *et al.*, 1998; Durica *et al.*, 2002). However, El Haj *et al.* (1996) found that ecdysteroid treatment did not affect total RNA synthesis and suggested that changes in muscle protein synthesis might largely be due to control of translation.

Crustaceans possess several different muscle types that have varying mechanical properties and levels of fatigue resistance. In lobsters, at least three identifiable muscle types are present: fast, slow twitch (S_1), and slow tonic (S_2) (Silverman *et al.*, 1987; Neil *et al.*, 1993; Mykles, 1997; West, 1997). Fast fibers have sarcomere lengths of about 4 μm; they also have high rates of ATP hydrolysis and are more susceptible to fatigue than slow fibers. Slow fibers can be further divided into at least two groups: S_1 fibers are characterized by intermediate sarcomere lengths (6–10 μm), intermediate ATPase activities and shortening velocities, and intermediate fatigue resistance; whereas S_2 fibers possess long sarcomeres (up to 12 μm), low ATPase activity and fiber shortening velocities, and the highest levels of fatigue resistance. S_2 fibers are generally thought to play a role in providing long-term postural support.

Lobster claw closer muscles are dimorphic: the large crusher claw contains slow fibers and the slim cutter claw contains, predominantly, fast fibers (Govind, 1992). In a previous study (Medler and Mykles, 2003), we used sequence-specific primers for fast and S_1 myosin heavy chain (MHC) with real-time PCR to measure expression patterns in different muscle types. We demonstrated that different muscles display unique patterns of myofibrillar gene expression, although many fibers co-express multiple MHC genes.

In the current study, we have employed these methods to measure the effects of elevated 20E on myofibrillar gene expression. The eyestalks of adult lobsters were amputated, causing the levels of ecdysteroids in the hemolymph to rise. At varying times after eyestalk ablation, muscle tissues from the claws and abdomen were harvested, and mRNA levels for actin, fast MHC, and S_1 MHC were measured. We also compared the expression of polyubiquitin in intact lobsters with that of the eyestalk-ablated animals with elevated ecdysteroids.

Materials and Methods

Animals and tissue preparation

Adult lobsters, *Homarus americanus*, were raised in the culture facility at the Bodega Marine Laboratory from larvae (Chang and Conklin, 1993). Both eyestalks were ablated at their bases with scissors, and the animals were maintained for 1 to 29 days before they were sacrificed and their muscle tissues were collected for analysis. Animals from the same group, but with the eyestalks left intact, served as controls. Hemolymph samples, taken at the time of sacrifice, were drawn from the base of the last pair of walking legs with a 1-ml syringe fitted with a 26-gauge needle. Muscles from the dimorphic cutter and crusher claws, and from the deep-abdominal flexor muscles, were quickly frozen in liquid N_2 and then stored at -80 °C until analysis (see below).

In independent analyses, muscles from lobsters at different phases of the natural molt cycle (intermolt, premolt, or postmolt) were collected for study. Premolt animals were identified by the synthesis of new exoskeleton and by pleopod setal development (Aiken, 1973), and postmolt animals (2–10 days postmolt) were identified on the basis of records of the last molt. Muscles from these animals were collected and quickly frozen as described above.

Measurement of hemolymph ecdysteroids

Hemolymph samples (100 μl) were mixed with 300 μl of methanol and centrifuged. Supernatants were then dried under vacuum and assayed for ecdysteroids by radioimmunoassay (Chang and O'Connor, 1979; Yu *et al.*, 2002). Values are reported as picograms of ecdysteroid per microliter of hemolymph.

Real-time PCR quantification of myofibrillar protein mRNAs

Total RNA from lobster muscles was isolated using TRIzol Reagent (Invitrogen). Tissues (50–200 mg) were placed in 1 ml of TRIzol Reagent for each 50–100 mg of tissue in a handheld glass homogenizer and were ground until completely homogenized. Insoluble materials were removed by centrifugation at 12,000 × *g* for 10 min at 4 °C. After a 5-min incubation at room temperature, chloroform (0.2 ml per 1 ml TRIzol Reagent) was added to each supernatant. Samples were shaken by hand for 30 s, allowed to stand at room temperature for 5 min, and then centrifuged at 12,000 × *g* for 10 min at 4 °C. RNA in the aqueous phase was precipitated by the addition of isopropanol (0.5 ml per 1 ml TRIzol Reagent) and was then allowed to stand at room temperature for 10 min. The precipitated RNA was collected by centrifugation at 12,000 × *g* for 10 min at 4 °C and then washed with 75% ethanol. After air-drying, the RNA samples were dissolved in water and stored at −80 °C.

The RNA samples were treated with DNase (Invitrogen) for 15 min at room temperature to remove any genomic DNA contamination. First-strand cDNA was synthesized from total RNA using M-MLV reverse transcriptase (Invitrogen) and oligo dT primers. The reaction contained 2.5 μg of oligo(dT) 12–18, 2.5 m*M* dNTP, 1× first-strand buffer, 5 m*M* DTT, 2.5 units of RNase inhibitor, 1–2 μg of RNA, and 200 units of M-MLV reverse transcriptase.

cDNA synthesized from different tissues was used as a template for subsequent real-time PCR. Single cDNA samples were divided for use in separate reactions to measure the copy numbers of fast MHC, slow (S_1) MHC, and α-actin. Thus, three distinct transcripts were monitored for each sample and served as internal controls. The Light Cycler DNA Master SYBR Green I reaction mix for PCR (Roche Molecular Biochemicals) was used to amplify target cDNA with a Cepheid Smart Cycler instrument. PCR master mix was added to 25-μl sample tubes containing 5 μl of the first-strand cDNA reaction. The master mix consisted of 1× LightCycler-DNA Master Green I (contains dNTP mix, FastStart Taq DNA polymerase, SYBR Green I dye), 2.5 m*M* $MgCl_2$, and 0.5 μ*M* of each primer. PCR amplification consisted of denaturation of template and activation of the HS Taq (95 °C for 5 min), followed by amplification of the cDNA target (30 cycles of denaturation at 95 °C for 15 s, annealing at 60 °C for 6 s, and extension at 72 °C for 20 s). Primers for fast and slow (S_1) MHCs, as well as those for α-actin, were the same as those reported previously (Koenders *et al.*, 2002; Medler and Mykles, 2003). Plasmid DNA containing the specific cDNA sequences for each of the target sequences was used as the template for PCR to optimize reaction conditions. The fast MHC primers amplified a 315-bp product, while the S_1 MHC primers amplified a 453-bp product (Medler and Mykles, 2003). The actin primers were designed to amplify α-actin from lobster skeletal muscles as previously described, yielding a 401-bp product (Koenders *et al.*, 2002). Standard curves were constructed by using serially diluted purified plasmid DNA as the template and plotting the number of template copies as a function of the threshold cycle during which product began to accumulate exponentially. The melting temperature, which is a measure of the GC content and the length of the product, was used to identify the specificity of the PCR product. In addition, reaction products were usually separated on 1% agarose gels to verify product size. The cycle thresholds from reactions containing unknown amounts of cDNA were converted to number of copies with the standard curves (Medler and Mykles, 2003). The numbers of mRNA copies of the different sequences were standardized to micrograms of total RNA.

RT PCR of polyubiquitin mRNA

In the current study, a semiquantitative method was used to measure the difference in polyubiquitin mRNA between intact animals and eyestalk-ablated animals with elevated ecdysteroid concentrations (> 200 pg/μl). PCR amplification of the polyubiquitin cDNA is incompatible with real-time PCR, because the head-to-tail orientation of the individual ubiquitin mRNA sequences leads to multiple ubiquitin PCR products of differing sizes (Koenders *et al.*, 2002). Therefore, we used a standard PCR and monitored the amount of product at the end of a different number of cycles. PCR conditions were those used previously by Koenders *et al.* (2002). We determined that the most prominent, 225-base-pair product in samples from intact and eyestalk-ablated animals could best be discriminated following 21 cycles of amplification. Ethidium-bromide-stained PCR products separated on 1% agarose gels were saved as digital images and quantified by densitometry (NIH Image 1.62).

Analysis of actin and MHC proteins

Muscle tissues from eyestalk-ablated and intact controls were collected as described. Samples used for protein analyses were processed according to the methods of Mykles (1985). Briefly, frozen muscles were glycerinated for 2–3 h, with stirring, in ice-cold buffer containing 20 m*M* Tris-HCl (pH 7.5), 50% glycerol, 100 m*M* KCl, 1 m*M* EDTA, and 0.1% Triton X-100. Single fibers or fiber bundles were removed from the muscle and solubilized in 250 μl of SDS sample buffer containing 62.5 m*M* Tris-HCl (pH 6.8), 12.5% glycerol, 1.25% SDS, and 1.25% β-mercaptoethanol. Muscle samples were left in this solution overnight at room temperature with occasional vortexing. To analyze myofibrillar isoform assemblages, SDS-PAGE was performed with a discontinuous gel system, as described in Mykles

(1985). Briefly, 10% separating gels (37.5:1 acrylamide: N,N-methylenebisacrylamide) were used to separate about 4–6 μg myofibrillar proteins, using a Bio-Rad Mini-Protean 3 gel system. The gels were stained with Coomassie blue or silver (Wray *et al.*, 1981), and the relative amounts of actin and MHC from the silver-stained gels were determined by scanning densitometry (NIH Image 1.62).

Statistical analyses

For regression analyses, the numbers of myofibrillar mRNA copies were log-transformed to reduce variance and regressed against ecdysteroid concentrations. In addition, we examined these values as a function of the number of days after eyestalk ablation. The number of myofibrillar mRNA copies and the MHC/actin ratios were compared among fiber types with a one-way ANOVA, followed by Bonferroni post-ANOVA tests (experiment-wise $\alpha = 0.05$).

For analysis of gene expression in muscles from intact animals at different molt stages, the numbers of myofibrillar mRNA copies were log-transformed and analyzed by ANOVA. A factorial ANOVA was used to analyze the number of copies of mRNA, with the factors being molt stage (intermolt, premolt, or postmolt), muscle type (deep-abdominal flexor, crusher, or cutter), and specific myofibrillar gene (actin, S_1 MHC, fast MHC). Between four and seven samples were taken for each unique treatment group (molt stage × muscle type × myofibrillar gene). Statview 5.0.1 (SAS Institute Inc.) was used for all statistical analyses.

Results

Effects of eyestalk ablation on ecdysteroid titers

Ecdysteroid concentrations in the hemolymph increased significantly as a function of the number of days after eyestalk ablation ($P = 0.001$; Fig. 1). Elevated levels of hormones were detected within the first few days after ablation, but these levels were quite variable. Overall, eyestalk-ablated animals, collectively, had significantly higher ecdysteroid concentrations than the intact controls, as determined by an unpaired Student's *t*-test ($P = 0.009$). The mean (± SD) ecdysteroid concentration was 13.4 ± 12.8 pg/μl for the intact control lobsters *versus* 156.4 ± 145 pg/μl for the eyestalk-ablated animals.

Effect of ecdysteroid concentration on myofibrillar mRNAs

Levels of mRNAs for actin, fast MHC, and S_1 MHC were quantified by real-time PCR for muscles from the crusher and cutter claws and for the deep abdominal flexors. When these levels were examined as a function of the time since eyestalk ablation, only actin message expressed in the deep-abdominal flexor muscles changed, decreasing significantly as a function of the number of days since ablation ($P = 0.002$; Fig. 2). About 30 days after eyestalk ablation, the amount of actin message was more than 10-fold lower than in intact animals. However, these genes encoding actin, fast MHC, and S_1 MHC showed no significant changes in expression as a function of ecdysteroid concentration in any of the muscles sampled (Fig. 3A–C, E–G, I–K).

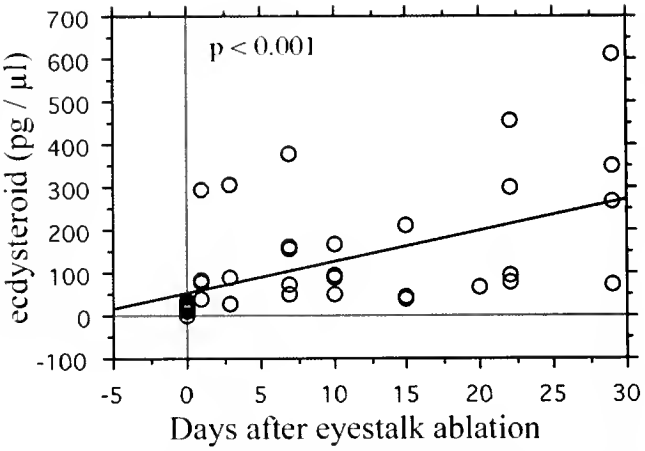

Figure 1. Effect of eyestalk ablation on hemolymph ecdysteroid concentration. Ecdysteroids significantly increased following eyestalk ablation ($P = 0.001$). Animals were eyestalk-ablated on day 0, and concentrations of ecdysteroids in the hemolymph were measured at the time of tissue collection at various times over the following weeks. Control animals with intact eyestalks are shown at day 0. Although the linear increase in ecdysteroid titer is significant, the values from different animals are highly variable.

Effect of muscle type on myofibrillar mRNAs

When intact and eyestalk-ablated animals were combined into a single group, significant differences in mRNA levels were detected among muscle types for all three myofibrillar genes (Fig. 3D, H, L). Actin expression was highest in slow muscles of the crusher claw, being almost 7 times higher than in the fast cutter claw, and more than 1000 times higher than in the fast deep flexors (Fig. 3D). Fast MHC expression was highest in the deep flexors, being almost 4 times higher than in the cutter claw muscle, and more than 3000 times higher than in the crusher claw muscle (Fig. 3H). Slow (S_1) MHC expression was highest in the crusher claw muscle, being almost 15 times higher than in the cutter claw muscle, and almost 3000 times higher than in the deep flexors (Fig. 3L).

When these expression levels were grouped by muscle type, characteristic patterns were observed for each muscle (Fig. 4). In the crusher muscles, actin expression was almost 1000 times higher than S_1 MHC expression and more than 1500 times the level of fast MHC expression (Fig. 4A). Fast cutter muscles expressed more copies of fast MHC than the other genes, being more than 3 times higher than actin

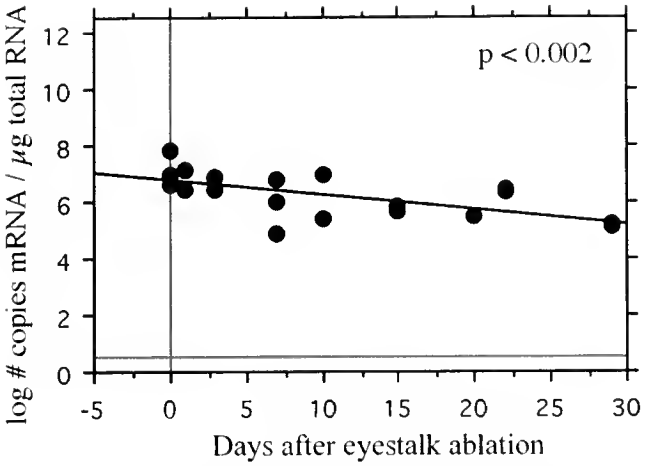

Figure 2. Level of actin mRNA in deep-abdominal flexor muscles as a function of the time following eyestalk ablation. After nearly 30 days without eyestalks, actin expression fell by about one order of magnitude ($P = 0.002$). Actin mRNA data are the same as those in Figure 3C.

expression and more than 7000 times higher than S_1 MHC expression (Fig. 4B). In the fast deep flexors, fast MHC expression was almost 2000 times greater than actin expression and more than 6 orders of magnitude higher than S_1 MHC expression (Fig. 4C). Each of the three muscle types expressed both the fast and S1 MHC isoforms. This co-expression was more prominent for the cutter and crusher claw muscles, but less dramatic for the deep-abdominal muscle (Figs. 3E–L, 4, 5D–I).

Effect of molt stage on myofibrillar mRNAs

Premolt and postmolt muscles consistently exhibited slightly higher levels of myofibrillar gene expression than intermolt muscles (Fig. 5). Although these differences were not dramatic, they were significant when molt-stage muscles (premolt and postmolt combined) were compared with intermolt muscles ($P = 0.0422$; Table 1). The effect of molt stage was not significant when pre- and postmolt muscles were treated as separate groups ($P = 0.13$; data not shown). The average myofibrillar gene expression in molt-stage animals (premolt and postmolt) was about 4 times greater than that observed in intermolt animals; but given the level of variability, this is not a precise value. As expected, significant differences were also detected with respect to the muscle type and the specific gene of interest ($P < 0.0001$; Table 1, "Muscle" and "Gene," respectively). In addition, the interaction between muscle type and gene expressed was significant ($P < 0.0001$; Table 1, "Muscle * Gene"). Each of these effects reflects the muscle-specific expression patterns described above—namely that each muscle type expresses different myofibrillar genes in unique proportions.

Effects of eyestalk ablation on myofibrillar protein composition

Relative concentrations of MHC and actin proteins were assessed by SDS-PAGE and densitometry. Significant differences in the myosin/actin ratio were observed among all three muscles, with the fast deep-abdominal muscle having the highest MHC/actin ratio, followed by the cutter muscles and finally the crusher muscles (Bonferroni post-ANOVA test; experiment-wise $\alpha = 0.05$) (Fig. 6). However, the myosin/actin ratio in none of the three muscle fiber types changed as a function of time after eyestalk ablation ($P = 0.30$; data not shown), indicating that a selective loss of thin filament proteins did not occur during the experiment.

Effects of elevated ecdysteroids on polyubiquitin expression

Previous studies have shown that polyubiquitin protein and mRNA increase in crustacean muscles during premolt, when ecdysteroids are elevated (Shean and Mykles, 1995; Koenders *et al.*, 2002; Spees *et al.*, 2003). As a positive control for the systemic effects of elevated ecdysteroids, we used a semiquantitative PCR method to compare polyubiquitin expression in claw muscles from intact control animals and eyestalk-ablated animals with elevated ecdysteroid titers (> 200 pg/μl). We detected a significant elevation (about 2-fold) in polyubiquitin expression in those animals with elevated ecdysteroids, when they were compared with intact control animals ($P < 0.0001$; Fig. 7).

Discussion

We have shown that experimentally elevated ecdysteroid concentrations triggered in lobsters by eyestalk ablation have little or no effect on myofibrillar gene expression. In contrast, animals undergoing natural molting exhibit slightly elevated myofibrillar gene expression. Overall, the data reported here are consistent with previous studies indicating that myofibrillar gene expression is elevated during molting, but these changes are not dramatic and are sometimes difficult to detect. These same data also confirm that patterns of gene expression among muscle fiber types differ, and that many fibers are polymorphic, expressing multiple myofibrillar isoforms.

Over time, eyestalk ablation significantly elevated ecdysteroids to levels comparable to those observed in premolt lobsters experiencing a natural molt cycle (Fig. 1) (Snyder and Chang, 1991; Chang *et al.*, 2001). Although ecdysteroid concentrations were quite variable in eyestalk-ablated animals, this pattern is not surprising: ecdysteroid levels fluctuate significantly over time even in intact animals (Snyder and Chang, 1991). Ecdysteroids coordinate a number of physiological processes involved with molting in crustaceans, and several studies have suggested that these

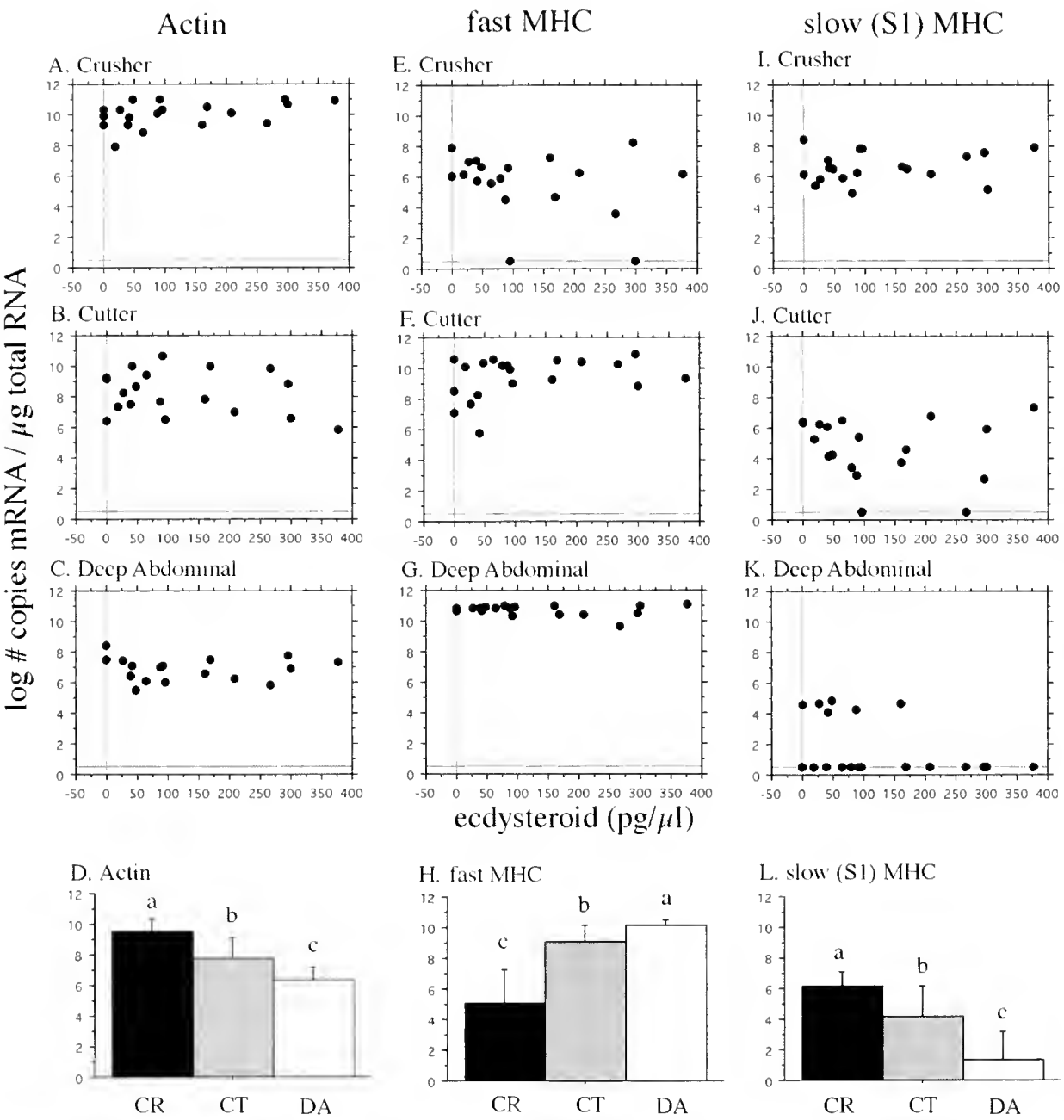

Figure 3. Myofibrillar gene expression as a function of ecdysteroid concentration. (A–C) Actin expression did not significantly change with increasing levels of ecdysteroids in any of the muscles examined. (D) But when the same data were grouped by muscle type, significant differences were found among the three muscle types: expression was highest in the slow crusher (CR) muscles, followed by the cutter (CT) and the deep-abdominal muscles (DA). (E–G) Fast MHC expression was not affected by ecdysteroid concentration in any of the three muscles. (H) But when grouped by muscle type, fast MHC expression was significantly higher in the deep-abdominal muscles than in the cutter or crusher claw muscles, and the fast cutter muscles expressed higher levels of fast MHC than the slow crusher claw muscles. (I–K) Slow (S_1) MHC expression was unaffected by ecdysteroids in the muscles examined. (L) When the data were grouped by muscle type, S_1 MHC expression was significantly highest in the slow crusher muscles, followed by the cutter muscles and the deep-abdominal muscles. Means with different letters in (D), (H), and (L) are significantly different from one another, as determined by a Bonferroni post-ANOVA test (experiment-wise $\alpha = 0.05$; $n = 16–20$; values are means ± SD).

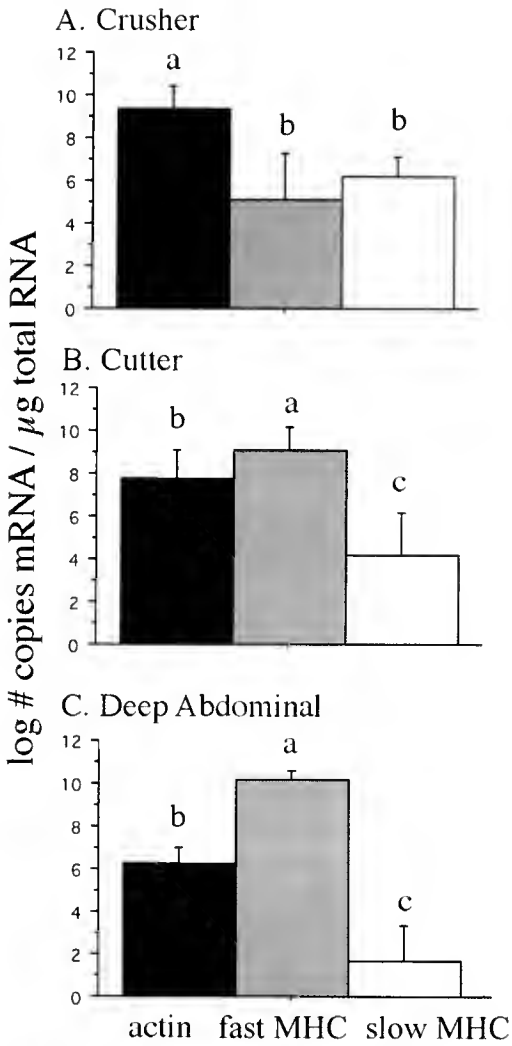

Figure 4. Different muscle types exhibit distinct myofibrillar protein expression patterns. (A) Slow muscles in the crusher claw expressed significantly higher levels of mRNA encoding actin than the mRNAs encoding either fast or slow MHC. Although slow (S_1) MHC expression was higher than fast MHC expression, the difference was not significant. In general, the expression of the fast MHC was much more variable than S_1 MHC in the slow muscles of the crusher claw. (B, C) Both fast muscle phenotypes exhibited significantly higher expression of fast MHC than of either actin or slow MHC, and actin expression fell between those of fast and slow MHC. In both muscle types, slow MHC expression was quite variable. Means with different letters are significantly different from one another as determined by a Bonferroni post-ANOVA test (experiment-wise $\alpha = 0.05$; $n = 16–20$; values are means ± SD). (Data are from the eyestalk-ablation experiment, which included both intact and ablated animals.)

hormones are responsible for such molt-related changes in skeletal muscles as the atrophy of the large cheliped muscles in some decapod crustaceans (El Haj and Houlihan, 1987; Ismail and Mykles, 1992; El Haj *et al.*, 1996; El Haj and Whiteley, 1997; Whiteley and El Haj, 1997). Moreover, an ecdysteroid receptor has been detected in lobster muscle (El Haj *et al.*, 1994). Other studies have reported increases in protein synthesis in crustacean muscles during premolt and postmolt periods (Skinner 1965, 1966; El Haj *et al.*, 1996), but whether these changes result from changes in myofibrillar gene expression is equivocal (Whiteley *et al.*, 1992; El Haj *et al.*, 1996; Mykles, 1997; Whiteley and El Haj, 1997). We detected no significant changes in myofibrillar gene expression in response to elevated ecdysteroid concentrations (Fig. 3). In contrast, muscles taken from intact lobsters demonstrated modest, but significant, increases in myofibrillar gene expression in premolt and postmolt animals when compared to intermolt animals (Fig. 5; Table 1). These results indicate that myofibrillar gene expression can increase before and after molting.

In this study, the expression patterns detected in intact lobsters experiencing a natural molt cycle provide a useful comparison for patterns observed in eyestalk-ablated animals. In both cases, myofibrillar gene expression is relatively constant, but the intact premolt and postmolt lobsters exhibited significantly higher expression when compared with the intermolt animals (Fig. 5; Table 1). This difference indicates that the physiological events following eyestalk ablation are not precisely equivalent to those occurring during the natural molt cycle. This conclusion is supported by diverse earlier findings. The X-organ/sinus gland complex located in the eyestalks is an important neuroendocrine center involved in several physiological processes, including molting, reproduction, osmoregulation, and energy metabolism (Van Herp and Kallen, 1991; Landau *et al.*, 1997). Indeed, eyestalk ablation is known to have significant effects on osmoregulatory processes (Jackson *et al.*, 1987; Charmantier-Daures *et al.*, 1994; Wheatly and Hart, 1995), energy metabolism (Rosas *et al.*, 1993; Chang, 2001), and reproductive processes (Khalaila *et al.*, 2002) in crustaceans. The peptide hormones released from the sinus gland probably have complex, broad physiological effects. We conclude, therefore, that eyestalk ablation is an experimental procedure with the potential to affect most important physiological systems in decapod crustaceans. As such, it is certainly not simply equivalent to increases in ecdysteroids during molting (Wheatly and Hart, 1995), and as an experimental tool, it should be used judiciously.

Our analysis of the relative amounts of MHC and actin revealed no changes at the protein level as a result of eyestalk ablation. In contrast, studies of molt-associated atrophy in crabs demonstrated that thin filament proteins were selectively lost during atrophy (Ismail and Mykles, 1992; Mykles, 1997, 1998; West, 1997). Consistent with established patterns in crustacean muscles (Jahromi and Atwood, 1969; Ismail and Mykles, 1992; West, 1997), we detected significant differences in the myosin/actin ratio among the different fiber types, with the fast muscles having proportionately more myosin (Fig. 6). But these ratios were

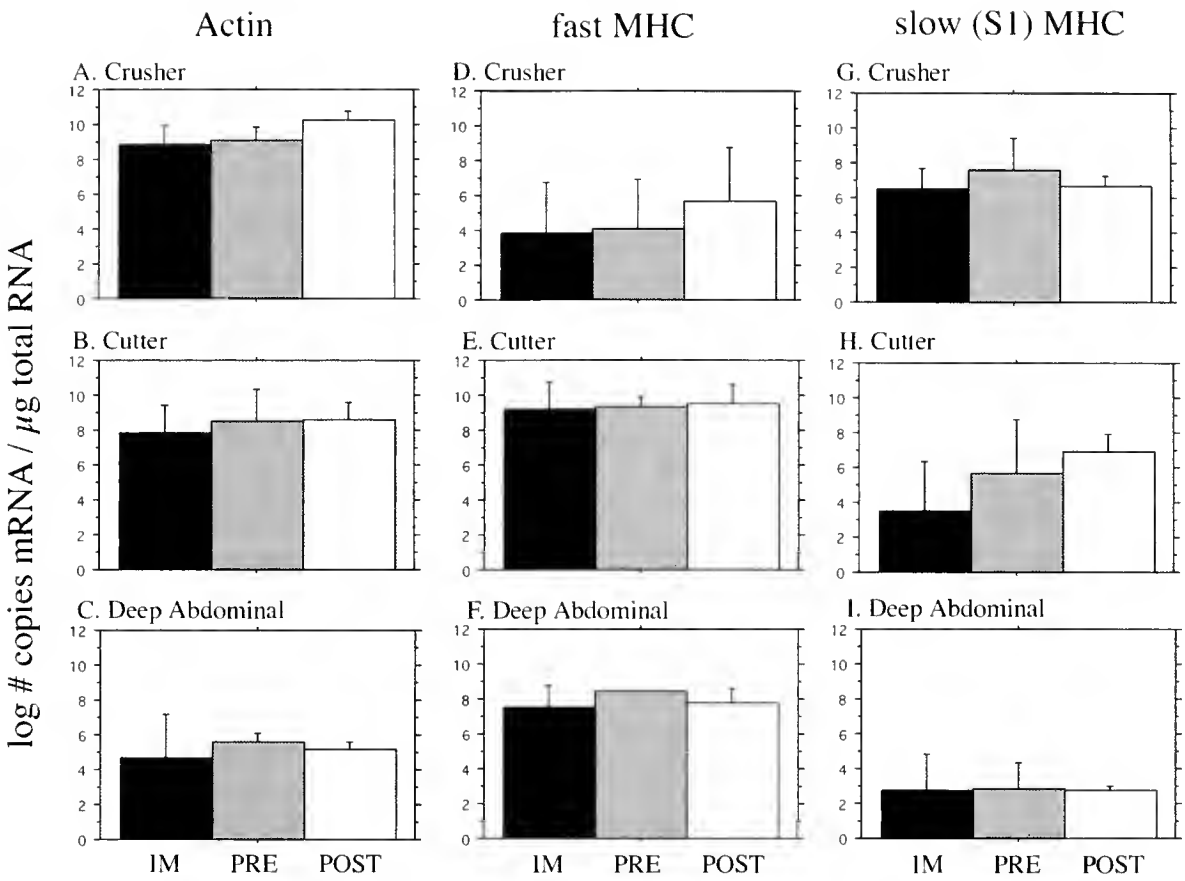

Figure 5. Myofibrillar gene expression in claw and deep-abdominal muscles as a function of molt stage in intact animals (intermolt: IM; premolt: PRE; postmolt: POST). (A–C) Actin expression, (D–F) fast MHC expression, and (G–I) slow (S_1) MHC expression. Expression of each gene was slightly, but not significantly, higher in the premolt and postmolt muscles. When the data were pooled and analyzed by factorial ANOVA, the premolt and postmolt muscles had significantly higher expression than muscles from intermolt animals (Table 1).

affected neither by ecdysteroid concentration nor by the duration of eyestalk ablation (data not shown).

The failure of elevated ecdysteroids to affect myofibrillar protein levels was also evident when gene expression was examined. Lobsters with elevated ecdysteroids following eyestalk ablation did not show the increased gene expression that might have been expected from the slight elevation of myofibrillar gene expression in premolt and postmolt lobsters. In 1966, Skinner had already proposed that molt-induced atrophy is not under the direct control of ecdysteroids, suggesting instead that the complex process probably involves changes in motor neuron activity. Similarly, others have suggested that the control of skeletal muscle growth and remodeling is complex, and not under the direct control of ecdysteroids alone (El Haj and Houlihan, 1987; Whiteley *et al.*, 1992; El Haj and Whiteley, 1997; Whiteley and El Haj, 1997). Our analysis of muscle proteins, together with the mRNA data, indicates that lobster skeletal muscles are largely unaffected by the ecdysteroid elevation alone.

Table 1

ANOVA of intact lobsters from intermolt, premolt, and postmolt stages (premolt and postmolt combined as one group)

Source of Variation	DF	Sum of Squares	Mean Square	*F*-value	*P*-value
Stage	1	10.50	10.50	4.23	**0.0422**
Muscle	2	115.33	57.66	23.25	**<0.0001**
Gene	2	114.61	57.03	23.10	**<0.0001**
Stage*Muscle	2	3.09	1.55	0.62	0.5381
Stage*Gene	2	0.57	0.29	0.12	0.8916
Muscle*Gene	4	290.69	72.67	29.30	**<0.0001**
Stage*Muscle*Gene	4	3.45	0.86	0.35	0.8449
Residual	103	255.49	2.48		

Dependent variable: log # RNA copies/μg total RNA. Factors: Stage (intermolt and pre/postmolt); Muscle (slow (S_1) crusher claw, fast cutter claw, fast deep abdominal); Gene (actin, slow (S_1), fast MHC). **Bold** values indicate significant effects ($P < 0.05$).

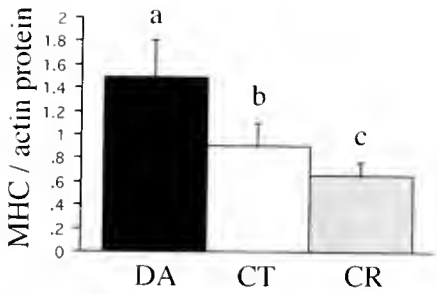

Figure 6. The ratio of MHC to actin proteins in fast and slow fibers from deep abdominal (DA), cutter (CT), and crusher (CR) claw muscles in eyestalk-ablated and intact control animals. Means with different letters are significantly different from one another as determined by a Bonferroni post-ANOVA test (experiment-wise $\alpha = 0.05$; $n = 16$; values are means ± SD). No changes in these ratios were detected for any of the three muscle types following eyestalk ablation (data not shown).

The natural molting process likely involves not only increased ecdysteroid titers, but also permissive events that prepare the tissues for molting. One such possibility is that ecdysteroid receptors in the muscles are not available under the conditions of experimental ecdysteroid elevation (El Haj *et al.*, 1994).

The different muscles were clearly distinguished by the patterns of MHC and actin expression, consistent with previously observed expression levels in adult lobsters (Medler and Mykles, 2003). Slow (S_1) MHC expression is highest in the slow crusher claw muscles, intermediate in the fast cutter claw muscles, and low to absent in the fast muscles of the deep abdominal flexors (Fig. 3L). A similar correlation was observed for actin expression, while fast MHC expression followed a reverse pattern (Fig. 3D, H). As we and others have previously suggested, differences in actin expression probably reflect differences in thin-to-thick filament ratios in the different fiber types, as slow muscles have significantly higher proportions of thin filaments (Jahromi and Atwood, 1969; Medler and Mykles, 2003). This pattern was confirmed in the present study: the significant differences detected in the relative amounts of MHC and actin in the different fiber types (Fig. 6) mirrored the differences in mRNA levels for the different fiber types (Figs. 3D, H, L; 4). Significant differences were found between the fast cutter muscles and fast abdominal muscles, both in terms of mRNA levels and the ratio of MHC and actin proteins (Figs. 3D, H, L; 6). A recent study of freshwater crayfish muscles demonstrated subtle differences in these fast muscles in terms of sarcomere length, troponin proteins, and Ca^{2+} activation kinetics (Koenders *et al.*, 2004). These findings suggest that, notwithstanding the nomenclature, the fast muscles of the claw and the abdomen are physiologically distinct.

Another interesting pattern is the co-expression of multiple MHC isoforms in the same muscles. Although this may be due in part to the presence of multiple fiber types within the intact muscle, we have observed co-expression in single fibers (Medler and Mykles, 2003; Medler *et al.*, 2004). This type of co-expression has also been noted in a number of other animals and seems to represent the rule rather than the exception with respect to profiles of isoform expression in muscle (Peuker and Pette, 1997; Lutz *et al.*, 1998, 2001; Stevens *et al.*, 1999; Stephenson, 2001; Caiozzo *et al.*, 2003). A newly emerging challenge for skeletal muscle biologists is to define the extent and significance of single-fiber polymorphism (Stephenson, 2001; Caiozzo *et al.*, 2003). The role of motor nerves on factors that affect the expression of specific myofibrillar isoforms is suggested by the developmental changes in lobster claw muscles (Govind, 1992).

In contrast to the lack of effect on myofibrillar gene expression, elevated ecdysteroid levels were associated with higher levels of polyubiquitin mRNA. Polyubiquitin expression increases in premolt claw muscles when these muscles experience atrophy (Shean and Mykles, 1995; Koenders *et*

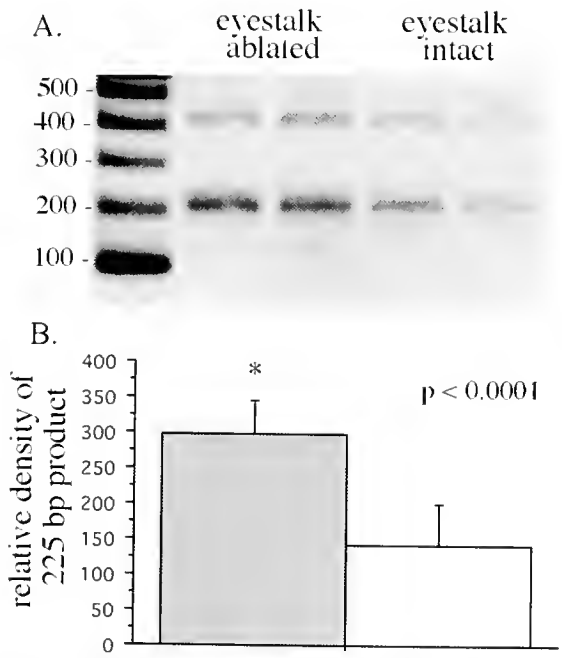

Figure 7. Polyubiquitin expression in animals with elevated ecdysteroid concentrations after eyestalk ablation. (A) PCR products following 21 cycles of eyestalk-ablated (left two lanes) compared with intact control (right two lanes) muscles (inverse image of ethidium-bromide-stained gel). The most prominent band was the smallest, a 225-bp product, which was subsequently quantified by densitometry (lane on far left consists of standards). (B) Quantification of the relative density of the most prominent (225-bp) PCR product from the muscles from eyestalk-ablated (left) and intact control (right) animals ($n = 8$; values are means ± SD). Cutter and crusher muscles from animals with elevated ecdysteroids (above 200 pg/μl) had significantly (*) ($P < 0.0001$) higher expression of polyubiquitin as compared with intact control animals.

al., 2002; Spees *et al.*, 2003), and this expression was therefore used in the current study as an alternative measure of the effects of elevated ecdysteroids. Ubiquitin is a highly conserved protein that becomes covalently bound to other proteins by an ATP-dependent conjugating system. Further addition of ubiquitin monomers (polyubiquitin) targets the bound protein for degradation by the proteasome (Mykles, 1998). The ubiquitin/proteasome system is clearly involved in atrophic processes in mammalian skeletal muscle (Mitch and Goldberg, 1996) and appears to be involved in crustacean muscle atrophy as well (Shean and Mykles, 1995; Mykles, 1998; Koenders *et al.*, 2002). In the present study, comparison of eyestalk-intact animals and eyestalk-ablated animals with high ecdysteroid levels confirms significantly higher polyubiquitin expression in the eyestalk-ablated group. These results indicate that the ablation—and possibly the ensuing ecdysteroid exposure—was affecting select cellular processes, although myofibrillar gene expression was not one of these.

Another exception to the general lack of effect of the elevated ecdysteroids was the reduced actin expression in the deep flexors as a function of the duration of eyestalk ablation. In these muscles, actin expression fell by about an order of magnitude 30 days post-ablation ($P = 0.002$; Fig. 2). We might dismiss this finding as a statistical artifact but for the level of statistical significance and because it is consistent in certain respects with previously reported data. Molting crabs and crayfish claw muscles selectively lose actin filaments as they atrophy, but it is not known whether this also occurs in the abdominal muscles (Mykles and Skinner, 1990; Ismail and Mykles, 1992; West, 1997). Previous studies have shown that synaptic efficacy in these muscles is significantly reduced by acute 20E application, and that escape responses in postmolt lobsters are less forceful than in non-molting animals (Cooper and Ruffner, 1998; Cromarty and Kass-Simon, 1998). These results were muscle-specific, as the effect of 20E in the claw opener muscles was opposite to that in the abdominal muscle, namely to enhance synaptic efficacy (Cromarty *et al.*, 1991). Further work is needed to establish whether the decline in actin expression in the phasic abdominal muscles is a general response to eyestalk ablation in lobsters.

Overall, the data reported here are consistent with previous studies indicating that myofibrillar gene expression is elevated during molting, but these changes are not dramatic and sometimes difficult to detect (Whiteley *et al.*, 1992; El Haj *et al.*, 1996; Whiteley and El Haj, 1997; El Haj, 1999). Molting is a complex process that involves not only increases in ecdysteroid concentrations, but other processes as well. Further study is needed to understand the complex factors involved in molt-associated changes in skeletal muscle growth and differentiation.

Acknowledgments

We sincerely thank Luisa Bautista, Rachelle Doran, and Travis Lilly for their dedicated technical assistance. We also thank Dr. Kara Lee for critically reviewing the manuscript. This research was supported by a grant from the National Science Foundation to DLM (IBN-0077422) and an NRSA postdoctoral fellowship from the National Institute of Arthritis and Musculoskeletal and Skin Diseases to SM (AR 08597-01A1).

Literature Cited

Aiken, D. E. 1973. Proecdysis, setal development, and molt prediction in the American lobster (*Homarus americanus*). *J. Fish Res. Board Can.* **30:** 1337–1344.

Caiozzo, V. J., M. J. Baker, K. Huang, H. Chou, Y. Z. Wu, and K. M. Baldwin. 2003. Single fiber myosin heavy chain polymorphism: how many patterns and what proportions? *Am. J. Physiol. Regul. Integr. Comp. Physiol.* **285:** R570–R580.

Chang, E. S. 2001. Crustacean hyperglycemic hormone family: old paradigms and new perspectives. *Am. Zool.* **41:** 380–388.

Chang, E. S., and M. J. Bruce. 1980. Ecdysteroid titers of juvenile lobsters following molt induction. *J. Exp. Zool.* **214:** 157–160.

Chang, E. S., and D. E. Conklin. 1993. Larval culture of the American lobster (*Homarus americanus*). Pp. 489–495 in *CRC Handbook of Mariculture*, 2nd ed., J. P. McVey, ed. CRC Press, Boca Raton, FL.

Chang, E. S., and J. D. O'Connor. 1979. Arthropod molting hormones. Pp. 797–814 in *Methods of Hormone Radioimmunoassay*, B. M. Jaffe and H. R. Behrman, eds. Academic Press, New York.

Chang, E. S., S. A. Chang, and E. P. Mulder. 2001. Hormones in the lives of crustaceans: an overview. *Am. Zool.* **41:** 1090–1097.

Charmantier-Daures, M., G. Charmantier, P. C. Janssen, D. E. Aiken, and F. Van Herp. 1994. Involvement of eyestalk factors in the neuroendocrine control of osmoregulation in adult American lobster *Homarus americanus*. *Gen. Comp. Endocrinol.* **94:** 281–293.

Chung, A. C.-K., D. S. Durica, and P. M. Hopkins. 1998. Tissue-specific patterns and steady-state concentrations of ecdysteroid receptor and retinoid-X-receptor mRNA during the molt cycle of the fiddler crab, *Uca pugilator*. *Gen. Comp. Endocrinol.* **109:** 375–389.

Cooper, R. K., and M. E. Ruffner. 1998. Depression of synaptic efficacy at intermolt in crayfish neruromuscular junctions by 20-hydroxyecdysone, a molting hormone. *J. Neurophysiol.* **79:** 1931–1941.

Cromarty, S. I., and G. Kass-Simon. 1998. Differential effects of a molting hormone, 20-hydroxyecdysone, on the neuromuscular junctions of the claw opener and abdominal flexor muscles of the American lobster. *Comp. Biochem. Physiol.* **120A:** 289–300.

Cromarty, S. I., J. S. Cobb, and G. Kass-Simon. 1991. Behavioral analysis of the escape response in the juvenile lobster *Homarus americanus* over the molt cycle. *J. Exp. Biol.* **158:** 565–581.

Durica, D. S., X. Wu, G. Anilkumar, P. M. Hopkins, and A. C. K. Chung. 2002. Characterization of crab EcR and RXR homologs and expression during limb regeneration and oocyte maturation. *Mol. Cell. Endocrinol.* **121:** 119–132.

El Haj, A. J. 1999. Regulation of muscle growth and sarcomeric protein gene expression over the intermolt cycle. *Am. Zool.* **39:** 570–579.

El Haj, A. J., and D. F. Houlihan. 1987. *In vitro* and *in vivo* protein synthesis rates in a crustacean muscle during the moult cycle. *J. Exp. Biol.* **127:** 413–426.

El Haj, A. J., and N. M. Whiteley. 1997. Molecular regulation of muscle growth in Crustacea. *J. Mar. Biol. Assoc. UK* **77:** 95–106.

El Haj, A. J., P. Harrison, and E. S. Chang. 1994. Localization of ecdysteroid receptor immunoreactivity in eyestalk and muscle tissue of

the American lobster, *Homarus americanus*. *J. Exp. Zool.* **270:** 343–349.

El Haj, A. J., S. R. Clarke, P. Harrison, and E. S. Chang. 1996. *In vivo* muscle protein synthesis rates in the American lobster *Homarus americanus* during the moult cycle and in response to 20-hydroxyecdysone. *J. Exp. Biol.* **199:** 579–585.

Govind, C. K. 1992. Claw asymmetry in lobsters: a case study in developmental neuroethology. *J. Neurobiol.* **23:** 1423–1445.

Ismail, S. Z. M., and D. L. Mykles. 1992. Differential molt-induced atrophy in the dimorphic claws of male fiddler crabs, *Uca pugnax*. *J. Exp. Zool.* **263:** 18–31.

Jackson, S. A., M. J. Bruce, E. S. Chang, and J. S. Clegg. 1987. Effects of eyestalk ablation upon water relations in the American lobster, *Homarus americanus*. *J. Exp. Zool.* **244:** 389–393.

Jahromi, S. S., and H. L. Atwood. 1969. Correlation of structure, speed of contraction, and total tension in fast and slow abdominal muscle fibers of the lobster (*Homarus americanus*). *J. Exp. Zool.* **171:** 25–38.

Khalaila, I., R. Manor, S. Weil, Y. Granot, R. Keller, and A. Sagi. 2002. The eyestalk-androgenic gland-testis endocrine axis in the crayfish, *Cherax quadricarinatus*. *Gen. Comp. Endocrinol.* **127:** 147–156.

Koenders, A., X. Yu, E. S. Chang, and D. L. Mykles. 2002. Ubiquitin and actin expression in claw muscles of land crab, *Gecarcinus lateralis*, and American lobster, *Homarus americanus*: differential expression of ubiquitin in two slow muscle fiber types during molt-induced atrophy. *J. Exp. Zool.* **292:** 618–632.

Koenders, A., T. M. Lamey, S. Medler, J. M. West, and D. L. Mykles. 2004. Two fast-type fibres in the claw closer and abdominal deep muscles of the Australian freshwater crustacean, *Cherax destructor*, differ in Ca^{2+}-sensitivity and troponin I isoforms. *J. Exp. Zool.* **301A:** 588–598.

Landau, M., W. J. Biggers, and H. Laufer. 1997. Invertebrate endocrinology. Pp. 1291–1390 in *Handbook of Physiology, Comparative Physiology*, Vol. 2. American Physiological Society, Bethesda, MD.

Lutz, G. J., D. B. Cuison, A. F. Ryan, and R. L. Leiber. 1998. Four novel myosin heavy chain transcripts define a molecular basis for muscle fibre types in *Rana pipiens*. *J. Physiol.* **508:** 667–680.

Lutz, G. J., S. N. Bremner, M. J. Bade, and R. L. Leiber. 2001. Identification of myosin light chains in *Rana pipiens* skeletal muscle and their expression patterns along single fibres. *J. Exp. Biol.* **204:** 4237–4248.

Medler, S., and D. L. Mykles. 2003. Analysis of myofibrillar proteins and transcripts in skeletal muscles of the American lobster, *Homarus americanus*: variable expression of myosins, actin, and troponins in fast, slow-twitch, and slow-tonic fibres. *J. Exp. Biol.* **206:** 3557–3567.

Medler, S., T. Lilley, and D. L. Mykles. 2004. Fiber polymorphism in lobster skeletal muscles: continuum between slow phasic (S_1) and slow tonic (S_2) muscle fibers. *J. Exp. Biol.* **207:** 2755–2767.

Mitch, W. E., and A. L. Goldberg. 1996. Mechanisms of muscle wasting: the role of the ubiquitin-proteasome pathway. *New Engl. J. Med.* **335:** 1897–1905.

Mykles, D. L. 1985. Multiple variants of myofibrillar proteins in single fibers of lobster claw muscles: evidence for two types of slow fibers in the cutter closer muscle. *Biol. Bull.* **169:** 476–483.

Mykles, D. L. 1997. Crustacean muscle plasticity: molecular mechanisms determining mass and contractile properties. *Comp. Biochem. Physiol.* **117B:** 367–378.

Mykles, D. L. 1998. Intracellular proteinases of invertebrates: calcium-dependent and ubiquitin/proteasome-dependent systems. *Int. Rev. Cytol.* **184:** 157–289.

Mykles, D. L., and D. M. Skinner. 1990. Atrophy of crustacean somatic muscle and the proteinases that do the job: a review. *J. Crustac. Biol.* **104:** 577–594.

Neil, D. S., W. S. Fowler, and G. Tobasnick. 1993. Myofibrillar protein composition correlates with histochemistry in fibres of the abdominal flexor muscles of the Norway lobster *Nephrops norvegicus*. *J. Exp. Biol.* **183:** 185–201.

Peuker, H., and D. Pette. 1997. Quantitative analysis of myosin heavy-chain mRNA and protein isoforms in single fibers reveal pronounced fiber heterogeneity in normal rabbit muscles. *Eur. J. Biochem.* **247:** 30–36.

Rosas, C., I. Fernandez, R. Brito, and E. Diaz-Iglesia. 1993. The effect of eyestalk ablation on the energy balance of the pink shrimp, *Penaeus notialis*. *Comp. Biochem. Physiol.* **104A:** 183–187.

Shean, B. S., and D. L. Mykles. 1995. Polyubiquitin in crustacean striated muscle: increased expression and conjugation during molt-induced claw muscle atrophy. *Biochim. Biophys. Acta* **1264:** 312–322.

Silverman, H., W. J. Costello, and D. L. Mykles. 1987. Morphological fiber type correlates of physiological and biochemical properties in crustacean muscle. *Am. Zool.* **27:** 1011–1019.

Skinner, D. M. 1965. Amino acid incorporation into protein during the molt cycle of the land crab, *Gecarcinus lateralis*. *J. Exp. Zool.* **160:** 225–234.

Skinner, D. M. 1966. Breakdown and reformation of somatic muscle during the molt cycle of the land crab, *Gecarcinus lateralis*. *J. Exp. Zool.* **163:** 115–124.

Skinner, D. M. 1985. Molting and regeneration. Pp. 43–146 in *The Biology of Crustacea*, Vol. 9, D. E. Bliss and L. H. Mantel, eds. Academic Press, New York.

Snyder, M. J., and E. S. Chang. 1991. Ecdysteroids in relation to the molt cycle of the American lobster, *Homarus americanus*. *Gen. Comp. Endocrinol.* **81:** 133–145.

Spees, J. L., S. A. Chang, D. L. Mykles, M. J. Snyder, and E. S. Chang. 2003. Molt cycle-dependent molecular chaperone and polyubiquitin gene expression in lobster. *Cell Stress Chaperones* **8:** 258–264.

Stephenson, G. M. M. 2001. Hybrid skeletal muscle fibres: a rare or common phenomenon? *Clin. Exp. Pharmacol. Physiol.* **28:** 692–702.

Stevens, L., B. Gohlsch, Y. Mounier, and D. Pette. 1999. Changes in myosin heavy chain mRNA and protein isoforms in single fibers of unloaded rat soleus muscle. *FEBS Lett.* **463:** 15–18.

Van Herp, F., and J. L. Kallen. 1991. Neuropeptides and neurotransmitters in the X-organ sinus gland complex, an important neuroendocrine integration centre in the eyestalk of Crustacea. Pp. 211–221 in *Comparative Aspects of Neuropeptide Function*, Manchester University Press, New York.

West, J. M. 1997. Ultrastructural and contractile activation properties of crustacean muscle fibres over the moult cycle. *Comp. Biochem. Physiol.* **117B:** 333–345.

Wheatly, M. G., and M. K. Hart. 1995. Hemolymph ecdysone and electrolytes during the molting cycle of crayfish: a comparison of natural molts with those induced by eyestalk removal or multiple limb autotomy. *Physiol. Zool.* **68:** 583–607.

Whiteley, N. M., and A. J. El Haj. 1997. Regulation of muscle gene expression over the moult in Crustacea. *Comp. Biochem. Physiol.* **117B:** 323–331.

Whiteley, N. M., E. W. Taylor, and A. J. El Haj. 1992. Actin gene expression during muscle growth in *Carcinus maenas*. *J. Exp. Biol.* **167:** 277–284.

Wray, W., T. Boulikas, V. P. Wray, and R. Hancock. 1981. Silver staining of proteins in polyacylamide gels. *Anal. Biochem.* **118:** 197–203.

Yu, X., E. S. Chang, and D. L. Mykles. 2002. Characterization of limb autotomy factor—proecdysis (LAF_{pro}), isolated from limb regenerates, that suspends molting in the land crab, *Gecarcinus lateralis*. *Biol. Bull.* **202:** 204–212.

Reference: *Biol. Bull.* **208:** 138–144. (April 2005)

Evolutionary and Acclimation-Induced Variation in the Thermal Limits of Heart Function in Congeneric Marine Snails (Genus *Tegula*): Implications for Vertical Zonation

EMILY STENSENG, CAREN E. BRABY*, AND GEORGE N. SOMERO

Hopkins Marine Station, Department of Biological Sciences, Stanford University, Pacific Grove, California 93950-3094

Abstract. We analyzed the thermal limits of heart function for congeneric species of the marine snail *Tegula* that have different patterns of vertical zonation. *T. funebralis* is found in the low to mid-intertidal zone, and *T. brunnea* and *T. montereyi* live in the low-intertidal or subtidally. As indices of thermal limits of heart function, we used the temperature at which heart rate initially decreased rapidly during heating (the Arrhenius break temperature, or ABT) and the temperature at which heart ceased to beat with either heating or cooling (the flatline temperature, or FLT_{hot} or FLT_{cold}, respectively). These three indices provide an estimate of the thermal range within which *Tegula* heart function is maintained. For field-acclimatized specimens, the thermal range of the high-intertidal *T. funebralis* was greater than those of its two lower-occurring congeners (higher ABT, higher FLT_{hot}, lower FLT_{cold}). We also demonstrated the effects of constant thermal acclimation on the heart rate response to heat stress. Acclimation to 14 °C and 22 °C resulted in increases in ABT and FLT_{hot}, with the largest changes in *T. brunnea* and *T. montereyi*. Although *T. funebralis* is more heat tolerant and eurythermal than its two lower-occurring congeners, it can encounter field body temperatures that exceed ABT, indicating that *T. funebralis* faces a larger threat from heat stress, *in situ*. These findings are consistent with recent studies on other taxa of marine invertebrates that have shown, somewhat paradoxically, that warm-adapted, eurythermal intertidal species may be more impacted by global warming than congeneric subtidal species that are less heat tolerant.

Received 3 September 2004; accepted 22 December 2004.

* To whom correspondence should be addressed, at Monterey Bay Aquarium Research Institute, 7700 Sandholdt Road, Moss Landing, CA 95039. E-mail: caren@mbari.org

Abbreviations: ABT, Arrhenius break temperature, or the temperature at which heart rate decreases rapidly as temperature rises; FLT, flatline temperature, or the temperature at which heart beat ceases, at either high or low temperatures.

Introduction

Physiological adaptations to temperature in ectothermic species are pervasive and have long been regarded as important in establishing biogeographic patterning along latitudinal thermal gradients (Bullock, 1955). Studies of many taxa of marine invertebrates have documented that physiological adaptations to temperature also play key roles in establishing vertical zonation along the subtidal to intertidal gradient (reviewed in Newell, 1979; Somero, 2002). In these analyses of how temperature-adaptive physiological variation contributes to biogeographic and vertical patterning, congeneric species are especially powerful study systems (Stillman and Somero, 1996; Stillman, 2002, 2003; Tomanek, 2002). These closely related species allow the effects of temperature to be discerned because confounding influences due to phylogeny are absent (Stillman and Somero, 2000). Along the gradient of subtidal to intertidal habitats, a wide range of phyla have congeneric species with different vertical zonation ranges, which allows the linkages between adaptation and zonation to be compared.

Studies of congeneric species of the turban snail *Tegula* from central California (Tomanek and Somero, 1999) have shown that a low-to-mid-intertidal species, *T. funebralis* (A. Adams 1855), is more tolerant of high temperatures than two congeners, *T. brunnea* (Philippi, 1848), and *T. montereyi* (Kiener, 1850), that occur exclusively in the very

low intertidal zone or subtidally (hereafter referred to as subtidal species). In an effort to understand the mechanistic bases of these differences in thermal tolerance, we examined the abilities of these three congeners of *Tegula* to sustain heart function at high and low temperatures. We determined the temperature at which heart function initially showed a sharp decrease with rising temperature, the Arrhenius break temperature (ABT) (Dahlhoff *et al.*, 1991; Stillman and Somero, 1996), and the temperature at which heart rate fell to zero, the flatline temperature (FLT_{hot}). The effects of cold stress on heart rate were compared by recording the temperature at which the heart ceased beating during chilling (FLT_{cold}). To determine the relative acclimatory capacities (physiological plasticity) of the three congeners, animals were acclimatized to 14 °C and 22 °C. In agreement with recent studies of porcelain crabs (genus *Petrolisthes*) from subtidal and intertidal habitats (Stillman and Somero, 1996, 2000; Stillman, 2003), the low- to mid-intertidal species *T. funebralis* is significantly more heat tolerant and eurythermal than the subtidal species. Nonetheless, *T. funebralis* faces the largest threat from heat stress *in situ* because its body temperature may routinely reach levels at which heart function is impaired and because it is less able to acclimate to higher temperatures than its more cold-adapted, low-occurring congeners. Thus, somewhat paradoxically, species with relatively high abilities to tolerate heat may be the most threatened by global warming.

Materials and Methods

Study organisms and acclimation protocols

Tegula funebralis has a broad biogeographic distribution in the eastern Pacific. It occurs in the low- to mid-intertidal zone from Vancouver Island, British Columbia, Canada (48°25′N) to central Baja California, Mexico (28°0′N) (Abbott and Haderlie, 1980; Riedman *et al.*, 1981). *Tegula brunnea* occurs in the subtidal to low-intertidal zones of the eastern Pacific Ocean from Cape Arago, Oregon (43°C25′N) to the Santa Barbara Channel Islands, California (34°17′N) (Abbott and Haderlie, 1980; Riedman *et al.*, 1981; Watanabe, 1984). *Tegula montereyi* occurs almost exclusively in the subtidal zone from Sonoma County, California (38°17′N) to the Santa Barbara Channel Islands (Abbott and Haderlie, 1980; Riedman *et al.*, 1981; Watanabe, 1984). Specimens used in these studies were collected in May and June 2004 at Hopkins Marine Station of Stanford University in Pacific Grove, California (36°36′N, 121°54′W). All specimens were adults of medium to large size (20–25 mm basal diameter). Specimens designated as "field acclimatized" were held in recirculating aquaria containing ambient seawater (13–14 °C) for 24 h prior to experimentation.

Acclimation experiments were conducted in two recirculating seawater aquaria with water temperatures set to 14°C and 22 °C (±0.2 °C). Fifteen snails of each species were acclimated for 15–19 days. Animals were fed fresh kelp (*Macrocystis pyrifera*) every 3 days during the acclimation period. Water levels in the tanks were kept high enough to prevent emersion.

Measurements of heart rate

A hand-held drill was used to make two small holes (diameter about 1 mm) in the shell of each snail, adjacent to the pericardial space. Ceramic-coated copper electrodes were inserted into these holes, placed as close as possible to the heart, and secured with cyanoacrylate adhesive. The impedance between the two electrodes, which changed as a function of distance as the heart beat, was converted to a voltage signal using impedance converters (model 2991, UFI, Morro Bay, CA) and recorded using a PowerLab data acquisition system (ADI Instruments, Castle Hill, Australia). To prevent the snails from emerging from their shells during experimentation, the outer lip of the shell was glued to a clean glass microscope slide. Corks were then glued to the top of the shell, and the animals were suspended, by metal clamps attached to the corks, in a temperature-controlled water bath containing filtered and aerated seawater. The temperature of the water bath was controlled by a programmable, computer-controlled Lauda refrigerated water bath whose temperature could be ramped up or down at the desired rate. Six animals were run concurrently in each experiment. A gelatin-filled snail shell in which a thermocouple was implanted was placed in the experimental water bath to monitor the rate of change in "body" temperature during heating or cooling. The heating or cooling of gelatin-filled shells occurs at the same rate as in intact snails (Tomanek and Somero, 1999). Thermal equilibration was essentially instantaneous; that is, there was no measurable difference between the temperatures of the immersion water bath and the gelatin-filled snail shell (data not shown).

For heat-stress experiments, the water bath temperature was held constant at 13 °C for 1 h and then increased by 1 °C every 15 min (see Fig. 1A) a rate that is environmentally realistic (Tomanek and Somero, 1999). Heart rate was measured every 7 min during the experiment. After reaching 40 °C, or once all specimens' hearts had failed, water temperature was decreased rapidly to 13 °C to assess recovery of cardiac function.

For cold-stress experiments, 6 specimens of each species were maintained at 13 °C for 1 h, and then the water temperature was decreased at a rate of 1 °C per 10 min, down to a temperature near 0 °C. After cessation of heart beat, the water temperature was quickly returned to 13 °C to assess recovery of cardiac function.

Following the heat- and cold-stress experiments, snails were removed from the experimental water bath and placed in an aquarium containing 13–15 °C seawater. Survivorship was recorded over a 72-h period.

In addition to temperature ramps, control runs were performed to ensure that the stress of experimentation (drilling, electrode placement and gluing) did not contribute to heart failure or mortality. In the control experiments, heart rates were monitored for 7 h at 13 °C, the ambient seawater temperature during the time of these studies. Survival of the control snails was monitored for a week after the experiments. All snails survived (data not shown).

Data analysis

Heart rates were expressed as beats per minute (bpm). Arrhenius plots (ln bpm *versus* reciprocal temperature (*K*)) were generated, and the Arrhenius break temperature (ABT)—defined as the temperature at which the Arrhenius plot exhibited a sharp discontinuity in slope (*i.e.*, a rapid decrease in bpm once a certain temperature was reached)—was calculated as described by Dahlhoff *et al.* (1991) and Stillman and Somero (1996). ABT was determined, using a standard spreadsheet program by drawing two best-fit regression lines, one on either side of the putative inflection point on the Arrhenius plot (Fig. 1B). The intersection of these two regression lines was used to determine the ABT in degrees Celsius.

Flatline temperatures (FLT_{hot} or FLT_{cold}) were recorded as the temperatures at which the heart beat ceased, at either high or low temperatures.

The effects of temperature and species on ABT and FLT were evaluated using analysis of variance (ANOVA). For analyzing data from field-acclimatized snails, we used one-factor ANOVA (with species as the only factor), while for the data from acclimated specimens we used two-factor ANOVA (with species and acclimation temperature as the two factors). Significant ANOVA results were followed by *post hoc* comparisons to discern the differences among species (Tukey test, $\alpha = 0.05$). Data are given as means ± standard error.

Results

Habitat and body temperatures

During the animal collection period (May–June 2004), sea surface temperatures at our study site (Hopkins Marine Station) were near 13 °C and ambient air temperatures seldom exceeded 20 °C. Thus, the subtidal species, *Tegula brunnea* and *T. montereyi*, were probably exposed to a near-constant temperature of 13 °C prior to experimentation. *T. funebralis*, in contrast, undergoes substantial changes in body temperature in concert with alternating periods of immersion and emersion during the tidal cycle. During a several week period in March and April of 1996, Tomanek and Somero (1999) recorded body temperatures at the same site as ours; they showed that body temperatures were as high as 33 °C for *T. funebralis*, and that temperatures in the range of 27–33 °C were common. In April 2000, Tomanek and Sanford (2003) recorded body temperatures as high as 34.5 °C for *T. funebralis*, consistent with the earlier measurements. During the 1996 study, body temperatures of *T. brunnea* only rarely reached 24 °C. *T. montereyi*, which has a lower vertical position than *T. brunnea*, would not experience body temperatures in excess of ambient water temperatures unless an unusual emersion event occurred. Although our study site on Monterey Bay is near the middle of the distribution ranges of the species, our conclusions about the thermal conditions of the subtidal species during immersion would apply over their full biogeographic ranges, because both species are restricted to cool, mid-latitude habitats in which surface seawater temperature rarely reaches 20 °C (National Climatic Data Center: http://www.ncdc.noaa.gov/oa/ncdc.html.)

Field-acclimatized snails

We initially measured the effects of temperature on the heart rate of field-acclimatized snails. The response of all specimens was qualitatively similar: beats per minute (bpm) initially rose with increasing experimental temperature and then abruptly decreased as a species-specific high temperature, the ABT, was reached (Fig. 1A). ABT values (mean ± SE) for the three congeners were 31.1 ± 0.7 °C for *T. funebralis*, 25.0 ± 0.5 °C for *T. brunnea*, and 24.2 ± 0.7 °C for *T. montereyi* (Fig. 2). ABT values differed significantly by species (one-factor ANOVA, $P < 0.0001$), with *T. funebralis* exhibiting a higher ABT than the two subtidal species; ABTs for the latter two species are not significantly different from each other. In heating experiments, FLT_{hot} values (temperatures at which heart rate fell to zero) for the three congeners were 39.4 ± 0.2 °C for *T. funebralis*, 32.4 ± 0.2 °C for *T. brunnea*, and 33.1 ± 0.1 °C for *T. montereyi* (Fig. 2). As with ABT, FLT_{hot} values differed significantly by species (one-factor ANOVA, $P < 0.0001$), with *T. funebralis* exhibiting a higher FLT_{hot} than the two subtidal species.

When heat-stressed snails taken to the FLT_{hot} were returned to 13 °C, they regained cardiac activity (Fig. 1A). However, within 24–48 h after return to 13 °C, 92% of the *T. funebralis* specimens and 100% of the *T. brunnea* and *T. montereyi* died.

As specimens were cooled from 13 °C down to about 0 °C, heart beat gradually decreased in rate and eventually ceased. No distinct ABT could be determined from the data, but FLTs could be discerned and were significantly different among species (one-factor ANOVA, $P = 0.0005$). *Tegula funebralis* had a significantly greater tolerance of low temperatures, as well as high temperatures; its FLT_{cold} was 2.1 ± 0.2 °C, compared to values of 3.5 ± 0.3 °C and 4.8 ± 0.5 °C for *T. brunnea* and *T. montereyi*, respectively, which were not significantly different from each other. All speci-

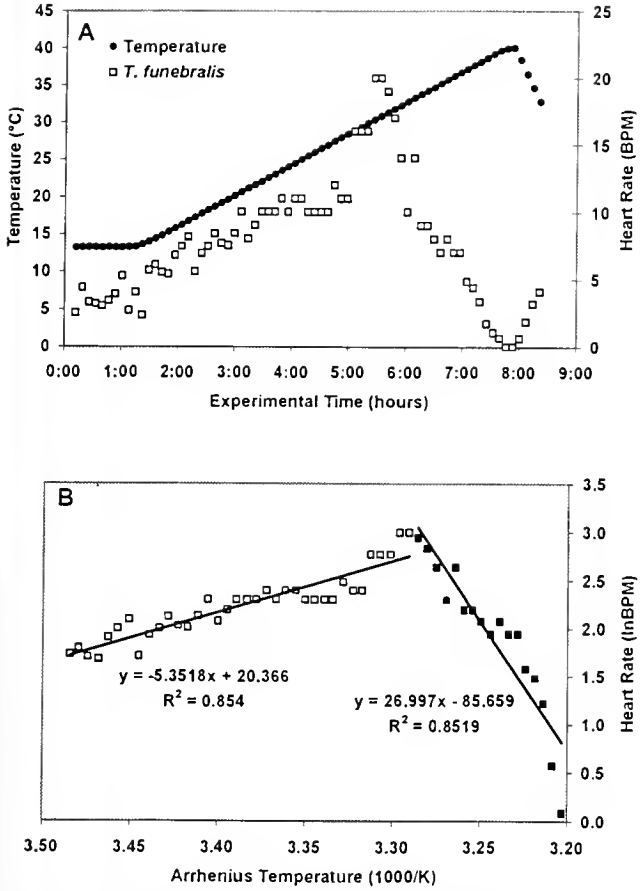

Figure 1. Effects of increasing measurement temperature on heart rate of field-acclimatized *Tegula funebralis*. (A) Typical response of heart rate to increasing temperature. (B) Arrhenius plot of the same data, indicating the method for calculating Arrhenius break temperature (ABT) (see Materials and Methods).

mens subjected to cold stress recovered, and no mortality was observed during the subsequent 3-day holding period.

At a common measurement temperature, the heart rate of *T. funebralis* was significantly higher than those of the other two species. At 13 °C, heart rates were as follows: *T. funebralis*, 6.8 ± 1.3 bpm; *T. brunnea:* 2.0 ± 0.3 bpm; and *T. montereyi*, 3.6 ± 0.4 bpm.

Laboratory-acclimated snails

To examine phenotypic plasticity in ABT and FLT_{hot}, we acclimated the three species to two temperatures, 14 °C and 22 °C. The former temperature corresponds closely to the average water temperature and thus the average body temperatures of the two lower-occurring species) at the season of study (spring); the latter temperature reflects the highest temperatures recorded for *T. brunnea* (Tomanek and Somero, 1999). Both acclimation temperature and species contributed significantly to the patterns of ABT and FLT_{hot} (two-factor ANOVA, $P < 0.0001$ for both ABT and FLT).

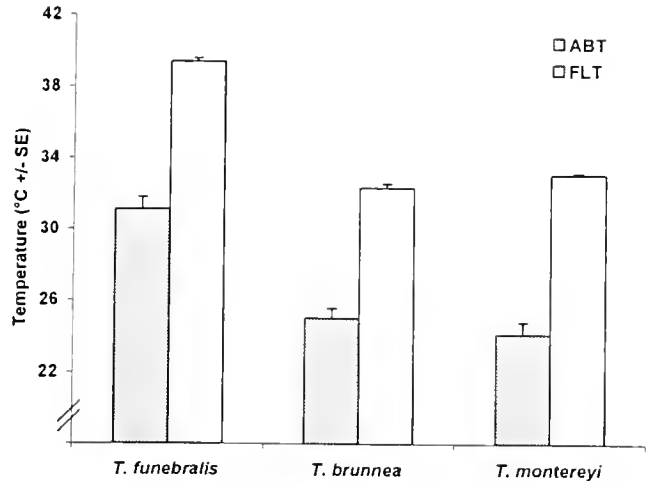

Figure 2. Arrhenius break temperature (ABT) and flatline temperature (FLT_{hot}) values for three congeners of field-acclimatized *Tegula* subjected to heating. Numbers of specimens: *T. funebralis* (13), *T. brunnea* (11), and *T. montereyi* (10). Error bars represent standard errors of the mean.

In all species, the higher acclimation temperature increased both ABT and FLT_{hot}. However, acclimation had stronger effects on the ABT values of the two lower-occurring species, which increased their ABT values by 4 °C (*T. montereyi*) or 6.6 °C (*T. brunnea*), than on that of *T. funebralis*, which increased its ABT by only 1.6 °C (Table 1). Only very small increases in FLT_{hot} were noted (Table 1) but all species were significantly different from each other.

Discussion

The differences in thermal effects on cardiac function among these three congeners of *Tegula* provide insights into

Table 1

Values for Arrhenius break temperature (ABT) and flatline temperature (FLT) (°C) for congeners of Tegula *acclimated to temperatures of 14 °C or 22 °C for 15–19 d or taken directly from the field*

Variable	Acclimation type	*T. funebralis*	*T. brunnea*	*T. montereyi*
Heat stress				
ABT	14 °C	28.5 ± 0.5 °C	20.2 ± 0.8 °C	21.7 ± 0.8 °C
	22 °C	30.1 ± 0.7 °C	26.8 ± 0.7 °C	25.7 ± 0.6 °C
	Field	31.0 ± 0.7 °C	25.0 ± 0.5 °C	24.2 ± 0.7 °C
FLT	14 °C	39.8 ± 0.2 °C	31.7 ± 0.4 °C	33.6 ± 0.3 °C
	22 °C	40.6 ± 0.2 °C	32.8 ± 0.3 °C	34.1 ± 0.2 °C
	Field	39.4 ± 0.2 °C	32.4 ± 0.2 °C	33.1 ± 0.1 °C
Cold stress				
FLT	Field	2.1 ± 0.2 °C	3.5 ± 0.3 °C	4.8 ± 0.5 °C

Number of individuals in each group: acclimated to temperatures of 14 °C or 22 °C (*T. funebralis* = 6; *T. brunnea* = 5; *T. montereyi* = 6) or taken directly from the field (heat stress — *T. funebralis* = 13, *T. brunnea* = 11, *T. montereyi* = 10; cold stress — *T. funebralis* = 6, *T. brunnea* = 6, *T. montereyi* = 6).

the determinants of vertical zonation and the differential effects that climate change may have on these species. We measured two variables to determine thermal effects: the Arrhenius break temperature (ABT), or the temperature at which heart rate decreases rapidly as temperature rises; and the flatline temperature (FLT_{hot} or FLT_{cold}), or the temperature at which heart beat ceases, at either high or low temperatures. The observation that the cardiac function of *T. brunnea* and *T. montereyi* becomes impaired at body temperatures near 24–25 °C, the ABTs for both species, and ceases near 32–33 °C, the FLT_{hot} values of the two species (Fig. 2), shows that neither species is adapted to function at the body temperatures that are common for *T. funebralis* during emersion (Tomanek and Somero, 1999, 2000; Tomanek and Sanford, 2003). Even though the ABTs and, to a lesser extent, the FLT_{hot} values of the two subtidal species were increased during acclimation to high temperature, *T. brunnea* and *T. montereyi* still lack the ability to withstand temperatures that *T. funebralis* encounters during emersion. Although all individuals recovered cardiac function immediately when temperature was reduced to values below the FLT_{hot} (Fig. 1A), no individuals of *T. brunnea* and *T. montereyi* survived during subsequent incubation at 13 °C. Thus, even though cessation of heart activity is not immediately lethal, thermal damage done during exposure to temperatures as high as the FLT_{hot} eventually proved lethal to both subtidal species. Studies of thermal effects on protein synthesis and expression of heat-shock proteins showed that these processes, too, were fully inhibited at temperatures near 33 °C in *T. brunnea* and *T. montereyi* (Tomanek and Somero, 1999). For *T. funebralis*, protein synthesis and production of heat-shock proteins continued to temperatures near 38 °C. Interspecific differences in thermal tolerance were also observed in field experiments in which specimens of *T. brunnea* were caged and transplanted to intertidal sites at which *T. funebralis* is common. During the one month of exposure to intertidal conditions within the cages, no mortality was observed for *T. funebralis*, but 8.5% of the *T. brunnea* specimens died (Tomanek and Sanford, 2003).

The impairment of cardiac function noted in these experiments, which involved only submerged specimens, may underestimate the stress encountered in the field, especially by the intertidal species *T. funebralis*. During emersion, it is possible that stress from desiccation or restricted gas exchange could exacerbate the effects resulting from temperature. For example, if respiratory stress during emersion reduces oxygen supply to the heart, lower ABT and FLT_{hot} values than those reported here may result. We are unaware of any studies of marine invertebrates that have measured thermal limits of heart function in air *versus* water. Santini *et al.* (1999) reported that heart rate in the intertidal limpet *Patella caerulea* was the same in emersed and submerged specimens at temperatures up to about 25 °C, but thermal limits were not determined. A multifactorial analysis of the effects of thermal, respiratory, and desiccation stress could provide a more refined characterization of the limits of cardiac function in intertidal species.

Another possible determinant of cardiac thermal sensitivity that merits further study is the role that variation in temperature, as opposed to average temperature, plays in setting ABT values. Here we show that ABT values for the field-acclimatized specimens of *T. brunnea* and *T. montereyi* (which experience average sea surface temperatures of about 13° C) were more similar to those of the 22 °C-acclimated snails than to those of the 14 °C-acclimated individuals. This suggests that laboratory acclimation studies done at a constant temperature (and thus simulating the average field temperature) may yield data that differ substantially from those obtained from specimens that are field-acclimatized to a similar average, but more variable, temperature. Although we did not determine the ranges of body temperature experienced by the field-acclimatized specimens of the subtidal species, perhaps even short periods at elevated temperatures were sufficient to elicit an adaptive response, that is, an increase in the ABT to values higher than expected on the basis of average temperature.

The increases in ABT noted following acclimation to 14 °C and 22 °C were not paired with equivalent changes in FLT_{hot}. The basis of this discrepancy in the phenotypic plasticity of the two traits is not known, but it might reflect different mechanistic bases for ABT and FLT_{hot}. ABT effects are commonly attributed to alterations in the biophysical properties of membranes (Hochachka and Somero, 2002). Because the composition of membranes can be adaptively altered during thermal acclimation through processes termed homeoviscous and homeophasic adaptation, it is likely that the shifts in ABT reflect such alterations. Dahlhoff and Somero (1993) found correlated changes in the ABT of mitochondrial respiration and membrane biophysical state (fluidity) during thermal acclimation of abalone (genus *Haliotis*). FLT_{hot} values may, in contrast to ABT, reflect thermal effects on cellular constituents such as proteins that are unable to alter their temperature sensitivities during acclimation.

The differences in heat tolerance of cardiac function found among congeners of *Tegula* reveal that interspecific differences in vulnerability to heat death *in situ* exist. The most heat-tolerant and eurythermal species studied, *T. funebralis*, is most threatened by extremes of high temperature. The ABT for cardiac function is slightly below the upper body temperatures encountered during emersion on hot days at a site near the middle of the species' latitudinal distribution range (Tomanek and Somero, 1999). Thus, unlike the two subtidal species, which are unlikely to experience seawater temperatures as high as their ABTs throughout their biogeographic ranges (National Climatic Data Center: http://www.ncdc.noaa.gov/oa/ncdc.html), *T. funebralis* occasionally encounters these temperatures during em-

ersion. Moreover, *T. funebralis* has a lower ability to increase its ABT during acclimation to warmer temperatures. Thus, even though it is more tolerant to heat, *T. funebralis* seems more likely than its subtidal congeners to encounter damaging, if not lethal, temperatures *in situ*. Its limited ability to acclimate to increased temperatures suggests that *T. funebralis* will be more imperiled by global warming than are its lower-occurring congeners. And, as indicated above, if respiratory and desiccation stresses compound the effects of stress from high temperature, *T. funebralis* may be even more threatened by warming than is suggested by these studies done with submerged specimens.

These same interspecific trends were observed in subtidal and low-to-mid-intertidal porcelain crabs (Stillman and Somero, 1996, 2000; Stillman, 2003). The highest occurring temperate porcelain crab had ABTs for heart function that essentially coincided with the highest body temperatures it encounters in the field, and it had a lower ability to increase ABT during warm acclimation. Another parallel with porcelain crabs is found in the interspecific differences in cold tolerance. The more heat-tolerant intertidal species in each genus also sustain heart function at lower body temperatures than do subtidal species (Table 1); that is, they are significantly more eurythermal than subtidal species. The differences in cold tolerance of intertidal and subtidal species may also contribute to vertical zonation, because mid-latitude winter temperatures for emersed intertidal organisms may fall below 0 °C. The mechanistic basis of heart stoppage at low temperatures is not clear. However, the effects of low temperature seem consistent with a gradual reduction in metabolic rate (*i.e.*, in the supply of ATP to support cardiac activity) that eventually leads to cessation of heart beat.

One additional difference between *T. funebralis* and the two subtidal congeners merits noting: the significantly higher rate of heart beat in the intertidal species. Other marine molluscs exhibit a significant positive correlation between heart rate and rate of oxygen consumption (metabolism)(see Santini *et al.*, 1999, for references). Our findings suggest, then, that under identical thermal conditions, *T. funebralis* may have a higher rate of metabolism than its subtidal congeners. Because *T. funebralis* grows significantly more slowly than either *T. brunnea* or *T. montereyi* (Frank, 1965; Watanabe, 1982; Somero, 2002), its higher rate of energy turnover may reflect increased costs of repairing thermal damage. Supporting this hypothesis is evidence from studies of the expression of heat-shock proteins in field-acclimatized individuals of these three species (Tomanek and Somero, 2002). Compared to *T. brunnea* and *T. montereyi*, *T. funebralis* had higher standing stocks of the heat-inducible isoform of heat-shock protein 70 (Hsp72) as well as a higher ratio of Hsp72 to Hsp74, a constitutively expressed chaperone. Similarly, field-acclimatized specimens of *T. funebralis* also had higher standing stocks of the transcription factor, heat-shock factor-1, which modulates expression of heat-shock genes.

In summary, the differences in the responses of heart activity to increases or decreases in body temperature found in three congeneric turban snails having different vertical distributions at a common latitude illustrate the importance of physiological adaptation in establishing vertical zonation in marine species. As in the case of porcelain crabs, the species that lives highest in the intertidal zone and is subject to prolonged periods of emersion is more tolerant of high and low temperatures than are the low-intertidal or subtidal species. However, the most eurythermal and heat-tolerant congeners are also the most threatened by heat stress because the upper value of their temperatures are close to the temperatures that stop their hearts, and because they have limited abilities to extend the heat tolerance of heart function during acclimation to higher temperatures.

Acknowledgments

This study was supported by National Science Foundation grant IBN-0133184 and the Partnership for the Interdisciplinary Study of Coastal Oceans (PISCO). These experiments benefited from the aid of Dr. James Watanabe and Maxine Chaney. This is PISCO contribution number 166.

Literature Cited

Abbott, D. P., and E. C. Haderlie. 1980. Prosobranchia: marine snails. Pp. 230–307 in *Intertidal Invertebrates of California*, R.H. Morris, D.P. Abbott, and E.C. Haderlie, eds. Stanford University Press, Stanford, CA.

Bullock, T. H. 1955. Compensation for temperature in the metabolism and activity of poikilotherms. *Biol. Rev.* **30:** 311–342.

Dahlhoff, E., and G. N. Somero. 1993. Effects of temperature on mitochondria from abalone (genus *Haliotis*): adaptive plasticity and its limits. *J. Exp. Biol.* **185:** 151– 168.

Dahlhoff, E., J. O'Brien, G. N. Somero, and R. D. Vetter. 1991. Temperature effects on mitochondria from hydrothermal vent invertebrates: evidence for adaptation to elevated and variable habitat temperatures. *Physiol. Zool.* **64:** 1490–1508.

Frank, P. W. 1965. Shell growth in a natural population of the turban snail, *Tegula funebralis*. *Growth* **29:** 395–403.

Hochachka, P. W., and G. N. Somero. 2002. *Biochemical Adaptation: Process and Mechanism in Physiological Evolution.* Oxford University Press, Oxford, UK.

Newell, R. C. 1979. *Biology of Intertidal Animals.* Marine Ecological Surveys, Faversham, UK.

Riedman, M. L., A. H. Hines, and J. S. Pearse. 1981. Spatial segregation of four species of turban snails (genus *Tegula*) in central California. *Veliger* **24:** 97–102.

Santini, G., M. DePirro, and G. Chelazzi. 1999. *In situ* and laboratory assessment of heart rate in a Mediterranean limpet using a noninvasive technique. *Physiol. Biochem. Zool.* **72:** 198–204.

Somero, G. N. 2002. Thermal physiology and vertical zonation of intertidal animals: optima, limits, and costs of living. *Integr. Comp. Biol.* **42:** 780–789.

Stillman, J. H. 2002. Causes and consequences of thermal tolerance limits in rocky intertidal porcelain crabs, genus *Petrolisthes*. *Integr. Comp. Biol.* **42:** 790–796.

Stillman, J. H. 2003. Acclimation capacity underlies susceptibility to climate change. *Science* **301:** 65.

Stillman, J. H., and G. N. Somero. 1996. Adaptation to temperature stress and aerial exposure in congeneric species of intertidal porcelain crabs (genus *Petrolisthes*): correlation of physiology, biochemistry and morphology with vertical distribution. *J. Exp. Biol.* **199:** 1845–1855.

Stillman, J. H., and G. N. Somero. 2000. A comparative analysis of the upper thermal tolerance limits of eastern Pacific porcelain crabs, genus *Petrolisthes:* influences of latitude, vertical zonation, acclimation and phylogeny. *Physiol. Biochem. Zool.* **73:** 200–208.

Tomanek, L. 2002. The heat-shock response and patterns of vertical zonation in intertidal *Tegula* congeners. *Integr. Comp. Biol.* **42:** 797–807.

Tomanek, L., and E. Sanford. 2003. Heat-shock protein 70 (Hsp70) as a biochemical stress indicator: an experimental field test in two congeneric intertidal gastropods (Genus: *Tegula*). *Biol. Bull.* **205:** 276–284.

Tomanek, L., and G. N. Somero. 1999. Evolutionary and acclimation-induced variation in the heat-shock responses of congeneric marine snails (genus *Tegula*) from different thermal habitats: implications for limits of thermotolerance and biogeography. *J. Exp. Biol.* **202:** 2925–2936.

Tomanek, L., and G. N. Somero. 2000. Time course and magnitude of synthesis of heat-shock proteins in congeneric marine snails (genus *Tegula*) from different tidal heights. *Physiol. Biochem. Zool.* **73:** 249–256.

Tomanek, L., and G. N. Somero. 2002. Interspecific- and acclimation-induced variation in levels of heat-shock proteins 70 (hsp70) and 90 (hsp90) and heat-shock transcription factor-1 (HSF1) in congeneric marine snails (genus *Tegula*): implications for regulation of *hsp* gene expression. *J. Exp. Biol.* **205:** 677–685.

Watanabe, J. M. 1982. Aspects of community organization in a kelp forest habitat: factors influencing the bathymetric segregation of three species of herbivorous gastropods. Ph.D. dissertation, University of California, Berkeley.

Watanabe, J. M. 1984. The influence of recruitment, competition, and benthic predation on spatial distributions of three species of kelp forest gastropods (Trochidae: *Tegula*). *Ecology* **65:** 920–936.

Reference: *Biol. Bull.* **208:** 145–155. (April 2005)

Characterization of Symbiont Populations in Life-History Stages of Mussels From Chemosynthetic Environments

JENNIFER L. SALERNO[1], STEPHEN A. MACKO[2], STEVE J. HALLAM[3], MONIKA BRIGHT[4], YONG-JIN WON[5], ZOE McKINESS[6], AND CINDY L. VAN DOVER[1,*]

[1] *Biology Department, The College of William & Mary, Williamsburg, Virginia 23187;* [2] *Department of Environmental Sciences, University of Virginia, Charlottesville, Virginia 2290;* [3] *Monterey Bay Aquarium Research Institute, 7700 Sandholdt Road, Moss Landing, California 95039;* [4] *Department of Marine Biology, Institute of Ecology and Conservation Biology, University of Vienna, Althantstrasse 14, 1090 Vienna, Austria;* [5] *Dept. of Life Sciences, Ewha Womans University, Science C Building, 11-1 Daehyon-Dong, Sodaemun-Ku, Seoul, 120–750, Korea; and* [6] *Department of Organismic and Evolutionary Biology, Harvard University, Cambridge, Massachusetts 02138*

Abstract. The densities of chemoautotrophic and methanotrophic symbiont morphotypes were determined in life-history stages (post-larvae, juveniles, adults) of two species of mussels (*Bathymodiolus azoricus* and *B. heckerae*) from deep-sea chemosynthetic environments (the Lucky Strike hydrothermal vent and the Blake Ridge cold seep) in the Atlantic Ocean. Both symbiont morphotypes were observed in all specimens and in the same relative proportions, regardless of life-history stage. The relative abundance of symbiont morphotypes, determined by transmission electron microscopy, was different in the two species: chemoautotrophs were dominant (13:1–18:1) in *B. azoricus* from the vent site; methanotrophs were dominant (2:1–3:1) in *B. heckerae* from the seep site. The ratio of CH_4:H_2S is proposed as a determinant of the relative abundance of symbiont types: where CH_4:H_2S is less than 1, as at the Lucky Strike site, chemoautotrophic symbionts dominate; where CH_4:H_2S is greater than 2, as at the seep site, methanotrophs dominate. Organic carbon and nitrogen isotopic compositions of *B. azoricus* ($\delta^{13}C = -30‰$; $\delta^{15}N = -9‰$) and *B. heckerae* ($\delta^{13}C = -56‰$; $\delta^{15}N = -2‰$) varied little among life-history stages and provided no record of a larval diet of photosynthetically derived organic material in the post-larval and juvenile stages.

Received 17 December 2003; accepted 9 February 2005.
* To whom correspondence should be addressed. E-mail: clvand@wm.edu

Introduction

Mussels in the genus *Bathymodiolus* are biomass dominants at many known deep-sea hydrothermal vent and cold seep habitats, where they are host to endosymbiotic, autotrophic bacteria in their gills. Anatomical and nutritional relationships between the symbionts and their adult hosts is well documented (*e.g.*, Distel *et al.*, 1995; Robinson *et al.*, 1998; Southward *et al.*, 2001; Fiala-Médioni *et al.*, 2002; Raulfs *et al.*, 2004). Although bathymodiolin mussels may be able to obtain some nutrition by suspension feeding (Le Pennec *et al.*, 1990; Page *et al.*, 1991; Fujiwara *et al.*, 1998), most of the nutrition of adult mussels is derived from their symbionts (Fisher *et al.*, 1988; reviewed in Fisher, 1990; Childress and Fisher, 1992; Kochevar *et al.*, 1992). Larval stages of vent mussels are pelagic and have been described as planktotrophic (Lutz *et al.*, 1980; Berg, 1985; LePennec and Beninger, 2000), but the distribution of mussel larvae in the water column, the nature of their planktonic diet, and the trophic transition that takes place as they become benthic are all unknown.

Some mussel species host only chemoautotrophic (also referred to as thiotrophic), sulfur-oxidizing bacterial symbionts (Nelson *et al.*, 1995; Fujiwara *et al.*, 2000); other species host only methanotrophic symbionts (Fujiwara *et al.*, 2000; Barry *et al.*, 2002); and still others host both types of bacteria ("dual symbionts"; Fisher *et al.*, 1993; Robinson *et al.*, 1998; Fiala-Médioni *et al.*, 2002). Dual symbionts

provide obvious advantages to host individuals recruiting to environments where the availability of substrates is unpredictable or fluctuating (Cavanaugh *et al.*, 1992; Robinson *et al.*, 1998; Fiala-Médioni *et al.*, 2002), but the host is also challenged to recognize and sequester two different microbial types within its cells, while excluding pathogenic or otherwise harmful bacteria. There is some empirical evidence that the relative abundance of dual symbionts within adult mussels of a given species can vary in response to environmental parameters (Trask and Van Dover, 1999; Fiala-Médioni *et al.*, 2002), although *in situ* studies involving transplant experiments have yet to be reported, and the manner through which these symbiont populations are regulated is unclear. Although the mode or modes of acquisition of dual symbionts in the earliest life-history stages of mussels is also uncertain, a recent report (Won *et al.*, 2003) provides evidence for environmental acquisition of chemoautotrophic symbionts in *Bathymodiolus azoricus* von Cosel *et al.*, 1999; and *B. puteoserpentis* von Cosel *et al.* 1994 from hydrothermal vents. If symbionts are acquired from the environment, rather than by maternal transfer, then acquisition of dual symbionts need not be simultaneous and may be a response to ontogenetic or environmental conditions of the host mussels. Furthermore, it is not inconceivable that juveniles and adults might use sulfide and methane in different proportions so as to minimize intraspecific competition, or that juveniles and adults occupy different microzones within diffuse flow vents with different relative availabilities of sulfide and methane, and that these conditions might be reflected in the relative abundance of the symbiont types (Trask and Van Dover, 1999; Colaço *et al.*, 2002; Fiala-Médioni *et al.*, 2002).

Adults of *B. azoricus* from the Lucky Strike vent site on the Mid-Atlantic Ridge (Fig. 1) are known to host chemoautotrophic and methanotrophic symbionts in their gills; the evidence is based on ultrastructural, biochemical, isotopic, and immunological characterization (Fiala-Médioni *et al.*, 2002). Adults of *B. heckerae* from the Blake Ridge seep site off the coast of South Carolina (Fig. 1) are also reported to host dual symbionts; this report is based on ultrastructural and isotopic evidence (Van Dover *et al.*, 2003). In this study, we used transmission electron microscopy (TEM) to explore the composition and density of symbionts in early life-history stages (*i.e.*, post-larvae and juveniles) of these species, as well as in adults. Mussel recruits often occur in large numbers (>1000 m^{-2}) in mussel beds (CLVD, pers. obs.). The most recent arrivals (post-larvae) are between 0.6 and 1.2 mm in shell length and are recognizable by the presence of prodissoconch I and II shells and the lack of dissoconch shell growth. In addition to lines of demarcation, prodissoconch and dissoconch shells are conveniently differentiated by shell color: prodissoconch shells are pink or red; dissoconch shell material is yellow.

We aimed in this study to determine whether chemoautotrophic and methanotrophic symbionts are present in the very earliest benthic stages, which would indicate simultaneous or near-simultaneous acquisition of both symbiont types early in the life history of the mussels. We also asked whether the relative abundance of chemoautotrophs and methanotrophs includes an ontogenetic factor. In addition to using transmission electron microscopy for quantitative assessment of symbiont populations, we used carbon and nitrogen stable isotopes in an attempt to detect isotopic remnants of a photosynthetically based larval diet in post-larval tissues, to interpret the relative abundance of symbiont types within and between mussel species, and to determine whether the contribution of chemoautotrophic and methanotrophic production to host nutrition varied with the size of the mussel.

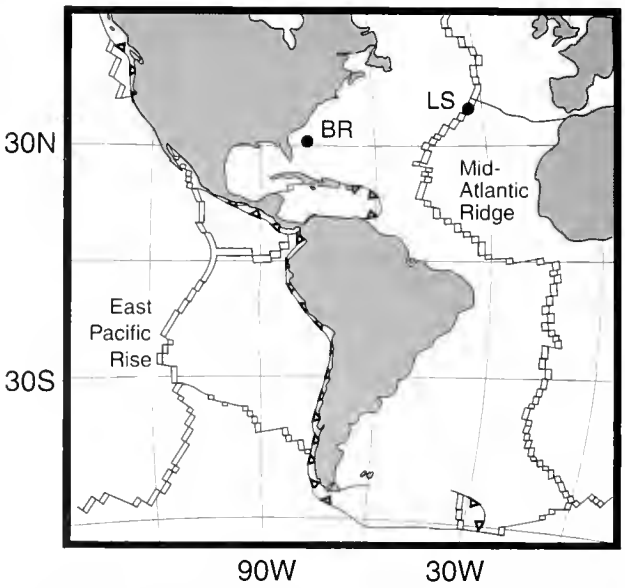

Figure 1. Location of sampling sites. LS = Lucky Strike hydrothermal vent, Mid-Atlantic Ridge; BR = Blake Ridge cold seep.

Materials and Methods

Sample collection

The deep-submersible vehicle *Alvin* was used to collect samples of adult mussels and their associated fauna. *Bathymodiolus azoricus* mussels were collected in July 2001 from Eiffel Tower at the Lucky Strike hydrothermal vent field [Mid-Atlantic Ridge, 37°17.5′N, 32°16.5′W; 1687 m; see Van Dover *et al.* (1996) for site description]. *Bathymodiolus heckerae* was collected in September 2001 from the Blake Ridge methane-hydrate seep [western Atlantic, 32°31′N, 76°12′W; 2170 m; see Van Dover *et al.* (2003) for site description]. The mussels were rinsed over a 250-μm sieve with chilled (4 °C), 10-μm filtered seawater. To collect

post-larval and juvenile mussels, fresh, sieved material was sorted under a dissecting microscope.

Mussels were separated into classes based on shell color, shell morphology, and shell length. The smallest size class consisted of post-larval mussels with pinkish-red prodissoconchs (I and II) and with shell lengths within the range of 0.12 to 0.60 mm. Early juveniles, herein referred to as "J1", were characterized by the presence of a narrow band of yellow dissoconch shell and by shell lengths within the range of 0.6 to 1.2 mm. Four additional juvenile size classes were designated, with shell lengths in the following ranges: J2: 1.2–2.4 mm; J3: 3.6–4.8 mm; J4: 4.8–6.0 mm; and J5: 6.0–8.4 mm.

Transmission electron microscopy

A 0.5-cm-wide section of tissue was dissected from the middle of the gill of adult and larger juvenile specimens. Where mussels were too small to be dissected (*i.e.*, post-larvae and juvenile stages J-1 and J-2), the shells were cracked to allow fixative to penetrate the tissue. *Bathymodiolus azoricus* tissues were fixed for about 3 weeks in 3% glutaraldehyde with 0.1 *M* cacodylate buffer and 0.4 *M* NaCl (pH 7.8). *Bathymodiolus heckerae* tissues were fixed for about 48 hours in 3% glutaraldehyde with 0.1 *M* phosphate buffer and 0.25 *M* sucrose (pH 7.4). Samples were rinsed in 0.1 *M* phosphate buffer containing 0.25 *M* sucrose and were post-fixed in a 1% osmium tetroxide solution. The shells of post-larvae and juveniles were dissolved by a 24-h immersion in 2.5 g EDTA/100 ml buffer solution. Specimens were dehydrated in a graded acetone series and stained *en bloc* with 2% uranyl acetate. Gill tissue or whole individuals were infiltrated with Embed 812 epoxy embedding medium, polymerized, cut into 70-nm to 80-nm thin sections, and stained with lead citrate. Gill sections were viewed with a Zeiss 109 transmission electron microscope.

Densities of bacterial morphotypes

The density of bacterial morphotypes is defined here as the number of methanotrophic or chemoautotrophic cells per 15.5 μm^2 within the apical region of bacteriocytes in transverse section (Fig. 2). The areal dimension and location were chosen because they approximately cover the region of a bacteriocyte that contains symbionts. For each specimen, three transverse sections were cut through the middle of the gill filaments (3 to 6 gill filaments per section) at intervals greater than the maximum diameter of the bacteria (*i.e.*, > 2.0 μm) to ensure that a particular bacterial cell was counted only once. Fifteen 15.5-μm^2 areas per section were haphazardly selected at low magnification (240×) for bacterial cell counts. Where an area selected haphazardly at low magnification was not located in the apical region of a bacteriocyte, the specimen was adjusted until the apical region of that bacteriocyte filled the field of view. Counts were carried

Figure 2. Transmission electron micrograph mosaic of a transverse section through a post-larval specimen of *Bathymodiolus azoricus* (0.12 to 0.60 mm in shell length) gill filament. cc, ciliary cell; fc, frontal cilia; lc, lateral cilia; lu, lumen; ly, lysosomal-like residual body; n, nucleus; m, methanotrophic morphotypes; arrowheads, chemoautotrophic morphotypes; double-ended arrow, apical region of bacteriocyte. Scale bar = 2 μm.

out at high magnification (48,000×) and included all bacterial cells that were in the field of view and those cells that were intersected by the upper and right margins.

The density of bacterial morphotypes was estimated for mussels of different sizes within each species, as follows: *Bathymodiolus azoricus*—3 post-larvae, 5 J1, 5 J2, 5 J3, and 4 adults; *B. heckerae*—3 post-larvae, 5 J1, 4 J2, 5 J3, and 4 adults. The Kruskal-Wallis nonparametric test for a one-way design was used to assess variations in median density of each morphotype within a mussel species ($\alpha = 0.05$).

Stable isotope analyses

Foot, gill, and mantle tissue was dissected, variously, from adult mussels (>20 mm in shell length) and placed in a drying oven (70 °C) for 24 h. Due to their small size, post-larval and juvenile mussels (<8 mm in shell length) were pooled [post-larvae: 35 individuals per pooled sample; juvenile size classes (J1 through J5): 2 individuals per pooled sample]. These pooled samples were dried whole, then soaked in 10% HCl to remove the shell carbonate, and then re-dried. Subsamples of dried, acidified tissues were

ground to a fine powder and packaged in tin capsules. Samples were transformed to CO_2 and N_2 for isotope analysis with a Carlo Erba elemental analyzer coupled to an OPTIMA stable isotope ratio mass spectrometer (Micromass, Manchester, UK). Carbon and nitrogen isotopes were determined with a single combustion in a dual-furnace system composed of an oxidation furnace at 1020 °C and a reduction furnace at 650 °C. The resulting gases were purified by gas chromatography, chemically dried, and injected into the source of the mass spectrometer by continuous flow.

Stable isotope ratios are reported in the following notation: $\delta^X E = [R_{sample}/R_{standard} - 1]\ 10^3$ (‰), where X is the heavy isotope of element E, and R is the abundance ratio of the heavy to light isotopes of that element (*i.e.*, $^{13}C/^{12}C$ and $^{15}N/^{14}N$). Stable isotope compositions were calculated relative to the international standards for carbon (Pee Dee Belemnite limestone, PDB) and nitrogen (atmospheric N_2, air), which have defined $\delta^X E$ values of 0.0‰. Isotope values are reported as means (± standard deviation). Statistical comparisons of isotopic compositions between small and large mussels were made after defining a *post hoc* 8-mm boundary based on the relationship between isotopic composition and shell length.

Results

Gill ultrastructure

The number of gill filaments and the length of the dorsal-ventral axis of the gill filaments increase with shell length and volume of the individual. The increase in gill-filament length reflects an increase in the number of bacteriocytes and intercalary cells constituting the gill filament. Cells exhibiting two distinct morphotypes were observed with transmission electron microscopy within gill epithelial cells (bacteriocytes) of all stages of *Bathymodiolus azoricus* and *B. heckerae* (total number of specimens examined = 43) and were interpreted to be bacteria (Figs. 2, 3). Both bacterial morphotypes, either singly or in groups of two or more cells, were contained in vacuoles surrounded by a peribacterial membrane. The larger, round-to-oval-shaped morphotypes did not differ in size within the different host mussel species, and had an overall mean diameter of 1.1 μm (± 0.06 SE; n = 165). These large cells contained stacks of complex intracytoplasmic membranes, characteristic of type I or type X methanotrophic bacteria (Cavanaugh *et al.*, 1992). The smaller morphotype was also similar in size within the different host mussel species, and had an overall mean diameter of 0.31 μm (± 0.05 SE; n = 165). This smaller cell type was coccid or, less frequently, rod-shaped, lacked intracellular membranes, and resembled chemoautotrophic bacteria (Cavanaugh *et al.*, 1992). Because these two morphotypes were of the same general size and ultrastructure as the two types of symbionts described from other bathymodiolin mussels (Cavanaugh *et al.*, 1987; Fisher *et al.*, 1993; Distel *et al.*, 1995; Fiala-Médioni *et al.*, 2002), we refer to them herein as chemoautotrophic and methanotrophic symbiont morphotypes, or simply as chemoautotrophs and methanotrophs.

Divisional stages of chemoautotrophic and methanotrophic bacterial morphotypes were observed in all size classes of both mussel species. Transverse sections of bacteriocytes that contained only a single symbiont type were rarely observed. Apparent lysosomal digestion of symbionts (Fiala-Médioni *et al.*, 1986, 2002; Kochevar *et al.*, 1992) was indicated by the presence of cellular components resembling lysosomal residual bodies in the basal portion of the bacteriocytes (Figs. 2, 3). These bodies appeared to contain remnants of partially digested bacterial cells of both types and were observed regularly in both species of mussel and in all size classes examined.

Possible instances of endo- or exocytosis of symbionts (*e.g.*, Fig. 4A) were observed in several *B. azoricus* and *B. heckerae* individuals, but, due to the static nature of transmission electron microscopy, we could neither infer which of these two processes was taking place nor even eliminate the possibility that this observation was an artifact of fixation. Abnormally large vacuoles filled with chemoautotrophic or methanotrophic bacterial morphotypes, or both, were occasionally observed in *B. azoricus* mussels (Fig. 4B).

In several *B. azoricus* individuals, bacteriocytes seemed to be separated from adjacent bacteriocytes and were rounded off at their basal portion (Fig. 4C). In other cases, bacteriocyte cell membranes and most of the peribacterial membranes were disrupted (Fig. 4D).

Chemoautotrophic and methanotrophic bacterial morphotypes were also observed in the mantle epithelium of post-larval and juvenile *B. azoricus* and *B. heckerae* mussels (Fig. 4E, F). Mantle epithelial cells containing symbiont morphotypes were similar in ultrastructure to gill bacteriocytes. Cellular components resembling lysosomal residual bodies were also observed near the basal nuclei of mantle bacteriocytes. Bacteria-like bodies, with dimensions and ultrastructural characteristics resembling those of chemoautotrophic and methanotrophic symbiont morphotypes of the gill and mantle, were also observed in the gut lumen of several post-larvae.

Density of bacterial symbiont morphotypes

Total average density of symbionts was 4 to 5 times greater in *B. azoricus* than in *B. heckerae* (Fig. 5). Methanotrophic morphotype densities in *B. azoricus* were uniformly low (mean density < 4 cells per 15.5 μm^2) in all size classes examined; chemoautotrophic morphotype densities (mean density between 23 and 40 cells per 15.5 μm^2 in 17 of 22 specimens) were an order of magnitude greater than

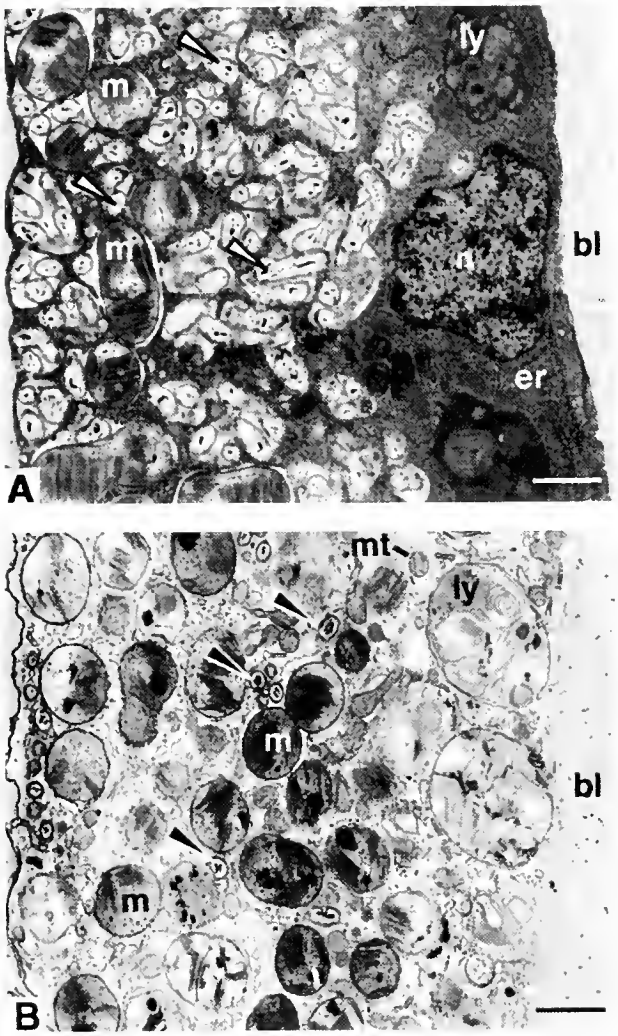

Figure 3. Transmission electron micrographs of transverse sections through (A) *Bathymodiolus azoricus* and (B) *B. heckerae* mussel gill filaments of juveniles (J1 size class). bl, basal lamina; er, endoplasmic reticulum; ly, lysosomal-like residual body; mt, mitochondrion; n, nucleus; m, methanotrophic morphotypes; arrowheads, chemoautotrophic morphotypes. Scale bars = 1 μm.

methanotrophic morphotype densities (Fig. 5A). Variation in densities of both morphotypes was maximal in the smallest, post-larval size class. No significant differences in median symbiont densities were detected in Kruskal-Wallis comparisons of size-class pairs within *B. azoricus* (chemoautotrophs, $P = 0.115$; methanotrophs, $P = 0.383$).

Methanotrophic symbionts accounted for more than 60% of the total bacterial symbiont density in *B. heckerae*, compared to less than 10% in *B. azoricus* (Fig. 5). Methanotrophic and chemoautotrophic densities were uniformly low in *B. heckerae* (mean density of both morphotypes combined, < 15 cells per 15.5 μm^2) in all size classes examined (Fig. 5B). The median density of symbionts in *B. heckerae* did not differ among the size-classes examined (chemoautotrophs, $P = 0.67$; methanotrophs, $P = 0.342$).

Stable isotopic compositions

A difference of more than 25‰ was measured in the $\delta^{13}C$ compositions (Fig. 6) of *B. azoricus* (~ -30‰) and *B. heckerae* (~ -56‰). Within *B. azoricus*, the $\delta^{13}C$ composition was enriched in ^{13}C (by 3‰) in juvenile mussels (<8 mm shell length) compared with larger mussels (>20 mm shell length). Average $\delta^{15}N$ values of mussel tissues (Fig. 6) were also different in the two species (*B. azoricus:* ~ -9‰; *B. heckerae:* ~ -2‰), and there was a small ($\sim$1.6‰) difference in the nitrogen isotopic composition of small and large individuals of *B. azoricus*. Average $\delta^{15}N$ values were enriched in ^{15}N by $\sim$5.5‰ in large individuals of *B. heckerae* (>20 mm) compared to small ones (<8 mm), whether the comparison was made using values for gill or mantle in the larger individuals.

Discussion

Descriptive characteristics of the symbionts

Gill tissues of *Bathymodiolus azoricus* and *B. heckerae* post-larvae from vent and seep mussel beds contain cells that we infer to be methanotrophic and chemoautotrophic endosymbionts on the basis of their size and ultrastructural characters. The presence of both symbiont morphotypes in the earliest, post-larval benthic stage of the mussels suggests that the mussels are autotrophically competent to oxidize sulfide and methane as soon as they arrive at a vent site or very shortly thereafter. The absence of symbionts in post-larvae would have been consistent with a horizontal mode of transmission; the presence of symbionts in post-larvae does not allow us to resolve the mode of symbiont transmission.

The presence of chemoautotrophic and methanotrophic symbiont types was not limited to gill tissues; symbionts were also found in mantle epithelial cells of post-larvae and juveniles. Bacteriocytes located along that surface of the mantle exposed to the mantle cavity, and thus to the water flow generated by gill cilia in post-metamorphic mussels, were morphologically indistinguishable from bacteriocytes in the gill epithelium. Qualitative observations indicate that bacteriocytes in both locations contain similar densities and ratios of endosymbionts. Mantle and gill bacteriocytes also contained cellular components resembling lysosomal residual bodies, consistent with digestion of bacteria and nutritional reliance on symbionts by host mussels (Fisher, 1990; Cavanaugh *et al.*, 1992; Fiala-Médioni *et al.*, 2002; Barry *et al.*, 2002). The observation of mantle bacteriocytes is not unprecedented, although this is, to our knowledge, the first record for a vent mussel. Streams *et al.* (1997) observed coccid bacteria resembling gill endosymbionts in the mantle

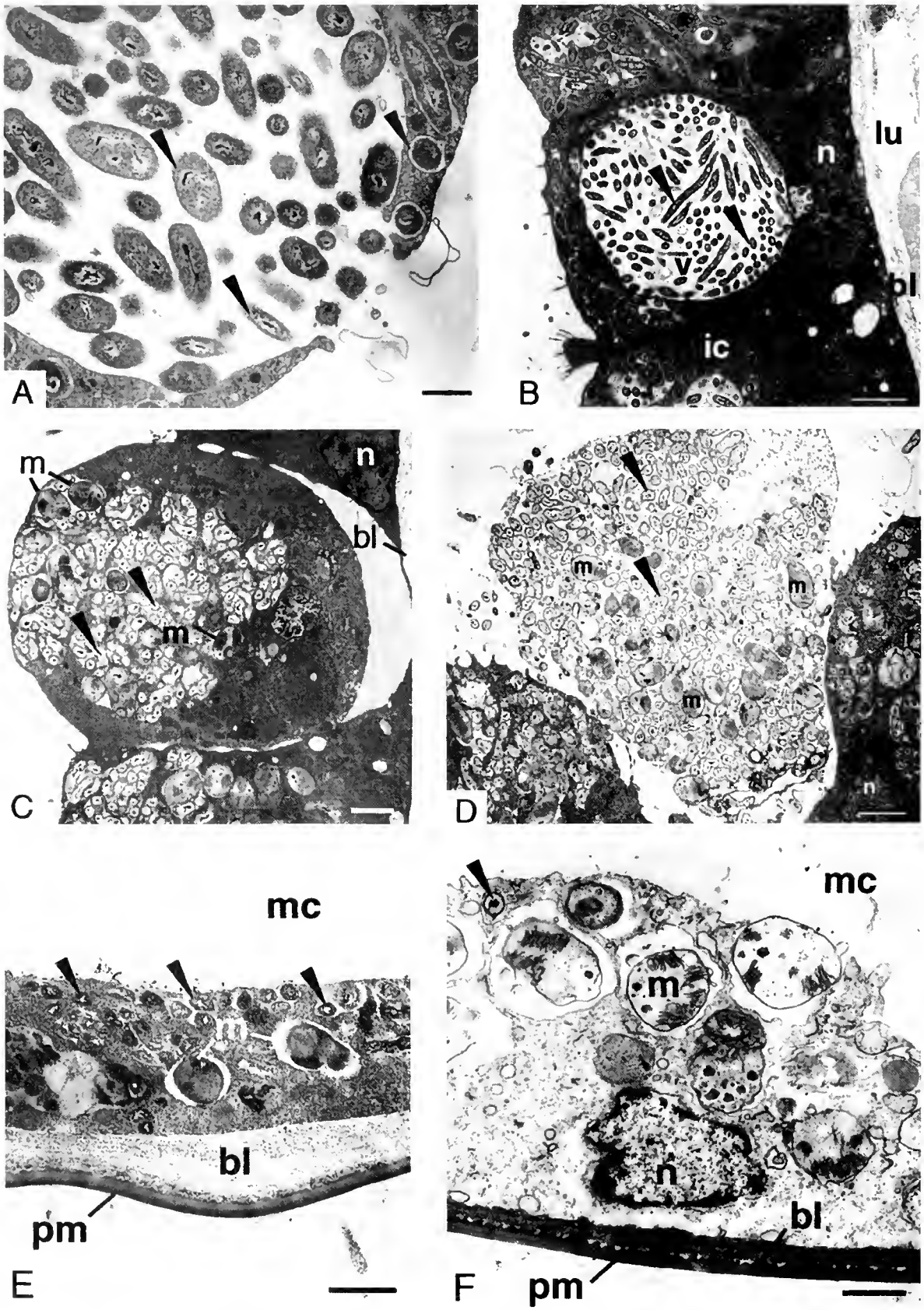
A
B
lu
n
v
bl
ic
C
m
n
bl
m
D
m
m
m
n
E
mc
bl
pm
F
mc
m
n
bl
pm

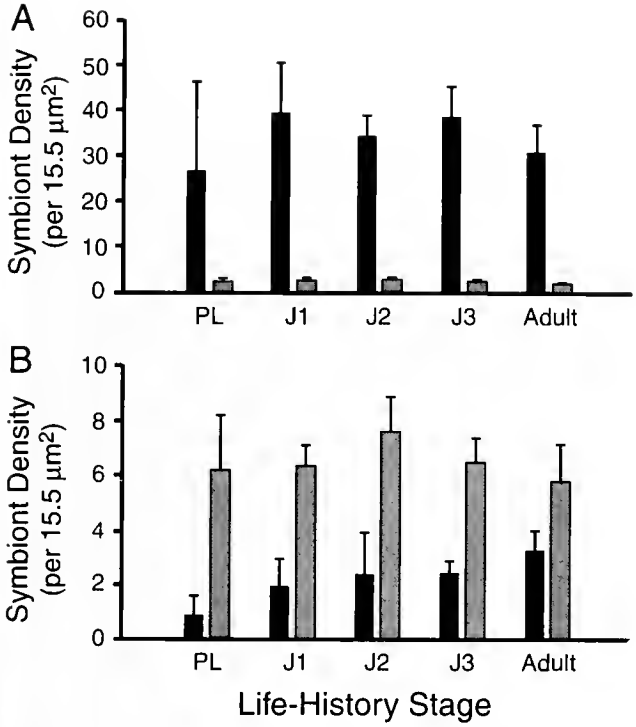

Figure 5. Symbiont densities per 15.5 μm^2 ($\pm$ SD) in gill tissues. (A) *Bathymodiolus azoricus*. (B) *B. heckerae*. PL = post-larvae; J1–J3 = juvenile size classes 1–3 (see text). Black bars, chemoautotrophic morphotype; grey bars, methanotrophic morphotypes.

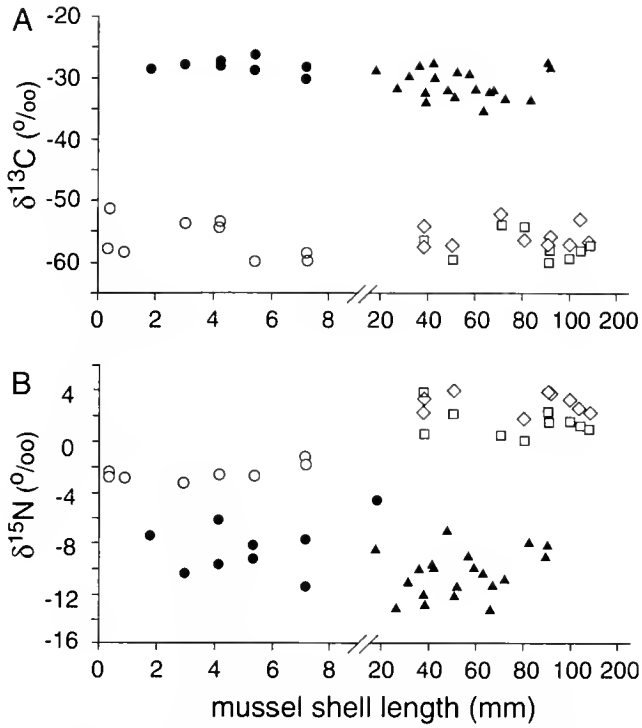

Figure 6. *Bathymodiolus* spp. stable isotopic composition of tissues. (A) $\delta^{13}C$ (‰) *vs.* shell length; (B) $\delta^{15}N$ (‰) *vs.* shell length. *B. azoricus:* filled symbols; *B. heckerae:* open symbols. For whole mussels < 8 mm (○ or ●), whole animals (acid-treated to dissolve shells) were pooled and analyzed (see Materials and Methods). For mussels > 20 mm, ▲ = foot tissue; ◇ = gill tissue; □ = mantle tissue.

and foot tissue of juvenile (shell length = 4 to 8 mm) seep mussels (*Bathymodiolus childressi*) from the Gulf of Mexico. All symbionts exhibited morphotypes of type I methane-oxidizing bacteria and actively incorporated carbon from methane during ^{14}C tissue autoradiography experiments. Given the origins of gill primordia as epithelial protuberances of the mantle at the base of the foot during larval development in some bivalve species (Chaparro *et al.*, 2001), mantle cells, rather than gill cells, may be the locus of initial infection of environmentally acquired symbionts (Streams *et al.*, 1997). Furthermore, the volume of gill bacteriocytes is limited in smaller individuals. Mantle symbionts may provide an important additional source of nutrition to post-larval and juvenile mussels.

In addition to possible lysosomal digestion of gill and mantle symbionts, we occasionally observed gill and mantle bacteriocytes associated with large clusters of extracellular symbionts in both mussel species, but we could not tell whether the host cells were engaged in endocytosis or exocytosis at the time of fixation (but see also Won *et al.*, 2003, wherein endocytosis in a bathymodiolin species is inferred from ultrastructural studies).

Bacteriocytes in apparent stages of degradation were occasionally observed, although we cannot discount the possibility that the degraded cells are artifacts of the fixation process. In some cases, degrading cells are round and separate laterally from adjacent bacteriocytes, but host cytoplasm and organelles and symbionts remain intact. In other degrading cells, host cell membranes and peribacterial membranes are disrupted, host cytoplasm and organelles are lost, and symbionts appear to be released from the host cell. If these "abnormal" bacteriocytes indeed represent a degradation sequence, the intact nature of the symbionts stands in

Figure 4. (A) Example of a breach in a gill bacteriocyte membrane, indicative of endo- or exocytosis; scale bar = 2.0 μm. (B) Large vacuole filled with chemoautotrophic morphotypes in a gill bacteriocyte; scale bar = 1.0 μm. (C) Gill bacteriocyte separating from surrounding bacteriocytes; scale bar = 1.0 μm. (D) Bacteria expelled from a gill bacteriocytes; scale bar = 0.5 μm. (E, F) Mantle tissue of post-larval specimens of *Bathymodiolus azoricus* and *B. heckerae*, respectively; scale bar (E) = 1.0 μm, scale bar (F) = 1.5 μm. bl, basal lamina; ic, intercalary cell; lu, lumen; mc, mantle cavity; n, nucleus; v, vacuole; m, methanotrophic morphotypes; pm, protein matrix; arrowheads, chemoautotrophic morphotypes.

contrast to digested symbionts observed during the process of cell death in *Riftia pachyptila* (Bright and Sorgo, 2003). The specific processes of cell death, as well as the fate of the symbiotic bacteria, remain to be studied in bathymodiolin mussels.

Quantitative comparisons of symbiont densities

Symbiont population densities are consistently different in the host species studied. Total (*i.e.*, chemoautotrophic and methanotrophic) symbiont density within gill bacteriocytes was 4 to 5 times greater in *B. azoricus* than in *B. heckerae* and was independent of size class. The ratio of chemoautotrophs to methanotrophs was also species-specific and independent of size class, with chemoautotrophs much more numerous than methanotrophs (13:1 to 18:1) in *B. azoricus*, and with methanotrophs nearly equal to, or moderately more numerous than, chemoautotrophs (2:1 to 3:1) in *B. heckerae*. Although the total symbiont densities are different in the two species, the volume of a gill bacteriocyte occupied by symbionts is qualitatively similar, because the two symbiont morphotypes differ in their size and relative abundance.

The lack of significant differences in symbiont densities and relative abundances among the size classes examined within the two mussel species suggests that there is no niche separation at the level of symbiont populations between the juvenile mussels and the adults. Density data also offer no evidence for an acquisition priority for one symbiont type over the other in either mussel species, or for a systematic ontogenetic shift in the relative density of symbiont morphotypes. We infer that gill symbionts of post-larvae, juveniles, and adults within a mussel population compete for methane and sulfide in the same relative proportions, and that the symbiont densities are regulated. The mode of that regulation—whether by host control mechanisms, by density-dependent control mechanisms elicited by the bacterial symbionts, or by the environment—remains unknown.

Relationships among symbiont densities, stable isotope compositions, life-history stages, and the environment

The dominance of chemoautotrophs over methanotrophs in *B. azoricus*, and of methanotrophs over chemoautotrophs in *B. heckerae*, is consistent with the limited data available on sulfide and methane availability at the Lucky Strike vent and the Blake Ridge seep. At the Eiffel Tower site (Lucky Strike), sulfide concentrations (2.1 m*M*) were higher than methane concentrations (0.68 m*M*; Charlou *et al.*, 2000) in end-member fluids (*i.e.*, high-temperature fluids [350 °C] emanating from black smokers). At the methane-hydrate seep site, pore-water methane concentrations were as much as 3.4 m*M*, while dissolved sulfide concentrations in pore-waters were 1.3 m*M* (Paull *et al.*, 1996). The only estimates available thus suggest that the ratio of CH_4:H_2S is less than 1 at the Lucky Strike site, where chemoautotrophic symbionts dominate, and greater than 2 at the seep site, where methanotrophs dominate. While the relative dominance of chemoautotrophs and methanotrophs can be site-specific within a species, presumably in response to environmental availabilities of sulfide and methane (Trask and Van Dover, 1999; Fiala-Médioni *et al.*, 2002), coordinated measurements of symbiont density and the chemical environment of the host mussels have yet to be undertaken.

Stable carbon and nitrogen isotopic compositions of mussel tissues were also species-specific. The 25‰ difference in $\delta^{13}C$ between the tissues of seep mussels and vent mussels reflects differences in the source of methane at the seep (bacterially derived; $\delta^{13}C_{methane} = -67.8‰$; Paull *et al.*, 1995, 2000) and at the vent (thermogenically derived; $\delta^{13}C_{methane} = -13.7‰$ to $-12.7‰$; Radford-Knoery *et al.*, 1998; Charlou *et al.*, 2002), as well as the relative contributions of methanotrophs and chemoautotrophs to mussel nutrition. The range of $\delta^{13}C$ values reported here for *B. azoricus* adult and juvenile mussels collected from Eiffel Tower in 2001 ($-26.3‰$ to $-35.6‰$) is very close to the range of values reported for adult mussels ($-28.7‰$ to $-33.4‰$) collected from Eiffel Tower in 1996 (Trask and Van Dover, 1999) and is within the range reported for bathymodiolin mussels that host only chemoautotrophic endosymbionts (Fisher, 1990). The methanotroph-to-chemoautotroph ratio for *B. azoricus* from Eiffel Tower at Lucky Strike (this study) is identical to that of *B. azoricus* adults sampled from the same locale in 1996 (Trask and Van Dover, 1999). Because carbon stable-isotope ratios in mussel tissues and ratios of methanotrophs to chemoautotrophs in *B. azoricus* remained essentially unchanged between sampling periods, and assuming that ratios of methanotrophs to chemoautotrophs shift in response to fluid chemistry, it seems likely that the relative availability of methane and sulfide at Eiffel Tower was the same in 1996 and 2001.

The relationships among relative symbiont density, relative availability of CH_4 and dissolved H_2S, and carbon stable-isotopic compositions may prove to be relatively straightforward in mussels with dual symbionts on the Mid-Atlantic Ridge, and independent of the mussel species (Trask and Van Dover, 1999; Colaço *et al.*, 2002; Fiala-Médioni *et al.*, 2002). The carbon isotopic composition of the source methane varies from site to site on the Mid-Atlantic Ridge, but falls in a range of roughly $-13‰$ to $-18‰$ (Charlou *et al.*, 2002), and cannot explain much of the observed variation in the carbon isotopic composition of mussel gills at these vent sites. Interpretation of carbon isotopic fractionation associated with dual symbioses in mussels may be complicated by the availability of methane-derived CO_2 as a substrate for sulfide-based autotrophic metabolism within the bacteriocytes (Fisher, 1993; Fiala-Médioni *et al.*, 2002). Nevertheless, $\delta^{13}C$ values reported

for *B. azoricus* and *B. puteoserpentis* from Mid-Atlantic Ridge vents are positively related to the ratio of CH_4 to H_2S in the end-member fluids (Fig. 7). Ratios of methanotrophs to chemoautotrophs are so far reported only for *B. azoricus* from Lucky Strike and Menez Gwen (Trask and Van Dover, 1999; Fiala-Médioni *et al.*, 2002; this study) and for *B. heckerae* from the Blake Ridge seep (this study), and are consistent with the model of increasing density of methanotrophs as the ratio of CH_4 to H_2S increases (Fig. 7). The relationships in Figure 7 are intriguing, but low-temperature fluid chemistry, symbiont densities, and isotopic compositions of fluids and host mussel tissues remain to be determined in a systematic manner across a range of CH_4:H_2S values for any given species. These relationships should ultimately prove powerful in the analysis of energy flow in dual-symbiont mussel systems.

Tissues from *B. heckerae* were consistently more enriched in ^{15}N than tissues from *B. azoricus*. Lacking any information about the isotopic composition of the nitrogen source used by these symbioses at either the seep or the vent site, we cannot interpret these differences. Within *B. heckerae*, larger mussels (> 40 mm in shell length) had nitrogen isotopic compositions about 5.5‰ more enriched in ^{15}N than post-larval and juvenile mussels (Fig. 6), consistent with an increased contribution of photosynthetically derived organic material in larger mussels. Nevertheless, alternative explanations, including variation in the isotopic composition of the nitrogen source available to the different-sized mussels, seem just as likely.

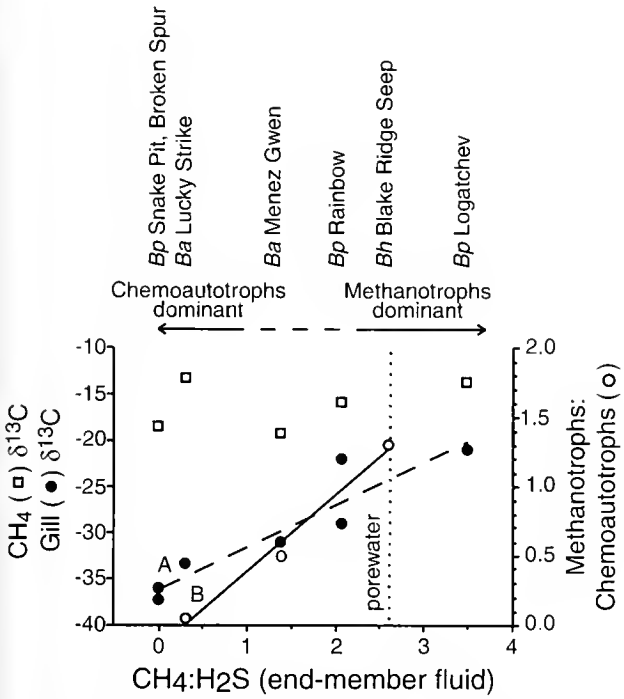

Figure 7. Relationship between the $\delta^{13}C$ of source methane, the $\delta^{13}C$ of mussel gill tissue, the ratio of methanotrophs to chemoautotrophs in gill bacteriocytes of mussels (identified as *Bp*: *Bathymodiolus puteoserpentis*; *Ba* = *B. azoricus*; *Bh* = *B. heckerae*), and the ratio of methane to sulfide (CH_4:H_2S) in end-member fluids of vent sites. CH_4:H_2S for seep porewater is indicated by the dotted vertical line. Sites are identified at the top of the figure. Line A: $\delta^{13}C_{gill}$ = 4.5 (CH_4:H_2S)—36‰; r^2 = 0.87. Line B: Ratio of methanotrophs to chemoautotrophs = 0.55 (CH_4:H_2S)—0.17‰; r^2 = 0.98. CH_4:H_2S regimes where chemoautotrophs or methanotrophs are predicted to dominate in mussels with dual symbionts are identified by the horizontal arrows; the dashed line connecting the arrows emphasizes the fact that this is a model. Methane isotope data and CH_4:H_2S ratios are from Charlou *et al.* (2002) and Paul *et al.* (1995, 1996); ratios of methanotroph to chemoautotroph are from Fiala-Médioni *et al.* (2002) and this study.

The small oocyte size and morphology of the prodissoconch II shells of *B. thermophilus* led Lutz *et al.* (1980) to conclude that *B. thermophilus* (found at vents on the East Pacific Rise) has a planktotrophic larval stage with long-distance dispersal capabilities. The similarly small oocyte size (50 μm in diameter) and prodissoconch II size and morphology (shell length = 100 to 600 μm) of *B. azoricus* and *B. heckerae* (this study) led us to a similar conclusion about their larval development strategies. We expected that the post-larval tissues of species with planktotrophic larvae would thus retain a history of a diet of photosynthetically derived organic carbon and nitrogen (*i.e.*, $\delta^{13}C$ of ~ −25.2‰; $\delta^{15}N$ of +8.5 to +9.7‰; Benner *et al.*, 1997). Indeed, diets of photosynthetic origin have been documented for the dispersive stages of vent species. Vent shrimp, for example, have planktonic larvae (Herring and Dixon, 1998), and juveniles of *Mirocaris fortunata* newly arrived at vent sites contain high concentrations of wax ester and (n-3) poly-unsaturated fatty acids, which are presumed to be of photosynthetic origin (Pond *et al.*, 1997). Juveniles of the shrimp species *Rimicaris exoculata* have bulk carbon isotopic compositions that are distinct from adults, but that approach values expected for photosynthetically derived organic material (Polz *et al.*, 1998, Van Dover, 2000).

In this study, however, we found no convincing isotopic evidence for a larval diet of photosynthetically derived organic material in post-larval specimens of either mussel species that we examined. The nitrogen isotopic compositions of post-larvae of both species were so negative (−2.5‰ to −9‰) as to seem difficult, if not impossible, to derive from a diet dominated by photosynthetically derived organic material. The surprising lack of a compelling photosynthetic isotopic signal, together with evidence from transmission electron microscopy that post-larval mussels have well-developed symbiont populations, suggests that the diet of mussel larvae merits further attention. Lipid biomarker analysis of mussel larvae collected in plankton nets or sediment traps away from vent sites, and transmission electron microscopy of gill and mantle tissues in these larvae, should help to resolve the nutritional status and timing of acquisition of endosymbionts in bathymodiolin mussels.

Acknowledgments

We thank the captain and crew of the R/V *Atlantis*, the pilots and technicians of the DSV *Alvin*, and members of the scientific party for their assistance in obtaining biological specimens at sea. We also thank Dr. Joe Scott and Jewel Thomas for their assistance with TEM, and the reviewers of the manuscript for their thoughtful suggestions for improvements. Field collections and laboratory studies were supported by grants to CLVD from the National Science Foundation (Biological Oceanography OCE-988550, OCE-9982999), NOAA's Ocean Exploration Program, the University of North Carolina-Wilmington National Undersea Research Center, and by the College of William and Mary.

Literature Cited

Barry, J. P., K. R. Buck, R. K. Kochevar, D. C. Nelson, Y. Fujiwara, S. K. Goffredi, and J. Hashimoto. 2002. Methane-based symbiosis in a mussel, *Bathymodiolus platifrons*, from cold seeps in Sagami Bay, Japan. *Invertebr. Biol.* **121:** 47–54.

Benner, R., B. Biddanda, B. Black, and M. McCarthy. 1997. Abundance, size distribution, and stable carbon and nitrogen isotopic compositions of marine organic matter isolated by tangential-flow ultrafiltration. *Mar. Chem.* **57:** 243–263.

Berg, C. J., Jr. 1985. Reproductive strategies of mollusks from abyssal hydrothermal vent communities. *Biol. Soc. Wash. Bull.* **6:** 185–197.

Bright, M., and A. Sorgo. 2003. Ultrastructural reinvestigation of the trophosome in adults of *Riftia pachyptila* (Siboglinidae, Annelida). *Invertebr. Biol.* **122:** 345–366.

Cavanaugh, C. M., P. R. Levering, J. S. Maki, R. Mitchell, and M. E. Lidstrom. 1987. Symbiosis of methylotrophic bacteria and deep-sea mussels. *Nature* **325:** 346–348.

Cavanaugh, C. M., C. O. Wirsen, and H. W. Jannasch. 1992. Evidence for methylotrophic symbionts in a hydrothermal vent mussel (Bivalvia: Mytilidae) from the Mid-Atlantic Ridge. *Appl. Environ. Microbiol.* **58:** 3799–3803.

Chaparro, O. R., J. A. Videla, and R. J. Thompson. 2001. Gill morphogenesis in the oyster *Ostrea chilensis*. *Mar. Biol.* **138:** 199–207.

Charlou, J. L., J. P. Donval, E. Douville, P. Jean-Baptiste, J. Radford-Knoery, Y. Fouquet, A. Dapoigny, and M. Stievenard. 2000. Compared geochemical signatures and the evolution of Menez Gwen (37°50′N) and Lucky Strike (37°17′N) hydrothermal fluids, south of the Azores Triple Junction on the Mid-Atlantic Ridge. *Chem. Geol.* **171:** 49–75.

Charlou, J. L., J. P. Donval, Y. Fouquet, P. Jean-Baptiste, and N. Holm. 2002. Geochemistry of high H_2 and CH_4 vent fluids issuing from ultramafic rocks at the Rainbow hydrothermal field (36°14′N, MAR). *Chem. Geol.* **191:** 345–359.

Childress, J. J., and C. R. Fisher. 1992. The biology of hydrothermal vent animals: physiology, biochemistry, and autotrophic symbioses. *Oceanogr. Mar. Biol. Annu. Rev.* **30:** 337–441.

Colaço, A., F. Dehairs, D. Desbruyères, N. Le Bris, and P.-M. Sarradin. 2002. $\delta^{13}C$ signature of hydrothermal mussels is related with the end-member fluid concentrations of H_2S and CH_4 at the Mid-Atlantic Ridge hydrothermal vent fields. *Cah. Biol. Mar.* **43:** 259–263.

Distel, D. L., H. K.-W. Lee, and C. M. Cavanaugh. 1995. Intracellular coexistence of methano- and thioautotrophic bacteria in a hydrothermal vent mussel. *Microbiology* **92:** 9598–9602.

Fiala-Médioni, A., C. Metivier, A. Herry, and M. Le Pennec. 1986. Ultrastructure of the gill of the hydrothermal-vent mytilid *Bathymodiolus* sp. *Mar. Biol.* **92:** 65–72.

Fiala-Médioni, A., Z. P. McKiness, P. Dando, J. Boulegue, A. Mariotti, A. M. Alayse-Danet, J. J. Robinson, and C. M. Cavanaugh. 2002. Ultrastructural, biochemical, and immunological characterization of two populations of the mytilid mussel *Bathymodiolus azoricus* from the Mid-Atlantic Ridge: evidence for a dual symbiosis. *Mar. Biol.* **141:** 1035–1043.

Fisher, C. R. 1990. Chemoautotrophic and methanotrophic symbioses in marine invertebrates. *Rev. Aquat. Sci.* **2:** 399–436.

Fisher, C. R. 1993. Oxidation of methane by deep sea mytilids in the Gulf of Mexico. Pp. 606–618 in *Biogeochemistry of Global Change: Radiatively Active Trace Gases*, R.S. Oremland, ed. Chapman and Hall, New York.

Fisher, C. R., J. J. Childress, A. J. Arp, J. M. Brooks, D. Distel, J. A. Favuzzi, H. Felbeck, R. Hessler, K. S. Johnson, M. C. Kennicutt II, S. A. Macko, A. Newton, M. A. Powell, G. N. Somero, and T. Soto. 1988. Microhabitat variation in the hydrothermal vent mussel, *Bathymodiolus thermophilus*, at the Rose Garden vent on the Galapagos Rift. *Deep-Sea Res. A* **35:** 1769–1791.

Fisher, C. R., J. M. Brooks, J. S. Vodenichar, J. M. Zande, J. J. Childress, and R. A. Burke, Jr. 1993. The co-occurrence of methanotrophic and chemoautotrophic sulfur-oxidizing bacterial symbionts in a deep-sea mussel. *Mar. Ecol.* **14:** 277–289.

Fujiwara, Y., K. Uematsu, S. Tsuchida, T. Yamamoto, J. Hashimoto, K. Fujikura, Y. Horii, and M. Yuasa. 1998. Nutritional biology of a deep-sea mussel from hydrothermal vents at the Myojin Knoll Caldera. *JAMSTEC J. Deep Sea Res.* **14:** 237–244.

Fujiwara, Y., K. Takai, K. Uematsu, S. Tsuchida, J. C. Hunt, and J. Hashimoto. 2000. Phylogenetic characterization of endosymbionts in three hydrothermal vent mussels: influence on host distributions. *Mar. Ecol. Prog. Ser.* **208:** 147–155.

Herring, P. J., and D. R. Dixon. 1998. Extensive deep-sea dispersal of postlarval shrimp from a hydrothermal vent. *Deep-Sea Res. Part I* **45:** 2105–2118.

Kochevar, R. E., J. J. Childress, C. R. Fisher, and E. Minnich. 1992. The methane mussel: roles of symbiont and host in the metabolic utilization of methane. *Mar. Biol.* **112:** 389–401.

Le Pennec, M., and P. G. Beninger. 2000. Reproductive characteristics and strategies of reducing-system bivalves. *Comp. Biochem. Physiol. A* **126:** 1–16.

Le Pennec, M., A. Donval, and A. Herry. 1990. Nutritional strategies of the hydrothermal ecosystem bivalves. *Prog. Oceanogr.* **24:** 71–80.

Lutz, R. A., D. Jablonski, D. C. Rhoads, and R. D. Turner. 1980. Larval dispersal of a deep-sea hydrothermal vent bivalve from the Galapagos Rift. *Mar. Biol.* **57:** 127–133.

Nelson, D. C., K. D. Hagen, and D. B. Edwards. 1995. The gill symbiont of the hydrothermal vent mussel *Bathymodiolus thermophilus* is a psychrophilic, chemoautotrophic, sulfur bacterium. *Mar. Biol.* **121:** 487–495.

Page, H. M., A. Fiala-Medioni, C. R. Fisher, and J. J. Childress. 1991. Experimental evidence for filter-feeding by the hydrothermal vent mussel, *Bathymodiolus thermophilus*. *Deep-Sea Res. A* **38:** 1455–1461.

Paull, C. K., W. Ussler III, W. Borowski, and F. Spiess. 1995. Methane-rich plumes on the Carolina continental rise: associations with gas hydrates. *Geology* **23:** 89–92.

Paull, C. K., R. Matsumoto, P. J. Wallace, N. R. Black, W. S. Borowski, T. S. Collett, J. E. Damuth, G. R. Dickens, P. K. Egeberg, K. Goodman, and others. 1996. Site 996. *Proceedings of the Ocean Drilling Program, Initial Reports* **164:** 241–275.

Paull, C. K., R. Matsumoto, P. J. Wallace, and W. P. Dillon, eds. 2000. *Proceedings of the Ocean Drilling Program*, Scientific Results 164, Ocean Drilling Program, College Station, TX.

Polz, M. F., J. J. Robinson, C. M. Cavanaugh, and C. L. Van Dover.

1998. Trophic ecology of massive shrimp aggregations at a Mid-Atlantic Ridge hydrothermal vent site. *Limnol. Oceanogr.* **43:**1631–1638.

Pond, D. W., D. R. Dixon, and J. R. Sargent. 1997. Wax-ester reserves facilitate dispersal of hydrothermal vent shrimps. *Mar. Ecol. Prog. Ser.* **143:**45–63.

Radford-Knoery, J., J. L. Charlou, J. P. Donval, M. Aballea, Y. Fouquet, and H. Ondreas. 1998. Distribution of dissolved sulfide, methane, and manganese near the seafloor at the Lucky Strike (37°17′N) and Menez Gwen (37°50′N) hydrothermal vent sites on the Mid-Atlantic Ridge. *Deep-Sea Res. I* **45:**367–386.

Raulfs, E. C., S. A. Macko, and C. L. Van Dover. 2004. Tissue and symbiont condition of mussels (*Bathymodiolus thermophilus*) exposed to varying levels of hydrothermal activity. *J. Mar. Biol. Assoc. UK* **84:** 229–234.

Robinson, J. J., M. F. Polz, A. Fiala-Médioni, and C. M. Cavanaugh. 1998. Physiological and immunological evidence for two distinct C_1-utilizing pathways in *Bathymodiolus puteoserpentis* (Bivalvia: Mytilidae), a dual endosymbiotic mussel from the Mid-Atlantic Ridge. *Mar. Biol.* **132:**625–633.

Southward, E. C., A. Gebruk, H. Kennedy, A. J. Southward, and P. Chevaldonné. 2001. Different energy sources for three symbiont-dependent bivalve molluscs at the Logatchev hydrothermal site (Mid-Atlantic Ridge). *J. Mar. Biol. Assoc. UK* **81:**655–661.

Streams, M. E., C. R. Fisher, and A. Fiala-Médioni. 1997. Methanotrophic symbiont location and fate of carbon incorporated from methane in a hydrocarbon seep mussel. *Mar. Biol.* **129:** 465–476.

Trask, J., and C. L. Van Dover. 1999. Site-specific and ontogenetic variations in nutrition of mussels (*Bathymodiolus* sp.) from the Lucky Strike hydrothermal vent field, Mid-Atlantic Ridge. *Limnol. Oceanogr.* **44:**334–343.

Van Dover, C. L. 2000. *The Ecology of Deep-Sea Hydrothermal Vents.* Princeton University Press, Princeton.

Van Dover, C. L., D. Desbruyères, M. Segonzac, T. Comtet, L. Saldanha, A. Fiala-Médioni, and C. Langmuir. 1996. Biology of the Lucky Strike hydrothermal field. *Deep-Sea Res.* **43:** 1509–1529.

Van Dover, C. L., P. Aharon, J. M. Bernhard, M. Doerries, W. Flickinger, W. Gilhooly, S. K. Goffredi, K. Knick, S. A. Macko, S. Rapoport, and others. 2003. Blake Ridge methane seeps: characterization of a soft-sediment, chemosynthetically based ecosystem. *Deep-Sea Res. I* **50:**281–300.

Won, Y.-J., S. J. Hallam, G. D. O'Mullan, I. L. Pan, K. R. Buck, and R. C. Vrijenhoek. 2003. Environmental acquisition of thiotrophic endosymbionts in deep-sea mussels of the genus *Bathymodiolus*. *Appl. Environ. Microbiol.* **69:**6785–6792.

THE
BIOLOGICAL BULLETIN

2005 Subscription Rates

Volumes 208-209

Paid subscriptions include both print and online versions.

	Institutional	Individual
One year subscription (6 issues - 2 volumes)	**$360.00**	**$120.00**
Single Volume (3 issues)	$180.00	$70.00
Single Issues	$75.00	$25.00

Surface delivery included in above prices.

For prompt delivery, we encourage subscribers outside the U.S. to request airmail service.

Airmail Delivery Charges:

U.S. and Canada, $45.00 Mexico, $60.00 All other locations, $100.00

The Biological Bulletin
ISSN: 0006-3185
Frequency: Bimonthly
Number of issues per year: 6
Months of Publication: February, April, June, August, October, December
Subscriptions entered for calendar year
Volume indexes contained in June and December issues
Back issues available
Claims handled upon receipt

Please address orders to:

Subscription Administrator, *The Biological Bulletin*
Marine Biological Laboratory, 7 MBL Street
Woods Hole, MA 02543 U.S.A.
Fax: 508-289-7922 • Tel: 508-289-7402 • E-mail: lreuter@mbl.edu

Orders must be prepaid in U.S. Dollars, check payable to Marine Biological Laboratory
(with reference *The Biological Bulletin*)

www.biolbull.org

Published by the Marine Biological Laboratory
Woods Hole, Massachusetts, 02543 U.S.A.

THE

BIOLOGICAL BULLETIN

2005 Subscription Form

Volumes 208-209, 6 issues

Please print)

AME: _____

NSTITUTION: _____

DDRESS: _____

ITY: _____ STATE: _____ POSTAL CODE: _____

OUNTRY: _____ TELEPHONE: _____

AX: _____ E-MAIL ADDRESS: _____

Please send me a 2005 subscription to *The Biological Bulletin* at the rate indicated below:

Price includes both print and online versions. All subscriptions run on the calendar year.

❒ Individual: $120.00 (6 ISSUES) ❒ Institutional: $360.00 (6 ISSUES)

❒ Individual: $70.00 (3 ISSUES) ❒ Institutional: $180.00 (3 ISSUES)

Check one: ❒ February, April, June or ❒ August, October, December

ease send me the following back issue(s): _____

Individual: at $25.00 (PER ISSUE) ❒ Institutional: at $75.00 (PER ISSUE)

elivery Options

Surface Delivery (Surface delivery is included in the subscription price.)

Air Delivery (Please add the correct amount to your payment.)

U.S. and Canada: $45.00 Mexico: $60.00 All other locations: $100.00

yment Options

Enclosed is my check or U.S. money order for $ _____

payable to Marine Biological Laboratory (with reference *The Biological Bulletin*)

Please charge my ❒ VISA ❒ MasterCard ❒ Discover Card $ _____

Account No.: _____ Exp. Date: _____

Signature: _____ Date: _____

Please send me an invoice. (Note: Payment must be received before subscription commences.)

Return this form with your check or credit information to:

Subscription Administrator, *The Biological Bulletin*

Marine Biological Laboratory, 7 MBL Street

Woods Hole, MA 02543 U.S.A.

Fax: 508-289-7922 • Tel: 508-289-7402 • E-mail: lreuter@mbl.edu

www.biolbull.org

Published by the Marine Biological Laboratory
Woods Hole, Massachusetts, 02543 U.S.A.

MARINE RESOURCES CENTER

MARINE BIOLOGICAL LABORATORY • WOODS HOLE, MA 02543 • (508)289-7700
WWW.MBL.EDU/SERVICES/MRC/INDEX.HTML

zebrafish facilities

Animal and Tissue Supply for Education & Research

- 150 aquatic species available for shipment via online catalog: <http://www.mbl.edu/animals/index.html>; phone: (508)289-7375; or e-mail: specimens@mbl.edu
- zebrafish colony containing limited mutant strains
- custom dissection and furnishing of specific organ and tissue samples

MRC Services Available

- basic water quality analysis
- veterinary services (clinical, histopathologic, microbial services, health certificates, etc.)
- aquatic systems design (mechanical, biological, engineering, etc.)
- educational tours and collecting trips aboard the R/V Gemma

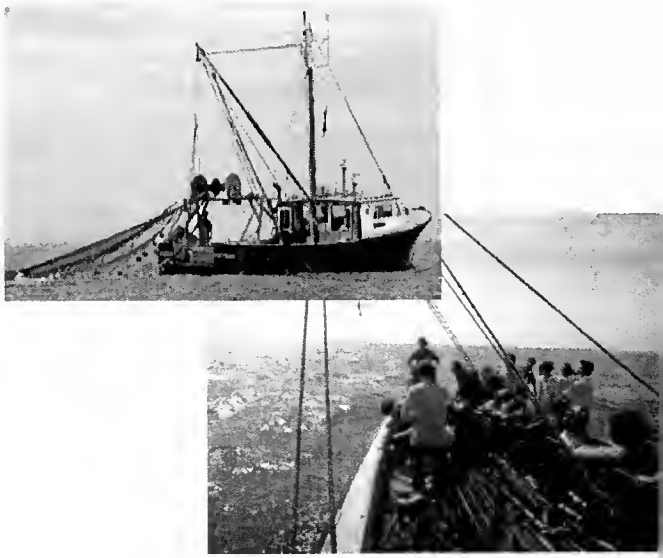

Using the MRC for Your Research

- capability for advanced animal husbandry (temperature, light control, etc.)
- availability of year-round, developmental life stages
- adaptability of tank system design for live marine animal experimentation

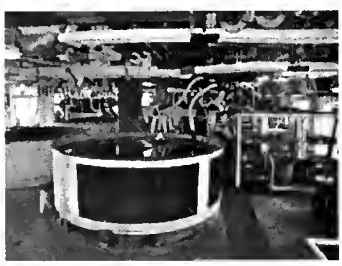

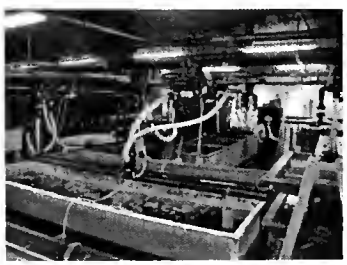

Better Images...Faster Answers

Developmental Biologists are Thrilled!

the developmental lab, be it working with Zebrafish, *C. elegans*, Mice, or Drosophila, better images lead to more curate conclusions.

ica introduces a new tool in the pursuit of **better images**, the MZ16 FA. This stereofluorescence microscope ovides greater resolution than ever before from whole embryo to the sub-cellular level. Your fluorescent specimens ll appear in high contrast on a jet-black background thanks to Leica's patented TripleBeam™ technology.

r experiments in time lapse, extended depth of focus, or multi-probe imaging, **faster answers** are obtained rough Leica's Intelligent Automation of the MZ16 FA's five motorized features.

tter Images...Faster Answers with the Leica MZ16 FA! Call 800-248-0123 today!

telligent Automation

ca Microsystems Inc.
45 Waukegan Road
nnockburn, IL 60015

Telephone (847) 405-0123 (800) 248-0123
Fax (847) 405-0164
In Canada call (800) 205-3422
www.stereomicroscopy.com

Leica
MICROSYSTEMS

June 2005 Volume 208 • Number 3

THE BIOLOGICAL BULLETIN

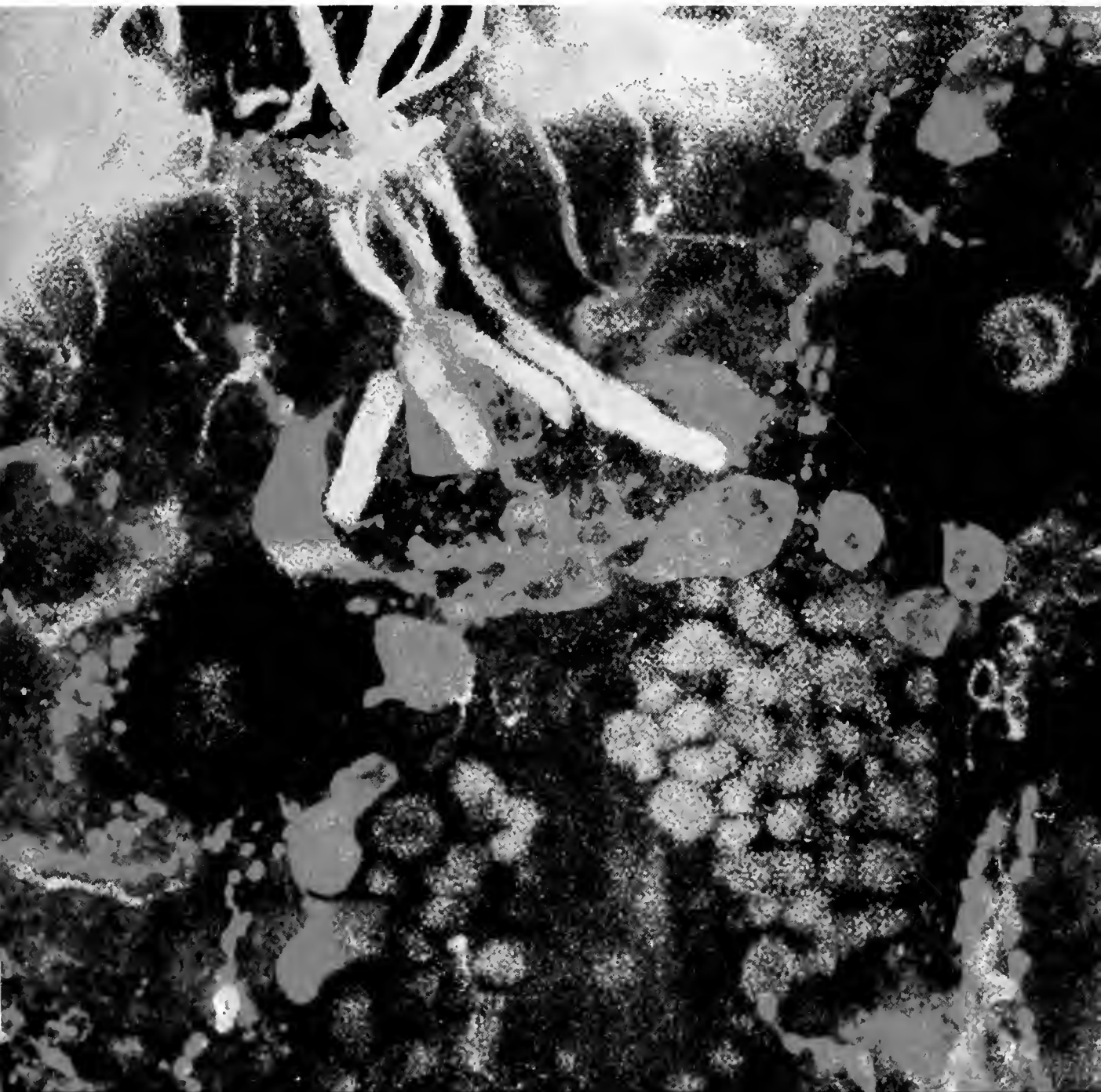

Published by the Marine Biological Laboratory

Woods Hole, Massachusetts

WHEN IT COMES TO SPEED AND HANDLING,

ABOUT THE ONLY THING NOT MOTORIZED IS YOU.

ROCKET SCIENCE.™

800 446 5967 olympusamerica.com/microscopes

Cover

The cover shows an anterior frontal view of a recently hatched, lecithotrophic larva of the aeolid nudibranch mollusc *Berghia verrucicornis*. This species of *Berghia* lives on shallow reef flats in the Caribbean in areas where its prey, the sea anemone *Aiptasia pallida*, is abundant. As is the case with other molluscan species, the larva of *Berghia* has a central nervous system that includes an apical ganglion. This ganglion contains the primary receptor (or receptors) for the inductive chemical signal that initiates settlement and metamorphosis in opisthobranch larvae.

In the laser scanning, confocal, maximum intensity projection shown, the larva has been double-labeled with antibodies that reveal cells or cell parts that contain serotonin or tubulin. This labeling reveals a number of serotonergic neurons (red) that are located between and below the larva's two black eyespots. Of these, the five largest are parampullary neurons within the apical ganglion, with the three closest to the top of the image possessing sensory dendrites (red), the ends of which are embedded in the larva's pretrochal epithelium. These sensory neurons, as well as the two interneurons of this group of five, extend axons into the central neuropil (red) of the ganglion. The axons originating from at least some of these neurons then exit the neuropil and project into the velum, a larval organ used for both swimming and feeding. This sensory serotonergic system is thought to be involved in modulating activities of the velar musculature and cilia.

In addition to the velar cilia at the top of the image, the tubulin antibody labels five tubular structures (bright green, two on the right superimposed) in the apical ganglion that are dense ciliary bundles. These are present within a deep invagination of the plasmalemma of sensory cells called ampullary neurons. As is apparent, the invaginated ampulla of each neuron communicates with the external environment *via* a long narrow canal. The ends of these canals are grouped in the pretrochal epithelium around and among the ciliary tuft cells, the ciliary tufts of which can be seen centrally at the top of the image. It has been suggested that the ampullary neurons are the actual primary receptors for the metamorphic inducer. Kempf and Page (p. 169 of this issue) use antitubulin labeling to examine the structure and organization of the ampullary neurons and of a new, putative apical nerve in larvae of a number of opisthobranch species.

Credits: Confocal data collected and processed by Stephen C. Kempf (Auburn University). Cover design: Beth Liles (Marine Biological Laboratory).

THE BIOLOGICAL BULLETIN

JUNE 2005

Published by
Marine Biological Laboratory
Woods Hole, Massachusetts

http://www.biolbull.org

CONTENTS

VOLUME 208, NO. 3: JUNE 2005

THE BIOLOGICAL BULLETIN

THE BIOLOGICAL BULLETIN is published six times a year by the Marine Biological Laboratory, 7 MBL Street, Woods Hole, Massachusetts 02543.

Subscriptions and similar matter should be addressed to Subscription Administrator, THE BIOLOGICAL BULLETIN, Marine Biological Laboratory, 7 MBL Street, Woods Hole, Massachusetts 02543. Subscription includes both print and online journals. Subscription per year (six issues, two volumes): $360 for libraries; $120 for individuals. Subscription per volume (three issues): $180 for libraries; $70 for individuals. Back and single issues (subject to availability): $75 for libraries; $25 for individuals.

Communications relative to manuscripts should be sent to James L. Olds, Editor-in-Chief, or Pamela Clapp Hinkle, Managing Editor, at the Marine Biological Laboratory, 7 MBL Street, Woods Hole, Massachusetts 02543. Telephone: (508) 289-7149. FAX: 508-289-7922. E-mail: pclapp@mbl.edu.

http://www.biolbull.org

THE BIOLOGICAL BULLETIN is indexed in bibliographic services including *Index Medicus* and MEDLINE, *Chemical Abstracts, Current Contents, Elsevier BIOBASE/Current Awareness in Biological Sciences,* and *Geo Abstracts.*

Printed on acid free paper,
effective with Volume 180, Issue 1, 1991.

POSTMASTER: Send address changes to THE BIOLOGICAL BULLETIN, Marine Biological Laboratory, 7 MBL Street, Woods Hole, MA 02543.

Periodicals postage paid at Woods Hole, MA, and additional mailing offices.
ISSN 0006-3185

INSTRUCTIONS TO AUTHORS

The Biological Bulletin accepts outstanding original research reports of general interest to biologists throughout the world. Papers are usually of intermediate length (10–40 manuscript pages). A limited number of solicited review papers may be accepted after formal review. A paper will usually appear within four months after its acceptance.

Very short, especially topical papers (less than 9 manuscript pages including tables, figures, and bibliography) will be published in a separate section entitled "Research Notes." A Research Note in *The Biological Bulletin* follows the format of similar notes in *Nature*. It should open with a summary paragraph of 150 to 200 words comprising the introduction and the conclusions. The rest of the text should continue on without subheadings, and there should be no more than 30 references. References should be referred to in the text by number, and listed in the Literature Cited section in the order that they appear in the text. Unlike references in *Nature*, references in the Research Notes section should conform in punctuation and arrangement to the style of recent issues of *The Biological Bulletin*. Materials and Methods should be incorporated into appropriate figure legends. See the article by Lee (October 2003, Vol. **205:** 99–101) for sample style. A Research Note will usually appear within two months after its acceptance.

The Editorial Board requests that regular manuscripts conform to the requirements set below; those manuscripts that do not conform will be returned to authors for correction before review.

1. ***Manuscripts.*** Manuscripts, including figures, should be submitted in quadruplicate, with the originals clearly marked. (Xerox copies of photographs are not acceptable for review purposes.) Please include an electronic copy of the text of the manuscript. Label the disk with the name of the first author and the name and version of the wordprocessing software used to create the file. If the file was not created in some version of Microsoft Word, save the text in rich text format (rtf). The submission letter accompanying the manuscript should include a telephone number, a FAX number, and (if possible) an E-mail address for the corresponding author. The original manuscript must be typed in no smaller than 12 pitch or 10 point, using double spacing (*including* figure legends, footnotes, bibliography, etc.) on one side of 16- or 20-lb. bond paper, 8 by 11 inches. Please, no right justification. Manuscripts should be proofread carefully and errors corrected legibly in black ink. Pages should be numbered consecutively. Margins on all sides should be at least 1 inch (2.5 cm). Manuscripts should conform to the *Council of Biology Editors Style Manual*, 5th Edition (Council of Biology Editors, 1983) and to American spelling. Unusual abbreviations should be kept to a minimum and should be spelled out on first reference as well as defined in a footnote on the title page. Manuscripts should be divided into the following components: Title page, Abstract (of no more than 200 words), Introduction, Materials and Methods, Results, Discussion, Acknowledgments, Literature Cited, Tables, and Figure Legends. In addition, authors should supply a list of words and phrases under which the article should be indexed.

2. ***Title page.*** The title page consists of a condensed title or running head of no more than 35 letters and spaces, the manuscript title, authors' names and appropriate addresses, and footnotes listing present addresses, acknowledgments or contribution numbers, and explanation of unusual abbreviations.

3. ***Figures.*** The dimensions of the printed page, 7 by 9 inches, should be kept in mind in preparing figures for publication. We recommend that figures be about 1 times the linear dimensions of the final printing desired, and that the ratio of the largest to the smallest letter or number and of the thickest to the thinnest line not exceed 1:1.5. Explanatory matter generally should be included in legends, although axes should always be identified on the illustration itself. Figures should be prepared for reproduction as either line cuts or halftones. Figures to be reproduced as line cuts should be unmounted glossy photographic reproductions or drawn in black ink on white paper, good-quality tracing cloth or plastic, or blue-lined coordinate paper. Those to be reproduced as halftones should be mounted on board, with both designating numbers or letters and scale bars affixed directly to the figures. All figures should be numbered in consecutive order, with no distinction between text and plate figures and cited, in order, in the text. The author's name and an arrow indicating orientation should appear on the reverse side of all figures.

Digital art: The Biological Bulletin will accept figures submitted in electronic form; however, digital art must conform to the following guidelines. Authors who create digital images are wholly responsible for the quality of their material, including color and halftone accuracy.

Format. Acceptable graphic formats are TIFF and EPS. Color submissions must be in EPS format, saved in CMKY mode.

Software. Preferred software is Adobe Illustrator or Adobe Photoshop for the Mac and Adobe Photoshop for Windows. Specific instructions for artwork created with various software programs are available on the Web at the Digital Art Information Site maintained by Cadmus Professional Communications at http://cpc.cadmus.com/da/

Resolution. The minimum requirements for resolution are 1200 DPI for line art and 300 for halftones.

Size. All digital artwork must be submitted at its actual printed size so that no scaling is necessary.

Multipanel figures. Figures consisting of individual parts (*e.g.,* panels A, B, C) must be assembled into final format and submitted as one file.

Hard copy. Files must be accompanied by hard copy for use in case the electronic version is unusable.

Disk identification. Disks must be clearly labeled with the following information: author name and manuscript number; format (PC or Macintosh); name and version of software used.

Color: The Biological Bulletin will publish color figures and plates, but must bill authors for the actual additional cost of printing in color. The process is expensive, so authors with more than one color image should—consistent with editorial concerns, especially citation of figures in order—combine them into a single plate to reduce the expense. On request, when supplied with a copy of a color illustration, the editorial staff will provide a pre-publication estimate of the printing cost.

4. ***Tables, footnotes, figure legends, etc.*** Authors should follow the style in a recent issue of *The Biological Bulletin* in preparing table headings, figure legends, and the like. Because of the high cost of setting tabular material in type, authors are asked to limit such material as much as possible. Tables, with their headings and footnotes, should be typed on separate sheets, numbered with consecutive Arabic numerals, and placed after the Literature Cited. Figure legends should contain enough information to make the figure intelligible separate from the text. Legends should be typed double spaced, with consecutive Arabic numbers, on a separate sheet at the end of the paper. Footnotes should be limited to authors' current addresses, acknowledgments or contribution numbers, and explanation of unusual abbreviations. All such footnotes should appear on the title page. Footnotes are not normally permitted in the body of the text.

5. ***Literature cited.*** In the text, literature should be cited by the Harvard system, with papers by more than two authors cited as Jones *et al.*, 1980. Personal communications and material in preparation or in press should be cited in the text only, with author's initials and institutions, unless the material has been formally accepted and a volume number can be supplied. The list of references following the text should be headed Literature Cited, and must be typed double spaced on separate pages, conforming in punctuation and arrangement to the style of recent issues of *The Biological Bulletin.* Citations should include complete titles and inclusive pagination. Journal abbreviations should normally follow those of the U. S. A. Standards Institute (USASI), as adopted by BIOLOGICAL ABSTRACTS and CHEMICAL ABSTRACTS, with the minor differences set out below. The most generally useful list of biological journal titles is that published each year by BIOLOGICAL ABSTRACTS (BIOSIS List of Serials; the most recent issue). Foreign authors, and others who are accustomed to using THE WORLD LIST OF SCIENTIFIC PERIODICALS, may find a booklet published by the Biological Council of the U.K. (obtainable from the Institute of Biology, 41 Queen's Gate, London, S.W.7, England, U.K.) useful, since it sets out the WORLD LIST abbreviations for most biological journals with notes of the USASI abbreviations where these differ. CHEMICAL ABSTRACTS publishes quarterly supplements of additional abbreviations. The following points of reference style for THE BIOLOGICAL BULLETIN differ from USASI (or modified WORLD LIST) usage:

A. Journal abbreviations, and book titles, all underlined (for *italics*)

B. All components of abbreviations with initial capitals (not as European usage in WORLD LIST *e.g., J. Cell. Comp. Physiol.* NOT *J. cell. comp. Physiol.*)

C. *All* abbreviated components must be followed by a period, whole word components *must not* (*i.e., J. Cancer Res.*)

D. Space between all components (*e.g., J. Cell. Comp. Physiol.*, not *J.Cell.Comp.Physiol.*)

E. Unusual words in journal titles should be spelled out in full, rather than employing new abbreviations invented by the author. For example, use *Rit Vísindafjélags Islendinga* without abbreviation.

F. All single word journal titles in full (*e.g., Veliger, Ecology, Brain*).

G. The order of abbreviated components should be the same as the word order of the complete title (*i.e.*, *Proc.* and *Trans.* placed where they appear, not transposed as in some BIOLOGICAL ABSTRACTS listings).

H. A few well-known international journals in their preferred forms rather than WORLD LIST or USASI usage (*e.g.*, *Nature, Science, Evolution* NOT *Nature, Lond., Science, N.Y.; Evolution, Lancaster, Pa.*)

6. ***Sequences.*** By the time a paper is sent to the press, all nucleotide or amino acid sequences and associated alignments should have been deposited in a generally accessible database (*e.g.*, GenBank, EMBL, SwissProt), and the sequence accession number should be provided.

7. ***Reprints, page proofs, and charges.*** Authors may purchase reprints in lots of 100. Forms for placing reprint orders are sent with page proofs. Reprints normally will be delivered about 2 to 3 months after the issue date. Authors will receive page proofs of articles shortly before publication. They will be charged the current cost of printers' time for corrections to these (other than corrections of printers' or editors' errors). Other than these charges for authors' alterations, *The Biological Bulletin* does not have page charges.

Reference: *Biol. Bull.* **208:** 157–158. (June 2005)

A Test for Larval Kin Aggregations

MATTHEW L. NICOTRA[1] AND LEO W. BUSS[1,2,*]

Departments of Ecology and Evolutionary Biology[1] and Geology and Geophysics[2], Yale University, New Haven, Connecticut 06520-8106

Hart and Grosberg (1) claimed that demersal larvae remain in kin aggregations. A simple test of this proposition has recently become possible. In the athecate colonial hydroid Hydractinia symbiolongicarpus, *allorecognition is controlled by a single chromosomal interval and fusion is expected only between closely related individuals (2). If* Hydractinia *larvae do aggregate in kin groups, then recruits from the same shell should fuse more frequently than those from different shells. We sampled a shallow subtidal population from Long Island Sound (Old Quarry Harbor, Guilford, CT) to identify hermit crab shells that bore two or more newly recruited* Hydractinia *colonies. The colonies were explanted from the shells, reared in the laboratory, and subsequently tested for fusibility. We observed fusion between 4.4% of co-occurring colonies and 1.8% of colonies from different shells—frequencies that do not differ significantly. These results provide no support for the claim that larvae remain aggregated in the field.*

Hydractinia symbiolongicarpus (Buss and Yund, 1989) occurs most frequently as an epibiont on the shells of hermit crabs and is, therefore, a sessile organism on mobile substrata. Colonies are dioecious, with the gametes freely shed into the water column on a diurnal light cue. This natural history suggests that larval kin aggregations are unlikely; nonetheless, egg release is restricted to a period of less than an hour each day, the eggs are negatively buoyant, and the larvae crawl but do not swim. Thus, larvae might conceivably remain in kin aggregations if a hermit crab remained immobile; if the larvae did not crawl away from one another; and if tidal movement, currents, or bioturbation did not resuspend the mud and sand for a period of 48–72 h.

Should this concatenation of conditions occur, hermit crabs might be expected occasionally to pick up two larvae as they pass through a single aggregation. In contrast, different crabs would not be likely to traverse the same aggregation; hence larvae recruiting to different shells would be expected to be unrelated. A direct test of the claim that demersal larvae remain in kin aggregations is provided by comparing new recruits found on the same shell with those on different shells.

To make this test, we exploit new findings on the genetics of allorecognition in *Hydractinia* (2). When recruits encounter one another, one of two genetically alternative results are obtained. Colonies either fuse, establishing a chimera with a continuous gastrovascular system, or they fail to fuse (2–5). The failure to fuse is called rejection and triggers a nematocyst-based effector system, which in turn results in either the elimination of one colony or the development of the oft-observed "suture-lines" separating colonies on the same shell (6–8).

We have recently demonstrated that the decision to fuse or reject is controlled by a single chromosomal interval and confirmed this result by both classical genetic techniques and the development of molecular markers spanning the interval (2). Fusion occurs only if colonies share alleles at one or more loci in this interval (2). Thus, field-collected colonies are expected to fuse only if they are related or if both carry an allele common in the population. The latter is expected to occur infrequently, as allorecognition loci are said to be highly polymorphic (9). If larvae are aggregated in kin groups, then fusion among recruits on a single shell must exceed fusion among recruits from different shells.

To test Hart and Grosberg's (1) larval kin aggregation hypothesis, we sought conditions most conducive to the formation of larval kin aggregations. Specifically, we avoided intertidal habitats and those with high currents, and we sampled from a calm, shallow subtidal embayment. Using scuba, we collected 1369 shells on four dates in 2002 (30 May, 4 June, 21 June, and 31 July) at a depth of 5 m on the seaward edge of One Tree Island, Old Quarry Harbor (Guilford, CT). Newly recruited colonies (<10 polyps) are

Received 20 July 2004; accepted 17 March 2005.
* To whom correspondence should be addressed.

easily identified by inspection of shells under a stereomicroscope (10). Forty-six shells clearly bearing two or more new recruits were identified. Colonies were removed from the shell with a scalpel blade, affixed to glass microscope slides with thread until they adhered, and maintained in 10-gallon glass aquaria filled with artificial seawater (Reef Crystals) where they were fed three times a week with 2- to 3-day-old *Artemia* nauplii. Explants were taken when the colonies had grown sufficiently, and the colonies were tested for their ability to fuse to one another, using colony-based or polyp-based fusibility assays. In the colony-based assay, small fragments cut from each colony were attached 2–3 mm apart with thread on a glass microscope slide and observed at daily intervals until they contacted; thereafter, daily observations continued until the assay was scored. In the polyp-based assay (11), one polyp cut from each colony was threaded onto a human hair and sandwiched between two agar blocks so that its cut end opposed that of the other polyp. After 2 h, the agar blocks and hair were removed, but the polyps continued to adhere. At 24 h, the assays were scored as fusions if the polyps fused to create a single gastric cavity and common ectoderm, or as rejections if they fell apart. Colony and polyp assays are interchangeable with respect to fusion and rejection (2); they differ only with respect to a third class of allorecognition phenotype in which colonies initially fuse but subsequently separate. This transitory fusion phenotype is detectable only in the colony assay; in the polyp assay it cannot be distinguished from fusion. Transitory fusion is also known to be controlled within the chromosomal interval (2), and it was not observed among our samples.

We performed 113 pairwise tests of fusibility between colonies recruited to a single shell. We compared these results to those obtained from an additional 110 pairwise assays performed with colonies derived from different shells. We observed fusion between 4.4% (5/113) of co-occurring colonies and 1.8% (2/110) of colonies from different shells. There is no significant difference between these two frequencies (G test for independence, $G = 1.201$, $P > 0.25$). The power of this analysis is low (0.23, $\alpha = 0.05$) because the frequency of fusion is so low. Indeed, if the frequency of fusion on the same shell actually exceeds that on different shells, a power of 0.8 would require a sample size of more than 1175 pairwise fusion assays to detect an effect as small that measured.

Our findings confirm the suggestion made by Hart and Grosberg (1) that fusion occurs at a detectable frequency in natural populations of *Hydractinia*. Moreover, our results are consistent with the extreme lower range of Hart and Grosberg's (1) estimate that 2%–18% of co-occurring colonies are full siblings. Recall, however, that fusion can occur either because encounters are biased toward kin or as a consequence of allelic diversity in the population. Our observation that frequencies of fusion between recruits onto the same shell do not differ from frequencies of fusion observed on different shells suggests that the extraordinary claim of larval kin aggregates is not warranted on the basis of the data now available.

Acknowledgments

D. T. Kysela, S. R. Rogal, and A. Y. Signorovitch assisted in animal care. Financial support provided by NSF MCB-9817380 and EF-0319076.

Literature Cited

1. **Hart, M. W., and R. K. Grosberg. 1999.** Kin interactions in a colonial hydrozoan (*Hydractinia symbiolongicarpus*): population structure on a mobile landscape. *Evolution* **53:** 793–805.
2. **Cadavid, L. F., A. Powell, M. L. Nicotra, M. Moreno, and L. W. Buss. 2004.** An invertebrate histocompatibility complex. *Genetics* **167:** 357–365.
3. **Hauenschild, C. 1954.** Genetische und entwichlungphysiologische Untersuchungen über Intersexuälitat und Gewebeverträlichkeit bei *Hydractinia echinata*. *W. Roux Arch. EntwMech. Org.* **147:** 1–114.
4. **Hauenschild, C. 1956.** Über die Vererbung einer Gewebeverträglichkeits-Eigenschaft bei dem Hydroid-polypen *Hydractinia echinata*. *Z. Naturforsch.* **11:** 132–174.
5. **Mokady, O., and L. W. Buss. 1996.** Transmission genetics of allorecognition in *Hydractinia symbiolongicarpus* (Cnidaria: Hydrozoa). *Genetics* **143:** 823–827.
6. **Müller, A. W. 1964.** Experimentalle Untersuchungen über Stockentwicklung, Polypendifferenzierung und Sexualchimären bei *Hydractinia echinata*. *W. Roux Arch. EntwMech. Org.* **155:** 181–268.
7. **Buss, L. W., C. S. McFadden, and D. R. Keene. 1984.** Biology of hydractiniid hydroids. 2. Histocompatibility effector system/competitive mechanism mediated by nematocyst discharge. *Biol. Bull.* **167:** 139–158.
8. **Lange, R., G. Plickert, and W. A. Müller. 1989.** Histocompatibility in a low invertebrate, *Hydractinia echinata:* analysis of the mechanism of rejection. *J. Exp. Zool.* **249:** 284–292.
9. **Grusberg, R. K. 1988.** The evolution of allorecognition specificity in clonal invertebrates. *Q. Rev. Biol.* **63:** 377–412.
10. **Yund, P. O., C. W. Cunningham, and L. W. Buss. 1987.** Recruitment and post-recruitment interactions in a colonial hydroid. *Ecology* **68:** 971–982.
11. **Lange, R., M. Dick, and W. A. Müller. 1992.** Specificity and early ontogeny of historecognition in the hydroid *Hydractinia*. *J. Exp. Zool.* **262:** 307–316.

Reference: *Biol. Bull.* **208:** 159–168. (June 2005)

Effects of Hypoxia and Hypercapnic Hypoxia on the Localization and the Elimination of *Vibrio campbellii* in *Litopenaeus vannamei*, the Pacific White Shrimp

JOSEPH E. BURGENTS, KAREN G. BURNETT, AND LOUIS E. BURNETT*

Grice Marine Laboratory, College of Charleston, 205 Fort Johnson, Charleston, South Carolina 29412

Abstract. Low oxygen (hypoxia) and elevated CO_2 (hypercapnia, are characteristic of estuarine environments. Although hypoxia and hypercapnic hypoxia decrease the resistance of shrimp to bacterial pathogens, their direct effects on the immune system are unknown. Here we present evidence demonstrating in the penaeid shrimp *Litopenaeus vannamei* that both hypoxia and hypercapnic hypoxia affect the localization of bacteria, their conversion from culturable to non-culturable status (bacteriostasis), and their elimination from hemolymph and selected tissues. Shrimp were injected with a sublethal dose of a pathogenic strain of *Vibrio campbellii* expressing green fluorescent protein and resistance to kanamycin. Real-time polymerase chain reaction was used to determine the number of intact *V. campbellii* in hemolymph, gills, hepatopancreas, heart, and lymphoid organ. Selective plating was used to quantify the injected bacteria that remained culturable. We found that both hypercapnic hypoxia and hypoxia increased the percentage of culturable bacteria recovered from the hemolymph and tissues, suggesting an overall decrease in bacteriostatic activity. Hypoxia and hypercapnic hypoxia generally increased the distribution of intact *V. campbellii* to the hepatopancreas and the gills, which are major targets for the pathogenic effects of *Vibrio* spp., without affecting the number of intact bacteria in the lymphoid organ, a main site of bacterial accumulation and bacteriostatic activity.

Received 9 December 2004; accepted 29 March 2005.

* To whom correspondence should be addressed. E-mail: BurnettL@cofc.edu

Abbreviations: ANOVA, analysis of variance; CFU, colony-forming unit; HS, Holm-Sidak method for pairwise multiple comparison tests; PCR, polymerase chain reaction; ROS, reactive oxygen species.

Introduction

Penaeid shrimp are often exposed to large fluctuations in dissolved oxygen that are characteristic of the estuarine environments in which they live. Globally, the severity of hypoxia in coastal waters is increasing at a drastic rate (Diaz and Rosenberg, 1995; Diaz, 2001). In addition, hypoxia often co-occurs with increased levels of CO_2 (hypercapnia) produced by respiration, causing a decrease in water pH (Cochran and Burnett, 1996; Burnett, 1997; Ringwood and Keppler, 2002). Although not always the primary cause of mortality, hypoxia and hypercapnic hypoxia decrease the resistance of shrimp to bacterial pathogens. Hypoxia (P_{O_2} = 3.1 kPa, 1 mg O_2 l^{-1}) decreased the survival of *Penaeus stylirostris*, the black tiger shrimp, following injection of the bacterial pathogen *Vibrio alginolyticus* (Le Moullac *et al.*, 1998). Hypercapnic hypoxia (P_{CO_2} = 1.8 kPa; P_{O_2} = 4 kPa) increased mortality in the shrimp *Litopenaeus vannamei* and *Palaemonetes pugio* injected with the bacterial pathogen *V. parahaemolyticus* (Mikulski *et al.*, 2000). The specific effects of oxygen and pH on the susceptibility of shrimp to these invading bacterial pathogens remain unclear, but may involve changes in mechanisms of immune defense such as the number of circulating hemocytes, the production of reactive oxygen species (ROS), and the activity of prophenoloxidase (Le Moullac *et al.*, 1998; Mikulski *et al.*, 2000; Cheng *et al.*, 2002). In addition, other physiological responses to hypoxia and hypercapnia, such as changes in cardiac stroke volume and heart rate and the redistribution of hemolymph flow (McMahon and Burnett, 1990; Burnett 1992, 1997), may alter the access of bacterial pathogens to tissues involved in disease or immune defense (see Discussion).

When introduced by injection, bacteria not trapped at the injection site quickly appear in the hemolymph and other

tissues of crustaceans, but are rapidly eliminated (*e.g.*, Smith and Ratcliffe, 1980; White and Ratcliffe, 1982; Clem *et al.*, 1984). Under well-aerated, normoxic conditions ($P_{O_2} \approx 20$ kPa), penaeid shrimp also quickly remove bacteria from their hemolymph (Martin *et al.*, 1993; Burgents *et al.*, 2005). Suppression of pathogen growth, as detected by culture on artificial media, occurs much more rapidly than the removal of bacterial degradation products, as monitored by a variety of other techniques, including histology, radiolabel tracing, or real-time PCR (Martin *et al.*, 1993; van de Braak *et al.*, 2002; Burgents *et al.*, 2005).

Exposure to hypoxia or hypercapnic hypoxia decreases the rate at which culturable bacteria are eliminated from the hemolymph in a number of crustaceans. When *Penaeus monodon* was exposed to hypoxia (P_{O_2} = 5.4–6.4 kPa, 1.8–2.0 mg O_2 l^{-1}), the shrimp had significantly higher numbers of culturable *Vibrio harveyi* in their hemolymph 30 min after bacterial injection than did animals in well-aerated water (Direkbusarakom and Danayadol, 1998). Similar results were obtained when the freshwater prawn *Macrobrachium rosenbergii* was exposed to hypoxia (Cheng *et al.*, 2002). Holman *et al.* (2004) observed a significant increase in the number of culturable *Vibrio campbellii* that remained in the hemolymph of *Callinectes sapidus*, the blue crab, in hypercapnic hypoxia (P_{CO_2} = 1.8 kPa; P_{O_2} = 4 kPa) compared with animals held in normoxic conditions. In these studies, the increased retention of culturable bacteria in hemolymph that is associated with hypoxia and hypercapnic hypoxia could be the result of a decrease in the inactivation of culturable bacteria, a decrease in the physical removal of bacteria from the hemolymph, or a combination of both mechanisms.

Bacteria that accumulate in a variety of tissues are subsequently eliminated, although their rates of accumulation, conversion to non-culturable status (bacteriostasis), and degradation differ as a function of the crustacean host, the bacterial pathogen, and the tissue examined. Penaeid shrimp, unlike most crustacean species, possess a lymphoid organ that is apparently involved in the elimination of foreign material (reviewed by van de Braak *et al.* (2002). Burgents *et al.* (2005) quantified the bacteriostatic activity of four tissues of the penaeid shrimp *Litopenaens vannamei* and found that the lymphoid organ was the main site of active uptake and bacteriostasis of pathogenic *V. campbellii* injected intramuscularly. Although the gills and the hepatopancreas were also major sites of bacterial accumulation, these tissues had lower levels of bacteriostatic activity (Burgents *et al.*, 2005). To clarify the role of each of these tissues in immune defense and to better understand how low oxygen and high carbon dioxide decrease the resistance of shrimp to bacterial pathogens, we examined the effects of hypoxia and hypercapnic hypoxia on the tissue accumulation and bacteriostasis of pathogenic *V. campbellii* injected into *L. vannamei*.

Materials and Methods

Animals

The present study was performed in conjunction with that described by Burgents *et al.* (2005). Individuals of *Litopenaeus vannamei* (Kona Specific Pathogen Free Stock, Oceanic Institute, Kona, HI) weighing between 5 and 9 g were obtained from Waddell Mariculture Center, Bluffton, South Carolina, and held at the Grice Marine Laboratory in Charleston, South Carolina. Shrimp were held in well-aerated recirculating seawater at 30 ppt salinity, 23–25 °C, and pH 7.8–8.1. They were fed daily with commercial shrimp pellets (Rangen Inc., Buhl, ID) and held for at least 2 weeks before use in experiments.

Experimental design

We tested the influence of ambient pressures of oxygen and carbon dioxide on the tissue distribution and the fates of the bacterial pathogen *Vibrio campbellii* injected into the shrimp. In all treatments, shrimp injected with saline were used as controls. Shrimp were transferred from their holding tanks to 19-l glass aquariums in which concentrations of oxygen and carbon dioxide were regulated. Treatments consisted of different levels of ambient oxygen and carbon dioxide in the water in which the shrimp were held (Table 1). Shrimp were held in treatment conditions for 4 h before the injection of bacteria or saline as well as for the duration of the experiment (up to 4 h) after injection. The level of hypoxia (P_{O_2} = 4 kPa) used in the present study is not lethal in *L. vannamei*, but it is below the critical oxygen pressure (5.6 to 6.9 kPa, unpubl. data) for the species — that is, the oxygen pressure below which the shrimp are not able to regulate their oxygen uptake.

Hypoxia and hypercapnic hypoxia were established by continuous gassing of water with either N_2 (hypoxia) or a combination of N_2 and CO_2 (hypercapnic hypoxia). Specific oxygen levels were maintained by gassing the water intermittently with air. The oxygen pressure in the water was monitored using an oxygen electrode (YSI Model 58, Yellow Springs, OH), the output of which was fed into a data acquisition system (Sable Systems International, Las Vegas, NV). The data acquisition system was programmed to maintain a specific oxygen pressure by activating an aerator as

Table 1

Oxygen and carbon dioxide pressures in the three experimental treatments

Treatment	P_{O_2} (kPa)	P_{CO_2} (kPa)
Normoxia	19–20.6	<0.05
Hypoxia	4	<0.05
Hypercapnic hypoxia	4	1.8

needed. In the hypercapnia experiments, CO_2 pressures were held at 1.8 kPa by gassing the water constantly with 2% CO_2. Normoxia was maintained by vigorous aeration with ambient air.

Bacterial challenge

Vibrio campbellii 90-69B3 used in the present study were transformed with pMSB6, a plasmid that bears genes encoding green fluorescent protein (GFP) and resistance to the antibiotic kanamycin (kan), as described by Burgents *et al.* (2005). The injection dose was prepared as described by Burgents *et al.* (2005), and the shrimp were injected intramuscularly in the third abdominal segment with 2 μl g^{-1} body weight of 1×10^7 colony-forming units (CFU) ml^{-1} of *V. campbellii*, for a final injection dose of 2×10^4 CFU g^{-1} shrimp. This bacterial dose is approximately one-tenth of the LD_{50} for *L. vannamei* (Mikulski *et al.*, 2000) and was selected in order to profile a successful defense against the bacterial pathogen. At 15, 60, or 240 min after injection, hemolymph was sampled, and the gills, the heart, the lymphoid organ, the hepatopancreas, and the injection site (third abdominal segment) were dissected, weighed, and homogenized individually in 5 ml of sterile HEPES-buffered saline (2.5% NaCl, 10 m*M* HEPES; pH 7.5). Tissues were taken from 7–10 bacteria- or saline-injected animals for each treatment and time point; the numbers of tissues used in each statistical analysis (n) are given in Tables 2 and 3. Aliquots of the tissue homogenates were stored at −70 °C until they were used for real-time PCR, while the remainder of the homogenates were diluted and plated on selective plates.

Shrimp serving as saline controls were injected with equivalent volumes of sterile HEPES-buffered saline (2.5% NaCl; 10 m*M* HEPES; pH 7.5).

Real-time polymerase chain reaction

Real-time PCR was used to quantify the total number of intact *V. campbellii* in the tissues of *L. vannamei*. Briefly, as described by Burgents *et al.* (2005), tissue homogenates were centrifuged at 5,000 × g and resuspended in distilled water. Samples were incubated at 95 °C, and the resultant supernatants, containing the plasmids from lysed *V. campbellii*, were analyzed. A 129-bp fragment of the kanamycin-resistance gene was amplified using 200 n*M* forward primer RTKnF 5′-TGATGCGCTGGCAGTGTT-3′, 200 n*M* reverse primer RTKnR 5′-CTCGCATCAACCAAACCGTTA-3′, and 200 n*M* Taqman probe 5′-TGCGCCGGTTGCATTCGATTCCTGT-3′, 5′ labeled with 6-carboxyfluorescein (FAM) and 3′ labeled with Black Hole Quencher-1 (Integrated DNA Technologies, Inc., Coralville, IA). Reaction mixtures (25 μl) were prepared using the QIAGEN QuantiTect Probe PCR Kit (catalog # 204343). The amplification was monitored using Applied Biosystem's 7000 Sequence Detection System and consisted of a 15-min incubation at 95 °C to activate the hot-start polymerase, followed by 50 cycles of denaturation at 95 °C for 30 s, annealing at 56 °C for 45 s, and elongation at 72 °C for 30 s.

Quantification using real-time PCR was limited to plasmids associated with intact *V. campbellii*. Detection of plasmids from lysed or degraded bacteria was not expected, due to the removal of the initial supernatant, as described above, and the short residence time of nucleic acids in the nuclease-rich environment of the tissue homogenate. As described by Burgents *et al.* (2005), water samples and tissue samples from saline-injected control shrimp were analyzed as negative controls to ensure that there was no amplification except that detected from the injected bacteria. Tissue samples from saline-injected control shrimp were also spiked with *V. campbellii* to test for any tissue-specific inhibition of the PCR. A standard curve was constructed on the basis of saline samples (2.5% NaCl, 10 m*M* HEPES; pH 7.5) with known numbers of CFU. The use of this standard curve allowed us to accurately compare the values obtained by real-time PCR and selective plating, since the number of injected bacteria would be the same whether enumerated by PCR or plating. Using this standard curve, we established that the real-time PCR could be used to quantify as few as one *V. campbellii* per 25-μl reaction volume. Threshold cycles of replicate samples differed by no more than one cycle, and the efficiency of all reactions was greater than 1.80, with most above 1.90.

Selective plating

Selective plating was used to quantify the number of culturable *V. campbellii* in each tissue. Homogenates were plated in marine agar supplemented with 1% NaCl and 100 μg ml^{-1} kanamycin overlaid on thiosulfate-citrate-bile-sucrose (TCBS) agar supplemented with 2% NaCl and 100 μg ml^{-1} kanamycin. Plates were incubated at 25 °C, and the number of culturable *V. campbellii* in each tissue was quantified by counting CFU 24 h after plating. The selectivity of the plates was confirmed by plating the parent strain of the transfected *V. campbellii*, which does not contain the kanamycin-resistance gene, as a negative control. Water samples were plated to ensure that kanamycin-resistant *Vibrio* spp. were not present in the water in which the shrimp were held. Tissue homogenates from saline-injected shrimp were also plated to ensure that kanamycin-resistant *Vibrio* spp. that might occur in the environment would not be detected. The identity of *V. campbellii*, expressing GFP, was confirmed by fluorescence microscopy. The injection dose was plated for each shrimp as a positive control and also for use in the standard curve in the real-time PCR analysis described above.

Statistical analysis

The effects of time after injection, tissue, and gas level on the total number of intact and culturable *V. campbellii* in the four tissues were analyzed using separate three-way analyses of variance (ANOVA). Using the experiment-wide three-way ANOVA instead of a series of individual tests minimized Type I error, which remained at 0.05. Time after injection, tissue, and gas level were treated as fixed effects, whereas individual shrimp were treated as a random effect to adjust for any variances among animals. The tests were modeled using R, a language for statistical computing (R Foundation for Statistical Computing, 2004). The use of R, and 'lme' within R, which differs from the normal least squares approach, allowed us to accurately estimate the parameters and significance of this unbalanced, mixed model. To meet assumptions of equal variance and normality, the weight-specific number of *V. campbellii*, either intact or culturable, was log-transformed, while the percentage of culturable *V. campbellii* was arc-sin square-root-transformed. SigmaStat 3.0 software (SPSS Inc.) was used to perform *post hoc* pairwise multiple comparisons on significant effects and interactions using the Holm-Sidak method (HS).

Results

Experiment-wide three-way analysis of variance

Injected bacteria that remained sufficiently intact to retain the pMSB6 plasmid were quantified by real-time PCR using primers directed against the plasmid kanR gene. The real-time PCR data were analyzed by a mixed-model three-way ANOVA to determine whether the numbers of intact bacteria in the target tissues of injected shrimp were significantly affected by each of three major factors: time after injection, tissue type, and treatment (normoxia, hypoxia, or hypercapnic hypoxia). By this analysis, time after injection and tissue type each had significant effects on the number of *Vibrio campbellii* in the tissues of *Litopenaeus vannamei* ($P < 0.0001$, degrees of freedom [df] = 229, for each factor). The effect of treatment on the accumulation of intact *V. campbellii* depended on the tissue type; that is, there was a significant interaction between treatment and tissue type ($P < 0.0001$, df = 229).

The number of culturable bacteria in the target tissues of injected shrimp represented a subset of intact bacteria that remained viable, could grow on selective medium, and retained the pMSB6 plasmid. A three-way ANOVA indicated that each of the three factors (time after injection, tissue type, and treatment) had significant effects on the number of culturable *V. campbellii* ($P < 0.001$, df = 235) as well as on the percentage of intact bacteria that were culturable ($P < 0.001$, df = 229). There was, however, a significant interaction between time and tissue type ($P < 0.0001$, df = 229) and between all three factors ($P = 0.0085$, df = 229), meaning that the effect of time differed within different tissues and within different tissues and treatments, respectively.

In subsequent analyses, the effects of time and treatment on the localization and elimination of bacteria were examined in two ways. First, to provide an overall picture of what happened to the total bacterial dose injected into shrimp, we calculated the total number of intact bacteria, culturable bacteria, and percent culturable bacteria in each of the tested tissues at each time point, then divided those values by the weight of the shrimp. Since the bacterial dose was weight-adjusted, this value — total bacteria in all tissues summed per gram of shrimp (Fig. 1) — could be compared among shrimp, regardless of the animal weight. Then, changes in bacterial numbers within a single tissue type were calculated as a function of treatment, yielding the number of intact bacteria, culturable bacteria, and percent culturable bacteria per gram tissue for each tissue type and each time point (Figs. 2–4). Significant effects of time and treatment, as well as the interaction of time and treatment, in the tested tissues (total and individual tissues) and in the hemolymph, were separately tested for significance by two-way ANOVA (significance level < 0.05). *Post hoc* pairwise multiple comparisons on significant effects and interactions were tested by the Holm-Sidak method (HS).

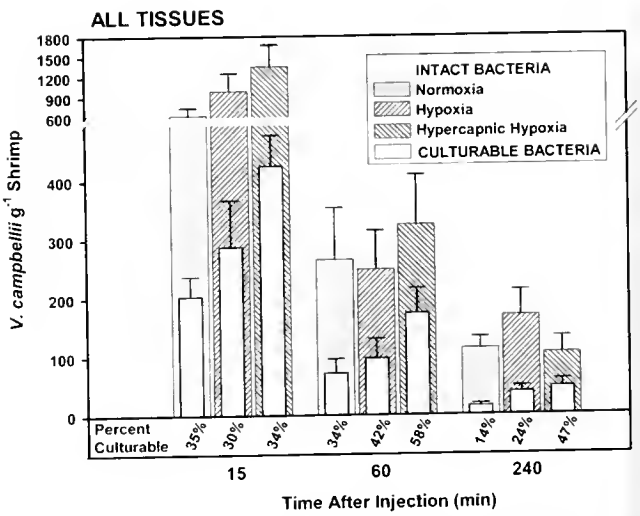

Figure 1. Mean total numbers (± SEM) of intact (shaded bars) and culturable (open bars) *Vibrio campbellii* in all tested tissues (gills, hepatopancreas, heart, and lymphoid organ) of *Litopenaeus vannamei* as a function of treatment (normoxia, hypoxia, hypercapnic hypoxia) and time after injection of 2×10^4 *V. campbellii* g^{-1} shrimp. The mean percentages of the intact *V. campbellii* that were culturable are reported on the *x*-axis below each respective bar. See the text and Tables 2 and 3 for detailed comparisons and statistical analyses.

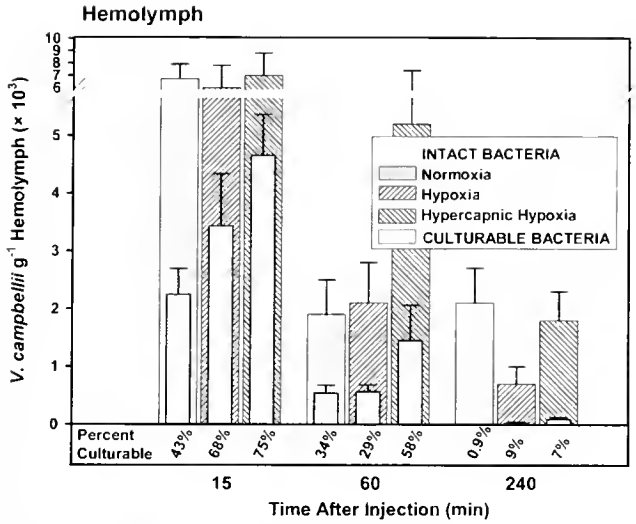

Figure 2. Mean number (± SEM) of intact (shaded bars) and culturable (open bars) *Vibrio campbellii* in the hemolymph of *Litopenaeus vannamei* 15, 60, and 240 min after injection of 2×10^4 *V. campbellii* g^{-1} shrimp. The mean percentages of the intact *V. campbellii* that were culturable are reported on the *x*-axis, below each respective bar. See the text and Tables 2 and 3 for detailed comparisons and statistical analyses.

Effect of time on all tissues

For significant effects of time (ANOVA $P < 0.05$), P values and corresponding degrees of freedom are given in Table 2. The average numbers (± SEM) of intact bacteria in all tissues summed (gills + hepatopancreas + heart + lymphoid organ) in *Vibrio*-injected animals are presented as shaded bars for each treatment group (normoxia, hypoxia, hypercapnic hypoxia) as a function of time (Fig. 1). Analysis by two-way ANOVA revealed a significant effect of time across all treatments on the number of intact bacteria in all tissues summed ($P < 0.001$, as shown in Table 2). Similarly, there was a significant effect of time on the number of intact bacteria in the hemolymph, as well as individually in the gills, the hepatopancreas, and the heart, across all treatments (Figs. 2, 3, 4; Table 2). In contrast, there was no significant effect of time across all treatments on the number of intact *V. campbellii* in the lymphoid organ (Fig. 4), but the two-way ANOVA revealed a significant interaction of time and treatment. *Post hoc* analysis showed a significant effect of time with exposure to hypercapnic hypoxia (HS, $P = 0.002$, Table 3), but not to hypoxia or normoxia, on intact bacteria in the lymphoid organ. The *post hoc* analysis does not reveal the direction of change, but data in Figure 4 indicate a decrease in intact bacteria in the lymphoid organ over time. The number of culturable *V. campbellii* also decreased over time, regardless of treatment, in all tissues summed (Fig. 1), as well as in the hemolymph and individual tissues, including the lymphoid organ (Figs. 2–4).

In all tissues summed and individually in the hemolymph, the heart, and the lymphoid organ, the percentage of intact bacteria that were culturable decreased over time (Figs. 1, 2, 4; Table 2). In contrast, the percentage of intact *V. campbellii* that could be cultured from the gills did not change over time, but in the hepatopancreas this value did increase with time (Fig. 3; Table 2). Pairwise analysis showed that the increase in the hepatopancreas occurred between 15 and 60 min after injection (HS, $P = 0.005$). The effect of time on the percentage of intact bacteria that were culturable did not significantly vary as a function of treatment (normoxia,

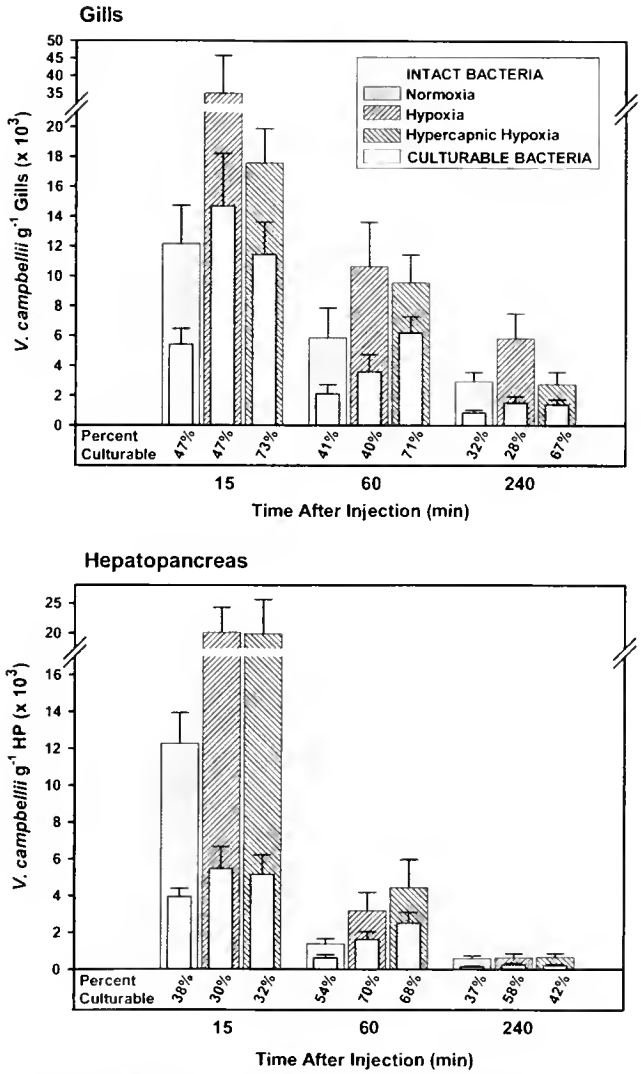

Figure 3. Mean number (± SEM) of intact (shaded bars) and culturable (open bars) *Vibrio campbellii* in the gills and the hepatopancreas (HP) of *Litopenaeus vannamei* per unit tissue weight at 15, 60, and 240 min after injection of 2×10^4 *V. campbellii* g^{-1} shrimp. The mean percentages of the intact *V. campbellii* that were culturable are reported on the *x*-axis, below each respective bar. See the text and Tables 2 and 3 for detailed comparisons and statistical analyses.

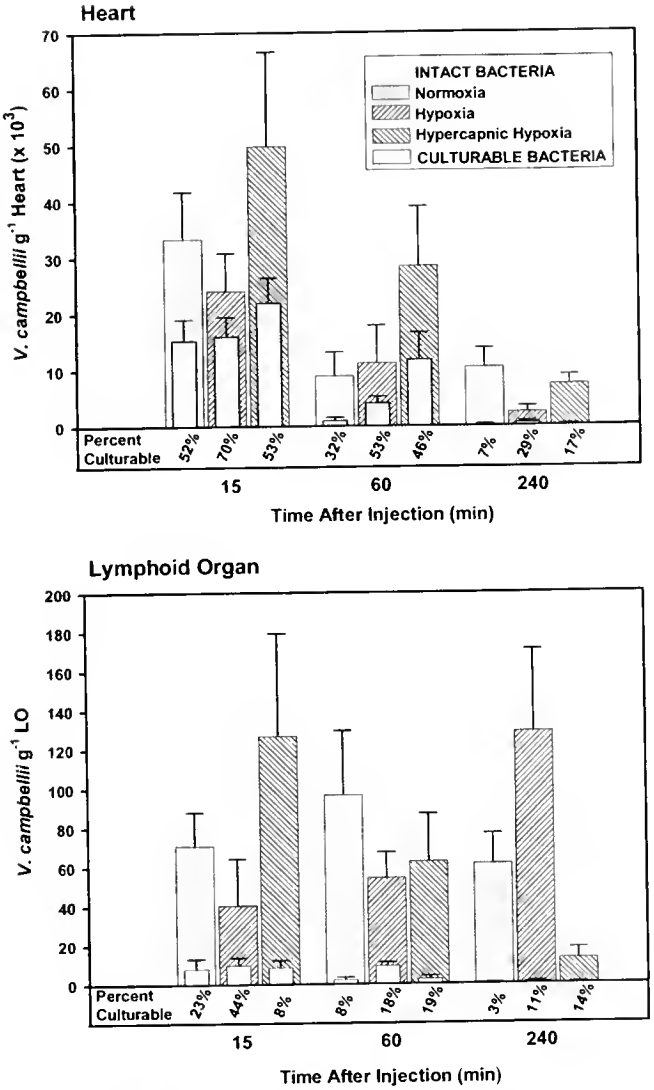

Figure 4. Mean number (± SEM) of intact (shaded bars) and culturable (open bars) *Vibrio campbellii* in the heart and the lymphoid organ (LO) of *Litopenaeus vannamei* per unit tissue weight at 15, 60, and 240 min after injection of 2×10^4 *V. campbellii* g^{-1} shrimp. The mean percentages of the intact *V. campbellii* that were culturable are reported on the *x*-axis, below each respective bar. See the text and Tables 2 and 3 for detailed comparisons and statistical analyses.

hypoxia, hypercapnic hypoxia) — neither in all tissues summed nor in individual tissues.

Effect of treatment on all tissues and hemolymph

As indicated above (*Experiment-wide three-way ANOVA*), treatment as a variable and independent of time and tissue type had significant effects on the number of culturable *V. campbellii* as well as on the percentage of intact bacteria that were culturable. The effect of treatment on the accumulation of intact bacteria depended on the tissue type; therefore, treatment effects are presented separately below for (1) all tissues summed and hemolymph, (2) gills and hepatopancreas, and (3) heart and lymphoid organ.

For significant effects across treatments (ANOVA $P < 0.05$), P values and corresponding degrees of freedom are given in the text below, while the HS P values from *post hoc* pairwise tests of hypoxia or hypercapnic hypoxia *versus* normoxia are provided in Table 3. The total numbers of intact *V. campbellii* recovered from all of the tissues (gills + hepatopancreas + heart + lymphoid organ) did not significantly vary with treatment; however, treatment significantly affected the number and percentage of culturable bacteria (ANOVA $P < 0.003$, $P < 0.001$, respectively; df = 53) (Fig. 1). In pairwise comparisons with normoxia, hypercapnic hypoxia, but not hypoxia, increased both the number and the percentage of culturable bacteria (Table 3).

The number of intact *V. campbellii* recovered from the hemolymph did not vary significantly with treatment (Fig. 2). Treatment significantly impacted both the number and the percentage of culturable bacteria in the hemolymph ($P = < 0.001$, df = 69 and $P = 0.034$, df = 61, respectively), although the effect varied among the treatments. Shrimp exposed to hypoxia had a greater number, but not a greater percentage of culturable *V. campbellii* in the hemolymph, while the animals in hypercapnic hypoxia had both a greater number and a greater percentage of intact bacteria that could be cultured in the hemolymph as compared to normoxic controls (Fig. 2; Table 3).

Effect of treatment on gills and hepatopancreas

Treatment had a significant effect on the numbers of intact and culturable *V. campbellii* in the gills ($P = 0.013$, $P = 0.002$, respectively; df = 71) and hepatopancreas ($P < 0.001$, df = 70 for both tests) and on the percent culturable bacteria in the gills ($P < 0.001$, df = 71). Exposure to hypoxia, but not to hypercapnic hypoxia, increased the number of intact bacteria in the gill, as compared to normoxia. Both hypoxia and hypercapnic hypoxia increased the number of intact *V. campbellii* in the shrimp hepatopancreas, as compared to normoxia. In both the gills and the hepatopancreas, there were also significantly more culturable *V. campbellii* in shrimp exposed to hypoxia and hypercapnic hypoxia than in normoxic animals. The percentage of culturable *V. campbellii* in the gills of shrimp exposed to hypercapnic hypoxia, but not to hypoxia, was higher than in animals held in normoxia. When compared to normoxia, neither hypoxia nor hypercapnic hypoxia had a significant effect on the percentage of culturable *V. campbellii* in the shrimp hepatopancreas (Fig. 3; Table 3).

Effect of treatment on heart and lymphoid organ

Neither hypoxia nor hypercapnic hypoxia had a significant effect on the number of intact, culturable, or percent culturable *V. campbellii* in the heart (Fig. 4; Table 3).

Table 2

Results of ANOVA for the significant effects of time on Vibrio campbellii *(intact, culturable, or percent culturable bacteria) in tested tissues and hemolymph across all treatments*

Tissue	Direction of change in bacteria with time and ANOVA P values (degrees of freedom)		
	Intact bacteria	Culturable bacteria	% Culturable bacteria
All tissues (gills + hepatopancreas + heart + lymphoid organ)	↓ $P = 0.001$ (53)	↓ $P = 0.001$ (53)	↓ $P = 0.022$ (53)
Hemolymph	↓ $P = 0.001$ (61)	↓ $P = 0.001$ (69)	↓ $P = 0.001$ (61)
Gills	↓ $P = 0.001$ (71)	↓ $P = 0.001$ (71)	NS (71)
Hepatopancreas	↓ $P = 0.001$ (70)	↓ $P = 0.001$ (70)	↑* $P = 0.017$ (70)
Heart	↓ $P = 0.001$ (61)	↓ $P = 0.001$ (61)	↓ $P = 0.001$ (61)
Lymphoid organ	NS** (58)	↓ $P = 0.002$ (70)	↓** $P = 0.028$ (58)

↓ and ↑ indicate a decrease or increase, respectively, in the direction of change of the variable with time. NS = no significant effect of time (ANOVA $P > 0.05$).

* Increase between 15 and 60 min (Holm-Sidak method, $P = 0.005$).

** Significant interaction with treatment; see Table 3 for the results of *post hoc* tests.

As mentioned previously, the lymphoid organ was the only tissue in which there was a significant interaction between treatment and time after injection for a measure of *V. campbellii* quantified in this study. Specifically, the effect of either hypoxia or hypercapnic hypoxia on the number of intact *V. campbellii* in the lymphoid organ depended on the time after injection ($P = 0.013$, df = 60 for the interaction). Only at 240 min were fewer intact *V. campbellii* detected in the lymphoid organ of shrimp exposed to hypercapnic hypoxia compared to shrimp exposed to either hypoxia or normoxia (Fig. 4). As compared to normoxia, neither hypoxia nor hypercapnic hypoxia had a significant effect on the

Table 3

Pairwise multiple comparison analysis of Vibrio campbellii *(intact, culturable, or percent culturable bacteria) in body compartments of shrimp testing the effects of hypoxia or hypercapnic hypoxia* versus *normoxia.*

Tissue	Treatment	Difference from normoxia, Holm-Sidak P values (n)		
		Intact bacteria	Culturable bacteria	% Culturable bacteria
All tissues (gill + hepatopancreas + heart + lymphoid organ)	Normoxia		NS (22)	NS (22)
	Hypoxia		NS (15)	NS (15)
	Hypercapnic hypoxia		$P < 0.001$ (17)	$P < 0.001$ (17)
Hemolymph	Normoxia		NS (30)	NS (27)
	Hypoxia		$P = 0.008$ (21)	NS (18)
	Hypercapnic hypoxia		$P < 0.001$ (19)	$P = 0.011$ (17)
Gills	Normoxia	NS (30)	NS (30)	NS (30)
	Hypoxia	$P = 0.003$ (21)	$P = 0.004$ (21)	NS (21)
	Hypercapnic hypoxia	NS (21)	$P = 0.002$ (21)	$P < 0.001$ (21)
Hepatopancreas	Normoxia	NS (30)	NS (30)	NS (30)
	Hypoxia (21, all tests)	$P = 0.043$ (21)	$P = 0.010$ (21)	NS (21)
	Hypercapnic hypoxia	$P = 0.013$ (20)	$P = 0.004$ (20)	NS (20)
Heart	Normoxia			
	Hypoxia			
	Hypercapnic hypoxia			
Lymphoid organ	Normoxia	NS (26)		NS (26)
	Hypoxia	NS (17)		$P = 0.013$ (17)
	Hypercapnic hypoxia	NS* (18)		NS (18)

The Holm-Sidak method for multiple comparisons (significance level = 0.05) was performed only on data sets for which two-way ANOVA showed a significant effect of treatment or a significant interaction with time ($P < 0.05$). Shaded areas = no significant treatment effect and no interaction of treatment with time as determined by two-way ANOVA. NS = no significant effect by the Holm-Sidak method ($P > 0.05$). Values in parentheses are numbers of samples tested from each treatment group.

* Significant interaction between time and treatment. At 240 min, ANOVA, $P < 0.014$, df = 60.

number of culturable *V. campbellii* recovered from the lymphoid organ; however, exposure to hypoxia significantly increased the percentage of culturable *V. campbellii* in this tissue (Fig 4; Table 3).

Discussion

In the present study, we demonstrate that hypercapnic hypoxia and, to a lesser extent, hypoxia inhibit the overall ability of the shrimp *Litopenaeus vannamei* to reduce the numbers of culturable *Vibrio campbellii* in its hemolymph and tissues during the first 4 h after injection. Across all timepoints examined, hypoxia and hypercapnic hypoxia did not significantly alter the numbers of intact bacteria in whole animals (all tissues summed), as compared to normoxia. Examination of individual tissues, however, revealed significant treatment effects on the numbers of intact bacteria in gills, hepatopancreas, and lymphoid organ (Table 3). Where significant effects of hypoxia, hypercapnic hypoxia, or both were detected, there were increases in gills and hepatopancreas and decreases in the lymphoid organ (Table 3). These results are consistent with a shift in the distribution of bacteria in the major tissues away from the lymphoid organ towards the gills and the hepatopancreas.

Our data confirm the results of previous studies showing that both hypoxia and hypercapnic hypoxia impair the removal of live, culturable bacteria from the hemolymph of decapod crustaceans (Direkbusarakom and Danayadol, 1998; Cheng *et al.*, 2002; Holman *et al.*, 2004). To our knowledge, this study provides the first demonstration that hypoxia and hypercapnic hypoxia suppress bacteriostasis but do not impair the physical removal of intact bacteria from the hemolymph.

Although numerous mechanisms are likely to be involved in the bacteriostasis of *V. campbellii*, the present data suggest that at least some of these mechanisms are inhibited by hypoxia and hypercapnic hypoxia. Low dissolved oxygen and pH suppress several specific immune functions, such as phagocytosis, the production of ROS, and the prophenoloxidase cascade (Smith, 1991; Muñoz *et al.*, 2000; Bachère *et al.*, 2004; Cerenius and Söderhäll, 2004). Antimicrobial peptides (Bachère *et al.*, 2004) as well as the *in vivo* formation of hemocyte-bacterial nodules (Martin *et al.*, 1998) are believed to contribute to suppressing the growth of bacterial pathogens in shrimp. The sensitivities of the antimicrobial peptides and nodule formation to hypoxia and hypercapnic hypoxia have yet to be assessed.

Recent evidence suggests that, in penaeid shrimp, the lymphoid organ is a major site of active uptake of bacteria from the hemolymph (van de Braak *et al.*, 2002; Burgents *et al.*, 2005). After bacteria are injected, hemocytes migrate from the hemolymph to the lymphoid organ, where they phagocytose invading bacteria (van de Braak *et al.*, 2002). Hypoxia and hypercapnic hypoxia are believed to decrease the activity of shrimp hemocytes, as measured by a decrease in ROS production (Le Moullac *et al.*, 1998) and phagocytosis (Cheng *et al.*, 2002), which consequently would reduce the accumulation of bacteria at sites of active hemocyte uptake. The latter findings are consistent with the results of the present study — higher numbers of culturable *V. campbellii* remaining in the hemolymph and changes in the lymphoid organ — that indicate both reduced accumulation of intact bacteria under hypercapnic hypoxia and reduced bacteriostatic activity in hypoxia. Both the hepatopancreas and the gills are target tissues of *Vibrio* infection in penaeid shrimp (Lightner, 1996). The elevated number of culturable bacteria circulating in the hemolymph may allow additional time for these pathogens to accumulate in the hepatopancreas and the gills, explaining the elevated mortality rates associated with exposure to hypoxia and hypercapnic hypoxia.

In decapod crustaceans, the gills are a major site of bacterial accumulation under normoxic conditions (Smith and Ratcliffe, 1980, 1981; White and Ratcliffe, 1982; Martin *et al.*, 1993; Alday-Sanz, 2002). The results of the present study suggest that, if the gills actively take up bacteria from the hemolymph, then the mechanisms responsible for this sequestration are not inhibited by either hypoxia or hypercapnic hypoxia. Instead, significantly more intact *V. campbellii* per unit tissue weight were recovered from the gills after exposure to hypoxia compared to normoxia, and significantly more culturable *V. campbellii* per unit tissue weight were recovered from the gills after exposure to either hypoxia or hypercapnic hypoxia. Since the gills are a target for the pathogenic effects of vibriosis (Lightner, 1996), the enhanced accumulation of *V. campbellii* we observed in the gills provides a logical explanation for the increased pathogenicity of *Vibrio* spp. in shrimp exposed to hypoxia and hypercapnic hypoxia (Le Moullac *et al.*, 1998; Mikulski *et al.*, 2000).

It is possible that the observed increase in bacterial accumulation at the gills is mediated by changes in virulence factors expressed by the bacteria or by gill-surface receptors that mediate the adherence of *Vibrio* spp. to their target tissues. Alternatively, an increase in bacterial accumulation at the gills might be related to hemodynamic changes associated with responses to hypoxia. Decapod crustaceans generally increase cardiac output in response to environmental hypoxia (reviewed by McMahon, 2001). The elevated perfusion of the gills improves oxygenation of the hemolymph but, as suggested by Martin *et al.* (1993), it may also provide more opportunity for the entrapment of nodules formed by hemocytes and bacteria. Furthermore, elevated hydrostatic pressures driving the hemolymph through the gills cause the hemolymph spaces within the gills to expand (McMahon and Burnett, 1990), a property known as compliance. Simultaneously, hydrostatic pressures in the chamber surrounding the gills, which are already negative, be-

come more negative with increased activity of the water pumping mechanism (reviewed by McMahon, 2001). Thus, the increased positive pressure in the hemolymph space within the gill and the increased negative pressure outside the gill both act to lower vascular resistance, resulting in a preferential shunting of hemolymph through the gill. In general, hemolymph flow during hypoxia appears to be shunted away from the viscera (Airriess and McMahon, 1994).

In all tissues combined (gills + hepatopancreas + heart + lymphoid organ) and in the hemolymph, hypercapnic hypoxia had a greater impact than hypoxia alone on the number and percentage of culturable bacteria (Table 3). Most studies investigating the effects of hypoxia on the immune system have ignored the associated increase in CO_2, or hypercapnia, which causes a decrease in water pH. Although not previously documented in shrimp, a decrease in pH has an independent and negative effect on the *in vitro* production of ROS by oyster hemocytes (Boyd and Burnett, 1999) as well as a negative effect on the bacteriostatic activity of fish phagocytes (Boleza *et al.*, 2001). The data presented here further document the importance of considering both dissolved oxygen levels and pH when assessing the immunological competence of marine organisms.

The results of the present study suggest that the decreased resistance to bacterial pathogens associated with exposure to hypoxia and hypercapnic hypoxia at levels that are normally sublethal may be partly due to decreases in the accumulation of bacteria and the bacteriostatic activity in the lymphoid organ, a tissue that converts a large percentage of accumulated bacteria from a culturable to a non-culturable state (Burgents *et al.*, 2005). Exposure to hypoxia and hypercapnic hypoxia also increases the number of culturable bacteria that remain in the hemolymph over the first 4 hours after exposure to the pathogen. The increased presence of intact and culturable bacteria in the hemolymph is consistent with the greater uptake of bacteria in the gills and hepatopancreas and the increased exposure of these target organs to *V. campbellii* under conditions of hypoxia and hypercapnic hypoxia. It is clear that these levels of hypoxia and hypercapnic hypoxia have an effect on immune defense mechanisms that results in a decreased resistance to invading pathogens.

Acknowledgments

This paper was based upon work supported by the National Science Foundation under Grant No. IBN-0212921 to Dr. Karen Burnett and Dr. Lou Burnett. We wish to acknowledge Dr. Eric Stabb for providing the transformed *V. campbellii* strain and for real-time PCR technical support, Dr. Erin Burge for technical advice, and Dr. Allan Strand for statistical analysis. Contribution # 271 of the Grice Marine Laboratory.

Literature Cited

Airriess, C. N., and B. R. McMahon. 1994. Cardiovascular adaptations enhance tolerance of environmental hypoxia in the crab *Cancer magister*. *J. Exp. Biol.* **190:** 23–41.

Alday-Sanz, V. 2002. Clearing mechanisms on *Vibrio vulnificus* biotype I in the black tiger shrimp *Penaeus monodon*. *Dis. Aquat. Org.* **48:** 91–99.

Bachère E., Y. Gueguen, M. Gonzalez, J. de Lorgeril, J. Garnier, and B. Romestand. 2004. Insights into the anti-microbial defense of marine invertebrates: the penaeid shrimps and the oyster *Crassostrea gigas*. *Immunol. Rev.* **198:** 149–168.

Boleza, K. A., L. E. Burnett, and K. G. Burnett. 2001. Hypercapnic hypoxia compromises bactericidal activity of phagocytic cells against opportunistic environmental pathogens. *Fish Shellfish Immunol.* **11:** 395–410.

Boyd, J. N., and L. E. Burnett. 1999. Reactive oxygen intermediate production by oyster hemocytes exposed to hypoxia. *J. Exp. Biol.* **202:** 3135–3143.

Burgents, J. E., L. E. Burnett, E. V. Stabb, and K. G. Burnett. 2005. Localization and bacteriostasis of *Vibrio* introduced into the Pacific white shrimp, *Litopenaeus vannamei*. *Dev. Comp. Immunol.* **29:** 681–691.

Burnett, L. E. 1992. Integrated function of the respiratory pigment hemocyanin in crabs. *Am. Zool.* **32:** 438–446.

Burnett, L. E. 1997. The challenges of living in hypoxic and hypercapnic aquatic environments. *Am. Zool.* **37:** 633–640.

Cerenius L., and K. Söderhäll. 2004. The prophenoloxidase-activating system in invertebrates. *Immunol. Rev.* **198:** 116–126.

Cheng, W., C. H. Liu, J. P. Hsu, and J. C. Chen. 2002. Effect of hypoxia on the immune response of giant freshwater prawn *Macrobrachium rosenbergii* and its susceptibility to pathogen *Enterococcus*. *Fish Shellfish Immunol.* **13:** 351–365.

Clem, L. W., K. Clem, and L. McCumber. 1984. Recognition of xenogeneic proteins by the blue crab: dissociation of the clearance and degradation reactions and lack of involvement of circulating hemocytes and humoral factors. *Dev. Comp. Immunol.* **8:** 31– 40.

Cochran, R. E., and L. E. Burnett. 1996. Respiratory responses of the salt marsh animals, *Fundulus heteroclitus*, *Leiostomus xanthurus*, and *Palaemonetes pugio* to environmental hypoxia and hypercapnia and to the organophosphate pesticide, azinphosmethyl. *J. Exp. Mar. Biol. Ecol.* **195:** 125–144.

Diaz, R. J. 2001. Overview of hypoxia around the world. *J. Environ. Qual.* **30:** 275–281.

Diaz, R. J., and R. Rosenberg. 1995. Marine benthic hypoxia: a review of its ecological effects and the behavioural responses of benthic macrofauna. *Oceanogr. Mar. Biol. Annu. Rev.* **33:** 245–303.

Direkbusarakom, S., and Y. Danayadol. 1998. Effect of oxygen depletion on some parameters of the immune system in black tiger shrimp (*Penaeus monodon*). Pp. 147–149 in *Advances in Shrimp Biotechnology*, T. W. Flegel, ed. National Center for Genetic Engineering and Biotechnology, Bangkok, Thailand.

Holman J. D., K. G. Burnett, and L. E. Burnett. 2004. Effects of hypercapnic hypoxia on the clearance of *Vibrio campbellii* in the Atlantic blue crab, *Callinectes sapidus* Rathbun. *Biol. Bull.* **206:** 188–196.

Le Moullac, G., C. Soyez, D. Saulnier, D. Ansquer, J. C. Avarre, and P. Levy. 1998. Effect of hypoxic stress on the immune response and the resistance to vibriosis of the shrimp *Penaeus stylirostris*. *Fish Shellfish Immunol.* **8:** 621–629.

Lightner, D. V. 1996. *A Handbook of Shrimp Pathology and Diagnostic Procedures for Diseases of Cultured Penaeid Shrimp*. World Aquaculture Society, Baton Rouge, LA.

Martin G. G., D. Poole, C. Poole, J. E. Hose, M. Arias, L. Reynolds, N. McKrell, and A. Whang. 1993. Clearance of bacteria injected into the hemolymph of the penaeid shrimp, *Sicyonia ingentis*. *J. Invertebr. Pathol.* **62:** 308–315.

Martin G. G., J. Kay, D. Poole, and C. Poole. 1998. *In vitro* nodule formation in the ridgeback prawn, *Sicyonia ingentis*, and the American lobster, *Homarus americanus*. *Invertebr. Zool.* **117:** 155–168.

McMahon, B. R. 2001. Respiratory and circulatory compensation to hypoxia in crustaceans. *Respir. Physiol.* **128:** 349–364.

McMahon, B. R., and L. E. Burnett. 1990. The crustacean open circulatory system: a reexamination. *Physiol. Zool.* **63:** 35–71.

Mikulski, C. M., L. E. Burnett, and K. G. Burnett. 2000. The effects of hypercapnic hypoxia on the survival of shrimp challenged with *Vibrio parahaemolyticus*. *J. Shellfish Res.* **19:** 301–311.

Muñoz M., R. Cedeno, J. Rodriguez, W. P. W. van der Knaap, E. Mialhe, and E. Bachère. 2000. Measurement of reactive oxygen intermediate production in haemocytes of the penaeid shrimp, *Penaeus vannamei*. *Aquaculture* **191:** 89–107.

R Foundation for Statistical Computing. 2004. *The R Project for Statistical Computing*. R vers. 2.0.1 [Online]. Available: http://www.r-project.org. [accessed 2 August 2004].

Ringwood, A. H., and C. J. Keppler. 2002. Water quality variation and clam growth: Is pH really a non-issue in estuaries? *Estuaries* **25:** 901–907.

Smith, V. J. 1991. Invertebrate immunology: phylogenetic, exotoxicological and biomedical implications. *Comp. Haematol. Int.* **1:** 60–76.

Smith, V. J., and N. A. Ratcliffe. 1980. Host defense reactions of the shore crab, *Carcinus maenas* (L.): clearance and distribution of injected test particles. *J. Mar. Biol. Assoc. UK* **60:** 89–102.

Smith, V. J., and N. A. Ratcliffe. 1981. Pathological changes in the nephrocytes of the shore crab, *Carcinus maenas*, following injection of bacteria. *J. Invertebr. Pathol.* **38:** 113–121.

van de Braak, C. B. T., M. H. A. Botterblum, N. Taverne, W. B. van Muiswinkel, J. H. W. M. Rombout, and W. P. W. van der Knaap. 2002. The roles of haemocytes and the lymphoid organ in the clearance of injected *Vibrio* bacteria in *Penaeus monodon* shrimp. *Fish Shellfish Immunol.* **13:** 293–309.

White, K. N., and N. A. Ratcliffe. 1982. The segregation and elimination of radio- and fluorescent-labelled marine bacteria from the hemolymph of the shore crab, *Carcinus maenas*. *J. Mar. Biol. Assoc. UK* **62:** 819–833.

Reference: *Biol. Bull.* **208:** 169–182. (June 2005)

Anti-Tubulin Labeling Reveals Ampullary Neuron Ciliary Bundles in Opisthobranch Larvae and a New Putative Neural Structure Associated With the Apical Ganglion

STEPHEN C. KEMPF[1,*] AND LOUISE R. PAGE[2]

[1] *Department of Biological Sciences, 331 Funchess Hall, Auburn University, Auburn, Alabama 36849; and* [2] *Department of Biology, University of Victoria, British Columbia V8W 3N5, Canada*

Abstract. This investigation examines tubulin labeling associated with the apical ganglion in a variety of planktotrophic and lecithotrophic opisthobranch larvae. Emphasis is on the ampullary neurons, in which ciliary bundles within the ampulla are strongly labeled. The larvae of all but one species have five ampullary neurons and their associated ciliary bundles. The anaspid *Phyllaplysia taylori,* a species with direct development and an encapsulated veliger stage, has only four ampullary neurons. The cilia-containing ampulla extends to the pretrochal surface *via* a long, narrow canal that opens to the external environment through a very small pore (0.1 μm diameter). Cilia within the canal were never observed to project beyond the opening of the apical pore. The ampullary canals extend toward and are grouped with the ciliary tuft cells and remain in this location as planktotrophic larvae feed and grow. If, as has been reported, the ciliary tuft is motile, the pores may be continually bathed in fresh seawater. Such an arrangement would increase sensitivity to environmental chemical stimuli if the suggested chemosensory function of these neurons is correct. In general, ciliary bundles of newly hatched veligers are smaller in planktotrophic larvae than in lecithotrophic larvae. In planktotrophic larvae of *Melibe leonina,* the ciliary bundles increase in length and width as the veligers feed and grow. This may be related to an increase in sensitivity for whatever sensory function these neurons fulfill. An unexpected tubulin-labeled structure, tentatively called the apical nerve, was also found to be associated with the apical ganglion. This putative nerve extends from the region of the visceral organs to a position either within or adjacent to the apical ganglion. One function of the apical nerve might be to convey the stimulus resulting from metamorphic induction to the visceral organs.

Received 17 December 2004; accepted 23 March 2005.

* To whom correspondence should be addressed. E-mail: kempfsc@auburn.edu

Abbreviations: AG, apical ganglion; AN, apical nerve; MFSW, Millipore-filtered seawater; SCP, small cardioactive peptide.

Introduction

The planktonic larval stages of marine invertebrates are confronted with the need to metamorphose in a habitat appropriate for successful juvenile and adult life. However, in an ocean covering over 70% of the earth's surface, it is nearly always the case that far less than 1% of the available habitats will meet this need. Thus, the larvae of many species have evolved the ability to "delay" metamorphosis (*e.g.,* Kempf, 1981; Kempf and Hadfield, 1985; Pechenik and Eyster, 1989; Pechenik, 1990; Pechenik and Cerulli, 1991) until they sense a chemical inductive cue (the inducer) that identifies their presence in a suitable habitat (*e.g.,* Crisp, 1974; Kriegstein *et al.,* 1974; Hadfield, 1978; Harrigan and Alkon, 1978; Morse and Morse, 1984; Hadfield *et al.,* 2001; Harder *et al.,* 2002a,b; Zhao and Qian, 2002). Pires *et al.* (2000) point out that many larvae are initially unresponsive to the inducer, so the ability to sense it must develop during the planktonic larval period. The apical ganglion is a larval structure that was previously suggested to serve this purpose (Bonar, 1978; Chia and Koss, 1984) and is now known to do so (Hadfield *et al.,* 2000).

Conklin (1897) provides what is perhaps the first description of the apical ganglion (AG) in an invertebrate larva. Bonar (1978) presents the seminal ultrastructural analysis of the AG in larvae of the aeolid nudibranch *Phestilla sibogae.*

He describes it as being composed of three cell types. Chia and Koss (1984) give a more detailed account of AG ultrastructure in larvae of the nudibranch *Rostanga pulchra* and provide the terminology currently used for the cell types of this organ (*i.e.*, ampullary cells, parampullary cells, and ciliary tuft cells). Both Bonar (1978) and Chia and Koss (1984) describe some of the AG cell types as sensory neurons, with Bonar (1978) suggesting that the ampullary cells (hereinafter ampullary neurons) might be responsible for sensing the inductive cue for metamorphosis. Chia and Koss (1984) concur on this point, but also note that more than one sensory cell type is present, thus the AG probably has more than one sensory function.

Recent investigations using immunohistochemical and neurophysiological techniques allow the neurochemical and possible functional properties of the AG cell types to be determined (*e.g.*, Kempf *et al.*, 1997; Marois and Carew, 1997a,b,c; Leise and Hadfield, 2000; Dickinson and Croll, 2003). Kempf *et al.* (1997) and Marois and Carew (1997b, c) analyze the serotonergic and other components of the AG's neuronal circuitry in detail. Their results indicate that the sensory serotonergic neurons of the AG are involved in modulating muscular and ciliary activity in the velum. Kempf *et al.* (1997) also suggest that these AG components may form a compensatory system of control that would allow the larva to orient each velar lobe relative to changes in the other.

Experiments by Leise and Hadfield (2000) demonstrate that in larval *P. sibogae* the central nervous system responds to the inductive cue with a change in the activity pattern of action potentials. Further investigations by Hadfield *et al.* (2000) provide crucial insight into at least one sensory function of the AG. Using photoablation of AG cells or cell parts that are stained by the vital dye DASPEI, they demonstrate that the AG contains the primary receptor for the chemical cue that induces metamorphosis in nudibranch (and possibly other types of spiralian) larvae. Hadfield *et al.* (2000) suggest that DASPEI may be staining the ampullary neurons described in earlier research (*e.g.*, Bonar, 1978; Chia and Koss, 1984) and that these cells may be the primary receptor for the inductive cue; as yet, however, conclusive evidence is lacking.

All previous examinations of the AG ampullary neurons have been ultrastructural. While this work provides information on the cytology of these neurons and some insight into their structural relationships with other cells of the AG (Bonar, 1978; Chia and Koss, 1984; Kempf *et al.*, 1997; Marois and Carew, 1997a), ultrastructural examinations are time-consuming, difficult, and subject to potentially substantial artifacts from shrinkage and other problems associated with dehydration and embedding. A means of examining ampullary neurons in whole larvae, using methods that eliminate such difficulties, would be useful. The ampullary neurons in a variety of invertebrate larvae have characteristics that suggest a combination of confocal imaging and fluorescently tagged tubulin antibodies might be useful for identifying them in whole-mount preparations and examining their morphology and associated structures for clues about function. First, ampullary neurons are characterized by thick, dense bundles of internalized, modified cilia (Bonar, 1978; Chia and Koss, 1984; Lacalli, 1981, 1982; Uthe, 1995; Kempf *et al.*, 1997; Marois and Carew, 1997a; Schaefer and Ruthensteiner, 2001; Page, 2002; Ruthensteiner and Schaefer, 2002). Second, they are the only cells in the AG that contain internalized dense, ciliary bundles (Bonar, 1978; Chia and Koss, 1984; Kempf *et al.*, 1997; Page and Parries, 2000). Third, they are adjacent to easily identified, serotonergic parampullary neurons (Kempf *et al.*, 1997; Marois and Carew, 1997a, b). This paper describes the successful use of a tubulin antibody to identify the ampullary neurons in opisthobranch larvae as well as a new structure associated with the AG. Whereas previous studies have dealt mainly with newly hatched larvae, we have also examined later stages in the development of planktotrophic larvae.

Materials and Methods

Adults of the nudibranch *Berghia verrucicornis* (Aeolidiidae) were collected in the Florida Keys and maintained in laboratory culture at Auburn University, Alabama, using the methods of Carroll and Kempf (1990). Those of the nudibranchs *Melibe leonina*, *Tritonia diomedea* (Tethyidae), *Armina californica* (Arminidae), *Janolus fuscus* (Zephyrinidae), and *Phyllaplysia taylori* (Aplysiidae) were collected in the waters of the San Juan Islands and maintained in flow-through seawater tables at the University of Washington's Friday Harbor Laboratories. Egg masses of the nudibranch *Phestilla sibogae* (Aeolidiidae) were kindly provided by Dr. M. G. Hadfield, Kewalo Marine Laboratory, Pacific Biomedical Research Center, University of Hawaii. Of these, the embryo of *P. taylori* undergoes direct development with an encapsulated, embryonic veliger stage, and the newly hatched larvae of *B. verrucicornis* and *P. sibogae* are lecithotrophic and ready to metamorphose a few days after hatching (Bonar and Hadfield, 1974; Harris, 1975; Carroll and Kempf, 1990). The other species all have planktotrophic larvae that must undergo a period of feeding and growth in the plankton before they reach metamorphic competence. Larvae examined were either decapsulated veliger stages (*P. taylori*), newly hatched (*B. verrucicornis*, *P. sibogae*, *J. fuscus*, *A. californica*), or veligers that were either newly hatched or at subsequent stages of growth during planktonic feeding in culture (*M. leonina*, *T. diomedea*).

Egg masses of all species were cultured in glass or plastic beakers with either artifical seawater (Reef Crystals, Aquarium Systems) at about 30 ppt from well-established aquaria (*B. verrucicornis*, *P. sibogae*) or fresh seawater (all other species and *P. sibogae*). In all cases, 0.45-μm Millipore-

filtered seawater (MFSW) was used and cultures were aerated (Kempf *et al.*, 1997; Miller and Hadfield, 1986). Planktotrophic larvae of *M. leonina* and *T. diomedea* were cultured in the laboratory using previously published methods (Kempf and Willows, 1977; Bickell and Kempf, 1983).

In preparation for fixation, veliger-stage embryos of *P. taylori* were decapsulated by tearing apart egg masses with forceps and collecting larvae that were released from their capsules. Larvae of the other species were collected either at hatching or at various stages of growth during feeding in culture. All embryos or larvae were decalcified, as described by Pennington and Hadfield (1989), in an MES buffered, ~pH 5.5, MBL seawater solution for a few hours to overnight in a refrigerator or a 17 °C incubator. Decalcified veliger stages of *P. taylori* were transferred directly to fixative (see below). Larval stages of the other species were relaxed in a 1:3 mixture of chlorotone-saturated seawater and MFSW at room temperature (Bonar and Hadfield, 1974). Embryos and larvae were fixed in 4% paraformaldehyde containing 0.2 *M* Millonig's phosphate buffer and 0.14 *M* NaCl, rinsed in 20 m*M* phosphate-buffered saline (PBS), permeabilized by ethanol dehydration and rehydration, and stored in a refrigerator, all as described for light microscopy in Kempf *et al.* (1997).

Antibody labeling was performed as described by Kempf *et al.* (1997). Primary antibodies were mouse anti-acetylated tubulin (Sigma, Cat. # 6-11B-1) diluted 1:500, rabbit anti-serotonin (Diasorin) diluted 1:1000, and as a positive control, mouse anti-small cardioactive peptides (anti-SCP, Masinovsky *et al.*, 1988) diluted 1:20. Secondary antibodies were either goat anti-mouse or anti-rabbit IgG (MT Biomedicals) conjugated to fluorescene (FITC) or rhodamine (RITC), or donkey anti-mouse or anti-rabbit IgG (Molecular Probes) conjugated to Alexafluor 488 or 594. Tissues labeled with one or more primary antibodies were incubated in the appropriate secondary antibody or antibodies at dilutions of 1:1000 for goat anti-mouse or anti-rabbit IgG and 1:200–1:400 for donkey anti-mouse or anti-rabbit IgG. Antibodies were diluted in 20 m*M* PBS containing 5% heat-inactivated goat serum, 0.1% NaN_3, and 0.1% Triton X-100. Larvae unlabeled with primary antibody were incubated in secondary antibody or antibodies only as a negative control. In addition to the species already mentioned, we also attempted to label the ampullary cilia in larvae of the bivalve *Crassostrea virginica* and the prosobranchs *Ilyanassa obsoleta* (kindly provided by Dr. E. Leise), *Trichotropis cancellata*, *Crepipatella dorsalis*, and *Fusitriton oregonensis* with the Sigma anti-acetylated tubulin antibody.

Labeled larvae were mounted under coverslips in either DPX mountant (Electron Microscopy Sciences) after ethanol dehydration or in a glycerol mounting medium containing 5% *n*-propyl gallate (Giloh and Sadat, 1982). Larvae of *B. verrucicornis* and *P. sibogae* were examined with a Bio-Rad MRC-1024 confocal, laser-scanning system mounted on a Zeiss Axioskop microscope. Larvae of *M. leonina*, *T. diomedea*, *J. fuscus*, *A. californica*, and *P. taylori* were examined on a Bio-Rad Radiance confocal, laser scanning system mounted on a Nikon Eclipse E800 microscope. Both 40× dry and 40× and 60× oil immersion objectives were used to collect data with Bio-Rad Lasersharp 2000 software (ver. 5.2). Images were processed for contrast and color with Adobe Photoshop.

Newly hatched larvae of *T. diomedea* were relaxed and then fixed in phosphate-buffered 2.5% glutaraldehyde with post-fixation in 2% bicarbonate-buffered osmium tetroxide for ultrastructural examination. Details of the procedures and methods for fixation, embedment, sectioning, and staining are described by Page (1995). In the region of the apical ganglion where the ampullary neurons are located, serial sections were cut to locate the pores of the ampullary canals. Stained sections were examined and images collected using a Hitachi 7000 electron microscope. Images of the ampullary pores were processed for contrast using Adobe Photoshop.

To assess differences in the size of the ciliary bundles of ampullary neurons in newly hatched larvae of various species and in 13-day post-hatch larvae of *M. leonina*, the length and width of the central and lateral ciliary bundles were measured using maximum intensity projections of the original data from the serial optical sections and the line function in Bio-Rad Lasersharp analysis software. Only larvae presenting a near-frontal view of the ciliary bundles were measured. Widths were measured across the center of each ciliary bundle. Lengths were measured from the base of the ampulla to the point at the apex where the bundle narrows into a canal that extends to the pretrochal surface (Fig. 1). If the ciliary bundles were bent, the length was measured as the sum of the connected lengths of the straight portions of the bundle (Fig. 1). The significance of differences in length and width was tested using a two-way analysis of variance run on the SAS statistical software package (ver. 8.2).

Results

Ampullary neurons

The apical ganglion (AG) of the larvae of all opisthobranch species and developmental stages examined had ampullary neurons, the ciliary bundles of which were labeled by Sigma's anti-acetylated tubulin antibody. In each species, the ciliary bundles could be seen centrally positioned between the velar lobes and beneath the pretrochal epidermis (Fig. 2A). In all species except *Phyllaplysia taylori*, five labeled ciliary bundles were clearly evident at hatching and in subsequent larval stages. These ciliary bundles were grouped as two lateral pairs to the left and right of a central ciliary bundle (Fig. 2A–E, G–I). In *P. taylori*, the central ciliary bundle appeared to be missing, but the four ciliary bundles of the lateral pairs were present (Fig. 2F). In

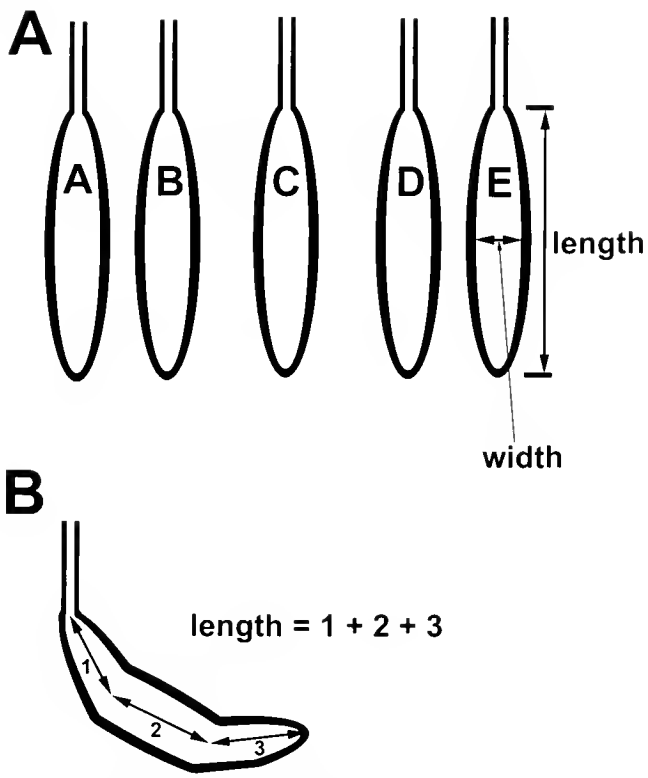

Figure 1. Measurement of ampullary neuron ciliary bundles. (A) Width and length in unbent ciliary bundles were measured as shown. (B) Length in bent ciliary bundles was measured as the sum of the linear components of the bent bundle.

newly hatched larvae of planktotrophic species, it was often difficult to discern the projection of labeled bundle cilia into the ampullary canal that extends to the pretrochal surface (Fig. 2D, G, H); however, this projection was clearly evident, as revealed by intense tubulin labeling, in newly hatched larvae of lecithotrophic species (Fig. 2B, C) and in later stage planktotrophic larvae of *Melibe leonina* (*e.g.*, Fig. 2E). Later planktotrophic larval stages of *Armina californica* and *Janolus fuscus* were not examined. Sigma's anti-acetylated tubulin antibody did not label ampullary cilia in larvae of the bivalve *Crassostrea virginica* or the prosobranchs *Ilyanassa obsoleta, Trichotropis cancellata, Crepipatella dorsalis,* and *Fusitriton oregonensis,* though other cilia, such as those of the velum and digestive tract, were labeled.

The projection of ampullary cilia within the ampullary canal extending to the pretrochal surface was clearly evident in newly hatched lecithotrophic larvae of *Berghia verrucicornis* (Fig. 2B) and *Phestilla sibogae* (Fig. 2C), as well as in later stage planktotrophic larvae of *M. leonina* (Fig. 2E). Both at hatching and in the later stage planktotrophic larvae, the ampullary canals of all the ampullary neurons were closely grouped around the central ciliary tuft cells (*e.g.*, Fig. 2B, C, E). Despite a previous report (Bonar, 1978), it was not possible to detect cilia projecting beyond the opening of the ampullary pore. Transmission electron microscopic examination of ampullary neurons in newly hatched larvae of *Tritonia diomedea* clearly revealed the ampullary pore (Fig. 3) and indicated that the ampullary cilia do not extend above the pretrochal surface at hatching.

Sufficient tubulin antigen was sometimes present in the perikarya of the ampullary neurons to make them visible in confocal optical sections. The perikarya were always closely grouped and had basal nuclei (Fig. 4A, B). The ciliary bundles within each ampullary neuron were in a cylindrical pocket that extended toward the pretrochal surface. The final portion of the ampulla consisted of a long, thin, tubular conduit (the ampullary canal) that extended between the ciliary bundle and the apical pore at the pretrochal surface (Fig. 2B, C, E). Measurement of appropriately oriented neuronal perikarya in Figure 4A and B gave maximum cell widths of 7.0 ± 1.3 μm (n = 3) for 13-day-old *M. leonina* and 6.6 ± 0.7 μm (n = 3) for 15-day-old *T. diomedea*. Total cell lengths (perikaryon + ciliary bundle) were 21.2 ± 1.4 μm (n = 2) for *M. leonina* and 18.1 ± 0.8 μm (n = 3) for 15-day-old *T. diomedea*.

Measurement of ciliary bundles (Table 1) in ampullary neurons of newly hatched larvae revealed that their length ranged from 8.5 ± 1.1 μm (*T. diomedea*) to 12.7 ± 1.5 μm (*P. sibogae*) and width from 1.2 ± 0.2 μm (*T. diomedea, A. californica*) to 2.6 ± 0.6 μm (*P. sibogae*). The planktotrophic larvae of *T. diomedea* had the shortest ciliary bundles, while those of the lecithotrophic larvae of *P. sibogae* were the longest.

When ciliary bundle lengths of the five ampullary neurons in larvae of *M. leonina* were compared within groups of newly hatched (F = 0.06; P = 0.9938) or 13-day-old (F = 1.03; P = 0.4000) larvae, there were no significant differences. The only significant difference in a comparison of ciliary bundle widths for the five ampullary neurons in newly hatched larvae was between the central bundle and lateral bundles (F = 8.55; $P < 0.0001$). There were no significant differences in length or width among ciliary bundles of 13-day-old larvae (F = 0.30; P = 0.8755). A comparison of both ciliary bundle length and width between newly hatched and 13-day-old larvae of *M. leonina* revealed that bundles were significantly longer (F = 93.97; $P < 0.0001$) and wider (F = 264.37; $P < 0.0001$) in 13-day-old larvae.

Positive controls using anti-SCP had typical labeling (Kempf *et al.*, 1987) of SCP-containing neurons and axons in central nervous system ganglia, commissures, and connectives and no labeling in the region of the apical ganglion (Fig. 4C). Larvae incubated in secondary antibody only showed no specific labeling (*e.g.*, Fig. 4D, E). Positive controls using anti-serotonin antibody labeled the characteristic serotonergic neurons and associated axons of the AG, but not the ampullary neurons (Fig. 5A).

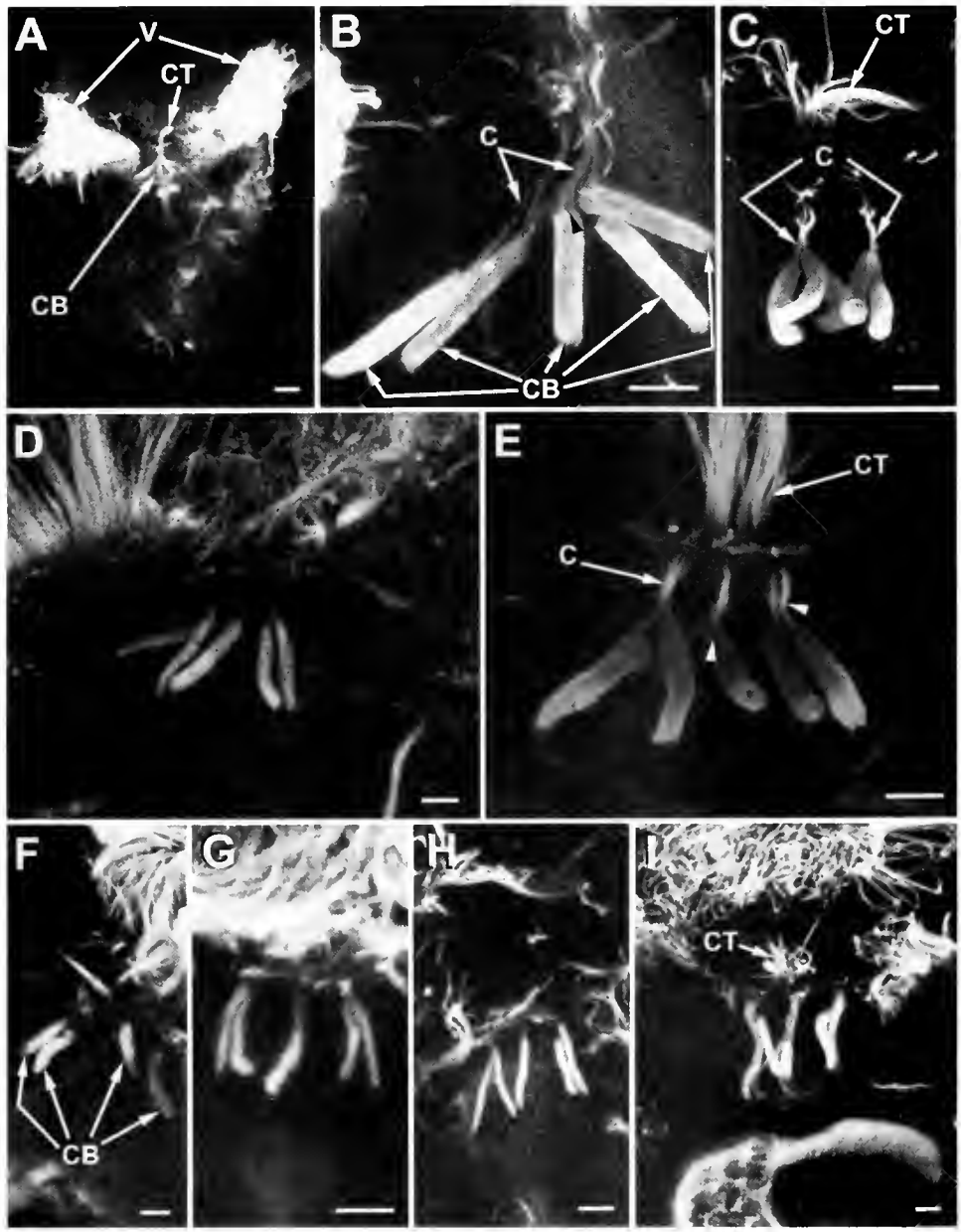

Figure 2. Ciliary bundles of ampullary neurons in seven species of opisthobranchs. Abbreviations: C, labeled cilia; CB, ciliary bundles; CT, ciliary tuft; V, velar lobes. (A) Low-magnification image of a newly hatched, competent larva of *Berghia verrucicornis* in frontal view. The ciliary bundles of the five ampullary neurons lie beneath the ciliary tuft and between the velar lobes. (B) High-magnification image of the five ampullary neurons in a newly hatched, competent larva of *B. verrucicornis*. Note the very long ampullary canals that are defined by the labeled cilia within. In some cases (*e.g.*, arrowhead) anti-tubulin labeling of the cilia suggests that more than one canal may arise from a single ampullary neuron. (C) The ciliary bundles of the five ampullary neurons in a newly hatched, near-competent larva of *Phestilla sibogae*. Note that the canals of the ampullary neurons appear to form two tight groups on the left and right sides of the ciliary tuft. (D) The five ciliary bundles of the ampullary neurons in a newly hatched planktotrophic larva of *Melibe leonina*. As indicated by very weak labeling, few cilia are present in the apical canals of this planktotrophic species at hatching. (E) High-magnification image of the five ciliary bundles in a 13-day-old larva of *M. leonina* (~19 days before competence; Bickell and Kempf, 1983). This larva is a little over halfway to metamorphic competence. As in *B. verrucicornis*, very long apical canals are revealed by labeling of cilia within. Also, as in *B. verrucicornis*, in some instances anti-tubulin labeling of the cilia suggests that more than one canal extends from a single ampullary neuron (arrowheads). (F) The ciliary bundles in a veliger-stage embryo of *Phyllaplysia taylori*. Only four ampullary neurons are present in encapsulated veligers of this species. (G, H) Ciliary bundles of the five ampullary neurons in a newly hatched, planktotrophic larva of *Armina californica* (G) and *Janolus fuscus* (H). (I) Ciliary bundles of the five ampullary neurons in a 15-day-old planktotrophic larva of *Tritonia diomedea*. Scale bars: A = 20 μm; B–I = 5 μm.

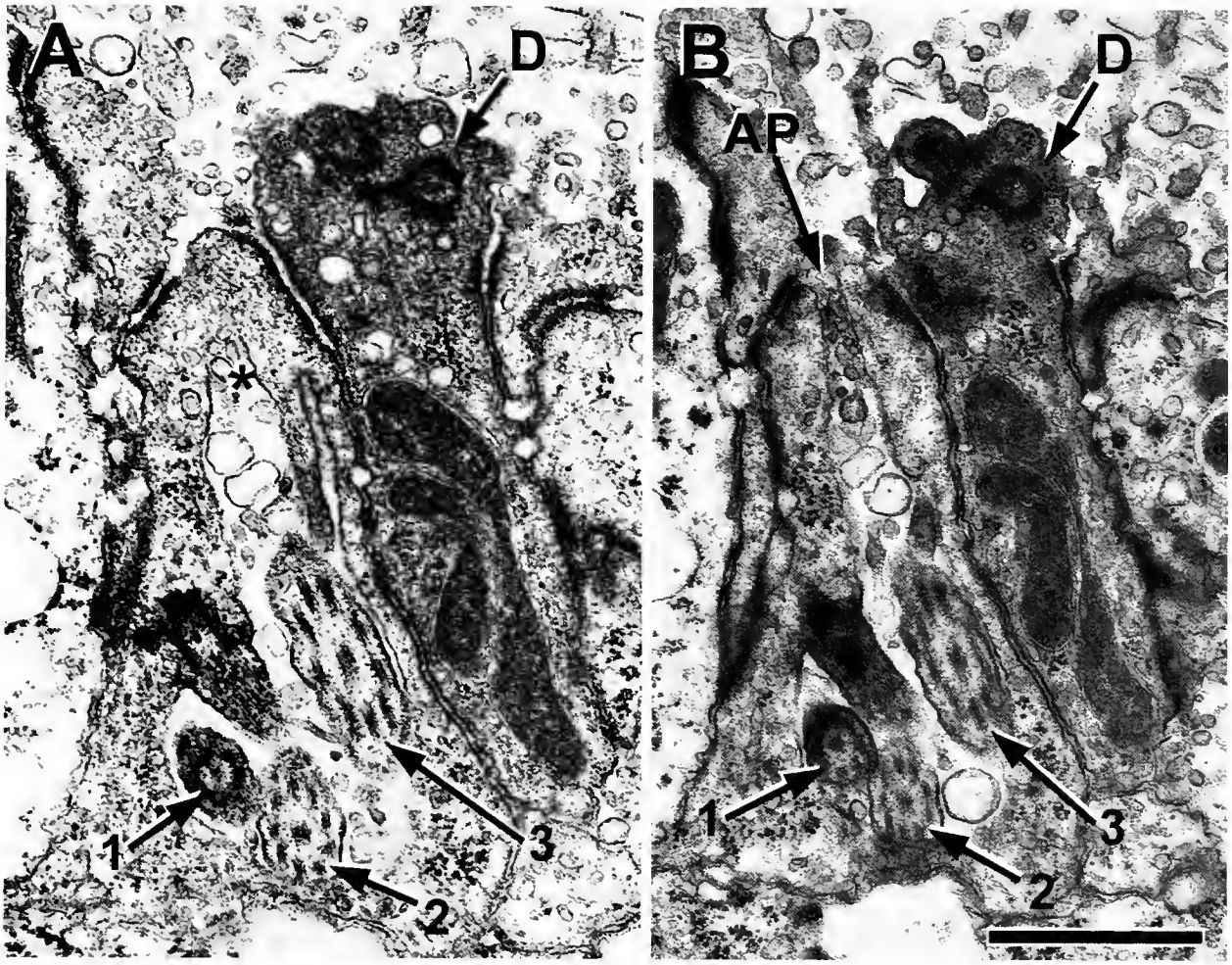

Figure 3. Electron micrographs from the apical ganglion of a newly hatched larva of *Tritonia diomedea*, showing the opening of the ampullary canal at the pretrochal surface that forms the ampullary pore. (A) The asterisk marks the ampullary canal in a section just before its opening at the pretrochal surface. Three cilia (1, 2, 3) within the canal are indicated. The dendrite (D) of a type I parampullary neuron lies directly adjacent to the ampullary neuron. The basal bodies of the two cilia characteristic of this type of dendrite can be seen at its tip. (B) The next section following that in (A) shows the ampullary pore (AP) opening at the pretrochal surface. As is evident, the pore is exceedingly small. Scale bar = 1 μm.

Apical nerve

In addition to the ciliary bundles of ampullary neurons, the Sigma anti-acetylated tubulin antibody also labeled a new structure, tentatively called the apical nerve (AN). This structure was observed in newly hatched planktotrophic larvae of *M. leonina* and newly hatched lecithotrophic larvae of *B. verrucicornis*, as well as in later stages of both *M. leonina* and *T. diomedea*. Larvae of *A. californica*, *J. fuscus*, *P. sibogae*, and *Phyllaplysia taylori* were not specifically examined for the presence of this structure. The best examples of the AN were observed in 13-day-old larvae of *M. leonina*. Serial confocal, optical sections of larvae double-labeled with anti-serotonin and anti-acetylated tubulin revealed that the termini of the AN were dorsal to the serotonergic parampullary neurons and ampullary neurons and either within or associated with the apical ganglion (see Fig. 5A–G). The AN consisted of a long twisted process that originated in the region of the larval viscera and extended to just below the pretrochal epidermis. At its end, beneath the pretrochal epidermis, the process split into three branches that ended in swollen termini (Fig. 5F, G). One branch had a long thin appendage extending from its swollen terminus (Fig. 5 F, G, asterisk-arrow). In 13-day-old larvae of *M. leonina*, the AN could be seen to end dorsal to the ciliary bundles of the ampullary neurons that were closely grouped around the ciliary tuft cells. The serotonergic parampullary neurons were ventral to this grouping, with the dendrites of the lateral, sensory, parampullary neurons extending to the

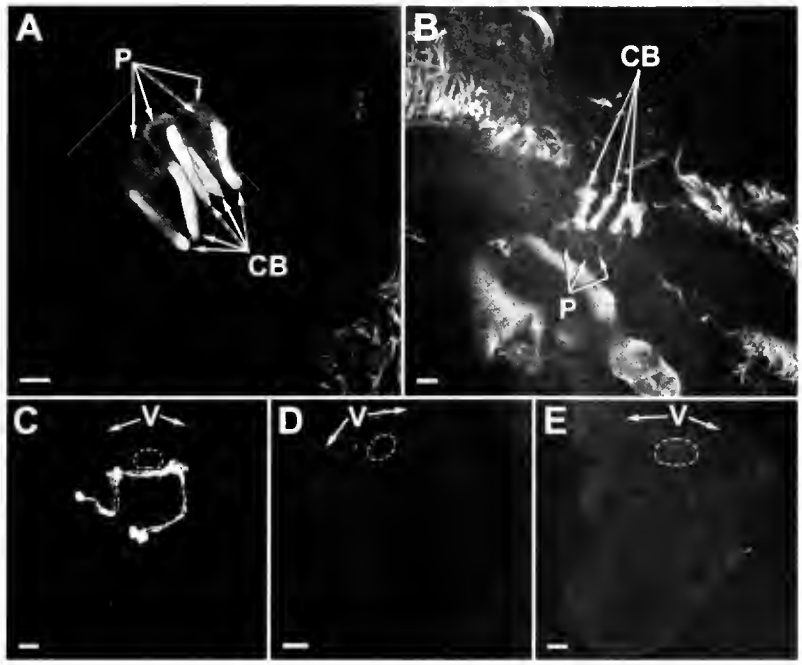

Figure 4. Ampullary neuron perikarya and control labeling. (A) Ampullary neuron perikarya (P) and ciliary bundles (CB) in a 13-day-old larva of *Melibe leonina* (~19 days before competence; Bickel and Kempf, 1983). (B) Ampullary neuron perikarya and ciliary bundles in a 15-day-old larva of *Tritonia diomedea* (~19 days before competence; Kempf and Willows, 1977) (C) Positive control, newly hatched larva of *M. leonina* labeled with a mouse monoclonal antibody that binds to small cardioactive peptides (anti-SCP). Axons crossing the cerebral commissure and extending from posterior neurons on either side of the larva are labeled. The dashed oval indicates the position of the apical ganglion and its associated ampullary neurons. (D) Example of secondary antibody control. Note lack of labeling by secondary, RITC-conjugated, goat anti-mouse IgG antibody in a newly hatched larva of *T. diomedea*. The dashed oval indicates the position of the apical ganglion and its associated ampullary neurons. (E) Example of secondary antibody control. Note lack of labeling by secondary, Alexafluor 594-conjugated donkey anti-mouse IgG antibody in a newly hatched larva of *Armina californica*. The dashed oval indicates the position of the apical ganglion and its associated ampullary neurons. Scale bars: A, B = 5 μm; C, D, E = 10 μm.

pretrochal surface some distance to the left and right of the central ampullary neuron-ciliary tuft cell grouping (Fig. 5A–C, D, E). The general position of the apical nerve relative to the ampullary and serotonergic parampullary type I neurons is shown in Figure 6.

Discussion

Apical ganglion and ampullary neurons

The apical ganglion (AG) of molluscs (Leise, 1996; Lin and Leise, 1996a, b; Marois and Carew, 1997a, b) is also known by a variety of other names, *e.g.,* apical sense organ (Conklin, 1897), apical organ (Pelseener, 1911; Werner, 1955; Tardy, 1974; Page, 1992), cephalic sensory organ (Bonar, 1978; Uthe, 1995), apical sensory organ (Chia and Koss, 1984; Kempf *et al.,* 1997), and apical complex (Tardy and Dongard, 1993). Previous studies on the morphology of this ganglion (Bonar, 1978; Chia and Koss; 1984; Tardy and Dongard, 1993; Uthe, 1995; Kempf *et al.,* 1997; Marois and Carew, 1997a, b, c) suggest that the ampullary and parampullary neurons play a sensory and modulatory role that affects larval behavior. Morphological studies by Kempf *et al.* (1997) and Marois and Carew (1997b, c) indicate that serotonergic sensory neurons in and innervation arising from the apical ganglion may modulate muscle contractility, ciliary activity, or both in the velum of larval opisthobranchs. Recent experiments by Hadfield *et al.* (2000) demonstrate that DASPEI-labeled cellular structures of the apical ganglion are critical for primary recognition of the chemical inductive cue that initiates metamorphosis in larvae of the aeolid mollusc *Phestilla sibogae*. These structures have not yet been identified, but Hadfield *et al.* (2000) suggest that they may be the ampullary neurons, which are located in the apical ganglion and are morphologically similar to putative chemoreceptors in the cephalopod olfactory organ (Emory, 1975, 1976; Bonar, 1978). If this is correct, the organization of the pores of the ampullary neurons around the bases of the ciliary tuft cells (as revealed by our anti-tubulin labeling) may be important. This juxta-

Table 1

Length and width of ciliary bundles in ampullary neurons

Species* P, Planktotrophic L, Lecithotrophic E, Embryonic	Ciliary bundle length†		Ciliary bundle width†	
	Newly hatched	13 d post-hatch	Newly hatched	13 d post-hatch
Melibe leonina	11.6 ± 1.0	14.1 ± 1.4	1.8 ± 0.2	2.5 ± 0.3
P	(9, 45)	(9, 45)	(11, 54)	(11, 54)
Tritonia diomedea	8.5 ± 1.1	—	1.2 ± 0.2	—
P	(8, 28)		(8, 29)	
Janolus fuscus	9.5 ± 1.3	—	1.4 ± 0.2	—
P	(4, 16)		(4, 15)	
Armina californica	8.8 ± 0.9	—	1.2 ± 0.2	—
P	(4, 16)		(4, 18)	
Berghia verricicornis	11.1 ± 1.0	—	2.1 ± 0.3	—
L	(4, 10)		(3, 9)	
Phestilla sibogae	12.7 ± 1.5	—	2.6 ± 0.6	—
L	(3, 5)		(2, 4)	
Phyllaplysia taylori	10.3 ± 0.3	—	2.2 ± 0.2	—
L, E	(1, 4)		(1, 4)	

* All stages labeled were hatched larval stages except for those of *Phyllaplysia taylori*, which were veliger stage embryos. *P. taylori* is a direct-developing species that has an encapsulated embryonic veliger but lacks a free-living larval stage. This species hatches as a fully metamorphosed slug.

† Values (in micrometers) are mean ± standard deviation. The first number in parentheses is the number of larvae in which measurements were made. The second number is the total number of individual ciliary bundles that were measured.

position with the ciliary tuft cells is maintained throughout larval development. Since the ciliary tuft appears to be motile (Page and Parries, 2000; unpubl. obs.), it may act to constantly bathe the ampullary pores in fresh seawater, thus enhancing their exposure to dissolved metamorphic inducer when a larva encounters a suitable habitat for the juvenile and adult.

Using figure 2 in Hadfield *et al.* (2000), we determined that the DASPEI-labeled structures that they describe are about 2 μm in diameter. Our results provide a width of about 7 μm and a length of 18–21 μm for ampullary neurons in 13-day-old larvae of *Melibe leonina* and 15-day-old larvae of *Tritonia diomedea*. Since our measurements of ciliary bundles in these species and in *P. sibogae* are similar, we would expect the same for the size of ampullary neurons. This being the case, if the DASPEI labeling reported by Hadfield *et al.* (2000) is associated with the ampullary neurons, then only a small portion of each of these cells, presumably a cytoplasmic "cloud" of mitochondria, was labeled. Nevertheless, photoablation of DASPEI-labeled structures in the AG (Hadfield *et al.*, 2000) is still sufficient to eliminate inductive sensing ability and demonstrate that the AG contains the primary receptor or receptors for the inductive cue.

Ciliary bundle length and width varied among newly hatched larvae of different species. Those with lecithotrophic development (including encapsulated veligers of direct-developing species) usually had the longest and widest ciliary bundles—that is, *P. sibogae, Berghia verrucicornis, Phyllaplysia taylori;* however, this was not an absolute rule since the ciliary bundles in newly hatched *M. leonina* were similar in length to or longer than those in species with lecithotrophic development. As larvae of *M. leonina* grew, their ciliary bundles increased in length and width. In larvae cultured for 13 days, ciliary bundles were longer than at hatching and had increased in width such that they were similar to those of newly hatched lecithotrophic larvae. That being the case, the differences in ciliary bundle length and width observed at hatching between lecithotrophic and planktotrophic larval stages appear to be related to the fact that planktotrophic larvae are not as well developed at hatching (see Table 2) rather than to intrinsic and perhaps functional differences in the ampullary neurons of different species. The increase in length and width of the ciliary bundles as larvae of *M. leonina* grow toward metamorphic competence suggests either that the cilia increase in length and width during larval growth or that new, and possibly longer, cilia are added to the bundle. If the ampullary neurons are the primary receptor for the metamorphic inducer, this increase in length and width of the bundles may reflect an increase in sensitivity in preparation for the metamorphic event.

Previous investigations (Bonar, 1978; Kempf *et al.*, 1997; Marois and Carew, 1997a; Page and Parries, 2000) describe the ampullary neurons as having a tapering ampulla that extends to the pretrochal surface and, in some cases, illustrate it as such (Bonar, 1978; Kempf *et al.*, 1997; Marois and Carew, 1997a; Page and Parries, 2000). Only Chia and Koss (1984) describe the ampulla's connection with the pretrochal surface as a "long narrow channel or neck" similar to what we observed in later stage planktotrophic larvae and newly hatched lecithotrophic larvae. We suspect this discrepancy in structure between different species is an artifact caused by shrinkage during fixation and embedding for ultrastructural examination. In addition, it is likely that the ampulla's canal is shorter in newly hatched planktotrophic larvae than in later stage larvae of the same species.

The ampullary pore is very small, on the order of 0.1 μm in diameter (see Fig. 3). It can be visualized only in well-fixed tissue that has good preservation of membranes and an absence of excessive shrinkage. Bonar (1978) reports that cilia of the ampullary neurons in a nudibranch veliger extend through the canal (neck) of the ampulla and also through and above the pore at the pretrochal surface. At the opposite extreme, Schaefer and Ruthensteiner (2001) and Ruthensteiner and Schaefer (2002) found no evidence of an external pore for ampullary neurons in a selection of

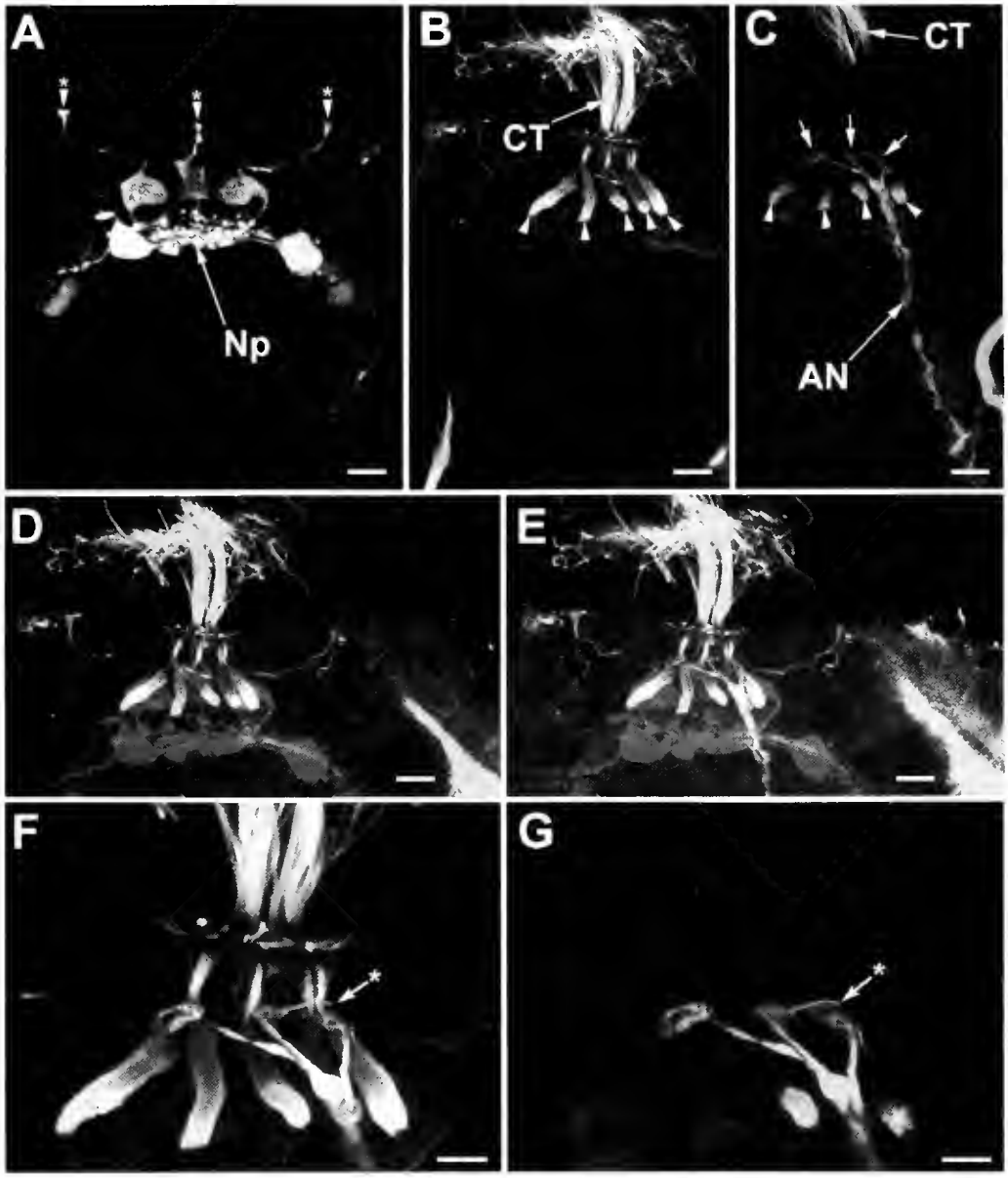

Figure 5. Known components associated with the apical ganglion and the newly described apical nerve in 13-day-old larva of *Melibe leonina*. All images are from a frontal view as seen from the dorsal side of the same larva. (A) Serotonergic neurons in the apical ganglion. The perikarya of the five serotonergic neurons are brightly labeled and situated with three above and one on either side of the apical ganglion neuropil (Np). The more weakly labeled neurons lateral to these are presumably in the edges of the cerebral ganglia. Asterisk-arrowheads identify the dendritic termini of the three sensory serotonergic neurons. (B) Ampullary neuron ciliary bundles (arrowheads) and ciliary tuft (CT) cells in the apical ganglion. (C) The apical nerve (AN) extends from the visceral region of the larva (not in picture) to a position slightly dorsal to the ampullary neuron ciliary bundles, the bases of which are identified by the arrowheads. Beneath the pretrochal epithelium, the end of the apical nerve splits into three branches with swollen termini (arrows). Note the irregular twisted appearance of the apical nerve. A portion of the ciliary tuft (CT) is visible at the top of the picture. (D) Double labeling of the ciliary bundles of the ampullary neurons (bright white) situated adjacent and slightly dorsal to the sensory serotonergic neurons (grey). (E) The terminal branches of the apical nerve are dorsal to the ampullary neuron ciliary bundles. (F) High-magnification image of the ciliary bundles of the ampullary neurons. The ampullary canals project to the pretrochal surface and are grouped around the base of the ciliary tuft. The terminal branches of the apical nerve are visible dorsal to the ampullary neurons. A narrow appendage extends to the right from the swollen terminus of the central terminal branch (asterisk-arrow). (G) A projection constructed from the optical sections that pass through the terminal branches of the apical nerve illustrates that this process is dorsal to the narrow necks of the ampullary neuron ciliary bundles. The bases of two ciliary bundles can be seen below the terminal branches and on either side of the apical nerve. Scale bars: A–E = 10 μm; F, G = 5 μm.

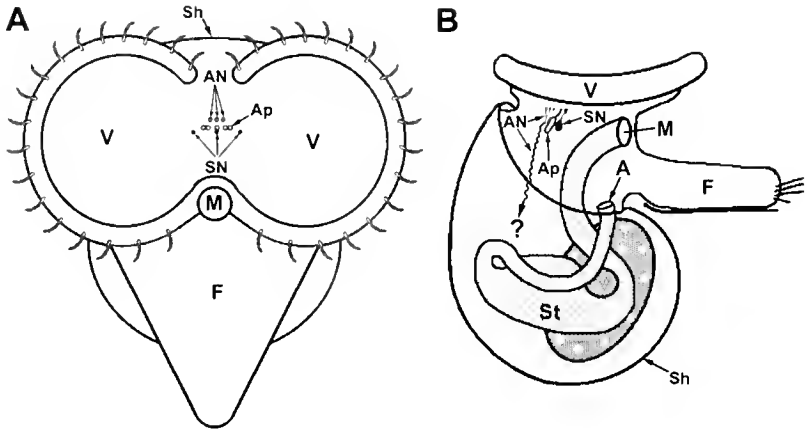

Figure 6. Relative positions of the serotonergic parampullary neurons, ampullary neurons, and apical nerve. (A) Transverse view showing the dendrites of the serotonergic neurons (SN) as most ventral, with the pores of the ampullary canals (Ap) directly above and the terminal branches of the apical nerve (AN) most dorsal. (B) Sagittal view showing the apical nerve extending toward an unknown origin in the visceral region. A, anus; F, foot; M, mouth; Sh, shell; St, stomach; V, velum..

cephalaspid and pulmonate veligers. We observed either few or no labeled cilia within the ampullary canal of newly hatched planktotrophic larvae, whereas tubulin labeling was strong in the ampullary canals of later stage planktotrophic larvae and newly hatched lecithotrophic larvae. Nonetheless, we never observed labeled cilia projecting through the ampullary pore and above the pretrochal epithelium. Assuming that the chemosensory function hypothesized for these cells is correct (Bonar, 1978; Chia and Koss, 1984; Hadfield *et al.*, 2000), the presence of this pore is essential if receptors for chemical ligands reside on the membranes of cilia within the ampulla. The very small size of the pore would augment the ability to discriminate between suitable and unsuitable habitats by effectively increasing the concentration of inducer necessary to elicit a response from the ampullary receptor neurons. An analogous situation is seen in mammalian tastebuds, where molecules defining specific taste sensations must enter a small taste pore to contact receptors on taste cell microvilli (Junqueira and Carneiro, 2003).

Larval organs and tissues present at hatching in both planktotrophic and lecithotrophic larvae are oriented toward sustaining the larva through a planktonic period that may include both feeding and growth to metamorphic competence. A number of structures critical to the metamorphic event or subsequent juvenile and adult life develop as the larva grows and attains competence; these include the radula, most ganglia of the adult nervous system, the propodium, and the primary cerata in some species (Thompson, 1958, 1962; Bonar and Hadfield, 1974; Kempf and Willows, 1977; Bickell and Kempf, 1983; Carroll and Kempf, 1994). Some such structures (*e.g.*, eyespots, digestive organs, propodium, certain nervous system components) serve multiple roles concerned with larval growth, settlement and metamorphosis, and juvenile and adult life (see Table 3). Since the cellular composition of the AG is unchanged as planktotrophic larvae of *Rostanga pulchra* grow from hatching to competence, Chia and Koss (1984) suggest that it is important both in general larval functions and in settlement and metamorphosis. It is possible that this attribute applies to specific cell types as well as to the AG as a whole. The ampullary neurons have characteristics in common with photosensory (Arendt *et al.*, 2004), mechanosensory (Emory, 1976; Altner and Prillinger, 1980), and chemosensory (Emory, 1975, 1976) receptors. They are present at hatching (and undoubtedly before), and they show little change in their structure other than small increases in the length and width of the ciliary bundles (in planktotrophic larvae) during larval life. These facts suggest that they serve one or more important sensory functions throughout the larval period. It may be that all four to five ampullary neurons mediate, for example, chemoreceptive functions related to needs during general larval life, as well as those related to sensing the metamorphic inducer once competence is attained. It is also possible that one or more of the ampullary neurons serve general sensory needs while others function in more specific modalities such as sensing the metamorphic cue. Final, though unlikely, possibilities are that some ampullary neurons act as photoreceptors or mechanoreceptors while others perform chemoreception, or that sensory modality shifts—for example, from photo- or mechanoreception to chemoreception—as the larva attains metamorphic competence.

The absence of labeling in the ampullary cilia of bivalve (*Crassostrea virginica*) and prosobranch (*Ilyanassa obsoleta, Trichotropis cancellata, Crepipatella dorsalis,* and *Fusitriton oregonensis*) larvae suggests either that the spe-

Table 2

Developmental characteristics of labeled larvae when cultured at temperatures similar to those found in their normal environment

Species (type of larval development)	Embryonic period (days)	Larval shell length: At hatching (μm)	Larval shell length: When labeled (days after hatching, μm)	Development period from oviposition to earliest competence (days)	% of development from ovi-position to competence at time of labeling*	Size at competence (μm)
Melibe leonina (planktotrophic)	10[a]	150[a]	0 d-150[a] 13 d-205[a]	42[b]	10 d-24% 23 d-55%	255[a]
Tritonia diomedea (planktotrophic)	11 (10–12[c])	145[c]	0 d-145[c] 15 d-290[c]	45[c]	11 d-24% 26 d-58%	329[c]
Janolus fuscus (planktotrophic)	?	?	?	?	?	?
Armina californica (planktotrophic)	17–23[d]	160[d]	0 d-160[d]	?	?	?
Berghia verrucicornis (lecithotrophic)	12[e]	255[e]	~0 d[‡]-255[e]	13[e]	~12d-92%	255[e]
Phestilla sibogae (lecithotrophic)	7 (6–8[f])	264[g]	~0 d[‡]-264[g]	8 (7–9[f])	~7d-~88%	264[g]
Phyllaplysia taylori (direct development‡)	27[h]	NA	?	?	?	300[h,†]

Values were taken from the literature as indicated by the following footnotes: [a]Bickell and Kempf (1983); [b]personal observation (SCK); [c]Kempf and Willows (1977); [d]Strathmann (1987); [e]Carroll and Kempf (1990) (shell does not grow after hatching in this lecithotrophic larva); [f]Hadfield *et al.* (2000); [g]Harris (1975)—the shell does not grow after hatching in this lecithotrophic larva; [h]Bridges (1975). A question mark indicates that no measurements were taken and no published data are available; NA indicates that the measurement is not applicable for that species.

* % of development = days since oviposition ÷ days from oviposition to competence. Where a range of days for hatching is given, the mean was used to calculate % development.

† Intracapsular metamorphosis.

‡ Larvae were artificially hatched and then fixed at a time close to the normal hatching period.

cific tubulin antigen bound by the acetylated tubulin antibody used (Sigma) is "hidden" or that the antigenic makeup of ampullary cilia tubulin is different in these species. It may be that other tubulin antibodies that bind to different tubulin antigens will label the ciliary bundles in ampullary neurons of bivalves and prosobranchs. We also suspect that similar differences in antigenicity may be found in the larval ampullary cilia of other invertebrate phyla.

A final observation about labeling of ampullary neuron cilia with a tubulin antibody is that the apical canals and pores of these neurons remain closely grouped around the ciliary tuft cells throughout planktotrophic larval development. Thus, tubulin labeling within the apical canals may provide a useful landmark for determining functionally related changes in the relative position of other AG components as a larva develops to metamorphic competence.

The "apical nerve"

An unexpected result of labeling with tubulin antibody was the observation of what appears to be a nerve extending from the visceral region to a position beneath the pretrochal epithelium either in or near the AG. This putative nerve ends in three processes that presumably arise from one or more axons. The ends of these processes are swollen, suggesting that they are in contact with a cell or cells within or next to the AG. As is the case for the apical ganglion, the "apical nerve" is present in the larvae of newly hatched and later stage planktotrophs, as well as in metamorphically competent lecithotrophs. This implies that it is functionally important throughout larval life; however, its close association with the AG also suggests possible involvement in the metamorphic event.

Superficially, metamorphosis in gastropod larvae appears to involve a "simple" loss of the velum (and in some cases the shell and operculum) and rearrangement of the larval body to accommodate a benthic crawling existence; however, it also involves significant internal changes at the organ, tissue, and cellular levels that are necessary for the newly formed juvenile to survive in the adult environment. In part, these needs are met by functional activation of adult-specific organs such as the radula, primary cerata, and adult CNS ganglia that have developed in the larva prior to metamorphosis (Thompson, 1958, 1962; Bickell and Kempf, 1983). In addition, some previously used larval organs must undergo changes at the cellular and genetic level that enable them to perform needed functions in the juvenile and adult; such changes include a shift in digestive tract enzymes to accommodate a change from a vegan or lecithotrophic food source to a carnivorous life style (Kempf and Todd, 1989).

Past research provides ample evidence that metamorphic changes are, in many respects, mediated by the nervous system (Hadfield, 1978, 1998; Hadfield and Pennington, 1990). This is emphasized by the fact that Hadfield *et al.* (2000) conclusively demonstrate that the AG contains the primary receptors for the chemical cue that induces meta-

Table 3

Periods during which organs or structures of planktotrophic opisthobranch larvae appear to have a critical function

Organ or structure	Present at hatching	Pre-metamorphic larval growth and/or behavior	Settlement and metamorphosis	Juvenile and adult functions
Velum	yes	yes	no*	lost
Larval shell	yes	yes	no	lost**
Larval foot other than propodium	yes	yes	yes	yes
Statocyst	yes	yes	?	yes
Operculum	yes	yes	no	lost***
Digestive tract	yes	yes	no	yes
Nephrocysts	yes	yes	no	lost
Eye spots	no	yes	yes	yes
Larval heart	no	yes	no	lost
Propodium	no	no	yes	yes
Apical ganglion	yes	yes	yes	lost
Cerebral ganglia	yes	yes	?	yes
Pleural ganglia	no	?	?	yes
Visceral ganglion	no	?	?	yes
Pedal ganglia	no	?	yes	yes
Buccal ganglia	no	?	?	yes

Question marks indicate that there is currently no basis for the determination of function at that stage of development.

* It might be said that the slowing or cessation of velar ciliary beating causes the larva to settle; however, this appears to be under nervous control, possibly mediated by the apical ganglion (see Mackie *et al.*, 1969, 1976; Kempf *et al.*, 1997; Marois and Carew, 1997c).

** Larval shell acts as the initial template upon which the adult shell is laid down in some opisthobranch species (*e.g.*, Anaspidea).

*** May act as the initial template upon which the adult operculum is laid down in a few opisthobranch groups (*e.g.*, Pyramidellidae).

morphosis in larvae of the nudibranch *P. sibogae* and probably in the larvae of other opisthobranchs. The impetus for induction must be conveyed from the AG receptors to the organs, tissues, and cells that will undergo changes to bring about metamorphosis. While at this point the purpose of the "apical nerve" must remain the subject of conjecture, one cannot help but ask if it might be a sensory pathway that conveys the metamorphic stimulus to the visceral organs, resulting in a shift from larval to juvenile function.

Acknowledgments

The authors thank Dr. Esther Leise, University of North Carolina Greensboro, for providing larvae of *Ilyanassa obsoleta;* Dr. M. G. Hadfield, University of Hawaii, for providing fertile egg masses of *Phestilla sibogae;* and Dr. Michael C. Wooten, Auburn University, for assistance with statistical analyses. We also thank Dr. A. O. D. Willows, Director of Friday Harbor Laboratories (FHL), University of Washington, and Dr. William Fitt of the Key Largo Marine Research Laboratory for providing laboratory space and equipment for some of this research; the FHL Center for Cell Dynamics for generously allowing us to use their Bio-Rad Radiance confocal microscope; the Auburn University Advanced Microscopy & Imaging Facility for the use of their Bio-Rad MRC-1024 confocal microscope; and two anonymous reviewers whose comments provided direction for improvement of the originally submitted manuscript. This research was supported by grants from the Alabama Agricultural Experiment Station (SCK) and a research grant from NSERC of Canada (LRP). This work is AU Marine Biology Program contribution #2.

Literature Cited

Altner, H., and L. Prillinger. 1980. Ultrastructure of invertebrate chemoreceptors, thermoreceptors and hygroreceptors, and its functional significance. *Int. Rev. Cytol.* **67:**69–140.

Arendt, D., K. Tessmar-Raible, H. Snyman, A. W. Dorresteijn, and J. Wittbrodt. 2004. Ciliary photoreceptors with a vertebrate-type opsin in an invertebrate brain. *Science* **306:**869–871.

Bickell, L. R., and S. C. Kempf. 1983. Larval and metamorphic morphogenesis in the nudibranch *Melibe leonina* (Mollusca: Opisthobranchia). *Biol. Bull.* **165:**119–138.

Bonar, D. B. 1978. Ultrastructure of a cephalic sensory organ in larvae of the gastropod *Phestilla sibogae* (Aeolidacea, Nudibranchia). *Tissue Cell* **10:**153–165.

Bonar, D. B., and M. G. Hadfield. 1974. Metamorphosis of the marine gastropod *Phestilla sibogae* Bergh (Nudibranchia: Aeolidacea). I. Light and electron microscopic analysis of larval and metamorphic stages. *J. Exp. Mar. Biol. Ecol.* **16:**227–255.

Bridges, C. B. 1975. Larval development of *Phyllaplysia taylori* Dall, with a discussion of development in the Anaspidea (Opisthobranchia: Anaspidea). *Ophelia* **14:**161–184.

Carroll, D. J., and S. C. Kempf. 1990. Laboratory culture of the aeolid nudibranch *Berghia verrucicornis* (Mollusca, Opisthobranchia): some aspects of its development and life history. *Biol. Bull.* **179:**243–253.

Carroll, D. J., and S. C. Kempf. 1994. Changes occur in the central nervous system of the nudibranch *Berghia verrucicornis* (Mollusca, Opisthobranchia) during metamorphosis. *Biol. Bull.* **186:**202–212.

Chia, F.-S., and R. Koss. 1984. Fine structure of the cephalic sensory organ in the larva of the nudibranch *Rostanga pulchra* (Mollusca, Opisthobranchia, Nudibranchia). *Zoomorphology* **104:**131–139.

Conklin, E. G. 1897. The embryology of *Crepidula. J. Morphol.* **13:**1–226.

Crisp, D. J. 1974. Factors influencing the settlement of marine invertebrate larvae. Pp. 177–265 in *Chemoreception in Marine Organisms,* P. T. Grant and A. M. Mackie, eds. Academic Press, New York.

Dickinson, A. J. G., and R. P. Croll. 2003. Development of the larval nervous system of the gastropod *Ilyanassa obsoleta. J. Comp. Neurol.* **466:**197–218.

Emory, D. 1975. The histology and fine structure of the olfactory organ of the squid *Lolliguncula brevis* Blainville. *Tissue Cell* **7:**357–367.

Emory, D. 1976. Observations on the olfactory organ of adult and juvenile *Octopus joubini. Tissue Cell* **8:**33–46.

Giloh, H., and J. W. Sedat. 1982. Fluorescence microscopy: reduced photobleaching of rhodamine and fluorescein protein conjugates by *n*-propyl gallate. *Science* **217:**1252–1255.

Hadfield, M. G. 1978. Metamorphosis in marine molluscan larvae: an analysis of stimulus and response. Pp. 165–175 in *Settlement and Metamorphosis of Marine Invertebrate Larvae,* F.-S. Chia and M. E. Rice, eds. Elsevier, New York.

Hadfield, M. G. 1998. The D. P. Wilson lecture: research on settlement

and metamorphosis of marine invertebrate larvae: past, present and future. *Biofouling* **12:**9–29.

Hadfield, M. G., and J. T. Pennington. 1990. The nature of the metamorphic signal and its internal transduction in larvae of the nudibranch *Phestilla sibogae*. *Bull. Mar. Sci.* **46:**455–464.

Hadfield, M. G., E. A. Meleshkevitch, and D. Y. Boudko. 2000. The apical sensory organ of a gastropod veliger is a receptor for settlement cues. *Biol. Bull.* **198:**67–76.

Hadfield, M. G., E. J. Carpizo-Ituarte, K. del Carmen, and B. T. Nedved. 2001. Metamorphic competence, a major adaptive convergence in marine invertebrate larvae. *Am. Zool.* **41:**1123–1131.

Harder, T., C. Lam, and P.-Y. Qian. 2002a. Induction of larval settlement of the polychaete *Hydroides elegans* (Haswell) by marine biofilms: an investigation of monospecific fouling diatoms as settlement cues. *Mar. Ecol. Prog. Ser.* **229:**105–112.

Harder, T., S. C. K. Lau, H-U. Dahms, and P-Y. Qian. 2002b. Isolation of bacterial metabolites as natural inducers for larval settlement in the marine polychaete *Hydroides elegans* (Haswell). *J. Chem. Ecol.* **28:**2029–2043.

Harrigan, J. F., and D. L. Alkon. 1978. Laboratory cultivation of *Haminoea solitara* (Say, 1822) and *Elysia chlorotica* (Gould, 1870). *Veliger* **21:**229–305.

Harris, L. G. 1975. Studies on the life history of two coral-eating nudibranchs of the genus *Phestilla*. *Biol. Bull.* **149:**539–550.

Junqueria, L. C., and J. Carneiro. 2003. *Basic Histology—Text and Atlas*, 10th ed. Lange Medical Books, McGraw-Hill, New York. Pp. 293–294.

Kempf, S. C. 1981. Long-lived larvae of the gastropod *Aplysia juliana:* do they disperse and metamorphose or just slowly fade away? *Mar. Ecol. Prog. Ser.* **6:**61–65.

Kempf, S. C., and M. G. Hadfield. 1985. Planktotrophy by lecithotrophic larvae of a nudibranch, *Phestilla sibogae* (Gastropoda). *Biol. Bull.* **169:**119–130.

Kempf, S. C., and C. D. Todd. 1989. Feeding potential in the lecithotrophic larvae of *Adalaria proxima* and *Tritonia hombergi:* an evolutionary perspective. *J. Mar. Biol. Assoc. UK* **69:**659–682.

Kempf, S. C., and A. O. D. Willows. 1977. Laboratory culture of the nudibranch *Tritonia diomedea* Bergh (Tritoniidae: Opisthobranchia) and some aspects of its behavioral development. *J. Exp. Mar. Biol. Ecol.* **30:**261–276.

Kempf, S. C., B. M. Masinovsky, and A. O. D. Willows. 1987. A simple neuronal system characterized by a monoclonal antibody to SCP neuropeptides in embryos and larvae of *Tritonia diomedea* (Gastropoda, Nudibranchia). *J. Neurobiol.* **18:**217–236.

Kempf, S. C., L. R. Page, and A. Pires. 1997. Development of serotonin-like immunoreactivity in the embryos and larvae of nudibranch mollusks with emphasis on the structure and possible function of the apical sensory organ. *J. Comp. Neurol.* **386:**507–528.

Kriegstein, A. R., V. Castellucci, and E. R. Kandel. 1974. Metamorphosis of *Aplysia californica* in laboratory culture. *Proc. Natl. Acad. Sci. USA* **71:**3654–3658.

Lacalli, T. C. 1981. Structure and development of the apical organ in trochophores of *Spirobranchus polyserus, Phyllodoce maculata* and *Phyllodoce mucosa* (Polychaeta). *Proc. R. Soc. Lond. B* **212:**381–402.

Lacalli, T. C. 1982. The brain and central nervous system of Muller's larva. *Can. J. Zool.* **61:**39–51.

Leise, E. M. 1996. The fluorescent dye DASPEI selectively stains the apical ganglion in larval *Ilyanassa obsoleta* (Mollusca, Gastropoda). *Microsc. Res. Tech.* **33:**496–500.

Leise, E. M., and M. G. Hadfield. 2000. An inducer of molluscan metamorphosis transforms activity patterns in a larval nervous system. *Biol. Bull.* **199:**241–250.

Lin, M.-F., and E. M. Leise. 1996a. Gangliogenesis in the prosobranch gastropod *Ilyanassa obsoleta*. *J. Comp. Neurol.* **374:**180–193.

Lin, M.-F., and E. M. Leise. 1996b. NADPH-diaphorase activity changes during gangliogenesis and metamorphosis in the gastropod mollusk *Ilyanassa obsoleta*. *J. Comp. Neurol.* **374:**194–203.

Mackie, G. O., A. N. Spencer, and R. Strathmann. 1969. Electrical activity associated with ciliary reversal in an echinoderm larva. *Nature* **223:**1384–1385.

Mackie, G. O., C. L. Singla, and C. Thiriot-Quievreux. 1976. Nervous control of ciliary activity in gastropod larvae. *Biol. Bull.* **151:**182–199.

Marois, R., and T. J. Carew. 1997a. Fine structure of the apical ganglion and its serotonergic cells in the larva of *Aplysia californica*. *Biol. Bull.* **192:**388–398.

Marois, R., and T. J. Carew. 1997b. Ontogeny of serotonergic neurons in *Aplysia californica*. *J. Comp. Neurol.* **386:**477–490.

Marois, R., and T. J. Carew. 1997c. Projection patterns and target tissues of the serotonergic cells in larval *Aplysia californica*. *J. Comp. Neurol.* **386:**491–506.

Masinovsky, B., S. C. Kempf, J. C. Calloway, and A. O. D. Willows. 1988. Monoclonal antibodies to the molluscan small cardioactive peptide SCP_B: immunolabeling of neurons in diverse invertebrates. *J. Comp. Neurol.* **273:**500–512.

Miller, S. E., and M. G. Hadfield. 1986. Ontogeny of phototaxis and metamorphic competence in larvae of the nudibranch *Phestilla sibogae* Bergh (Gastropoda: Opisthobranchia). *J. Exp. Mar. Biol. Ecol.* **97:**95–112.

Morse, A. N. C., and D. E. Morse. 1984. Recruitment and metamorphosis of *Haliotis* larvae induced by molecules uniquely available at the surfaces of crustose red algae. *J. Exp. Mar. Biol. Ecol.* **75:**191–215.

Page, L. R. 1992. New interpretation of a nudibranch central nervous system based on ultrastructural analysis of neurodevelopment in *Melibe leonina*. I. Cerebral and visceral loop ganglia. *Biol. Bull.* **182:**348–365.

Page, L. R. 1995. Similarities in form and developmental sequence for three larval shell muscles in nudibranch gastropods. *Acta Zool.* **76:**177–191.

Page, L. R. 2002. Apical sensory organ in larvae of the Patellogastropod *Tectura scutum*. *Biol. Bull.* **202:**6–22.

Page, L. R., and S. C. Parries. 2000. Comparative study of the apical ganglion in planktotrophic caenogastropod larvae: ultrastructure and immunoreactivity to serotonin. *J. Comp. Neurol.* **418:**383–401.

Pechenik, J. A. 1990. Delayed metamorphosis by larvae of benthic marine invertebrates: Does it occur? Is there a price to pay? *Ophelia* **32:**63–94.

Pechenik, J. A., and T. R. Cerulli. 1991. Influence of delayed metamorphosis on survival, growth, and reproduction of the marine polychaete *Capitella* sp. 1. *J. Exp. Mar. Biol. Ecol.* **151:**17–27.

Pechenik, J. A., and L. S. Eyster. 1989. Influence of delayed metamorphosis on growth and metabolism of young *Crepidula fornicata* (Gastropoda) juveniles. *Biol. Bull.* **176:**14–24.

Pelseener, P. 1911. Recherches sur l'embryologie des gastropods. *Mem. Acad. R. Belg. Cl. Sci.* **3:**1–167.

Pennington, J. T., and M. G. Hadfield. 1989. A simple non-toxic method for the decalcification of living invertebrate larvae. *J. Exp. Mar. Biol. Ecol.* **130:**1–7.

Pires, A., R. P. Croll, and M. G. Hadfield. 2000. Catecholamines modulate metamorphosis in the opisthobranch gastropod *Phestilla sibogae*. *Biol. Bull.* **198:**319–331.

Ruthensteiner, B., and K. Schaefer. 2002. The cephalic sensory organ in veliger larvae of pulmonates (Gastropoda: Mollusca). *J. Morphol.* **251:**93–102.

Schaefer, K., and B. Ruthensteiner. 2001. The cephalic sensory organ in pelagic and intracapsular larvae of the primitive opisthobranch genus *Haminoea*. *Zool. Anz.* **240:**69–82.

Strathmann, M. F. 1987. Reproduction and development of marine invertebrates of the northern Pacific coast. University of Washington Press, Seattle. 670 pp.

Tardy, J. 1974. Morphogenese du system nerveux chez les mollusques nudibranchs. *Haliotis* **4:**61–75.

Tardy, J., and S. Dongard. 1993. Le complexe apical de la veligere de *Ruditapes philippinarum* (Adams et Reeve, 1850) mollusque bivalve Veneride. *C.R. Acad. Sci. Paris.* **316:**177–184.

Thompson, T. E. 1958. The natural history, embryology, larval biology, and postlarval development of *Adalaria proxima* (Alder and Hancock) (Gastropoda, Opisthobranchia). *Philos. Trans. R. Soc. Lond. B* **242:**1–58.

Thompson, T. E. 1962. Studies on the ontogeny of *Tritonia hombergi* Cuvier (Opisthobranchia). *Philos. Trans. R. Soc. Lond. B* **245:**171–218.

Uthe, D. 1995. Fine structure of the cephalic sensory organ in veliger larvae of *Littorina littorea.* (L.) (Mesogastropoda, Littorinidae). *Hydrobiologia* **309:**45–52.

Werner, B. 1955. Über die Anatomie, die Entwickling und Biologie des Veligers und der Veliconcha von *Crepidula fornicata* (L.) (Gastropoda Prosobranchia). *Helgol. Wiss. Meeresunters.* **4:**260–316.

Zhao, B., and P. Y. Qian. 2002. Larval settlement and metamorphosis in the slipper limpet *Crepidula onyx* (Sowerby) in response to conspecific cues and the cues from biofilm. *J. Exp. Mar. Biol. Ecol.* **269:**39–51.

Reference: *Biol. Bull.* **208:** 183–188. (June 2005)

Exploration in a T-Maze by the Crayfish *Cherax destructor* Suggests Bilateral Comparison of Antennal Tactile Information

ADRIAN McMAHON†, BLAIR W. PATULLO, AND DAVID L. MACMILLAN*

Department of Zoology, The University of Melbourne, Parkville, Victoria 3010, Australia

Abstract. Many crayfish species inhabit murky waters or have a crepuscular lifestyle, which forces them to rely on chemical and mechanical information rather than visual input. Information on how they use one form of mechanical information—tactile cues—to explore their local environment is limited. We observed the exploratory behavior of the crayfish *Cherax destructor* in a T-maze under red light. Animals moved forward along the long arm of the maze and then moved equally in one of two available directions. The arm chosen by one crayfish did not affect that selected by a second crayfish tested immediately after in an unwashed maze. Previous experience in the maze also did not affect the choice. We found, however, that crayfish with one antenna denervated or splinted back to the carapace turned more often toward the unaltered side. Our data support the hypothesis that crayfish bilaterally compare information from their antennae.

Introduction

Crayfish are found in a variety of habitats including springs, ephemeral lakes, creeks, rivers, and alpine and subtropical streams (Merrick, 1991; Lawrence and Jones, 2002). Many species are crepuscular and make regular excursions from their shelters in the first few hours after dark and before dawn (Page and Larimer, 1972; Reynolds, 1980; Corotto and O'Brien, 2002). As a result, these animals rely heavily upon nonvisual stimuli such as chemical and mechanical, including tactile, cues for moving about and orienting (Basil and Sandeman, 2000). The major appendages for these sensory tasks are the antennules and antennae. Although these appendages are both chemosensory and mechanosensory, the antennules are the primary olfactory chemosensory organs (Cate and Derby, 2002; Grasso and Basil, 2002), while the antennae respond primarily to mechanosensory stimuli (Bush and Laverack, 1982). Each antenna consists of five basal segments and a long segmented flagellum. In some species, the antennae are as long as the body and extremely flexible (Sandeman, 1985, 1989; Zeil *et al.*, 1985). These attributes assist crayfish to locate the position of objects by using information from receptors on the flagellum (Zeil *et al.*, 1985; Sandeman, 1989).

The physiological evidence that the antennae are important in tactile responses is substantial (Bush and Laverack, 1982). Proprioceptive organs at the base of the flagellum monitor antennal movement and position (Bush and Laverack, 1982; Mellon, 2000). Changes in tactile or hydrodynamic stimulation of sensilla on the flagellum assist to determine the direction of a stimulus (Masters *et al.*, 1982). This detailed information allows the animal to determine the type of object and the distance to it (Zeil *et al.*, 1985; Sandeman and Varju, 1988). Mechanical, including tactile, input from the antennae is therefore likely to be important for navigation and exploration of terrain in the wild. In spite of this, behavioral evidence on the use of antennae during exploration of novel environments is limited (Basil and Sandeman, 2000), and there is no information on how crayfish explore or navigate in confined spaces. In streams, crayfish are often exposed to habitats that contain crevices and wooded debris. These and other features restrict or impede movement and force animals to make decisions about moving over or around obstacles.

This study investigates the exploratory behavior of the

Received 14 September 2004; accepted 25 March 2005.

* To whom correspondence should be addressed: Dr. David Macmillan, Department of Zoology, University of Melbourne, Parkville VIC 3010, Australia. E-mail: dlmacm@unimelb.edu.au

† Present address: School of Tropical Environment Studies and Geography, James Cook University, Townsville, Queensland 4811, Australia.

crayfish *Cherax destructor* (Clark 1936) in a restricted space. We used an experimental choice apparatus based on a traditional Y-maze to mimic a simple exploratory decision that crayfish might make in their natural habitat. In the maze, we compared the effects of crayfish scent, memory, and removal of sensory input from the antennae with the normal exploratory behavior of control animals.

Materials and Methods

Animals

Crayfish, *Cherax destructor*, of 6–10 cm rostrum to tail-fan, were obtained from a commercial supplier and maintained in fiberglass aquaria (120 × 50 × 20 cm) at 18 °C ± 1 °C and an artificial 12 h/12 h light/dark cycle. Animals were fed pellets *ad libitum*.

Apparatus

A T-maze was constructed from PVC pipe (diameter 10 cm). An entrance arm (120 cm) and two side arms (55 cm each) were joined with a T-joint, and each arm was capped to make the maze watertight (Fig. 1). A 3-cm-wide cut was made along the top of each arm to allow us to view the crayfish. After each trial, the maze was cleaned twice with a high-pressure hose and refilled with tap water. Trials commenced 30 min after the onset of the dark period of the artificial light/dark cycle and continued for 3–6 h, a period when other species of crayfish are most active (Page and Larimer, 1972). A 15-W light equipped with a red darkroom filter (Ilford) was suspended 1.8 m above the maze, producing 0.8 ± 0.1 lux of illumination at maze level. This light enabled the animals to be viewed during trials but was relatively undetectable to them (Cronin and Goldsmith, 1982). To verify that the light was too dim for crayfish vision, we placed 10 crayfish, one at a time, in a plastic container (20 × 20 × 10 cm) and waved our hands back and forth 1 m above each animal. None of the 10 crayfish responded to the movement as the animals do in daylight and as described for other species (Beall *et al.*, 1990).

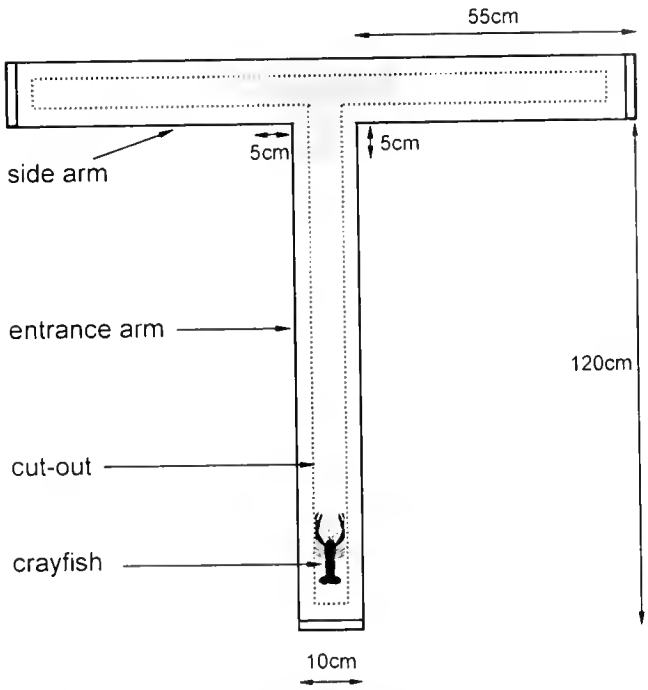

Figure 1. The T-Maze. **Crayfish** were placed in the bottom of the **entrance arm** and viewed through the **cut-out** as they proceeded to the junction (**shaded area**) and into a **side arm.**

Trials

Crayfish were held in a plastic container (20 × 20 × 10 cm) for 2–4 min (except where otherwise stated) and then placed in the base of the maze. They proceeded along the maze and, at the junction, moved into one of the two side arms. A crayfish was deemed to have entered the junction when its rostrum crossed a line 5 cm before the top of the entrance arm and to have exited the junction after crossing a line 5 cm into either side arm. When an animal exited the junction, it was recorded as having turned either left or right. Preliminary observations suggested that this was a reliable indicator of arm choice because crayfish seldom turned back. The time taken to reach the junction and the time spent in the junction were recorded with a stopwatch for each trial.

Crayfish were randomly divided into five groups: (1) 20 crayfish to test arm choice and general exploratory behavior; (2) 20 to test whether response is influenced by conspecific scent; (3) 10 that were tested 10 times each to determine whether arm choice is influenced by experience in the maze; (4) 80 to test whether removal of sensory input from the antennae affects exploratory behavior; and (5) 20 to test whether splinting back of one antenna had the same effect on exploratory behavior as removal of sensory input.

Denervation of antennal flagellum

A small flap, about 1 × 1 mm, was cut in the dorsal cuticle of the flagellum between the 1st and 10th annuli. A miniature wire hook was inserted into the flap, twisted around, and pulled out to sever the nerve. The antenna was not denervated in the basal segments, because proprioceptors between the articulations of these joints monitor antenna movement and denervation of these structures might disrupt the animal's thigmotactic behavior (Hartman and Austin, 1972; Sandeman, 1985; Basil and Sandeman, 2000). The level of the denervation was thus selected to remove the distal sensory information it supplies to the animal without disrupting the proximal proprioceptors. Crayfish were sacrificed after experiments and dissected to confirm the status of the denervation.

To control for any surgical effects, sham denervations were performed identically, except that the nerves were neither hooked nor severed, and care was taken to avoid severe bleeding in case this could produce clotting and damage the nerve.

Splinting of antennal flagellum

The antennal flagellum was splinted to the top of the crayfish's carapace. A small plastic tube (6–8 mm length) was attached with cyanoacrylate adhesive to the carapace centrally at the fusion between head and thorax. Crayfish were then given 24 h to adapt before experimentation. Thirty minutes prior to a trial the crayfish was placed in a plastic container (20 × 20 × 10 cm), and its left or right antenna was splinted by feeding it through the plastic tube on the carapace. The flagellum was held in place with a small amount of adhesive at the distal end of the tube to secure it to the animal's back. The splint was checked after the experiment to confirm that it was still in place.

Analysis

General exploratory behavior. Arm choice was scored as either left or right and analyzed with a chi-square test. A Yate's correction was applied because there were only two alternatives in the maze (Fowler *et al.*, 1998).

Influence of scent. A runs test for dichotomized data was used to compare right and left choices for randomness (Sokal and Rohlf, 1995). This test determines whether events occur in a random sequence or whether the probability of a given event is a function of the outcome of a previous event.

Influence of memory. To check for any patterns in each trial, time taken to walk up the entrance arm and time spent in the junction were analyzed for each crayfish with a runs test above and below the median.

Removal of sensory input. Arm choice was compared with a Yate's corrected chi-square test for each group of left and right denervated animals. Time taken to walk up the entrance arm of the maze and time spent in the junction were pooled for denervated and sham groups, log transformed to normalize data, and compared with a Student's *t*-test using Systat 10.2.

Results

General exploratory behavior

When placed in the T-maze, crayfish spread their antennae to touch the sides before starting to walk. They then walked up the middle of the tube with both antennae held out in front, touching the walls on either side of the maze, to guide themselves (thigmotaxis). The tubular arms of the maze meant that animals walked roughly in the center with no apparent deviation. At the junction, they scanned left and right with their antennae before turning into one arm of the maze. Animals entered the side arms without preference for a particular direction: 11 animals turned right and 9 turned left ($n = 20$, df = 1, $\chi^2 = 0.25$, $P = 0.617$).

Influence of conspecific scent

Twenty crayfish were tested in the maze when it was not washed between trials. These animals were selected randomly from a densely populated communal holding tank (≈60 animals/m^2) to minimize differences in social status between individuals and to ensure some group familiarity. The result of a trial was recorded as a choice between the same or different arm chosen by the animal in the immediately preceding trial. A "dummy" crayfish was run in the maze at the start of the experiment but excluded from the analysis. If a crayfish failed to walk through the junction and returned down the entrance arm, it was excluded and another dummy crayfish was used before the experiment continued. Once a crayfish had entered a side arm, a mesh fence was inserted by hand into that arm, between the junction and the animal, to prevent the crayfish from turning back during capture. The crayfish was then removed with a net. In these experiments, 9 crayfish went in the same direction as the previous animal and 11 went into the opposite arm (runs test, $P > 0.05$). This result suggests that either no scent was left by other crayfish in the maze or there was no preference for animals to follow the preceding individual.

Influence of memory

Ten crayfish were each tested in 10 consecutive trials. Between all trials, the maze was washed and animals were rested for 2–4 min in the plastic container. There was no significant difference in arm choice for any crayfish in its 10 repeated trials (runs test, all $P > 0.05$; see Fig. 2). Seven crayfish showed random behavior in time taken to reach the junction (runs test, $P > 0.05$), whereas three showed a significant pattern over their 10 trials (runs test, $P < 0.05$). Nine of the crayfish showed random behavior for time spent in the junction (runs test, $P > 0.05$), and only one displayed a significant pattern (runs test, $P < 0.05$).

Effect of the removal of antennal sensory information

Removal of sensory input from one of the antenna had a pronounced effect on behavior and arm choice. Crayfish with a denervated flagellum often trailed that appendage behind when they walked. They walked down the center of the maze with the intact antenna touching the side, similar to the intact animals. These animals turned toward the side of the intact antenna. The response was consistent whether

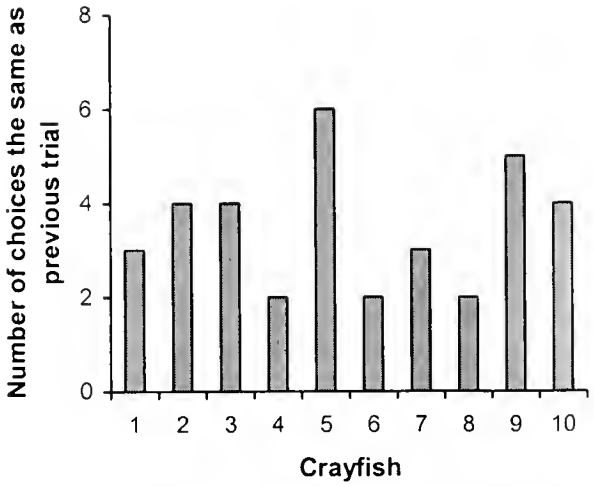

Figure 2. The number of choices out of 9 that each crayfish made that were the same as in its previous trial in the maze.

the right ($n = 20$) or left ($n = 20$) flagellum was denervated. Of the 20 animals with the right antenna intact, 15 turned into the right arm (df = 1, $\chi^2 = 5.05$, $P = 0.025$); of the 20 with left antenna intact, 16 turned left and 4 right (df = 1, $\chi^2 = 7.25$, $P = 0.007$).

The sham-operated animals showed no preference for either side arm. Crayfish with a sham-denervated left flagellum turned left 11 times and right 9 ($n = 20$, df = 1, $\chi^2 = 0.25$, $P = 0.617$); those with the right flagellum sham-denervated turned left and right 10 times each ($n = 20$, df = 1, $\chi^2 = 0.05$, $P = 0.823$). There was no noticeable difference in behavior of this group compared to unoperated crayfish, and we concluded that the surgery itself did not affect the behavior.

Because arm choice was not different between the left and right groups in each category of surgery, the data on time in the maze were pooled to compare the denervated flagellum group with the sham group. Time taken to walk to the junction was not different between the two groups ($n = 80$, df = 78, $t = -0.312$, $P = 0.756$; Fig. 3A). Crayfish with a denervated flagellum spent less time in the junction than sham-operated animals ($n = 80$, df = 78, $t = 3.102$, $P = 0.003$; Fig. 3B).

Effect of immobilizing one antenna on exploratory behavior

Splinting either the left or right antenna behind the crayfish's head had a pronounced effect on arm choice in the maze. These crayfish, like the denervated group, turned toward the side of the unmanipulated antenna: 16 crayfish turned toward the side of the free antenna and 4 to the splinted side ($n = 20$, df = 1, $\chi^2 = 6.050$, $P = 0.025$).

Discussion

When individuals of *Cherax destructor* were placed in a T-maze, they used thigmotactic information to navigate. This behavior was used to test directional responses of animals under conditions that may reflect situations in the wild. The antennae were important in exploration of the maze. When tactile information was removed from one antenna by denervation or was altered by splinting one antenna back, the crayfish explored the maze on the side of the unaltered appendage.

Crayfish may have moved to the maze arm of the side of the intact antenna because they could detect surrounding stimuli in that arm. This may signify a tendency to move toward a safer, known sensory environment. Basil and Sandeman (2000) observed that crayfish follow walls in preference to open space and closely hug objects that jut out

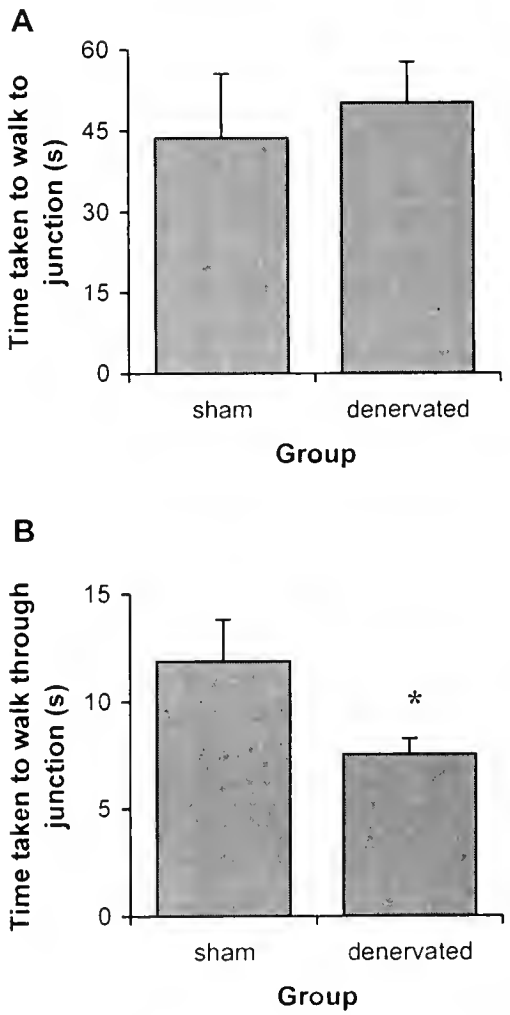

Figure 3. Mean time (± SEM) taken to reach the junction (A) and spent in the junction (B) for crayfish with one denervated flagellum and for sham-operated crayfish. Asterisk (*) indicates a significant difference.

from a straight wall. In those situations, animals compared known tactile information from the wall with no information from the water on the other side, which supports the idea that crayfish prefer to explore identified environments. This is also supported in our experiments by the finding that denervated animals make a decision in the junction of the maze faster than intact animals.

Our data suggest that crayfish compare tactile input from the two antennae. The finding that both denervated and splinted crayfish turned toward their unaltered side suggests that the response was not some artifact due to the artificial removal of sensory information from the denervation procedure, but rather that they were comparing inputs from both antennae. When both antennae detected tactile cues in the maze, animals explored randomly; however, when input was removed from one appendage, turns were biased toward the side from which information was still arriving.

It has been proposed that crayfish and other decapod crustaceans use bilateral comparison between the antennae or antennules to orientate toward chemical cues (lobsters: Reeder and Ache, 1980; Atema, 1996; Beglane *et al.*, 1997; crayfish: Kraus-Epley and Moore, 2002; review: Grasso and Basil, 2002). When considered in conjunction with these studies, our results suggest subtle differences between the way chemical information and tactile information are used for this comparison. We observed that animals moved faster in the junction when tactile input was reduced, whereas there is evidence to suggest that selective absence of chemical input produces slower movement (Kraus-Epley and Moore, 2002).

Crayfish encounter a variety of scents in the wild. Some decapod crustaceans are sensitive to chemical cues at nanomolar and picomolar concentrations (Derby and Atema, 1982). Crayfish release urine in bursts (Breithaupt and Eger, 2002), and thus animals may be able to detect other individuals in the maze. It is known that crayfish and shrimp are attracted to the scent of familiar conspecifics (Ward *et al.*, 2004; Crook *et al.*, 2004). In our experiment, we administered scent in a way that crayfish may encounter it in the wild; however, this was not sufficient to affect the direction explored by an individual. This may have been because they could detect the residual scent of previous trials in both arms, or because no scent trail was laid in the short time that animals were in the maze. Given that crayfish were maintained in high-density communal tanks, individuals were likely to be familiar with each other in our experiments, or at least to have recognized that they were from the same cohort. Testing with scents added in a more guaranteed manner, albeit also more artificial, may reveal a different result.

When compared to other studies, our research suggests that the learning mechanisms of crayfish may differ depending on the topography of the environment. Basil and Sandeman (2000) found that crayfish learned the environment of a large open test arena and moved more rapidly through it as it became more familiar. If crayfish had remembered their previous choice in the T-maze, one would predict that they would make a choice more quickly in subsequent trials. However, our time data suggest that this is unlikely. Furthermore, we would expect arm choice to be the same. It remains possible that crayfish remembered the maze, but that the memory did not result in a response to move to a familiar environment. The result might be different when a chosen direction is reinforced by some resource such as food or shelter. In such situations, animals would be expected to turn in the direction that rewards a particular choice.

The extent that vision interacts with the tactile system is unclear. Antennal movement appears to be different between sighted and blinded crayfish (Zeil *et al.*, 1985). The combination of additional sensory input and tactile information may influence exploration in spaces such as the T-maze or in the wild, but our darkened conditions eliminated this factor. This situation has a parallel in haptic perception in humans. The haptic sense refers to the movement of limbs to gather information about their position in space and about objects they encounter by touch. The crayfish system presents a model that may help explain how visually impaired people gain conscious knowledge of position (Zeil *et al.*, 1985).

This study highlights the importance of the antennae to crayfish performing directional responses in restricted spaces. The role of the antennae may have implications for crayfish living in a dynamic environment where all senses may not always be available. It remains to be determined whether the effect of denervation is temporary or persists until the crayfish grows a new antenna.

Acknowledgments

We thank Robyn Crook, Garry Jolly-Rogers, Luke Finley, and Theresa Jones for their input in discussions and experimental design. This research was supported by funding from the Australian Research Council to D. L. Macmillan.

Literature cited

Atema, J. 1996. Eddy chemotaxis and odor landscapes: exploration of nature with animal sensors. *Biol. Bull.* **191:** 129–138.

Basil, J., and D. Sandeman. 2000. Crayfish (*Cherax destructor*) use tactile cues to detect and learn topographical changes in their environment. *Ethology* **106:** 247–259.

Beall, S. P., D. J. Langley, and D. H. Edwards. 1990. Inhibition of escape tailflip in crayfish during backward walking and the defense posture. *J. Exp. Biol.* **152:** 577–582.

Beglane, P. F., F. W. Grasso, J. A. Basil, and J. Atema. 1997. Far field chemo-orientation in the American lobster, *Homarus americanus:* effects of unilateral ablation and lesioning of the lateral antennule. *Biol. Bull.* **193:** 214–215.

Breithaupt, T., and P. Eger. 2002. Urine makes the difference: chem-

ical communication in fighting crayfish made visible. *J. Exp. Biol.* **205:** 1221–1231.

Bush, B.M.H., and M. S. Laverack. 1982. Mechanoreceptors. Pp. 369–468 in *Biology of Crustacea,* Vol. 3. D. H. Bliss, H. L. Atwood, and D. C. Sandeman, eds. Academic Press, New York.

Cate, H. S., and C. D. Derby. 2002. Ultrastructure and physiology of the hooded sensillum, a bimodal chemo-mechanosensillum of lobsters. *J. Comp. Neurol.* **442:** 293–307.

Corotto, F., and M. R. O'Brien. 2002. Chemosensory stimuli for the walking legs of the crayfish *Procambarus clarkii*. *J. Chem. Ecol.* **28:** 1117–1130.

Cronin, T. W., and T. H. Goldsmith. 1982. Photosensitivity spectrum of crayfish rhodopsin measured using fluorescence of metarhodopsin. *J. Gen. Physiol.* **79:** 313–332.

Crook, R., B. W. Patullo, and D. L. Macmillan. 2004. Multimodal individual recognition in the crayfish *Cherax destructor*. *Mar. Freshw. Behav. Physiol.* **37:** 271–285.

Derby, C. D., and J. Atema. 1982. The function of chemo- and mechanoreceptors in lobster (*Homarus americanus*) feeding behaviour. *J. Exp. Biol.* **98:** 317–327.

Fowler, J., L. Cohen, and P. Jarvis. 1998. *Practical Statistics for Field Biology.* John Wiley, New York.

Grasso, F. W., and J. A. Basil. 2002. How lobsters, crayfishes, and crabs locate sources of odor: current perspectives and future directions. *Curr. Opin. Neurobiol.* **12:** 721–727.

Hartman, H. B., and W. D. Austin. 1972. Proprioceptor organs in antennae of Decapoda Crustacea. 1. Physiology of a chordotonal organ spanning two joints in spiny lobster *Panulirus interruptus* (Randall). *J. Comp. Physiol.* **81:** 187.

Kraus-Epley, K. E., and P. A. Moore. 2002. Bilateral and unilateral antennal lesions alter orientation abilities of the crayfish, *Orconectes rusticus*. *Chem. Senses* **27:** 49–55.

Lawrence, C., and C. Jones. 2002. *Cherax.* Pp. 635–670 in *Biology of Freshwater Crayfish,* D. L. Holdich, ed. Blackwell Science, Victoria, Australia.

Masters, W. M., B. Aicher, J. Tautz, and H. Markl. 1982. A new type of water vibration receptor on the crayfish antenna. *J. Comp. Physiol. A* **149:** 409–422.

Mellon, DeF., Jr. 2000. Convergence of multimodal sensory input onto higher-level neurons of the crayfish olfactory pathway. *J. Neurophysiol.* **84:** 3043–3055.

Merrick, J. R. 1991. *The Biology, Conservation and Management of Australian Freshwater Crayfishes. A Bibliography.* Macquarie University, NSW, Australia.

Page, T., and J. L. Larimer. 1972. Entrainment of the circadian locomotor activity rhythm in crayfish. The role of the eyes and caudal photoreceptor. *J. Comp. Physiol.* **78:** 107–120.

Reeder, P. B. and B. W. Ache. 1980. Chemotaxis in the Florida spiny lobster, *Panulirus argus*. *Anim. Behav.* **28:** 831–839.

Reynolds, K. M. 1980. Aspects of the biology of the freshwater crayfish, *Cherax destructor* in farm dams in far-western NSW. M.Sc. thesis, University of New South Wales, Australia.

Sandeman, D. C. 1985. Crayfish antennae as tactical organs: their mobility and the responses of their proprioceptors to displacement. *J. Comp. Physiol. A* **157:** 363–373.

Sandeman, D. C. 1989. Physical properties, sensory receptors and tactile reflexes of the antenna of the Australian freshwater crayfish *Cherax destructor*. *J. Exp. Biol.* **141:** 197–217.

Sandeman, D. C., and D. Varju. 1988. A behavioural study of tactile localization in the crayfish *Cherax destructor*. *J. Comp. Physiol. A* **163:** 525–536.

Sokal, R. R., and F. J. Rohlf. 1995. *Biometry: The Principles and Practice of Statistics in Biological Research.* 3rd ed. W. H. Freeman, New York.

Ward, J., N. Saleh, D. W. Dunham, and N. Rahman. 2004. Individual discrimination in the big-clawed snapping shrimp, *Alpheus heterochelis*. *Mar. Freshw. Behav. Physiol.* **37:** 35–42.

Zeil, J., R. Sandeman, and D. C. Sandeman. 1985. Tactile localization: the function of active antennal movements in the crayfish *Cherax destructor*. *J. Comp. Physiol. A* **157:** 607–617.

Reference: *Biol. Bull.* **208:** 189–199. (June 2005)

Cell Differentiation Is a Primary Growth Process in Developing Limbs of *Artemia*

JOHN A. FREEMAN*

Department of Biological Sciences, University of South Alabama, Mobile, Alabama 36688

Abstract. The limb of the brine shrimp *Artemia* develops over a four-instar period when the protopod, endite, exopod, endopod, and epipod are defined and cell differentiation (change in cell shape) occurs. To understand the importance of cell differentiation in limb growth, development of the epidermis was studied in the first thoracopod of instar V–VIII larvae. Each region was established by instar V, and the larval epidermal cells developed into general epidermal (GEC), tendinal, setal, or transport cells by instar VI. Basal extensions of the GECs formed pillar structures. The epidermal cells decreased in height from 10 to 4 μm by instar VI. Increase in length and width resulted from both cell replication and expansion of the apical cell surface in differentiating cells. Growth occurred mainly by cell replication in instar V, whereas expansion of the cell surface in GEC and setae was the major growth process in instar VII. Increase in apical cell surface area occurred primarily by change in cell shape from columnar to squamous during instar V and by increase in total cell surface in subsequent instars. The results demonstrated that cell differentiation is a significant component of growth during limb development.

Introduction

Crustacean larvae grow by increase in tissue mass during the molt cycle and the periodic shedding of the restrictive exoskeleton. Nutrients stored during the intermolt period support cell growth during the premolt period (Hartnoll, 1982; Freeman, 1991). The increase in dimension and change in shape is realized after ecdysis when the newly formed cuticle unfolds and stretches (Cheng and Chang, 1993, 1994). Moreover, regions of the integument may grow at different rates (Blake, 1979; Hartnoll, 1982).

Received 19 August 2004; accepted 28 February 2005.
* E-mail: jafreema@jaguar1.usouthal.edu

In developing crustaceans, new structures formed during one instar become evident after the molt to the next instar (Schrehardt, 1987). The apical surface area increases when columnar larval cells flatten, becoming squamous general epidermal cells (GECs). Later these cells continue to grow by increasing the total surface area. Both processes lead to a larger cuticle-forming surface (Freeman 1989, 1993, 1995). As the GECs differentiate, they may produce basal pillar structures that maintain the paddle shape of the limb (Benesch, 1969; Taylor and Taylor, 1992). Other specialized cells include tendinal cells that attach muscles to the cuticle (Freeman *et al.*, 1995), cells that form the setal shaft (Tchernigovtzeff, 1976; MacRae and Freeman, 1995), and cells that are modified for respiratory and osmoregulatory functions in the epipod (Copeland, 1967).

Many of these cell types change shape as they differentiate, and this change may contribute to growth of the appendage by increasing the area of the apical surface. To understand the role of cell differentiation in limb growth and development, cell replication, cell shape change, and apical surface expansion were examined in the first thoracic limb of *Artemia* during instars V–VIII. In addition, the amount of new plasma membrane needed to support growth by cell replication and cell enlargement was estimated for two growth periods. The results demonstrate that change in cell shape during differentiation leads to growth of the integument and formation of the limbs.

Materials and Methods

Brine shrimp were reared in filtered seawater, salinity 30 ppt, at 23 °C. Limb structures were measured in live larvae or in specimens fixed in 3:1 ethanol-acetic acid and stained for nuclei with Hoechst 33258 (Sigma Chemical, St. Louis, MO) or for plasma membranes with C_{10}-Bodipy$_{500/515}$-C_3 (Molecular Probes, Eugene, OR) (Freeman, 1995; Macho *et al.*, 1996). Linear measurements were made using an ocular

micrometer or through an imaging system calibrated using a slide micrometer. Images were acquired with Inspector software ver. 2.1 (Matrox Electronic Systems, Quebec, Canada).

For determinations of length (proximal-distal axis) and width (medial-lateral axis), the region was measured in the widest part of each axis (see Fig. 1C). Although this method may lead to a slight overestimate due to the shape of some of the lobes, it does compensate for any underestimation due to the convexity of the curved surface. The number of cells was determined by counting the nuclei in the region. The mean apical surface area (cuticle-secreting) per cell was determined by dividing the area of the region by the number of cells. The cellular data were determined for the anterior face of the limb only. Cell height was determined by taking the mean of five measurements in live larvae.

Morphometric determinations of cell height and mean cell surface area formed the basis for computations of membrane biosynthesis. To determine total surface area (apical, lateral, and basal) for each cell, the cell was considered to be a cylinder. Total surface area for the region was obtained by multiplying the value per cell by the number of cells in that region. The values in Table 1 indicate the differences between instars (total surface area for instar $n + 1$ minus the total surface area for instar n). For mitosis, the new membrane for cytokinesis was assumed to bisect the cell. For surface area determinations on setae, the height and base were used to compute the surface area of a cone. The diameter of the setal base was measured directly at high magnification, and the plasma membrane was evident at the tip of the setae. The amount of new surface membrane produced for mitosis or cell expansion is indicated as differences between instars (Table 1). Cells that increased their apical surface by becoming squamous (SC in Table 1) were considered to have changed shape without an increase in total cell surface area.

Results

Limb morphology

The adult limb is shown in Figure 1. The protopod has medial (endites, endopod) and lateral (exopod, epipod) lobes. Setae and muscles can be seen in Figure 1A, and differences in cell (nuclei) density are shown in Figure 1B. The adult limb reached 1100 μm, and the length and width of each region (Fig. 1C) are indicated in Figure 1D. In instars V through VIII, the limb grew primarily in length, and by instar VIII the limb dimensions were 25% that of the adult (Fig. 1E).

Growth and regional differentiation

At the beginning of instar IV, the limb is a phyllopod with 150 cells on the anterior surface (Fig. 2A). After apolysis, invaginations separating prospective lobes were evident at the distal edges. Cell division in the proximal-distal axis of each lobe (Fig. 2B) doubled the number of cells in the lobe by late instar IV (Fig. 2C). At the molt to instar V, the endites and endopod became evident on the medial edge, and the exopod and epipod formed on the lateral edge of the protopodite (Fig. 2D, E). Each of these regions was composed of densely packed larval cells 10–12 μm in height (Fig. 2E).

Differentiated cell types began to develop in instars V and VI. Larval cells became squamous general epidermal cells (GECs) in the protopod in instar V as their height decreased from 10 μm to 3–5 μm (Fig. 2F, G). The tendinal cells, setal cells, and pillar structures were clearly defined early in instar VI (Fig. 2G, H, I). The general form of the limb with all cell types in each region was attained by instar VIII (Fig. 2J).

As the phyllopod developed, growth of the limb resulted in a marked increase in length and width (Fig. 1E). However, due to presence of numerous pillar structures, each an extension of the basal surface on the anterior surface that attaches to a like process extending from the GECs on the posterior surface, the maximum depth of the limb remained at 60–80 μm through instar VIII (Fig. 2I). Based on a diameter of 2 μm and a length of 20 μm, each pillar extension had a surface area of 63 μm^2 per cell. Although the absolute number of pillars was not determined for each lobe, the number of pillars in some regions equaled the number of GECs, suggesting that, in these regions, each GEC produced a pillar extension.

The protopod grew in length at each instar. The region was wider than long in instar V but doubled in length by instar VI (Fig. 3A, E). By instar VIII the region had grown 3-fold in length and 30% in width (Fig. 3E). With the exception of a few tendinal cells, GECs populated the protopod surface. Initially, these cells were arranged in four medial-lateral rows (Fig. 3A). There were about 24 cells in the protopod of instar IV, 100 cells in late instar VI, and 160 cells in instar VIII (Fig. 3F). The height of the cells declined from 10 to 4 μm by instar VI, and the apical surface grew during premolt; these changes resulted in undulations in the epidermal surface in late premolt (Fig. 3B, C). The mean apical surface area per cell decreased slightly from instar V to VI, when over half the cells replicated, but it then increased continuously for the next two instars (Fig. 3F). By the adult stage, the mean surface area increased to 597 μm^2 (Fig. 3D). Tendinal cells were evident by instar VI. The results indicate that growth of the protopod was a result of cell replication, shape change, and apical surface expansion.

The endites include four setated lobes on the medial edge of the limb bud (Fig. 1). Setae were evident by instar V and increased in number and length through instar VIII (Fig. 4A, F). Setal cells developed in distal regions associated with high cell density, whereas GECs formed in more proximal

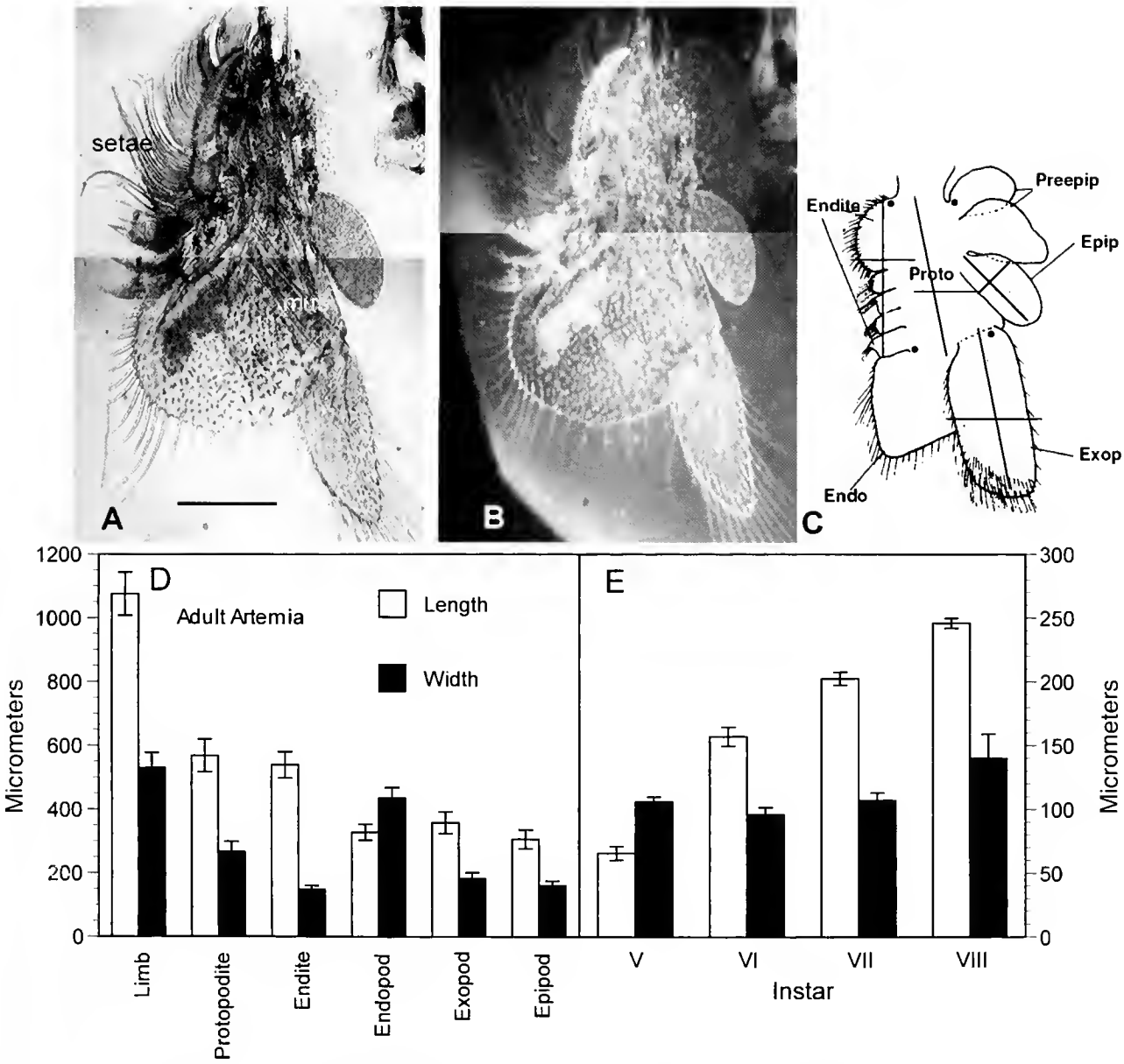

Figure 1. The adult thoracopod of segment 1 as seen in light (A) and fluorescence (B, for nuclei) images. Setae and muscles (mus) are indicated in A. The different regions are indicated in the diagrammatic view (C, adapted from McLaughlin, 1980, with permission from W.H. Freeman and Company), and the corners of the protopod are delineated by black dots. The axes used for length and width determinations are indicated. For clarity, only the bases of the setae are shown. Medial is to the left in each view. Abbreviations in C: proto, protopod; endo, endopod; exop, exopod; epip, epipod; preepip, preepipod. Bar in A (=B) represents 200 μm. (D) Length and width of the adult limb and the lobes. Each bar in D indicates the mean ± 1 SD of 8–16 larvae. (E) Dimensions of the first thoracopod in instars V–VIII. Each bar in E indicates the mean ± 1 SD of 10–18 measurements.

regions adjacent to the protopod (Fig. 4A, B, C). The region increased in length, with a slight increase in width through instars V–VIII (Fig. 4E). The medial endite region had grown to 500 μm in length and was 140 μm in width in adults (Fig. 1D). Most of this growth was due to cell replication (Fig. 4B, F). The apical surface area increased slowly during instars V–VIII and then increased 3-fold by the adult (Fig. 4B, D, F). Newly formed setae had a mean length of 25 μm, an increase in apical surface area of 100 μm (Fig. 4F). By instar VIII the number of setae increased to 43 and the length reached 87 μm, attaining a surface area of 547 μm^2 per seta. In adults, the number of setae had

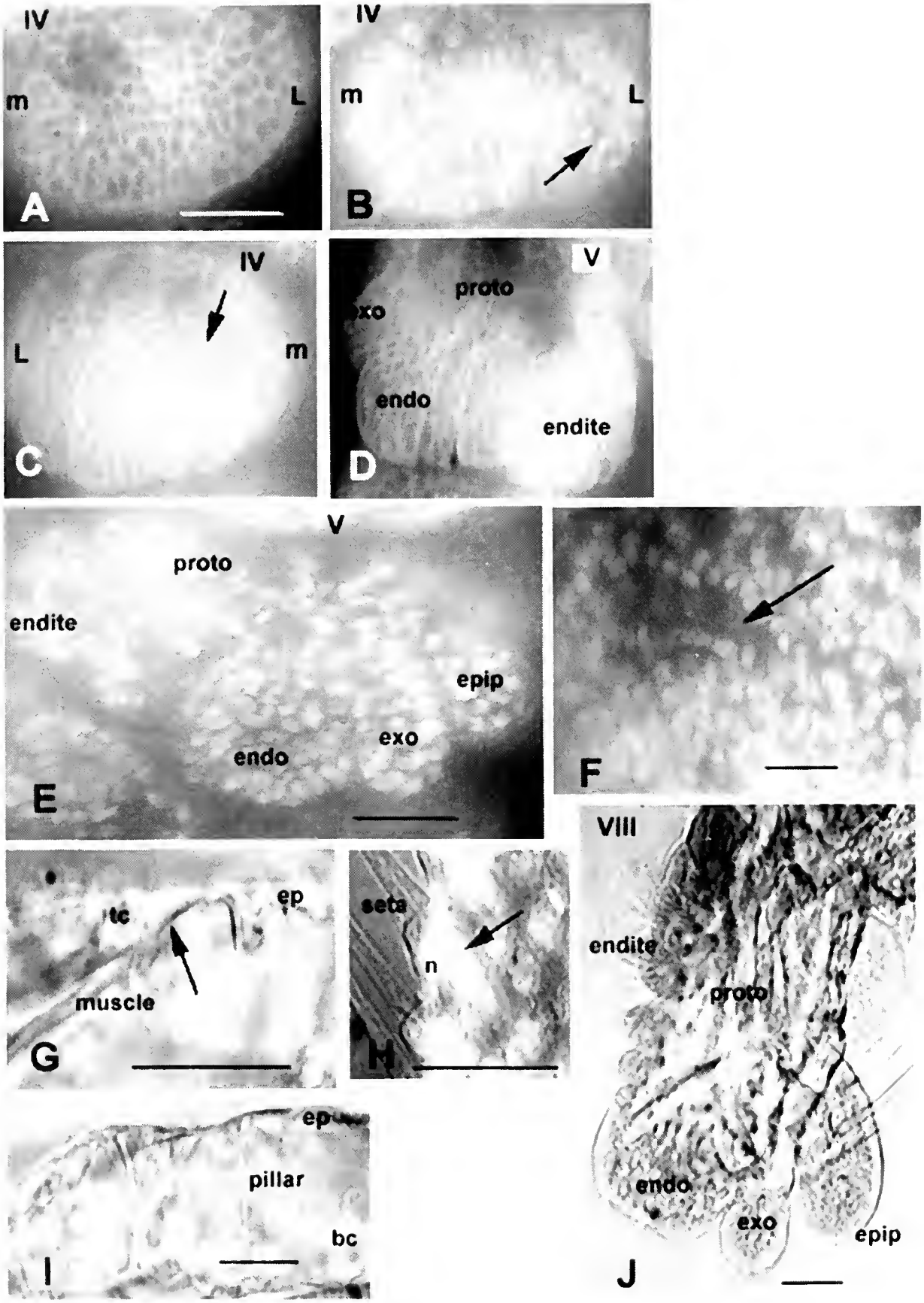
IV
m
L
A
IV
m
L
B
IV
L
m
C
V
proto
xo
endo
endite
D
V
proto
endite
epip
exo
endo
E
F
tc
ep
muscle
G
seta
n
H
VIII
endite
proto
endo
exo
epip
J
ep
pillar
bc
I

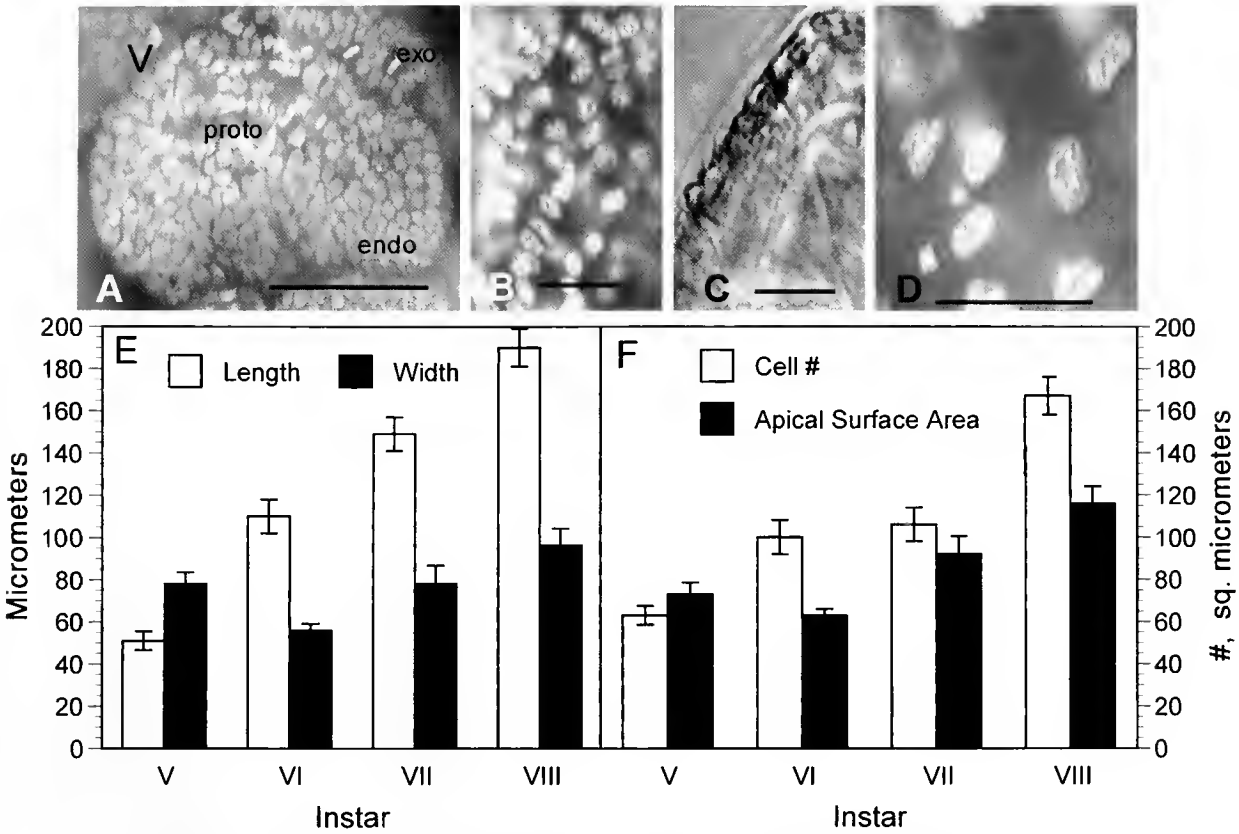

Figure 3. Development of the protopod. (A) Cell division and increased apical surface area in instar V. For comparison, the endopod (endo) and the exopod (exo) are labeled. (B) Instar VI stained for nuclei, showing increased surface area (decreased nuclear density) in GECs to the right in the image. (C) Transverse view of epidermal cells, showing undulations of the apical surface late in instar VI. (D) Fluorescent images of GECs in adult limb, showing increased apical surface area. The small nuclei are in blood cells below the plane of the epidermis. Bars in A = 40 μm; B = 30 μm; C = 10 μm; D = 20 μm. (E) Dimensions of the protopodite in instars V–VIII. Each bar indicates the mean ± 1 SD of 7–15 larvae. (F) Cell number and mean apical surface area during instars V– VIII. Each bar represents the mean ± 1 SD of 5–7 larvae.

almost doubled, reaching 71, and the length increased to 250 μm. The endites grew by cell replication, increase in surface area, and setal enlargement.

The endopod was a broad lobe with numerous pillars (Figs. 2E, J; 5A, B). It grew in width more than in length, becoming a thin paddle 98 μm wide by instar VIII (Fig. 5C). It reached 317 μm long and 420 μm wide by the adult (Figs. 1D, 5B). While the number of GECs increased from 34 in instar VI to 50 in instar VIII, reaching 90 cells per surface in the adult, the surface area increased from 42 μm^2

Figure 2. Development of limb regions in instars IV–VIII. A–C. Instar IV (m, medial; L, lateral). (A) Cell borders early in the instar. (B) Fluorescent image of late instar IV showing mitoses (arrow). (C) Late instar IV limb showing invaginations (arrow) separating lobes late in the instar. (D) Postmolt instar V stained for plasma membrane, showing major regions of the limb. The epipodite is out of focus behind the exopodite. (E) Instar V stained for nuclei. Mitotic figures are evident in the protopod, exopod, and epipod. (F) Increase in apical surface area (lower density of nuclei, arrow) is seen in the protopod in instar V. (G) The tendinal cell (tc) in instar VI connects the muscle to the cuticle secreted by the epidermis (ep). The arrow indicates the region of the cell enriched for microtubules and actin (Freeman *et al.*, 1995). (H) Setae are apical extensions of the epidermal cells (n = nucleus of setal cell) and have polyploid accessory cells (arrow, nucleus of accessory cell) below the epithelium that aid in the expansion of the seta as it grows during late premolt. (I) Pillar structures extend basally from epidermal cells (ep) on opposite faces of the limb. A blood cell (bc) is present in the spaces between pillar structures. (J) Instar VIII limb. Abbreviations as in Figure 1. Bars in A (=B–D) = 25 μm; E–I = 20 μm; J = 35 μm.

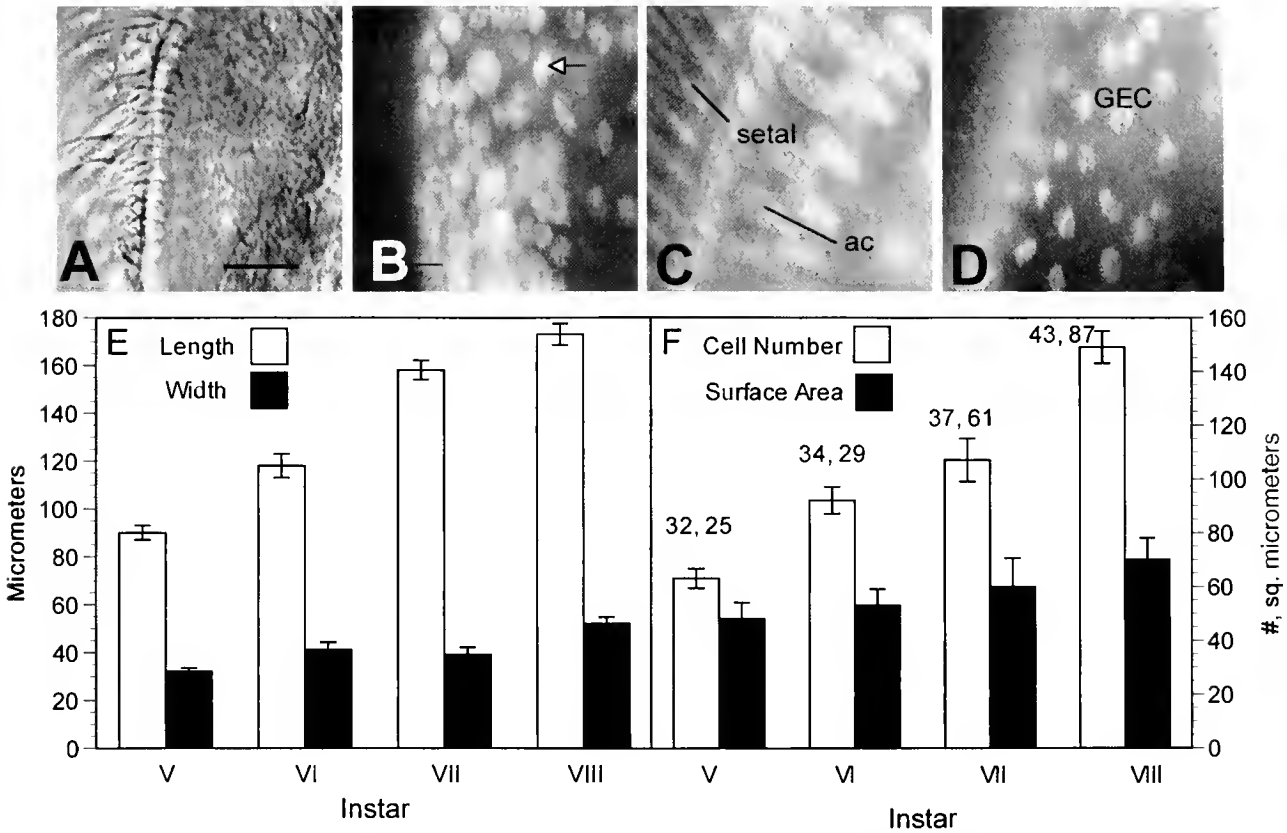

Figure 4. Development of the endites. (A, B) Light and fluorescent (for nuclei) images, respectively, of instar VI endite. The setal cells are to the left and the GECs are to the right in each image. Line in B indicates the edge of the region where setae are forming. The arrow indicates a mitotic figure. (C, D) Same adult endite viewed at different focal planes, showing setal cell nuclei (setal), accessory cells (ac), and GEC nuclei. Bar in A (=B–D) = 20 μm. (E) Dimensions of the endite during instars V–VIII. Each bar indicates the mean ± 1 SD of 6–10 larvae. (F) Cell number and mean apical surface area in endite epidermal cells during instars V–VIII. Numbers above bars indicate number of setae and mean length (μm) of the setae for that instar. Each bar represents the mean ± 1 SD of 4–6 larvae.

in instar V to 131 μm^2 in instar VIII and 542 μm^2 by the adult (Fig. 5B, D). Setae began to form during instar VII and increased from four 24-μm-long setae in instar VIII to 22 setae with a mean length of 172 μm in the adult. Tendinal cells formed at least seven muscle attachments during instar V. Apical surface expansion was the primary means of growth in this region.

The exopod was first evident as a small bud of 15 cells per surface in instar V (Figs. 2E, 6A). It continued to grow more in length than in width, becoming a thin blade by instar VIII (Fig. 6B, C). It grew from 20 μm in instar V to 51 μm at instar VIII and to 300 μm in the adult (Figs. 1D; 6E). Cell replication increased the cell number from 18 in instar V to 30 by instar VIII (Fig. 6F). Ninety GECs were present in the adult. The apical surface area doubled by instar VIII and reached 212 μm^2 by the adult (Fig. 6D, F). The GECs became arranged in proximal-distal rows that alternated with setal cells (Fig. 6D). There were three or four small setae in instar VIII. In the adult, the number increased to 21 setae, and the mean length reached 363 μm. Two muscles attached to tendinal cells. This region grew primarily by expansion of the cell surface.

The epipod was first evident as a small lobe in instar V (Fig. 2E). As the GECs differentiated, the limb grew through cell replication and apical surface expansion to form a flattened sac (Fig. 7A, B). The lobe grew to 96 μm in length by instar VIII (Fig. 7D), reaching 300 μm in the adult (Fig. 1D). The number of cells increased slightly in instars V–VIII and increased to 50 per surface in the adult (Fig. 7E). The height of the cells decreased from 8–10 μm in instar V to 4 μm in instar VI. There was a gradual change in apical cell surface from 44 μm^2 in instar V to 162 μm^2 in instar VIII, eventually reaching 1020 μm^2 in the adult (Fig. 7C, E). The cells appeared to be arranged in two populations, one forming the narrow edge of the lobe and the other forming the flat surface supported by pillar structures (Fig. 7A, C). There were about 60 pillars in the adult. No muscles attached to this lobe and no setae formed. Most of the growth was a result of expansion of the apical surface.

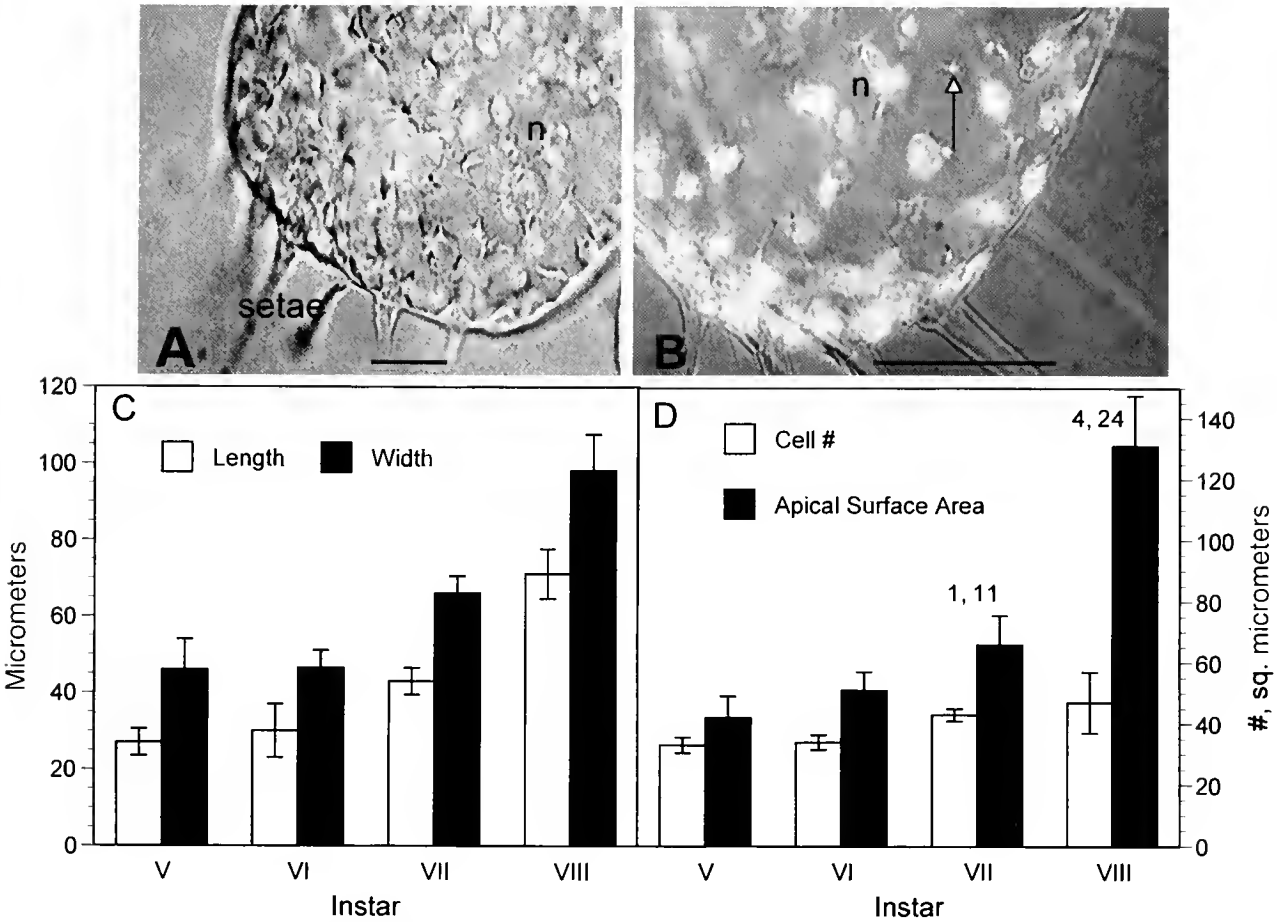

Figure 5. Development of the endopod. (A) Endopod in instar VIII, showing newly formed setae and GEC nuclei (n). (B) Light/fluorescent image of adult endopod, showing nucleus of GECs (n) and pillar structure (arrow). Bars in A and B = 20 and 50 μm, respectively. (C) Dimensions of the endopod during instars V–VIII. Each bar indicates the mean ± 1 SD of 8–12 larvae. (D) Cell number and mean apical surface area for instars V–VIII. Numbers above bars indicate the mean number and length of new setae. Each bar represents the mean ± 1 SD of 6–12 larvae.

Production of new cell surface

The morphometric findings demonstrated that development of the limb involved both cell replication and expansion of the apical surface. Cytokinesis, expansion of the apical membrane surface in GECs, and formation of setae require production of new plasma membrane. To assess the importance of new membrane production associated with the growth and developmental processes, the morphometric data (Figs. 3–7) were used to estimate the amount of increased cell surface area needed to support cytokinesis and increased apical surface area in each region of the limb (Table 1).

Growth from instar V to VI (total surface area of instar VI − total surface area of instar V) involved synthesis of new membrane for cytokinesis. Elongation of the setae occurred in the endites. Cells in the endites also produced new membrane for the cell surface as the region elongated in the proximal-distal axis while cells in the protopod, endopod, and epipod changed shape from cuboidal to squamous, presumably increasing the apical surface area without significant production of new plasma membrane (SC, Table 1). In instar VII, all regions demonstrated production of membrane for cytokinesis, and the level was 33% greater than in instar V. The increase in total cell surface, however, was much greater than that observed in instar V and 4 times the area formed by mitosis. The setae continued to grow in the endites, and new setae developed in the endopod and exopod. Overall, cell surface expansion in instar VII was over 6 times that found for instar V.

Discussion

The crustacean integument grows during the molt cycle, resulting in an expanded cuticle at the next ecdysis. General patterns included cell replication early in the molt cycle

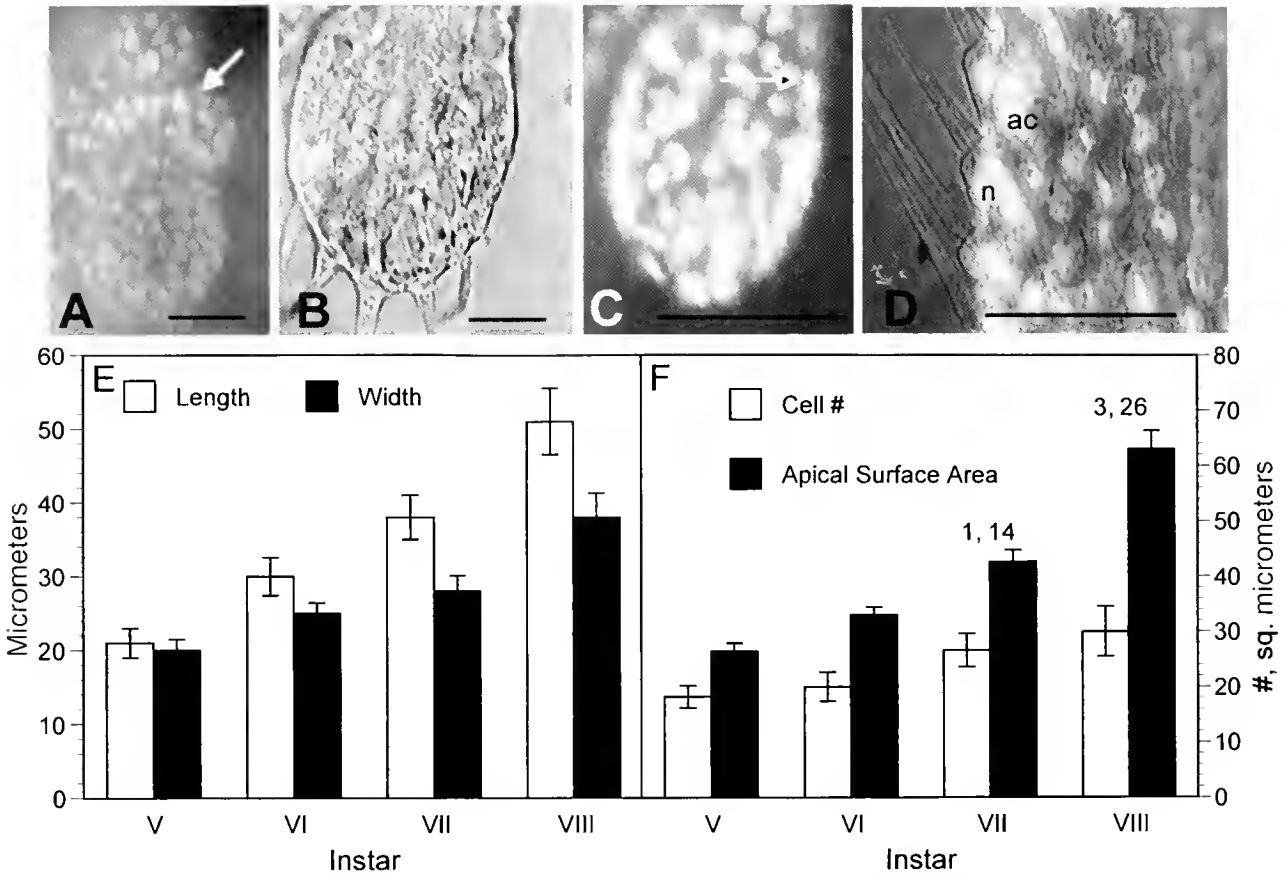

Figure 6. Development of the exopod. (A) Exopod in instar V limb. (B, C) Light and fluorescence images, respectively, of exopod in instar VIII, showing new setae and nuclei of GECs. Arrows in A and C indicate mitotic figures. (D) Exopod of adult, showing the setal region at the edge of the lobe. Nucleus (n) of a setal cell and an accessory cell (ac) are shown. Bars in A = 20 μm, B = 15 μm, C = 40 μm, D = 50 μm. (E) Dimensions of the exopod during instars V–VIII. Each bar indicates the mean ± 1 SD of 6–12 larvae. (F) Cell number and mean apical surface area for GECs in instars V–VIII. Numbers above the bars indicate the mean number and length of setae for those instars. Each bar represents the mean ± 1 SD of 5–12 limbs.

with subsequent growth during late premolt (Freeman, 1991), or replication during mid-premolt that resulted in an undulated apical surface (Cheng and Chang, 1994). The results reported here reveal another process, expansion of the apical surface as the cell differentiates to a general epidermal cell (GEC) or a setal cell. These changes complement cell replication and are essential to growth and development of form in larval crustaceans. Of the four cell types studied, the GEC, setal, and transport cells contributed to growth as they differentiated. Another morphogenic force, evident in the transition from instar V to instar VI, involved a change in cell shape (SC in Table 1) from columnar to squamous, with minimum formation of new plasma membrane. It is possible that the elongation of the limb in the proximal-distal axis involved flattening of some of the GECs and a reorganization of cell neighbors in the plane of the epithelium (Schöck and Perrimon, 2002). The mechanisms by which these changes occur and new membrane is integrated into the plasma membrane remain to be studied.

Each of the regions of the phyllopod grew in a different spatial and temporal pattern. The protopod grew by cell replication and cell shape change early, and differentiation and cell surface expansion of GECs later. The endites grew by replication, apical surface expansion, and development of setae, although the contribution of each process was different in each instar. The endopod demonstrated apical expansion early, followed by growth in all categories in later instars. The exopod and epipod, by contrast, grew by mitosis initially but by cell surface expansion later on. The results demonstrate that apical surface expansion associated with differentiation contributes significantly to growth of the limb. Further, these differences suggest that form in the limb is determined by the patterns of cell replication and cell differentiation in the epidermis. The limb is not the only region to demonstrate both growth processes; similar results

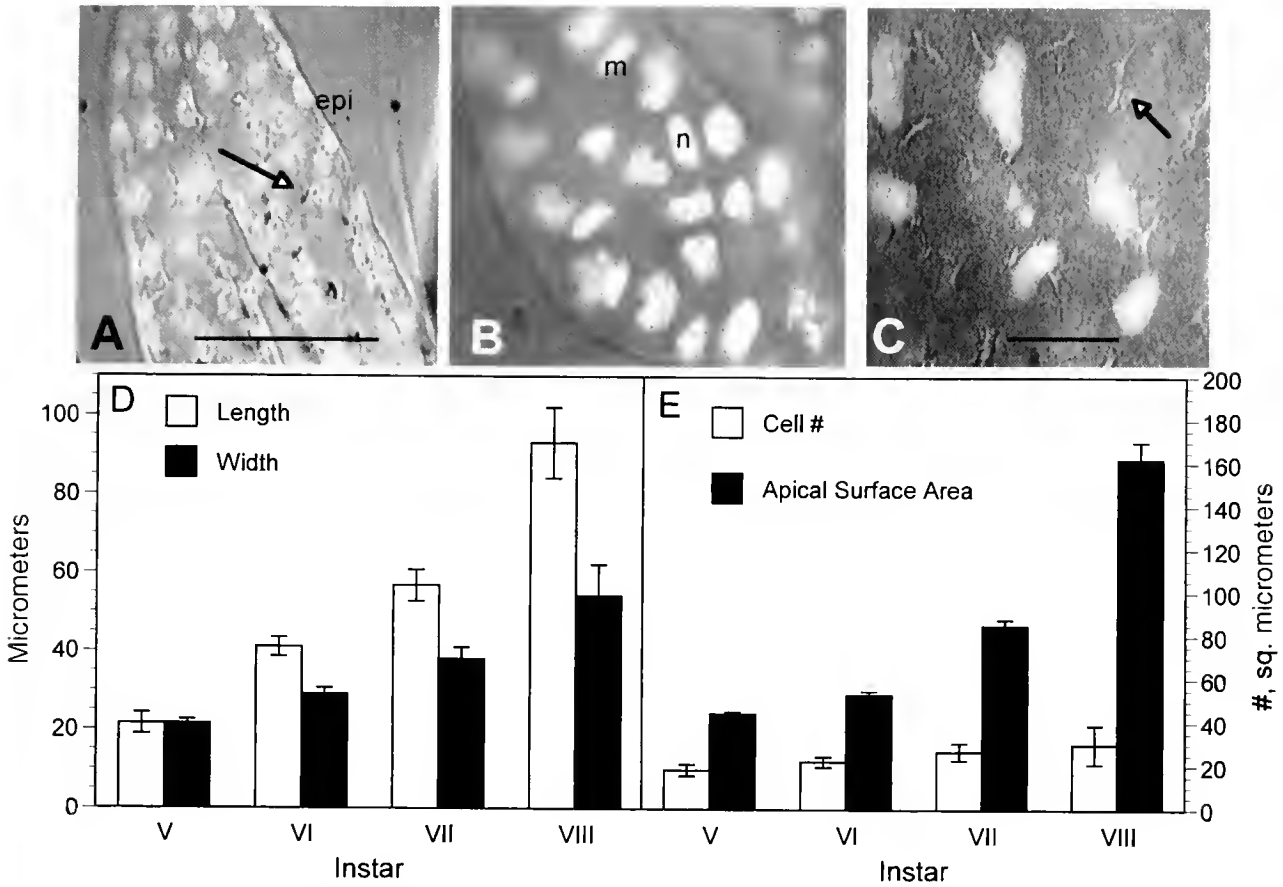

Figure 7. Development of the epipod. (A, B) Light and fluorescent images, respectively, of instar VIII epipod, showing epidermis (epi), mitotic figure (m), and GEC nucleus (n). (C) Epipod of adult. Arrows in A and C indicate pillar structures. Bars in A (=B) = 40 μm; C = 20 μm. (D) Dimensions of the epipod in instars V–VIII. Each bar indicates the mean and ± 1 SD of 4–15 limbs. (E) Cell number and mean apical surface area for GECs in instars V–VIII. Each bar represents the mean ± 1 SD of 2–15 limbs.

were found in the lateral surfaces of the first segment (Freeman, 1995).

GECs formed by shape change and increased apical surface area. Some cells also expanded the basal surface, forming pillar structures connecting the anterior and posterior surfaces of the limb. A few pillars were observed in instar IV. As each region developed, new pillar processes formed, maintaining the paddle-like structure of the appendage as it grew and as it changed shape in the transition from instar V to VI. Formation of a pillar would be one of the first stages of differentiation of the GECs in all the regions of the limb and probably requires a concentration of microtubules and microfilaments in the basal region (MacRae *et al.*, 1991; Taylor and Taylor, 1992; MacRae and Freeman, 1995; Cieluch *et al.*, 2004). Although tendinal cells did not markedly increased the apical surface, their formation also involves reorganization of the basal membrane and cytoplasm as the cells form tonofibrillae and muscle attachments (Freeman *et al.*, 1995).

The larval epidermal cell is polarized, producing the cuticle at the apical surface, a region enriched with microtubules and microfilaments (MacRae *et al.*, 1991). As the apical surface of the cell expands by insertion of new membrane, the cytoskeleton may be active in supporting the expanded cell borders, the enlarged apical plasma membrane, and the biosynthesis of the new cuticle.

Analysis of changes in surface area during cell differentiation and growth demonstrated the remarkable amount of plasma membrane biosynthesis during cytokinesis and differentiation. When a molt cycle duration of 1 to 2 days is considered, it becomes clear that a large proportion of the nutrients in the diet must be used to produce the protein and phospholipids for new membrane. About 50% of plasma membrane is lipid, and 10%–45% of the essential fatty acids acquired in the diet are incorporated in polar lipid fractions (Navarro *et al.*, 1991, 1992). The importance of these compounds has been demonstrated in studies showing that the level of polar lipids was enhanced in larvae fed diets enriched with polyunsaturated fatty acids and that the levels were maintained when the larvae were subsequently starved

Table 1

Production of new plasma membrane (μm^2) by epidermal cells in the developing limb of Artemia *during two larval instars*

	Period of Growth					
	Instar V to VI			Instar VII to VIII		
Region	Mitosis	Expansion	Setal area	Mitosis	Expansion	Setal area
Protopod	4,662	SC	NA	5,856	24,519	NA
Endites	3,654	1,080	1,166	5,880	5,181	11,653
Endopod	88	SC	NA	293	9,007	535
Exopod	185	None	NA	222	2,334	402
Epipod	480	SC	NA	250	6,774	NA
Total=	9,069	1,080	1,166	12,501	47,815	12,590
		(11,315)			(72,906)	

Expansion indicates an increase in apical surface area supported by biosynthesis of new plasma membrane. Setal area was determined as the area of a cone, using setal height and base diameter minus the original apical surface area. SC indicates an increase due to cell shape change without synthesis of additional plasma membrane. Values in parentheses at bottom indicate the grand total for the period of growth. NA indicates that the region lacks setae.

(Coutteau and Mourente, 1997; Sakamoto *et al.*, 1982). Similar results have been obtained with other crustaceans (Kanazawa and Koshio, 1994). Considering the rapid rate of cellular growth observed in this study, the level of essential fatty acids in the diet becomes critical for optimum cell differentiation.

Several studies have demonstrated variation in the number of larval instars in *Artemia*, and some of the observations shown here are slightly different from those seen in previous studies (Schrehardt, 1987). Variation in instar number has also been shown in other groups of crustacean larvae (Williamson, 1982). Although these differences could be ascribed to different strains of cysts, it is equally possible that the feeding regime affects the number of instars. Knowlton (1974) and McConaugha (1985) have suggested that nutrient allocation for general maintenance, molting, growth, and differentiation occurs during each instar and that there may be a hierarchy in the allocation such that cell differentiation does not occur when the levels of essential nutrients (fatty acids) are low. The cells may allocate nutrients to maintenance and molting at the expense of growth and differentiation. Moreover, cells may replicate but not expand the apical surface (*e.g.*, differentiation of GECs), resulting in less growth for that instar. If so, these differences could account for variation in the development of structures such as setae, differences in dimension of some of the limb structures, or presence of supernumerary instars. This would be particular evident in species such as *Artemia* that do not have a well-developed hepatopancreas for long-term nutrient storage and that exhibit many instars in which there is a greater chance of experiencing periods when nutrients are scarce.

Literature Cited

Benesch, R. 1969. Zur Ontogenie und Morphologie von *Artemia salina* L. *Zool. Jahrb. Abt. Anat. Ontog. Tiere* **86:** 307–458.

Blake, R. W. 1979. The development of the brine shrimp *Artemia salina* (L.): a morphometric approach. *Zool. J. Linn. Soc.* **65:** 255–260.

Cheng, J.-H., and F. S. Chang. 1993. Determinants of postmolt size in the lobster *Homarus americanus*. III. Scute density. *Invertebr. Reprod. Dev.* **24:** 169–178.

Cheng, J.-H., and F. S. Chang. 1994. Determinants of postmolt size in the American lobster (*Homarus americanus*). II. Folding of premolt cuticle. *Can. J. Fish. Aquat. Sci.* **51:** 1774–1779.

Cieluch, U., K. Anger, F. Aujoulat, F. Buchholz, M. Chamantier-Daures, and G. Charmantier. 2004. Ontogeny of osmoregulatory structures and functions in the green crab *Carcinus maenas* (Crustacea, Decapoda). *J. Exp. Biol.* **207:** 3225–3236.

Copeland, D. E. 1967. A study of salt secreting cells in the brine shrimp (*Artemia salina*). *Protoplasma* **63:** 363–384.

Coutteau, P., and G. Mourente. 1997. Lipid classes and their content of *n*-3 highly unsaturated fatty acids (HUFA) in *Artemia franciscana* after hatching, HUFA-enrichment and subsequent starvation. *Mar. Biol.* **130:** 81–91.

Freeman, J. A. 1989. The integument of *Artemia* during early development. Pp. 233–256 in *Biochemistry and Cell Biology of Artemia*, T.H. MacRae, J.C. Bagshaw, and A.H. Warner, eds. CRC Press, Boca Raton, FL.

Freeman, J. A. 1991. Growth and morphogenesis in crustacean larvae. *Mem. Queensl. Mus.* **31:** 309–319.

Freeman, J. A. 1993. The crustacean epidermis during larval development. Pp. 193–219 in *The Crustacean Integument: Morphology and Biochemistry*, M.N. Horst and J.A. Freeman, eds. CRC Press, Boca Raton, FL.

Freeman, J. A. 1995. Epidermal cell cycle and region-specific growth during segment development in *Artemia*. *J. Exp. Zool.* **271:** 285–295.

Freeman, J. A., C. Whittington, and T. H. MacRae. 1995. Relative growth of the tendinal cell and muscle in larval *Artemia*. *Invertebr. Reprod. Dev.* **28:** 205–210.

Hartnoll, R. G. 1982. Growth. Pp. 111–196 in *The Biology of Crustacea, Vol. 2, Embryology, Morphology, and Genetics*, L.G. Abele, ed. Academic Press, New York.

Kanazawa, A., and S. Koshio. 1994. Lipid nutrition of the spiny lobster *Panulirus japonicus* (Decapoda, Palinuridae): a review. *Crustaceana* **67:** 226–232.

Knowlton, R. E. 1974. Larval developmental processes and controlling factors in decapod Crustacea, with emphasis on Caridea. *Thallasia Jugosl.* **10:** 138–158.

Macho, A., Z. Mishal, and J. Uriel. 1996. Molar quantification by flow cytometry of fatty acid binding cells using dipyrromethene boron difluoride derivatives. *Cytometry* **23:** 166–173.

MacRae, T. H., and J. A. Freeman. 1995. Organization of the cytoskeleton in brine shrimp setal cells is molt-dependent. *Can. J. Zool.* **73:** 765–774.

MacRae, R. H., C. M. Langdon, and J. A. Freeman. 1991. Spatial distribution of posttranslationally modified tubulins in polarized cells of developing *Artemia*. *Cell Motil. Cytoskelet.* **18:** 189–203.

McConaugha, J. R. 1985. Nutrition and larval growth. Pp. 127–154 in *Crustacean Issues. 2: Larval Growth*, A. M. Wenner, ed. A. A. Balkema, Boston.

McLaughlin, P. A. 1980. *Comparative Morphology of Recent Crustacea*. W.H. Freeman, San Francisco. p. 13.

Navarro, J. C., F. Amat, and J. R. Sargent. 1991. A study of the variations in lipid levels, lipid class composition and fatty acid composition in the first stages of *Artemia* sp. *Mar. Biol.* **111:** 461–465.

Navarro, J. C., M. V. Bell, F. Amat, and J. Sargent. 1992. The fatty acid composition of phospholipids from brine shrimp, *Artemia* sp., eyes. *Comp. Biochem. Physiol.* **103B:** 89–91.

Sakamoto, M., D. L. Holland, and D. A. Jones. 1982. Modification of the nutritional composition of *Artemia* by incorporation of polyunsaturated fatty acids using micro-encapsulated diets. *Aquaculture* **28:** 311–320.

Schöck, F., and N. Perrimon. 2002. Molecular mechanisms in epithelial morphogenesis. *Annu. Rev. Cell Dev. Biol.* **18:** 463–493.

Schrehardt, A. 1987. A scanning electron-microscope study of the postembryonic development of *Artemia*. Pp. 5–32 in *Artemia Research and its Applications. Vol. 1. Morphology, Genetics, Strain Characterization, Toxicology. Proceedings of the Second International Symposium on the Brine Shrimp Artemia*, P. Sorgeloos, D.A. Bengston, W. Decleir, and E. Jaspers, eds. Universa Press, Wetteren, Belgium.

Taylor, H. H., and E. W. Taylor. 1992. Gills and lungs: the exchange of gases and ions. Pp. 203–293 in *Microscopic Anatomy of Invertebrates, Vol. 10: Decapod Crustacea*, R. Harrison, ed. Wiley-Liss, New York.

Tchernigovtzeff, C. 1976. Sur l'organisation des matrices sétigères chez deux Crustacés Malacostracés, étudiée au microscope électronique. *C.R. Acad. Sci. Paris* **282:** 727–729.

Williamson, D. I. 1982. Larval morphology and diversity. Pp. 43–110 in *The Biology of Crustacea. Vol. 2. Embryology, Morphology, and Genetics*, L.G. Abele, ed. Academic Press, New York.

Reference: *Biol. Bull.* **208:** 200–212. (June 2005)

Gill Anatomy and the Evolution of Symbiosis in the Bivalve Family Thyasiridae

SUZANNE C. DUFOUR*

Marine Biology Research Division, Scripps Institution of Oceanography, La Jolla, California 92093-0202

Abstract. Among families of bivalves with chemoautotrophic symbionts, the Thyasiridae may vary the most in their anatomical characters and in the extent of their nutritional reliance upon symbionts. Since only a fraction of thyasirid species are symbiotic, and the symbionts are mostly observed to be extracellular, this group may be representative of early stages in the evolution of bacterium-bivalve symbioses. To better understand the distribution of symbiosis among thyasirid genera, and the relationships between gill structure and symbiont occurrence, the gills of 26 thyasirid species were studied by light and electron microscopy. Observations revealed three gill types, which are generally constrained within genera or subgenera. Symbionts were found in two gill types: the most simple, homorhabdic filibranch morphotype, and the most derived and thickened morphotype, which resembles the gill structure of other chemosymbiotic bivalves. In all observable cases, the symbionts were located extracellularly among the microvilli of the bacteriocytes. Among individuals of the species *Thyasira* (*Parathyasira*) *equalis*, the quantity of symbionts varied. The results suggest an evolutionary sequence: a homorhabdic filibranch gill structure with few symbionts among the epithelial cell microvilli eventually thickened abfrontally, and thereby offered a larger surface for colonization by symbionts. Eventually, the symbionts persisted and grew in vacuoles within epithelial cells.

INTRODUCTION

Among the families of bivalves that receive a nutritional benefit from their association with symbiotic, chemoautotrophic bacteria (see Le Pennec *et al.*, 1995, for review), the Thyasiridae (subclass Heterodonta) stand out in several ways. (1) Whereas the bacteria in all other known bivalves are endosymbionts, those of studied thyasirids (with the exception of *Maorithyas hadalis*, see Fujiwara *et al.*, 2001) are extracellular (Southward, 1986). (2) Thyasirid symbionts that have been phylogenetically characterized fall into separate clades, rather than clustering as in most other groups of chemosymbiotic bivalves (Imhoff *et al.*, 2003). (3) Only within the Thyasiridae is there a genus, *Thyasira*, in which some species contain symbionts and others lack them (Southward, 1986). (4) Thyasirids have a much wider distribution than other chemosymbiotic bivalve families; they are found from coastal to hadal depths, in different types of sediments, and from both poles to the equator. However, the distribution of symbiotic thyasirids may be more restricted. (5) Thyasirids, as opposed to many other bivalves with chemoautotrophic symbionts, are small; most are less than a centimeter long.

The gills of thyasirids are also distinctive. The family Thyasiridae is the only one in which demibranch number is a variable character. Whereas the outer demibranch is reduced in some thyasirids, it is absent in others; this absence may be explained by paedomorphy (Stasek, 1963; Reid and Brand, 1986; Payne and Allen, 1991). Thyasirid gills also vary in the extent to which the filaments are expanded abfrontally (Southward, 1986; Payne and Allen, 1991). Typically, bivalves with symbiotic chemoautotrophic bacteria have modified gill filaments, in which the abfrontal end is expanded, its epidermis is increased in area and thickness, and the cells, called bacteriocytes, are modified to house the symbionts (Distel, 1998). Some thyasirids with symbionts have such expanded gill filaments, with a bacteriocyte zone similar to that of some lucinids (Southward, 1986). But the filaments in one symbiotic species, *Thyasira equalis*, are

Received 21 June 2004; accepted 29 March 2005.

* Present address: Institut des Sciences de la Mer de Rimouski, Université du Québec à Rimouski, 310, allée des Ursulines, C.P. 3300, Rimouski, QC G5L 3A1, Canada. E-mail: suzanne.dufour@uqar.qc.ca

thin, transparent, and unmodified (Southward, 1986); thus they resemble, in transverse section, many homorhabdic filibranch gill filaments. Because symbiotic thyasirids have gills with variable degrees of abfrontal differentiation, the family provides a unique opportunity for addressing evolutionary questions related to symbiosis.

The relationship between the structure of thyasirid gills and the occurrence of bacterial symbionts has, in fact, been described in seven species (Southward, 1986; Le Pennec *et al.*, 1988; Fujiwara *et al.*, 2001). In this study, to explore these relationships more thoroughly, gill structure and symbiont occurrence were examined in 26 thyasirid species, either freshly collected or obtained from museum collections, and varying, not only in anatomical characters, but also in size and habitat. Given the paucity of phylogenetic data on this family and the anatomical variability within this group, we must consider that the Thyasiridae may be polyphyletic. Even so, the patterns of variation in gill complexity and symbiont location found within thyasirids may suggest the gradual changes that can lead to endosymbiosis in epithelial cells.

MATERIALS AND METHODS

Live specimens and specimens obtained from museum collections were used in this study (Table 1). The nomenclature used follows Oliver and Killeen (2002); therefore, *Axinulus* and *Mendicula*, which other authors have determined to be subgenera of *Thyasira*, are here considered to be genera. The taxonomic affiliation of some species being unclear, they were classified with the taxon which they most resemble in shell character and demibranch number.

Within an hour after collection, live specimens were removed from their shells, and the gills were fixed for a minimum of 1 h in 3% glutaraldehyde in 0.1 *M* sodium phosphate buffer (pH 7.3) with 0.35 *M* sucrose. The tissues were then rinsed in the 0.1 *M* sodium phosphate buffer and postfixed for 1 h in 1% osmium tetroxide in the same buffer. After fixation, the gills were dehydrated in an ethanol gradient and embedded in Spurr resin.

Most of the specimens obtained from museum collections had been immersed in formaldehyde with their shells closed, so the gill epithelia were in a relatively poor state of preservation. However, these specimens could still provide useful information about gill anatomy, and symbionts could sometimes be detected and located. The gills of these specimens were removed and processed in the same manner as the live specimens.

Semi-thin (1–2 μm), transverse sections of the gills of all specimens were stained with toluidine blue, and ultra-thin sections (approximately 70 nm) were stained with uranyl acetate for 15 min, and with lead citrate for 7 min. Observations and micrographs were made on a LEO EM 912 or a Philips 410A transmission electron microscope.

A few museum specimens from the San Diego Trough (*Conchocele excavata, Thyasira (Thyasira)* sp., and *Adontorhina cyclia;* Table 1) were prepared for scanning electron microscopy. Following the removal of one valve, the specimens were post-fixed in 2.5% glutaraldehyde in a 0.1 *M* sodium cacodylate buffer (osmolarity $\approx$ 1050 mosmol). The half-shell preparations were dehydrated in an ascending ethanol gradient, critical-point-dried from CO_2, mounted on stubs, and sputter-coated with a gold/palladium mixture. Observations were made on a Cambridge Instruments 350 scanning electron microscope.

When bacteria were observed in association with abfrontal surfaces of a given species, they were assumed to be symbionts if they were abundant, found on most abfrontal cells, and on more than one individual of a species (ideally, from different collection sites). In four species, symbiont presence was inferred from observations of only one individual; but those were species with a highly derived gill structure which, in all other observed cases, represented an adaptation to symbiosis.

RESULTS

The semi-thin gill sections revealed wide variations in gill filament morphology within the family (Fig. 1). Thyasirid gills have either a homorhabdic filibranch design (type 2) or a structure derived from it, with more interfilamentar tissue fusion in the abfrontal area (type 1), or with filaments expanded abfrontally and extensive epithelial surfaces accomodating bacteria (type 3).

Gill type 1

Only the three species in the genus *Axinopsida* had gill type 1 (Table 2). This type is characterized by filaments without abfrontal expansion and with a high degree of inter-filamentar fusion throughout most ($\sim$ 70%) of the dorsoventral length of the filaments (Fig. 1a). This extensive fusion precludes water flow through the gill, except in the dorsalmost part where filaments are separate (as in Fig. 1b), allowing the flow of water from the infrabranchial to the suprabranchial chambers. In the highly fused areas of the gill, water currents must be parallel to the dorsoventral axis of the filaments; they are likely to be directed dorsalward, as in all suspension-feeding bivalves examined (Beninger and St-Jean, 1997). The tissue joining individual filaments contains many mucocytes (Fig. 1a, 2), which may secrete to the frontal surface *via* ducts, as in some lucinids (Duplessis *et al.*, 2004). In one of four specimens of *Axinopsida serricata, Rickettsia*-like nodules were seen, both in the abfrontal area and among the lateral and laterofrontal ciliated cells (Fig. 2). No bacterial symbionts were observed in the specimens with gill type 1.

Table 1

Summary of collection information for thyasirid specimens examined

Species[1]	n[2]	Size (mm)	Collection site[3]	Depth (m)
Specimens collected in the field				
Axinulus croulinensis	1	2.2	Raunefjord, Norway (60° 16.235′N, 5°08.631′E)	220–253
Mendicula ferruginea	2	2–3	Raunefjord, Norway	220–253
Thyasira (?) obsoleta	5	2–3	Raunefjord, Norway	220–253
Thyasira (Parathyasira) equalis	71	2–5	Raunefjord, Norway	220–253
Thyasira (Thyasira) sarsi	49	3–8.5	Dolviken, Norway (60°19.185′N, 5°15.344′E)	50–54
Thyasira (Thyasira) flexuosa	61	3–9	Dolviken, Norway	50–54
	46	2–6	La Coruña, Spain (43°21.449′N, 8°22.404′W, 43°21.880′N, 8°23.220′W)	13–16
	2	4–6	Long Beach, CA, USA (33°40.886′N, 118°19.313′W)	151
Specimens from museums				
Axinopsida orbiculata	2	2–5	Tatar Strait[A]	30
	3	2	E. Greenland[B]	3–9
Axinopsida serricata	2	4	Bering Sea[C]	36
	2	5	Vancouver Island[D]	58–190
Axinopsida subquadrata	1	4.5	Okhotsk Sea[A]	25
	1	4.5	Japan Sea[A]	48
*Axinulus croulinensis**	2	2	North Sea[B]	200
Axinulus eumyaria	3	2	North Sea oil field[B]	300–350
Axinulus sp.	1	1	Doubtful Sound, NZ[E]	376
*Mendicula ferruginea**	1	3	North Sea[B]	200
Mendicula pygmaea	1	2	North Sea[B]	200
Adontorhina cyclia	2	2	San Diego Trough[F]	1199–1250
Genaxinus debilis	1	1	South Orkney Islands[C]	298–403
	1	2	Anvers Island, Antarctica[E]	18
Genaxinus sp.	1	2	South Orkney Islands[C]	298–403
*Thyasira (?) obsoleta**	2	2–3	North Sea[B]	200
	1	2	Off Beaufort, NC[G]	198
Thyasira (Parathyasira) granulosa	1	7	North Sea oil field[B]	300–350
*Thyasira (Parathyasira) equalis**	2	3	Barents Sea[A]	195–380
	3	4	North Sea[B]	200
Thyasira (Parathyasira) neozelanica	1	4	Doubtful Sound, NZ[E]	376
Thyasira (Thyasira) dearboni	1	4	Shetland Islands[C]	?
Thyasira (Thyasira) n. sp.	1	5	W. Greenland[B]	641
Thyasira (Thyasira) trisinuata	3	8–11	off Daytona Beach, FL[C]	185
*Thyasira (Thyasira) sarsi**	1	6	White Sea[A]	17–19
	2	7–14	North Sea[B]	200
*Thyasira (Thyasira) flexuosa**	3	5	North Sea[B]	200
	2	5	Tatar Strait[A]	30
Thyasira (Thyasira) gouldi	1	5	W. Greenland[H]	37
	1	5	Faroe Islands[H]	15
	1	5	N. Greenland[H]	10.5
	1	4	Pechorskoye Sea[A]	106
	1	4	Kuril Islands[A]	75
Thyasira (Thyasira) peregrina	1	4	Pegasus Bay, NZ[E]	505
Thyasira (Thyasira) bongraini	1	7	Anvers Island, Antarctica[E]	39
Thyasira (Thyasira) falklandica	1	18	Anvers Island, Antarctica[E]	5
Thyasira (Thyasira) sp.	2	3.5	San Diego Trough[F]	1215–1244
Conchocele excavata	1	15	San Diego Trough[F]	1250

[1] Asterisks (*) identify museum species that were also collected live.

[2] n represents the number of specimens examined.

[3] A, Zoological Institute, Russian Academy of Sciences; B, Swedish Museum of Natural History; C, Smithsonian National Museum of Natural History; D, Royal British Columbia Museum; E, Museum of New Zealand; F, Scripps Institution of Oceanography Benthic Invertebrates Collection; G, Museum of Comparative Zoology, Harvard University; H, Zoological Museum, Copenhagen.

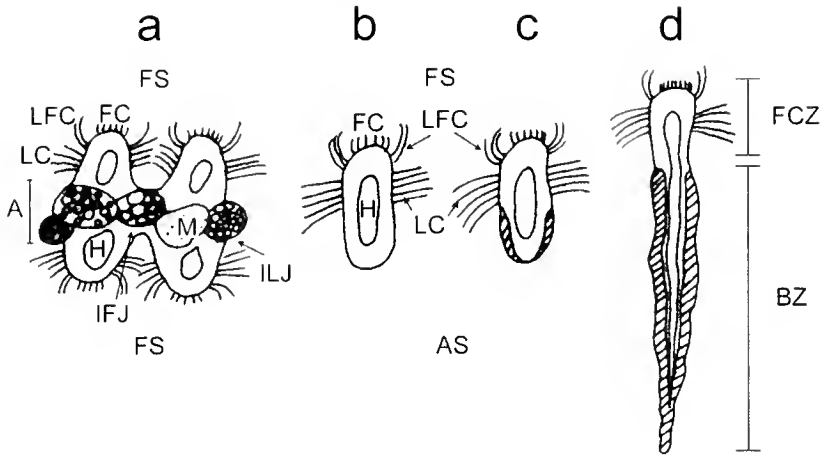

Figure 1. Schematic representation of transverse sections of gill filaments in the Thyasiridae. **(a)** Gill type 1. The ascending and descending arms of two neighboring filaments, interconnected by inter-filamentar (IFJ) and inter-lamellar (ILJ) tissue junctions. The frontal surface (FS) bears frontal cilia (FC), laterofrontal cirri (LFC), and lateral cilia (LC). In the abfrontal zone (A), several mucocytes (M) are present. At their dorsal end, the filaments are separate, as in (b). H, hemocoel. **(b, c)** Gill type 2. Filaments sectioned at the dorsal end of a demibranch. The frontal surface (FS) contains frontal cilia (FC), laterofrontal cirri (LFC), and lateral cilia (LC). Hatched areas at the abfrontal surface (AS) are occupied by symbionts in (c). H, hemocoel. **(d)** Gill type 3. Section through one arm of a gill filament. All cells in the bacteriocyte zone (BZ), below the frontal ciliated zone (FCZ), contain symbionts (hatched areas).

Gill type 2

Thyasirids within this group have simplified gill filaments with no apparent expansion of the abfrontal tissue (Fig. 1b, c; 3a). The frontal surface bears frontal cilia, laterofrontal cirri, and lateral cilia (Fig. 3a, b). Scanning electron micrographs (SEM) revealed the presence of several particles on the gill frontal surfaces, between filaments, and on the ventral food tract (Fig. 3b). Species with gill type 2 had either one or two demibranchs (Table 2); only specimens of the genera *Axinulus, Mendicula,* and *Adontorhina* had no outer demibranch (the presence of the gill axis on the outer side of the descending lamella of the lone demibranch confirms that it is the inner demibranch).

Transmission electron micrographs (TEM) revealed three types of cells in the abfrontal area of type 2 gill filaments: cells (C1) containing either several large mitochondria or, in *Mendicula ferruginea,* large electron-dense organelles (Fig. 3c, d); epithelial cells (C2) with more or less elongate microvilli (among which there may be symbionts — if so, these cells are called bacteriocytes); and mucocytes. When present, the mitochondria-rich cells (C1) seem to always be covered apically by thin extensions of C2 epithelial cells (Fig. 3c, d; 4a, b).

Only two species with gill type 2 were found to have symbiotic bacteria in the abfrontal zone (Table 2). These bacteria were located in the extracellular space between the apical cell membrane and microvillar extensions of the membrane (Fig. 4a, c). In TEMs, the density of symbionts within this extracellular space varied with species, and in *Thyasira (Parathyasira) equalis,* among individuals of a species (Fig. 4a, d). In one *T. (Parathyasira) equalis* specimen, symbionts were visible within bacteriocytes, perhaps having been taken up by endocytosis (Fig. 4b); in another specimen, careful survey of several filaments, on two grids prepared from separate gill areas, revealed a lack of symbionts (Fig. 4d). Other species with type 2 gills had no visible bacterial symbionts (Fig. 3c, d).

Gill type 3

Species with this gill type belong to the genera *Conchocele* and *Thyasira (Thyasira).* The gill filaments in these species are expanded abfrontally and have a distinct bacteriocyte zone (Fig. 1d; 5a–c). The frontal surface of the gills of *Conchocele excavata* and *T. (Thyasira)* sp. bears cilia typical of many suspension-feeding bivalves: frontal cilia, laterofrontal cirri, and lateral cilia can be seen (Fig. 5a, d). No cilia were visible on the surfaces of bacteriocytes or other abfrontal cells in these species (Fig. 5a, e).

In all specimens examined, the extracellular space occupied by bacterial symbionts was relatively large compared to the bacteriocyte cytoplasm (Fig. 5b, c). Symbionts were more abundant in association with the frontal-most bacteriocytes; their number (and occupied volume) decreased in cells having a more abfrontal position.

The cytological position of the symbionts was examined by transmission electron micrography. In all species where unambiguous observations could be made, the symbionts were extracellular—maintained in spaces delimited basally

Table 2

Summary of data for the thyasirid species studied

Species	Gill type	Number of demibranchs	Symbiont abundance*	Maximum size† (mm)	Depth range† (m)
Axinopsida orbiculata	1	2	−	8 (1)	2–944 (2)
Axinopsida serricata	1	2	−	8 (3)	0–275 (3)
Axinopsida subquadrata	1	2	−	3 (4)	25–48 (4)
Axinulus croulinensis	2	1	+	2.5 (1)	24–3861 (5, 6)
Axinulus eumyaria	2	1	−	2.5 (1)	42–2663 (5)
Axinulus sp.	2	1	−	1 (4)	376 (4)
Mendicula ferruginea	2	1	−	4.5 (1)	40–4825 (3, 5)
Mendicula pygmaea	2	1	−	2 (1)	22–1470 (5, 7)
Adontorhina cyclia	2	1	−	3 (3)	12–3000 (3)
Genaxinus debilis	2	2	−	3 (8)	9–1000 (8,9)
Genaxinus sp.	2	2	−	2 (4)	298–403 (4)
Thyasira (?) obsoleta	2	2	−	4 (1)	24–2900 (5)
Thyasira (Parathyasira) granulosa	2	2	−	10 (1)	100–1800 (1)
Thyasira (Parathyasira) equalis	2	2	+	8 (1)	10–4734 (1,5)
Thyasira (Parathyasira) neozelanica	2	2	−	4 (4)	137–201 (10)
Thyasira (Thyasira) dearboni	2	2	−	5 (8)	222–1100 (8)
Thyasira (Thyasira) n. sp.	2	2	−	5 (4)	641 (4)
Thyasira (Thyasira) trisinuata	3	2	++	18 (5)	18–2359 (5, 11)
Thyasira (Thyasira) sarsi	3	2	++	25 (1)	50–340 (4, 12)
Thyasira (Thyasira) flexuosa	3	2	++	12 (3)	6–3000 (3, 13)
Thyasira (Thyasira) gouldi	3	2	++	10 (1)	5–732 (7)
Thyasira (Thyasira) peregrina	3	2	++	5 (14)	4–505 (4, 10)
Thyasira (Thyasira) bongraini	3	2	++	7 (4)	9–512 (15)
Thyasira (Thyasira) falklandica	3	2	++	18 (15)	5–344 (15)
Thyasira (Thyasira) sp.	3	2	++	3.5 (4)	1215–1244 (4)
Conchocele excavata	3	2	++	24 (3)	800–2520 (3)

* ++, abundant symbionts; +, few symbionts; −, no symbionts seen.

† Numbers in parentheses indicate source from which the data were taken: (1) Oliver and Killeen, 2002; (2) Ockelmann, 1958; (3) Coan *et al.*, 2000; (4) present study; (5) Payne and Allen, 1991; (6) Verrill and Bush, 1898; (7) Aitken and Gilbert, 1996; (8) Cattaneo-Vietti *et al.*, 2000; (9) Dell, 1990; (10) Fleming, 1950; (11) Dall, 1899; (12) Zimmermann *et al.*, 1997; (13) López-Jamar and Parra, 1997; (14) Iredale, 1930; (15) Nicol, 1966.

by the bacteriocyte membrane and apically by microvilli (Fig. 6a–c). Extensions of the bacteriocyte cytoplasm among the symbionts were visible (Fig. 6b). In some individuals, material resembling lysed bacterial remains could be seen in the bacteriocytes (Fig. 6d, e). One *Thyasira (Thyasira) flexuosa* individual from off Long Beach contained viral particles, both within bacterial symbionts and in intracellular lysed remains (Fig. 6d).

Symbionts with different morphologies were observed: some appeared ovoid (Fig. 6a, b, e), whereas others were spherical (Fig. 6f) or rod-shaped (Fig. 6c). Empty spaces within the bacteria (Fig. 6b) may have been sulfur stores, which were washed out during specimen preparation (Vetter, 1985). In one specimen of *Thyasira (Thyasira) sarsi*, bacteria with different appearances were seen in association with different bacteriocytes (Fig. 6f). In one specimen of *T. (Thyasira) flexuosa* from a North Sea oil field, one or two electron-dense spheres were seen at the extremities of the symbionts (Fig. 6c); they appeared to be located between the external and internal bacterial membranes. Observation without prior osmium tetroxide fixation or heavy-metal staining revealed that these structures probably do not contain metals and may be organic (they were not electron-dense under those conditions).

DISCUSSION

The results of this study improve our knowledge of thyasirid gills by covering a wider taxonomic range and nearly four times as many species as previously described. Overall, the data show an unusual amount of variation in gill anatomy and symbiont presence for bivalves at the family level, suggesting adaptations to different environments and lifestyles. Within genera and subgenera, gill characters are more conservative. The results appear to illustrate an evolutionary sequence, from a typical homorhabdic filibranch gill structure, with a few bacteria among abfrontal cell microvilli, to a modified gill with abfrontal thickening and a greater surface available to symbionts, the latter eventually becoming intracellular.

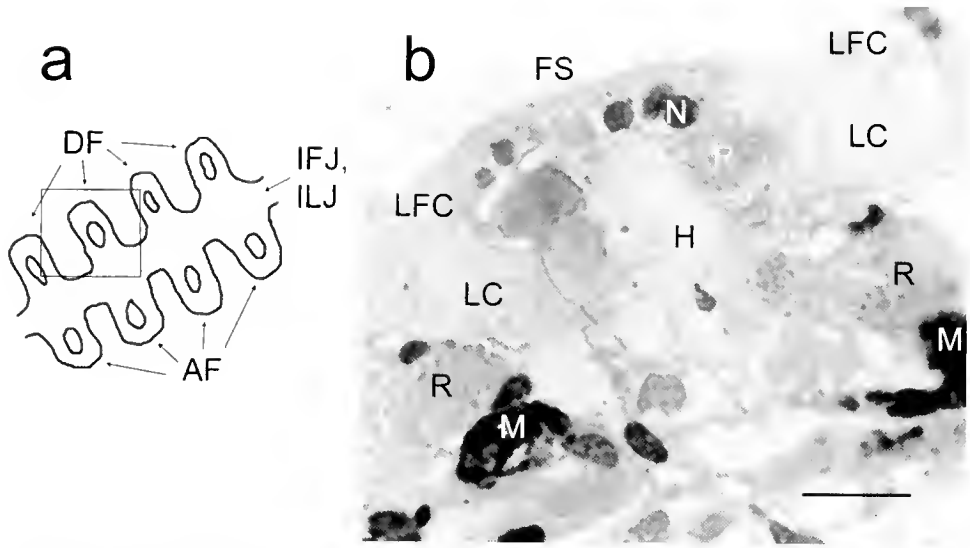

Figure 2. Type 1 gill filaments of *Axinopsida serricata*. **(a)** Diagram of a transverse section through the gill, with a square framing the location and orientation of the section depicted in (b). AF, ascending filaments; DF, descending filaments; IFJ, inter-filamentar junctions; ILJ, interlamellar junctions. **(b)** Light micrograph of a semi-thin section, showing nuclei (N) of cells at the frontal surface (FS), laterofrontal cirri (LFC) and lateral cilia (LC), and gill hemocoel (H). *Rickettsia*-like nodules (R) are visible among lateral ciliated cells and in the abfrontal zone, where several mucocytes (M) are also visible. Frontal cilia are not visible here, but were seen on other sections. Bar = 10 μm.

Gill structure and symbiont presence

The gill types are constrained within genera or subgenera: only *Axinopsida* species have gill type 1, and only *Conchocele*, *Thyasira (Thyasira)*, and *Maorithyas* (Fujiwara *et al.*, 2001) have gill type 3. Among the genera studied, *Thyasira* is most diverse, having type 2 and type 3 gills; for the most part, type 2 gills are found in the subgenus *Parathyasira*, and type 3 gills in the subgenus *Thyasira*. Whether gill structure may be used as a taxonomic character to distinguish subgenera of *Thyasira* is still unclear, since a global-scale taxonomy of this group based on other characters is not yet resolved.

Symbionts were identified in *Conchocele* and *Thyasira (Thyasira)* species (type 3), and in *Thyasira (Parathyasira) equalis* and *Axinulus croulinensis* (type 2). Judging from published figures, the symbiotic thyasirid *Maorithyas hadalis* has type 3 gills (Fujiwara *et al.*, 2001), and initial observations of *Conchocele bisecta* (data not shown) reveal even more complex gills, with cylindrical structures underlying the frontal ciliated layer, as in many lucinids (Distel and Felbeck, 1987). The gill types suggest an evolutionary sequence associated with the acquisition of symbionts, as described below.

Demibranch number is another variable character in thyasirids. From the present data, only species from the genera *Axinulus*, *Mendicula*, and *Adontorhina* do not have two demibranchs. This is not surprising given that demibranch number has been used as a taxonomic character (Payne and Allen, 1991). Although most symbiotic species from this survey have two demibranchs, *Axinulus croulinensis*, as well as a symbiotic thyasirid from the deep-sea (Southward, 1986), have only one. Thus, demibranch number seems unrelated to symbiont presence. As noted by Payne and Allen (1991), demibranch number is probably related to body size: thyasirids with only one demibranch are all less than 5 mm long. In bivalves, small body size and simple gill structure are common in species inhabiting the deep-sea (Allen, 1979). Hence, Payne and Allen (1991) suggested that, in thyasirids, the loss of a demibranch and small body size are adaptations for deep-sea life. A survey of thyasirid depth distribution (Table 2) reveals that many of the larger species can nonetheless be found at bathyal depths; but among asymbiotic thyasirids, most of the deep-sea dwelling species are small and have only one demibranch.

Of the thyasirid species studied here, those with symbionts are larger and live at somewhat shallower depths than those without symbionts (Table 2). The larger size could be due to their having a greater nutritional input than strict suspension-feeders, especially in the deep-sea, where particulate food is less abundant. If the symbionts described here are chemoautotrophic sulfide-oxidizing bacteria, as in other thyasirids (Dando and Southward, 1986), the apparent preference of symbiotic thyasirids for shallower depths may be based on a bacterial requirement for reduced sulfur, which is more common in sediments on the continental

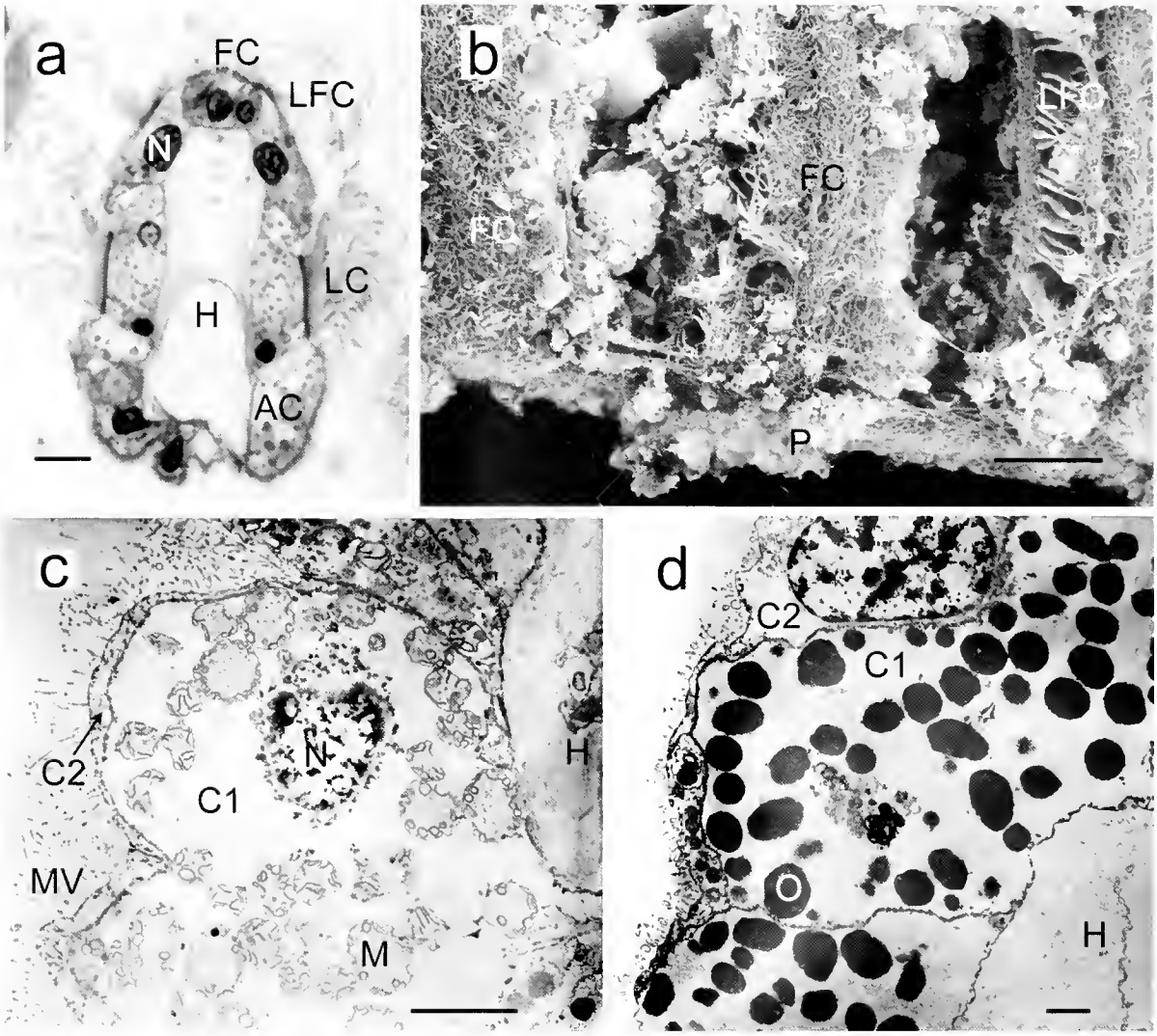

Figure 3. Light and electron micrographs of Type 2 gill filaments. **(a)** *Thyasira (Parathyasira) equalis.* Light micrograph of a semi-thin, transverse section of a gill filament, showing frontal cilia (FC), laterofrontal cirri (LFC), lateral cilia (LC), hemocoel (H), and abfrontal cells (AC). N, nucleus. **(b)** *Adontorhina cyclia.* SEM of the ventral extremity of three gill filaments. Frontal cilia (FC) and laterofrontal cirri (LFC) are visible. Numerous particles can be seen on the frontal tracts, between filaments, and along the ventral food tract (P). **(c)** *T. (?) obsoleta.* TEM of cells in the abfrontal zone of a gill filament. Thin cells (C2) with microvilli (MV) cover the apical surface of cells (C1) with numerous mitochondria (M). N, nucleus; H, hemocoel. **(d)** *Mendicula ferruginea.* TEM of cells (C1) with electron-dense organelles (O); these cells are covered at their apical end by thin cells (C2). H, hemocoel. Bars: (a) = 25 μm; (b) = 20 μm; (c, d) = 1 μm.

shelf, where organic matter is more abundant. At deeper sites, thyasirids (some of which may have symbionts) have been found at hydrothermal vents (Gebruk *et al.*, 2000), at cold seeps (Clarke, 1989; Lewis and Marshall, 1996; Imhoff *et al.*, 2003), and in oxygen-minimum zones (L. Levin, Scripps Institution of Oceanography; pers. comm.), where sulfide is more abundant. Elsewhere in the deep-sea, symbiotic thyasirids could rely on sparser amounts of sulfide: even at coastal depths, symbiotic thyasirids are often found in sediments where sulfide levels are low or undetectable (Dando and Southward, 1986). The ability of symbiotic thyasirids to mine for sulfide by using their superextensible foot allows them to access patches of sulfide in such environments (Dufour and Felbeck, 2003).

Symbiont density varied among specimens of *Thyasira (Parathyasira) equalis* (Fig. 4a, b, d). This may be related to seasonal or spatial variations in available sulfide in the sediment, differentially affecting the fitness and growth of symbionts among thyasirid individuals. Dando and Spiro (1993) noted that *T. (Thyasira) sarsi* and *T. (Parathyasira) equalis* exhibited seasonal variability in $^{13}C/^{12}C$ ratios, and concluded that their nutritional dependence upon their sym-

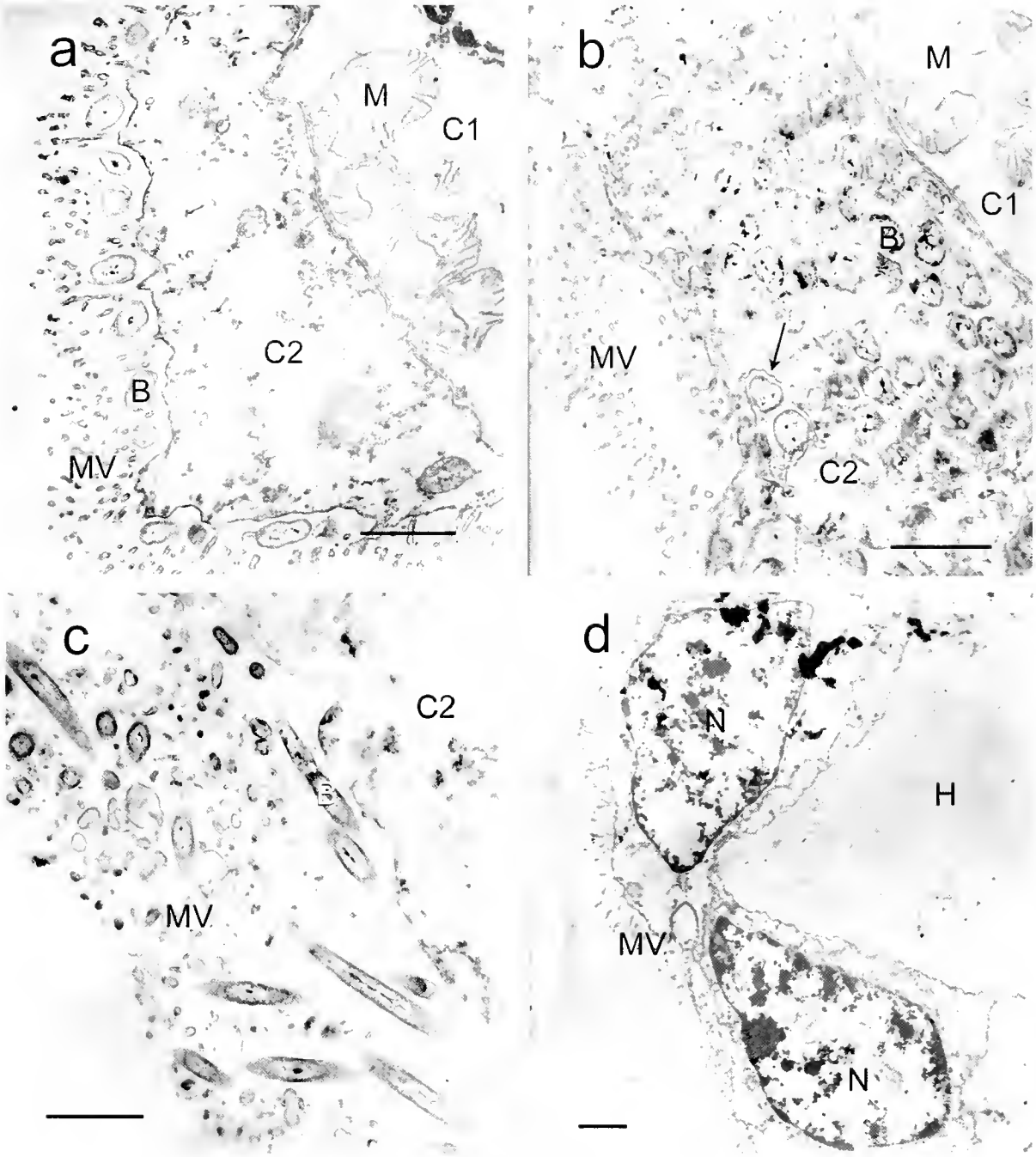

Figure 4. TEM of cells in the abfrontal zone of thyasirids with gill type 2. **(a)** *Thyasira (Parathyasira) equalis*. Bacteria (B) are present among the microvilli (MV) of thin epithelial cells (C2) in the abfrontal zone. Underlying cells (C1) contain several mitochondria (M). **(b)** *T. (Parathyasira) equalis*. Thin epithelial cell (C2), with degrading bacteria (B) in the cytoplasm (none are visible among the microvilli [MV]). Arrow points to symbionts within a vacuole. Mitochondria (M) are visible in the underlying cell (C1). **(c)** *Axinulus croulinensis*. Apical end of an abfrontal cell (C2), with bacterial symbionts (B) among the microvilli (MV). **(d)** *T. (Parathyasira) equalis*. Abfrontal cells in an individual without symbionts. H, hemocoel; MV, microvilli; N, nucleus. Bars = 1 μm.

bionts varied with changing sulfide content in the sediment. Perhaps this change in carbon isotope ratios is caused, not by a lower rate of symbiont digestion when organic matter is low, but rather by the sparseness of symbionts at these times. Although not reported, symbiont density may vary similarly in other chemosymbiotic bivalves; moreover, spe-

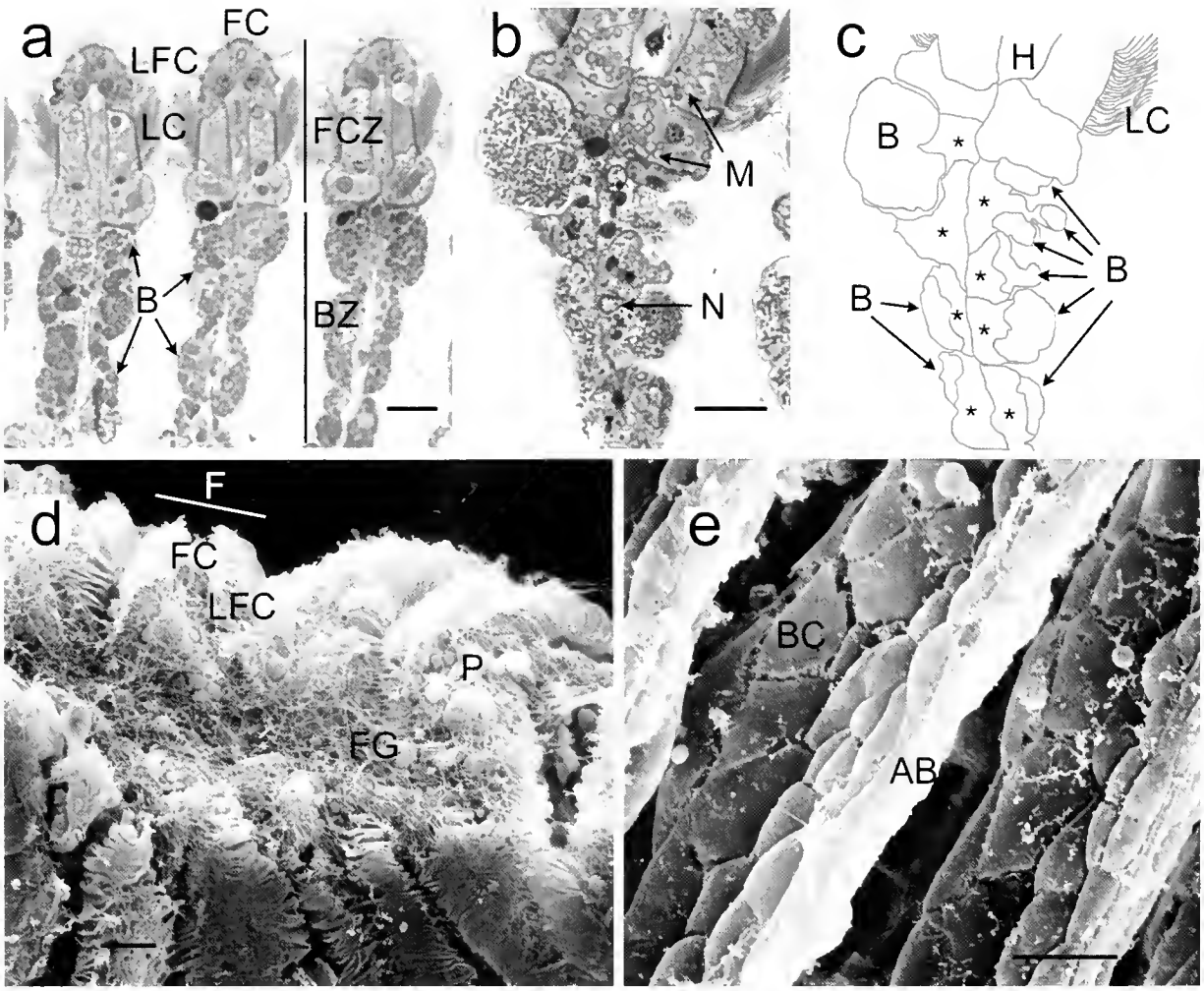

Figure 5. Light and electron micrographs of type 3 gill filaments. **(a)** Light micrograph of a semi-thin, transverse section of three gill filaments of *Thyasira (Thyasira) flexuosa*, showing frontal ciliated zone (FCZ) and bacteriocyte zone (BZ). Frontal cilia (FC), laterofrontal cirri (LFC), and lateral cilia (LC) are visible. Darker stained areas within bacteriocytes are symbionts (B). **(b,c)** Light micrograph of a semi-thin, transverse section and diagram of a gill filament of *T. (Thyasira) flexuosa*. Asterisks show the cytoplasm of bacteriocytes, at the apical end of which are kept the bacteria (B). Mitochondria (M) are visible in cells of the frontal ciliated zone. H, hemocoel; LC, lateral cilia; N, nucleus. **(d)** SEM of the ventral food groove (FG) of gill filaments (F) of *T. (Thyasira)* sp., revealing frontal cilia (FC) and rows of laterofrontal cirri (LFC). P, particles. **(e)** SEM of the abfrontal end (AB) in the bacteriocyte zone of *T. (Thyasira)* sp. gill filaments. The outlines of individual bacteriocytes (BC) are visible. Bars: (a) = 35 μm; (b) = 25 μm; (d, e) = 20 μm.

cies observed here as having no symbionts could in fact possess them at different times or locations. The implication of this variation in symbiont density is that the symbiosis may be facultative in some thyasirids, serving more as a nutritional supplement than a primary food source.

The symbionts themselves showed variation in size and structure: seen in sections, some were rod-shaped, while others appeared ovoid or spherical. The various morphologies may indicate that the symbionts in different thyasirids are different species; further examination using molecular techniques would resolve this issue.

One specimen of *Thyasira (Thyasira) sarsi* had what appeared to be two morphotypes of symbionts within two neighboring bacteriocytes; this would not be the first report of two different symbionts within a thyasirid, as they were also seen in *Maorithyas hadalis* (Fujiwara *et al.*, 2001) and in two unidentified deep-sea thyasirids (Southward, 1986).

The evolution of chemosymbiosis

The different gill structures observed in the family Thyasiridae, when related to the presence and cytological location of symbionts, are suggestive of the pathways of gill evolution in chemosymbiotic autobranch bivalves. It is

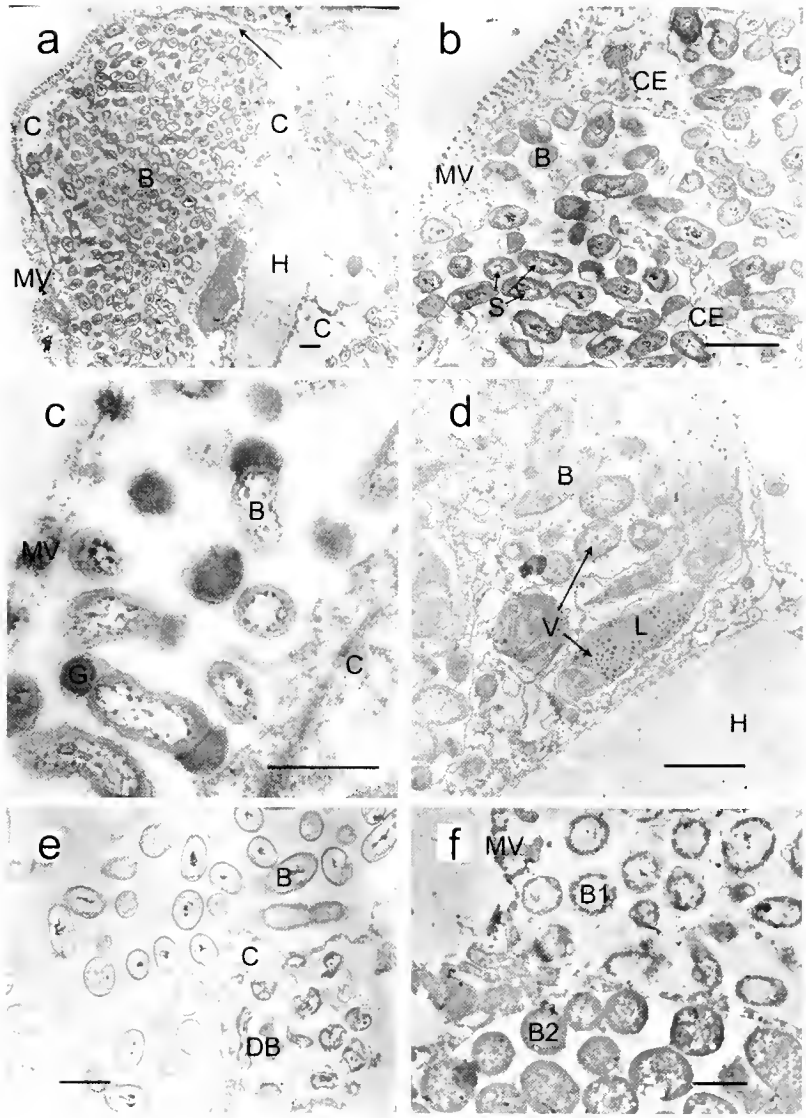

Figure 6. TEM of bacteriocytes in thyasirids with gill type 3. **(a)** Oblique section of *Thyasira (Thyasira) flexuosa* bacteriocytes. Bacteria (B) are extracellular and distinct from cytoplasm (C). Arrowhead points to a cytoplasm extension. H, hemocoel; MV, microvilli. **(b)** Apical end of a *T. (Thyasira) flexuosa* bacteriocyte, showing detail of cytoplasm extension (CE), microvilli (MV), and bacteria (B). Translucent areas within bacteria may have contained sulfur deposits (S), which washed out during TEM preparation. **(c)** Bacterial symbionts (B) in *T. (Thyasira) flexuosa* from an oil field in the North Sea. Electron-dense granules (G) are visible at one or both ends of the rod-shaped bacteria. C, bacteriocyte cytoplasm; MV, microvilli. **(d)** The basal end of a *T. (Thyasira) flexuosa* bacteriocyte, with lysosomes (L) containing the remains of bacteria (B) and viruses (V). H, hemocoel. **(e)** Bacteriocyte cytoplasm (C) of *T. (Thyasira) sarsi* and associated bacteria (B). DB, degrading bacteria. **(f)** Two neighboring bacteriocytes in *T. (Thyasira) sarsi*, each cell having a different morphotype of bacteria (B1 and B2). MV, microvilli. Bars: (a, b, d–f) = 1 μm; (c) = 0.5 μm.

plausible that, with time, symbionts progressed from an extracellular location to an intracellular one (Fig. 7), and that gills became more elongate.

In all the thyasirids observed, the symbionts were normally located extracellularly, within spaces delimited by the cell membrane and microvilli (except when presumably taken up by endocytosis). This is believed to be a simple state (Smith, 1979; Hickman, 1994; Cavanaugh, 1994), with bacteria being taken up by endocytosis and digested within the host epithelial cells (Le Pennec *et al.*, 1988). Evidence for this digestion include the presence of lysosomal bodies with accumulated bacterial membranes within the cells, which have been seen, not only in thyasirids, but also in mytilids, vesicomyids, lucinids, and solemyids with endosymbionts (Fiala-Médioni *et al.*, 1986; Fiala-Médioni and Le Pennec, 1987; Le Pennec *et al.*, 1988; Fisher, 1990;

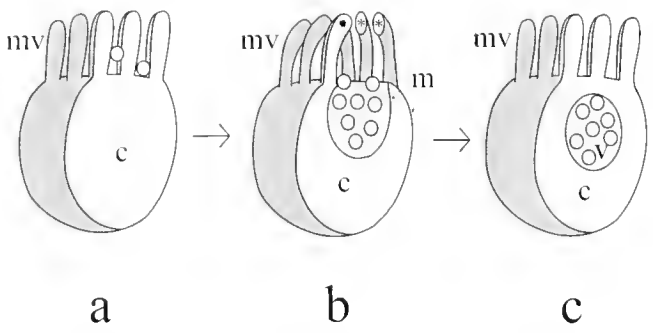

Figure 7. Diagram, based on thyasirid gill data, showing the evolution of symbiosis from an extracellular to an intracellular mode. Each diagram represents a bacteriocyte, sectioned along the apical-basal plane (revealing, in white, what is typically seen in transverse sections of gills). Bacteria are represented by small circles. **(a)** Bacteriocyte in thyasirids with gill type 2, with bacteria present among the microvilli (mv), but separate from the cytoplasm (c). **(b)** Bacteriocyte in a gill type 3, with bacteria (circles) still maintained outside the cytoplasm (c), but in a space delimited by the bacteriocyte membrane (m), and microvilli (mv). In sections, the microvilli appear either entire (star) or partial (asterisks). **(c)** Bacteriocyte in the type 3 gill of *Maorithyas hadalis* (or other bivalves with endosymbionts) maintained in a vacuole (v), within the cytoplasm (c). mv, microvilli.

Barry *et al.*, 2002). The endocytosis of bacteria is not a phenomenon restricted to epithelial cells of the gills of chemosymbiotic bivalves; it is an inherent defense mechanism of almost all eukaryotic cells (Silverstein *et al.*, 1977). The likelihood of bacteria passing between gill filaments and reaching the abfrontal surfaces without prior interception by laterofrontal cilia appears high, given the relatively large space between filaments, as seen by naked eye upon dissection, and on scanning electron micrographs (Fig. 3b; although the position of particles on these specimens may be artifactual, the wide spaces between filaments, coupled with laterofrontal cirri that are not abnormally large, suggest that bacteria can easily reach abfrontal surfaces).

In the species *Maorithyas hadalis*, as well as in some species of *Bathymodiolus*, and in the symbiotic gastropods *Ifremeria nautilei* and *Alviniconcha hessleri*, apically situated vacuoles containing bacteria often have an open connection to the external water (Le Pennec and Hily, 1984; Endow and Ohta, 1989; Windoffer and Giere, 1997; Dubilier *et al.*, 1998; Fujiwara *et al.*, 2001). This arrangement was suggested to be an intermediate state between extracellular and intracellular symbionts (Windoffer and Giere, 1997), where only bacteria in vacuoles close to the apical end of bacteriocytes are in contact with seawater (Endow and Ohta, 1989). In the gills of symbiotic gastropods, the bacteria are enclosed within a vacuolar network, which may allow exchange with external water (Windoffer and Giere, 1997). Extracellular bacteria may receive some benefit (such as dissolved gases or nutrients) from being in contact with flowing seawater. On the other hand, when symbionts are enclosed by host-cell microvilli, the latter may exercise some control on the nature of the fluid bathing the symbionts.

The microvilli of symbiotic thyasirids appear more elongated than those of typical bivalve gill epithelial cells (Morse and Zardus, 1991). Elaborate microvillar layers are typical of surfaces involved in symbiosis, such as the light organ of squids (Montgomery and McFall-Ngai, 1993; McFall-Ngai, 1998) or enteric epithelia (Woolverton *et al.*, 1992). Interestingly, some of the nonsymbiotic thyasirids had similarly elongated microvilli; this suggests that they may have the ability to retain bacteria, and that an examination of additional specimens might reveal symbionts in some specimens.

In thyasirids, the uptake of symbionts within epithelial cells is predated by the abfrontal development of gill filaments, which increases the space available for bacterial colonization. Only in the thyasirid *Maorithyas hadalis* have intracellular symbionts been observed (Fujiwara *et al.*, 2001); this species has a type 3 gill. Perhaps intracellular symbionts are present in other species in the genus *Maorithyas*, as well as in certain *Conchocele;* the structure of the gill of *C. bisecta*, with its bacteriocyte cylinders, certainly suggests a more advanced state. The presence of symbionts in the simpler type 2 gill of *Thyasira (Parathyasira) equalis* suggests that this species has acquired its symbionts relatively recently.

The abfrontal elaboration of gill filaments appears to be a more efficient way to increase the overall space available for bacterial housing, compared to an increase in the number of unmodified filaments per gill: in the second case, the bivalves have to elaborate and maintain not only extra bacteriocytes, but also additional frontal ciliated zones.

ACKNOWLEDGMENTS

I am grateful to H. Felbeck, J.B.C. Jackson, N.D. Holland, and W. Newman at the Scripps Institution of Oceanography (SIO), and K. Roy at the University of California, San Diego, for their advice and support. P.V. Scott at the Santa Barbara Museum of Natural History provided assistance with thyasirid identifications. D. Cadien at the County Sanitation Districts of Los Angeles County; S. Parra and I. Frutos at the Instituto Español de Oceanografía, in La Coruña; T. Hoisæter, P. Johannessen, and staff at the University of Bergen and the Marine Biological Station, Espegrend, were involved in the collection of specimens. F. Gaill, J.-P. Lechaire, and G. Frebourg at the Université Pierre et Marie Curie, Paris; L. Rudee at the Materials Sciences Department at the University of California, San Diego; and S. Barlow at the San Diego State University provided transmission electron microscopy facilities and resources. C. Graham from the SIO Analytical Facility assisted with scanning electron microscopy. The American

Malacological Society and the SIO provided financial support.

LITERATURE CITED

Aitken, A. E., and R. Gilbert. 1996. Marine mollusca from Expedition Fiord, Western Axel Heiberg Island, Northwest Territories, Canada. *Arctic* **49**:29–43.

Allen, J. A. 1979. The adaptations and radiation of deep-sea bivalves. *Sarsia* **64**:19–27.

Barry, J. P., K. R. Buck, R. K. Kochevar, D. C. Nelson, Y. Fujiwara, S. K. Goffredi, and J. Hashimoto. 2002. Methane-based symbiosis in a mussel, *Bathymodiolus platifrons*, from cold seeps in Sagami Bay, Japan. *Invertebr. Biol.* **121**:47–54.

Beninger, P. G., and S. D. St-Jean. 1997. The role of mucus in particle processing by suspension-feeding marine bivalves: unifying principles. *Mar. Biol.* **129**:389–397.

Cattaneo-Vietti, R., M. Chiantore, S. Schiaparelli, and G. Albertelli. 2000. Shallow- and deep-water mollusc distribution at Terra Nova Bay (Ross Sea, Antarctica). *Polar Biol.* **23**:173–182.

Cavanaugh, C. M. 1994. Microbial symbiosis: patterns of diversity in the marine environment. *Am. Zool.* **34**:79–89.

Clarke, A. H. 1989. New molluscs from undersea oil seep sites off Louisiana. *Malacol. Data Net* **2**:122–134.

Coan, E. V., P. V. Scott, and F. R. Bernard. 2000. *Bivalve Seashells of Western North America.* Santa Barbara Museum of Natural History, Santa Barbara, CA. 764 pp.

Dall, W. H. 1899. Synopsis of the Lucinacea and of other American species. *Proc. U.S. Natl. Mus.* **23**:779–833.

Dando, P. R., and A. J. Southward. 1986. Chemoautotrophy in bivalve molluscs of the genus *Thyasira*. *J. Mar. Biol. Assoc. UK* **66**:915–929.

Dando, P. R., and B. Spiro. 1993. Varying nutritional dependence of the thyasirid bivalves *Thyasira sarsi* and *T. equalis* on chemoautotrophic symbiotic bacteria, demonstated by isotope ratios of tissue carbon and shell carbonate. *Mar. Ecol. Prog. Ser.* **92**:151–158.

Dell, R. K. 1990. Antarctic mollusca, with special reference to the fauna of the Ross Sea. *R. Soc. N.Z. Bull.* **27**:1–311.

Distel, D. L. 1998. Evolution of chemoautotrophic endosymbioses in bivalves. *BioScience* **48**:277–286.

Distel, D. L., and H. Felbeck. 1987. Endosymbiosis in the lucinid clams *Lucinoma aequizonata, Lucinoma annulata* and *Lucina floridana*: a reexamination of the functional morphology of the gills as bacteria-bearing organs. *Mar. Biol.* **96**:79–86.

Dubilier, N., R. Windoffer, and O. Giere. 1998. Ultrastructure and stable carbon isotope composition of the hydrothermal vent mussels *Bathymodiolus brevior* and *B.* sp. affinis *brevior* from the North Fiji Basin, western Pacific. *Mar. Ecol. Prog. Ser.* **165**:187–193.

Dufour, S. C., and H. Felbeck. 2003. Sulphide mining by the superextensile foot of symbiotic thyasirids. *Nature* **426**:65–67.

Duplessis, M. R., S. C. Dufour, L. E. Blankenship, H. Felbeck, and A. A. Yayanos. 2004. Anatomical and experimental evidence for particulate feeding in *Lucinoma aequizonata* and *Parvilucina tenuisculpta* (Bivalvia: Lucinidae) from the Santa Barbara Basin. *Mar. Biol.* **145**:551–561.

Endow, K., and S. Ohta. 1989. The symbiotic relationship between bacteria and a mesogastropod snail, *Alviniconcha hessleri*, collected from hydrothermal vents of the Mariana Back-Arc Basin. *Bull. Jap. Soc. Microb. Ecol.* **3**:73–82.

Fiala-Médioni, A., and M. Le Pennec. 1987. Trophic structural adaptations in relation to the bacterial association of bivalve molluscs from hydrothermal vents and subduction zones. *Symbiosis* **4**:63–74.

Fiala-Médioni, A., C. Métivier, A. Herry, and M. Le Pennec. 1986. Ultrastructure of the gill of the hydrothermal-vent mytilid *Bathymodiolus* sp. *Mar. Biol.* **92**:65–72.

Fisher, C. R. 1990. Chemoautotrophic and methanotrophic symbioses in marine invertebrates. *Rev. Aquat. Sci.* **2**:399–436.

Fleming, C. A. 1950. New Zealand Recent Thyasiridae (Mollusca). *Trans. R. Soc. N.Z.* **78**:251–254.

Fujiwara, Y., C. Kato, N. Masui, K. Fujikura, and S. Kojima. 2001. Dual symbiosis in the cold-seep thyasirid clam *Maorithyas hadalis* from the hadal zone in the Japan Trench, western Pacific. *Mar. Ecol. Prog. Ser.* **214**:151–159.

Gebruk, A. V., P. Chevaldonné, T. Shank, R. A. Lutz, and R. C. Vrijenhoek. 2000. Deep-sea hydrothermal vent communities of the Logatchev area (14°45′N, Mid-Atlantic Ridge): diverse biotopes and high biomass. *J. Mar. Biol. Assoc. UK* **80**:383–393.

Hickman, C. S. 1994. The genus *Parvilucina* in the Eastern Pacific: making evolutionary sense of a chemosymbiotic species complex. *Veliger* **37**:43–61.

Imhoff, J. F., H. Sahling, J. Süling, and T. Kath. 2003. 16S rDNA-based phylogeny of sulphur-oxidising bacterial endosymbionts in marine bivalves from cold-seep habitats. *Mar. Ecol. Prog. Ser.* **249**:39–51.

Iredale, T. 1930. Mollusca from the continental shelf of Eastern Australia. *Rec. Aust. Mus.* **17**:384–407.

Le Pennec, M., and A. Hily. 1984. Anatomie, structure et ultrastructure de la branchie d'un Mytilidae des sites hydrothermaux du Pacifique oriental. *Oceanol. Acta* **7**:517–523.

Le Pennec, M., M. Diouris, and A. Herry. 1988. Endocytosis and lysis of bacteria in gill epithelium of *Bathymodiolus thermophilus, Thyasira flexuosa* and *Lucinella divaricata* (Bivalve, Molluscs). *J. Shellfish Res.* **7**:483–489.

Le Pennec, M., P. G. Beninger, and A. Herry. 1995. Feeding and digestive adaptations of bivalve molluscs to sulphide-rich habitats. *Comp. Biochem. Physiol.* **111A**:183–189.

Lewis, K. B., and B. A. Marshall. 1996. Seep faunas and other indicators of methane-rich dewatering on New Zealand convergent margins. *N.Z. J. Geol. Geophys.* **39**:181–200.

López-Jamar, E., and S. Parra. 1997. Distribución y ecología de *Thyasira flexuosa* (Montagu, 1803) (Bivalvia, Lucinacea) en las rías de Galicia. *Publ. Espec. Inst. Esp. Oceanogr.* **23**:187–197.

McFall-Ngai, M. J. 1998. The development of cooperative associations between animals and bacteria: establishing detente among domains. *Am. Zool.* **38**:593–608.

Montgomery, M. K., and M. J. McFall-Ngai. 1993. The inductive role of bacterial symbionts in the morphogenesis of a squid light organ. *Am. Zool.* **35**:372–380.

Morse, M., and J. Zardus. 1991. Bivalvia. Pp. 7–118 in *Microscopic Anatomy of Invertebrates, Vol. 6A, Mollusca II.* F.W. Harrison and A.J. Kohn, eds. Wiley-Liss, New York.

Nicol, D. 1966. Description, ecology, and geographic distribution of some Antarctic pelecypods. *Bull. Am. Paleontol.* **51**:1–102.

Ockelmann, K. W. 1958. The zoology of east Greenland, marine Lamellibranchiata. *Medd. Grønl.* **122**:1–256.

Oliver, P. G., and I. J. Killeen. 2002. *The Thyasiridae (Mollusca: Bivalvia) of the British Continental Shelf and North Sea Oil Fields: An Identification Manual.* Studies in marine biodiversity and systematics from the National Museum of Wales. Biomôr Reports, Vol. 3 Cardiff, Wales. 73 pp.

Payne, C. M., and J. A. Allen. 1991. The morphology of deep-sea Thyasiridae (Mollusca: Bivalvia) from the Atlantic Ocean. *Philos. Trans. R. Soc. Lond. B* **334**:481–562.

Reid, R. G. B., and D. G. Brand. 1986. Sulfide-oxidizing symbiosis in Lucinaceans: implications for bivalve evolution. *Veliger* **29**:3–24.

Silverstein, S. C., R. M. Steinman, and Z. A. Cohn. 1977. Endocytosis. *Annu. Rev. Biochem.* **46**:669–722.

Smith, D. C. 1979. From extracellular to intracellular: the establishment of a symbiosis. *Proc. R. Soc. Lond. B* **204**:115–130.

Southward, E. C. 1986. Gill symbionts in thyasirids and other bivalve molluscs. *J. Mar. Biol. Assoc. UK* **66:**889–914.

Stasek, C. R. 1963. Orientation and form in the bivalved Mollusca. *J. Morphol.* **112:**195–214.

Verrill, A. E., and K. J. Bush. 1898. Revision of the deep-water mollusca of the Atlantic coast of North America, with descriptions of new genera and species. Part 1. Bivalvia. *Proc. U.S. Natl. Mus.* **20:** 775–901.

Vetter, R. D. 1985. Elemental sulfur in the gills of three species of clams containing chemoautotrophic symbiotic bacteria: a possible inorganic energy storage compound. *Mar. Biol.* **88:**33–42.

Windoffer, R., and O. Giere. 1997. Symbiosis of the hydrothermal vent gastropod *Ifremeria nautilei* (Provannidae) with endobacteria—structural analyses and ecological considerations. *Biol. Bull.* **193:**381–392.

Woolverton, C. J., L. C. Holt, D. Mitchell, and R. B. Sartor. 1992. Identification and characterization of rat intestinal lamina propria cells—consequences of microbial colonization. *Vet. Immunol. Immunopathol.* **34:**127–138.

Zimmermann, S., R. G. Hughes, and H. J. Flügel. 1997. The effect of methane seepage on the spatial distribution of oxygen and dissolved sulphide within a muddy sediment. *Mar. Geol.* **137:**149–157.

Reference: *Biol. Bull.* **208:** 213–220. (June 2005)

Holopelagic *Poeobius meseres* ("Poeobiidae," Annelida) Is Derived From Benthic Flabelligerid Worms

ADRIENE B. BURNETTE, TORSTEN H. STRUCK, AND KENNETH M. HALANYCH*

Auburn University, Department of Biological Sciences, Auburn, AL 36830, USA

Abstract. Phylogenetic relationships among and within the more than 70 recognized families of Annelida are poorly understood. In some cases, such as the monotypic Poeobiidae, derived morphology hinders the ability to find convincing synapomorphies that help elucidate evolutionary origins. In such cases, molecular data can be useful. Poeobiidae consists of the holopelagic polychaete *Poeobius meseres*, which is typically found in midwater depths off California. Morphologists have speculated that it is close to or within Flabelligeridae, but definitive evidence was lacking. Herein we use maximum likelihood phylogenetic reconstruction methods to examine the nuclear 18S rDNA (SSU) gene and the mitochondrial cytochrome *b* gene. Our results strongly support the hypothesis that *P. meseres* is a highly derived flabelligerid annelid closely related to *Therochaeta*. Thus, Poeobiidae is a junior synonym for Flabelligeridae. This result raises interesting questions about the evolution of the holopelagic *P. meseres* from a benthic ancestral flabelligerid.

Introduction

The holopelagic polychaete *Poeobius meseres*, which is up to 27 mm in length and has 11 poorly defined segments, is the sole recognized representative of Poeobiidae (Annelida; Fig. 1). It has been recorded from the eastern Pacific at depths of 350–1300 m (Rouse and Pleijel, 2001). The body is largely gelatinous with a thick mucus sheath, and segmentation is not clearly visible. The anterior end bears retractable pale green "tentacles," which consist of a pair of grooved palps and branchiae. Individuals of this species can be overlooked when taken because they are easily damaged by net tows and are amorphous out of water. However, some aspects of their biology are known (*e.g.*, metabolism—Thuesen and Childress, 1993; diet—Uttal and Buck, 1996). A second species, *Enigma terwillei*, has been attributed to Poeobiidae (Rouse and Pleijel, 2001), but it has only been collected once and the type material was lost. Therefore, it should be considered *incertae sedis* (of uncertain taxonomic position) as suggested by Fauchald (1977). The evolutionary origins of *P. meseres* are unclear, but there is speculation of a relationship to or within Flabelligeridae.

Flabelligeridae, known as bristle-cage worms, contains about 130 species in 14 recognized genera. These occupy many habitats ranging from intertidal zones to deep-sea muds, and are from 5 mm to 220 mm in length (Rouse and Pleijel, 2001). Members of Flabelligeridae are typically recognized by their unique and complex anterior end. The prostomium and peristomium are fused, forming a retractable head that in most cases (*e.g.*, *Flabelligera*, *Pherusa*, and *Diplocirrus*) is protected by a cage of modified setae from the first few parapodia (Spies, 1975; Blake, 2000). The body is often coated with sediment granules or a mucus sheath (Fauchald and Rouse, 1997).

Information on flabelligerid biology is limited. Spies (1977) found that *Flabelligera commensalis* retains gametes in the coelomic peritoneum until just before spawning. For comparison, many polychaetes shed their gametes directly into the coelom to mature. Studies of flabelligerid and *P. meseres* larvae are lacking (but see Spies, 1977). Some flabelligerids (*e.g.*, *Flabelligera affinis*) are motile surface-deposit feeders, whereas most others (*e.g.*, *Pherusa plumosa* and *Brada villosa*) are discretely motile, feeding in cracks and crevices (Fauchald and Jumars, 1979). Grooved palps and current-generating branchial fields are thought to be used in feeding (Fauchald and Jumars, 1979). Flabelligerids have a fossil record from about 295 million years ago in the Francis Creek Shale of Illinois (Carbondale Formation, Desmoinesian Series, Middle Pennsylvanian System of North America; Hay, 2002). Fossils have been placed into

Received 17 September 2004; accepted 22 February 2005.
* To whom correspondence should be addressed. E-mail:ken@auburn.edu

Figure 1. Individual of *Poeobius meseres* floating in the water column. Photo credit: MBARI ROV *Tiburon* and Karen Osborn.

one species, *Mazopherusa primosi*, which is most similar to the extant *Pherusa* on the basis of the cephalic cage. One additional worm that deserves mention is *Flota flabelligera*, another pelagic polychaete. Hartman (1967) initially considered it a flabelligerid, but she later transferred it to Fauveliopsidae (1971). Recently, *Flota* has been considered to be closely related to taxa in Terebellida and especially to *Poeobius* (Rouse and Pleijel, 2001, 2003). Under the Linnean system, *Flota* is still considered a separate family. Neither *F. flabelligera* nor *P. meseres* is known to have a fossil record.

To our knowledge, a formal phylogenetic hypothesis has never been proposed for relationships within Flabelligeridae. The first flabelligerid (*Amphitrite plumosa*, now *Pherusa plumosa*) was formally described in 1776 by Müller, and the family was erected in 1894 by Saint-Joseph. The current taxonomic scheme for the group is based largely on the works of Haase (1915), Fauvel (1927), Stop-Bowitz (1948), Day (1961, 1967), and Hartman (1961, 1969). Recent morphological cladistic analyses (Rouse and Fauchald, 1997; Rouse and Pleijel, 2001) place Flabelligeridae within Cirratuliformia, Terebellida, and Canalipalpata. Relationships within this putative clade (also including Acrocirridae, Cirratulidae, Ctenodrilidae, Fauveliopsidae, Poeobiidae, and Sternaspidae) remain unclear.

With the recognition of Poeobiidae Heath 1930, the monophyly of Flabelligeridae has been called into question. There are morphological similarities between these two groups, such as the presence of a retractable head, a pair of grooved palps, an anterior ring of branchiae, and a gelatinous mucus sheath, although some of these features are not exclusive to these taxa. Fauchald and Jumars (1979) also thought that these two groups belong to the same feeding guild—filter-feeding, discretely motile, tentacular—because the palps of Poeobiidae resemble those of flabelligerids. *P. meseres* was originally thought by Heath (1930) to be the link between the Annelida and "Echiuroidea," but later Pickford (1947, cited in Robbins, 1965) labeled it an aberrant polychaete. Hartman (1955) first pointed out the remarkable resemblance *P. meseres* has to flabelligerids—for example, the cephalic structure and the thick gelatinous membrane around the trunk region. Dales (1962) considered *P. meseres* to be an offshoot of the flabelligerids, leading Robbins (1965) to suggest that the relationship between Flabelligeridae and *P. meseres* be assessed in detail due to morphological similarities. Rouse and Fauchald's (1997) morphological cladistic analysis consistently placed Flabelligeridae closer to Fauveliopsidae and Sternaspidae than to Poeobiidae. Later, Rouse and Pleijel (2003) suggested that the recognition of Poeobiidae renders Flabelligeridae paraphyletic by presenting a strict consensus tree in which *Poeobius* and *Flota* are nested among three flabelligerid taxa (*Brada*, *Pherusa*, and *Flabelligera*). They present an anterior branchial cluster as the only non-homoplastic morphological apomorphy to support the *Poeobius*/*Flota*/flabelligerid clade. Rouse and Pleijel acknowledge that "the exact nature of . . .[the extreme anterior branchial cluster] is still unresolved" (p. 181), and given that several other polychaete taxa have anterior branchiae/palps/tentacles, the nature of this apomorphy is tenuous. Furthermore, their analysis fails to assess the robustness of their recovered topologies over alternative hypotheses. Thus, the question of whether *P. meseres* falls within Flabelligeridae is still open to debate.

The purpose of this study is to examine the position of *P. meseres*. In doing so, we hope to begin examining relationships within Flabelligeridae. We examined data from two molecular markers, 18S rDNA and cytochrome *b*, using maximum likelihood. Our phylogenetic results will allow us to look for changes that accompany the transition from a benthic to a holopelagic mode of life.

Materials and Methods

Specimens

The taxa sampled in this study, their collection locality, voucher specimen number, and GenBank numbers are listed in Table 1. Limited taxon sampling in this study was due to the difficulty in obtaining samples from deeper waters. Three outgroups, *Sternaspis* sp., *Fauveliopsis glabra*, and *Cirratulus spectabilis* were chosen on the basis of recent studies (Rouse and Fauchald, 1997; Rouse and Pleijel, 2001). All specimens were stored at −80° C or at 4 °C in ethanol immediately after collection. For most specimens, species identification was made at the time of collection and subsequently confirmed by Sergio Salazar-Vallejo (Unidad

Table 1

Taxonomic inclusion, locality information and GenBank accession numbers

Taxon	GenBank Accession No. 18S	GenBank Accession No. Cyt *b*	Museum number	Collection site	Latitude	Longitude
Ingroup Taxa						
Brada villosa 1	AY708535		USNM 1073349	Central California, USA	36°50.860′N	121°53.749′W
Brada villosa 2*		AY727748	USNM 1073357	Trondheimsfjord, Norway	63°32.745′N	10°14.910′E
Diplocirrus glaucus 1	AY708533	AY727750	completely used	Geitnstranda, Trondheim, Norway	63°24.00′N	9°58.67′E
Diplocirrus glaucus 2*	AY708534	AY727751	USNM 1073353	West Gullmarsfjorden, Sweden	58°13.30′N	11°20.20′E
Flabelligera affinis 1	AY708531	AY727755	USNM 1073355	Central California, USA	36°49.847′N	122°01.729′W
Flabelligera affinis 2*	AY708532		USNM 1073354	Gullmarsfjorden, Sweden	58°13.154′N	11°24.416′E
Ilyphagus octobranchus	AY708530	AY727749	USNM 1073351	South of Woods Hole, Massachusetts, USA	39°54.134′N	70°35.054′W
Pherusa plumosa 1	AY708529	AY727756	USNM 1073348	South of Woods Hole, Massachusetts, USA	40°53.019′N	70°25.003′W
Pherusa plumosa 2	AY708528	AY727752	USNM 1073356	Central California, USA	36°49.847′N	122°01.729′W
Therochaeta collarifera	AY708527	AY727753	USNM 1073350	South of Woods Hole, Massachusetts, USA	39°54.134′N	70°35.054′W
Poeobius meseres	AY708526	AY727754	USNM 1073358	Monterey Canyon, California, USA	36°41.228′N	122°01.965′W
Outgroup Taxa						
Cirratulus spectabilis	AY708536	AY727746	USNM 1073359	Snug Harbor, Washington, USA	48°34.317′N	123°10.115′W
Fauveliopsis glabra	AY708537		USNM 1073352	South of Woods Hole, Massachusetts, USA	39°54.085′N	69°54.601′W
Sternaspis sp. '*Banyuls*'†	AB106264					

* Sample kindly provided by Fredik Pleijel.

† 18S rDNA *Sternaspis* data are from Hall *et al.* (2004).

Chetumal, Mexico). Fredrik Pleijel identified the three specimens that he kindly provided (Table 1). Herein we have decided to follow the taxonomy of Blake (2000). However, Salazar-Vallejo has noted that both *Brada villosa* and *Fabelligera affinis* may be over-synonymized. He mentioned that, given the older literature, the following designations are probably correct and may be re-erected in the near future: our *Brada villosa* 1 = *B. pluribranchiata* and our *Flabelligera affinis* 1 = *F. infundibularis*. Also *B. villosa* from Norway is probably referable to *B. pilosa*. Voucher specimens have been deposited in the Smithsonian Museum of Natural History (Washington DC).

Data collection

For most tissues, DNA was extracted using the DNeasy Tissue Extraction Kit (Qiagen, Valencia, CA) according to the manufacturer's protocol. However, for *Poeobius meseres*, a standard phenol/chloroform with proteinase K extraction procedure was used (Hillis *et al.*, 1996). The 18S rDNA gene and approximately 420 basepairs of the cytochrome *b* (cyt *b*) mitochondrial gene were amplified and sequenced using the primers listed in Table 2. Amplification *via* HotStart-PCR of 18S (thermocycler profile: 3 min 94 °C; addition of polymerase; 3 min 94 °C; 40 cycles: 1 min 94 °C, 1 min 30 s 40 °C, 2 min 30 s 72 °C; 1 cycle: 7 min 72 °C; reaction-mix: 10 m*M* Tris-HCl pH 9.0, 50 m*M* KCl, 0.1% Triton X-100, 2.5 m*M* $MgCl_2$, ~ 1 ng/μl genomic DNA, 0.4 m*M* dNTPs, 0.8 μM of each primer, 0.03 U/μl *Taq* DNA Polymerase (Promega, Madison, WI)) was carried out in a volume of 25 μl. The cyt *b* protocol used the same recipe but a different thermocycling protocol (3 min 94 °C; addition of polymerase; 2 min 94 °C; 15 cycles: 30 s 94 °C, 30 s 42 °C, 30 s 72 °C; 20 cycles: 30 s 94 °C, 30 s 37 °C, 45 s 72 °C; 1 cycle: 7 min 72 °C). PCR products were isolated on 1% agarose gels. The appropriate-sized bands were excised and purified using the QIAquick Gel Extraction Kit (Qiagen, Valencia, CA). Purified products were quantified using a mass standard on 1% agarose gels. Bi- directional Sequences were determined on an ABI Prism 3100 (using the BigDye ver. 3.0 kit, Applied Biosystems, Foster City, CA) or a Beckman CEQ 8000 (using one-half reactions of the CEQ DTCS Quick Start Kit, Beckman Coulter, Fullerton, CA).

Sequences were assembled and edited using the LaserGene package (DNAStar, Inc., Madison, WI). The sequences were then aligned using ClustalX (Thompson *et al.*, 1997). The alignment was corrected by eye in MacClade ver. 4.06 (Maddison and Maddison, 2003). Regions of the 18S data that could not be unambiguously aligned were excluded from the analyses. The cyt *b* alignment was translated to inferred amino acid sequence using the *Drosophila* mitochondrial DNA code to check for sequencing errors. Alignments (Accession #S1268 and #M2212–2214) are available at TREEBASE (www.treebase.org).

Phylogenetic analysis

Phylogenetic analyses used maximum likelihood (ML) methods for both data sets individually and for combined

Table 2

Nucleotide primers used in amplification and sequencing

Primer	Sequence 5′-3′	Reference
18S rDNA		
Amp. & Seq.		
18e	CTG GTT GAT CCT GCC AGT	Hillis and Dixon, 1991
18R	GTC CCC TTC CGT CAA TTY CTT TAA G	Halanych, unpublished
18O	GGA ATR ATG GAA TAG GAC C	Halanych *et al.*, 1998
18R1779	TGT TAC GAC TTT TAC TTC CTC TA	Struck *et al.*, 2002
18P	TAA TGA TCC TTC CGC AGG TTC ACC T	Hillis and Dixon, 1991
Sequencing only		
18L	GAA TTA CCG CGG CTG CTG GCA CC	Hillis and Dixon, 1991
18H	AGG GTT CGA TTC CGG AGA GGG AGC	Hillis and Dixon, 1991
18F509	CCC CGT AAT TGG AAT GAG TAC A	This study
18F997	TTC GAA GAC GAT CAG ATA CCG	This study
18R925D	GAT CYA AGA ATT TCA CCT CT	This study
18R993D	CTT GRC AAA TGC TTT CGC	This study
18Q	TGT CTG GTT AAT TCC GAT AAC	Halanych *et al.*, 1998
18Qϕ	GTT ATC GGA ATT AAC CAG ACA	Halanych *et al.*, 1998
18F1435	AGG TCT GTG ATG CCC TTA GAT	This study
Cytochrome b		
Amp. & Seq.		
Cytb 424F (RT-1)	GGW TAY GTW YTW CCW TGR GGW CAR AT	Boore and Brown, 2000
Cytb 876R (RT-2)	GCR TAW GCR AAW ARR AAR TAY CAY TCW GG	Boore and Brown, 2000
Sequencing only		
cobr825	AAR TAY CAY TCI GGY TTR ATR TG	Jennings and Halanych, 2005

data. For cyt *b*, nucleotide data with and without third positions were analyzed. Combined analyses used cyt *b* without third positions. ML analyses with a heuristic search of 100 random sequence addition replicates and tree-bisection-reconnection (TBR) were conducted using PAUP* 4.0b10 (Swofford, 2002). ModelTest 3.06 (Posada and Crandall, 1998) was used to select the model of evolution with the best fit for each data set (see below). Nodal support was estimated using a bootstrap analysis consisting of 1000 heuristic iterations with random sequence addition.

In addition, using MrBayes (Huelsenbeck and Ronquist, 2001), we conducted a Bayesian inference analysis on the inferred amino acid data to determine if there was additional phylogenetic information in the cyt *b* data. To do this, we inferred amino acid residues using the *Drosophila* mtDNA translation code. The Bayesian search employed the amino acid model with all the priors set to default settings. Two million generations were run with four chains (3 cold and 1 hot) that were sampled every 200 generations.

The constraints option within an ML heuristic search (as above) was used to generate topologies consistent with alternative hypotheses. Resultant trees were compared with unconstrained ML results using the Shimodaira-Hasegawa test (Shimodaira and Hasegawa, 1999) implemented in PAUP* 4.0b10. Only the 18S data set was used because multiple outgroups allowed for testing the monophyly of Flabelligeridae, including *P. meseres*.

Results

The 18S rDNA data set included 13 terminal taxa and 2106 characters. Of the 1474 nucleotide positions that could be unambiguously aligned, 28.1% (414 positions) were variable and 18.3% (270 positions) were parsimony informative. ModelTest indicated a TrNef+Γ model (nucleotide frequencies equal; rates A⇔C 1.0000, A⇔G 2.2477, A⇔T 1.0000, C⇔G 1.0000, C⇔T 3.6285, G⇔T 1.000; gamma shape parameter = 0.2552) for the ML analysis. The single best ML tree (Ln likelihood = −6283.79641) is shown in Figure 2. A monophyletic Flabelligeridae clade including *Poeobius meseres* was recovered with a bootstrap value of 100%. Specifically, *P. meseres* falls as a sister taxon to *Therochaeta collarifera* (bootstrap 100%). The result that *Ilyphagus octobranchus* appears to be very closely related to *Diplocirrus glaucus* (bootstrap = 98%) is noteworthy.

The cytochrome *b* nucleotide data set consisted of 11 terminal taxa and 404 characters; the number of characters was reduced to 318 once the ends were trimmed. Of those, 57.2% (182 positions) were variable and 42.1% (134 positions) were parsimony informative. ModelTest indicated a TVM + Γ + I model (nucleotide frequencies A = 0.28290, C = 0.24680, G = 0.09230, T = 0.37800; rates A⇔C 3.3592, A⇔G 34.9373, A⇔T 15.4450, C⇔G 8.4295, C⇔T 34.9373, G⇔T 1.000; proportion of invariant sites = 0.3275; gamma shape parameter = 0.9565) for this analysis.

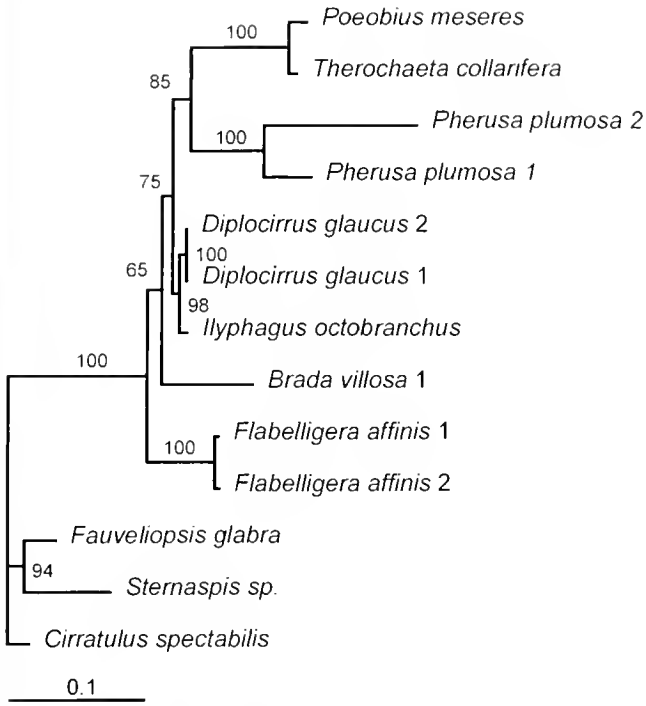

Figure 2. The single best 18S maximum likelihood tree (Ln likelihood = −6283.79641) based on 18SrDNA data set (see text for details). Bootstrap support values (>50%) out of 1000 iterations are represented at each node.

When third positions were included, a single best ML tree (Ln likelihood = −2157.13859) placed *P. meseres* within Flabelligeridae, but there was only weak (50%) bootstrap support (not shown). However, third positions appeared saturated because 94.3% (100 of 106 positions) of them displayed variation. Therefore, an ML analysis minus the third position was also performed, using a K81uf + Γ model with nucleotide frequencies A = 0.24400, C = 0.22550, G = 0.15250, T = 0.37800, rates A⇔C 1.0000, A⇔G 5.2849e+06, A⇔T 2.0229e+06, C⇔G 2.0229e+06, C⇔T 5.2849e+06, G⇔T 1.000, and gamma shape parameter = 0.2079. This tree (Ln likelihood = −962.14976; Fig. 3A) also grouped *P. meseres* with *Therochaeta collarifera*, but with a low bootstrap value (62%). As in the 18S analysis, *Ilyphagus octobranchus* and *Diplocirrus glaucus* are sister taxa, but with a bootstrap support less than 50%. Similarly, the Bayesian analysis of the amino acid data was poorly supported. Thus, for the sake of simplicity, that analysis is not described herein.

For the cyt *b* dataset, the percent divergence of the European and North American *Pherusa plumosa* is notable (10.8% for uncorrected distance). Further analysis is needed to assess whether the current nomen "*Pherusa plumosa*" represents multiple species.

The combined dataset consisted of 10 taxa with 2424

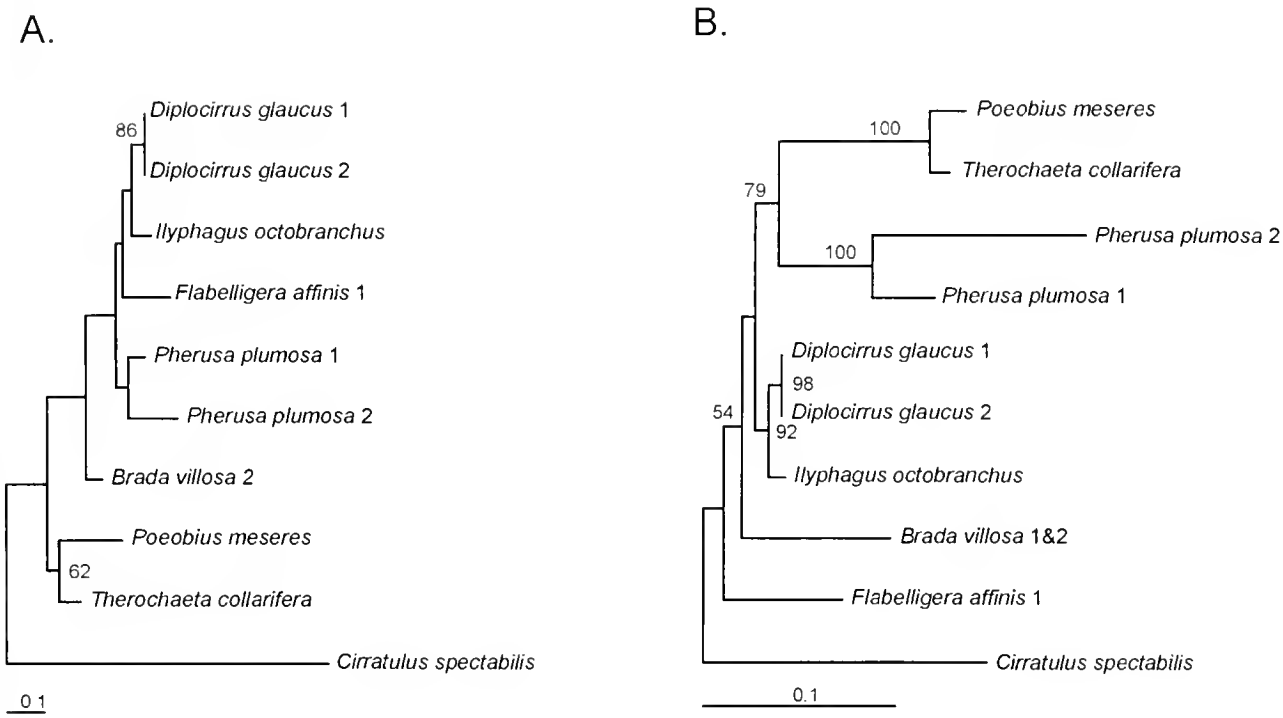

Figure 3. (A) The single best maximum likelihood tree (Ln likelihood = −962.14976) based on the cyt *b* nucleotide data set minus third positions (see text for details). (B) The single best maximum likelihood tree (Ln likelihood = −5810.60410) based on a combined data set of 18SrDNA and cyt *b* minus third positions (see text for details). For both trees, bootstrap support values (>50%) out of 1000 iterations are represented at each node.

Table 3

Shimodaira-Hasegawa results comparing alternative hypotheses[1]

Alternative hypotheses tested	Ln likelihood score	*P* value
Best Tree	−5369.97048	
Poeobius meseres outside Flabelligeridae	−5754.28014	<0.001*
Poeobius meseres & *Therochaeta collarifera* not sisters	−5466.10841	<0.001*
Hyphagus octobranchus & *Diplocirrus glaucus* not sisters	−5376.96342	0.666

[1] Alternative hypotheses are written contrary to what is observed in best tree. Thus *P* values represent significance of support for relationships observed in the "best tree" over these alternatives.

* $P < 0.05$.

nucleotide characters. When ambiguously aligned positions and cyt *b* third positions were excluded (1687 nucleotides remaining), 28.1% (474 positions) were variable and 14.5% (245 positions) were parsimony informative. Because of data availability, only one outgroup (*Cirratulus spectabilis*) was used, accounting for the lower number of variable sites when compared to the 18S dataset. The model for the combined data was a GTR + Γ + I using the following parameters: nucleotide frequencies A = 0.26400, C = 0.21870, G = 0.25330, T = 0.26400; rates A⇔C 1.2605, A⇔G 2.4146, A⇔T 3.2160, C⇔G 0.7243, C⇔T 7.5504, G⇔T 1.000; proportion of invariant sites = 0.393; gamma shape parameter = 0.5704. Given the absence of *Fauveliopsis glabra, Sternaspis* sp., and *Flabelligera affinis*, the topology of the combined data tree (Ln likelihood = −5810.60410; Fig. 3B) was identical to the 18S results, with a monophyletic Flabelligeridae including *P. meseres* as sister to *Therochaeta collarifera*. There was also strong support for *Hyphagus octobranchus* with *Diplocirrus glaucus* (bootstrap = 92%).

Table 3 presents Shimodaira-Hasegawa results of the hypotheses tested. The alternative hypotheses that *P. meseres* is neither a flabelligerid ingroup taxon nor the sister taxon of *Therochaeta collarifera* are significantly worse than the best hypothesis. However, the hypothesis that *Hyphagus octobranchus* and *Diplocirrus glaucas* are not sister taxa to each other is not significantly worse than the best tree.

Discussion

All analyses described herein are consistent with placement of the holopelagic *Poeobius meseres* within Flabelligeridae, and specifically as sister taxon to *Therochaeta collarifera*. Even though only about half (6) of the recognized flabelligerid genera are included in our study, support that *P. meseres* is within the Flabelligeridae is very strong on the basis of bootstrap proportions (100%) and a Shimodaira-Hasegawa test ($P < 0.001$). Morphological studies suggest that *P. meseres* falls within or close to the flabelligerids (Hartman, 1955; Robbins, 1965; Rouse and Fauchald, 1997; Rouse and Pleijel, 2001, 2003; S. Salazar-Vallejo, Unidad Chetumal, Mexico, pers. comm.). Because of the agreement in morphological and molecular data, we formally propose that *Poeobius meseres* be referred to Flabelligeridae Saint-Joseph, 1894. This action makes "Poeobiidae" (Heath, 1930) a junior synonym of Flabelligeridae Saint-Joseph, 1894.

Two additional holopelagic worms, *Enigma terwillei* and *Flota flabelligera*, deserve mention in making this placement of *P. meseres*. First, as stated earlier, *E. terwillei* should be considered *incertae sedis*. However, if the initial and only description was accurate, it should also be referred to Flabelligeridae in the spirit of Rouse and Pleijel (2003). Second, although the suggestion that *Flota* is closely related to *Poeobius* (Rouse and Pleijel, 2003) awaits confirmation by definitive synapomorphies or a well-supported phylogenetic hypothesis, if it is correct, we must consider the possibility that there has been a radiation of holopelagic forms within Flabelligeridae.

The placement of *P. meseres* within Flabelligeridae is evolutionarily interesting because it suggests that this holopelagic species evolved from a benthic form. A notable change that presumably accompanied this transition was a reduction in thickness of the body wall that allowed *P. meseres* to be largely transparent. Many animals have transparent planktonic forms in which subcellular structures are arranged to reduce their reflectivity and scattering of light (Johnsen, 2001). For example, many transparent organisms cover the external surface with microscopic protrusions to reduce reflectivity. "Extracellular tissues" also help to lower scattering. On the basis of Johnsen's work, we predict that similar subcellular rearrangement will be observed in *P. meseres*.

The evolutionary origins of *P. meseres* may be the result of heterochrony during development. Although little is known about larval development in most flabelligerids, Spies (1977) investigated *Flabelligera commensalis* and concluded that there was evidence for midwater spawning. During the 11-setiger stage of *F. commensalis*, bristles form on the anterior end, and development of adult setae progresses from the anterior to the posterior. Additionally, *F. commensalis* has feeding larvae (Spies, 1977). How much similarity exists between the adult form of *P. meseres* and, for example, a larval stage of *Therochaeta* is not clear, and more complete larval and developmental studies need to be completed. Nonetheless, what is known is suggestive of heterochrony, specifically progenesis. *P. meseres*, in the transition from a benthic to a pelagic form, has lost all obvious external segmentation, including setae. Hartman (1955) observed that the only evidence of segmentation is the midventral ganglia with 11 apparent segments (see also

Heath, 1930). If the development of *F. commensalis* can be generalized to other flabelligerids, then the ancestor of *Poeobius* may have been a benthic flabelligerid with midwater spawning and relatively late development of setae (*i.e.*, at or after the 11-setiger stage). Given a feeding larvae as seen in *F. commensalis*, then selective forces favoring a prolonged planktonic stage (*e.g.*, lower risk of predation than metamorphosed juveniles, more consistent food supply, better opportunity to encounter mates) could have easily favored the evolution of a *Poeobius*-like organism.

Among annelids, there are presumably other examples of transition from benthic to pelagic form; these include *Flota*, alciopids, lopadorhynchids, isopilids, *Pontodora*, typhloscolecids, and tomopterids. All of these forms have retained segments with well-developed parapodia. Most of them are presumed to be active swimmers in the water column. These attributes are characteristic of Phyllodocida, the major annelid clade in which these taxa are placed (except *Flota;* Rouse and Pleijel, 2001). Because we do not understand the exact phylogenetic placement of these groups, it is hard to hypothesize the mechanism by which they evolved a holopelagic lifestyle. Although progenesis cannot be ruled out, some of these organisms may have evolved directly from an adult form (*e.g.*, tomopterids). In the case of *P. meseres*, the lack of adult structures argues for a larval origin.

Even though cyt *b* data are largely unresolved, 18S provides information that allows us to begin to address flabelligerid systematics. *Ilyphagus* groups with *Diplocirrus*, a result consistent with observed morphology (Hartman, 1965; S. Salazar-Vallejo, pers. comm.). Furthermore, these taxa displayed the lowest cyt *b* intergeneric divergence values (7.08%, range of others 9.0%–19.3%) within Flabelligeridae. In the Shimodaira- Hasegawa tests, the best tree that did not have *Ilyphagus octobranchus* and *Diplocirrus glaucus* as sister taxa made them a polytomy rather than splitting them apart. This may explain the disparity between high bootstrap support and a nonsignificant Shimodaira-Hasegawa value. To better elucidate the relationships within Flabelligeridae, we are currently working on obtaining a wider representation of taxa for molecular analyses.

We had hoped that the combination of a more conserved gene (18S) and a more quickly evolving gene (cyt *b*) would provide phylogenetic information at several levels. Unfortunately, cyt *b* seems to provide little information at either the nucleotide or amino acid levels. For the question at hand, synonymous positions have apparently experienced saturation by multiple mutations, thereby obliterating the phylogenetic signal, and the nonsynonymous positions have not changed enough to record shared history. This situation has been reported previously in cyt *b* (Halanych and Robinson, 1999). The only other polychaete paper that we know to have employed cyt *b* for evolutionary history is Breton *et al.* (2003), but those authors used mainly third positions to infer history within a species in a phylogeographic context. Cyt *b* was not useful in our study, but it has potential for being a useful phylogentic marker, and we would encourage others to explore the gene in other annelid groups.

In summary, our results provide strong support for placement of *P. meseres* within a monophyletic Flabelligeridae. Thus, "Poeobiidae" (Heath, 1930) is an invalid name because it is a junior synonym to Flabelligeridae Saint-Joseph, 1894.

Acknowledgments

The crews of the R/V *Point Sur* and R/V *Oceanus* were most helpful in obtaining samples. For both cruises, we also acknowledge the help of the scientific crews (which are too numerous to list here). We are grateful for research support at Friday Harbor Laboratories, University of Washington. Fredrik Pleijel kindly provided samples, and Karen Osborn helped with the figures. Early drafts of this paper were greatly improved by discussion with Sergio Salazar-Vallejo. Constructive comments from Jim Blake, an anonymous reviewer, and a not-so- anonymous reviewer were most helpful. This work was supported by the WormNet grant (EAR-0120646) from the National Science Foundation to KMH. This work is AU Marine Biology contribution #1.

Literature Cited

Blake, J. A. 2000. Family Flabelligeridae Saint Joseph, 1894. Pp. 1–23 in *Taxonomic Atlas of the Benthic Fauna of the Santa Maria Basin and Western Santa Barbara Channel. Volume 7 - The Annelida Part 4, Polychaeta: Flabelligeridae to Sternaspidae*, J. A. Blake, B. Hilbig, and P. V. Scott, eds. Santa Barbara Museum of Natural History, Santa Barbara, CA.

Boore, J. L., and W. M. Brown. 2000. Mitochondrial genomes of *Galathealinum, Helobdella*, and *Platynereis:* sequence and gene arrangement comparisons indicate that Pogonophora is not a phylum and Annelida and Arthropoda are not sister taxa. *Mol. Biol. Evol.* **17:** 87–106.

Breton, S., F. Dufresne, G. Desrosier, and P. U. Blier. 2003. Population structure of two northern hemisphere polychaetes, *Neanthes virens* and *Hediste diversicolor* (Nereididae), with different life-history traits. *Mar. Biol.* **142:** 707–715.

Dales, R. P. 1962. The polychaete stomodeum and the interrelationships of the families of the Polychaeta. *Proc. Zool. Soc. Lond.* **139:** 289–328.

Day, J. H. 1961. The polychaete fauna of South Africa. Part 6. Sedentary species dredged off Cape coasts with a few new records from the shore. *J. Linn. Soc. Lond. (Zool.)* **10:** 463–560.

Day, J. H. 1967. A monograph on the Polychaeta of southern Africa. Part 1. Errantia. British Museum of Natural History, London.

Fauchald, K. 1977. *The Polychaete Worms: Definitions and Keys to the Orders, Families, and Genera.* Los Angeles County Natural History Museum, Los Angeles.

Fauchald, K., and P. Jumars. 1979. The diet of worms: a study of polychaete feeding guilds. *Oceanogr Mar. Biol.* **17:** 193–284.

Fauchald, K., and G. W. Rouse. 1997. Polychaete systematics: past and present. *Zool. Scr.* **26:** 71–138.

Fauvel, P. 1927. Polychetes Sedentaires. Addenda aux Errantes, Archiannelides, Myzostomaires. *Faune Fr.* **16:** 1–494.

Haase, P. 1915. Boreale und arktische Chloraemiden. *Wiss. Meeresunters. Kiel* **17:** 169–228.

Halanych, K.M., and T.J. Robinson. 1999. Multiple substitutions affect the phylogenetic utility of cytochrome *b* and 12S rDNA data: examining a rapid radiation in leporid (Lagomorpha) evolution. *J. Mol. Evol.* **48:** 369–379.

Halanych, K. M., R. A. Lutz, and R. C. Vrijenhoek. 1998. Evolutionary origins and age of vestimentiferan tube-worms. *Cah. Biol. Mar.* **39:** 355–358.

Hall, K. A., P. A. Hutchings, and D. J. Colgan. 2004. Further phylogenetic studies of the Polychaeta using 18S rDNA sequence data. *J. Mar. Biol. Assoc. UK* **84:** 949–960.

Hartman, O. 1955. Endemism in the North Pacific Ocean, with emphasis on the distribution of marine annelids, and descriptions of new or little known species. Pp. 39–57 in *Essays in the Natural Sciences in Honor of Captain Allan Hancock,* University of Southern California Press, Los Angeles.

Hartman, O. 1961. Polychaetous annelids from California. *Allan Hancock Pacific Exped.* **25:** 1–226.

Hartman, O. 1965. *Deep-water Benthic Polychaetous Annelids off New England to Bermuda and Other North Atlantic Areas.* University of Southern California Press, Los Angeles.

Hartman, O. 1967. Poychaetous annelids collected by the USNS *Eltanin* and *Staten Island* cruises, chiefly from Antarctic seas. *Allan Hancock Monogr. Mar. Biol.* **2:** 1–387.

Hartman, O. 1969. *Atlas of Sedentariate Polychaetous Annelids from California.* Allan Hancock Foundation, University of Southern California, Los Angeles.

Hartman, O. 1971. Abyssal polychaetous annelids from the Mozambique basin off Southeast Africa, with a compendium of abyssal polychaetous annelids from world-wide areas. *J. Fish. Res. Board Can.* **28:** 1407–1428.

Hay, A. A. 2002. Flabelligerida from the Francis Creek Shale of Illinois. *J. Paleontol.* **76:** 764–766.

Heath, H. 1930. A connecting link between the Annelida and the Echiuroidea (Gephyrea Armata). *J. Morphol.* **49:** 223–249.

Hillis, D. M., and M. T. Dixon. 1991. Ribosomal DNA: molecular evolution and phylogenetic inference. *Q. Rev. Biol.* **66:** 411–453.

Hillis, D. M., B. K. Mable, A. Larson, S. K. Davis, and E. A. Zimmer. 1996. Nucleic acids IV: sequencing and cloning. Pp. 321–381 in *Molecular Systematics,* D. M. Hillis, C. Mortiz, and B. K. Mable, eds. Sinauer Associates, Sunderland, MA.

Huelsenbeck, J. P., and F. Ronquist. 2001. MRBAYES: Bayesian inference of phylogenetic trees. *Bioinformatics* **17:** 754–755.

Jennings, R. M., and K. M. Halanych. 2005. Mitchondrial genomes of *Clymenella torquata* (Maldanidae) and *Riftia pachyptila* (Siboglinidae): evidence for conserved gene order in Annelida. *Mol. Biol. Evol.* **22:** 210–222.

Johnsen, S. 2001. Hidden in plain sight: the ecology and physiology of organismal transparency. *Biol. Bull.* **201:** 301–318.

Maddison, D., and W. Maddison. 2003. MacClade 4.06: a tool for phylogenetic analysis and character evolution. Sinauer Associates, Sunderland, MA.

Müller, O. F. 1776. *Zoologicae Danicae prodromus, seu Animalium Daniae et Norvegiae indigenarum characteres, nomina et synonyma imprimis popularium.* Hallageriis, Copenhagen.

Pickford, G. E. 1947. Histological and histochemical observations upon an aberrant annelid, *Poecobius meseres* Heath. *J. Morphol.* **80:** 287–319. (Cited in Robbins, 1965.)

Posada, D., and K. A. Crandall. 1998. Modeltest: testing the model of DNA substitution. *Bioinformatics* **14:** 817–818.

Robbins, D. E. 1965. The biology and morphology of the pelagic annelid *Poecobius meseres* Heath. *J. Morphol.* **146:** 197–212.

Rouse, G. W., and K. Fauchald. 1997. Cladistics and polychaetes. *Zool. Scr.* **26:** 139–204.

Rouse, G. W., and F. Pleijel. 2001. *Polychaetes.* Oxford University Press, Oxford.

Rouse, G. W., and F. Pleijel. 2003. Problems in polychaetes systematics. *Hydrobiologia* **496:** 175–189.

Saint-Joseph, A. 1894. Les Annelides polychetes des cotes de Dinard. Troisieme partie. *Ann. Sci. Nat. Zool. Paleontol. Ser. 7* **17:** 1–395.

Shimodaira, H., and M. Hasegawa. 1999. Multiple comparisons of Log-likelihoods with applications to phylogenetic inference. *Mol. Biol. Evol.* **16:** 1114–1116.

Spies, R. B. 1975. Structure and function of the head in flabelligerid polychaetes. *J. Morphol.* **147:** 187–207.

Spies, R. B. 1977. Reproduction and larval development of *Flabelliderma commensalis.* Pp. 323–345 in *Essays on Polychaetous Annelids in Memory of Dr. Olga Hartman,* D. J. Reish, and K. Fauchald, eds. The Allan Hancock Foundation, University of Southern California, Los Angeles.

Støp-Bowitz, C. 1948. Sur les polychètes arctiques. *Tromsø Mus. Årsh.* **66:** 1–58.

Struck, T. H., R. Hessling, and G. Purschke. 2002. The phylogenetic position of Aeolosomatidae and Parergodrilidae, two enigmatic oligochaete-like taxa of the "Polychaeta," based on molecular data from 18S rDNA sequences. *J. Zool. Syst. Evol. Res.* **40:** 155–163.

Swofford, D. L. 2002. *PAUP* Phylogenetic Analysis Using Parsimony (*and other Methods).* Version 4 Sinauer Associates, Sunderland, MA.

Thompson, J. D., T.J. Gibson, F. Plewniak, F. Jeanmougin, and D.G. Higgins. 1997. The ClustalX windows interface: flexible stategies for multiple sequence alignment aided by quality analysis tools. *Nucleic Acid. Res.* **24:** 4876–4882.

Thuesen, E. V., and J. J. Childress. 1993. Metabolic rates, enzyme activities and chemical compositions of some deep-sea pelagic worms, particularly *Nectonemertes mirabilis* (Nemertea; Holonemertinea) and *Poecobius meseres* (Annelida: Polychaeta). *Deep-Sea Res Part I* **40:** 937–953.

Uttal, L., and K. R. Buck. 1996. Dietary study of the midwater polychaete *Poecobius meseres* in Monterey Bay, California. *Mar. Biol.* **125:** 333–343.

Reference: *Biol. Bull.* **208:** 221–230. (June 2005)

A New Deepwater Species of Stauromedusae, *Lucernaria janetae* (Cnidaria, Staurozoa, Lucernariidae), and a Preliminary Investigation of Stauromedusan Phylogeny Based on Nuclear and Mitochondrial rDNA Data

ALLEN G. COLLINS[1,*] AND MARYMEGAN DALY[2]

[1]*NMFS, National Systematics Laboratory, National Museum of Natural History, MRC-153, Smithsonian Institution, P.O. Box 37012, Washington, DC 20013-7012; and* [2]*Department of Evolution, Ecology and Organismal Biology, The Ohio State University, Columbus, Ohio 43210*

Abstract. The deepwater stauromedusan *Lucernaria janetae* n. sp is described from adult and juvenile specimens collected from the East Pacific Rise. *Lucernaria janetae* is the first species in the genus recorded from the Pacific Ocean, and differs from its congeners in size and morphology. Mitochondrial (16S) and nuclear (SSU) ribosomal gene sequences from *L. janetae* were analyzed with those of representative stauromedusan taxa to evaluate stauromedusan monophyly. Both genes recovered a strongly monophyletic Stauromedusae that is the sister group to all other medusozoans. Support of these hypotheses is robust to method of phylogenetic reconstruction and to outgroup selection, buttressing the argument that Stauromedusae should be recognized as the class Staurozoa. The molecular markers used here favor the same topology of relationships among our samples and clearly distinguished between two species, *Haliclystus sanjuanensis* and *H. octoradiatus*, that have been considered synonymous by many workers. A stable systematic framework for Stauromedusae appears achievable through comprehensive study of both morphological and sequence data.

Introduction

Deep-sea hydrothermal vent communities have been intensively studied since their discovery (Ballard, 1977; Lonsdale, 1977), but continue to yield major new macrofaunal taxa and kinds of communities. Among some of these novel communities associated with areas of diffuse flow near active vents are spectacular fields of "stalked jellyfish" (Stauromedusae) up to 10 cm in height (Lutz *et al.*, 1998; Halanych *et al.*, 1999). Stauromedusans are typically small and solitary, and live in shallow near-shore habitats of temperate seas, highlighting the unusual nature of this deep-sea occurrence. Despite their benthic nature, members of Stauromedusae have traditionally been grouped as an order within the cnidarian class Scyphozoa. However, recent phylogenetic analyses of Cnidaria based on morphology (Marques and Collins, 2004) and molecular data (Collins, 2002) suggest that Stauromedusae is not more closely related to the scyphozoan taxa Coronatae, Rhizostomeae, and Semaeostomeae (herein united as Scyphozoa, following Marques and Collins, 2004) than it is to Cubozoa or Hydrozoa.

Evolutionary discussions of stauromedusans have largely focused on their relationship to other groups of Cnidaria (*e.g.*, Uchida, 1929, 1972; Thiel, 1966) rather than on the relationships among its component groups (but see Thiel, 1936; Uchida, 1972). Comparatively little effort has been put into determining the systematic relationships within Stauromedusae. As a result, families and genera are recognized by a mosaic of features, many of which are not exclusive, or which suggest contradictory groupings. As an example relevant to the findings reported here, *Lucernaria* is often grouped with *Haliclystus* to the exclusion of *Lucernariopsis* because both the former have muscles in the

Received 9 December 2004; accepted 19 April 2005.
* To whom correspondence should be addressed. E-mail: Collinsa@si.edu

peduncle. However, both *Lucernaria* and *Lucernariopsis* lack perradial anchors and have a single-chambered peduncle, whereas *Haliclystus* has anchors and a four-chambered peduncle. The taxonomy of Stauromedusae is further hindered by the fact that many species are rarely encountered. The group is in need of a thorough systematic revision.

In November 2003, a camera sled towed by the R/V *Atlantis* serendipitously captured footage of a stauromedusan aggregation near 8° 37′ North on the East Pacific Rise. This was not the first sighting of stauromedusans in the deep East Pacific (*e.g.*, Lutz *et al.*, 1998; Halanych *et al.*, 1999), but two subsequent dives in the DSV *Alvin* allowed for these animals to be collected and examined in detail. Our samples include individuals at several ontogenetic stages, allowing us to describe the morphology of both adults and juveniles. On the basis of our examinations, we find that these specimens belong to a new species, described here as *Lucernaria janetae*. This is the first species of *Lucernaria* described from the Pacific Ocean. In addition, we extracted DNA from a specimen of *L. janetae* and amplified two genes, one coding for the complete small subunit of the nuclear ribosome (SSU), the other for a region of the mitochondrial large ribosomal subunit (16S). Combining these data with data from five other species of Stauromedusae, we assess the usefulness of these markers for revealing historical relationships within Stauromedusae and present an initial investigation of stauromedusan phylogeny.

Materials and Methods

Footage from a camera sled towed by the R/V *Atlantis* of the Woods Hole Oceanographic Institution in November 2003 revealed dense aggregations of large stauromedusans in a previously undocumented area of weak hydrothermal activity at 8° 36.745′N, 104° 12.740′W. During two dives (3935, 3927) in the submersible *Alvin*, the extent of the aggregations was determined, populations were documented with still digital photography and video, and several specimens were collected by using suction samplers.

Live material was photographed and examined and then fixed in 20% formalin or 95% ethanol. Formalin-fixed material was transferred to 70% ethanol after 2 weeks. Additional material was frozen for molecular or isotopic analyses. All specimens have been deposited at the Field Museum of Natural History, Chicago, Illinois. Preserved specimens were examined whole and in dissection; some material was processed for histology with standard paraffin techniques. Histological slides were stained in Masson's trichrome (Presnell and Schreibman, 1997). Pieces of tissue from tentacles, subumbrellar vesicles, and gastric filaments were smeared on a slide; nematocysts in these smears were examined using differential interference contrast microscopy at 100× magnification. Cnidae terminology follows Mariscal (1974). Nematocyst type, size, and location are recorded because these data may be useful for future systematic studies of Stauromedusae.

The Invisorb extraction kit (Invitek GmbH, Berlin) was used to obtain DNA from one specimen each of *Lucernaria janetae* (FMNH 10329) preserved in 95% ethanol, *Craterolophus convolvulus* (Johnston, 1835), *Depastromorpha africana* Carlgren, 1935, and an undescribed species of *Haliclystus*. From these DNA preparations, as well as those from *Haliclystus octoradiatus* Clark, 1863, and *Haliclystus sanjuanensis* Hyman, 1940 (see Table 1 for locality data for all samples), a 530–560-bp region of mitochondrial 16S was amplified, using the forward primer from Cunningham and Buss (1993) combined with the reverse primer from Schroth *et al.* (2002). Products of the polymerase chain reaction (PCR) were purified and sequenced in both directions by using a Megabace 500 automated sequencer. Similarly, nearly complete sequences of the gene coding for SSU (or 18S) were obtained (except for *H. sanjuanensis*, which had already been sequenced for a prior study; Collins, 2002) by using standard PCR and sequencing primers (Medlin *et al.*, 1988). Edited 16S sequences were aligned by using ClustalW and then improved by eye with the software SeaView (Galtier *et al.*, 1996) along with sequences from two stauromedusans and six representatives of outgroup taxa obtained from GenBank; edited SSU sequences were aligned by eye into a dataset (derived from that used in Collins, 2002) comprising more than 150 other cnidarian species. All alignments used in this study are available upon request.

Phylogenetic analyses were carried out on three datasets using PAUP* 4.0 (Swofford, 2002). The first data set contains 230 characters of 16S that are hypothesized to be homologous across our stauromedusan samples and the six outgroup taxa representing Anthozoa, Cubozoa, Hydrozoa, and Scyphozoa. For the SSU sequences, we excluded regions that could not be reliably aligned across Stauromedusae and the eight outgroup taxa; the resulting alignment is 1746 bases. The third dataset comprises both 16S and SSU data from Stauromedusae; narrowing the taxonomic focus allowed us to include an additional 233 characters from 16S rDNA. For each dataset, we searched for optimal trees by using the criteria of maximum parsimony (MP) and maxi-

Table 1

Stauromedusans sampled for molecular data

Species	Locality of collection
Craterolophus convolvulus	Helgoland, Germany
Depastromorpha africana	False Bay, South Africa
Haliclystus octoradiatus	Northern Germany
Haliclystus sanjuanensis	Washington State, USA
Haliclystus sp.	Los Molinos (near Valdivia), Chile
Lucernaria janetae	8° 37′ North on the East Pacific Rise

mum likelihood (ML), with 500 and 100 replicate searches, respectively, and with sequences added randomly to the starting topology. Gaps were treated as missing data. We used likelihood ratio tests employed by ModelTest ver. 3.6 (Posada and Crandall, 1998) to determine an appropriate model of nucleotide evolution assumed for the ML searches. We assessed node support with bootstrap analyses of 500 and 200 pseudo-replicate data sets under MP and ML. In addition, we calculated decay indices (Bremer, 1988) by using constrained tree searches to measure the extent to which the parsimony criterion must be relaxed to compromise clades present in the most parsimonious topology. Finally, for the two data sets containing outgroup taxa, we conducted a series of MP analyses with all combinations of outgroups to determine their impact on rooting the portion of the topology containing Stauromedusae.

Results

Lucernaria janetae, Collins and Daly, new species

Lucernaria sp., Lutz *et al.*, 1998

Differential diagnosis. Exceptionally large, cream-colored stauromedusan with 8 adradial clusters of about 100 tentacles. Adults lack primary tentacles; small juveniles may bear small, ovate primary tentacles. Calyx goblet-shaped, equal in height to peduncle; peduncle monocameral and muscular. Gonads lanceolate, extending from base of calyx to base of arms.

Material examined. Holotype (FMNH 12492) 1 adult, East Pacific Rise, −2538 m, 8° 36.745′N, 104° 12.740′W, 6 Nov. 2003. Paratypes (FMNH 10328) 4 adults, 3 juveniles, East Pacific Rise, −2538 m, 8° 36.745′N, 104° 12.740′W, 6 Nov. 2003. Additional specimens (FMNH 10327) 8 adults, East Pacific Rise, −2553 m, 8°36.578′N, 104° 12.623′W, 8 Nov. 2003.

Adult external anatomy. Calyx goblet-shaped, creamy white with faint greenish or orange cast in life; all preserved specimens creamy white (Fig. 1). Calyx of live specimens to 100 mm wide, 50 mm deep; calyx width in preserved specimens to 30 mm, depth to 15 mm. Exumbrella smooth, without ridges or visible clusters of nematocysts. Mouth rectangular, slightly elongated at corners, opaque and lighter in color than calyx in life and in preservation. Inter- and per-radial notches approximately equal. Arms equidistant, identical in size and morphology, each with rounded cluster of about 100 monomorphic, capitate secondary tentacles. No anchors or primary tentacles. Rounded head of each secondary tentacle opaque cream, sharply demarcated from stalk. Secondary tentacles in center of cluster slightly longer than those on periphery.

Peduncle same color as calyx, tubular, length approximately equal to depth of calyx. Junction between peduncle and calyx abrupt rather than smoothly tapering (Fig. 1). Peduncle monocameral, divided by four septal cords (Fig. 2A) that may extend only midway down its length; each cord bears a pinnately branched longitudinal muscle (Fig. 2B). Basal disc not distinct; peduncle does not flare proximally. In one specimen, small juvenile attached to basal end (Fig. 3B).

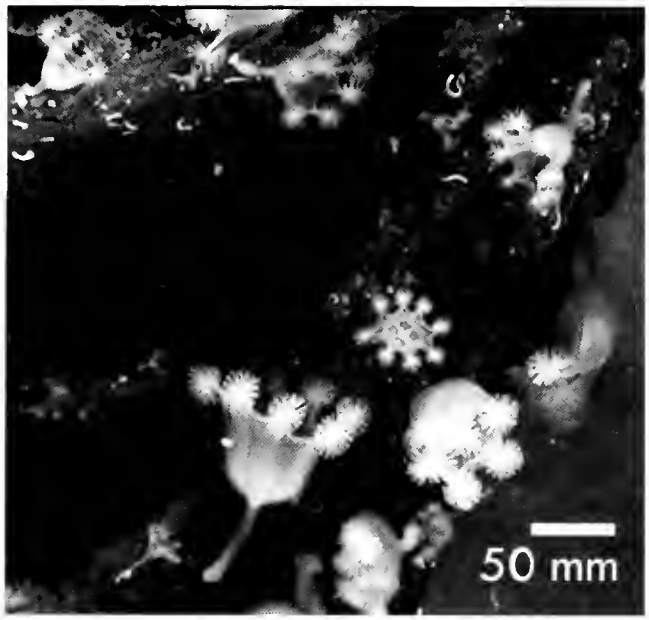

Figure 1. Living specimens of *Lucernaria janetae*, n. sp., *in situ*. Note variety of sizes represented in population.

Internal anatomy. Gamete-bearing tissue in 8 large, paired, lanceolate pads densely covered with bilobed, often U-shaped, vesicles that contain nematocysts and gametes (Fig. 2C). Vesicles on a single pad vary in size and shape, and are not arranged in rows. Coronal muscle separates paired sets of pads from one another. Each gametogenic pad extends from the base of the calyx into the base of the arms; proximal portion of pads separated by gastric filaments. Gastric filaments opaque cream, long, slender, bluntly pointed, restricted to base of calyx, between gametogenic pads.

Four equally developed, Y-shaped coronal muscles separate adjacent arms of calyx: stem of each Y runs between adjacent arms, arms of each Y belong to adjacent calyx arms. Radial muscles strong, discontinuous between arms.

Cnidom. Euryteles and holotrichs (Fig. 4). See Table 2 for size and distribution.

Morphology of juveniles. Smallest juvenile attached to underside of basal end of large adult (Fig. 3B); total height 2 mm, calyx width 1 mm, color uniformly white. Compared to adult or larger juvenile, calyx relatively tall and narrow,

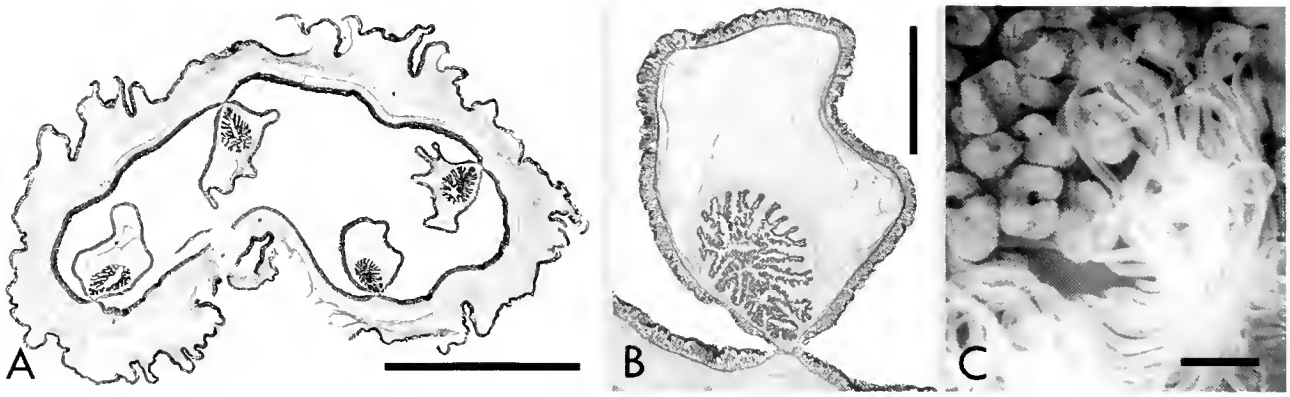

Figure 2. Internal anatomy of *Lucernaria janetae*, n. sp. (A) Transverse section through peduncle, showing four septal muscles. (B) Detail of a septal muscle. (C) Subumbrellar surface, showing U-shaped vesicles and slender gastric filaments. Scale bars: A = 2 mm; B, C = 0.5 mm.

more wedge- than goblet-shaped. Eight clusters of secondary tentacles; calyx not notched between each cluster. Secondary tentacle clusters with fewer members; tentacles relatively thicker, shorter, not capitate; opaque, round head at distal end not demarcated from stalk. Primary tentacles not visible.

Larger juveniles not attached to adult. Calyx width of larger of two specimens 3 mm, depth 3 mm; peduncle length 4 mm; smaller specimen calyx width 3 mm, depth 4 mm, peduncle length 2 mm. Color of both uniformly white. Calyx shape and proportions similar to those of adults (Fig. 3A): calyx goblet-shaped with rounded proximal end. Inter- and per-radial notches equal in depth, relatively shallower than in adults but clearly divide calyx into eight arms. Eight clusters of capitate secondary tentacles (Fig. 3A, C); compared to adults, clusters with fewer members. Small, oval, opaque primary tentacles (Fig. 3C); primary tentacles nodule-like, raised between secondary tentacles. No nematocysts found in primary tentacles; secondary tentacles with sparse, relatively

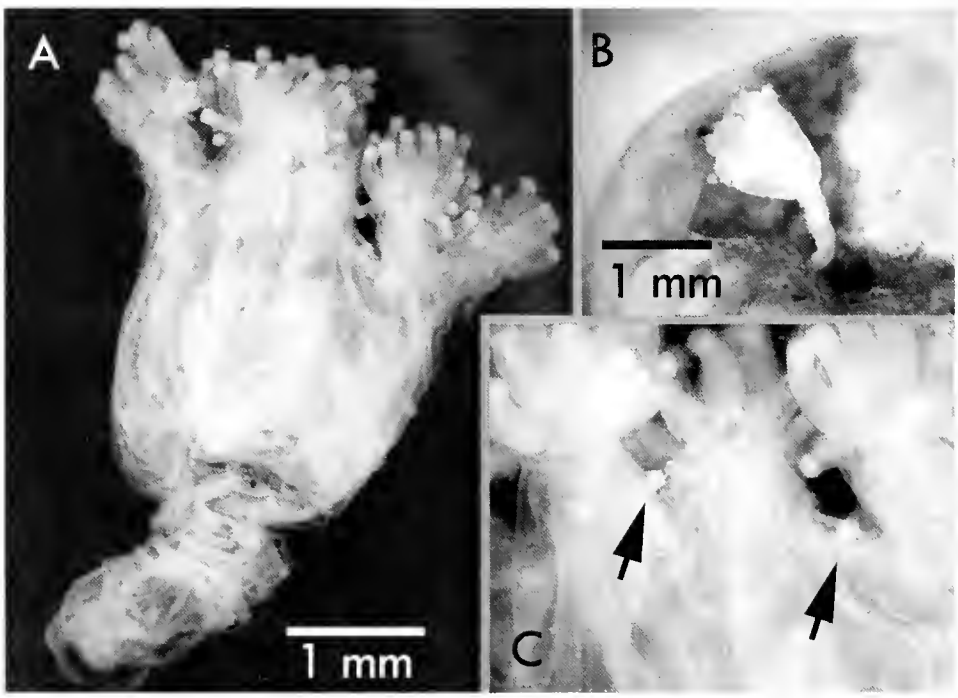

Figure 3. Morphology of juvenile specimens of *Lucernaria janetae*, n. sp. (A) One of the two larger juveniles; general shape and proportions as in adults. Scale bar = 1 mm. (B) Smallest juvenile, attached to basal end of an adult. Scale bar = 1 mm. (C) Primary tentacles (arrows) on specimen in A.

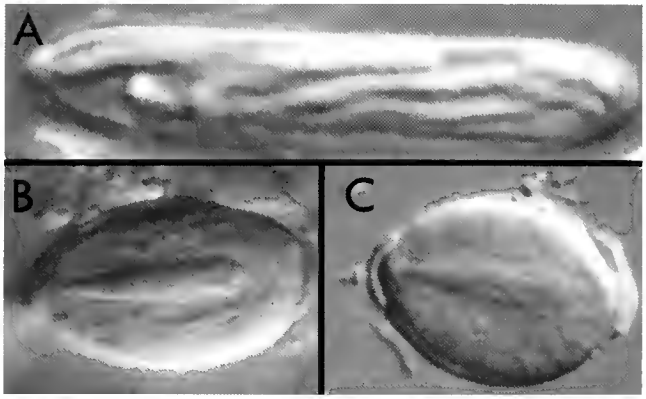

Figure 4. Representative cnidae from *Lucernaria janetae*, n. sp. (A) Holotrich. (B) Eurytele. (C) Eurytele.

smaller euryteles (5.4–9.5 × 3.3–5.6 μm, $n = 10$) and no holotrichs.

Etymology. Named for Dr. Janet Voight, The Field Museum, Chicago, in recognition of her commitment to discovering and describing deep-sea invertebrates.

Natural history and distribution. In terms of number of individuals and biomass, *Lucernaria janetae* is the dominant macrofaunal organism where it occurs. Asexual propagation is not known in Stauromedusae, but observations of dense aggregations and a juvenile attached to the base of the peduncle raise the question of whether *L. janetae* might be able to proliferate in this manner. Several specimens contained small pieces of crustacean legs and antennae, suggesting that *L. janetae* eats small pelagic crustaceans. The high density is likely the result of limited dispersal: most stauromedusans have nonciliated, creeping planulae (Otto, 1976, 1978). In the intertidal species *Haliclystus octoradiatus*, young settle together (Wietrzykowski, 1912); in *L. janetae*, the smallest specimen was associated with a large adult.

Lutz *et al.* (1998) and Halanych *et al.* (1999) observed *Lucernaria*-dominated communities at 20°50.304′N 109°05.422′W and 7°25.23′S 107°47.72′W, respectively. We tentatively identify these as *L. janetae*, but their identity cannot be definitely determined in the absence of specimens. Sea anemones (*Cynanthea* sp.) were noted by Lutz *et al.* (1998) and Halanych *et al.* (1999), but we did not observe any. Like Halanych *et al.* (1999), we found a few specimens of the tubeworm *Tevnia jerichonana* in the stauromedusan communities we sampled. A few specimens of mobile, vent-associated invertebrates were seen at the type locality, including galatheid (*Munidopsis squamosa*) and bythograeid (*Bythograea thermydon*) crabs.

Similar species. Most species of Stauromedusae are small (< 40 mm width or height); *Lucernaria* comprises all described species of Stauromedusae having an adult calyx diameter larger than 50 mm (Kramp, 1961). All species of *Lucernaria* except *L. janetae* are known only from the Atlantic Ocean. *L. janetae* is easily distinguished from *Lucernaria quadricornis* Müller, 1776, on the basis of habitat: *L. quadricornis* occurs in the shallow North Atlantic (*e.g.*, Hargitt, 1904; Mayer, 1910; Kramp, 1961; Cornelius *et al.*, 1990). Furthermore, the two differ noticeably in the shape of the gonads and the depth of the perradial notches. *Lucernaria bathyphilia* Haeckel 1880, the only other large, deep-water species in the genus, differs from *L. janetae* in the length of the peduncle and pairing of the arms. In *L. bathyphilia*, the peduncle is about one- tenth as long as the calyx; in *L. janetae*, the peduncle and calyx are about equal in length. Haeckel's (1881) drawings indicate that the arms of *L. bathyphilia* are extremely short—just barely separated from the margin of the bell; *L. janetae* has 8 distinct arms.

Gene sequences. New sequences generated for this study have been assigned GenBank accession numbers AY845338–AY845348. The region of mitochondrial 16S amplified from our stauromedusan samples is roughly 545 bases long. A number of insertion and deletion events (indels) were inferred during the alignment of stauromedusan 16S sequences, but none of these indels were longer than two bases. The near-complete SSU sequences from stauromedusans vary between 1750 and 1754 bases in length, and there are few indels. Not surprisingly, the mitochondrial 16S gene appears to evolve considerably faster than the nuclear SSU gene in Stauromedusae. For example, the uncorrected p-distance between the 16S of *L. janetae* and *Craterolophus convolvulus* is 21.4%, whereas that between their SSU is 1.39%. Similarly, our sampled representatives of *L. janetae* and *Haliclystus octoradiatus* differ by 24.0% and 1.33% for 16S and SSU, respectively. Within the genus *Haliclystus*, *H. sanjuanensis* and *H.* sp. from Chile have the least-diverged sequences (4.02% for 16S and identical for SSU). By these measures, both *H. sanjuanensis* and

Table 2

Size and distribution of nematocysts of Lucernaria janetae

Tissue	Nematocyst	*n*	*N*	Range
Subumbrellar vesicle	Eurytele B, C	34	3/3	19.3–12.2×6.2–8.9
	Holotrich A	34	3/3	20.4–16.4×2.2–4.3
Tentacle	Eurytele B, C	34	3/3	15.5–12.6×6.4–7.7
	Holotrich A	34	3/3	21.8–18.3×2.9–4.5
Gastric filament	Eurytele B, C	31	3/3	12.1–10.8×8–8.8

Letters refer to Figure 4; "*N*" is the proportion of examined specimens that had a particular type of nematocyst; "*n*" is the number of capsules measured; size presented as range of lengths by widths, in micrometers, for undischarged capsules.

H. sp. from Chile differ from *H. octoradiatus* by roughly 12% (16S) and 0.5% (SSU).

GenBank contains sequences of 16S and SSU for Stauromedusae that we infer to be erroneous. For 16S, the GenBank sequence U19376, identified as *Haliclystus* sp., is identical to the one we obtained from *C. convolvulus*. Our 16S sequence for *C. convolvulus* differs from a sequence in GenBank identified as *C. convolvulus* (U19375) by a single nucleotide change. The SSU sequence in GenBank purporting to be *Haliclystus* sp. (AF099103) is identical to our SSU sequence from *C. convolvulus*, whereas another GenBank sequence (AF099104) for *C. convolvulus* is highly similar to sequences from *Haliclystus*. The SSU sequences were generated as part of the same study (Kim *et al.*, 1999), and evidently the species names attached to them were inadvertently reversed at some point.

Phylogenetic relationships. Mitochondrial 16S and nuclear SSU data indicate identical sets of relationships among the stauromedusans sampled here (Figs. 5, 6). Both 16S and SSU sequences recover a monophyletic Stauromedusae. *Craterolophus convolvulus* is the sister taxon to a clade containing all other species. Within this clade, *L. janetae* appears at the base, and *D. africana* is sister to the three species of *Haliclystus*. *H. sanjuanensis* from the Northwest Pacific and *Haliclystus* sp. from Chile are more closely related to each other than either is to *H. octoradiatus* from northern Europe.

Inferred relationships among our samples are robust to the method used to reconstruct them. The topology of the ingroup based on 16S data does not change whether the optimality criterion is MP (Fig. 5) or ML (not shown). Similarly, the SSU-based MP topology (not shown) perfectly mirrors the topology for which our data are most likely (Fig. 6). In both the 16S and SSU analyses, the positions of all taxa are supported with bootstrap values greater than 75%, with the exception of *L. janetae* (Figs. 5, 6). Although its placement is unequivocal in all analyses, the position of *L. janetae* receives only limited support from both molecular markers. However, the placement of the root between *Craterolophus convolvulus* and the clade containing *L. janetae* at its base is remarkably stable to the use of different combinations of outgroup taxa. When 16S data are used, the root position shown in Figure 5 is found in all sets of most-parsimonious trees obtained using any combination of the outgroups as well as any used alone. Similarly, for SSU data, all possible combinations of outgroups, with the exception of hydrozoans used alone, yield a topology containing a root as shown in Figure 6.

Discussion

Diversity of Stauromedusae

We have added one to the total of roughly 50 known species of Stauromedusae (Mills, 2004). Stauromedusans form an easily distinguished group that is potentially united

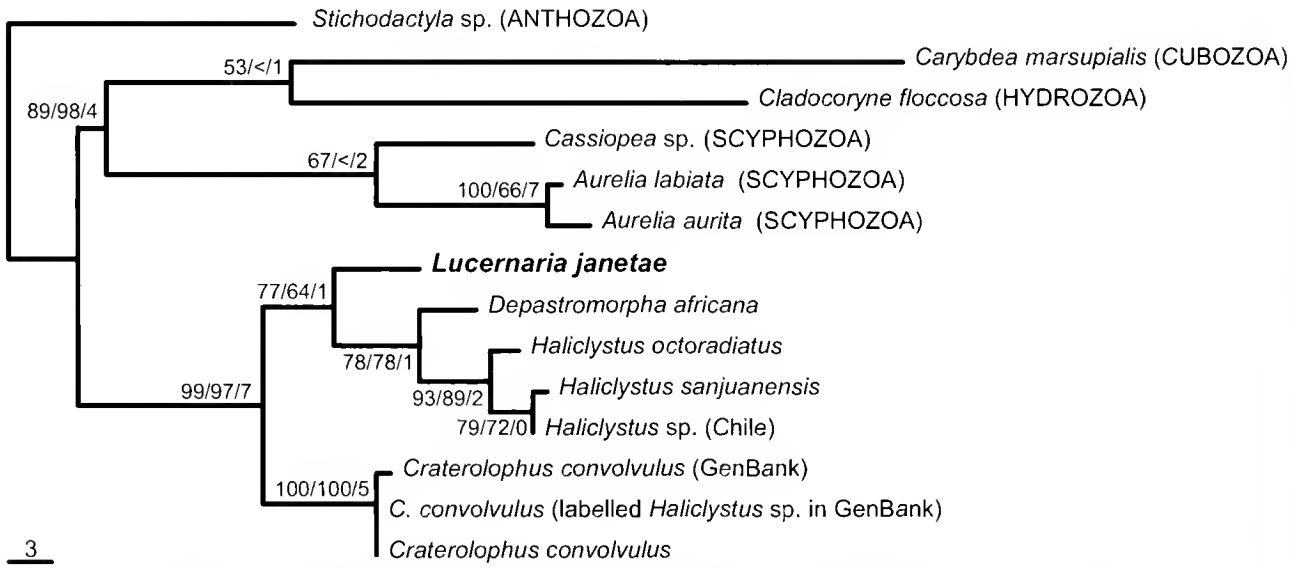

Figure 5. Maximum parsimony (MP) phylogram of relationships among sampled species of Stauromedusae based on mitochondrial 16S data, with MP and maximum likelihood (ML) bootstrap and decay indices shown at the nodes. "<" indicates a bootstrap index less than 50. The assumed model (TrNef+G) of nucleotide evolution for ML tree searches has one rate for transversions (1.0000), two rates for transitions (A–G, 1.6893; C–T, 3.3596), a gamma shape parameter (0.4330), and equal base frequencies. Listed in the order they appear in the figure, GenBank accession numbers for outgroups are as follows: Cm, AF360118; Cf, AY512535; Cs, U19374; Al, AF461401; Aa, U19373; and Ss, AY345874.

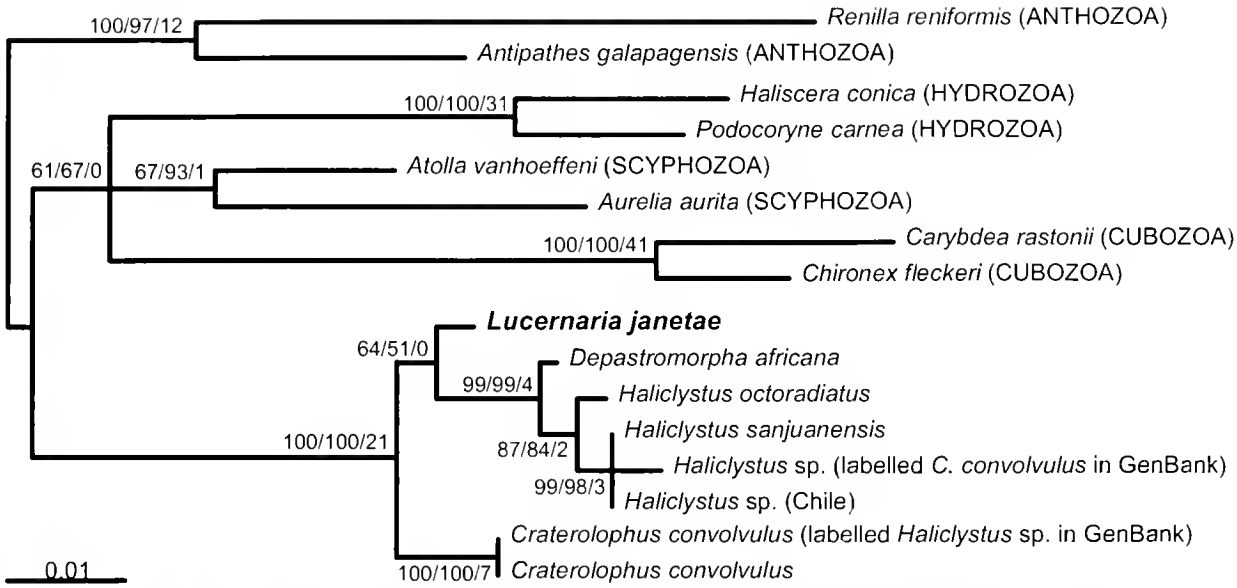

Figure 6. Maximum likelihood (ML) phylogram of relationships among sampled species of Stauromedusae based on nuclear SSU data, with maximum parsimony (MP) and ML bootstrap and decay indices shown at the nodes. "<" indicates a bootstrap index less than 50. The assumed model (TrN+I+G) of nucleotide evolution for ML tree searches has one rate for transversions (1.0000), two rates for transitions (A–G, 2.5175; C–T, 4.6618), an assumed proportion of invariant sites (0.5139), a gamma shape parameter (0.6443), and unequal base frequencies. Listed in the order they appear in the figure, GenBank accession numbers for outgroups are as follows: Hc, AF358064; Pc, AF358092; Av, AF100942; Aa, AY039208; Cr, AF358108; Cf, AF358104; Rr, AF052581; and Ag, AF100943.

by a nonciliated creeping planula with 16 rectangular endodermal cells (Otto, 1976, 1978), a four-chambered peduncle with an adhesive basal disk, eight clusters of capitate tentacles, and perhaps complex ovaries involving follicle cells. The generality of this last feature is somewhat tentative as it has been studied in only a single species, but it is dramatically different from what has been observed in coronates, rhizostomes, and semaeostomes (Eckelbarger and Larson, 1993). The molecular data presented here, though limited in terms of taxon sampling, indicate that Stauromedusae is indeed a clade.

As mentioned in the introduction, most discussions of the evolution of Stauromedusae have aimed to determine its phylogenetic position within Cnidaria. Members of Stauromedusae possess features that appear to be homologous with those of Cubozoa and Scyphozoa, such as intramesogleal muscles of the polyp, gastric filaments, hollow structures ontogenetically derived from primary polyp tentacles known as anchors or rhopalioids, and a metamorphosis from juvenile to adult morphology concentrated at their oral ends (Uchida, 1929; Hirano, 1986; Kikinger and Salvini-Plawen, 1995). Because of these similarities, Stauromedusae, Cubozoa, and Scyphozoa have classically been treated as a natural group. Indeed, a recent cladistic analysis of morphological and life-history characters (Marques and Collins, 2004) favored the recognition of this clade. In contrast, molecular data raise the possibility that these groups form a paraphyletic assemblage whose members share a set of characters that were lost in the lineage leading to Hydrozoa (Collins, 2002; Collins, unpubl data). Our 16S and SSU data add to the accumulating evidence that this is the case.

Specifically, accepting that Anthozoa is the sister group of Medusozoa (Haeckel, 1879; Werner, 1973; Salvini-Plawen, 1978; Schuchert 1993; Bridge *et al.*, 1995; Collins, 2002), Figures 5 and 6 reveal that Stauromedusae is the sister taxon to all other medusozoans. By comparison to medusozoan outgroups—particularly Cubozoa and the scyphozoan taxa Coronatae, Rhizostomeae, and Semaeostomeae—characters by which we recognize Stauromedusae can be sorted into likely synaporphies and symplesiomorphies (Fig. 7). For example, because four intramesogleal muscles associated with peristomial pits are characteristic of most species of Stauromedusae as well as of the polyps of scyphozoans, it seems likely that these characters are symplesiomorphies that have been lost in both Cubozoa and Hydrozoa. In the case of Cubozoa, polyps still possess intramesogleal muscles, but they are not united in four muscle bundles (Chapman, 1974). By similar reasoning, gastric filaments and a coronal muscle are features that were likely lost in the ancestry of Hydrozoa.

The relationship between the metamorphosis of primary tentacles into anchors or rhopalioids in Stauromedusae and the metamorphosis of primary tentacles into the rhopalia in

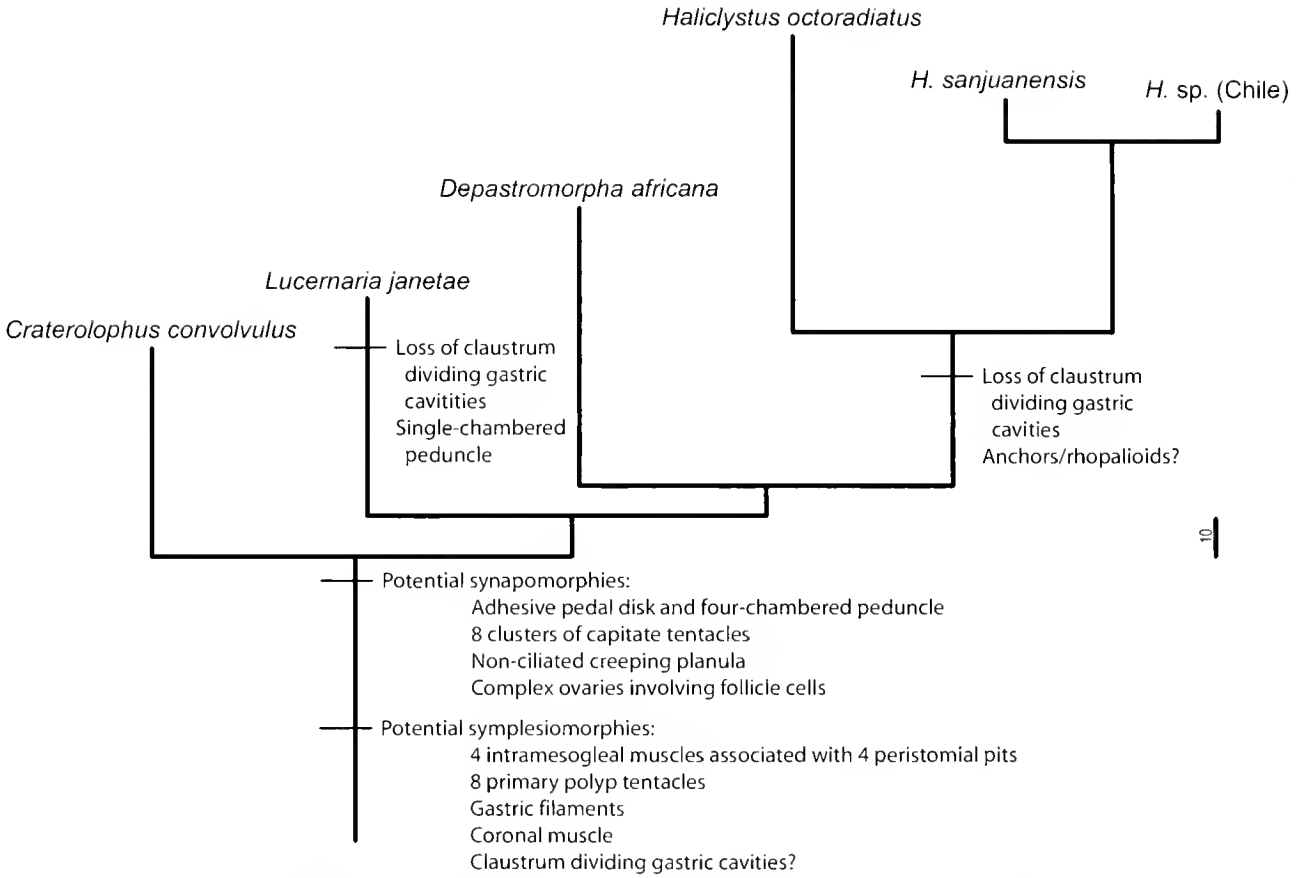

Figure 7. Maximum parsimony (MP) phylogram of relationships among sampled species of Stauromedusae based on combined 16S and SSU data, rooted as in Figures 5 and 6. Scale bar indicates 10 nucleotide character changes. Selected morphological and life-history features are mapped at various nodes. It is stressed that greater taxon sampling is a must to more fully understand the true history of character evolution within Stauromedusae.

Cubozoa and Scyphozoa is somewhat less clear, because anchors have a relatively limited distribution among stauromedusan species. Although the growth of eight perradial and interradial primary tentacles during ontogeny appears to be nearly universal within the group, species of just three genera, *Haliclystus*, *Stenoscyphus*, and *Halimocyathus*, have primary tentacles that are modified into rhopalioids (Kramp, 1961). It seems possible that anchors have been derived one or more times within Stauromedusae and that their evolutionary origin (or origins) is independent from that of cubozoan and scyphozoan rhopalia. That said, the presence of primary tentacles is likely to be a feature that is shared by cubozoans, scyphozoans, and stauromedusans as a result of their common history. If so, this character was lost in the ancestry of Hydrozoa.

A final character of considerable interest is the claustrum. As in adults of Cubozoa and Scyphozoa, in stauromedusans the gastrovascular chamber is divided by four interradial septa that separate a central gut from four radial gastric pockets. In some members of Stauromedusae, the gastrovascular system has an added level of complexity because the four gastric pockets are divided transversely by a piece of tissue, the claustrum. Just such an arrangement is also seen in adult cubozoans (Uchida, 1929), which raises the possibility that this character was present in the ancestral medusozoan and subsequently lost independently in lineages leading to Hydrozoa and Scyphozoa.

The claustrum has played a fundamental role in the systematics of Stauromedusae. The group has long been divided into two primary groups, Cleistocarpida and Eleutherocarpida (Clark, 1863), on the basis of its presence or absence, respectively. We have sampled two cleistocarpid species, *C. convolvulus* and *D. africana*, and found that not only do these species not form a clade, they also do not form a paraphyletic assemblage with respect to the remaining eleutherocarpid species. The species we describe here, *L. janetae*, does not possess a claustrum, and both molecular markers indicate that this species falls between *C. convolvulus* and *D. africana* (Figs. 5 and 6). Although more species of Stauromedusae need to be sampled for molecular data before the evolution of the claustrum can be settled conclusively, at this point it seems likely that the claustrum

is a more labile feature than suspected and that it may have been lost on more than one occasion (Fig. 7). No matter what the specific history of the evolution of the claustrum within Stauromedusae, it may turn out not to be a useful character for diagnosing subgroups within the clade.

From a molecular perspective, the mitochondrial 16S marker may be useful for determining species boundaries in future studies of Stauromedusae. For instance, species of *Haliclystus* have been difficult to distinguish. Kramp (1961) considered all three of the *Haliclystus* species sampled here to be synonyms, under the name *H. auricula* (Rathke, 1806). However, Hirano (1997) recently demonstrated that circumboreal representatives of *H. auricula* can be separated, on the basis of a set of morphological characters, into four types with differing, though somewhat overlapping, distributions. As names were available for each of these distinct types, she recommended the resurrection of *H. sanjuanensis* from the eastern North Pacific and *H. octoradiatus* from northern Europe and Iceland (in addition to *H. tenuis* Kishinouye, 1910, from the western North Pacific, not sampled here) as species separate from *H. auricula*. The significant divergences in both 16S and SSU data between our samples of *H. sanjuanensis* and *H. octoradiatus* support Hirano's assertion that the different morphotypes of circumboreal *Haliclystus* represent discrete species. Several important studies of stauromedusan features that used specimens referred to as *H. octoradiatus* from the northeastern Pacific probably present observations on *H. sanjuanensis* (*e.g.*, Otto, 1976, 1978; Eckelbarger and Larson, 1993). The name *H. auricula* has also been applied to all South American specimens of *Haliclystus* observed (Kramp, 1952; Grohman *et al.*, 1999; Zagal, 2004). Our data show that our specimens of *H.* sp. from Chile and *H. sanjuanensis* are relatively closely related, though more samples are of course necessary to determine whether they represent separate species. The molecular markers we have used to begin investigating stauromedusan phylogeny should prove helpful in moving toward a stable systematic framework for Stauromedusae based upon comprehensive study of both morphological and sequence data.

Finally, the evolution of mitochondrial genes has been observed to be notably slow in anthozoans (*e.g.*, Romano and Palumbi, 1997; Shearer *et al.*, 2002; Hebert *et al.*, 2003), raising the possibility that slow mitochondrial DNA evolution might be a widespread phenomenon within Cnidaria (Hebert *et al.*, 2003) or other early-diverging metazoan lineages (Shearer *et al.*, 2002). The data derived here, however, suggest that the mitochondrial 16S gene evolves rapidly enough in Stauromedusae to differentiate between relatively closely related species. Furthermore, other recent studies of non-anthozoan cnidarians (Schroth *et al.*, 2002; Collins *et al.*, 2005; Govindarajan *et al.*, 2005), and even placozoans (Voigt *et al.*, 2004), have used mitochondrial 16S data to distinguish among closely related lineages. Therefore, it appears more likely that slow mitochondrial DNA evolution is limited to Anthozoa, rather than being the general condition for early diverging metazoans. That said, investigating this question with additional data, especially from Ctenophora and Porifera, is certainly warranted.

Acknowledgments

These specimens were collected with the assistance of the crew of the R/V *Atlantis* and DSV *Alvin* and the science party of Cruise AT 11-03. The cruise was funded by NSF DEB-0072695 to J. Voight. T. Haney, J. McClain, and R. Zierenberg discovered the communities we sampled. We extend our thanks to G. Jarms and I. Straehler-Pohl for providing a DNA sample of *H. octoradiatus*, M. Dawson for providing tissue samples of *D. africana* and *H.* sp. from Chile, P. Schuchert for a tissue sample of *H. sanjuanensis*, and B. Bentlage for assistance deriving molecular sequences. D. Fautin generously supported MD's participation in AT 11-03 and provided invaluable help with the literature and taxonomy of stauromedusans. B. Schierwater, in whose laboratory our molecular sequences were generated, is gratefully acknowledged for his generosity. MD is supported by NSF 9978106 (to D. G. Fautin) and DEB 0415277.

Literature Cited

Ballard, R. D. 1977. Notes on a major oceanographic find. *Oceanus* **20:** 35–44.

Bremer, K. 1988. The limits of amino acid sequence data in angiosperm phylogenetic reconstruction. *Evolution* **42:** 795–803.

Bridge D., C. W. Cunningham, R. DeSalle, and L. W. Buss. 1995. Class-level relationships in the phylum Cnidaria: molecular and morphological evidence. *Mol. Biol. Evol.* **12:** 679–689.

Carlgren, O. 1935. Über eine neue südafrikanische Lucernariide, *Depastromorpha africana* n. gen., n. sp. *K. Svenska Vetenskapsakad. Handl.* Bd. 3, No. 15.

Chapman, D. M. 1974. Cnidarian histology. Pp. 1–92 in *Coelenterate Biology: Reviews and New Perspectives*, L. Muscatine and H. M. Lenhoff, eds. Academic Press, New York.

Clark, H. J. 1863. Prodromus of the history, structure, and physiology of the order Lucernariae. *J. Boston Soc. Nat. Hist.* **7:** 531–567.

Collins, A. G. 2002. Phylogeny of Medusozoa and the evolution of cnidarian life cycles. *J. Evol. Biol.* **15:** 418–432.

Collins, A. G., S. Winkelmann, H. Hadrys, and B. Schierwater. 2005. Phylogeny of Capitata (Cnidaria, Hydrozoa) and Corynidae in light of mitochondrial 16S rDNA data. *Zool. Scr.* **34:** 91–99.

Cornelius, P. F. S., R. L. Manuel, and J. S. Ryland. 1990. Hydroids, sea anemones, jellyfish, and comb jellies. Pp. 62–135 in *Handbook of the Marine Fauna of North-West Europe*, P. J. Hayward and J. S. Ryland, eds. Clarendon Press, Oxford.

Cunningham, C. W., and L. W. Buss. 1993. Molecular evidence for multiple episodes of pedomorphosis in the family Hydractiniidae. *Biochem. Syst. Ecol.* **21:** 57–69.

Eckelbarger, K. J., and R. J. Larson. 1993. Ultrastructural study of the ovary of the sessile scyphozoan *Haliclystus octoradiatus* (Cnidaria: Stauromedusae). *J. Morphol.* **218:** 225–236.

Galtier, N., M. Gouy, and C. Gautier. 1996. SEAVIEW and

PHYLO_WIN: two graphic tools for sequence alignment and molecular phylogeny. *Comput. Appl. Biosci.* **12:** 543–548.

Govindarajan, A.F., K.M. Halanych, and C.W. Cunningham. 2005. Mitochondrial evolution and phylogeography in the hydrozoan *Obelia geniculata* (Cnidaria). *Mar. Biol.* **146:** 213–222.

Grohman, P. A., M. P. Magalhães, and Y. M. Hirano. 1999. First record of the order Stauromedusae (Cnidaria, Scyphozoa) from the tropical southwestern Atlantic, with a review of the distribution of Stauromedusae in the southern hemisphere. *Species Div.* **4:** 381–388.

Haeckel, E. H. 1879. *Das System der Medusen: Erster Theil einer Monographie der Medusen.* G. Fischer, Jena.

Haeckel, E. H. 1880. *System der Acraspeden. Zweite Hälfte des System der Medusen.* Denkschriften, Jena.

Haeckel, E. H. 1881. Report on the deepsea medusae dredged by the H.M.S. Challenger during the years 1873–1876. *Rep. Challenger Exped. (Zoology)* **4:** 1–154.

Halanych, K. M., M. Tieger, G. D. O'Mullan, R. A. Lutz, and R. C. Vrijenhoek. 1999. Brief description of biological communities at 7° S on the East Pacific Rise. *InterRidge News* **8:** 23–27.

Hargitt, C. W. 1904. The medusae of the Wood's Hole region. *Bull. Bur. Fish.* **24:** 21–79.

Hebert, P. D. N., S. Ratnasingham, and J. R. de Waard. 2003. Barcoding animal life: cytochrome c oxidase subunit 1 divergences among closely related species. *Proc. R. Soc. Lond. B* **270:** S96–S99.

Hirano, Y. M. 1986. Species of Stauromedusae from Hokkaido, with notes on their metamorphosis. *J. Fac. Sci. Hokkaido Univ. Ser. VI Zool.* **24:** 182–201.

Hirano, Y. M. 1997. A review of a supposedly circumboreal species of stauromedusan, *Haliclystus auricula* (Rathke, 1806). *Proc. 6th Int. Conf. Coelenterate Biology 1995* 247–252.

Hyman, L. H. 1940. Observations and experiments on the physiology of medusae. *Biol. Bull.* **79:** 282–296.

Johnston, G. 1835. Illustrations in British zoology. *Loudon's Mag. Nat. Hist.* **6:** 320–322.

Kikinger, R., and L. v. Salvini-Plawen. 1995. Development from polyp to stauromedusa in *Stylocoronella* (Cnidaria: Scyphozoa). *J. Mar. Biol. Assoc. UK* **75:** 899–912.

Kim, J. H., W. Kim, and C. W. Cunningham. 1999. A new perspective on lower metazoan relationships from 18S rDNA sequences. *Mol. Biol. Evol.* **16:** 423–427.

Kishinouye, K. 1910. Some medusae of Japanese waters. *J. Coll. Sci. Tokyo* **27:** 1–35.

Kramp, P. L. 1952. Reports on the Lund University Chile Expedition 1948–49. 2. Medusae collected by the L. U. Exp. 1948–49. *Lunds Univ. Årsskrift, N. F. Avd. 2,* **Bd. 47:** 1–19.

Kramp, P. L. 1961. Synopsis of the medusae of the world. *J. Mar. Biol. Assoc. UK* **40:** 1–469.

Lonsdale, P. 1977. Clustering of suspension-feeding macrobenthos near abyssal hydrothermal vents at oceanic spreading centers. *Deep-Sea Res.* **24:** 857–863.

Lutz, R. A., D. Desbruyères, T. M. Shank, and R. C. Vrijenhoek. 1998. A deep-sea hydrothermal vent community dominated by Stauromedusae. *Deep-Sea Res. II* **45:** 329–334.

Mariscal, R. N. 1974. Nematocysts. Pp. 129–177 in *Coelenterate Biology: Reviews and New Perspectives,* L. Muscatine and H. M. Lenhoff, eds. Academic Press, New York.

Marques, A. C., and A. G. Collins. 2004. Cladistic analysis of Medusozoa and cnidarian evolution. *Invertebr. Biol.* **123:** 23–42.

Mayer, A. G. 1910. *Medusae of the World, Vol. 3. The Scyphomedusae.* Carnegie Institute of Washington, Washington D.C.

Medlin, L., H. J. Elwood, S. Stickel, and M. L. Sogin. 1988. The characterization of enzymatically amplified eukaryotic 16S-like ribosomal RNA-coding regions. *Gene* **71:** 491–500.

Mills, C. E. 2004. *Stauromedusae: List of All Valid Species Names.* [Online]. Available: http://faculty.washington.edu/cemills/Staurolist.html [January 2005].

Müller, O. F. 1776. *Zoologiae Danicae Prodromus, seu Animalium Daniae et Norvegiae Indigenarum Characteres, Nomina et Synonyma Imprimis Popularium.* Heineck & Faber, Havniae.

Otto, J. J. 1976. Early development and planula movement in *Haliclystus* (Scyphozoa: Stauromedusae). Pp. 319–329 in *Coelenterate Ecology and Behavior,* G. O. Mackie, ed. Plenum Press, New York.

Otto, J. J. 1978. The settlement of *Haliclystus* planulae. Pp. 13–22 in *Settlement and Metamorphosis of Marine Invertebrate Larvae,* F.-S. Chia and M. Rice, eds. Elsevier, New York.

Posada, D., and K. A. Crandall. 1998. MODELTEST: Testing the model of DNA substitution. *Bioinformatics* **14:** 817–818.

Presnell, J. K., and M. P. Shreibman. 1997. *Humason's Animal Tissue Techniques,* 5th ed. Johns Hopkins University Press, Baltimore.

Rathke, J. 1806. P. 35 in O. F. Müller, *Zoologiae Danica,* Bd. 4, Havniae.

Romano, S. L., and S. R. Palumbi. 1997. Molecular evolution of a portion of the mitochondrial 16S ribosomal gene region in scleractinian corals. *J. Mol. Evol.* **45:** 397–411.

Salvini-Plawen, L. v. 1978. On the origin and evolution of the lower metazoa. *Z. Zool. Syst. Evolutionsforsch.* **16:** 40–88.

Schroth, W., G. Jarms, B. Streit, and B. Schierwater. 2002. Speciation and phylogeography in the cosmopolitan marine moon jelly, *Aurelia* sp. *BMC Evol. Biol.* **2:** 1–10.

Schuchert, P. 1993. Phylogenetic analysis of the Cnidaria. *Z. Zool. Syst. Evolutionsforsch.* **31:** 161–173.

Shearer, T.L., M. J. Van Oppen, S. L. Romano, and G. Worheide. 2002. Slow mitochondrial DNA sequence evolution in the Anthozoa (Cnidaria). *Mol. Ecol.* **11:** 2475–2487.

Swofford, D. L. 2002. *PAUP*. Phylogenetic Analysis Using Parsimony (*and Other Methods). Version 4. Program and Documentation.* Sinauer Associates, Sunderland, MA.

Thiel, H. 1966. The evolution of Scyphozoa: A review. Pp. 77–118 in *The Cnidaria and Their Evolution,* W. J. Rees, ed. Academic Press, London.

Thiel, M. E. 1936. Scyphomedusae: Stauromedusae. *Bronns Klassen und Ordnungen des Tierreichs* **2:** 1–172.

Uchida, T. 1929. Studies on the Stauromedusae and Cubomedusae, with special reference to their metamorphosis. *Jpn. J. Zool.* **2:** 103–193.

Uchida, T. 1972. The systematic position of the Stauromedusae. *Publ. Seto Mar. Biol. Lab.* **20:** 133–139.

Voigt, O., A. G. Collins, V. B. Pearse, J. S. Pearse, H. Hadrys, and B. Schierwater. 2004. Placozoa — no longer a phylum of one. *Curr. Biol.* **14:** R944–R945.

Werner, B. 1973. New investigations on systematics and evolution of Scyphozoa and the phylum Cnidaria. *Publ. Seto Mar. Biol. Lab.* **20:** 35–61.

Wietrzykowski, W. 1912. Recherches sur le développement des lucernaires. *Arch. Zool. Exp. Gen.* 5e Série **10:** 1–95.

Zagal, C. J. 2004. Population biology and habitat of the stauromedusan *Haliclystus auricula* in southern Chile. *J. Mar. Biol. Assoc. UK* **84:** 331–336.

INDEX

F

G

H

I

J

K

L

M

N

O

THE
BIOLOGICAL BULLETIN

2005 Subscription Rates

Volumes 208-209

Paid subscriptions include both print and online versions.

	Institutional	Individual
One year subscription (6 issues - 2 volumes)	**$360.00**	**$120.00**
Single Volume (3 issues)	$180.00	$70.00
Single Issues	$75.00	$25.00

Surface delivery included in above prices.

For prompt delivery, we encourage subscribers outside the U.S. to request airmail service.

Airmail Delivery Charges:

U.S. and Canada, $45.00 Mexico, $60.00 All other locations, $100.00

The Biological Bulletin
ISSN: 0006-3185
Frequency: Bimonthly
Number of issues per year: 6
Months of Publication: February, April, June, August, October, December
Subscriptions entered for calendar year
Volume indexes contained in June and December issues
Back issues available
Claims handled upon receipt

Please address orders to:

Subscription Administrator, *The Biological Bulletin*
Marine Biological Laboratory, 7 MBL Street
Woods Hole, MA 02543 U.S.A.
Fax: 508-289-7922 • Tel: 508-289-7402 • E-mail: lreuter@mbl.edu

Orders must be prepaid in U.S. Dollars, check payable to Marine Biological Laboratory
(with reference *The Biological Bulletin)*

www.biolbull.org

Published by the Marine Biological Laboratory
Woods Hole, Massachusetts, 02543 U.S.A.

THE

BIOLOGICAL BULLETIN

2005 Subscription Form

Volumes 208-209, 6 issues

(Please print)

NAME: _____

INSTITUTION: _____

ADDRESS: _____

CITY: _____ STATE: _____ POSTAL CODE: _____

COUNTRY: _____ TELEPHONE: _____

FAX: _____ E-MAIL ADDRESS: _____

Please send me a 2005 subscription to *The Biological Bulletin* at the rate indicated below:

Price includes both print and online versions. All subscriptions run on the calendar year.

❒ Individual: $120.00 (6 ISSUES) ❒ Institutional: $360.00 (6 ISSUES)

❒ Individual: $70.00 (3 ISSUES) ❒ Institutional: $180.00 (3 ISSUES)

Check one: ❒ February, April, June or ❒ August, October, December

---

Please send me the following back issue(s): _____

❒ Individual: at $25.00 (PER ISSUE) ❒ Institutional: at $75.00 (PER ISSUE)

Delivery Options

❒ Surface Delivery (Surface delivery is included in the subscription price.)

❒ Air Delivery (Please add the correct amount to your payment.)

U.S. and Canada: $45.00 Mexico: $60.00 All other locations: $100.00

Payment Options

❒ Enclosed is my check or U.S. money order for $ _____

payable to Marine Biological Laboratory (with reference *The Biological Bulletin*)

❒ Please charge my ❒ VISA ❒ MasterCard ❒ Discover Card $ _____

Account No.: _____ Exp. Date: _____

Signature: _____ Date: _____

❒ Please send me an invoice. (Note: Payment must be received before subscription commences.)

Return this form with your check or credit information to:

Subscription Administrator, *The Biological Bulletin*
Marine Biological Laboratory, 7 MBL Street
Woods Hole, MA 02543 U.S.A.
Fax: 508-289-7922 • Tel: 508-289-7402 • E-mail: lreuter@mbl.edu

www.biolbull.org

Published by the Marine Biological Laboratory
Woods Hole, Massachusetts, 02543 U.S.A.

MARINE RESOURCES CENTER

MARINE BIOLOGICAL LABORATORY • WOODS HOLE, MA 02543 • (508)289-7700
WWW.MBL.EDU/SERVICES/MRC/INDEX.HTML

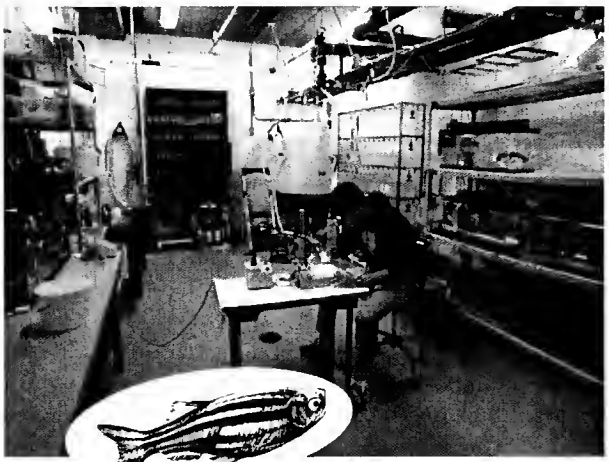

zebrafish facilities

Animal and Tissue Supply for Education & Research

- 150 aquatic species available for shipment via online catalog: <http://www.mbl.edu/animals/index.html>; phone: (508)289-7375; or e-mail: specimens@mbl.edu
- zebrafish colony containing limited mutant strains
- custom dissection and furnishing of specific organ and tissue samples

MRC Services Available

- basic water quality analysis
- veterinary services (clinical, histopathologic, microbial services, health certificates, etc.)
- aquatic systems design (mechanical, biological, engineering, etc.)
- educational tours and collecting trips aboard the R/V Gemma

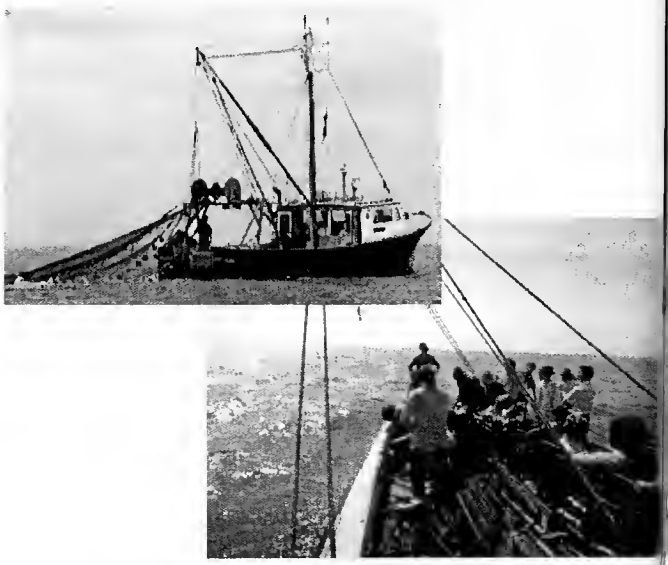

Using the MRC for Your Research

- capability for advanced animal husbandry (temperature, light control, etc.)
- availability of year-round, developmental life stages
- adaptability of tank system design for live marine animal experimentation

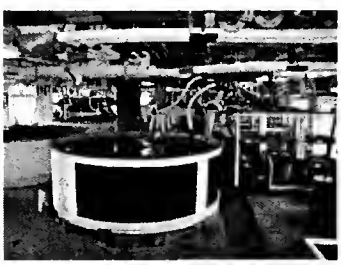

Zebrafish images from Talbot Laboratory, Stanford University

Whole Organism Macro Fluorescence

From the leader in 3-D optics comes the world's first Macroscopic Fluorescence zoom system for high-resolution, whole organism imaging, the NEW **Leica MacroFluo™**

In the past, capturing quality images of entire adult model organisms like mice, rats, zebrafish or stickleback fish was difficult due to their size. With the **MacroFluo™** this is no longer the case as this fluorescence imaging system is capable of capturing extra large fields. Add a Leica DFC digital camera and realize the system's true potential by capturing multiple large field-of-view images in a stack. These images are automatically rendered into an amazing composite photo where all planes, from top to bottom, are in focus at the same time (i.e. Image Stacking or MultiFocus).

Achieve Better Images... for Faster Answers with the **Leica MacroFluo™!** Call 800/248-0123 today for a free consultation!

Intelligent Automation

Leica Microsystems Inc
2345 Waukegan Road
Bannockburn, IL 60015

Telephone (847) 405-0123 (800) 248-0123
Fax (847) 405-0164
In Canada call (800) 205-3422
www.stereomicroscopy.com

Leica
MICROSYSTEMS